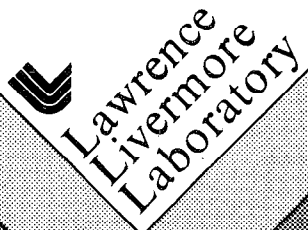
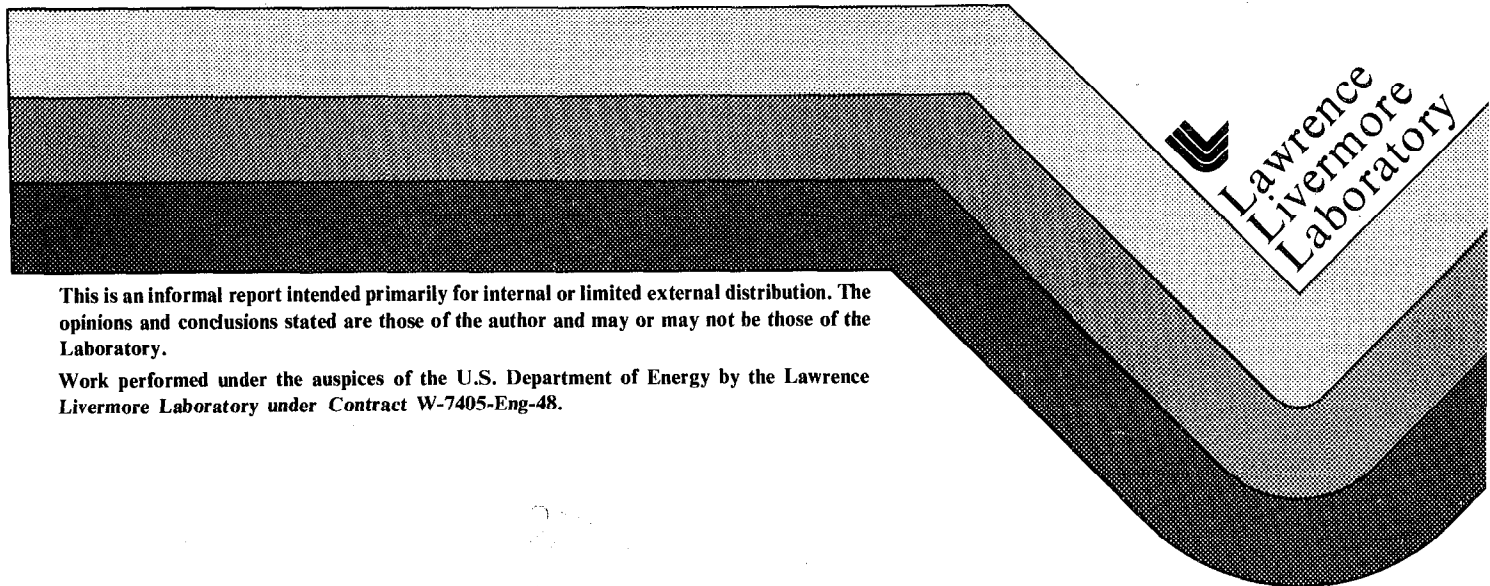


Tandem mirror hybrid reactor design study final report

R. W. Moir, B. M. Boghosian, R. S. Devoto,
J. L. Erickson, J. H. Fink, J. D. Lee, J. O. Myall,
W. S. Neef, Jr., J. W. Feldmann, A. E. Dubberley,
J. H. Germer, W. H. Harless, D. W. Jeter, S. Kraus,
M. Kangilaski, L. Nemeth, T. C. Osborne, G. R. Pflasterer,
C. Schatmeier, S. L. Stewart, K. R. Schultz, E. T. Cheng,
R. L. Creedon, V. H. Pierce, C. P. Wong, R. E. Aronstein,
S. K. Ghose, C. A. Shorts, M. H. Meleis, and M. G. Gadd

September 29, 1980



This is an informal report intended primarily for internal or limited external distribution. The opinions and conclusions stated are those of the author and may or may not be those of the Laboratory.

Work performed under the auspices of the U.S. Department of Energy by the Lawrence Livermore Laboratory under Contract W-7405-Eng-48.

DISCLAIMER

This document was prepared as an account of work sponsored by an agency of the United States Government. Neither the United States Government nor the University of California nor any of their employees, makes any warranty, express or implied, or assumes any legal liability or responsibility for the accuracy, completeness, or usefulness of any information, apparatus, product, or process disclosed, or represents that its use would not infringe privately owned rights. Reference herein to any specific commercial product, process, or service by trade name, trademark, manufacturer, or otherwise, does not necessarily constitute or imply its endorsement, recommendation, or favoring by the United States Government or the University of California. The views and opinions of authors expressed herein do not necessarily state or reflect those of the United States Government or the University of California, and shall not be used for advertising or product endorsement purposes.

This report has been reproduced
directly from the best available copy.

Available to DOE and DOE contractors from the
Office of Scientific and Technical Information
P.O. Box 62, Oak Ridge, TN 37831
Prices available from (615) 576-8401, FTS 626-8401

Available to the public from the
National Technical Information Service
U.S. Department of Commerce
5285 Port Royal Rd.,
Springfield, VA 22161

TANDEM MIRROR HYBRID REACTOR DESIGN STUDY
FINAL REPORT

Lawrence Livermore National Laboratory - R. W. Moir, Editor

B. M. Boghosian, R. S. Devoto, J. L. Erickson,
J. H. Fink, J. D. Lee, J. O. Myall, and
W. S. Neef, Jr.

General Electric Company

J. W. Feldmann, A. E. Dubberley, J. H. Germer,
W. H. Harless, D. W. Jeter, S. Kraus, M. Kangilaski,
L. Nemeth, T. C. Osborne, G. R. Pflasterer,
C. Schatmeier, and S. L. Stewart

General Atomic Company

K. R. Schultz, E. T. Cheng, R. L. Creedon,
V. H. Pierce, and C. P. Wong

Bechtel National, Inc.

R. E. Aronstein, S. K. Ghose, C. A. Shorts,
M. H. Meleis, and M. G. Gadd

September 29, 1980

*Formerly UCRL-52875.

CONTENTS

	<u>Page</u>
SECTION 1. INTRODUCTION	1-1
SECTION 2. EXECUTIVE SUMMARY	2-1
Mechanical Design of the Plant	2-4
Plasma Physics	2-6
Blanket Design	2-11
Helium-Cooled Blankets	2-12
Liquid Metal-Cooled Blankets	2-16
Water-Cooled Blanket	2-16
Beryllium and Molten Salt Blanket	2-21
Magnet Design	2-24
Injector Design	2-25
Microwave Heating	2-26
Plasma Direct Converter	2-26
Balance of Plant	2-32
Burner-Fission Reactor Description	2-34
Environment and Safety Analysis	2-36
System Modeling and Analysis	2-36
Resource and Market Economic Assessment	2-38
References	2-41
SECTION 3. PLASMA PHYSICS AND ENGINEERING	
Introduction	3-1
Magnetohydrodynamic (MHD) Instabilities	3-5
Microinstabilities	3-10
Thermal Fusion Mode of Operation	3-14
Two-Component Operation	3-19
Barrier Cell Operation	3-24
Future Work	3-31
References	3-32
SECTION 4. FUSION SYSTEMS DESIGN	
Neutral Beam Injectors	4-1
Neutral Beam Requirements	4-1

	<u>Page</u>
Injector Description	4-1
Development Requirements	4-5
Microwave Heaters	4-6
Microwave Requirements	4-6
Electron Heating by Microwaves	4-6
Magnet System	4-7
Introduction	4-7
Central Cell	4-9
Plug Coils	4-10
Transition Coils	4-10
A-Cell	4-11
Comparison with MFTF-B	4-12
Direct Converter - Mechanical Considerations	4-13
Introduction	4-13
End Tank Geometry	4-13
Vacuum Pumping	4-15
References	4-17
SECTION 5. ALTERNATE BLANKET COOLANT STUDIES	
Introduction	5-1
Helium	5-1
Gas-Cooled Reactor Technology	5-2
Advantages of Helium	5-2
Disadvantages of Helium	5-5
Gas-Cooled Blanket Options	5-6
Scoping Studying Evaluations	5-9
Mechanical Design	5-13
Recommendation	5-14
Liquid Metal-Cooled Blanket Design	5-17
Introduction and Summary	5-17
Blanket Configuration	5-19
Magnetic Field Considerations	5-22
Thermal-Hydraulic Analysis	5-24

	<u>Page</u>
Water-Cooled Blanket Design Concepts	5-25
Oblong Tube Concept	5-28
Cartridge Concept	5-28
Linked Assembly	5-33
Pool Concept	5-36
Beryllium/Molten Salt-Cooled Design	5-41
Concept and Justification	5-41
Molten Salt Technology Assessment	5-55
Conclusions	5-58
Water-Cooled Blankets	5-58
Molten Salt	5-59
Helium Cooling	5-59
References	5-60

SECTION 6. HELIUM-COOLED SYSTEM DESIGN

Introduction to Blanket Design	6-1
Large Module Approach	6-5
Design Philosophy and Concept	6-5
Mechanical Design	6-8
Reactor Orientation	6-8
Reactor Modularity	6-9
Vacuum Seal Configuration	6-11
Inflatable Cushion	6-12
Vacuum Seals	6-12
Summary of Vacuum Seal Systems	6-14
Shield Design	6-15
Blanket Changeout and Fuel Handling	6-15
Materials Considerations	6-22
Structural Material Requirements	6-22
First-Wall Structural Material	6-23
Cladding Material for Fuel	6-25
Tritium Breeding Material	6-27
Safety Aspects of Lithium Materials	6-30
Thorium Metal Fuel	6-31
Cartridge Design	6-33

	<u>Page</u>
Submodule Configuration	6-35
Submodule Flow Configuration	6-36
Submodule Fuel Configuration	6-36
Thermal-Hydraulics Design	6-38
Temperature and Pressure Drop Limits	6-39
Analysis	6-41
First-Wall Cooling	6-42
Fuel-Plate Thermal-Hydraulic Design	6-43
Plate Design and Mechanical Design Limits	6-43
Input from Neutronics Results	6-46
Flat Plate Fuel Design	6-46
Plate Design Thermal Hydraulics Results	6-51
Axially Oriented Rods With Cross Flow	6-55
Thermal-Hydraulic Results for Axial Rod, Radial Flow Design	6-57
Radial Rod, Radial Flow Design	6-60
Thermal Hydraulic Comparison	6-60
Blanket Coolant Pressure Drops	6-61
Nucleonics	6-64
Method of Calculations and Nuclear Data	6-64
Nucleonic Performance Comparisons of the Th Materials	6-67
Blanket Nucleonic Design Concepts	6-70
Final Blanket Design Calculations	6-73
Shield Design	6-82
Conclusions	6-85
Power Conversion System	6-85
Blanket Cost Estimates	6-86
Blanket Direct Cost	6-87
Annual Replacement Cost	6-87
Conclusions and Recommendations	6-90
Mechanical Design	6-92
Neutronics Design	6-93
Materials Selection	6-94
An Alternate Approach - The Linked Assembly Concept	6-95
Introduction - Philosophy and Concept	6-95
General Description	6-97

Fusion Reactor Requirements	6-99
Fuel Container Tubes	6-99
Lithium Tanks	6-100
Coolant Piping	6-101
Primary Shield	6-101
Solenoid Coils	6-102
Fuel Assemblies	6-102
Refueling and Maintenance	6-104
Design Development Requirements	6-106
Blanket Cost Estimate	6-106
Balance-of-Plant Design and Cost Estimate	6-107
Introduction	6-107
Heat Transport System	6-109
Energy Conversion System	6-112
Heat Rejection System	6-112
Plant Performance	6-114
Integrated Plant Design	6-114
Reactor Containment Building	6-126
Steam Generator Building	6-127
Reactor Service Building	6-128
Control Building	6-128
Auxiliary Building	6-129
Turbine Building	6-129
Conclusions and Recommendations	6-129
Basis and Scope Definition	6-133
Cost Scaling Algorithms	6-135
References	6-137

SECTION 7. MOLTEN SALT-COOLED SYSTEM DESIGN

Introduction	7-1
Study Objectives and Methodology	7-3
Blanket Design	7-4
Materials	7-6
First Wall	7-9
Blanket Structural Material	7-11

	<u>Page</u>
Neutron Multiplier and Cladding	7-16
Tritium Permeability	7-19
Corrosion Due to MHD Effects	7-21
Neutronics	7-21
Discussion	7-21
Conclusions	7-29
Mechanical Design	7-30
Design Input	7-31
Conceptual Design Description	7-32
Maintenance Access	7-39
Alternate Concept	7-40
Cost Estimate	7-40
Thermohydraulic and Performance Evaluation	7-43
Internal Description	7-43
Helium Coolant Performance	7-46
Magnetohydrodynamic (MHD) Effects	7-47
Molten Salt Coolant Performance	7-49
Conclusions	7-52
Molten Salt Chemical Processing	7-54
Introduction and Objectives	7-54
Evaluation of Molten Salt Processing System	7-55
Processing of Gaseous Products	7-55
Processing of Nongaseous Products	7-61
Evaluation of R&D Needs	7-63
Balance-of-Plant Design and Preconceptual Cost Estimate	7-65
Introduction and Overall Description	7-65
Heat Transport System	7-66
Energy Conversion System	7-69
Heat Rejection System	7-69
Emergency Cooling and Afterheat Removal	7-71
Plant Performance	7-71
Plant Arrangement	7-75
Conclusions and Recommendations	7-77
Preconceptual Cost Estimate	7-79
Basis and Scope Definition	7-81

	<u>Page</u>
Mechanical Equipment	7-81
Piping	7-81
Electrical	7-81
Exclusions	7-81
Cost Scaling Algorithms	7-82
Design Review and Critique	7-83
General Comments	7-84
Materials Comments	7-84
Expected Difficulties with Graphite	7-86
Reactions Between Tritium and Beryllium	7-86
Neutronics Considerations	7-86
Balance of Plant Comments	7-87
Mechanical, Maintenance, and Safety Considerations	7-88
Salt Flow and Recovery Systems	7-91
Molten Salt Chemistry/Chemical Processing and BOP Considerations	7-92
References	7-94
SECTION 8. SYSTEMS ANALYSIS	
System Modeling and Analysis	8-1
Objectives	8-1
System Model	8-1
System Model Detailed Description	8-4
System Modeling Results	8-8
Phase I Results	8-8
Phase II Results	8-14
Fissile Cost (\$/g)	8-26
Phase III Results	8-27
Phase IV Results	8-27
Fission Burner Reactor Assumptions	8-37
Light Water Reactors	8-38
High-Temperature, Gas-Cooled Reactor	8-45
Resource and Market Economic Assessment	8-51
Introduction	8-51
Market Place in Year 2010	8-52
Alternate Nuclear Fuel Supply Options	8-69

	<u>Page</u>
Hybrid's Impact on Fuel Resources	8-75
National Commitment Scenario	8-79
Economics	8-88
Economic Ground Rules	8-89
Converter Reactor	8-93
Converter Fuel Characteristics	8-95
Converter Capital Costs	8-96
Converter Fuel Service Costs	8-96
Conversion	8-101
Enrichment	8-101
Fabrication	8-102
Reprocessing	8-102
Shipping and Waste Disposal	8-104
Operation and Maintenance	8-104
Hybrid Reactor	8-105
Fusion Driver Performance	8-105
Blanket Performance Characteristics	8-106
Capital Cost Estimates	8-108
Fuel Service Cost Estimates	8-108
Power Costs and Fuel Sales	8-110
Bred Fuel Prices	8-110
Commercial Plant Rating	8-110
Hybrid Deployment Rates	8-113
Reprocessing and Fabrication Considerations	8-113
Economies in Construction	8-114
Marketability of Program	8-114
Research and Development Costs	8-116
Incentives for Hybrid	8-116
Reference Electrical Utility Forecast	8-117
Electrical Forecast With a Hybrid	8-125
Summary of Conclusions	8-125
References	8-131

SECTION 9. ENVIRONMENTAL AND SAFETY ANALYSIS

Introduction	9-1
Helium-Cooled Design Safety Aspects	9-1
Blanket Safety	9-2
Fuel Heat-Up Rate	9-3
Forces During Depressurization	9-4
Plant Safety	9-4
Plant Shutdown Cooling	9-5
Reactivity Insertion Accidents	9-8
Local Flow-Blockage Accidents	9-8
Partial Blockage Accidents	9-9
Detection of Local Flow-Blockage Accidents	9-10
Reactor-Coolant Leakage	9-10
Secondary-Coolant System Leakage	9-11
Fuel-Handling Accidents	9-12
Safety Conclusions and Recommendations	9-13
Molten Salt-Cooled Design	9-14
Compatibility of Molten Salt With Steam and Air	9-15
Tritium Handling and Safety Issues	9-15
Structure Radioactivity Due to Neutron Activation	9-15
Abnormal Operational Situations	9-16
Chemical Processing Safety and Environmental Considerations	9-17
Design Basis Accident	9-17
Conclusions and Recommendations	9-18
References	9-19

SECTION 10. COMPARATIVE EVALUATION

Introduction	10-1
Helium Case	10-3
Summary of Design Choice	10-3
Molten Salt Case	10-3
Fission-Suppressed Blanket	10-4
Conclusion	10-4

	<u>Page</u>
SECTION 11. CONCLUSIONS AND RECOMMENDATIONS	
System Performance	11-1
Blanket Coolant Technology	11-1
Water Cooling	11-1
Liquid Metal Cooling	11-1
Helium Cooling	11-4
Fission-Suppressed Blanket Concept	11-4
Blanket Design Philosophy	11-4
Tandem Mirror Operating Modes	11-5
APPENDIX A. CORROSION DUE TO MHD EFFECTS	A-1
APPENDIX B. MOLTEN SALT CHEMICAL CONSIDERATIONS	B-1
APPENDIX C. ARGONNE NATIONAL LABORATORY COMMENTS ON THE MIRROR HYBRID STUDY	C-1
APPENDIX D. REASONS FOR TERMINATION OF THE MOLTEN SALT REACTOR PROGRAM	D-1

ILLUSTRATIONS

<u>Figure</u>	<u>Page</u>
1-1. Standard mirror configuration.	1-5
1-2. Mirror Fusion Test Facility (MFTF).	1-6
1-3. Standard Mirror Hybrid Reactor.	1-7
1-4. Variation of fissile fuel cost with an increase in plasma Q for the standard mirror and tandem mirror. The solid curve was calculated by arbitrarily varying Q from the design point. The dashed curve was calculated using constrained operating model with its costs, magnetic fields, injection energies and other parameters interrelated. The two curves cannot be directly compared because different economic assumptions were made (different capital charge rates); however, the shapes of the curves can be compared, and clearly the tandem design point is less sensitive to Q variations than the standard mirror design point.	1-8
1-5. Tandem mirror magnetic flux surface shape and axial profiles of plasma density, electrostatic potential, and magnetic field strength.	1-10
1-6. Tandem Mirror Experiment (TMX).	1-11
1-7. Tandem mirror facility - version of MFTF-B.	1-12
1-8. Artist's drawing of the Tandem Mirror Hybrid Reactor (TMHR).	1-13
2-1. Artists drawing of the Tandem Mirror Hybrid Reactor (TMHR).	2-5
2-2. Schematic of variation of electrostatic potential and magnitude of magnetic field on the axis of a tandem mirror device.	2-7
2-3. Q vs Γ for 2500 MW fusion power.	2-8
2-4. Helium-cooled blanket module.	2-13
2-5. Liquid metal-cooled blanket.	2-17
2-6. Boiling water-cooled linked fuel assembly blanket.	2-19
2-7. Portion of TMHR central region molten salt concept.	2-22
2-8. Arrangement of magnets.	2-24
2-9. Injector for the TMHR.	2-27
2-10. TMHR end plug configuration.	2-29
2-11. Plasma direct converter and plasma dump.	2-30

<u>Figure</u>	<u>Page</u>
2-12 Main BOP systems for He-cooled blanket concept.	2-32
2-13. Main BOP systems for the He-cooled blanket concept (plant layout).	2-33
2-14. TMHR power flow diagram - He-cooled.	2-35
2-15. Variation of fissile fuel cost with an increase in plasma Q for the standard mirror and tandem mirror. The solid curve was calculated by arbitrarily varying Q from the design point. The dashed curve was calculated using constrained operating model with its costs, magnetic fields, injection energies and other parameters interrelated. The two curves cannot be directly compared because different economic assumptions were made (different capital charge rates); however, the shapes of the curves can be compared, and clearly the tandem design point is less sensitive to Q variations than the standard mirror design point.	2-39
3-1. Schematic of variation of electrostatic potential and magnitude of magnetic field on the axis of a tandem-mirror device.	3-2
3-2. Loss boundaries for hot ions.	3-3
3-3. Trajectory of two typical magnetic field lines in the tandem mirror.	3-7
3-4. β_c/β_p vs $\Delta B/B$ for stability to interchange modes for a typical coil set with barrier fields. ³⁻⁹	3-8
3-5. Plot of r_p/ρ_{iv} for stability against DCLC mode vs plasma β_v for deuterium energies of 200 and 600 keV.	3-11
3-6. Plot of n_w/n_H required for DCLC stability vs $S_v = r_p/\rho_{iv}$ for various plasma β .	3-12
3-7. Plot of optimized-Q vs Γ for 1500 MW _{fus} and 2500 MW _{fus} thermal fusion TMRs.	3-16
3-8. Plot of central cell length vs Γ for 1500 MW _{fus} and 2500 MW _{fus} , optimized-Q, thermal fusion TMRs.	3-16
3-9. Plot of first wall radius vs Γ for 1500 MW _{fus} and 2500 MW _{fus} , optimized Q, thermal fusion TMRs.	3-17
3-10. Plot of direct electron heating fraction vs Γ for 1500 MW _{fus} and 2500 MW _{fus} , optimized-Q, thermal fusion TMRs.	3-17
3-11. Plot of central cell ion temperature vs Γ for 1500 MW _{fus} and 2500 MW _{fus} , optimized-Q, thermal fusion TMRs.	3-18
3-12. Plot of electron temperature vs Γ for 1500 MW _{fus} , and 2500 MW _{fus} , optimized-Q, thermal fusion TMRs.	3-18

<u>Figure</u>	<u>Page</u>
3-13. Q vs Γ_w for two-component operation with $P_F = 2500$ MW.	3-22
3-14. Power to central cell and plugs vs Γ_w for two-component operation with $P_F = 2500$ MW.	3-22
3-15. Power ratio for central cell (Q_c) and for central cell plus plugs (Q_{tot}) vs Γ_w for two-component operation with $P_F = 2500$ MW.	3-23
3-16. Electron temperature (T_e) and tritium target temperature (T_t) vs Γ_w for two-component operation with $P_F = 2500$ MW.	3-23
3-17. Accessible Q/Γ parameter space; 500 MW fusion power Kelley mode Tandem Mirror Hybrid Reactor.	3-25
3-18. Accessible Q/Γ parameter space; 2500 MW fusion power Kelley mode Tandem Mirror Hybrid Reactor.	3-26
3-19. Insulation of the plug electrons from the central cell electrons by means of a potential drop between the plug and the central cell.	3-28
4-1. TMHR neutral beam injector design (24 MW).	4-3
4-2. TMHR end plug configuration.	4-4
4-3. Magnet arrangement for the 2500-MW hybrid reactor.	4-8
4-4. Hybrid-field magnitude $ B $ on machine axis.	4-9
4-5. TMHR yin yang plug flux fan.	4-14
4-6. TMHR cryopump panel location.	4-16
5-1. Liquid metal-cooled blanket configuration for TMHR.	5-20
5-2. Pool design--one-dimensional analytical model.	5-27
5-3. Oblong tube concept.	5-29
5-4. Oblong tube concept details.	5-30
5-5. Original cartridge concept--two rows.	5-32
5-6. Boiling water-cooled linked fuel assembly blanket.	5-34
5-7. Refueling and servicing layout--linked assembly concept.	5-35
5-8. Pool Concept No. 2.	5-38
5-9. Support ratios for blanket types. ($P_{fission}/P_{hybrid}$).	5-42

<u>Figure</u>	<u>Page</u>
5-10. Capacity expansion ratios for blanket types. (P_{fusion} per year/ P_{hybrid}).	5-43
5-11. Nuclear potential of Be blanket. [95% Be + 5% (^6Li + Th)].	5-45
5-12. Single-fluid, two-region, molten salt breeder reactor. For 1000 MW(e), the fuel salt flow rate through the core is 55,000 gpm, but less than 1 gpm passes through the processing plant. Electricity is produced from super- critical steam with an overall efficiency of 44% (from ORNL 4812).	5-47
5-13. Simplified flow diagram for processing a molten salt breeder reactor (from ORNL 4812).	5-48
5-14. Russian molten salt (fusion reactor) blanket.	5-50
5-15. Molten salt blanket concept--partial unassembled view.	5-52
5-16. Molten salt blanket concept--exploded view.	5-53
5-17. The system $\text{LiF-BeF}_2\text{-ThF}_4$.	5-54
6-1. Large module maintenance concept.	6-10
6-2. Module truck chassis.	6-11
6-3. Blanket changeout movement paths.	6-12
6-4. Omega point.	6-13
6-5. Module cross section.	6-13
6-6. Washer-shield concept.	6-16
6-7. Module service layout.	6-20
6-8. Allowable stresses for TMHR blanket module candidate materials.	6-24
6-9. Structural material strength.	6-26
6-10. Expected irradiation-induced swelling in candidate structural materials.	6-28
6-11. Module cross section.	6-34
6-12. Blanket pressure vessel and first wall.	6-35
6-13. TMHR He-cooled submodule.	6-37
6-14. Schematic of the He coolant temperature distribution in the blanket.	6-43

<u>Figure</u>	<u>Page</u>
6-15. First-wall cooling flow path.	6-44
6-16. Schematic of the wire-wrap fuel plates.	6-45
6-17. Blanket end-of-life power density.	6-47
6-18. Energy multiplication factor vs time.	6-50
6-19. Reynolds number versus multiplication factor (for plate thickness - 1.4 cm ave.).	6-50
6-20. Energy multiplication factor - pressure drop (mass flow rate vs time).	6-52
6-21. Nominal temperatures in the blanket.	6-53
6-22. Hot spot cladding temperature vs rod diameter for cross flow rods (average h).	6-58
6-23. Pressure drop vs rod diameter for cross flow rods.	6-59
6-24. Peak cladding hot spot temperature vs rod diameter for cross flow rods.	6-59
6-25. He coolant routing in the FRM blanket.	6-62
6-26. Breeding ratios vs fertile zone thickness at time = 0.	6-68
6-27. Blanket energy multiplication vs fertile zone thickness at time = 0.	6-68
6-28. Breeding ratio and blanket energy multiplication vs structural percent at time = 0.	6-69
6-29. One-dimensional schematic of the fusion-fission hybrid blanket neutronics calculational model.	6-74
6-30. Production of tritium or ^{233}U breeding ratio.	6-76
6-31. Burnup and fissile concentration vs exposure.	6-77
6-32. Blanket energy multiplication as a function of the Th zone thickness.	6-79
6-33. Tritium and ^{233}U breeding ratio as a function of first-wall exposure.	6-81
6-34. Blanket spatial distribution of volumetric nuclear heating.	6-82
6-35. Spatial distribution of ^{233}U enrichment as the end-of-life ($t = 9.6 \text{ MW-yr/m}^2$).	6-83
6-36. Linked assembly concept.	6-98

<u>Figure</u>	<u>Page</u>
6-37. Conceptual design--linked fuel assembly.	6-103
6-38. Linked assembly concept refueling and servicing layout.	6-105
6-39. TMHR He-cooled heat transport system heat balance.	6-109
6-40. Direct converter cooling and auxiliary blanket cooling system.	6-111
6-41. Energy conversion system heat balance.	6-113
6-42. Heat rejection system.	6-115
6-43. Integrated main BOP systems for He-cooled concept.	6-116
6-44. TMHR power flow diagram--He-cooled.	6-117
6-45. Artist's drawing of the Tandem Mirror Hybrid Reactor (TMHR).	6-119
6-46. General arrangement of reactor and support buildings (He-cooled).	6-121
6-47. Reactor and support buildings (He-cooled).	6-122
6-48. General Arrangement of reactor and support buildings--Section A-A (He-cooled).	6-123
6-49. Helium-cooled TMHR plot plan.	6-124
7-1. Block diagram of TMHR/molten salt concept.	7-2
7-2. TMHR/molten salt design effort logistics.	7-4
7-3. Cross-sectional view of TMHR/molten salt concept (central region).	7-7
7-4. Effect of irradiation temperatures of molybdenum alloys irradiated to 2.5×10^{22} m/cm ² . ⁵	7-10
7-5. Effect of postirradiation annealing on the ductility of irradiated austenitic stainless steel. ⁷	7-12
7-6. Estimated irradiation induced swelling in different structural alloys. ^{8,9}	7-13
7-7. Ultimate strength of selected alloys as a temperature function.	7-14
7-8. Effect of irradiation temperature on the ultimate strength of TMZ. ¹¹	7-14
7-9. Effect of irradiation temperature on the ductility of Mo. ¹¹	7-15
7-10. Pin design for graphite-clad beryllium rod.	7-16

<u>Figure</u>	<u>Page</u>
7-11. Helium release from beryllium as a function of irradiation temperature.	7-17
7-12. Irradiation-induced volume changes in different grades of graphite; irradiated at 705°C. ¹²	7-18
7-13. Dimensional changes vs fluence of high-density, five-grained isotropic graphites. ¹³	7-19
7-14. Permeation of tritium through various alloys. ¹⁷	7-20
7-15. Schematic diagram of repeating zone geometry for blanket heterogeneity study.	7-27
7-16. Portion of TMHR central region - molten salt concept.	7-33
7-17. Molten salt flow pattern in blanket segments.	7-37
7-18. Alternate concept - TMHR/molten salt central region.	7-41
7-19. Piping MHD effects.	7-50
7-20. Crossover MHD effects.	7-51
7-21. Simplified flow sheet for molten salt processing.	7-56
7-22. Schematic flow diagram of off-gas treatment system.	7-57
7-23. Gas recovery, if $3H$ and H pass through Pd separator.	7-59
7-24. Tritium recovery without Pd separator.	7-60
7-25. Continuous salt processing system for TMHR fuel-salt.	7-62
7-26. Heat transport system schematic.	7-68
7-27. Energy conversion system schematic.	7-70
7-28. Heat rejection system.	7-72
7-29. Integrated main BOP system for molten salt-cooled concept.	7-73
7-30. TMHR power flow diagram (molten salt-cooled concept).	7-74
7-31. Reactor and support building--general arrangement plan--molten salt-cooled concept.	7-76
7-32. Reactor and support building--section A-A.	7-77
8-1. System power flows.	8-2
8-2. Graphical solution of burner electric cost and hybrid fissile cost.	8-7

<u>Figure</u>	<u>Page</u>
8-3. System economics vs Q and wall loading (Γ) (base case is Th blanket and low technology driver).	8-12
8-4. Q vs wall loading trade off. The tandem driver was low technology (i.e., $B_{\max} = 12$ T, $E_{inj} = 200$ keV, with "A" cell). The blanket used Be and Th (molten salt).	8-13
8-5. Plasma Q vs first wall loading, Γ .	8-17
8-6. Central cell length vs Γ .	8-17
8-7. First wall radius vs Γ .	8-18
8-8. Fraction of input power in the form of direct electron heatin vs Γ .	8-18
8-9. Optimization of performance in Q, Γ space.	8-24
8-10. System power flows (Th/He case).	8-33
8-11. System power flows (Be/molten salt case).	8-34
8-12. U.S. electrical demand growth.	8-53
9-1. Standard fission-product decay-heat curve.	9-3
10-1. Blanket energy multiplication and fissile-fuel production are plotted vs neutron exposure. The energy multiplication for the fission-suppressed case is much less sensitive to exposure than the fast-fission case.	10-6
11-1. Physics and technology risk tradeoff.	11-7
11-2. Product fissile-fuel cost vs Q.	11-8
A-1. Electrical effects on corrosion.	A-2

TABLES

<u>Table</u>	<u>Page</u>
2-1. Fusion driver performance assumptions.	2-3
2-2. Hybrid plant parameters.	2-4
2-3. Operating modes for tandem mirror plasma parameters.	2-9
2-4. Helium cooled blanket characteristics--large module design.	2-14
2-5. Parameters for the lithium-cooled blanket.	2-18
2-6. Parameters for the boiling water-linked fuel blanket.	2-20
2-7. Perceived advantages of the Be/molten salt blanket.	2-21
2-8. Parameters for the molten salt-cooled blanket.	2-23
2-9. Magnet parameters.	2-25
2-10. Neutral beam injector microwave heating parameters.	2-28
2-11. Plasma direct converter parameters.	2-31
2-12. Burner fission reactor parameters (1000 MW _e).	2-36
3-1. Parameters for Kelley-mode operation.	3-27
3-2. Current and planned tandem mirror experiments and concepts to be tested.	3-31
4-1. TMHR injection requirements.	4-2
4-2. Comparison of hybrid with MFTF-B.	4-12
5-1. Gas-cooled reactor programs.	5-3
5-2. Advantages of helium-cooling.	5-4
5-3. Helium-cooled blanket concepts.	5-7
5-4. Blanket characteristics.	5-11
5-5. Helium-cooled blanket characteristics.	5-15
5-6. Helium-cooled TMHR characteristics.	5-16
5-7. Lithium blanket performance.	5-21
5-8. Water-cooled TMHR blanket performance.	5-40
5-9. Blanket neutronics--representative types and performance.	5-41

<u>Table</u>	<u>Page</u>
5-10. Materials used in the Molten Salt Reactor Experiment (MSRE) and the Molten Salt Fusion-Fission (MSFF) systems.	5-49
6-1. Automatic cushion seal development program.	6-14
6-2. Changeout affected equipment and conditions list.	6-17
6-3. Module changeout.	6-21
6-4. Allowable stresses for TMHR blanket module candidate materials.	6-24
6-5. Physical properties of thorium metal.	6-32
6-6. Hot spot factor variables, coefficients, and their values.	6-49
6-7. Breeder plate design parameters.	6-54
6-8. Fuel configuration thermal-hydraulic characteristics.	6-56
6-9. Identification of blanket coolant channels.	6-63
6-10. Pressure drops through different blanket sections.	6-63
6-11. Neutron 25 energy group structure (in eV).	6-65
6-12. Gamma 21 multigroup structure (in MeV).	6-66
6-13. Optimized fertile zone thicknesses and corresponding neutronic performance characteristics for Th fusion-fission blanket designs.	6-71
6-14. Helium cooled blanket performance at beginning and end-of-life (9.6 MW-yr/m ² exposure).	6-80
6-15. Direct cost of He-cooled TMHR blanket.	6-88
6-16. Helium-cooled blanket characteristics--large module design.	6-91
6-17. TMHR design base parameters.	6-108
6-18. Direct level capital cost summary (3Q 1979 pricing).	6-131
6-19. Direct level capital cost detail (3Q 1979 pricing).	6-132
6-20. Cost scaling algorithms--He-cooled case (in million \$).	6-136
7-1. Fusion driver performance assumptions.	7-5
7-2. Properties of TMHR/MS case molten salt.	7-6
7-3. Material choices for the TMHR/MS.	7-9

<u>Table</u>	<u>Page</u>
7-4. Analytical model and computer performance parameter values for TMHR molten salt reference design.	7-23
7-5. TMHR molten salt blanket heterogeneity study.	7-25
7-6. TMHR molten salt blanket Li-6 enrichment study.	7-26
7-7. TMHR molten salt blanket MS/Be volume % tradeoff study.	7-26
7-8. TMHR molten salt blanket miscellaneous parametric studies.	7-29
7-9. Input to mechanical design.	7-31
7-10. Descriptive data--first wall.	7-35
7-11. Descriptive data--blanket pressure boundary.	7-38
7-12. Central region cost estimates.	7-42
7-13. Blanket module description.	7-44
7-14. Multiplier Rod Description.	7-44
7-15. Blanket geometry and power model (2 MW/m ² first wall neutron loading).	7-45
7-16. Power split (MW)	7-46
7-17. Helium cooling system performance.	7-47
7-18. Molten salt cooling system performance.	7-53
7-19. Direct level capital cost summary (3Q 1979 pricing).	7-79
7-20. Direct level capital cost detail (3Q 1979 pricing).	7-80
7-21. Cost scaling algorithms molten salt-cooled case (in million \$).	7-83
7-22. ORNL review team.	7-84
8-1. Blanket neutronics--representative types and performance.	8-9
8-2. Driver performance parameters.	8-9
8-3. Burner related input data.	8-10
8-4. Summary of Phase I results.	8-11
8-5. Plasma variables for Q vs wall loading tradeoff.	8-14
8-6. Thermal plasma central-cell ECRH cases--2500 MW _f .	8-16

<u>Table</u>	<u>Page</u>
8-7. Thermal plasma central-cell ECRH cases--1500 MW _f .	8-16
8-8. Th/He blanket performance and cost.	8-19
8-9. Burner reactor performance and cost parameters.	8-20
8-10. BOP costs (in millions of dollars unless indicated otherwise).	8-21
8-11. Cost coefficients.	8-22
8-12. Summary of results.	8-25
8-13. Summary of blanket information.	8-28
8-14. Economic variables for the various blanket cases.	8-29
8-15. Performance comparison of boiling water, water, helium, and molten salt blankets.	8-30
8-16. Blanket performance and cost parameters.	8-32
8-17. Fusion driver component costs and performances.	8-32
8-18. Hybrid capital costs (in millions of dollars).	8-35
8-19. LWR parameters.	8-35
8-20. System performance comparison vs blanket type.	8-36
8-21. Plutonium-fueled LWR cycles with Pu-recycle (1000 MWe).	8-39
8-22. Denatured ²³³ U-fueled LWR cycle with Pu credit (1000 MWe).	8-40
8-23. Recommended LWR fuel characteristics (1000 MWe - 100% PWR).	8-40
8-24. Capital investment costs (1979 \$/kWe, including interest during construction).	8-41
8-25. LWR fabrication costs (1979 \$/kg HM).	8-43
8-26. Reprocessing cost for LWR fuels (1979 \$ kg HM).	8-43
8-27. Converter-spend fuel shipping and disposal costs (1979 \$/kg HM discharged from reactor).	8-44
8-28. Converter operation and maintenance costs (1979 \$).	8-44
8-29. One-cycle LWR fuel cycle costs--mills/kWh (\$220/kg U ₃ O ₈ basis, 1979 \$).	8-46
8-30. One-cycle LWR costs (1979 \$).	8-47

<u>Table</u>	<u>Page</u>
8-31. HTGR-SC total plant cost summary. First plant and follow-on unit 1 of a twin (January 1978, dollars in millions).	8-49
8-32. HTGR fuel consumption characteristics.	8-51
8-33. Future electrical use (as a multiple of 1978 electrical use).	8-54
8-34. Nuclear capacity projection.	8-55
8-35. Nuclear contribution (as a multiple of year 2010 total electrical usage).	8-56
8-36. Comparison of world nuclear forecasts.	8-57
8-37. Reference nuclear forecast.	8-58
8-38. 1978 DOE U.S. uranium resource estimate (tons U ₃ O ₈).	8-59
8-39. U.S. uranium resource estimate.	8-60
8-40. U.S. uranium price estimates (\$/lb U ₃ O ₈ - 1979 \$).	8-62
8-41. World uranium resources by continent.	8-63
8-42. Expanded world uranium resource estimate (millions of tons U ₃ O ₈).	8-64
8-43. World uranium resource basis.	8-64
8-44. U.S. uranium demand--thousands of short tons U _e O ₈ (75% capacity factor, 0.20% tails).	8-65
8-45. Domestic uranium prices - \$/lb U ₃ O ₈ (1979\$).	8-67
8-46. U.S. uranium demand--thousands of short tons U _e O ₈ (75% capacity factor, 0.20% tails).	8-68
8-47. Enriched uranium price for 93% ²³⁵ U--\$/gm ²³⁵ U.	8-69
8-48. Enriched uranium price for 3% ²³⁵ U--\$/gm ²³⁵ U.	8-69
8-49. Uranium savings-function of tails assay.	8-70
8-50. LWR uranium and enrichment requirements as a function tails assay.	8-71
8-51. Cost of uranium from advanced enrichment processes - \$/lb U ₃ O ₈ (feed at 0.3% ²³⁵ U).	8-71
8-52. Cost of uranium from advanced enrichment processes - \$/lb U ₃ O ₈ (feed at 0.2% ²³⁵ U).	8-71

<u>Table</u>	<u>Page</u>
8-53. Year 2010 domestic uranium requirements with advanced enrichment (thousands of short tons).	8-72
8-54. Reference LWR reprocessing industry growth scenario.	8-74.
8-55. Fuels available from reprocessing industry.	8-76
8-56. Sample hybrid deployment scenarios (4000 MW _{th} plants).	8-78
8-57. Fuel production schedule - with ²³⁹ U blanket.	8-80
8-58. Fuel production schedule - with Th blanket.	8-81
8-59. Fuel production schedule - with ²³⁸ U blanket.	8-82
8-60. Fuel production schedule - with Be + Th blanket.	8-83
8-61. Required fuel cycle services with ²³⁸ U blanket - thousands of MT/yr) (blanket enriched to 2%; new fuel fabricated at 3% enrichment).	8-84
8-62. Required fuel cycle services with Th blanket - thousands of MT/yr (blanket enriched to 2%; new fuel fabricated at 3% enrichment).	8-85
8-63. Required fuel cycle services with ²³⁸ U blanket - thousands of MT/yr (blanket enriched to 2%; new fuel fabricated at 3% enrichment).	8-86
8-64. Required fuel cycle services with Be + Th blanket - thousands of MT/yr (blanket enriched to 2%; new fuel fabricated at 3% enrichment).	8-87
8-65. Example of a hybrid reactor fabrication cost calculation.	8-91
8-66. Example of an LWR fuel cost calculations for uranium.	8-92
8-67. Coordinated financial assumptions for investor-owned utilities.	8-94
8-68. LWR fuel requirements (1000 MWe reactor @ 75% capacity factor).	8-97
8-69. CANDU fuel requirements (1000 MWe reactor @ 75% capacity factor).	8-98
8-70. LWR fuel characteristics (with fuel recycle).	8-99
8-71. CANDU fuel characteristics.	8-100
8-72. Capital investment costs (1979 \$/kWe, including interest during construction).	8-101
8-73. Converter fabrication costs (1979 \$/kg HM).	8-103

<u>Table</u>	<u>Page</u>
8-74. Converter reprocessing costs (1979 \$/kg HM).	8-103
8-75. Converter spent fuel shipping and disposal costs (1979 \$/kg HM discharged from reactor).	8-104
8-76. Converter operation and maintenance costs (1979 \$).	8-104
8-77. Fusion driver performance parameters.	8-107
8-78. TMHR blanket performance parameters.	8-107
8-79. Preliminary TMHR capital costs - millions of dollars (4000 MW _{th} plant).	8-108
8-80. Typical TMHR fuel service costs.	8-109
8-81. Typical bred fuel and system costs.	8-111
8-82. Fissile Pu and ²³³ U price.	8-112
8-83. Reference electrical capacity forecast.	8-118
8-84. Typical assumptions for incentives analysis.	8-120
8-85. Current dollar expenditure summary for utility industry (reference capacity case).	8-121
8-86. Discounted dollar expenditure summary for the utility industry (reference capacity case).	8-123
8-87. Electrical forecast with hybrid.	8-126
8-88. Discounted dollar expenditure summary for electrical utility industry (with hybrid).	8-128
10-1. Fuel configuration thermal-hydraulic characteristics for He case.	10-7
10-2. Helium-cooled blanket neutronics performance at beginning and end of Life (9.6 MW-yr/m ² exposure).	10-8
10-3. Shield parameters.	10-9
10-4. Helium blanket design characteristics.	10-10
10-5. Neutronics design, damage level, and material selection.	10-11
10-6. Conclusion and recommendations for a helium-cooled TMHR blanket.	10-12
10-7. Mechanical design.	10-12
10-8. TMHR molten salt coolant plant description.	10-13

<u>Table</u>	<u>Page</u>
10-9. TMHR molten salt design material considerations.	10-14
10-10. TMHR molten salt coolant neutronics considerations.	10-15
10-11. TMHR molten salt coolant mechanical design considerations.	10-16
10-12. TMHR molten salt coolant thermal hydraulic considerations.	10-17
10-13. TMHR molten salt coolant chemical processing and BOP considerations.	10-18
10-14. Comparisons of helium vs molten salt.	10-19
10-15. Perceived advantages of the Be molten salt blanket.	10-20
10-16. Problems with molten salt.	10-21
10-17. Other fission-suppressed blanket options.	10-22
10-18. Bred fuel isotopics (ppm).	10-23
10-19. Fission-suppressed blanket (relative to fast-fission blanket).	10-24
11-1. Parameters for the Th/He and Be/molten salt blankets.	11-2

ABSTRACT

This report describes the first year (October 1978 through September 1979) of a 2-year design study* of a tandem mirror fusion reactor designed to produce fissile fuel for fission power reactors, e.g., the light-water reactor and high temperature gas reactor. The design study is carried out jointly by Lawrence Livermore Laboratory (LLL), General Electric Company (GE), General Atomic Company (GA), and Bechtel National, Inc.

The tandem mirror concept lends itself to the development of an excellent hybrid reactor because of its cylindrical geometry and steady-state nature. The study uses the case method based on coolant and fuel cycle technology and plasma physics operating modes. The four technologies distinguished by coolant type are gas (either He or steam), water, liquid metal, and molten salt.

Four physics operating modes are considered: two-component, Kelley, thermal, and thermal barrier. We chose the thermal barrier mode because of its simultaneous high Q and low beam and magnet technologies gave superior performance. The design described in the report however uses the Q ~ 2 thermal mode because the thermal barrier concept was invented toward the end of the first year's studies. The neutral beam injectors are of the negative-ion type operated at 400 keV. The magnet technology under consideration is based on Nb₃Sn conductor operated at 12 to 15 T. The plasma exhaust is converted at 50% efficiency to electricity in a one-stage, direct energy converter.

For all cases the size of the commercial plant is 4000 MW nuclear. Primary emphasis is on ²³³U production after an initial investigation of the U-Pu fuel cycle. Water is eliminated as a coolant because of poor breeding resulting from neutron moderation. Liquid metal is dropped because of its safety related fire hazard and MHD design problems. After a more thorough study of plants based on molten salt and He coolant technology, molten salt is judged to require too much development with too great a risk of not finding

*The second half of the planned study has been deferred due to the lack of funds.

solutions to problems, such as fabrication of Mo structures. The He-cooled Th metal blanket performs well and results in a fuel cost of 70 \$/g ^{233}U (compared to 80 \$/g for molten salt). It has a support ratio of 9, which is not as high as for fission-suppressed molten salt (20), but is still satisfactory. The general class of fission suppressed blankets, of which molten salt is only one example, is judged to be well worth further study in combination with the He coolant.

The electric power capacity of ^{233}U -fueled, light-water fission reactors that can be supported by the hybrid of the same nuclear power is 11,000 MWe for the gas-cooled case and 28,000 MWe for the molten salt case at an electric add on cost of 24% for He and 14% for molten salt to account for the hybrid part of the system.

SECTION 1
INTRODUCTION

The fusion-fission hybrid is a combination of the fusion and fission processes having complementary features. The idea is to surround a fusion reaction region (in our case the cylindrical part of the tandem mirror) with fertile materials (U or Th) to allow the fusion-produced neutrons to convert fertile ^{232}Th or ^{238}U to fissile ^{233}U or ^{239}Pu by transmutation. This fissile material, after being appropriately processed, can be fed into a fission reactor, releasing more energy than that generated by fusion.

The deuterium-tritium (D-T) fusion process releases 17.6 MeV and 1 neutron per fusion event. Thus, a fusion reactor produces a large number of neutrons per unit of energy, and with modest neutron multiplication in the blanket can produce large quantities of fuel via its extra neutrons. These features complement the fission reactor characteristics of producing a large amount of energy per fission event (200 MeV) but relatively few neutrons so that fuel breeding is difficult to achieve. It has been said that fission is "energy-rich but neutron-poor," while fusion is "neutron-rich but energy-poor." These characteristics are complementary and appear to fit together nicely in the hybrid concept.

A hybrid which could produce fissile fuel commercially by the year 2000 would be quite timely, because a fuel shortage for fission power plants is predicted by many people. This shortage would prevent further expansion of fission power after the year 2000. Thus, the hybrid development would be insurance against the possibility of a fuel shortage. This fuel shortage has long been anticipated, and until recently the fission breeder has been the sole proposed solution. The hybrid has many advantages over the breeder.

The fusion power plant has long been considered the inexhaustible power source of the future, but it may be difficult for fusion to be made practical, and commercial and contribute significant amounts of energy until long after the year 2000. By this time the large-scale burning of fossil fuels may have to be abandoned due either to scarcity or to effects of CO_2 accumulation in the atmosphere. This CO_2 accumulation may result in a greenhouse effect with climatic changes, and other unknown consequences. The hybrid, on the other hand, can be developed with fusion technology that, according to some

estimates, is less demanding and will be achieved sooner than for a pure fusion power producer.

As a driver for a fusion-fission system, the fusion components can have lower performance, $Q < 5$ for example, and have higher cost while still maintaining an economic advantage over pure fusion. The development of lower performance/higher cost fusion components must surely be easier, less costly, and quicker than that required for pure fusion. This less demanding fusion technology, coupled with the fact that only a relatively small number of fusion breeders are required to supply fissile material to an expanding, contemporary fission industry, means that fusion as fissile-fuel producers can have a commercial impact much sooner than pure fusion. In addition, the hybrid fits into the present and anticipated fusion power infrastructure and is not a radical change for the energy industry.

The steady progress in fusion research suggests that $Q = 1$ operation¹ will most likely be achieved in the devices now being built in several laboratories.

An early practical hybrid can be based on fusion conditions corresponding to $Q = 1$, although its performance would be considerably improved if Q were a factor of 2 or better. $Q = 1$ is considerably short of the Q required for pure fusion electrical breakeven,² and a commercially-viable, pure fusion power plant will need to exceed electrical breakeven conditions by at least a factor of 3. Thus, if development is pursued, a practical low- Q hybrid could provide a fuel source for fission reactors in a timely manner and also provide an early application of fusion. The practical experience gained thereby may accelerate the development of pure fusion.

Design flexibility inherently results from the hybrid concept, since the fusion neutron source is separate from the fuel-producing zone. Some examples follow:

- Early hybrids that have more power consumption could improve power production at the expense of some fuel production (²³⁹Pu production results in more energy release than does ²³³U production).
- Small demonstration-of-principle facilities would be built soon, possibly even before the year 1990, with minimal design risk in the nonfusion portions of the plant.
- Better fusion conditions could lead to hybrids in which fission is largely suppressed, resulting in considerable safety advantages.

- Production of ^{233}U could provide a source of fuel, which with an admixture of ^{238}U could not readily be usable for weapons.

The hybrid can provide practically inexhaustible energy (fuel) source, as can the fast breeder reactor, the thermal neutron near-breeder, and the electro-nuclear breeder. Each of these is compared to the hybrid based on complete, steady-state (i.e., nonexpanding) energy producing systems. In the case of the hybrid the system includes the fission reactors, such as thermal neutron reactors (LWR, HTGR, HWR, LWBR), which consume the produced fuel. A thermal neutron near-breeder includes a makeup fuel system (mining and isotope separation). The fast breeder includes fission reactors (usually less than one per fast breeder) to consume excess fuel produced. The electronuclear breeder uses accelerator-produced particles to produce neutrons, which in turn produce fuel as in the hybrid. This system, like the hybrid, includes the fission reactors to consume the fuel. The final output of each system is electrical power.

The hybrid has an advantage over these alternatives in that it moves fusion development forward, which is highly desirable. The fast breeder, thermal neutron near-breeder, and hybrid can all supply fuel to fission reactors already developed and deployed. The fast breeder must generate electricity for sale to a load distribution network, whereas the hybrid because of its high fuel production rate can be a zero net electricity producer, i.e., be offline. The fast breeder needs large amounts of Pu to provide the initial core loading, and this fuel has to be bred in other reactors. Additionally, its low breeding ratio of about 1.3 will delay the ultimate economic advantage of the breeder. The hybrid, on the other hand, starts out using natural or depleted U and Th, and immediately begins to produce either Pu or ^{233}U , or both, and has a higher rate of fissile fuel production. The thermal neutron near-breeder also has logistic problems. It needs a great amount of ^{235}U , and therefore a lot of mined uranium and facilities for uranium isotope separation plus a developed Th fuel cycle to get started.

Cost comparisons are important, but highly uncertain at this time; however, some comparisons can be made. We expect fast breeders to cost significantly more—perhaps twice as much—as LWR's while supplying little fuel. Thus, the system capital cost (breeder plus burner) is approximately tripled, while the electric output is only approximately doubled. In comparison, the hybrid can cost considerably more than the breeder can cost because it supplies

fuel for many low-cost LWR's or near-breeders. The large allowable capital cost for hybrids will facilitate early introduction. The electronuclear breeder suffers a penalty similar to breeders in that about a factor of 2 fewer fuel atoms are produced per invested capital cost compared to the hybrid. The electronuclear breeder, on the other hand, can use linear accelerator technology, which is further developed than fusion technology.

The motivation for developing the hybrid is the possible shortfall of fissile fuel. To illustrate this shortfall, uranium resource projections can be compared with projected requirements. The following examples are taken from a study by Werner.³ In the U.S., the LWR's, either operating or under construction, are forecast to be about 200 by the year 1990. Assuming a 5% growth from 1990, there will be 325 by 2000, 530 by 2010, and 865 by 2020. Taking 171 tons of U_3O_8 per LWR-year for a 30-year life, and 480 tons for the initial core, then the cumulative uranium commitments are 1.7, 3.1, and 5.7 million tons for reactors starting up by year 2000, 2010, and 2020. United States uranium resource estimates vary from 2 to about 6 million tons at a forward cost of \$50/lb between the years 2002 and 2021. Resource depletion is thus indicated in the year 2014, the year 4 million tons are committed. (These figures account for uranium to last the remaining life of those reactors that are built.) If the growth rate is only 2.5%, then the date the resource is depleted (4 million tons) is prolonged until 2025.

If uranium recycle is employed, the resource base will expand by 10 to 15%; with Pu recycle also, the resource will expand 15 to 25%. Further, if the uranium-thorium cycle is utilized, the resource will last even longer. The point of these examples is to show that major reliance on nuclear fission for electrical power is not possible early in the next century without deployment of either near-breeders (U-Th reactors), breeders, or alternate breeding concepts such as the hybrid or the electronuclear breeder.

One of the first studies⁴ on the hybrid was carried out at LLL in 1954. With the discoveries of rich deposits of uranium in the 1950's, providing a relatively large, low cost resource of the fissile isotope ^{235}U compared to its demand, interest in the hybrid decreased. In the early 1970's, there was renewed interest^{5,6} in the hybrid due to the significant demand for ^{235}U in the commercial LWR's then operating and planned. The interest was also due to the reduced optimism about the fast breeder reactor and due to the slow progress toward pure fusion. A review article on hybrids was written

in 1973 summarizing current thoughts.⁷ Conceptual hybrid designs were completed for a mirror fusion driver,⁸ a tokamak driver,⁹ and a laser fusion driver.¹⁰ These designs tended to be primarily fuel producers (fuel factory); however, other designs emphasized power production^{11,12} and were sometimes called a fusion power amplifier.

The 1954 Imhoff, et al., study⁴ was based on a simple mirror concept (solenoid plus circular mirror coils at each end). As the mirror concept progressed, so did the sophistication of the design studies. The magnetic-well stabilized mirror using a so-called yin-yang coil (called a standard mirror), shown in Fig. 1-1, became the configuration of the large project at LLL called the Mirror Fusion Test Facility (MFTF), shown in Fig. 1-2. Its possible performance on D-D simulates Q of about 0.1 for the D-T reaction.

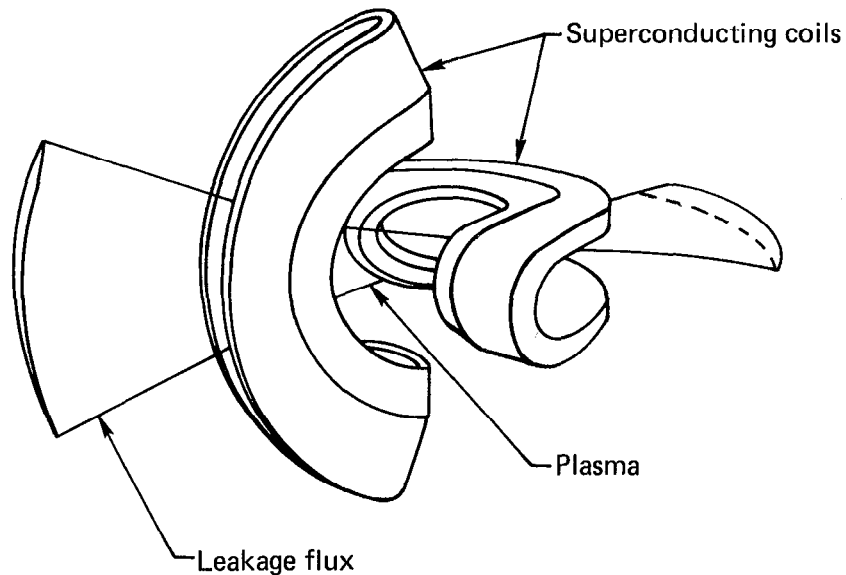


Fig. 1-1. Standard mirror configuration.

A 2-year reference design study¹³ was carried out on the hybrid version of this concept and is shown in Fig. 1-3. One feature of the design was its use of a large conventional, prestressed, concrete pressure vessel to enclose the magnet, beams, blanket, and helium coolant system. The coolant and fuel technology was similar to that of a gas-cooled fast reactor with, however, a lower power density in the fuel. The fuel form chosen was U_3Si .

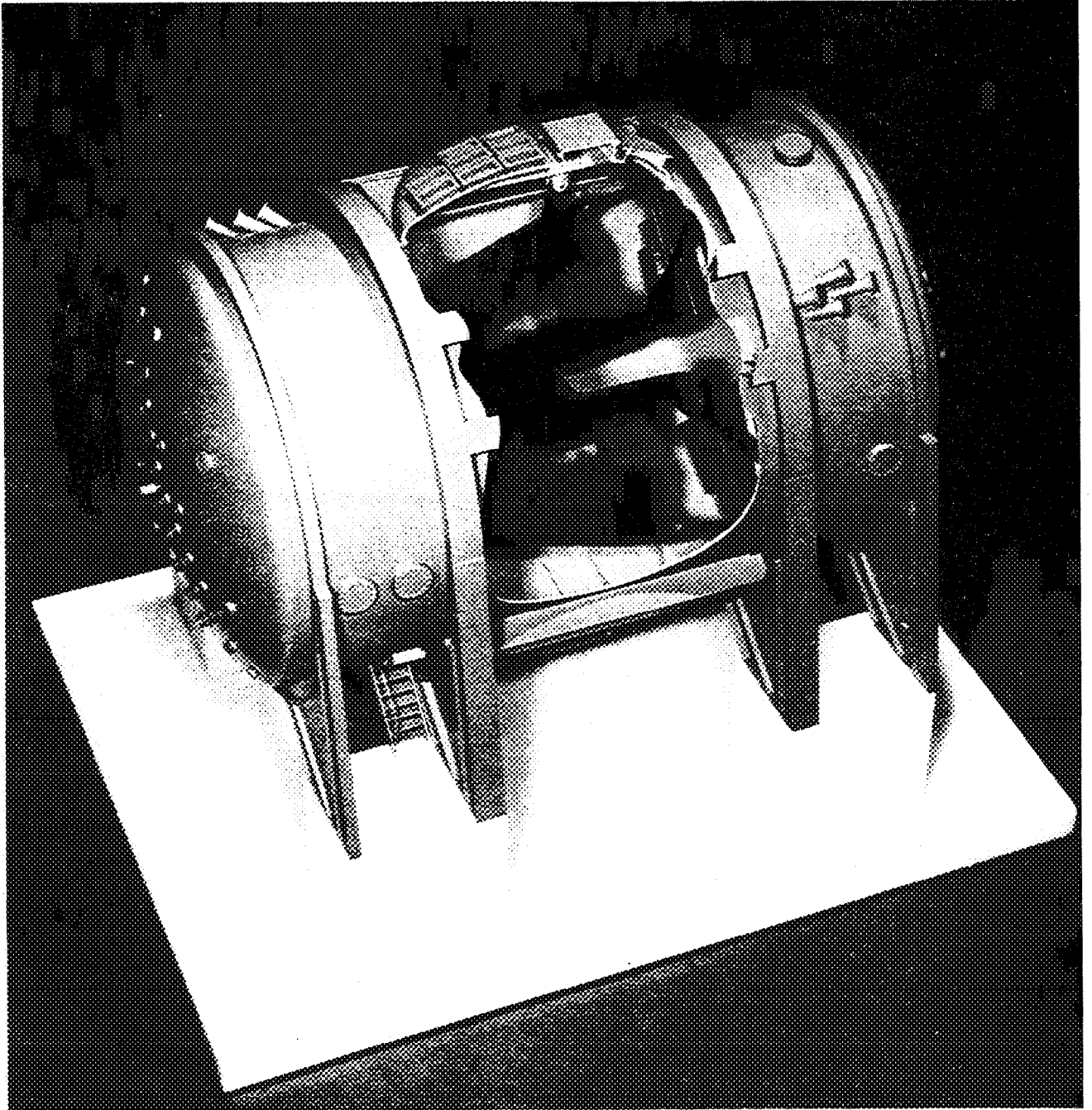


Fig. 1-2. Mirror Fusion Test Facility (MFTF).

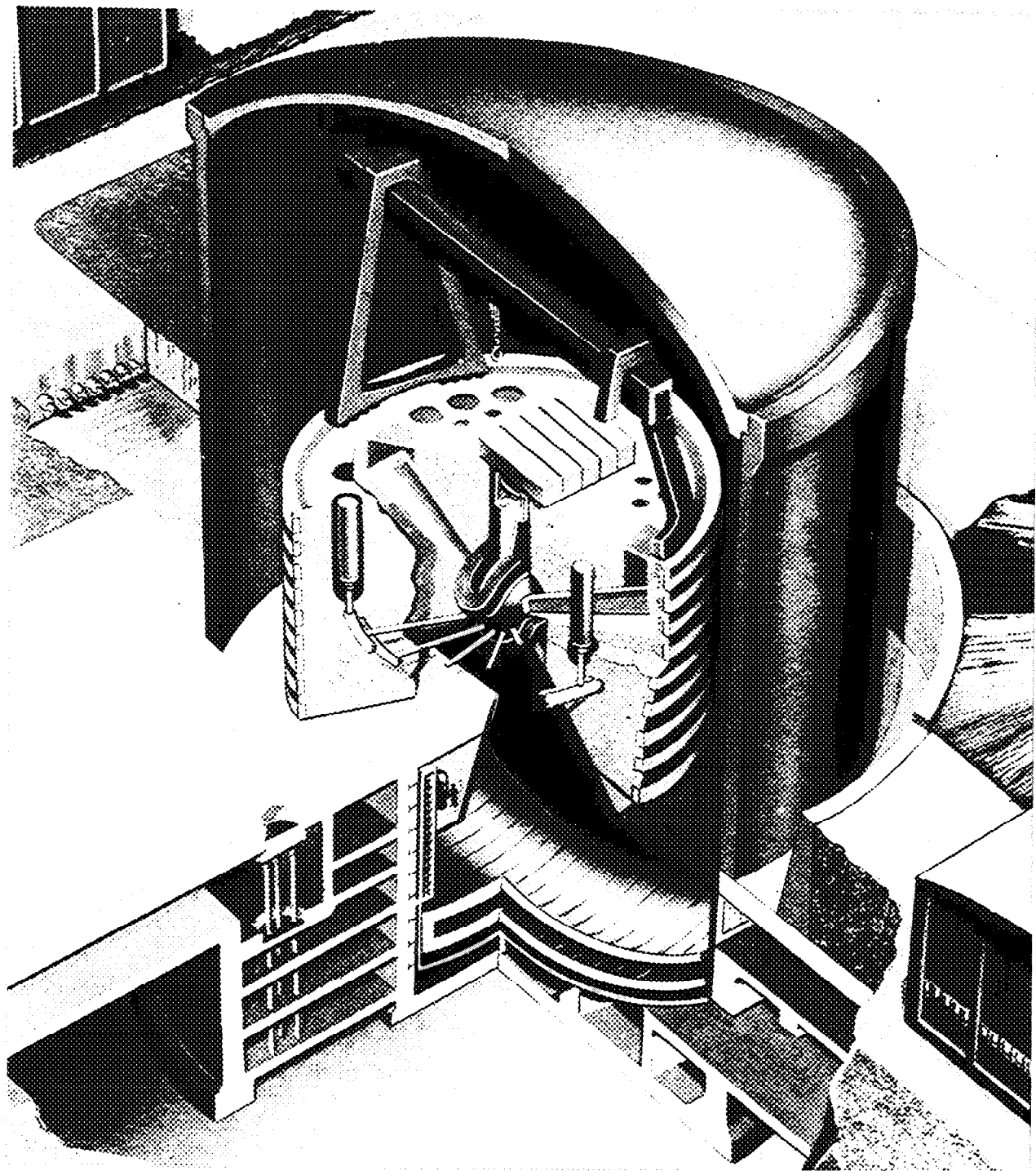


Fig. 1-3. Standard Mirror Hybrid Reactor.

Due to the high uranium density of U_3Si , a significantly higher fuel breeding resulted than for oxide fuel. A fuel-handling machine was conceptually designed to remove blanket modules from the inside of the reactor chamber. This machine was conceptually simple in that it operated on a spherical surface but was operationally complicated because of the necessity to make and break the vacuum and high pressure helium seals on each module. The performance of the standard mirror hybrid (whose design was constrained to use positive-ion beams and NbTi magnet technology), measured in \$/g of bred fuel was hurt by its low Q value of 0.6. The study showed the fuel cost versus Q relationship, given in Fig. 1-4. A clear advantage of higher Q was shown. Thus, the desire was strong for a new idea for improving the mirror hybrid reactor's performance and its simplicity.

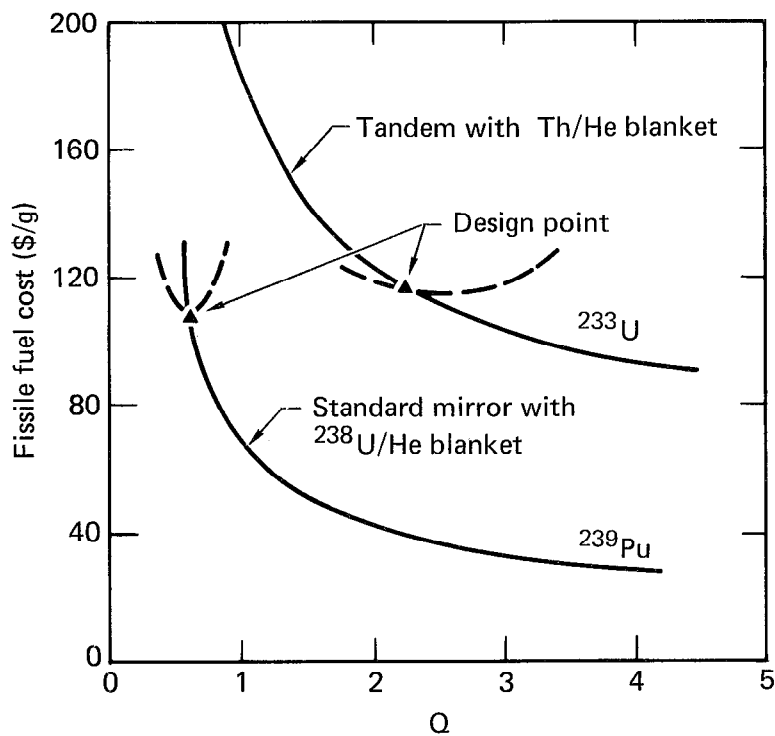


Fig. 1-4. Variation of fissile fuel cost with an increase in plasma Q for the standard mirror and tandem mirror. The solid curve was calculated by arbitrarily varying Q from the design point. The dashed curve was calculated using constrained operating model with its costs, magnetic fields, injection energies and other parameters interrelated. The two curves cannot be directly compared because different economic assumptions were made (different capital charge rates); however, the shapes of the curves can be compared, and clearly the tandem design point is less sensitive to Q variations than the standard mirror design point.

The tandem mirror concept was first invented in one form by G. Kelley¹⁴ in 1966. However, its high Q stable form was invented in 1976 by Dimov,¹⁵ Fowler, and Logan.¹⁶

The tandem mirror confinement idea (shown in Fig. 1-5) promised two distinct advantages over the standard mirror:

- The Q value could be higher by a factor of several from the 0.6 value for the standard mirror hybrid.
- The cylindrical geometry seems simpler than the spherical shell with its slots and beam holes of the standard mirror.

The tandem ideas are now being checked in an experiment called TMX (Tandem Mirror Experiment), shown in Fig. 1-6. Suggestions are pending to rebuild the MFTF into a large superconducting tandem mirror shown conceptually in Fig. 1-7.

The purpose of this study is to assess the usefulness and difficulty of breeding fission reactor fuel with tandem mirror fusion technology through the process of conceptual design. An artist's view of the anticipated Tandem Mirror Hybrid Reactor (TMHR) is shown in Fig. 1-8.

The hybrid is one possible development direction for tandem mirror fusion that involves production of radioactive nuclides resulting from nuclear transmutations and fission products in the region surrounding the fusion chamber. As progress is made in fusion research resulting in more output of fusion energy per input, the hybrid can evolve toward those designs, such as the molten salt hybrid where fission is largely suppressed.⁵ Further progress may result in pure fusion power, and still further progress might allow advanced fuel fusion reactions in which neutron production and tritium use is suppressed (clean fusion).

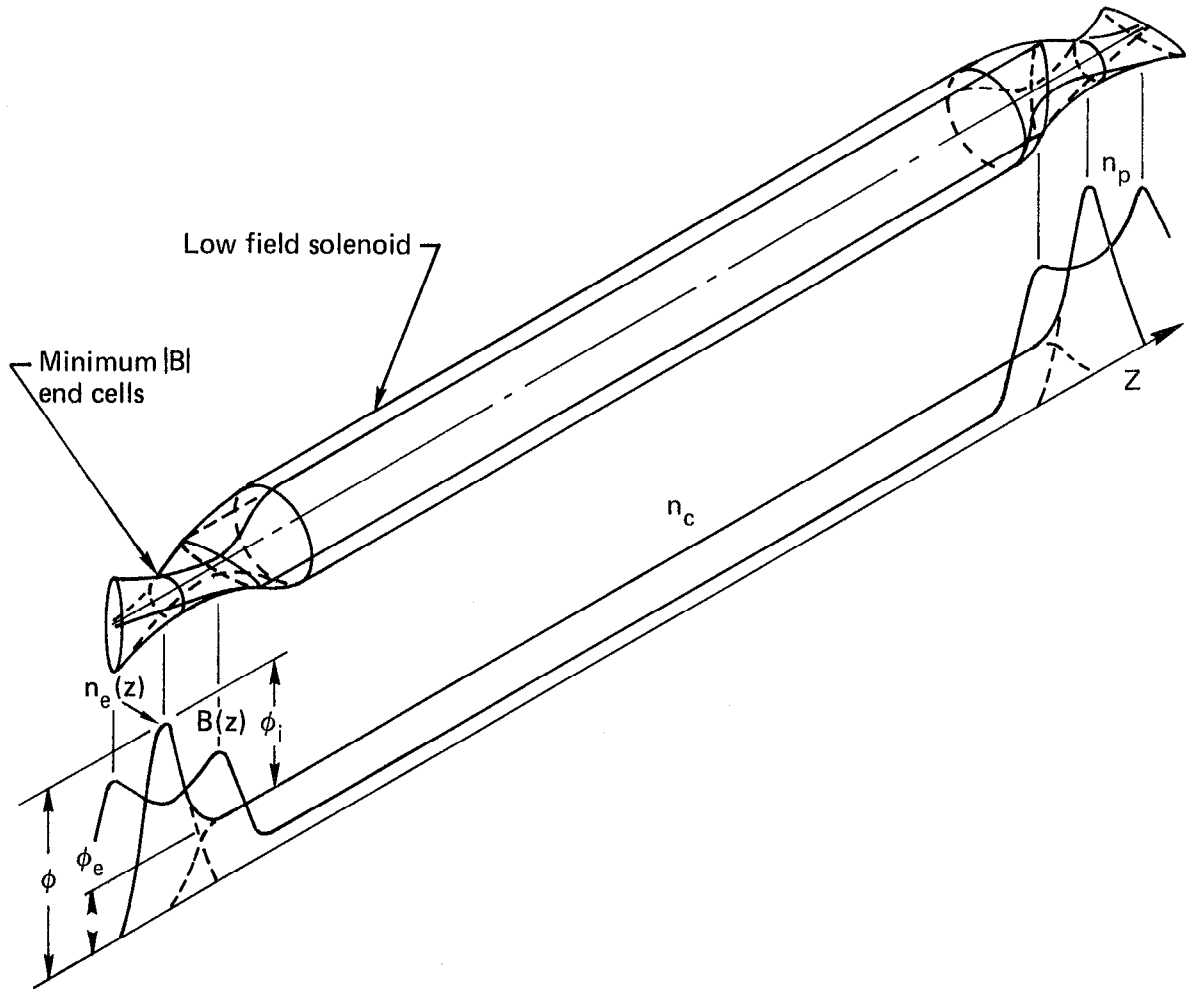


Fig. 1-5. Tandem mirror magnetic flux surface shape and axial profiles of plasma density, electrostatic potential, and magnetic field strength.

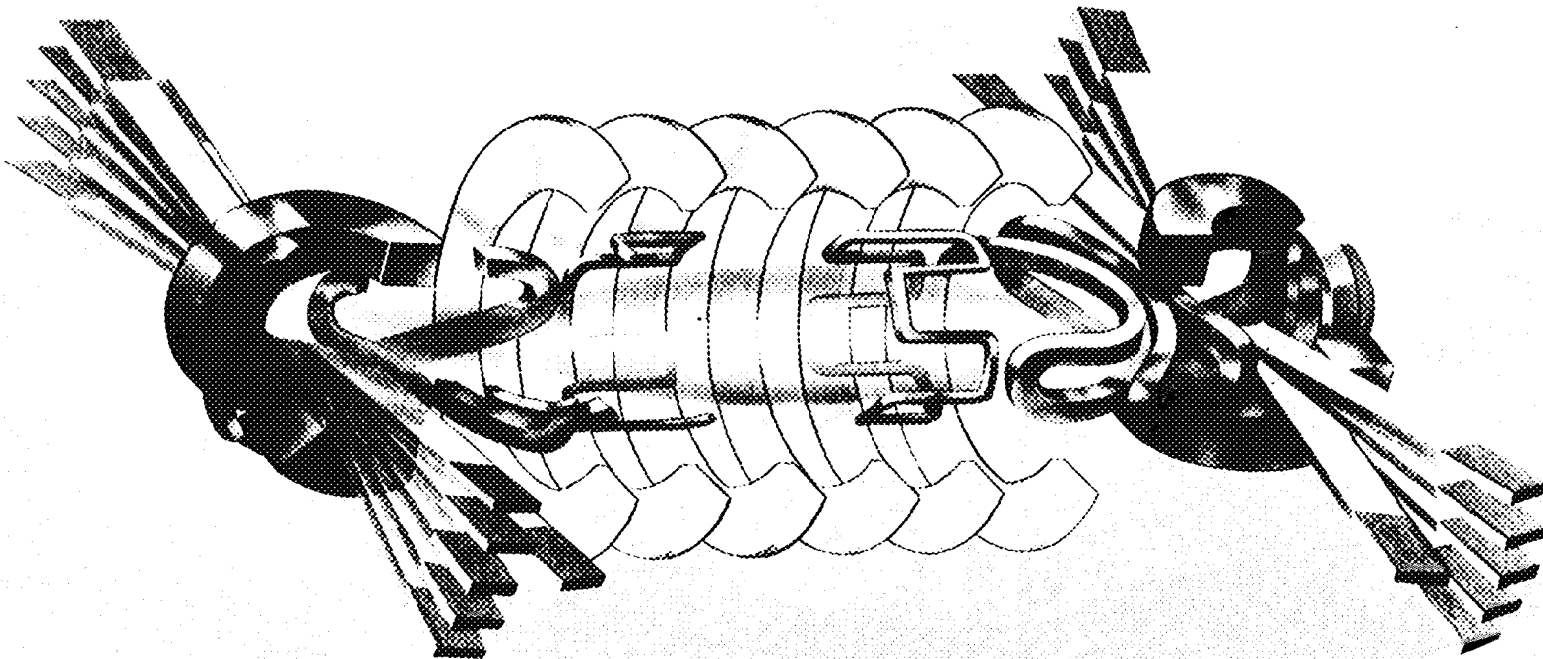


Fig. 1-6. Tandem Mirror Experiment (TMX).

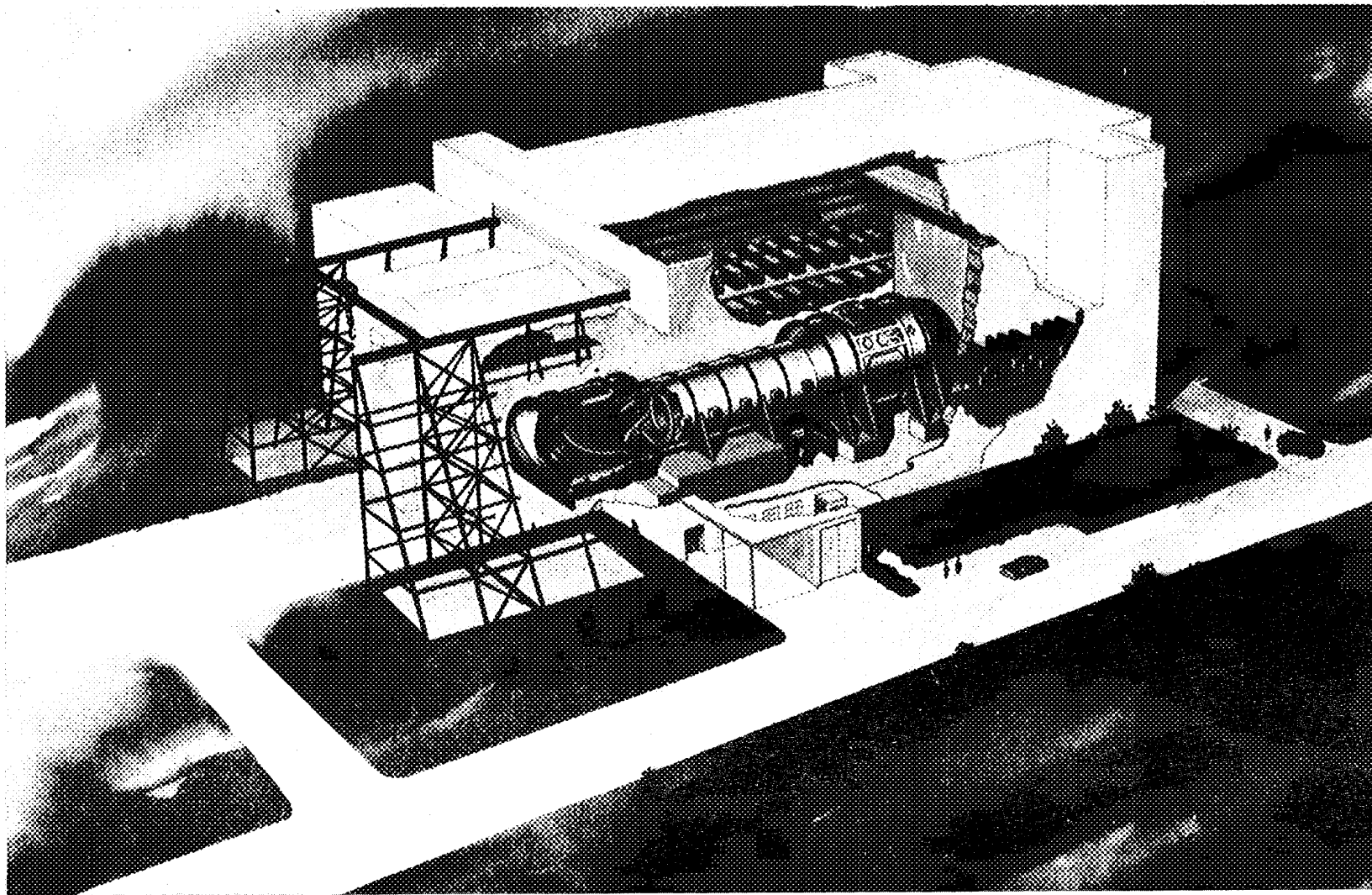


Fig. 1-7. Tandem mirror facility - version of MFTFB.

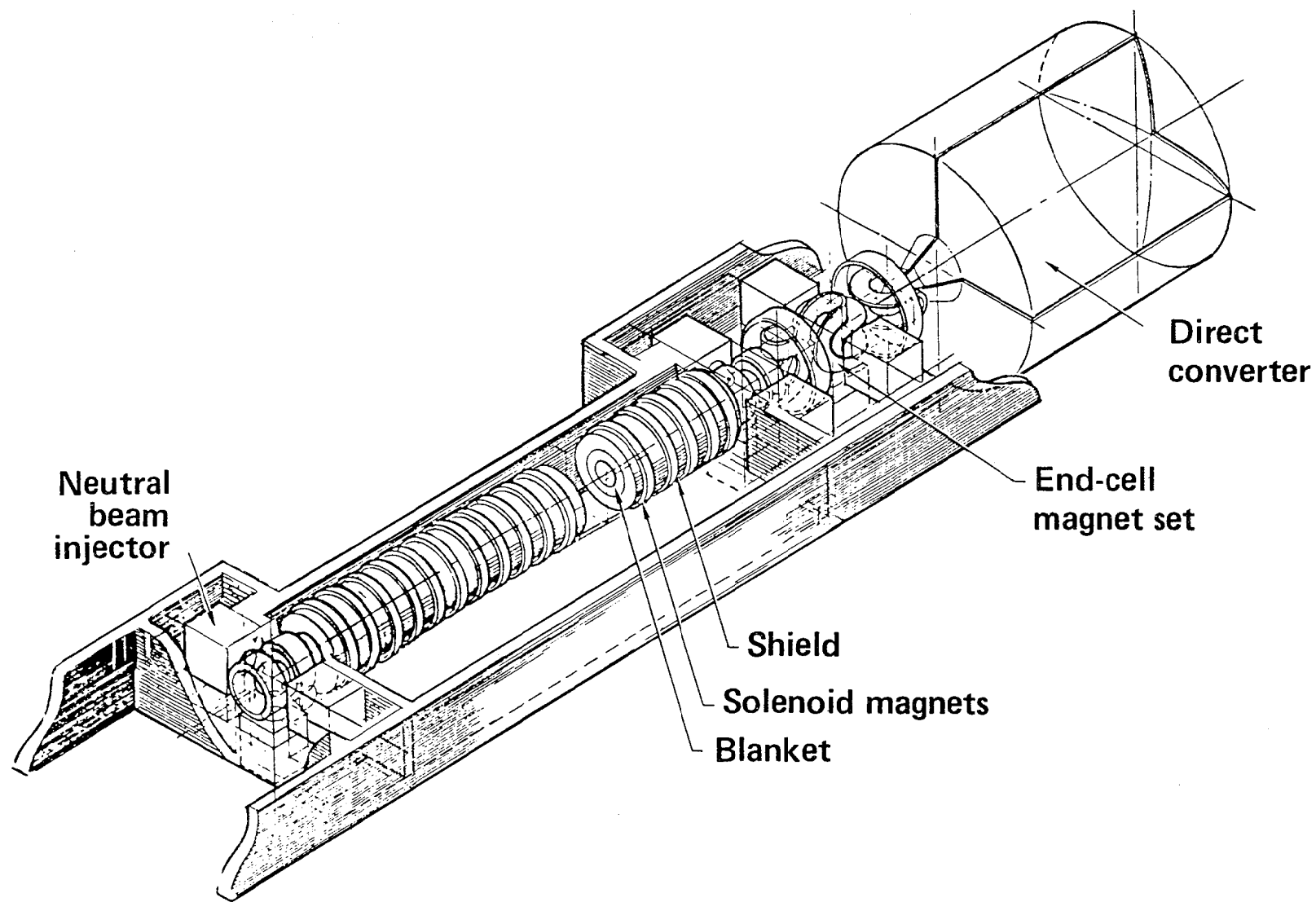


Fig. 1-8. Artist's drawing of the Tandem Mirror Hybrid Reactor (TMHR).

REFERENCES

1. Q is defined as the ratio of the energy of the fusion (17.6 MeV per DT reaction) to the energy invested in the fusing plasma for heating and maintaining losses. $Q = 1$ is called scientific feasibility. The definition of Q does not include the efficiencies of handling the input and output energies.
2. For electrical breakeven, the electrical energy recovered from the fusion process just exceeds the electrical energy supplied to the fusing plasma. The efficiencies of energy conversion are included here. $Q = 5$ corresponds to electrical breakeven for an efficiency of converting electrical energy into plasma energy and thermal conversion of 1/3. Q for electrical breakeven drops to 3.33 if a 50% efficient direct converter of plasma energy is practical. Commercialization of fusion is more difficult to achieve than electrical breakeven. It depends ultimately on the cost of delivered kilowatt hours.
3. R. W. Werner, "Cumulative Fuel Commitment for Light Water Reactors - Is There a "Uranium Crunch?" - "The Fusion-Fission Fuel Factory Can Help," Proceedings of the 4th Course "Driven Magnetic Fusion Reactors," Erice, Italy Sept. 18-26, 1978, also Lawrence Livermore Laboratory Report UCRL-81600(1978).
4. D. H. Imhoff, et al., "A Driven Thermonuclear Power Breeder," California Research and Development Corporation Report CR-6 (1954).
5. L. M. Lidsky, "Fission-Fusion Symbiosis: General Considerations and a Specific Example," in Proc. of British Nuclear Energy Society Nuclear Fusion Reactor Conference at Culham Laboratory, 1969, pp. 41-53, Culham Laboratory Report CLM-NFE (1969).
6. J. D. Lee, "Neutronics of Sub-Critical Fast Fission Blankets for D-T Fusion Reactors," in Proc. 7th Conf. Intersociety Energy Conversion Engineering, 1972 (American Chemical Society, 1972), p. 1294.
7. B. R. Leonard, Jr., "A Review of Fusion-Fission (Hybrid) Concepts," Nucl. Tech. 20, 161 (Dec. 1973).
8. R. W. Moir, et al., "Progress on the Conceptual Design of a Mirror Hybrid Fusion-Fission Reactor," Lawrence Livermore Laboratory Report UCRL-51797, p. 45 (1975).

9. R. P. Rose, et al., "Fusion-Driven Breeder Reactor Design Study," Final Report, WFPS-TME-043, May 1977.
10. Bechtel Corporation, "Laser Fusion-Fission Reactor Systems Study," U.S. ERDA Report UCRL-13796 pp. 1-8 (July 1977).
11. E. Greenspan, et al., "Natural Uranium Fueled Light Water Moderated Breeding Hybrid Power Reactors - a Feasibility Study," Princeton Plasma Physics Laboratory Report PPPL-1444 (1978).
12. F. H. Tenney, et al., "The Princeton Beam-Driven Tokamak Fusion-Fission Hybrid Reactor," TANS 024, 38 (1976).
13. D. J. Bender, editor, "Reference Design for the Standard Mirror Hybrid Reactor," a joint report by Lawrence Livermore Laboratory and General Atomic Company, UCRL-52489 and GA-A14796 (1978).
14. G. G. Kelley, Plasma Physics 9 p. 503 (1967).
15. G. I. Dimov, V. V. Zakaidakov, M. E. Kishinevskii, Sixth International Conference Plasma Phys. and Controlled Nuclear Fusion Research, Berchtesgaden, Fed. Rep. of Germany, 1976, Paper C4 (IAEA).
16. T. K. Fowler, B. G. Logan, Comments on Plasma Phys. and Controlled Fusion 2, 167 (1977).

SECTION 2.

EXECUTIVE SUMMARY

This report describes the first half (October 1978 through September 1979) of a planned 2-year study* of a tandem mirror fusion reactor designed to produce fissile fuel for light-water reactors (LWR's) and eventually for more advanced fission reactors. If the U.S. relies on fission power, a shortage of fissile fuel may occur early in the next century. Fusion-fission hybrid reactors offer a potentially economical and practically inexhaustible source of fissile fuel for fission reactors.

The goal of the U.S. fusion program is to develop fusion technology so that it is available in this time period. While it is quite possible that fusion may not be sufficiently advanced at that time to produce electrical power at an acceptable cost, fusion will probably be sufficiently developed to work well as a neutron source for breeding fissile fuel, ^{233}U from ^{232}Th or ^{239}Pu from ^{238}U . A hybrid could use a fusion system that may be a net energy consumer or produces power at a cost several times that of its fission counterparts—and could still make an economically viable power system by producing fissile fuel for consumption in relatively inexpensive fission power reactors.

The prospect for developing a fusion reactor with adequate performance for a hybrid system is quite good. The cost and safety aspects of the bulk of the power system, i.e., the 10 or more LWR's, are relatively well known and need little development. Also, the introduction of new capacity is much easier than for a fission breeder because the hybrid requires no initial fissile inventory.

We consider pure fusion power to be the ultimate goal of the U.S. fusion development program with a reliance on fission power based on fuel from mined uranium to support us until we attain economical fusion. Intended hybrid strategy is to develop the hybrid to the point where a relatively small number of them (one tenth or less of the number of supported fission reactors) could be built should a severe uranium shortage develop. This strategy fits well into an evolutionary philosophy of fusion. The application of fusion power would logically evolve from the hybrid fuel factory to pure deuterium-tritium

*The second half of the planned study has been deferred due to lack of funds.

(D-T) fusion to the ultimate objective of advanced fuel (clean) fusion as plasma confinement capability is gradually improved.

This study is based on the tandem mirror as the fusion part of the hybrid, mainly because LLL has a major program underway to develop the tandem mirror as a pure fusion reactor, and because another parallel DOE-sponsored hybrid study on the tokamak is underway by Westinghouse. The tandem mirror has desirable features such as steady state operation, simple cylindrical geometry, low first-wall power deposition, and a significant development program underway particularly if the tandem version of the Mirror Fusion Test Facility (MFTF) is built.

The study emphasis is on design of a commercial plant, although some parametric systems analysis is underway that will give size scaling information. Several operating regimes for the plasma are considered:

- The two-component operation, where an energetic beam (200 keV) of deuterium is injected into a cold background of tritium ions.
- The Kelley mode, where the end plugs are used to reduce the electric ambipolar field, but otherwise the ions are magnetically confined.
- The thermal mode, where the end-stopping is used to confine a thermal 50% deuterium and 50% tritium plasma.
- The thermal barrier mode, where confinement of the thermal mode is augmented by isolating the electron population with a negative electrostatic potential barrier.

We are still studying these cases to find either the best or an acceptable regime where Q should be at least between 1 and 2, and the wall load should be between 1 and 2 MW m⁻² (preferably the higher values for economic reasons as discussed later). Some design parameters based on the thermal mode are given in Table 2-1.

The magnet technology is based on Nb₃Sn conductor in the end plugs because the field strength at the conductor for most cases is about 12 T, which is over the 8 to 10 T capability of NbTi. The injector technology is based on the negative ion method of making neutral beams because the energies required are about 400 keV, and the injection efficiency for the positive-ion method is low at this energy level. It would be very desirable to develop ideas to lower both the field strength and injection energies to allow use of the better known technology of NbTi superconductor and the positive-ion-based neutral beam technology now widely employed in the fusion program.

Table 2-1. Fusion driver performance assumptions.

Parameter	He blanket	Molten salt blanket
Q	2	2.2
Γ , MW/m ²	1.5	2
R ^a _{first-wall} , m	2	2.1
R ^a _{solenoid magnet} , m	4	4.2
L ^a , m	39	90
P _{nuclear} , MW (max)	4000	4000
P _{fusion} , MW	915	3000
M _{blanket energy multiplication,} cycle average	5.2	1.4

*For comparison, the MFTF-B proposal employs similar magnets 2.2 m in radius, 25 m long with plasma radius of 0.4 m at 1.5 T (1.7 T for the hybrid).

Many breeding blanket varieties are considered. Both ²³⁹Pu and ²³³U production are possible, the latter being preferred in this study because less ²³³U is required in present-day fission reactors. Also, ²³³U can be isotopically denatured with ²³⁸U and would thus be more difficult to use in nuclear weapons.

At the beginning of this study, we set out to choose a blanket coolant technology for a reference design to be finished in the second year. During the scoping phase of this study, blankets based on He cooling, water cooling, liquid metal cooling, and molten salt cooling were investigated. The water-cooled blanket was dropped due to modest neutronic performance with the blankets. The liquid metal blanket was dropped because of perceived safety and magnetohydrodynamic (MHD) related concerns. The He and molten salt designs were carried further to develop preconceptual designs. The parameters of the hybrid plants are given in Table 2-2 for the He-cooled design and for two molten salt designs. One of the molten salt cases is the reference design discussed in Section 7, and the other is an improvement on this design.

Table 2-2. Hybrid plant parameters.

Parameter	He blanket	Molten salt blanket	
P_{nuclear}^a , MW	4000	4000	** (4000)
P_{fusion} , MW	915	3000	(2700)
P_{electric}^a , MW	890	270	(360)
Net electrical efficiency*, ^a %	25	7	(9)
kg ^{233}U /yr rate*	3310	8000	(9600)
kg ^{233}U /MW nuclear year	0.83	2.0	(2.4)
Total estimated direct cost, M\$	2000	4600	(4100)
Estimated \$/g	71	82	(59)
Number of fission reactors (LWR's) (at 303 kg/GWe yr) of 4000 MW nuclear supported	10.9	21	(25)

*Cycle average.

**Expected improvements from reference case.

The two reactors based on a He-cooled blanket and a molten salt blanket are quite different. The He-cooled design is a fast fission system with high power density and safety aspects similar to fission reactors. It uses conventional reactor technology and would need little additional unique materials or reactor technology development. The molten salt design has serious materials concerns and would require extensive development, but the fission-suppressed mode of operation offers significant design and safety advantages. In the end, neither of these two designs was selected for the reference design. With the improved plasma performance capability that now appears possible with the tandem mirror a low blanket energy multiplication can be accepted. Thus, it is recommended that further investigation of the fission-suppressed hybrid concept be pursued.

MECHANICAL DESIGN OF THE PLANT

The main part of the plant (Fig. 2-1) is composed of two distinct functional parts: the cylindrical section, where the fusion reaction and fuel breeding are the main function; and the end plug region, where fusion plasma

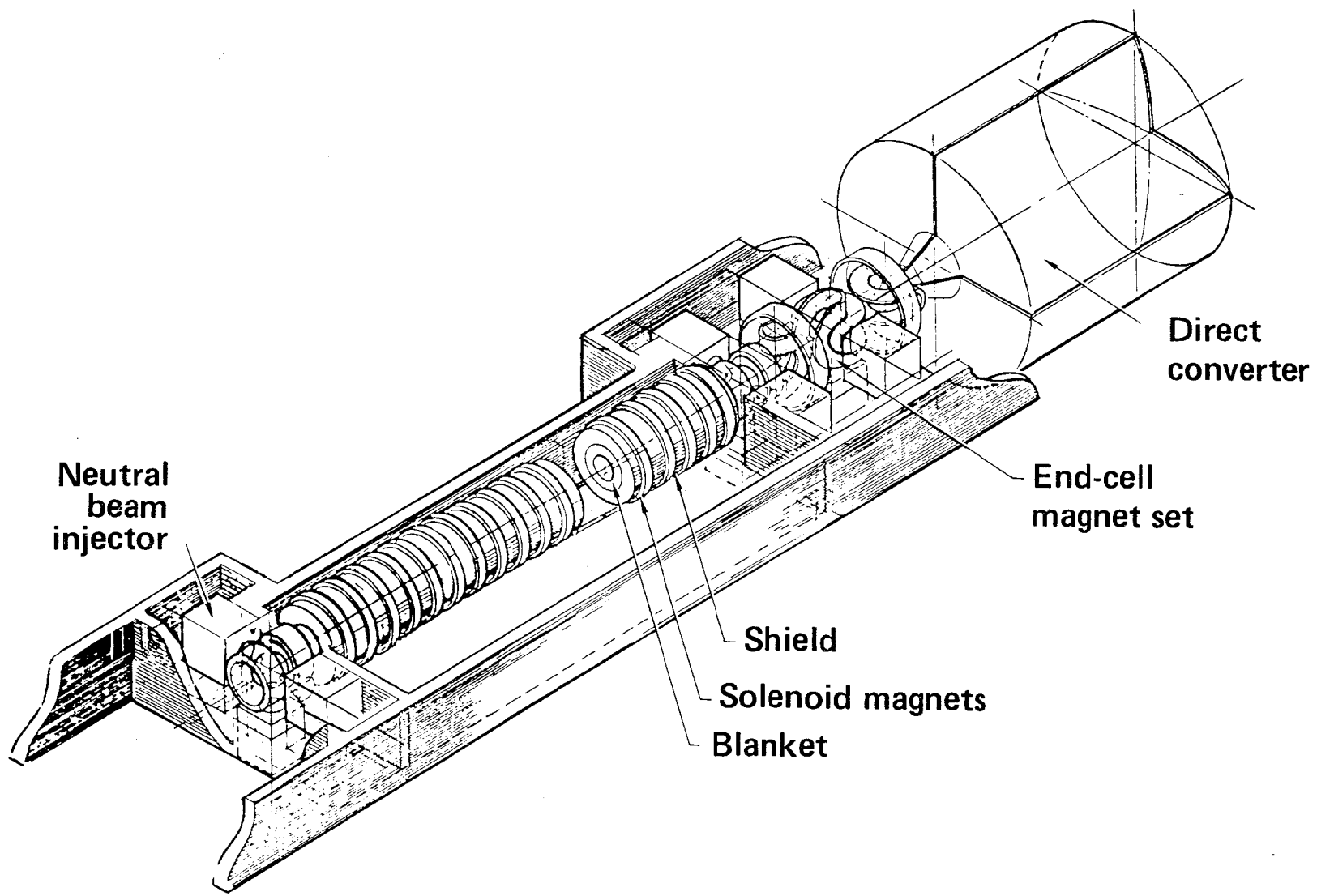


Fig. 2-1. Artists drawing of the Tandem Mirror Hybrid Reactor (TMHR).

confinement, heating, refueling, and dumping take place. The fusion reaction takes place along the 4-m diam, magnetically-confined plasma column that emits neutrons essentially as a line source. The breeding blanket surrounds this line source of neutrons. The blankets under consideration are characterized by geometric shape (pancakes, as shown in Fig. 2-1, or tube-type, not shown), by fuel form (Th) (solid or liquid), and by coolant type (He, water, steam, liquid metal, and molten salt).

The power level has been set at 4000 MW of nuclear power. Because some blanket types release more energy in the breeding reactions than others, the fusion power varies from 500 MW to 2500 MW and is accommodated by varying the length of the central section. The layout of the plant depends on the coolant selection and the detailed blanket design.

PLASMA PHYSICS

In previous reactor designs based on minimum-B mirrors (standard mirrors), we found that the large losses out the open ends limited the Q values (fusion power divided by input power) to about unity.¹ In 1976 Dimov et al.² and Fowler and Logan³ found it possible to essentially remove any limit on Q by placing three mirror devices in tandem as shown in Fig. 2-2. The two end devices (plugs) are, in effect, the standard mirror device operated at high density. The central device is cylindrical, which is a desirable shape for the incorporation of blankets. The plugs are maintained at a density higher than that of the central cell by neutral beam injection. As a result of the higher density, the electrostatic potential in the plugs is higher than in the central cell, thus forming a barrier to the leakage of central-cell ions. Because of this barrier, the central-cell ions are confined for much longer times, resulting in higher Q. Of course power must be expended in maintaining the plug plasma, which produces no power; but if the plug volume is much less than that of the central cell, the Q can be made quite high. A schematic of the potential and magnetic field distribution along the central axis of such a tandem mirror is shown in Fig. 2-2.

Several operating modes are possible for this tandem concept.

The potential at the end can be used to supplement magnetic mirror confinement in the central cell as suggested by Kelley.⁴ The results of parametric analysis for the Kelley mode are shown in Fig. 2-3, where we plot Q versus Γ , the neutron wall loading; both parameters play an important role in

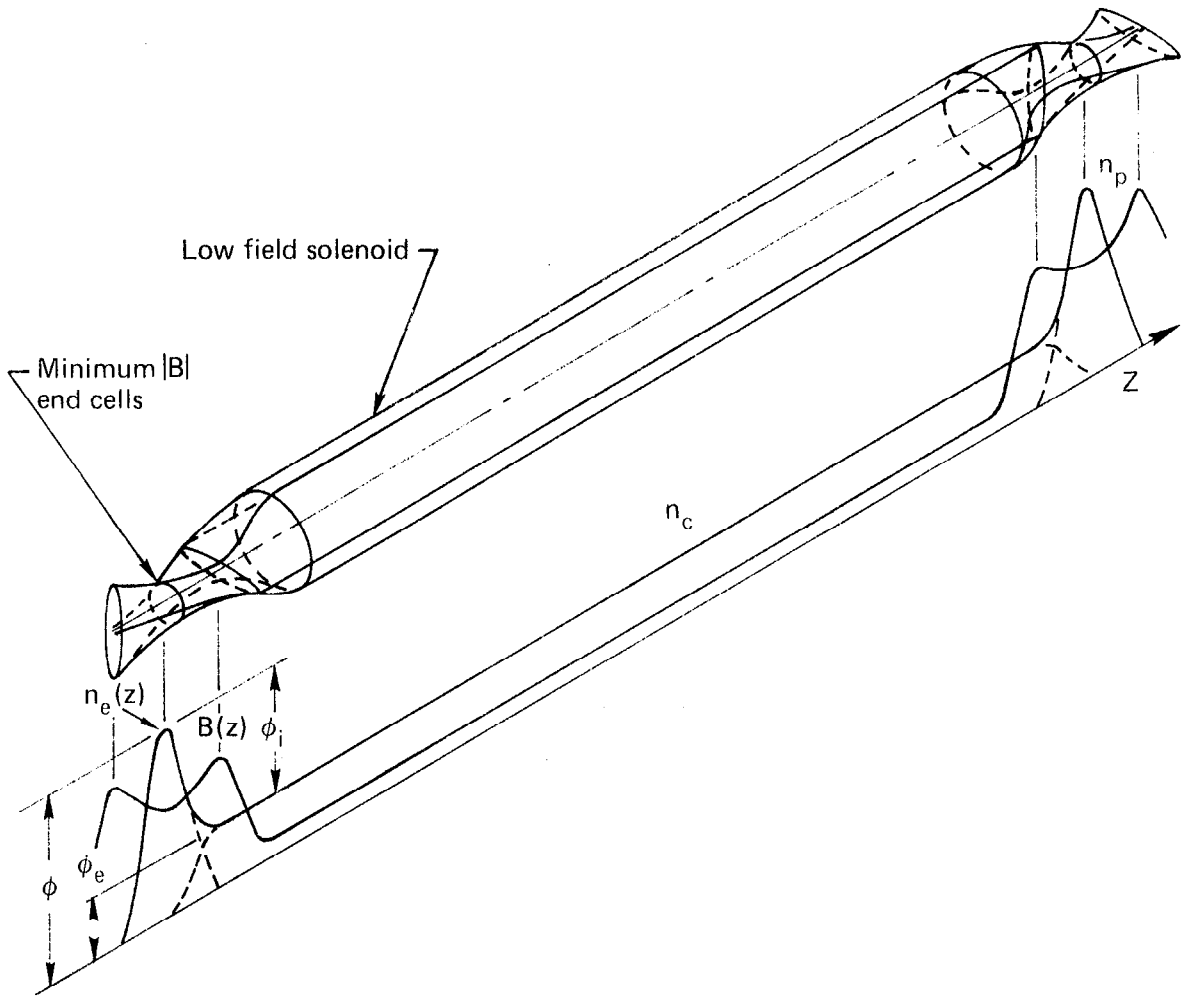


Fig. 2-2. Schematic of variation of electrostatic potential and magnitude of magnetic field on the axis of a tandem mirror device.

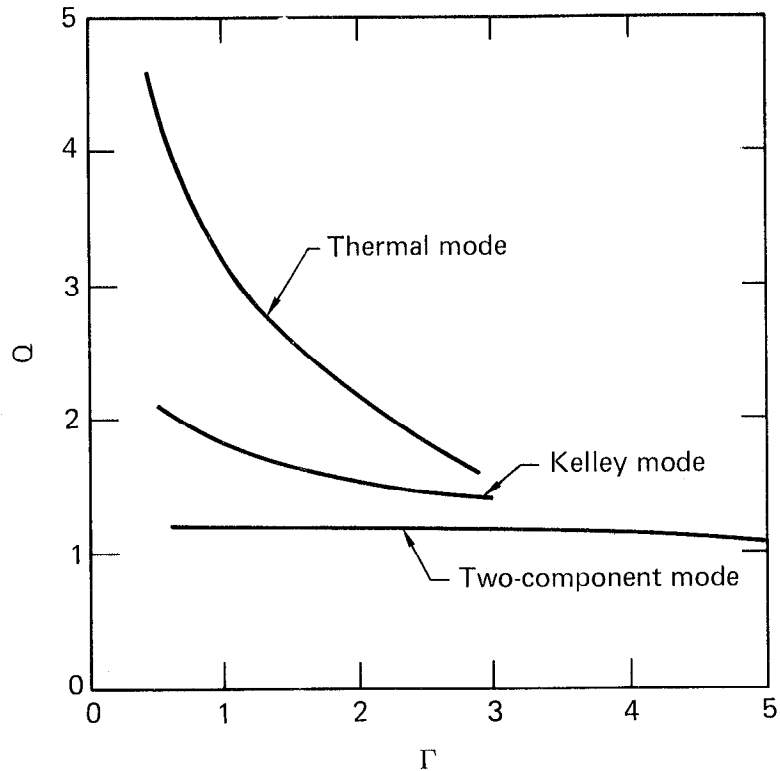


Fig. 2-3. Q vs Γ for 2500 MW fusion power.

economics. High Q decreases the cost of recirculating power equipment and allows for more revenue from the sale of electrical power. High Γ results in more fuel breeding and electrical energy production for a given capital investment. The nature of the curve indicates that a tradeoff between Q and Γ is necessary. The best operating point will be determined by systems analysis. A characteristic set of parameters is given in Table 2-3.

Another mode is the two-component mode, where a 200-keV deuterium beam is injected at one end of the solenoid into a cool (~ 6 keV) tritium background plasma that is electrostatically confined. The high throughput of T^+ ions through each end plug partially fills the volume in velocity space known as the loss-cone, thereby eliminating or greatly reducing microturbulence. The Q for this mode is limited to about 1.2. A disadvantage of the two-component mode is that the energy of the exiting ions over the potential barrier ($e\phi + T_i \approx 40$ keV) is in a low energy range where atomic collisions lead to production of cold ions and electrons in the expander region outboard of the plugs. This action results in cooling the plasma and makes direct energy conversion of this leakage plasma difficult.

Table 2-3. Operating modes for tandem mirror plasma parameters.

Plasma parameter	Two-component	Thermal	Kelley
P_{fusion} , MW	500	2500	500
Γ MW, m^{-2}	1	1	0.7
Q	0.9	1.1	1.5
$P_{\text{inj plug}}$, MW	160	580	15
Center cell, MW	530	2300	340
P_{ECRH} , MW	0	0	1200
$B_{\text{vac plug center}}$, T	6.9	6.9	6.9
Mirror, T	9.0	9.0	9.1
Center cell, T	2.2	2.5	1.7
β Plug	0.9	0.7	0.8
β Center cell	0.8	0.84	0.8
Radius, m, plug plasma	0.20	0.40	1.0
C-C plasma	0.39	0.85	2.2
C-C wall	0.59	1.03	2.7
Center cell length, m	53	103	104
E_{inj} , keV	300	300	200
E_{plug}	300	300	463
ϕ_{C} , kV	5.1	8.2	76
ϕ_{E} , kV	30	53	175
T_{e} , keV	6.0	11.3	56
T_{C} center cell, keV	1.5	3.9	25
E_{ion} center cell, keV	142	150	37

The thermal mode has an equal mixture of deuterium and tritium gas fed into the solenoidal section which is heated by the hotter electron population. This hot electron population is heated by the end plug neutral beams (via hot ions slowing by friction with the colder electrons) or by auxiliary heating such as electron-cyclotron heating using microwaves near the electron-cyclotron gyrofrequency.

Due to limited knowledge of the thermal barrier mode of plasma confinement, it is not considered in this study. The thermal barrier mode is similar to the thermal mode with the addition of an electrostatic potential depression located between the central cell and the end plug. The electron population is divided into three groups: those trapped in the end plug, those trapped in the central cell, and the passing ones. The electron temperature can be maintained considerably higher in the plug than in the central cell if the potential depression (electron barrier) is deep enough to decrease the electron thermal conductivity. Preliminary study shows that the benefit of the thermal barrier is so great that high Q (~ 15) and relatively low technology results. The Q values lie above all of those in the Q vs Γ plot of Fig. 2-3. Unfortunately the same studies show this particular design does not satisfy MHD stability. The parameters for this mode for a self-consistent design are expected to result in improvement in performance (raising the Q - Γ curves) and/or a reduction in technological requirements. A reduction in the neutral beam energy and power is clearly desirable.

Plasma stability of the tandem is always expected to be a problem to the designer, because attaining high performance will push the operating parameters to the very edge of instabilities. We are concerned with two classes of instabilities: the MHD and the microinstability. The MHD instability exists where the whole or part of the plasma column moves away from the equilibrium position toward the walls. High energy density (pressure) plasma in the magnetic wells in the end plugs can, in principle, stabilize the plasma column and connecting region. We feel confident that MHD stability can be assured at some value of plasma density in the solenoid. However, to increase the fusion reaction rate per unit volume, we must raise the plasma density as high as possible. The MHD instability has a threshold in density in the central cell, which limits the fusion rate and thereby, the neutron wall load.

The microinstability leads to turbulence-enhancing diffusive loss rates along and across the magnetic field. This instability is due to the deviation from thermodynamic equilibrium of the ion population in the end plugs. The

ion distribution is missing its low energy group, and the ion group whose velocity component parallel to the magnetic field is too high to be magnetically confined. The absence of these ion groups from an otherwise nearly Maxwellian distribution leads to strong turbulence driven by several so-called, loss-cone instabilities. Theory and experiment have shown, however, that this turbulence can be reduced to an innocuous level by making the plasma large in the radial direction and by providing a warm flowing plasma through the end plug to partially fill the otherwise empty region in velocity space. These microinstabilities, known as the drift-cyclotron-loss-cone (DCLC) mode, the convective loss-cone mode, and the Alfvén-ion cyclotron mode, are the subject of intense experimental and theoretical study at LLL. Their stability criteria, as they are now understood, are incorporated in the design parameters as a constraint.

Plasma transport (fusion fuel, D^+ and T^+) across the magnetic field and along the field out the ends is the determining process for energy loss and, therefore, is vital to determine Q . Plasma transport is also under intensive experimental (in TMX) and theoretical investigation at LLL, and the known criteria are being applied to the hybrid design. Further work is needed in both the stability and transport areas.

Plasma interaction with walls and, in particular, its disposal will be discussed in the direct energy converter subsection. Impurity contamination of the plasma is an important process that could jeopardize steady-state operation. This subject is not well understood and thus has received little attention to date, and is not explicitly considered in this study.

BLANKET DESIGN

One objective of the first year of this TMHR study is to evaluate alternative coolant technologies and to select one for use in the more detailed plant design study of the second year. As a result of early scoping studies, water and liquid metal coolants do not appear advantageous. On the other hand, both He and molten salt-cooled blankets hold enough promise to be further considered; thus, more detailed conceptual blanket designs for both coolant technologies are evaluated for comparison.

Considering fuel cycle tradeoffs, primary interest in this study is in the $Th-^{233}U$ cycle because of its superior performance in conventional

fission reactors, because it may be more nuclear weapons proliferation-resistant, and because the ^{238}U -Pu cycle has been previously studied. Thorex reprocessing is less well known and less advanced than the Purex process, and fuel cycle development would be required.

FISSION SUPPRESSED BLANKET CONCEPTS

In examining the molten salt case the outstanding fissile fuel production per unit reactor power and safety features of fission suppression become apparent. There are a number of possibilities for fission suppression, most of which have not been examined to know if they are feasible and perform well. Candidate nonfissioning neutron multipliers are Be, Pb^7 , and Li. Mobile fuels such as molten salt, balls, aqueous and slurry fuels allow removal of the bred fuel before fissile fuel buildup allows a significant fission rate. In the fast fission blanket concepts, the fission rate changes with time due to bred-in fissile material leading to an undesirable power swing in time. Removing the bred-fuel by online processing suppresses fission and reduces this power swing. The fuel produced in the fission suppressed concept has a higher purity of ^{233}U compared to the fast fission cases. Fission-suppressed blanket concepts have a high payoff, and therefore further work should be directed toward such blankets regardless of the coolant technology employed.

HELIUM-COOLED BLANKETS

The He-cooled TMHR blanket uses Th metal as the fertile material, provides an average nuclear power of 4000 MW, and produces 2.7 metric tons of U^{233} per year. The blanket module is shown in Fig. 2-4. The characteristics of this blanket are shown on Table 2-4. This design is based on the large module approach to maintenance and refueling, where the full central cell structure is handled as part of any refueling or maintenance operation. An alternative approach, the small module approach, where the first-wall and central-cell structure are not removed for refueling is discussed in Section 6.

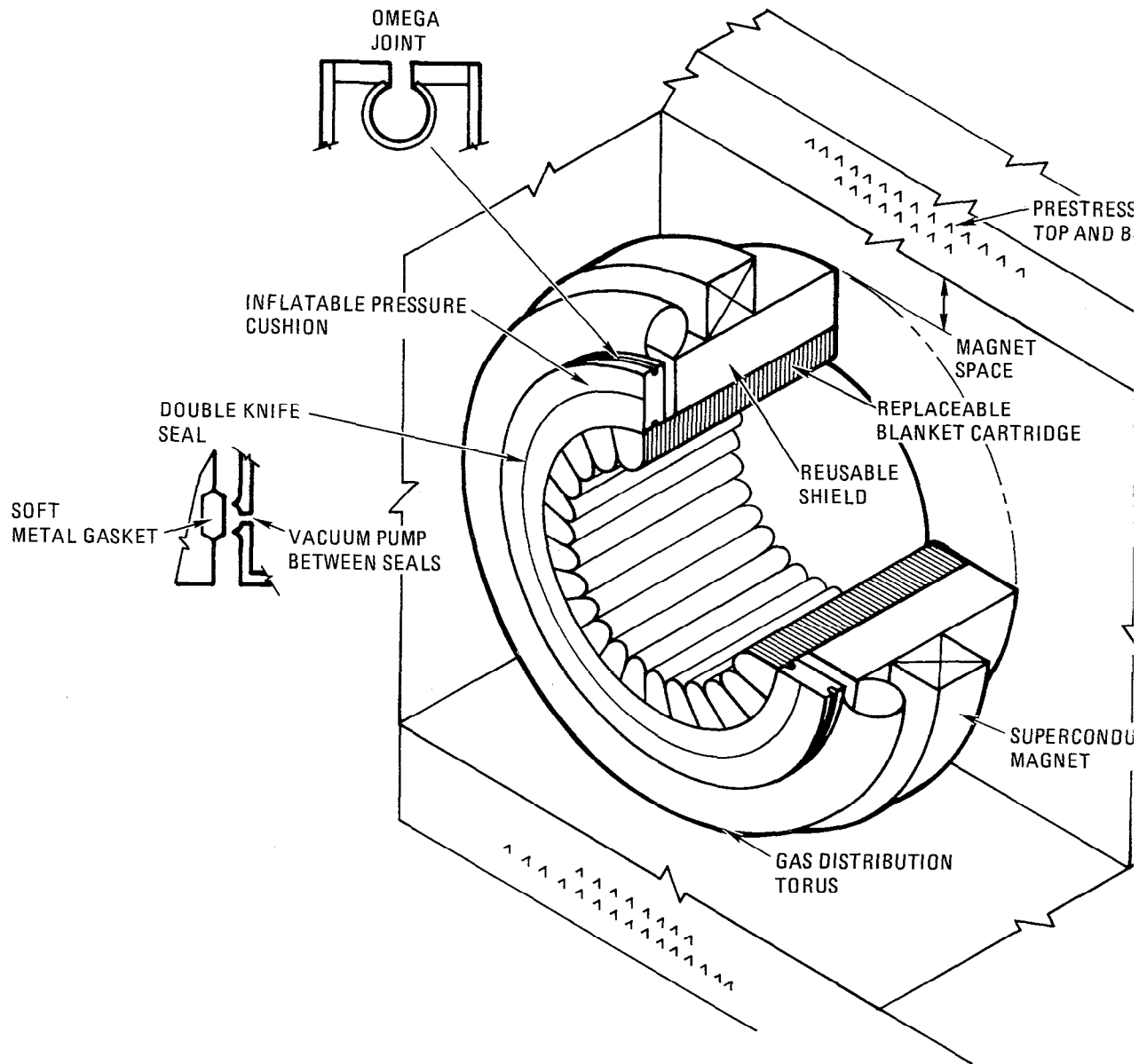


Fig. 2-4. Helium-cooled blanket module.

Table 2-4. Helium cooled blanket characteristics - large module design.

Axisymmetric cylindrical module configuration:

16 modules, each 2.4 m long, total length 39 m.

8 year module lifetime (6.4 full power years at 80% capacity factor), two replaced each year.

Helium coolant at 55 atm pressure, radial flow direction, $T_{in} = 285$ °C and $T_{out} = 515$ °C.

Inconel-718 first-wall.

Metallic thorium fuel plates, clad in HT-9, each ~1.2 cm thick, 12 cm deep.

Purged plates of Li₂O clad in HT-9 for tritium breeding, each ~1.5 cm thick, 45 cm deep.

Reflector/hot shield of SS-316, 10 cm deep.

Cold shield of SS-316/B₄C, 70 cm thick.

Blanket energy multiplication,^a $M = 5.2$

Reactor power = 4000 MW_t.

Blanket power = 3817 MW_t.

Thermal cycle efficiency ≈ 38%

Tritium production, $T/n = 1.07^a$

²³³U production, * $^{233}\text{U}/n = 0.84$

Annual production = 0.83 kg/MW_t·yr
= 2647 kg/yr^b

Burner reactors supported LWR (270 kg/GW_e yr) 10 GW_e
ACR (126 kg/GW_e yr) 21 GW_e

^a Reactor time and space average values.

^b 80% capacity factor has been assumed.

The design uses fairly conventional gas-cooled reactor technology to minimize the need for extensive development programs. The fuel mechanical design and thermal hydraulic performance are quite similar to that of gas-cooled fission reactor concepts. The blanket materials require extrapolation of the current state-of-the-art because there is presently only limited experience with use of metallic Th, Inconel-718, and HT-9 in nuclear power systems. The materials irradiation behavior uncertainty associated with a fusion neutron spectrum is, of course, a concern with this design as with all fusion systems studies. The Th fuel cycle is intended to interface with a Th/²³³U fuel cycle economy that is expected to be available in the early part of the 21st century. Although new head-end facilities will be needed for TMHR fuel, the reprocessing and recycle facilities expected to be in existence can be used directly. Thus, fuel cycle development will not be needed to implement the TMHR.

Gas-cooled power conversion system technology has been developed to the commercial stage, and the gas-cooled TMHR utilizes this technology. No new component development programs are expected to be needed. The blanket tritium systems will require new development as there is presently little experience in this area. By using a separate tritium purge flow system, tritium concerns in the fission zone and primary loop are minimized.

The mechanical design of the blanket system attempts to maximize the topological advantages of the simple cylindrical tandem mirror geometry. The ease of lateral access is utilized to provide the capability for rapid change-out of entire reactor modules. The cylindrical reactor is separated into 16 replaceable large modules connected by pressure-operated omega joints. The entire blanket and solenoid section of the reactor can be taken apart quickly. By using spare modules the reactor can be rapidly put back into operation while refurbishment or repair of spent modules is accomplished offline in the hot shop.

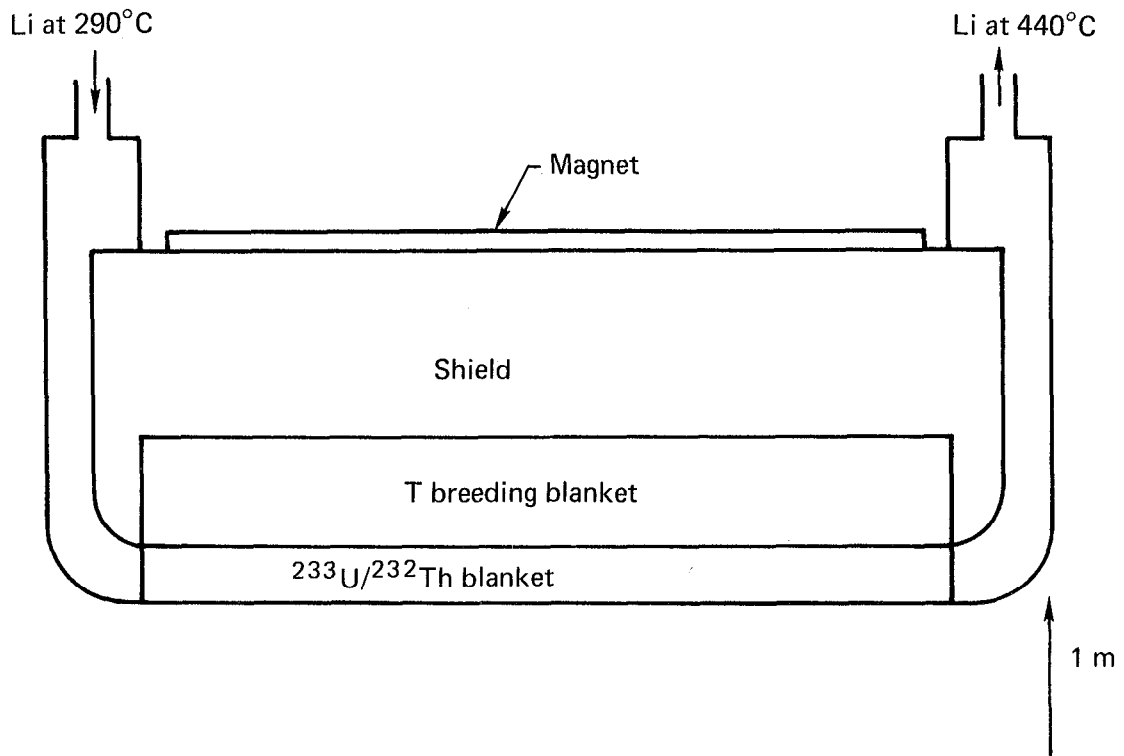
There are areas of technical uncertainty in the present design and areas where further analysis, design and optimization are needed. Nevertheless, the design as a whole appears to be technically feasible. The basic design requirements have been satisfied, and with optimization the design could be developed to become a practical fusion hybrid reactor, producing about 1000 MW_e of net electricity and about 3000 kg/year of high quality ²³³U fissile fuel for use in a fission burner reactor economy.

LIQUID METAL-COOLED BLANKETS

The excellent heat transfer properties of liquid metals along with the experience base from the LMFBR development make them a candidate for the hybrid. Lithium is one possibility because tritium breeding can be carried out simultaneously with heat removal. The addition of Pb would significantly lower the chemical reactivity of pure Li. Another possibility would be to use Na for heat removal and a separate loop of Li for tritium breeding and removal. Modular blanket designs with fuel rods oriented parallel to the axis of the magnetic field would allow use of economical fuel fabrication techniques. The blanket region used for inlet and outlet manifolds would have no fuel, which results in reduced breeding. MHD-related design problems are a disadvantage. A modular blanket is shown in Fig. 2-5. Typical parameters are given in Table 2-5. The design was carried out for a U blanket. A Th blanket would have had less of the aforementioned problems, because the energy release with Th is about half that with U. The liquid metal blankets were dropped because of MHD-related design problems and perceived safety problems; however, it is possible with further work this concept could be shown to be viable.

WATER-COOLED BLANKET

Four types of water-cooled blankets were considered: liquid water at 1 atm in a pool, boiling water, steam, and pressurized water. The pool design with its low water temperature is unacceptable because it consumes a large amount of power (~1.5 GWe) and generates no electricity. The steam designs have a fuel cladding corrosion problem. The pressurized water designs have low breeding because the water moderates the neutrons. Boiling water with better heat removal properties and lower hydrogen density results in designs having acceptable breeding on the U-Pu cycle but not on the Th-U cycle. Several blanket designs are considered. Each allows changing a fuel bundle without breaking the fusion system vacuum. The currently preferred linked assembly design is shown in Fig. 2-6. Typical parameters are given in Table 2-6. The short fuel rods (~0.5 m) in the linked assemblies results in a high fabrication cost. Water-cooled blankets are dropped primarily due to their limited performance on the Th/²³³U fuel cycle, but may deserve further study in a fission-suppressed mode.



Major features:

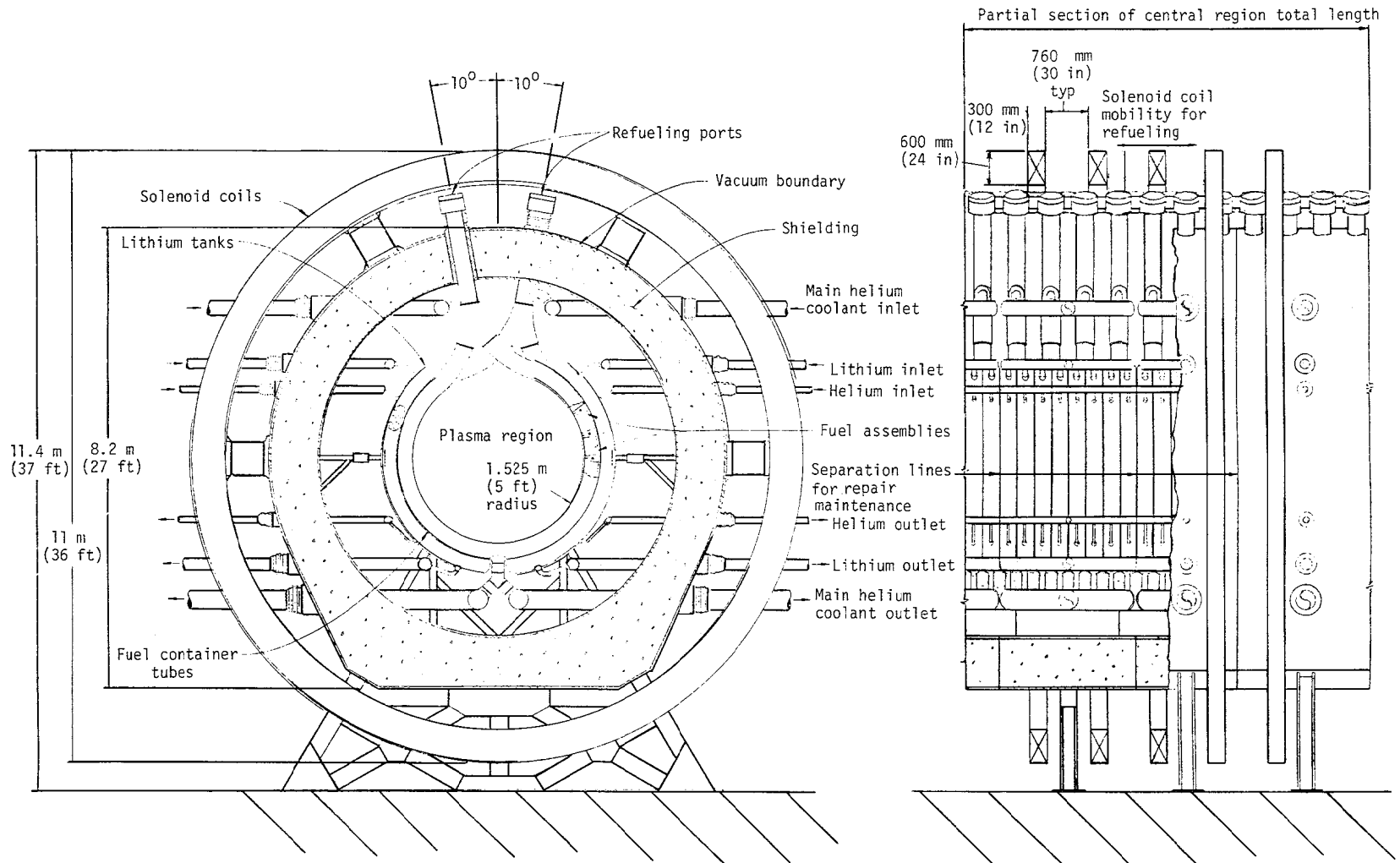
- Li (or Na) coolant.
- MHD limitations.
- Close reliance on LMFBR materials technology.

Fig. 2-5. Liquid metal-cooled blanket.

Table 2-5. Parameters for the lithium-cooled blanket.

Basis: 1 MW/m² neutron loading.
 1-m wall radius.
 UC fuel (depleted - 0.25% ²³⁵U).
 Tritium breeding ratio = 1.

Parameter	Reference design	High power design
Active length/solenoid length	0.53	0.9
Energy multiplication	3.8	6.4
Fissile breeding ratio	0.71	1.2
Nuclear power, MWt	4000	4000
Fusion power, MWt	1235	752
Blanket power, MWt	3754	3850
Length of solenoid, m	157	96
Total mass heavy metal, kg	15,100	25,400
Total fissile prod./FPY, kg Pu	3890	4000
Number of modules	53	32
Blanket power/module, MWt	71	120
Module pressure drop, psi	50	80



Central region cross section

Fig. 2-6. Boiling water-cooled linked fuel assembly blanket.

Table 2-6. Parameters for the boiling water-linked fuel blanket.

Parameter	U ₃ Si	Th metal
Fissile Breeding Ratio	1.2 ²³⁹ Pu	0.36 ²³³ U
T-breeding ratio	1.06	1.0
Energy multiplication	9.07	1.09
P _{nuclear} , MWt	4000	4000
P _{fusion} , MWt	535	3730
P _{electrical} , MWe		
Output (input)	+1000	-2500
Fissile production, kg/yr (100% plant factor)	3550	6000
Blanket length, m	39	225
Fertile zone thickness, cm		
Fissile	16	7.0
Fusile	17.5	17.5
Support of burner reactors, GW _e	-	-
LWR (270 kg ²³³ U/GW _e yr)	-	22
ACR (126 kg ²³³ U/GW _e yr)	-	47
LWR (400 kg ²³⁹ Pu/GW _e yr)	9	-

The beryllium/molten salt (Be/MS) blanket is fundamentally different from the other blanket types considered in this study. With the Be/MS blanket concept fission is suppressed by using Be for neutron multiplication via (n, 2n) reactions and by online removal of ^{233}Pa and/or ^{233}U . In the other blanket concepts neutron multiplication is via (n, fiss.), (n, 2n), (n, 3n) reactions in the ^{232}Th , and ^{233}U builds up to 2 to 3% in solid ^{232}Th fuel elements before being removed and processed. Such fuel buildup allows fissioning to build up a sizable fission product inventory in the blanket with attendant safety implications.

Because the initial results with the Be/MS blanket concept are so encouraging and other advantages (see Table 2-7) so attractive, more detailed feasibility study with particular considerations to materials, corrosion, and process requirements is necessary for comparison with the He design. To perform this assessment, a detailed reference conceptual design is developed and is used as a tool to address the technical feasibility questions. This design relies as much as possible on the ORNL molten salt technology base.

Table 2-7. Perceived advantages of the Be/molten salt blanket.

-
- High ratio of fissile material to energy production; therefore high support ratio (ratio of supported fission burner power to fusion hybrid power).
 - Continuous removal and sale of ^{233}U .
 - Low after heat.
 - Low fission product burden.
 - Long life.
 - Low radioactive waste generation.
 - Lower cost.
-

The blanket design that resulted is shown in Fig. 2-7. It consists of an independent, He-cooled, stainless-steel first-wall surrounded by a blanket region containing graphite-clad Be and flowing molten salt in Hastelloy-N structure. The first-wall is intended to last the life of the reactor. The

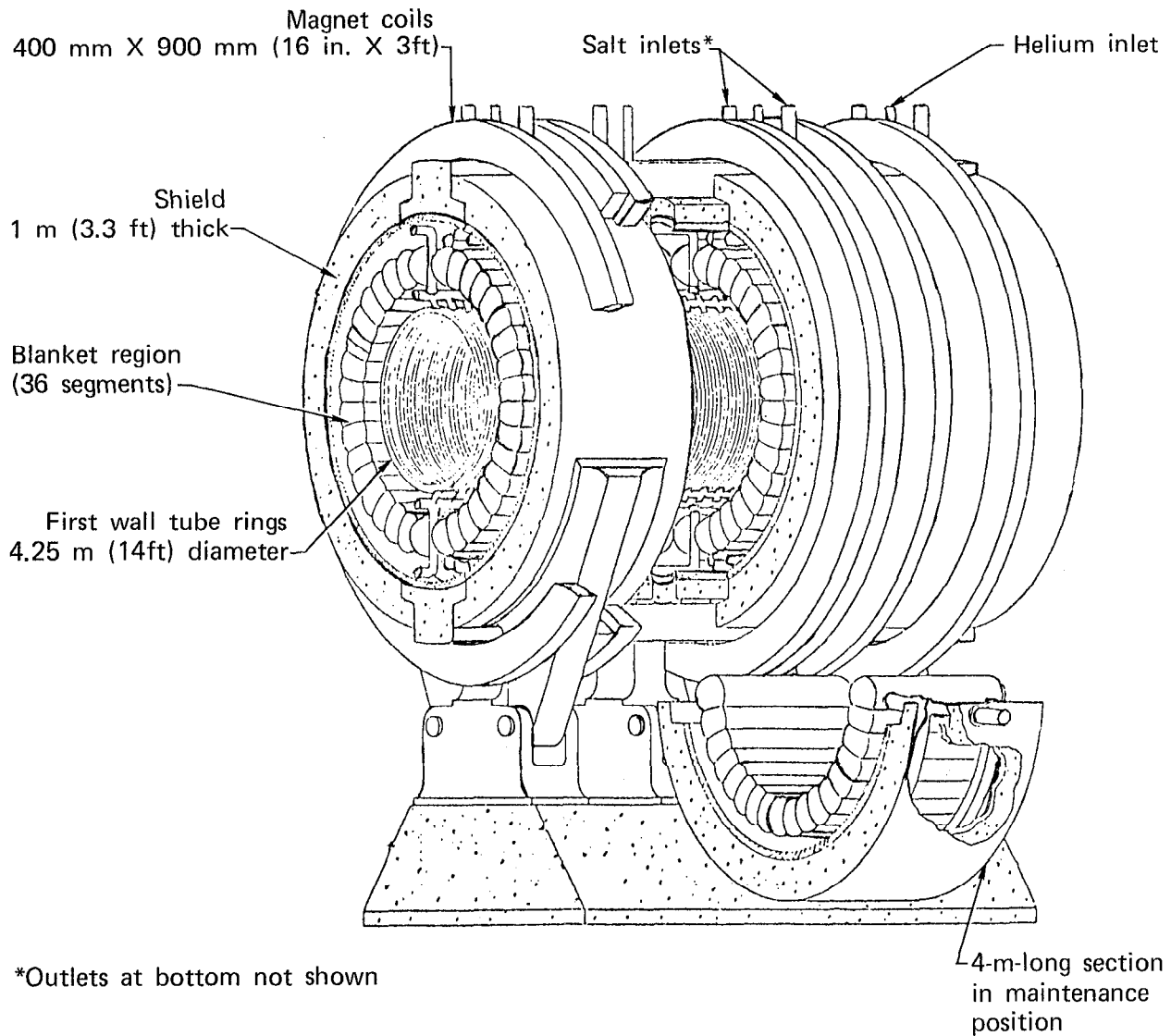


Fig. 2-7. Portion of TMHR central region molten salt concept.

blanket region consists of structural segments attached to pivoting clam shell shield segments to allow for maintenance. The composition and nuclear performance of this blanket are given in Table 2-8. An improved version of this design is included for comparison purposes.

The lower mole fraction of ThF_4 in the reference design, 12% vs 27% was chosen because that was the salt composition chosen by ORNL for their MSBR study. The salt composition used in the improved design gives better performance, and thus should be used in any future work. At elevated temperatures and in the high flux region of the blanket, Hastelloy proved unworkable, and thus TZM is the structural material in the improved design.

Table 2-8. Parameters for the molten salt-cooled blanket.

Parameter	Conceptual design	
	Reference	Improved
First-wall:		
Effective thickness, mm	6	6
Material	Ni	Ni
Blanket thickness, m	0.8	0.8
Blanket volume fractions:		
Be	0.65	0.75
C (cladding)	0.10	0.10
Molten salt	0.25	0.15
Structure	0	0
Molten salt composition, mole %:		
LiF	72 ^a	71 ^a
BeF ₂	16	2
ThF ₄	12	27
(Melting point, °C)	(~500)	(~550)
Performance:		
Tritium breeding	1.08 ^a	1.04 ^a
²³³ U breeding	0.64	0.83
M	1.47	1.62

^aNatural lithium.

The 50°C higher melting point of the improved salt should not effect the choice of TZM for blanket structure.

The molten salt chemical processing scheme proposed for the MSBR was found to be generally applicable to the molten salt hybrid. However, due to the large amount of tritium generated, additional processing requirements are necessary.

Another potential problem area involves control of the molten salt reductive/oxidative (Redox) nature. In the MSRE work the uranium (III)/uranium (IV) couple was used to control Redox, but in the molten salt hybrid the uranium inventory will be too small to perform this function. Cerium may possibly be used instead. A flow rate of about 60 l/min through the processing plant is needed to maintain the desired salt composition.

The Be/molten salt blanket design appears to realize the perceived advantages listed in Table 2-7; however, considerable development is required to bring molten salt technology to commercial status. Despite the materials concerns and development requirement, the molten salt concept is quite attractive because of the fission-suppressed mode of operation. It remains to be seen if the advantages of fission suppression can be achieved using more conventional reactor technology. If not, the molten salt concept may deserve further development.

MAGNET DESIGN

The performance of the tandem confinement concept (Q and Γ) is improved with higher magnetic field strength in the end plug resulting in a desire to employ the highest possible field strength at the conductor. The field strength is constrained to 12 T because there is a significant development program for Nb_3Sn underway with 12 T as the goal. The magnet configuration is shown in Fig. 2-8. The magnet is designed for the thermal mode. There are three general coil-functions: the solenoidal central cell, the plug set, and the expander coil, not shown. The function of the expander magnetic field is

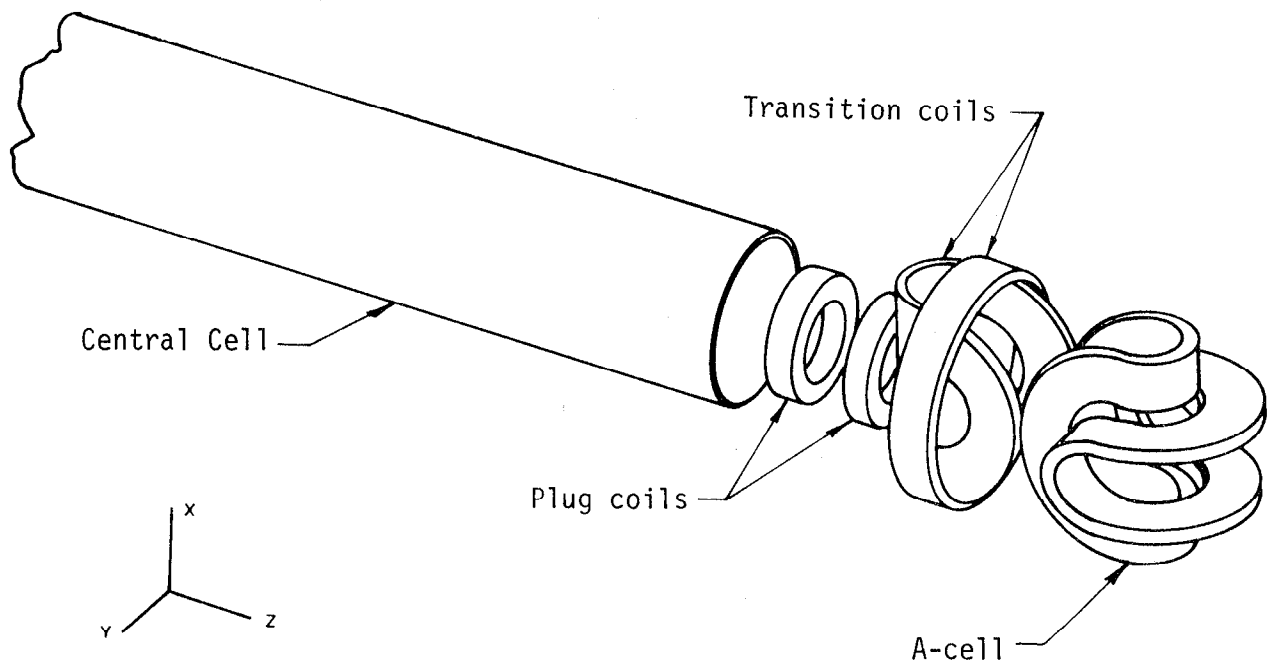


Fig. 2-8. Arrangement of magnets.

to guide the leaking plasma to the direct converter and in the process reduce the power density. The function of the solenoid is to confine the reacting plasma in the radial direction. The end plug magnet provides the special field shape to confine a high-energy density plasma, which in turn provides axial confinement and stability of the center-cell plasma. For the design shown the important magnet parameters are given in Table 2-9.

Table 2-9. Magnet parameters.

<u>End Plug - Nb₃Sn conductor/yin-yang type</u>	
B _{conductor}	12 T
B _{mirror}	9.1 T
B _{midplane (vacuum)}	7.0 T
Length	15 m
<u>Central Cell - MbTi conductor/solenoid type</u>	
B	1.7 T
Length	35 m
Radius	4.1 m

INJECTOR DESIGN

Neutral Beam Injection

The system study has shown an improving performance (Q and Γ) with increasing injection energy. In the range where positive ions can be used efficiently (<120 keV), the performance is too low; therefore, negative ions are called for. The reason for the switch over is the positive ions (D^+ , T^+) can be converted to neutral atoms (D^0 , T^0) by charge-exchange during transit through a gas cell. Ionization unfortunately competes with charge-exchange, and since the charge exchange cross section is dropping and the ionization cross section is rising with increasing energy, the fraction of ions that can be turned into neutral atoms drops dramatically beyond 100 keV. The efficiency of making D^0 is predicted to be about 70% at 100 keV, but drops to 40% at 150 keV. Conversely, negative ions (D^- , T^-) can be made into neutral

atoms by an electron stripping reaction that is almost completely energy-independent.

The efficiency of producing neutrals by the negative ion method is predicted to be about 60%. System studies show improving performance up to and beyond 600 keV. The development program now underway at Lawrence Berkeley Laboratory (LBL) and Brookhaven have as a goal a 1 MW-at-200 keV beam, which is planned for testing in the High Voltage Test Stand (HVTS) at LLL.

The injector designed for the He cooling case is shown in Fig. 2-9 with some typical parameters given in Table 2-10. The injector locations will have to be selected for the particular operating mode adopted. The two-component mode calls for most of the injection into the central cell with only a small fraction going into the plug, whereas the thermal mode calls for all of the injection into the plug.

MICROWAVE HEATING

For the thermal mode the input power is 3/4 microwaves and 1/4 neutral beam. A 466-MW microwave system has been studied. The system is based on 10-MW gyrotron tubes at 110 GHz and results in the end plug design, shown in Fig. 2-10.

PLASMA DIRECT CONVERTER

The magnetic expander discussed previously guides the plasma leaking from the central cell and end plugs into the direct converter electrodes. The direct converter is shown schematically in Fig. 2-11 with typical parameters given in Table 2-11. The functions performed by the direct converter are heat removal, gas pumping (these two are needed independently of direct conversion and are sometimes called plasma dumping), and direct conversion of ion kinetic energy into electrical energy.

As shown in Fig. 2-11, the leakage plasma is handled differently in three radial zones. The outer annulus is considered to be low temperature containing He^{++} (ash) and impurities and not suitable for energy recovery. This outer zone of plasma is directed into a plasma dump. The inner two zones contain high temperature particles suitable for recovery. The innermost zone is at a somewhat higher temperature and therefore has a separate set of collectors at different voltages than the intermediate zone.

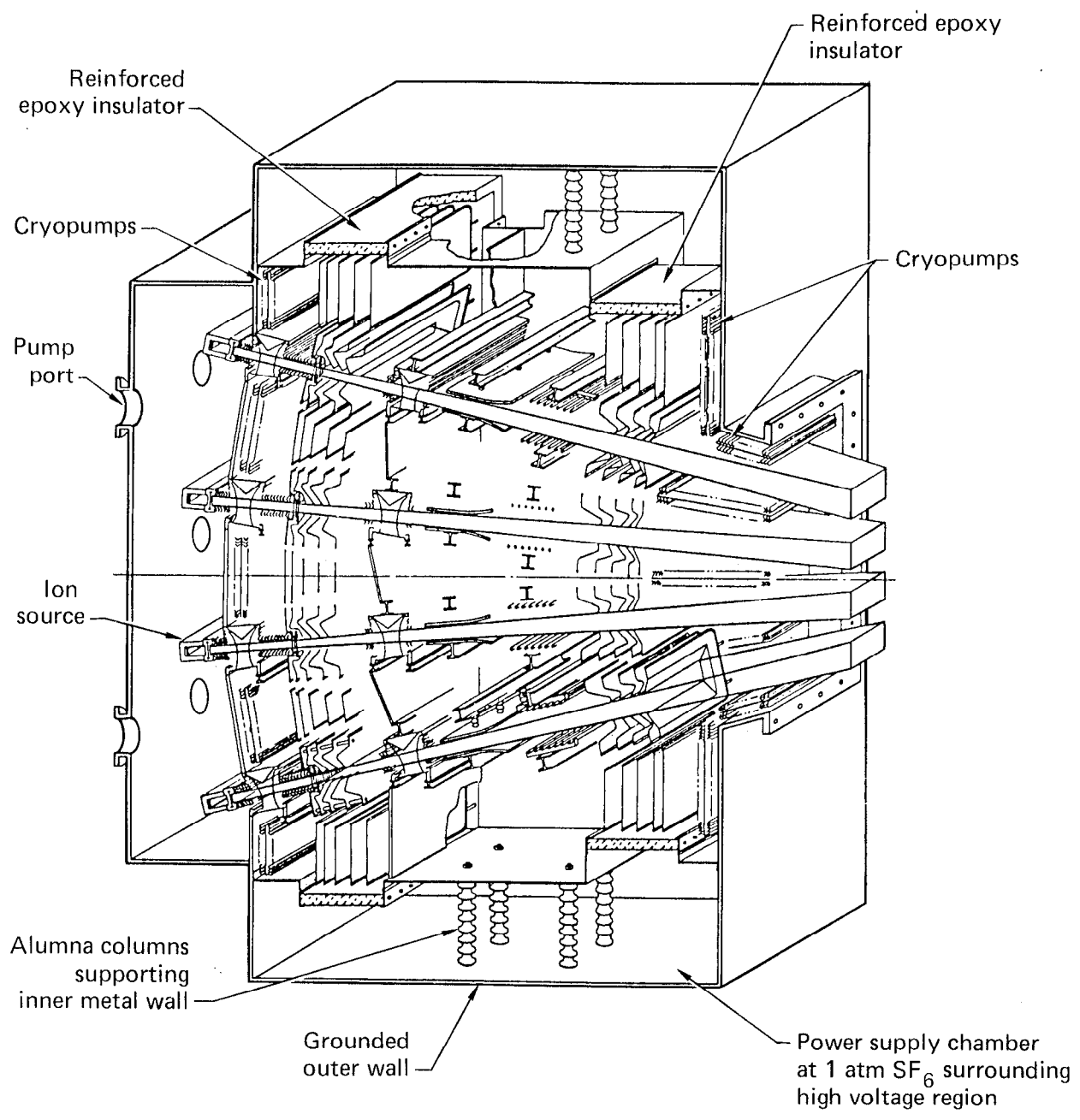


Fig. 2-9. Injector for the TMHR.

Table 2-10. Neutral beam injector microwave heating parameters.

Injector

Double charge-exchange type

Cs cell

400 keV

842 A (molten salt)

329 A (helium)

60% efficiency

Microwave System

Frequency 71 GHz

Power 1012 MW (molten salt)

466 MW (helium)

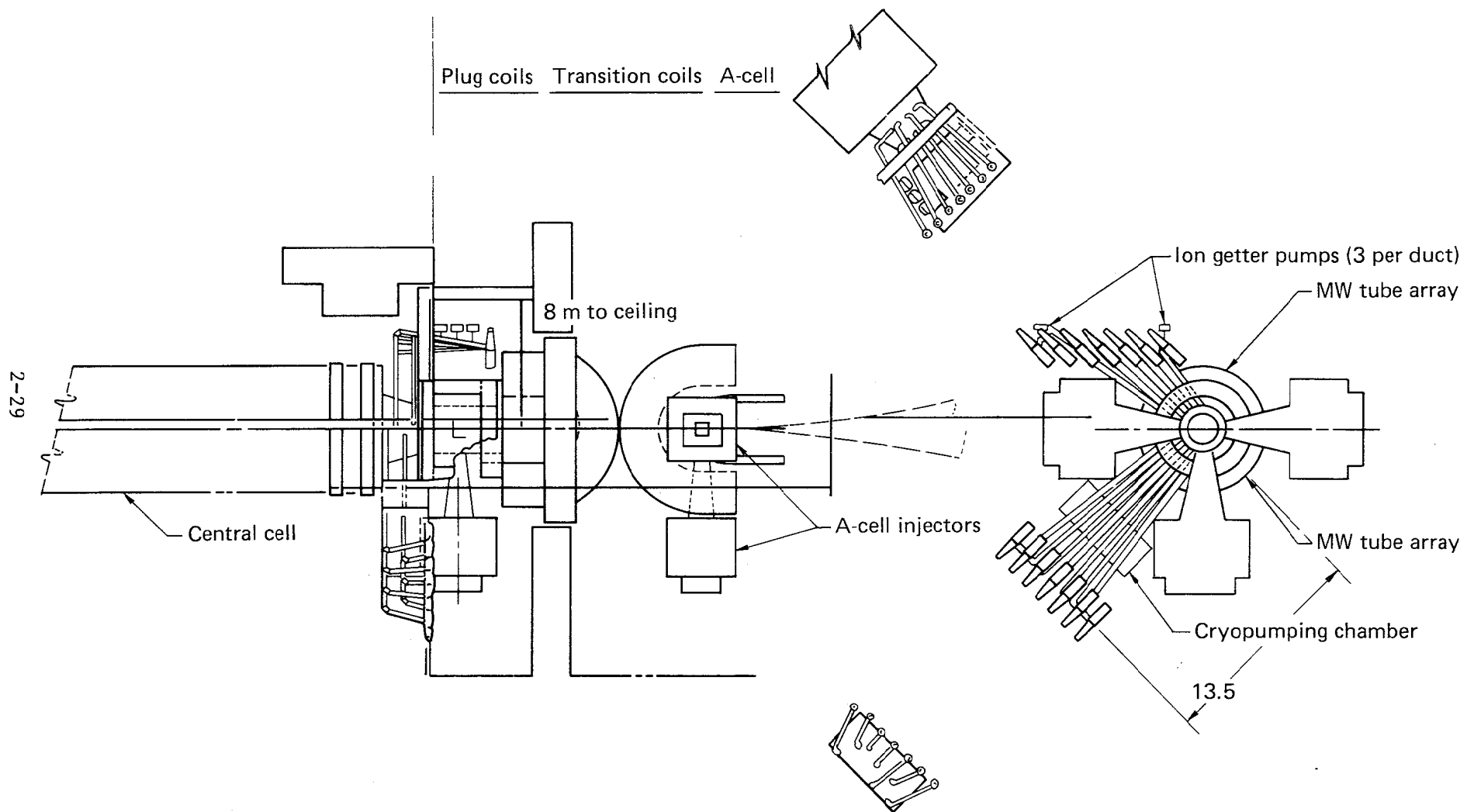


Fig. 2-10. TMHR end plug configuration.

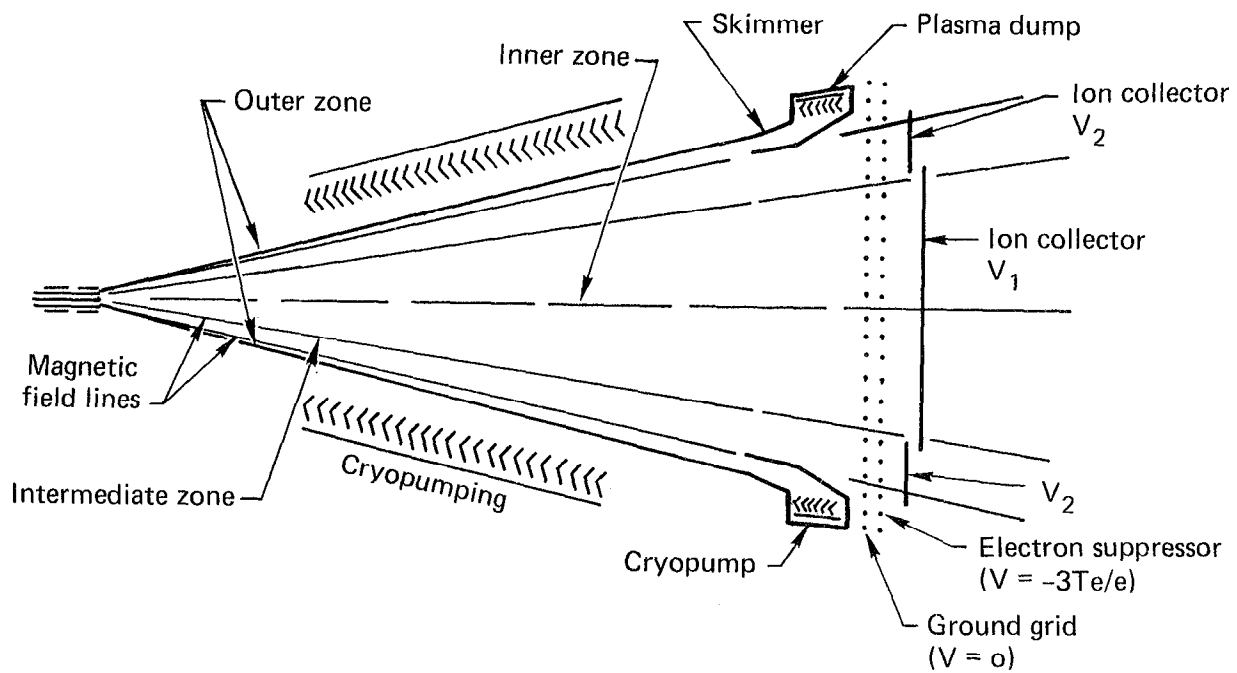


Fig. 2-11. Plasma direct converter and plasma dump.

Table 2-11. Plasma direct converter parameters.

Immersed grid	=	1-stage triode
Power density	=	100 W/cm ⁻²
V _{collector}	=	Peak electrostatic potential barrier

The magnetic expander field guides the leaking plasma ions and electrons to the collectors. Also the power density drops because the cross-sectional area is increasing as the square of the distance. The magnetic field is similarly dropping inversely with the square of the distance from the plug. Because of a conservation of magnetic moment ($\approx W_{\perp}/B$), the component of energy perpendicular to the magnetic field decreases with distance squared.

The magnetic field will drop from its value at the plugs of 9 T to the order of 0.01 T. The energy of the ions is virtually all in the direction of the magnetic field at the collectors and then is available to recovery.

The magnetic expansion leads to a density drop that leads to a potential drop ($\phi \sim \ln n$). This action results in an acceleration of ions and deceleration of electrons. The electrons' energy is largely transferred to ions, which means we only need to recover the ions' energy.

The grids perform several roles. The first grid establishes the potential. The next grid is made negative, as to reflect almost all electrons ($\sim 3T_e/e$, measured in volts). The electrons leaking out will make enough passes through the grounded grid to be removed. The grounded grid must dissipate heat from all the electrons hitting it (T_e per electron, measured in electron volts of energy), as well as a small fraction of ions being intercepted during one pass through this transparent grid (95% transparency). Once electron separation and removal are accomplished, the ions can be decelerated between the negative grid and the collector plate. The ion that impacts the collector buries a distance into the metal (0.1 μm), diffuses to the surface, recombines, and leaves as D_2 gas. The electron that neutralizes the ion must come from the grounded grid through the electrical circuit, doing work in the load and thus completing the circuit. Each collected ion gives up $eV_{\text{collector}}$ of energy. The excess energy $W - eV_{\text{collector}}$ (W is the kinetic energy of the ion as it entered the

grounded grid) is turned into heat upon striking the collector. If $W - eV_{\text{collector}}$ is negative, the ion did not have enough energy to strike the collector. These ions will be lost upon multiple transits on either the grounded or negative grid.

Gas pumping is assumed to be accomplished by cryopumps located out of the direct neutron and ion flux.

BALANCE OF PLANT

The balance of plant design includes parts of the primary coolant system, the remainder of the heat removal and power conversion system, the containment building, and other plant buildings. A plant layout has been made for each of the coolant choices. Figure 2-12 and 2-13 show the balance-of-plant flow

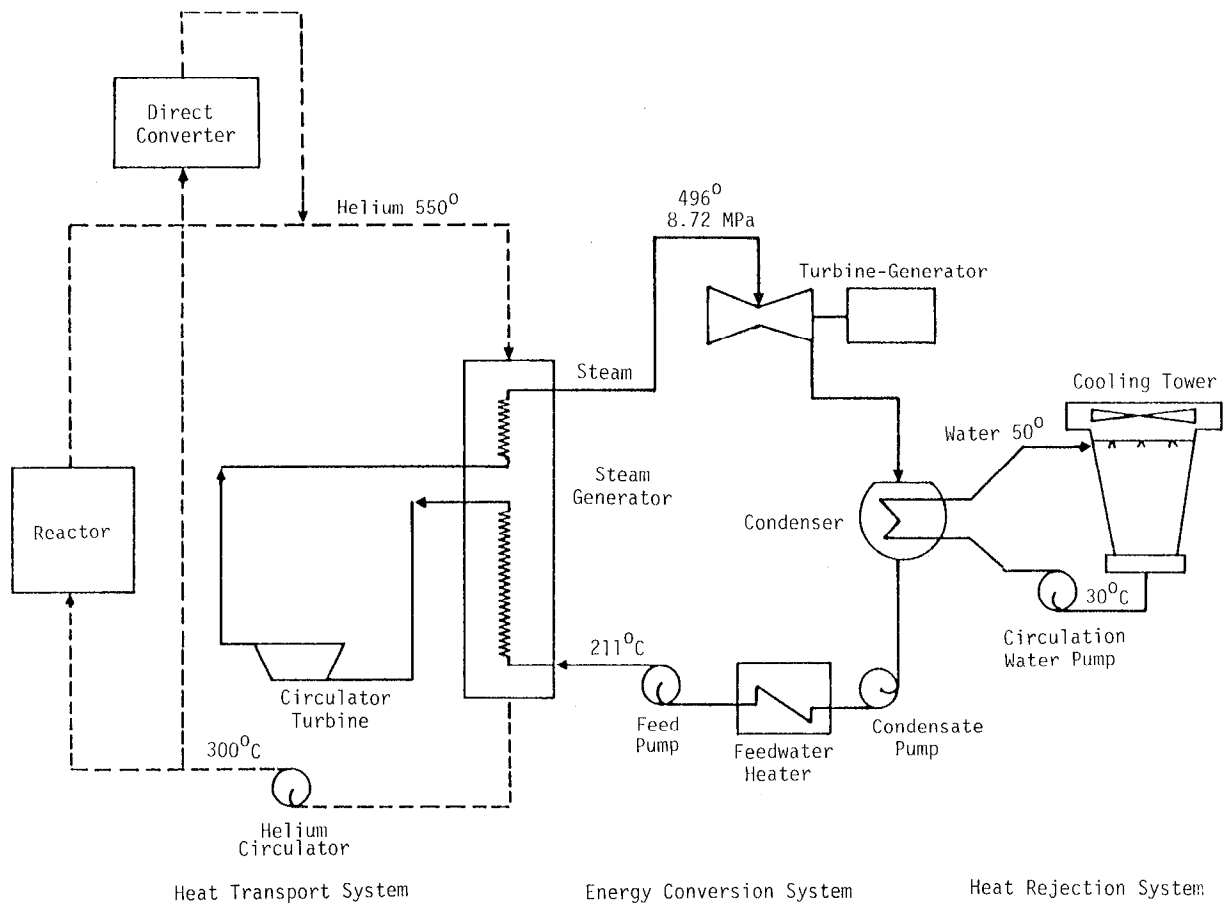


Fig. 2-12. Main BOP systems for He-cooled blanket concept.

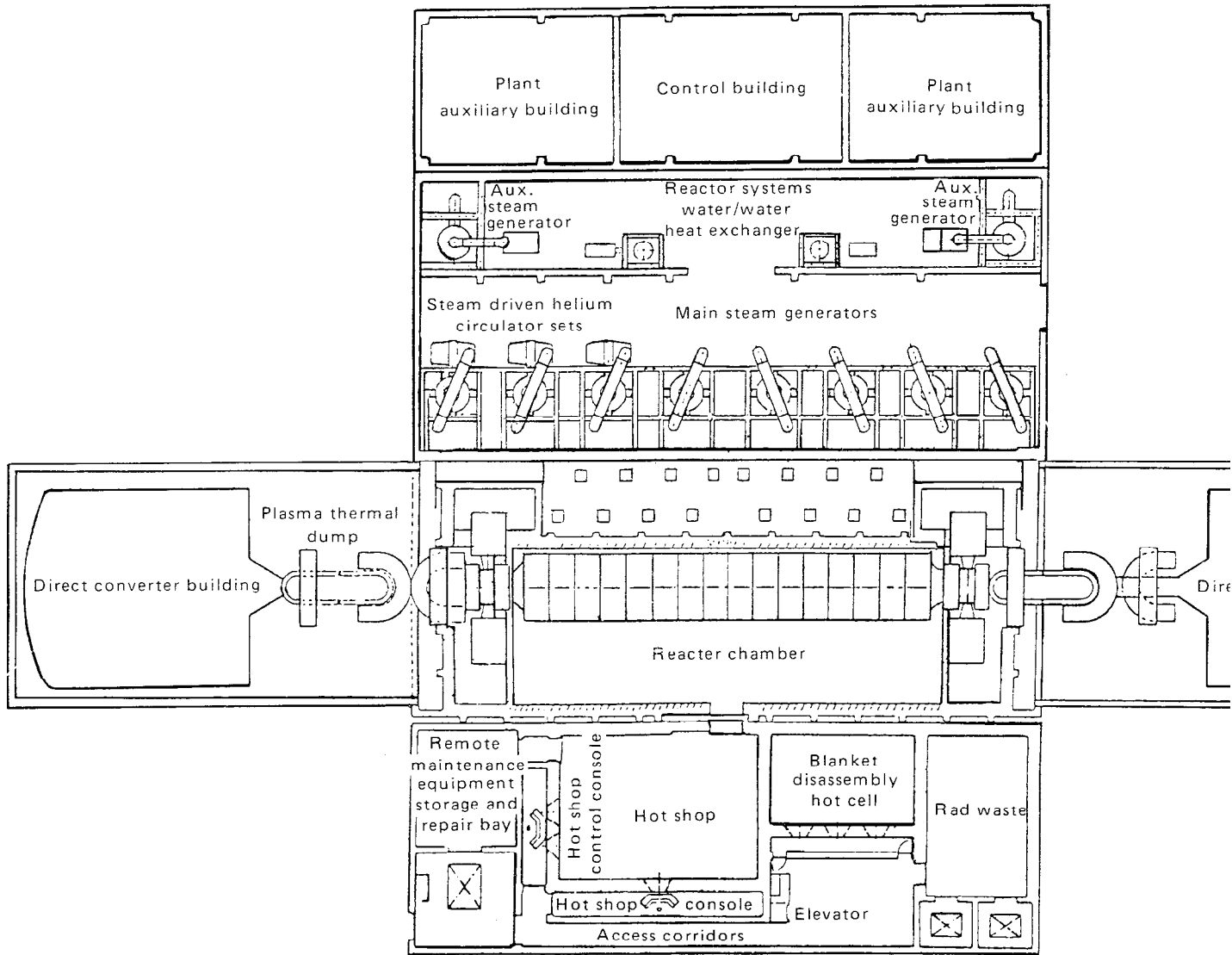


Fig. 2-13. Main BOP systems for the He-cooled blanket concept (plant layout)

schematic and plant layout for a typical coolant (He in this case). The power flow diagram for the helium case is shown as Fig. 2-14. The molten salt has several times more fusion power, and the containment building is correspondingly larger. Cost relationships have been developed for a number of subsystems for use in the systems code. Major balance-of-plant concerns for each coolant are:

<u>Key features</u>	<u>He</u>	<u>Molten salt</u>	<u>Li</u>
Reactor coolant, °C temperatures	550	650	440
Intermediate coolant temperature, °C	None	550	407
Heat transport system, IHX	None	Molten salt/He	Li/Na
Pumps/circulators	Gas compressors	Gas compressors and molten salt	Liquid metal
Technology extrapolators	Moderate	Major on molten salt	Moderate
Component cost	Expensive	Very expensive	Least expensive of these three
Materials for piping	SS	Hasteloy-N	2-1/4 Cr - 1 Mo
Development requirement	Minor	Major	Minor
Preheat problem	None	Major	Minor
Pipe and valve size	Large	Moderate	Moderate
Tritium control problem	Moderate	Can be major	Moderate
Maintainability	Some potential hands on	All remote	Primarily remote
Fuel reprocessing	Off site	On site	Off site

BURNER-FISSION REACTOR DESCRIPTION

The market for fissile fuel is assumed to be LWR's at first. It is also assumed that a fuel shortage will encourage later development and deployment of Advanced Converter Reactors (ACR) of the LWR, heavy-water or gas-cooled (HTGR) type. In addition, a supply of ^{233}U from hybrids would encourage ACR

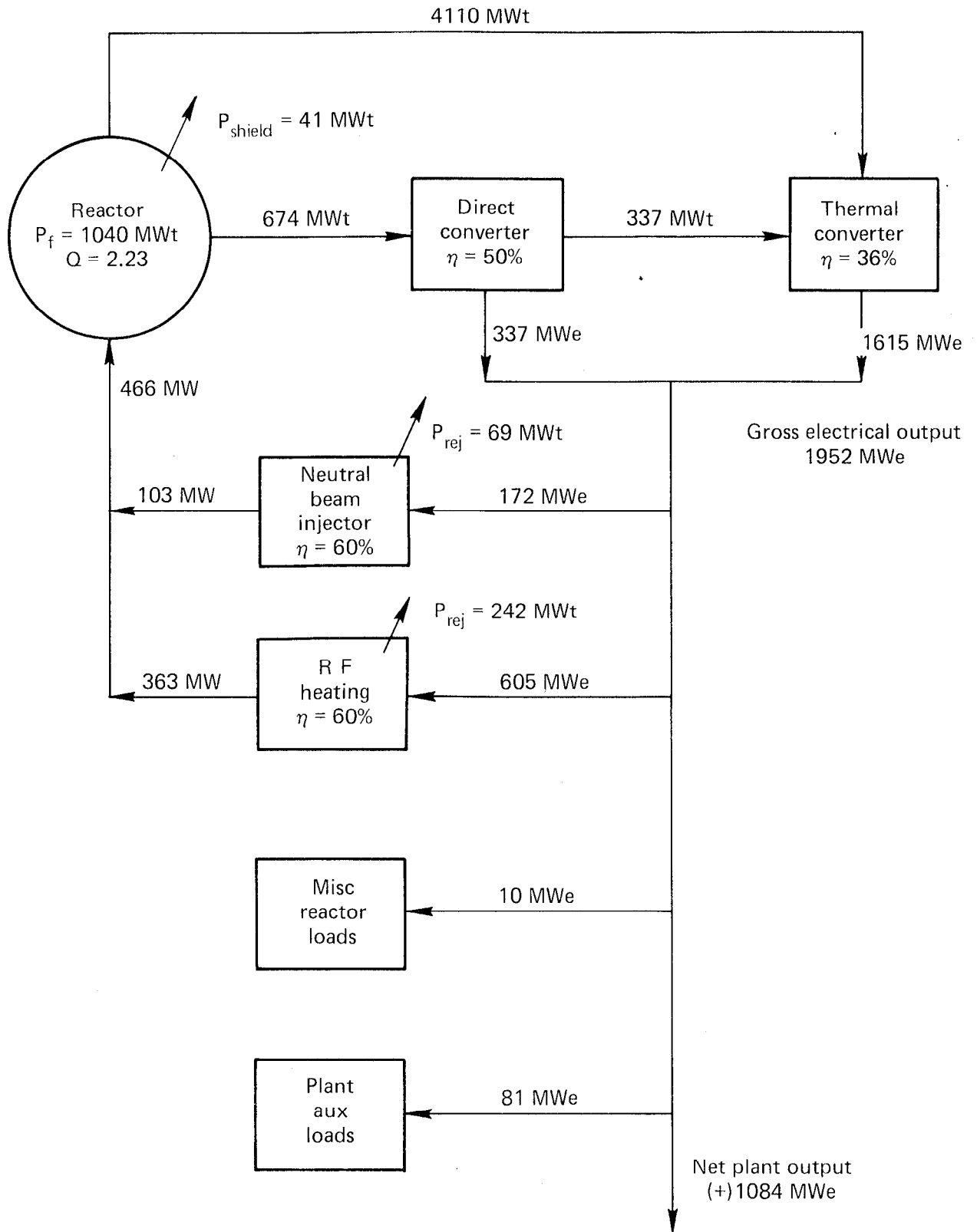


Fig. 2-14. TMHR power flow diagram - He-cooled.

deployment, and breeder reactors could use hybrid-bred fuel in order to speed up their introduction. This subsection summarizes the parameters for these burner reactors for use in our systems analysis modeling. Some of these results are given in Table 2-12. Since the single most important figure of merit for the economics of hybrids is the cost of fissile fuel generated, these plant characteristics are used in the systems code to determine the value of electricity. For hybrids, which neither produce nor consume electricity, the burner reactor would not affect the cost of fissile fuel generated.

Table 2-12. Burner fission reactor parameters (1000 MW_e).

LWR	Advanced HTGR (as an example of an ACR)
Cost = \$900 M	Somewhat more than an LWR
Inventory = 2400 kg ²³³ U	2000 kg ²³³ U
Makeup = 239 kg ²³³ U/yr	100 kg ²³³ U/yr
Capacity factor = 75%	75%

ENVIRONMENT AND SAFETY ANALYSIS

Environment and safety considerations will be weighed heavily in choosing the blanket technology for the reference design.

SYSTEM MODELING AND ANALYSIS

To aid in comparing the various blanket options and physics modes being considered, a tandem mirror fusion-fission system model was developed. The model includes the hybrid plant and all supported burner plants. It calculates power level and cost of the hybrid components, hybrid net output (electricity and fissile material), supported burner output and support ratios, capital cost information, and finally, dependent fissile material and electricity costs.

The development and use of the model occurred in four phases. During phase 1, we concentrated on developing the model and analyzing proposed fusion driver and blanket combinations. Since this was early in the study, blanket and driver (as well as burner) performances were estimated from previous studies. The principal result from phase 1 was that when blanket cost differences are relatively small, the blanket having the highest ratio of fissile fuel to power production is economically superior. The beryllium/molten salt blanket gave the lowest cost fissile fuel; thus, we were encouraged to look more intently at the molten salt blanket concept.

For phase 2, preliminary information on driver physics, Th/He blanket performance and costs, BOP and indirect costs generated for this study became available. These data were used to make economic comparisons of Th/He and Be/molten salt blankets coupled with two tandem physics modes and two burner types (LWR and HTGR). Also fuel reprocessing costs for the molten salt blanket were taken to be an order of magnitude less than for the solid Th blanket.

Comparing the combinations considered in phase 2 shows ^{233}U costs varying between 37 and 123 \$/g, system power cost varying between 14 and 23 mills/kWh_e, and nuclear support ratio varying between 39 and 9. The best performance belongs to the combination of the one component (or thermal) mode of tandem driver physics, the Be/molten salt blanket and the HTGR burner. The other end of the performance scale belongs to the two-component tandem physics, Th/He blanket, and LWR burner fusion-fission system combination.

For phase 3, system performance with water-cooled blankets was analyzed. Results for three water-cooled blankets are presented; two boiling water-cooled blankets, one fueled with thorium the other fueled with depleted uranium, and a thorium-fueled, water-cooled case. These three blankets were coupled with the one-component or thermal mode fusion driver at a Q of 2.23 and LWR burners. With the three water blankets (Th/BW, U/BW and Th/W), fissile costs were 141, 59, and 115 \$/g; nuclear support ratios were 8.9, 5.2, and 14; and system electricity costs were 24, 21, and 23 mills/kWh_e, respectively.

System performance parameters presented for the Th/He and Be/molten salt blankets are also based on one-component driver physics and LWR burners. Fissile costs were 71 \$/g and 82 \$/g, nuclear support ratios were 8 and 20, and system electricity costs were 20.5 mills/kWh_e and 21.1 from the Th/He and Be/molten salt blanketed cases, respectively. The Th/He blanket case is

economically superior while the Be/molten salt case has the support ratio advantage. Since the Be/molten salt blanket performance and cost data are based on an unoptimized initial design developed to look at the technological viability of the concept, we believe performance and cost improvements have a good chance of making the Be/molten salt blanket at least economically competitive if not superior to the He-cooled blanket. Also not accounted for is the batch nature of the Th/He blanket, which will increase its costs.

In summary, it appears the economics of Th/He and Be/molten salt blanketed hybrids might be similar. If that is the case, choosing between them will have to be based on other considerations such as support ratio, development cost and time, Be resource and cost questions, and safety and operational advantages.

The important question for any candidate fusion driver for a hybrid is the minimum Q required. Figure 2-15 illustrates the answer for the tandem. For Q values more than 2 to 3, diminishing returns set in, and the preference He design point was 2.0. For the standard minor on the Pu fuel cycle the diminishing returns Q values are about 1 to 2, but the design point had a Q of only 0.64. Thus, the higher Q (3 times in the examples) for the tandem makes its suitability for a hybrid much more favorable than the standard mirror.

RESOURCE AND MARKET ECONOMIC ASSESSMENT

The marketing assessment addresses a number of key economic and logistic issues that affect the design of the hybrid reactor from the point-of-view of the marketplace. This study includes a partial cost/benefit study to estimate the national benefit of some of the design options and of the program itself. Issues such as determining the optimum hybrid plant size and economics of the various fuel production modes are analyzed separately.

The market in the year 2010 for synthetic nuclear fuels and by-product electricity from fusion hybrid reactors will depend to a large degree on five key factors that influence the use of fission energy:

- Electrical load growth.
- Rate of addition of nuclear capacity.
- Extent of high grade U_3O_8 resources.
- Alternative nuclear fuel and reactor options.
- Public acceptance of nuclear energy.

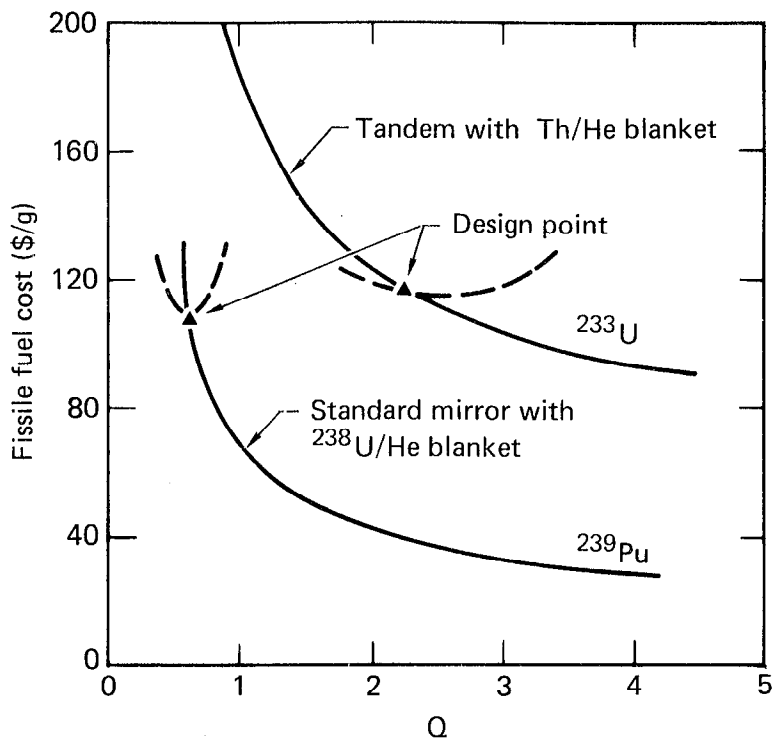


Fig. 2-15. Variation of fissile fuel cost with an increase in plasma Q for the standard mirror and tandem mirror. The solid curve was calculated by arbitrarily varying Q from the design point. The dashed curve was calculated using constrained operating model with its costs, magnetic fields, injection energies and other parameters interrelated. The two curves cannot be directly compared because different economic assumptions were made (different capital charge rates); however, the shapes of the curves can be compared, and clearly the tandem design point is less sensitive to Q variations than the standard mirror design point.

Domestic electrical use in 2010 is anticipated to be 2.3 to 6.6 times the 1978 level. Domestic nuclear capacity in 2010 is projected to range between 240 and 950 GW_e . World nuclear capacity in 2010 is projected to range between 1180 to 1380 GW_e . Domestic uranium resources are estimated between 2.5 and 4.5 million tons with prices between 40 and 110 \$/lb U_3O_8 - 1979 \$. World uranium resources are estimated between 5.8 and 10.6 million tons. Domestic uranium used and committed by 2010 is between 1.7 and 4.5 million tons. World cumulative demand by 2010 is between 7.4 and 8.3 million tons.

Comparing domestic uranium demand and supply estimates, a market for fusion bred fissile fuel will develop no later than 2030 and could develop as early as 1990. Successful development of the fusion-fission option allows

large scale long term deployment and use of fission burner reactors after minable uranium ore is exhausted.

The cost/benefit assessment showed that the benefit for a hybrid occurs in two parts. The first part is the benefit to the nation of lower cost nuclear fuel. This benefit is in the range 0 to \$20 billion (discounted to 1979), depending on the cost advantage of hybrid fuels over mined uranium. The second benefit however was found to be much larger. It stemmed from the conservation of the nation's uranium reserves and the availability of a nuclear alternative to coal as a source of electrical energy. This later benefit appeared to be in range of \$110 to 170 billion (discounted to 1979).

Competitors to the hybrid are also identified, such as the use of advanced LWR fuels, advanced enrichment processes, the reprocessing of existing spent nuclear fuel, and the development of more uranium conserving reactors such as ACR's and the LMFBR. All appear to be potential early year competitors to hybrid fuels, with only the later option having longer term potential. It is also suggested that a healthy reprocessing industry must be developed prior to the introduction of hybrids. It is believed that a stockpile of free, LWR-spent fuel would delay the commercialization of the hybrid.

The commercialization studies show that when blanket concepts are compared for sets of hybrid deployment scenarios, little difference in fuel production occurred. Each blanket concept, though some produce more fissile fuel than others, has a fuel supply schedule that is only 1 or 2 yr different from any other. This occurs because the rate of addition of new hybrids is larger than the fuel production differences of the blanket concepts. This discovery suggests that the selection of the fertile fuel in the blanket be made not on fuel production rates per reactor but on factors that will affect the deployment of hybrids, such as the availability of fuel cycle services and the size of the fusion driver.

The commercialization cases also suggest that small commercial plant ratings have merits worthy of further investigation. Small plant sizes could reduce problems in linking the hybrid with the reprocessing and bred fuel fabrication industries. Small sizes also have merit in reducing R&D costs and in increasing the marketability of the hybrid program.

The resource and market economic assessment finds that relatively few hybrids are needed to reduce the need for mined uranium. This advantage allows the hybrid to become a relatively fast acting solution to uranium

supply problems. Few other technologies could act as quickly to solve uranium supply problems.

REFERENCES

1. R. S. Devoto and D. J. Bender, Nucl. Fusion (to be published).
2. G. I. Dimov, V. V. Zukaidakov and M. E. Kishinevskii, Sov. J. Plasma Phys. 2, 326 (1976).
3. T. K. Fowler and B. G. Logan, Comm. Plasma Phys. Cont. Fusion 2, 167 (1977).
4. G. G. Kelley, Plasma Physics 9, 503 (1967).

SECTION 3

PLASMA PHYSICS AND ENGINEERING

(B. M. Boghosian and R. S. Devoto)

INTRODUCTION

In previous reactor designs based on minimum-B (standard) mirrors, it was found that the large losses out the open ends limited the Q values to about unity.¹ In 1976, Dimov et al.² and Fowler and Logan³ found it possible to essentially remove any limit on Q by placing three mirror devices in tandem. The two end devices (plugs) are, in effect, the standard mirror device operated at high density. The central device is cylindrical, which is a desirable shape for the incorporation of blankets. The plugs are maintained at a density higher than that of the central cell by neutral-beam injection. As a result of the higher density, the electrostatic potential in the plugs is higher than in the central cell, thus forming a barrier to the leakage of central-cell ions. Because of this barrier, the central-cell ions are confined for much longer times, resulting in higher Q. Of course power must be expended in maintaining the plug plasma, which produces no power, but if the plug volume is much less than that of the central cell, the Q can be made quite high. A schematic of the potential and magnetic field distribution along the central axis of such a tandem mirror is shown in Fig. 3-1.

The effect of the end plugs on the losses from the central cell can be further clarified with aid of Fig. 3-2. Figure 3-2(a) shows the regions of phase space (V_{\perp} = component of $\underline{v} \perp \underline{B}$) for ions confined or unconfined in a standard mirror. A typical ion is injected at $V_{\perp} = 1$ (arbitrary units) and diffuses in phase space under the action of collisions to the loss boundary. At high $V \equiv (V_{\perp}^2 + V_{\parallel}^2)^{1/2}$, the angle θ_{LC} of the loss boundary (loss cone) is given by

$$\sin^2 \theta_{LC} = 1/R_p, \quad (1)$$

where R_p is the ratio of mirror to central magnetic field, here taken as 2. The hole in phase space around $V_{\parallel} = 0$ is caused by the ambipolar potential ϕ ,

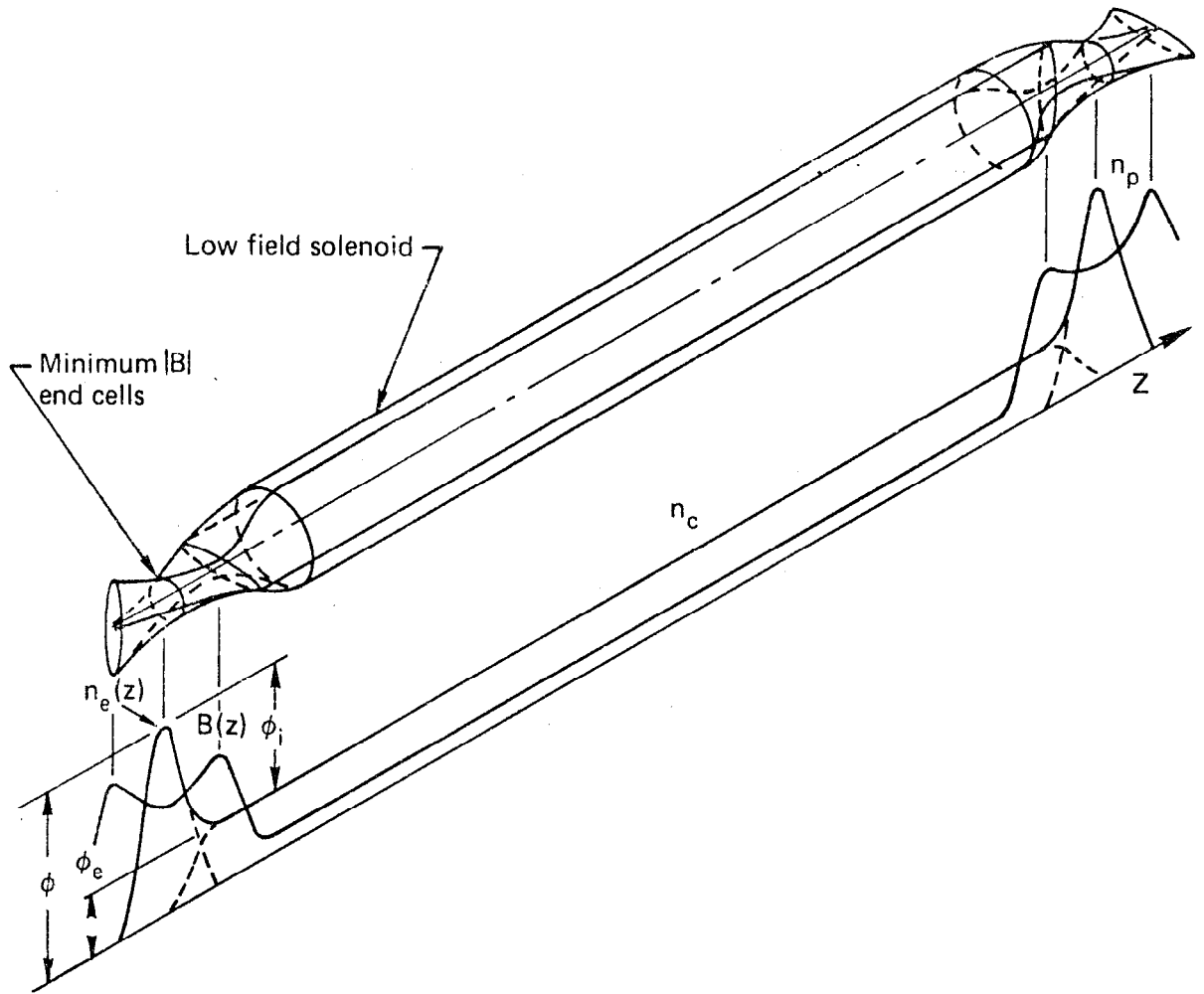


Fig. 3-1. Schematic of variation of electrostatic potential and magnitude of magnetic field on the axis of a tandem-mirror device.

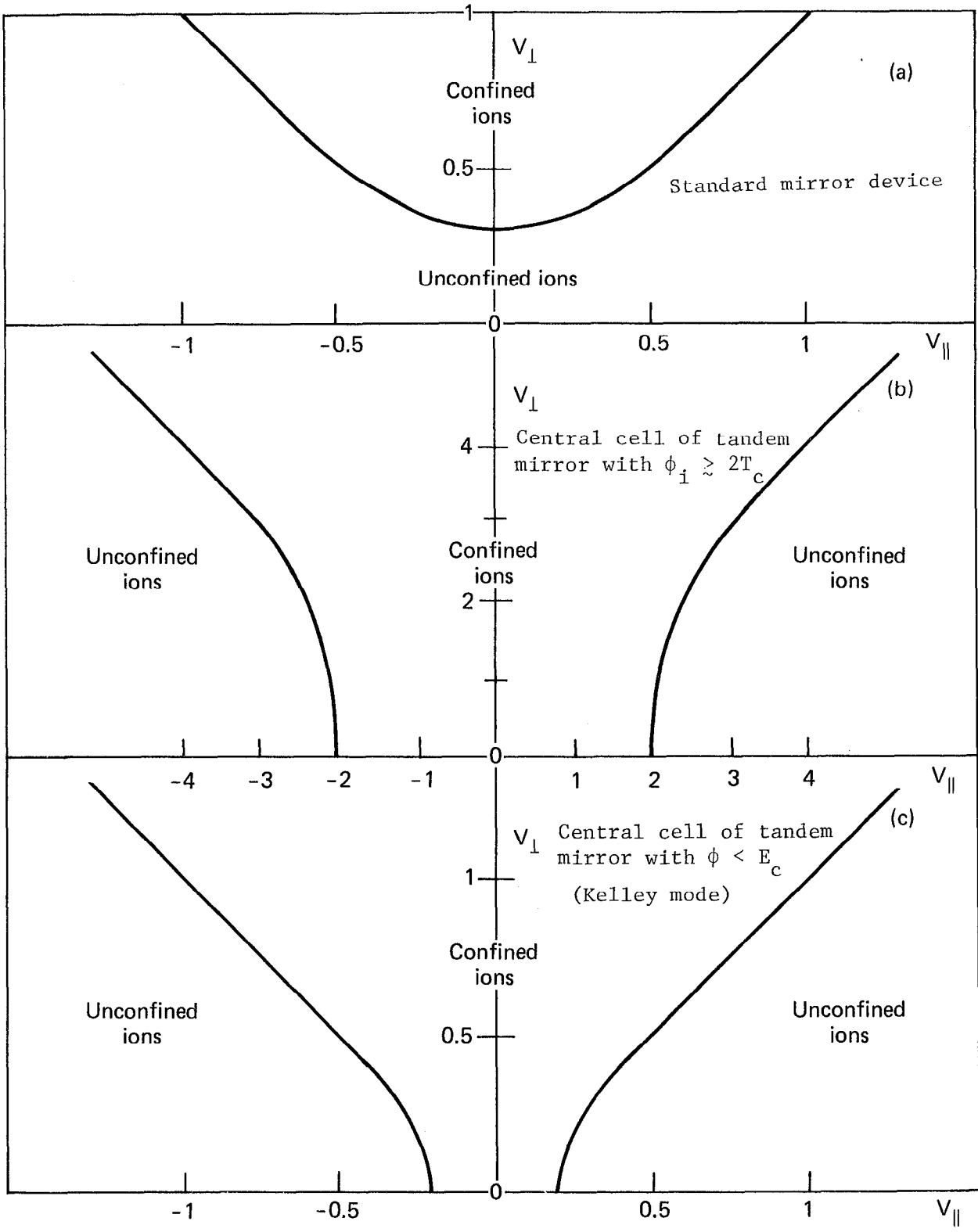


Fig. 3-2. Loss boundaries for hot ions.

which arises because electrons tend to leak out of the plasma much faster than ions. The intersection of the loss cone with the V_{\perp} axis is given by

$$V_{\perp 0}^2 = \frac{2\phi}{m_i (R_p - 1)} \quad (2)$$

Confinement time for the ions is the order of an ion-to-ion scattering time, provided the electron temperature is sufficiently high.

The situation in a tandem mirror where the ion confining potential ϕ_i is greater than the central-cell ion temperature T_c , is illustrated in Fig. 3-2(b).^{2,3} The plug and central-cell electron densities are n_p and n_c , respectively. In this case, ions are injected in the central cell at very low energies and are heated by interaction with hotter electrons that may be heated by interaction with plug ions or by imposed Electron Cyclotron Resonance Heating (ECRH), and, in two-component operation by hotter ions injected into the central cell. Confinement time of the central-cell ions can be several orders of magnitude larger than the ion-to-ion scattering time.

An alternative arrangement is to inject the central-cell ions at an energy much greater than confining potential ϕ_i (Kelley mode⁴). This case is illustrated in Fig. 3-2(c). The ions are essentially mirror-confined, however, without the "hole" in phase-space characteristic of Fig. 3-2(a). As a result, ions cannot simply drag into the loss region, but must also suffer sufficient angular deflection and are typically better confined than in the standard mirror.

A reactor design based on the tandem mirror with low-energy, central-cell ion injection has already been reported.⁵ In this design, the situation illustrated in Fig. 3-2(b) was invoked. Very high energy (600-1200 keV) neutral-beam injectors were required for the plugs in order to heat the electrons, which in turn heated the central-cell ions. The plug magnetic field was also quite high (16.5 T on axis). These values are necessary for the attainment of high Q values (ca. 5-10). However, Q values of only 1-2 are needed for hybrid reactors, which suggests that the requirements on magnetic field and neutral beam energies might be somewhat relaxed. But in order to attain fusion conditions in the central cell, the electrons and ions must be heated, if not by plug ions, then either by direct, high-energy injection into the central cell or by ECRH.

Two modes of high-energy, central-cell ion injection are possible. One mode is the Kelley scheme previously described. The other is the two-component

method in which even higher-energy ("hot") deuterium ions are injected into a colder target tritium plasma, and fusion reactions occur between the hot and cold components. This method has the advantage of furnishing a large low-energy streaming component out the ends, which can serve to stabilize the plugs against the drift-cyclotron loss-cone (DCLC) instability. The fact that the bulk of the losses are at low energy means lower power loss than if all losses were from a thermal fusion plasma.

These various methods of heating the fusing central cell ions have been considered for the hybrid reactor. Of these, injection of low-energy ions with ECRH or the two-component operation appear to be the most desirable. Details of the results obtained to date for these methods are given in this section.

A necessary requirement on any reactor is that it be free from magneto-hydrodynamic (MHD) instabilities. Early mirror devices used the magnetic field formed by two circular coils and were plagued by MHD interchange instabilities. The use of minimum-B magnets, for which field lines curve away from the plasma on the average, removed problems with this instability. In the tandem mirror the central section has straight field lines, and the plugs have field lines that curve away from the plasma; but the transition region between the plug and central cell produces lines with bad curvature. To ensure MHD stability, there must be sufficient good curvature in the plugs to balance the bad curvature in the transition region. Methods for deciding if a coil design is MHD-stable are discussed in this section. Other potential MHD instabilities and means for avoiding these are also discussed.

Consideration must also be given to potential microinstabilities in the tandem mirror. The most virulent appears to be the DCLC instability, which can severely limit confinement time in the plugs, thus increasing the input power required. Means for suppressing this instability are discussed in this section.

We also discuss current and future work and give a list of tandem mirror experiments and physics issues addressed in each.

MAGNETOHYDRODYNAMIC (MHD) INSTABILITIES

A sufficient criterion for stability against MHD interchange (flute) instabilities is⁶

$$\delta \int \frac{p_{\parallel} d\ell}{B} \leq 0 \quad . \quad (3)$$

With the aid of certain reasonable assumptions, Eq. (3) can be rewritten in a computationally more convenient form⁷ applicable at low β

$$\Gamma = \int (\hat{p}_{\perp} + \hat{p}_{\parallel}) (x''y + y''y) \frac{d\ell}{B_v} \geq 0 \quad . \quad (4)$$

Here $\hat{p}_{\perp, \parallel}$ are functions giving the dependence of pressure on the magnitude of the magnetic field; B_v is the vacuum magnetic field; and $x = x(\ell)$, $y = y(\ell)$ are coordinates of the field line.

Inequality (4) is the basic relation which the vacuum field generated by the coil design must satisfy. If the field lines curve away from the plasma, as they do in the minimum-B plugs of a tandem mirror, then the integral is positive and the criterion is satisfied. If the field lines are straight, as is approximately true in the central section, $x'' = y'' = 0$ and $\Gamma = 0$. However, at the transition from the plug to the central cell, the field lines necessarily curve toward the plasma (Fig. 3-3), resulting in a negative value for the integral. To ensure overall interchange stability, sufficient good curvature must be built into the plugs to compensate for this bad curvature.

The integral of Ineq. (4) has been coded for automatic computation by Johnston.⁸ Input to the code is a table of B_v for the coil set under consideration and the field line to be followed. In the transition and central sections of the tandem mirror $p_{\parallel} \approx p_{\perp} = \text{constant}$ while in the plug the following model field is employed:

$$\hat{p}_{\parallel} = p_0 \begin{cases} \frac{B_0 - B}{B_0 - B_{pv}} & , B < B_0 \\ 0 & , B \geq B_0 \end{cases} \quad (5)$$

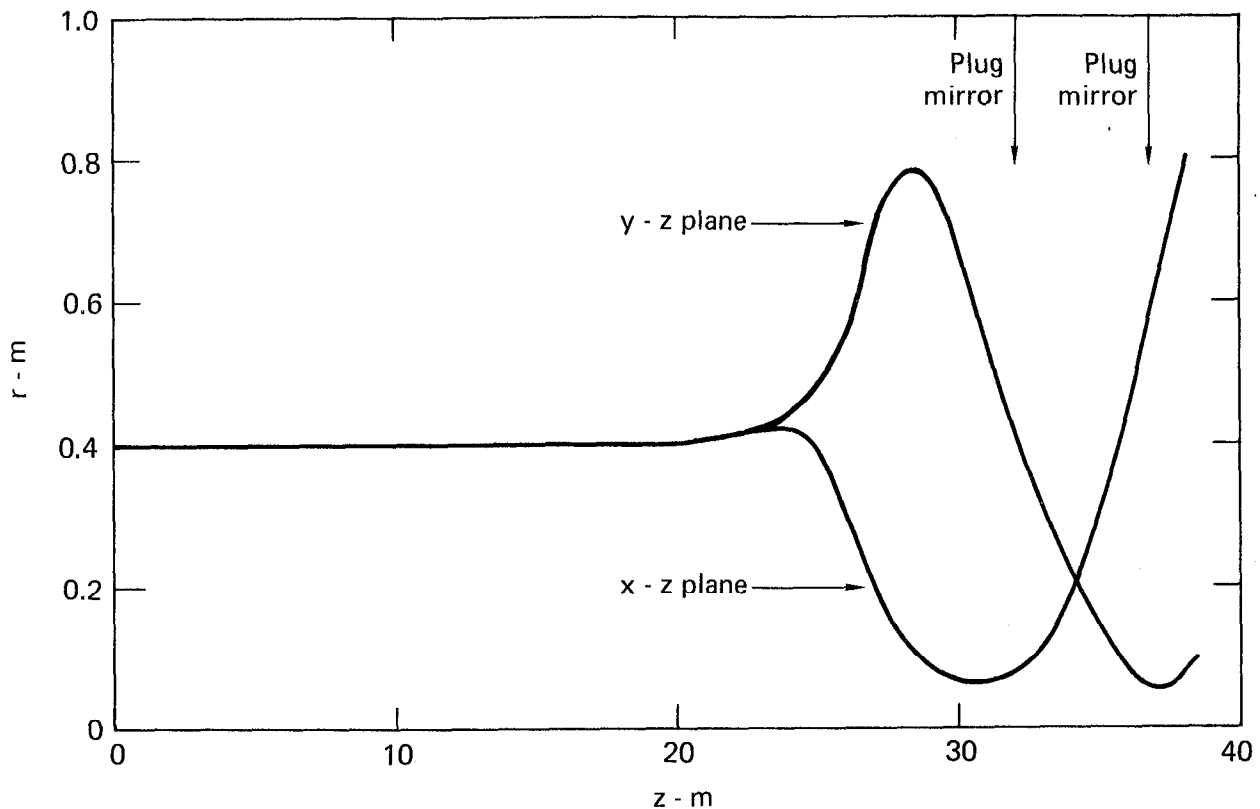


Fig. 3-3. Trajectory of two typical magnetic field lines in the tandem mirror.

$$\hat{p}_1 = \begin{cases} \hat{p}_1 - \frac{p_0 B}{B_0 - B_{pv}} \ln \left(\frac{B_0}{B} \right), & B < B_0 \\ 0, & B \geq B_0 \end{cases} \quad (6)$$

B_{pv} is the vacuum field at the plug midplane, B_0 is the field at which the pressure is assumed to vanish and satisfies $B_0 < B_{pm}$, where B_{pm} is the plug mirror field. The term p_0 is the value of p_1 at the midplane of the plug. However, since Γ is defined only within an arbitrary constant, we may measure the plug pressure in units of central-cell pressure. A convenient quantity for judging the suitability of a coil design is the ratio of β in the central cell to that in the plug,

$$\frac{\beta_c}{\beta_p} = \frac{p_{1c}}{B_{cv}^2} \frac{B_{pv}^2}{p_{1p}} = \left(\frac{B_{cv}}{B_{pv}} \right)^2 \frac{1}{p_0} . \quad (7)$$

Thus, a typical calculation varies p_0 until $\Gamma \approx 0$ and reports the quantity β_c/β_p at that value of p_0 . Clearly, lower values of β_c/β_p , i.e., where the integral of Ineq. (4) is more weighted by the good curvature in the plug, are even more stable.

As an example of the application of the interchange criterion, we study the effect of finite coil spacing in the central cell on the stability. Because of the finite spacing, field lines bulge outward between coils, resulting in bad curvature regions similar to the old simple mirror plasma device. We have varied the coil spacing in a typical tandem mirror coil set developed by Myall⁹ from zero, i.e., a continuous tube, to 4 m between coil centers. The field ripple at the plasma edge (1 m) vanishes in the former case and rises to 8% in the latter case for these coils of radius 2.64 m. Results for β_c/β_p are shown in Fig. 3-4 vs $\Delta B/B$ and coil spacing. Clearly, there is negligible effect on β_c/β_p for $\Delta B/B \lesssim 5\%$. Above this value, a somewhat reduced central-cell pressure is indicated. Such a reduction may be necessary to meet another criteria on central-cell β .

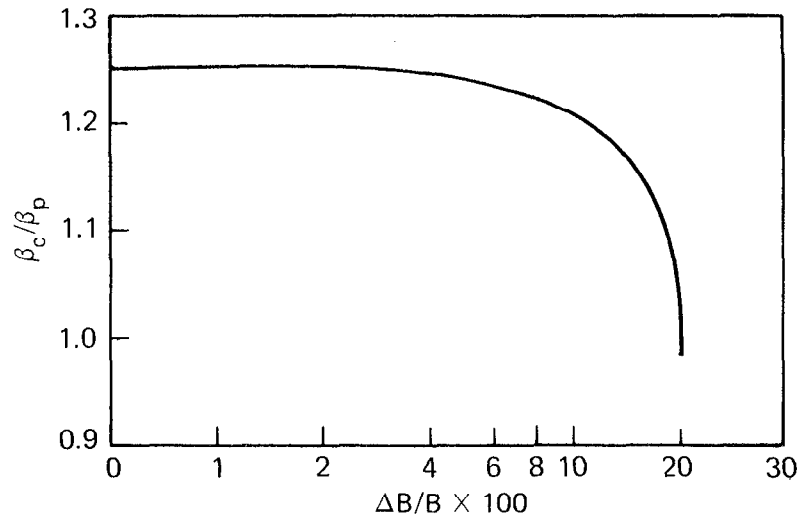


Fig. 3-4. β_c/β_p vs $\Delta B/B$ for stability to interchange modes for a typical coil set with barrier fields.³⁻⁹

The interchange instability effectively sets certain requirements on the coil design and on the β -ratio. Another closely related instability--ballooning, as driven by bad curvature--can arise as the pressure is increased. As the name implies, this instability is localized axially to a small region and typically occurs only in regions of bad vacuum-field curvature, although it can occur in the minimum-B plugs if the pressure is high enough to substantially alter the good curvature. Unfortunately, no simple criterion exists for the limiting β . Each case must be examined using a stability code developed by Kaiser.⁷ Typical β_c values computed for TMX are 40% and can be made higher with modification of the transition coils.

Another drive for ballooning is the rotation of the central column set up by the radial electric field (due to radial pressure gradients) interacting with the axial magnetic field. Friedberg and Pearlstein¹⁰ examined an approximation to the central cell--a straight rigid rotor with finite-Larmor radius effects included. The "worst" ballooning mode is found to limit the central-cell β to about

$$\beta_c \lesssim \pi^2 \frac{T_{ic}}{T_{ec}} \left(\frac{r_c^2}{L_c \rho_{icv}} \right)^2, \quad (8)$$

where T_{ic} and T_{ec} are the central-cell ion and electron temperatures, r_c and L_c are the central-cell radius and length, and ρ_{icv} is the central-cell vacuum Larmor radius. Consideration of typical parameters on the right-hand side of Ineq. (8) shows that rotation-driven ballooning should not be a problem for reactors.

Rotation can also drive interchange-like instabilities that were not considered in arriving at Ineq. (8). Theory is much less advanced in specifying criteria to avoid such instabilities. A simple comparison between the curvature-driven and rotation-driven interchange shows that the latter is less important if¹¹

$$\frac{T_{ec}}{T_{ic}} \left(\frac{T_{ec}}{T_{ic}} + 1 \right) \leq 2 \sqrt{R_{cm}} \frac{r_c^4}{\rho_{civ}^2 L_{tr} L_c}, \quad (9)$$

where $R_{cm} \equiv B_{cm}/B_c$ is the central-cell mirror ratio, and L_{tr} is the characteristic length of the transition region.

Two additional MHD instabilities can occur in nonisotropic regions such as the end plugs or in two-component operation of the central cell. These are the firehose and mirror modes. Criteria for avoidance of these instabilities are

$$B - \mu_0 \frac{\partial p_{\parallel}}{\partial B} > 0 \quad (10)$$

and

$$B + \mu_0 \frac{\partial p_{\perp}}{\partial B} > 0 \quad (11)$$

MICROINSTABILITIES

Past mirror experiments have suffered from DCLC instabilities that have severely limited ion confinement times. These can be suppressed by supplying sufficient warm plasma to partially fill the loss cone (Fig. 3-2a). Recent experiments in 2XII B show that the amount of warm plasma that must be supplied decreases with increasing plasma radius, as predicted by theory.¹² The same theoretical considerations also predict that the mirror plasma is free from DCLC oscillations if the ratio of plasma radius, r_p to ion vacuum Larmor radius, ρ_{iv} is large enough.¹³ To suppress this instability, we can take two approaches that: (1) build the plug large enough so the stability criterion is satisfied (gradient stabilization); or (2) ensure that the losses from the central cell are adequate to stream-stabilize the plugs.

The boundaries for stability of a deuterium plasma are shown vs r_p in Fig. 3-5. At a typical plug β (long-thin approximation) of 0.7 with 200-keV injection, the plug radius must satisfy $r_p \gtrsim 63 \rho_{iv}$. For a central plug field of 7 T, this requires $r_p \approx 0.78$ m. Such a large plug radius is possible only for large fusion power. At low fusion power, the power required for the plugs yields low Q .

Curves showing the ratio of warm (streaming)-to-hot plasma densities (n_w/n_H) for DCLC stability are given vs $S_v = r_p/\rho_{iv}$ in Fig. 3-6. The curves are applicable only for $(V_h/V_H)^2 = (\phi_e + \phi_i)/(R_p - 1) E_p = 0.1$, where ϕ_e and ϕ_i are the electron and ion confining potentials, R_p is the plug mirror ratio, and E_p is the plug ion energy. Theoretical estimates predict that n_w/n_H scales as $(V_h/V_H)^2$, which we use. Knowing the required n_w/n_H , we can then find the required stabilizing current density through the plug from

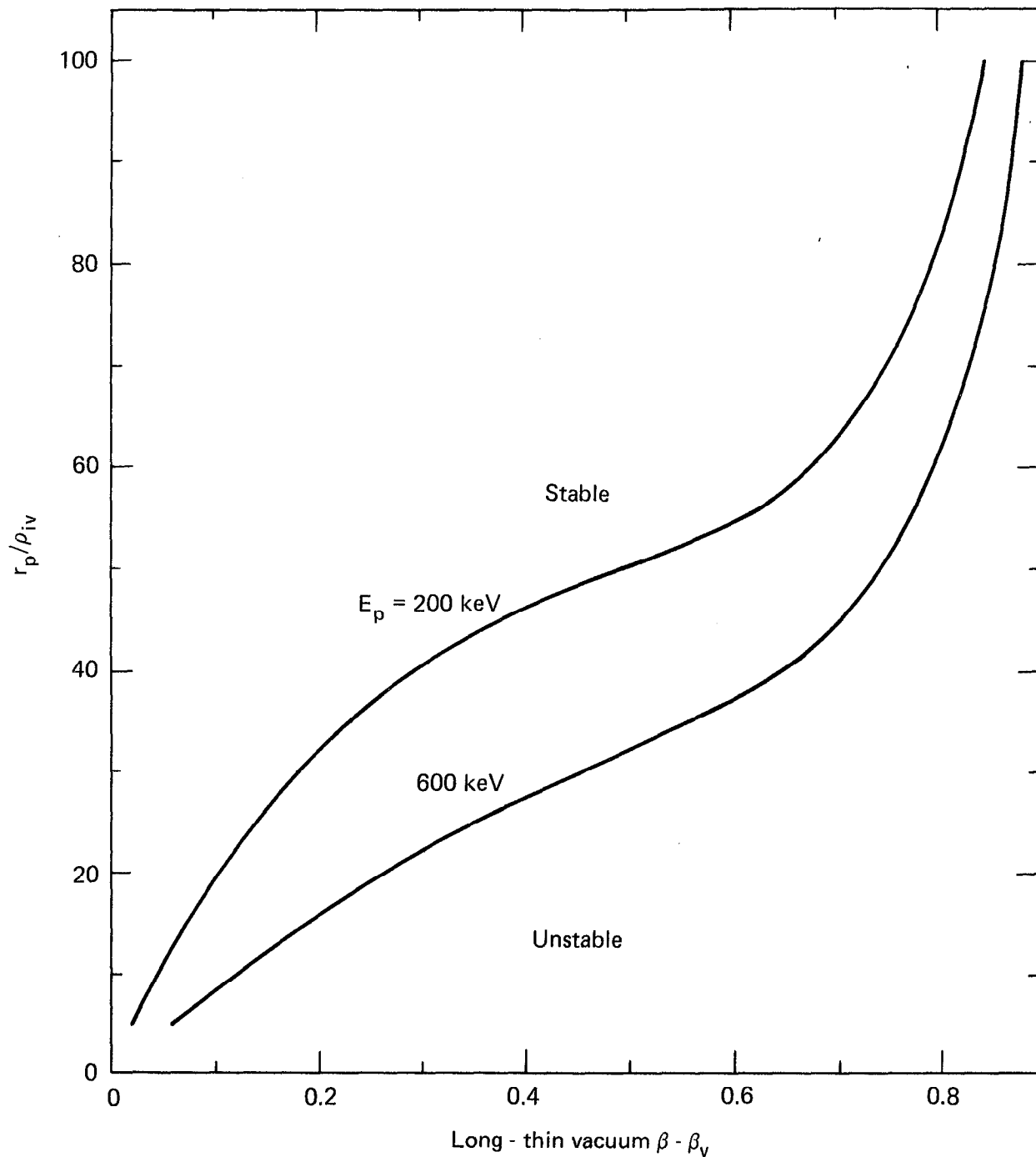


Fig. 3-5. Plot of r_p / ρ_{iv} for stability against DCLC mode vs plasma β_v for deuterium energies of 200 and 600 keV.

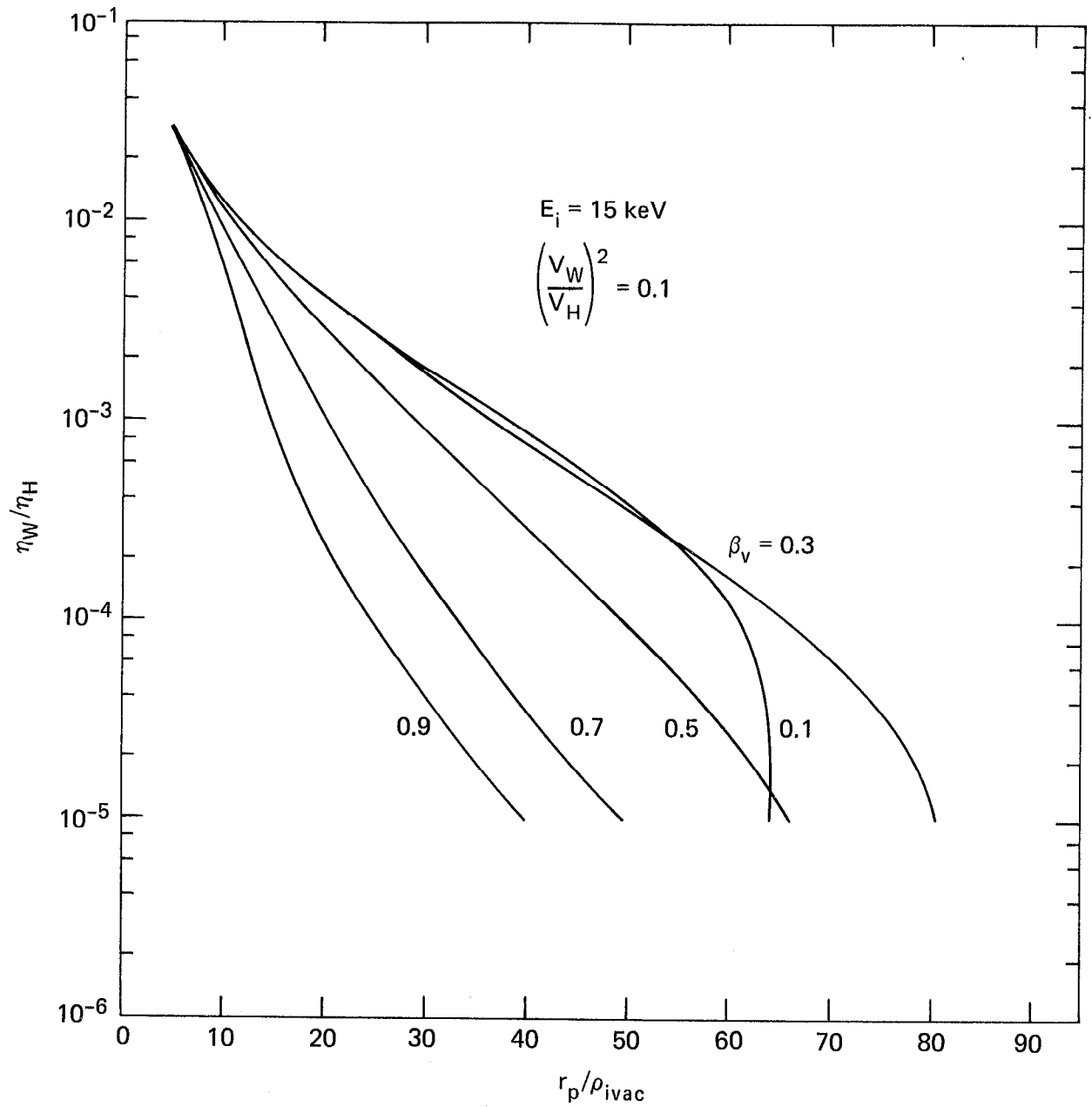


Fig. 3-6. Plot of n_w/n_H required for DCLC stability vs $S_v = r_p/\rho_{iv}$ for various plasma β .

$$j_{\text{STAB}} = en_w V_{w\parallel} \quad , \quad (12)$$

where $V_{w\parallel}$ is the speed of the streaming plasma along the field lines. Since the principal streaming plasma is that lost from the central cell, we find $V_{w\parallel}$ from

$$v_{w\parallel} = \alpha(2T_c/m_c)^{1/2} \quad , \quad (13)$$

where T_c and m_c are the temperature and mass of the central-cell ions. The factor α is near unity, which we take as 1/2 in accord with Correll, et al.¹² From the foregoing considerations, we find the following expression for required stabilizing current, where f is a fit to the curves in Fig. 3-6.

$$j_{\text{STAB}} = 2.48 \times 10^{-12} \frac{T_c^{1/2} (\phi_e + \phi_i) n_p}{M_c^{1/2} (R_p - 1) E_p} f(S_{pv}) \text{ A/cm}^2 \quad . \quad (14)$$

We use a standard form for f :

$$f = 10 \exp -(S_{pv} + \epsilon)/\rho \quad . \quad (15)$$

Constants for Eq. (15) are:

B	ϵ	ρ	S_{pv} range
0.5	17.6	6.21	5-14
0.5	26.5	7.99	14-30
0.7	11.4	4.55	5-20
0.7	17.3	5.46	20-35

Another instability, the Alfvén-Ion-Cyclotron (AIC) mode, can also arise in anisotropic pressure distributions, such as occur in the plugs and in two-component operation of the central cell. Theoretical studies¹³ indicate that with $\beta_{\perp} \approx 0.7$, the pressure ratio p_{\perp}/p_{\parallel} should be $\lesssim 7/4$. However, experiments in 2XIIB yielded much higher pressure ratios, perhaps because of the finite length and small radius (measured in terms of ρ_i). To date, we can not explain this discrepancy in a quantitative way. Nonetheless, it is possible that the AIC instability could place more severe restrictions on β than assumed in this study.

THERMAL FUSION MODE OF OPERATION

In the thermal fusion mode of operation, the central cell is not injected with any high-energy neutral beams. All power needed to sustain the central cell ions, therefore, comes from the electrons that pass between the plug and the central cell or from alpha heating. Since the former mechanism tends to dominate in most cases, it becomes preferable to channel as much input power as possible to the electrons. We wish to limit ourselves to plug neutral-beam injection energies that are at most equal to about 600 keV, and preferably in the vicinity of 200 keV; but injected neutrals at these energies tend to impart the greater fraction of their energy to ions (by scattering) rather than to electrons (by drag). It is therefore necessary to employ direct electron heating to make this a desirable operation. The fraction of the input power that is in the form of direct electron heating is an independent variable that we may optimize.

The physics model used incorporates new sophistication in tandem mirror parametric analysis, up to but not including the very new ideas of Baldwin, Logan, and Fowler involving thermal barrier cells.¹⁴ Though this latter concept now dominates the present effort in tandem mirror reactor design, its advantage is contingent upon more uncertain physics. Thus we shall assume central-cell (or transition region) direct electron heating only.

Key additions to the model and improvements in the code over and above what was described in the earlier report on tandem mirror reactors⁵ have been:

- The addition of A-cells on the outboard sides of the plugs, to decrease the maximum (outboard) axial potential drop seen by the plug ions, thus enhancing plug confinement.

- An option to automatically gradient-stabilize the plugs (and/or A-cells) by adjusting the value of the plug beta (and/or the A-cell beta) until marginal stability is achieved. This option uses results from Fig. 3-5, giving the maximum stable value of plug beta as a function of both the ion energy¹⁵ and the plug (and/or A-cell) radius expressed in units of ion Larmor radii.

- An optimizing controller program developed to maximize Q with respect to the plug-to-central cell mirror ratio and to the direct electron heating fraction, while constraining the system's wall loading to any desired value. The controller uses the simplex algorithm for function optimization.¹⁶

With regard to the first improvement, all results presented in this section use an A-cell to reduce the outboard plug potential drop ($\phi_e + \phi_i$) to equal the inboard plug potential drop (ϕ_i). If the outboard potential drop were reduced any more, the escaping ions from the main plug would go into the central cell rather than out of the machine. Though this may be desirable, the code is currently incapable of modeling such a case.

Since the minimum plug injection energy is equal to the maximum axial potential drop seen by the plug ions divided by $(R_p - 1)$, where R_p is the plug plasma mirror ratio, we see that the A-cell reduces this minimum plug injection energy. It is this fact that makes it possible for us to achieve potentially desirable tandem mirror hybrid drivers with only 200-400-keV plug injection energies. The A-cell has very little other effect on the tandem power flow and may be designed so that it consumes very little power.

The computational results from the code are displayed in Fig. 3-7 for fusion power outputs of 2500 MW and 1500 MW. The plug injection energy is taken as 400 keV, and the maximum field at the plug coils is 12 T. It is further assumed that the plugs can be axisymmetric coils since the minimum-B A-cell can provide all the good curvature necessary for MHD stabilization. These results give the maximum value of plasma Q attainable for a given wall loading, Γ_w . Since Q is a measure of plasma confinement and since Γ_w is a measure of plasma power density, we find that one may be traded for the other; in a tandem mirror there is always a fundamental tradeoff between confinement and power density.⁵

For each value of Γ_w , the value of Q was optimized with respect to the central-cell magnetic field strength, the fraction of input power in the form of direct-electron heating, and the central-cell fueling rate. Figures 3-8 through 3-12 give the central-cell length, first-wall radius⁵, direct electron heating fraction, central-cell ion temperature, and electron temperature, respectively, for the optimum-Q case at each value of Γ_w .

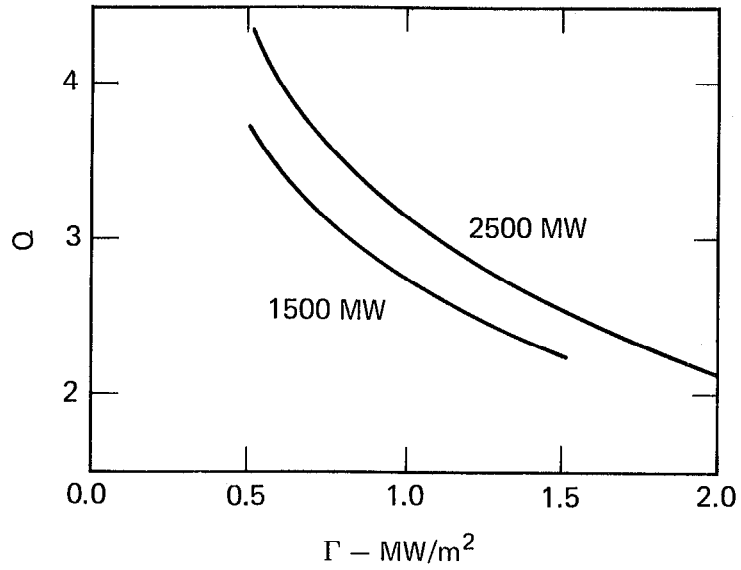


Fig. 3-7. Plot of optimized-Q vs Γ for 1500 MW_{fus} and 2500 MW_{fus} thermal fusion TMRS.

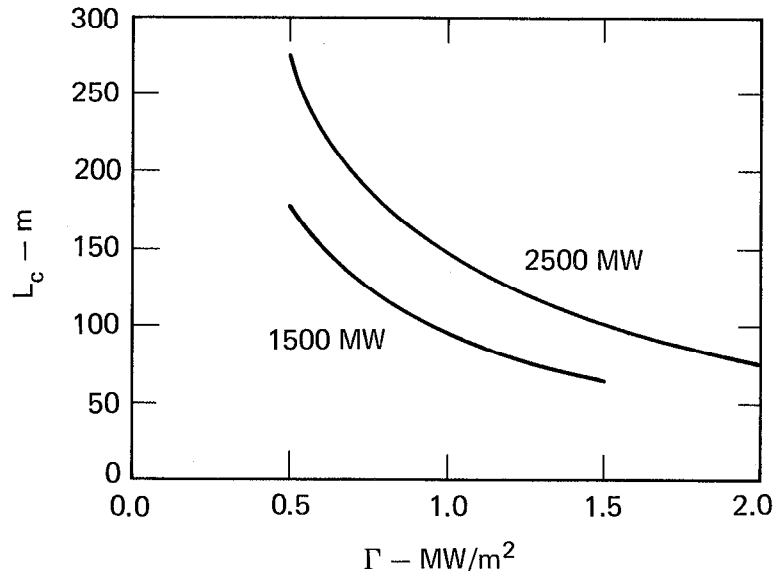


Fig. 3-8. Plot of central cell length vs Γ for 1500 MW_{fus} and 2500 MW_{fus}, optimized-Q, thermal fusion TMRS.

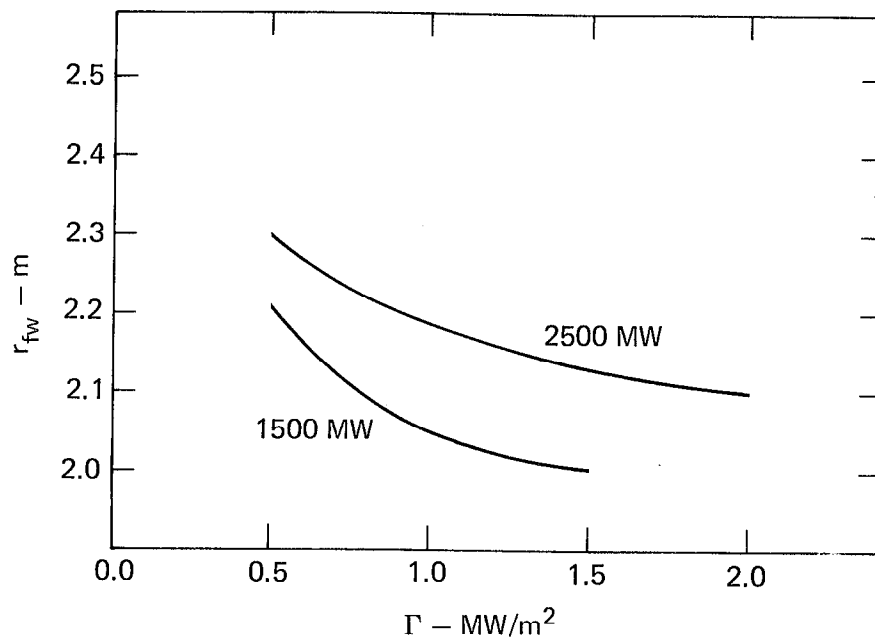


Fig. 3-9 Plot of first wall radius vs Γ for 1500 MW_{fus} and 2500 MW_{fus} , optimized Q, thermal fusion TMRs.

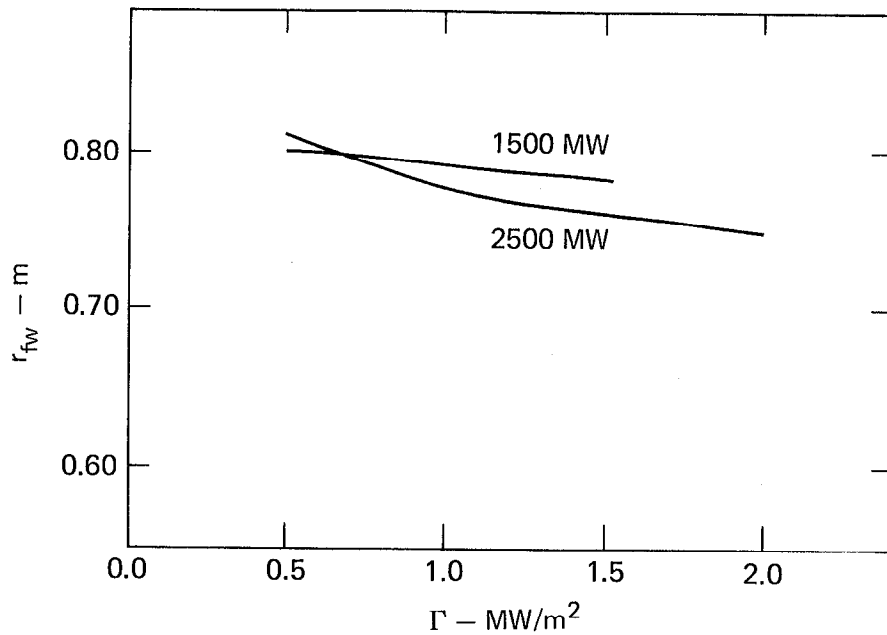


Fig. 3-10. Plot of direct electron heating fraction vs Γ for 1500 MW_{fus} and 2500 MW_{fus} , optimized-Q, thermal fusion TMRs.

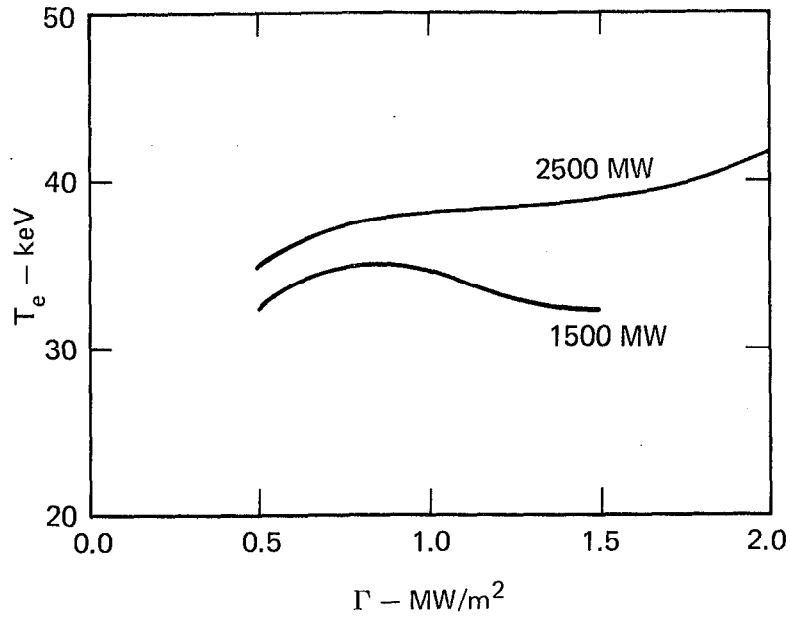


Fig. 3-11. Plot of central cell ion temperature vs Γ for 1500 MW_{fus} and 2500 MW_{fus} , optimized-Q, thermal fusion TMRs.

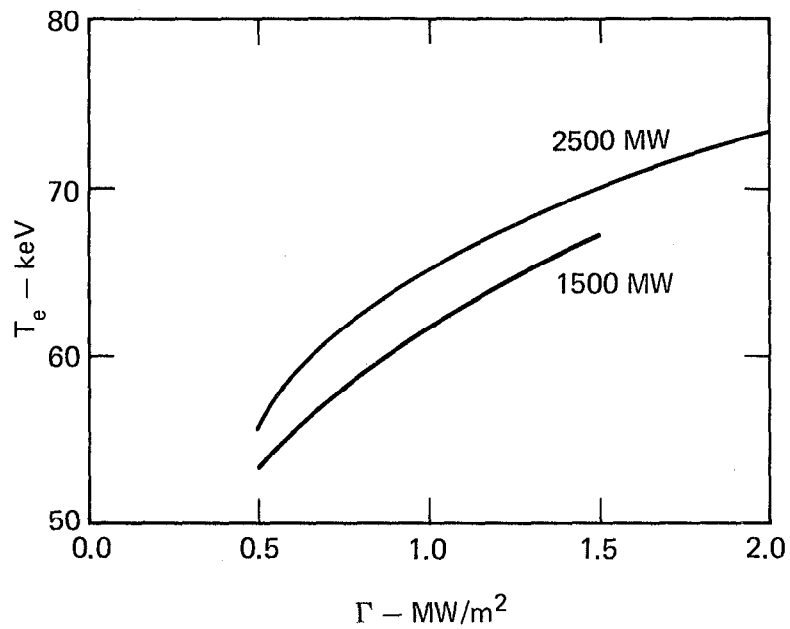


Fig. 3-12. Plot of electron temperature vs Γ for 1500 MW_{fus} , and 2500 MW_{fus} , optimized-Q, thermal fusion TMRs.

TWO-COMPONENT OPERATION

Gradient stabilization of tandem mirror plugs requires a large plug radius, r_p . The central-cell radius, r_c , is related to the plug radius by conservation of magnetic flux:

$$r_c = r_p \sqrt{B_p/B_c} . \quad (16)$$

Since $B_p > B_c$, to maintain a density difference between plug and central cell, $r_c > r_p$. A typical plug radius for gradient stabilization is 1 m, and for typical B_p/B_c of 3-5, the central-cell radius is about 2 m. For a total fusion power of 2500 MW, the central-cell length is about 100 m with Q of 2-5. To lower the fusion power, the length must be decreased, resulting in very rapid increase in Q since the plug-input power remains nearly constant. Thus, it is desirable to lower the plug radius, which can only be accomplished if stream stabilization is used.

We have investigated possible operating conditions for a reactor producing 500 MW of fusion power and first-wall neutron loads of 0.5 - 2.0 MW/m². The tool for these studies was a new zero-dimensional code written to enable the study of a variety of different possible operating scenarios for tandem mirrors. This code has not yet been documented,¹⁷ so we include a brief description here.

The code solves the density and energy equations for two central-cell and one plug-ion group, as well as electrons that are assumed to have the same energy in the plugs and central cell. One central-cell ion (tritium) is fed in at very low energy and is ionized and heated by the hot deuterium and electrons. The (equivalent) tritium current is adjusted to furnish sufficient losses out the end to satisfy

$$j_{loss} \gtrsim j_{STAB} , \quad (17)$$

where j_{STAB} is given by Eq. (14).

Confinement time of the tritium obeys the generalized Pastukhov expression¹⁸

$$\tau_{ccj} = \frac{(2\pi)^{3/2} \mu_0^2}{e^4 M_j^{1/2}} \sum_{ions} \frac{m_p^{1/2} T_j^{3/2}}{Z_k n_k \ln \Lambda_{jk}/M_k} Z_j \frac{\phi_i G(\zeta_j B_p/B_c) \exp(\phi_i/T_j)}{\zeta_j T_j I(T_j/\phi_i)} , \quad (18)$$

where M_j is the ion mass in units of proton mass (m_p),

$$G(x) = (2x + 1) \ln (4x + 2)/2x \quad , \quad (19)$$

$$I(x) = 1 + \frac{\sqrt{\pi x}}{2} e^{1/x} [1 - \operatorname{erf} (1/\sqrt{x})] \quad , \quad (20)$$

$$\zeta_j = \frac{\sum_{\text{ions}} Z_k^2 n_k \ln \Lambda_{jk}}{2M_j \sum_{\text{ions}} Z_k n_k \ln \Lambda_{jk}/M_k} \quad , \quad (21)$$

$$\phi_i = T_{ep} \ln (n_p/n_c) \quad , \quad (22)$$

and $\ln \Lambda_{jk}$ is the usual Coulomb factor.

Properties of the hot central-cell deuterium are computed from analytic distribution functions obtained by Heckrotte, et al.¹⁹ and

$$f(E) = j_h \begin{cases} r^{-1} (E r_0/E_0 r)^{1/p} \quad , \quad E < E_0 \\ (s_0/r_0 s) (E_0 r/E r_0)^{1/p} \exp [(E_0 - E)/T_{ec}] \quad , \quad E > E_0 \end{cases} \quad (23)$$

with $p \equiv 4 \log_{10} (B_m/B_c)$, j_h the trapped density of hot ions, E_0 their injection energy, and r and s are drag and dispersion rates for the ions.¹⁹ Mean ion properties are found by integration of appropriate moments over the distribution functions. Losses of electrons and electron energy from the central cell are found from bounce-average expressions for square-well magnetic fields¹⁸, and are too lengthy to reproduce here.

The plug is treated in steady state; specification of vacuum magnetic field, plug beta β_p , mean plug ion energy, and electron temperature serve to determine the density. Required injection power then follows when the confinement time is known. The latter computed from an expression incorporating both electron drag and ion scattering.²⁰

The initial studies for $P_F = 500$ MW (fusion power) and stream-stabilized plugs yielded a fairly constant Q of 0.9-1.0 for a neutron wall load (Γ_w) of 0.5-2.0 MW/m². Further studies then shifted to a fusion power of 2500 MW, suitable for a molten salt blanket with a lower neutron multiplication. With stream-stabilized plugs, a Q of about unity was also obtained. The stream-

stabilized mode of operation has the disadvantage of requiring the adjustment of the tritium gas feed to meet the stability requirement. This controllable parameter is then no longer available for maximizing Q . With the thought of possibly raising Q to economically more desirable values, it was decided to include an A-cell, thereby lowering the plug potential and reducing the losses required for DCLC stability. We found it possible to adjust the tritium gas feed to maximize Q , while always maintaining full plug stability.

Some results for this case are collected in Figs. 3-13 through 3-16. In Fig. 3-13, we see that the character of the Q vs Γ_w curve is markedly different than for the electron rf-heated reactor considered in the previous subsection. Rather than continuously increasing as $\Gamma_w \rightarrow 0$, it appears to flatten out. The explanation for this behavior may be found in Figs. 3-14 through 3-16. Figure 3-14 shows that the power to the plug does decrease as $\Gamma_w \rightarrow 0$, reflecting the smaller plug radius, but that the central cell power increases. Thus in Fig. 3-15 we see that the power ratio for the central cell alone (Q_c) decreases as $\Gamma_w \rightarrow 0$.

Figure 3-16 shows the electron and tritium target temperatures, T_e and T_t vs Γ_w . The higher temperatures are favorable for higher Q , since there is less drag on the high-energy beam components. The higher temperatures at larger Γ_w are a result of the increased neutral beam power input to the plug cells. Much of this power serves to heat the electrons, which helps to heat the target tritium ions.

The results in Figs. 3-14, 3-15, and 3-16 suggest that it might be desirable to raise the electron temperature by direct auxiliary heating. This option has not yet been explored.

KELLEY MODE OPERATION

In the Kelley mode of operation, both species of fuel ions are energetically injected into the central cell. The central-cell plasma is Maxwellian with a temperature typically anywhere from 2 to 20 times ϕ_c . In this regime, the Pastukhov expression for $(n\tau)_c$ is no longer valid and must be replaced with:

$$(n\tau)_c \approx T_c^{3/2} \left(1 + \frac{\phi_c}{T_c} \right) \exp \frac{\phi_c}{T_c} \quad (24)$$

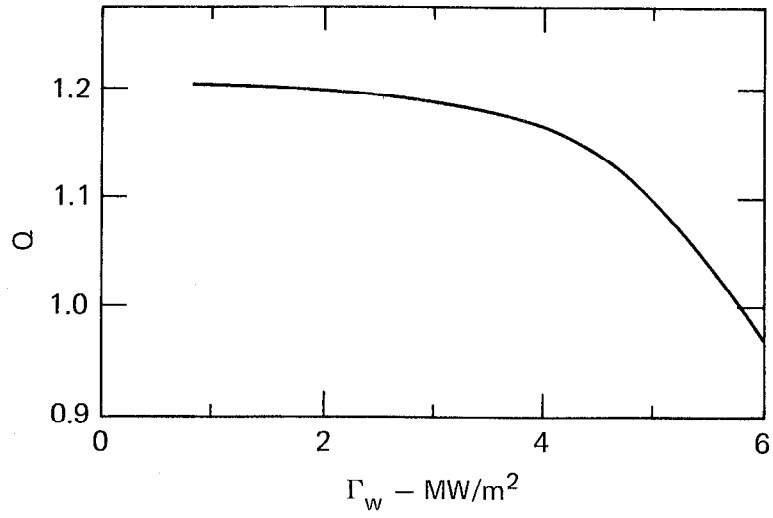


Fig. 3-13. Q vs Γ_w for two-component operation with $P_F = 2500$ MW.

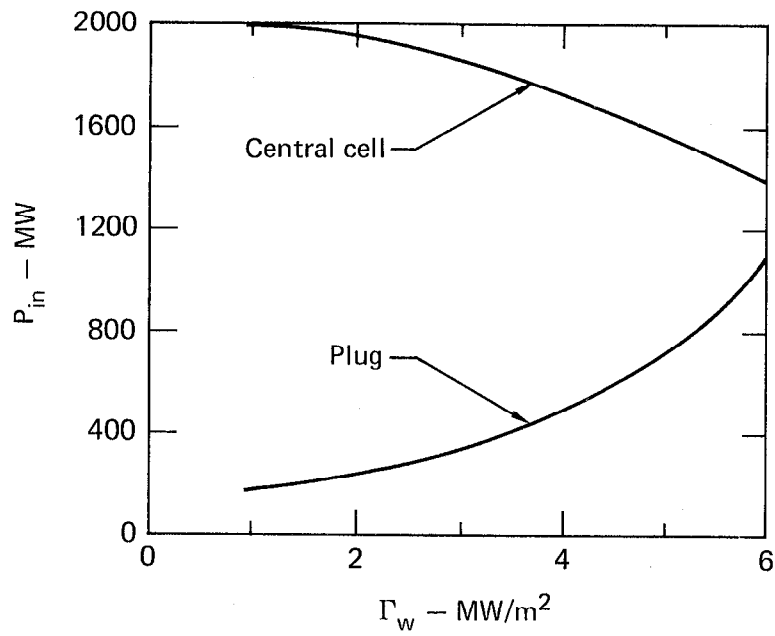


Fig. 3-14. Power to central cell and plugs vs Γ_w for two-component operation with $P_F = 2500$ MW.

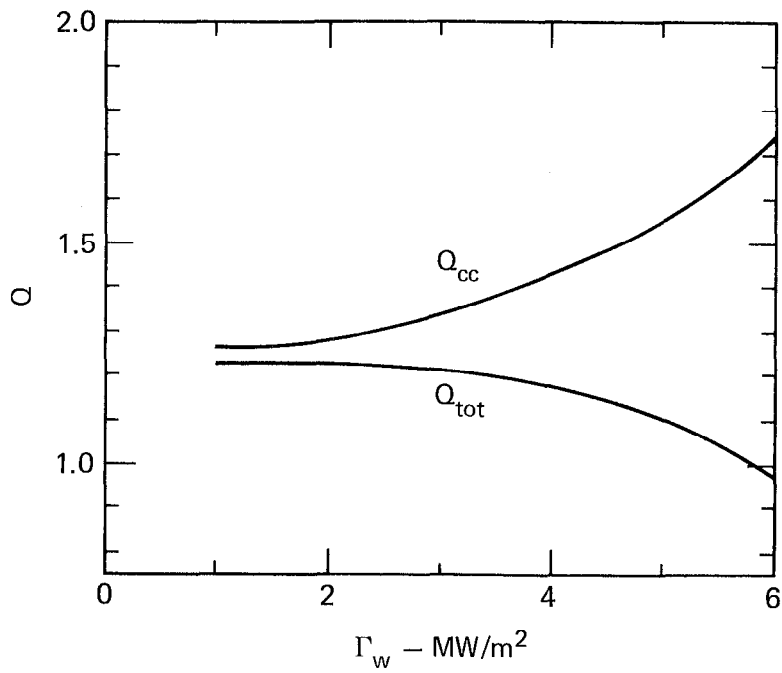


Fig. 3-15. Power ratio for central cell (Q_c) and for central cell plus plugs (Q_{tot}) vs Γ_w for two-component operation with $P_F = 2500$ MW.

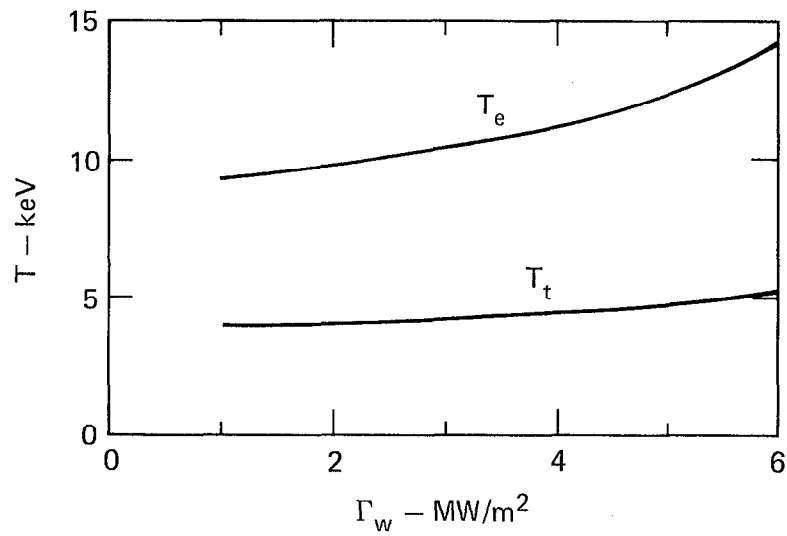


Fig. 3-16. Electron temperature (T_e) and tritium target temperature (T_t) vs Γ_w for two-component operation with $P_F = 2500$ MW.

There are two contributions to $\langle \sigma v \rangle_{DT}$: a thermal fusion contribution in the Maxwellian plasma, and a "slowing-down fusion" contribution from the beams interacting with the plasma. The latter of the two contributions is ignored in the calculations we present here.

Curves of optimum Q vs neutron first wall loading are given in Figs. 3-17 and 3-18 for fusion powers of 500 MW and 2500 MW. In all cases, the plug and central-cell injection energies are the same and are equal to 200 keV. The plug midplane vacuum fields are 7.0 T; since the plug mirror ratios are all 1.3, this corresponds to a field of approximately 12.1T at the Yin-Yang windings. Four point cases are selected and are been presented in detail in Table 3-1.

BARRIER CELL OPERATION

Although parametric physics studies of a tandem mirror hybrid reactor with barrier cells have not been conducted, we expect to proceed with this work in the near future. We present here a brief description of the physics underlying the barrier cell concept. Although this concept invokes more uncertain physics assumptions, it does appear to significantly improve performance while making fewer demands upon neutral beam and superconducting magnet technology in the end plugs.

The essential idea is to insulate the plug electrons from the central-cell electrons and to apply ECRH in the plugs so that the plug electron temperature T_{ep} becomes substantially larger than the central-cell electron temperature T_{ec} . To effect this insulation, we create a potential drop ϕ_b between the central cell and the plug (see Fig. 3-19). The Maxwell-Boltzman relations between the plug and the barrier cell may be written as

$$n_c = n_b \exp \left(\frac{\phi_b}{T_{ec}} \right) \quad (25)$$

and

$$n_p = n_b \exp \left(\frac{\phi_b + \phi_c}{T_{ep}} \right) , \quad (26)$$

respectively. Combining these to eliminate n_b , and solving for ϕ_c we get

$$\phi_c = T_{ep} \ln \left(\frac{n_p}{n_c} \right) + \left(\frac{T_{ep}}{T_{ec}} - 1 \right) \phi_b , \quad (27)$$

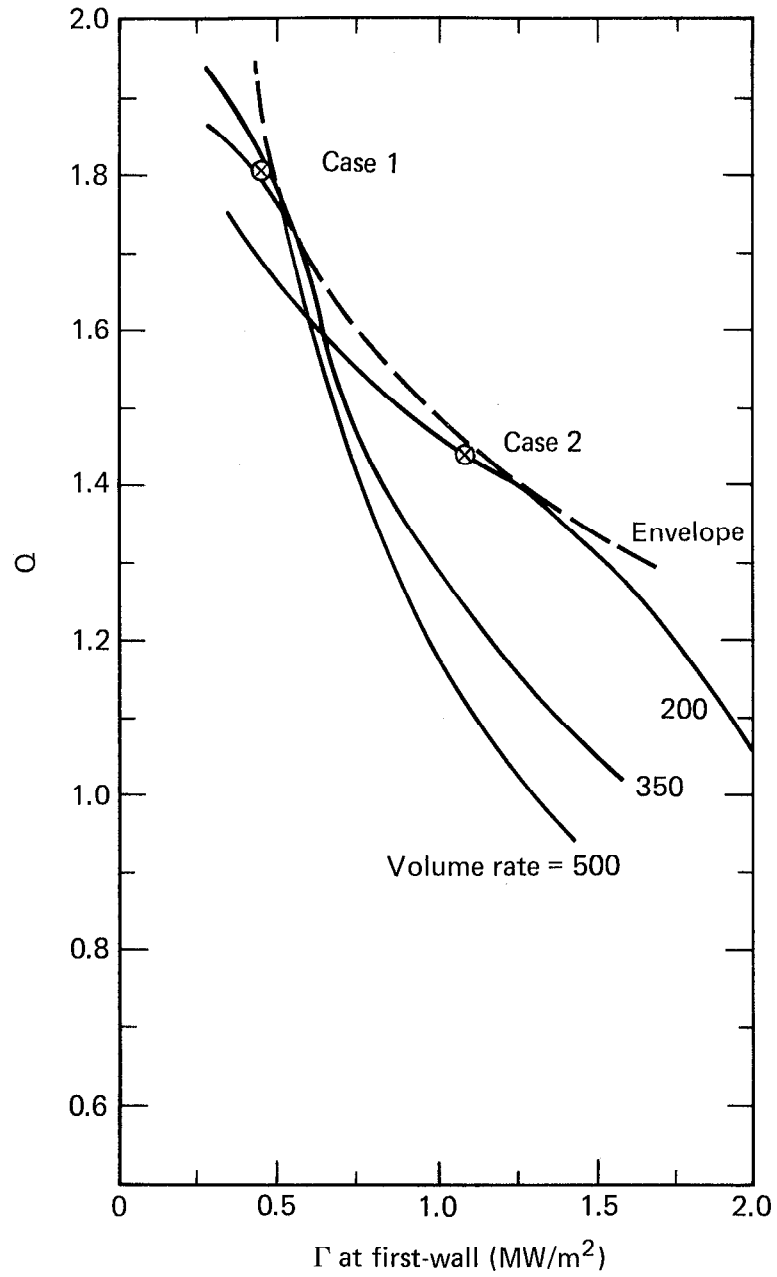


Fig. 3-17. Accessible Q/Γ parameter space; 500 MW fusion power Kelley mode Tandem Mirror Hybrid Reactor.

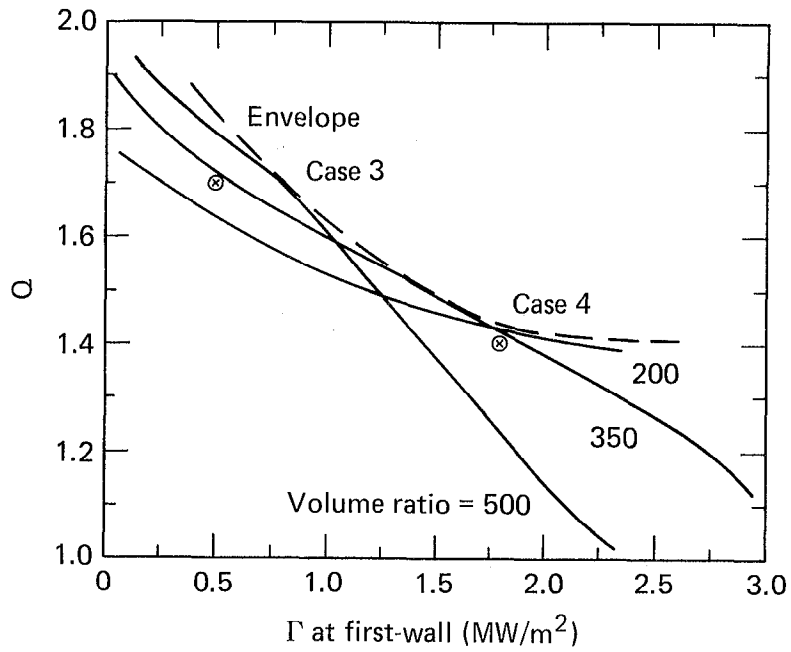


Fig. 3-18. Accessible Q/Γ parameter space; 2500 MW fusion power Kelley mode Tandem Mirror Hybrid Reactor.

Table 3-1. Parameters for Kelley-mode operation.

	Case 1	Case 2	Case 3	Case 4
Q	1.80	1.44	1.70	1.40
$\Gamma(\text{MW-m}^{-2})$	0.46	1.10	0.99	2.29
$L_{cc}(\text{m})$	38.9	19.9	70.2	36.7
$r_p(\text{m})$	0.47	0.45	0.71	0.70
$r_{cc}(\text{m})$	1.33	1.11	1.83	1.55
$r_{fw}(\text{m})^*$	1.79	1.45	2.29	1.90
$T_e(\text{keV})$	21.9	20.8	19.7	19.3
$T_c(\text{keV})$	101.7	110.6	84.6	94.3
$E_{\text{plug}}(\text{keV})$	258.0	251.8	244.5	242.2
$E_{\text{inj}}(\text{keV})$	200.0	200.0	200.0	200.0
$P_{\text{fus}}(\text{MW})$	500.0	500.0	2500.0	2500.0
$B_{p,vac}(\text{T})$	7.00	7.00	7.0	7.00
(T_c/ϕ_c)	5.906	18.585	2.681	4.404
$B_{cc,vac}(\text{T})$	1.75	2.33	1.75	2.33
$\phi_c(\text{keV})$	17.22	5.951	31.56	21.41
β_p	0.20	0.20	0.50	0.50
$n_p(\text{cm}^{-3})$	9.5777E13	9.8363E13	2.5377E14	2.5642E14
β_{cc}	0.80	0.80	0.80	0.80
$n_c(\text{cm}^{-3})$	4.3625E13	7.3887E13	5.1122E13	8.4571E13

*Note: First wall is situated 3 (3.52 MeV) alpha particle gyroradii away from plasma.

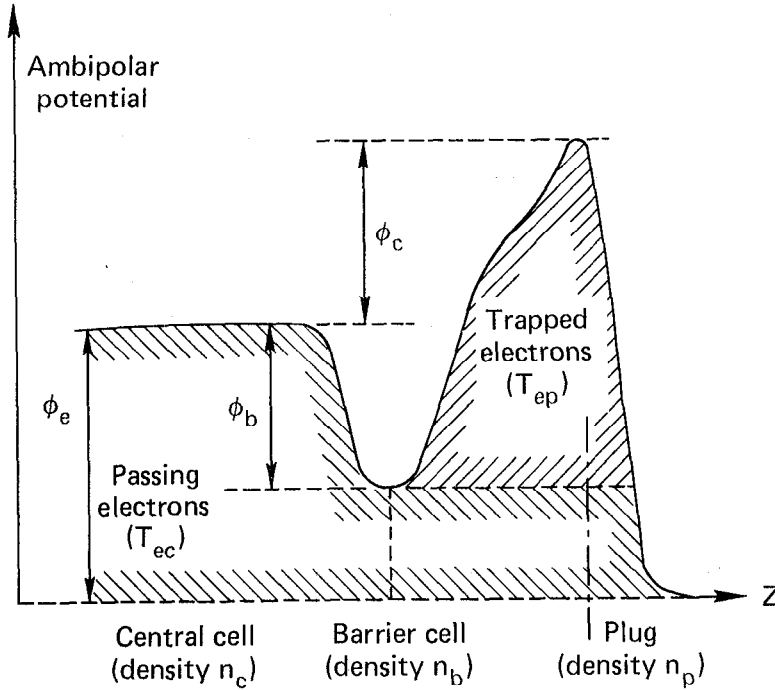


Fig. 3-19. Insulation of the plug electrons from the central cell electrons by means of a potential drop between the plug and the central cell.

which reduces to Eq. (3) if $\phi_b = 0$ and $T_e \equiv T_{ec} = T_{ep}$. We note that it is now possible to achieve $\phi_c > 0$, even if $n_p < n_c$. Since the expression for the Pastukhov confinement of central-cell ions may be written as

$$(n\tau)_c \approx T_c^{3/2} \left(\frac{\phi_c}{T_c} \right) \exp \left(\frac{\phi_c}{T_c} \right). \quad (28)$$

We may combine this with Eq. (27) to get

$$(n\tau)_c \approx T_c^{3/2} \left\{ \ln \left[\left(\frac{n_p}{n_c} \right)^{(T_{ep}/T_c)} \right] + \left(\frac{T_{ep}}{T_{ec}} - 1 \right) \frac{\phi_b}{T_c} \right\} \left(\frac{n_p}{n_c} \right)^{(T_{ep}/T_c)} \times \exp \left[\left(\frac{T_{ep}}{T_{ec}} - 1 \right) \frac{\phi_b}{T_c} \right] \quad (29)$$

It is instructive to briefly trace the evolution of the tandem mirror concept through the limiting forms of this equation.

The first tandem mirror experiment and reactor design studies had $T_e \equiv T_{ec} = T_{ep}$ and, of course, no barrier cell ($\phi_b = 0$). Under these circumstances Eq. (29) becomes:

$$(\pi\tau)_c \approx T_c^{3/2} \ln \left[\left(\frac{n_p}{n_c} \right)^{(T_e/T_c)} \right] \left(\frac{n_p}{n_c} \right)^{(T_e/T_c)} \quad (30)$$

A high T_e/T_c ratio has always been desirable, but limited by energetics considerations. Increasing (n_p/n_c) was the only way to control $(\pi\tau)_c$, but the required plug injection power increased as n_p^2 . This limited the first tandem mirror reactor designs to Q values of about 5.

Applying ECRH in the central cell, as presented in the Thermal Fusion Mode of Operation subsection, made it possible to increase the upper limit on (T_e/T_c) , and improved operation and/or lower plug technology demands. Since the ECRH is supplied to the central cell, which has a longer volume than the plugs, we are still justified in taking $T_{ep} = T_{ec}$.

Tandem mirror reactors in which ECRH is applied to the plugs were studied at LLL in early 1979. The thermal conductivity between trapped and passing electrons is large, but even without a barrier cell it is not infinite; so if all the ECRH is applied to the relatively small plug volume, we can get T_{ep} significantly greater than T_{ec} . In these studies ϕ_b was still zero, so Eq. (29) reduced to:

$$(\pi\tau)_c \approx T_c^{3/2} \ln \left(\frac{n_p}{n_c} \right)^{(T_{ep}/T_c)} \left(\frac{n_p}{n_c} \right)^{(T_{ep}/T_c)} \quad (31)$$

This looks identical to Eq. (30), but now, since T_{ec} and T_{ep} are decoupled, the upper bound on (T_{ep}/T_c) in Eq. (31) may be much higher than that on (T_e/T_c) in Eq. (30); this is true even if central-cell ECRH is considered in the latter case. Though tandem mirrors with plug ECRH were the most successful "pre-barrier cell" tandem concept, they necessitated high ECRH technology because of the high magnetic fields in the plugs.

From Eq. (29) we can see the obvious benefits of the barrier cell. The central cell ion confinement increases faster than exponentially with ϕ_b , and barrier cell tandem mirrors may have ignited central cells. Furthermore, we see that it is no longer necessary to have (n_p/n_c) greater than unity. Thus the plug density and magnetic field may be lowered so that high ECRH technology is no longer necessary to heat the plug electrons to $T_{ep} \gg T_{ec}$.

The potential barrier ϕ_b , which makes all of this work, is due to the fact that the magnetic field at the barrier midplane is lower than that of the central cell; although the field at the barrier mirror is much greater in order to achieve a high barrier mirror ratio R_b . The density of ions passing through the barrier is then

$$n_{\text{pass}} \approx \frac{n_c}{R_b} \left(\frac{T_c}{\pi\phi_b + T_c} \right)^{1/2} . \quad (32)$$

Now $n_b = n_{\text{pass}} + n_{\text{trap}}$, where n_{trap} is the density of ions that becomes trapped in the barrier due to the potential depression there. We define

$$g_b \equiv \frac{n_b}{n_{\text{pass}}} = 1 + \frac{n_{\text{trap}}}{n_{\text{pass}}} , \quad (33)$$

so Eqs. (30), (31) and (32) may be combined to eliminate n_c and n_{pass} to give:

$$\frac{\phi_b}{T_c} = \frac{T_{ec}}{T_c} \ln \left[\frac{R_b}{g_b} \sqrt{1 + \pi \frac{\phi_b}{T_c}} \right] \quad (34)$$

which may be solved numerically for ϕ_b . It is clear that if g_b becomes too large, the barrier potential disappears. Unfortunately, the natural accumulation of trapped ions in the barrier potential well reduces ϕ_b to zero on a time scale of a few tenths of a second unless some artificial means of pumping trapped ions out of the barrier is used.

Several pumping schemes are proposed. The most promising scheme is the injection of neutral beams into the barrier cell at an angle inside its loss cone. Charge exchange between trapped ions and the beam serves to replace each trapped ion with a passing ion; furthermore, those neutrals in the beam that are ionized may provide efficient fuel for the central cell. We think that several such beams will probably be used at different potentials as a sort of "multistage pumping" scheme; the details of this design are currently being worked out for the ongoing fusion reactor study.

In summary, the barrier cell concept greatly enhances performance and reduces technology, although it introduces new physics uncertainties (such as the rate of trapping of ions in the barrier cell, etc.) to which performance may be sensitive. It seems, however, that even under pessimistic physics assumptions the barrier cell's potential assets are intriguing enough to steer the course of future studies.

FUTURE WORK

Very few of the ideas described in the previous subsections have been tested in a single device, although most have been verified in different types of experiments. For reference purposes we collected a list of the tandem concepts and experiments currently under study in Table 3-2. Not listed in this table is the new idea for heating plug electrons to enhance the confining potential and a scheme for pumping of ions between the solenoid and plugs to insulate plug and central-cell electrons.¹⁴ Plans for MFTF-B include incorporation of this technique; it will probably be tried initially on TMX.

Table 3-2. Current and planned tandem mirror experiments and concepts to be tested.

Device/location	Concept	Date of tests
TMX/LLL	Electrostatic confinement. MHD stability of solenoid. Stream-stabilized plugs.	1979
	Plug stability scaling with r_p/a_i . Further MHD studies. Radial transport. Influence of impurities.	1980
	Two-component operation. ECRH.	1981
Gamma 6/Nagoya	Same as TMX in 1979.	1978-1979
Beta II/LLL	e-beam stabilization of plug against DCLC.	1980
MFTF/LLL	Plug-stability scaling with r_p/a_i . Alfven Ion-Cyclotron stability. Two-component operation. ECRH.	Mid 1980's

REFERENCES

1. R. S. Devoto and D. J. Bender, Nucl. Fusion 19, 1151 (1979).
2. G. I. Dimov, V. V. Zukaidakov and M. E. Kishinevskii, Sov. J. Plasma Phys. 2, 326 (1976).
3. T. K. Fowler and B. G. Logan, Comm. Plasma Phys. Cont. Fusion 2, 167 (1977).
4. G. G. Kelley, Plasma Phys. 9, 503 (1967).
5. TMR report, UCRL-52302.
6. L. S. Hall, Phys. Fluids 15, 882 (1972).
7. T. Kaiser, LLL UCID 18181 (1979).
8. B. Johnston, private communication (1979).
9. J. Myall, private communication (1979).
10. J. P. Freidberg and L. D. Pearlstein, Phys. Fluids 21, 1207 (1978).
11. D. E. Baldwin, et al., UCRL-80636 (1978).
12. D. Correll, et al., private communication (1978).
13. D. E. Baldwin, et al., UCID-17038 (1976).
14. D. E. Baldwin, et. al., UCID-18156 (1979).
15. L. D. Pearlstein, private communication (1978).
16. J. A. Nelder and R. Mead, Comput. J. 7, 308 (1965).
17. R. S. Devoto, LLL Report (in preparation).
18. R. H. Cohen, et al., Nuc. Fusion 18, 1229 (1978).
19. W. Heckrotte, et al., UCRL-75953, Rev. 1, (1974).
20. B. G. Logan and M. Rensink, private communication (1978).

SECTION 4
FUSION SYSTEMS DESIGN

NEUTRAL BEAM INJECTORS

(J. L. Erickson)

NEUTRAL BEAM REQUIREMENTS

The end plug design for the Tandem Mirror Hybrid Reactor (TMHR) is based on the Th/U, He-cooled base case. The total injected power for this case is 673 MW, which includes electron/cyclotron resonance heating, end plug neutral beam injection, and A-cell neutral beam injection, as outlined in Table 4-1.

Two neutral beam injector designs are used for TMHR. They are identical, except for physical dimensions and injected current; i.e., both the plug and A-cell injectors produce 400 keV D^0 beams using the same components. D^0 is produced by stripping a D^- beam, which is produced by double-charge exchange on a D^+ beam.

This injector is detailed elsewhere from a development standpoint¹ and an engineering design standpoint.² Figure 4-1 illustrates the injectors used in the TMHR plugs. Each of the four parallel beamlines produces 15 A of neutral beam. The A-cell injectors differ only in size, as shown in Fig. 4-2. These injectors inject 24 A of D^0 using three parallel beamlines, each producing 8 A.

INJECTOR DESCRIPTION

The end plug and A-cell injectors differ only in size. This description of the beamline elements applies to either injector. Positive deuterium(D^+) ions are produced in a continuously operating bucket-type source. A beam of D^+ is extracted at 1 - 1.5 keV through extraction grids of 50% transparency. This low energy D^+ beam then enters the first of two metal vapor cells in each beamline. The double-charge exchange cell converts an optimum of 20% (cesium vapor) of the D^+ ions to D^- . The D^- beam then enters the acceleration column to be brought up to 400 keV. The 400 keV D^- beam enters the second metal vapor cell, where an optimum of 60% (cesium) is stripped to form the neutral beam (D^0) at 400 keV. The resulting beam is injected into the

Table 4-1. TMHR injection requirements.

Item	Be/molten salt (case 1)	Th/U/He* (case 2)
Fusion power output, MW	2857	1333
Injected power, MW	1467	673
Q (ignoring A-cell requirements)	2.12	2.23
ECRH } heating plug NB } fraction	2.978	3.544
Total ECRH, MW	1012	466
Total plug NB at 0.4 MeV	842A	329A
Total NB injectors per plug	4	3
D ⁰ current per plug injector	105A	55A
Total A-cell NB at 0.4 MeV	298A	94A
Total injectors per A-cell	3	2
D ⁰ current per A-cell injector	50A	24A

* Parameters used in present plug design

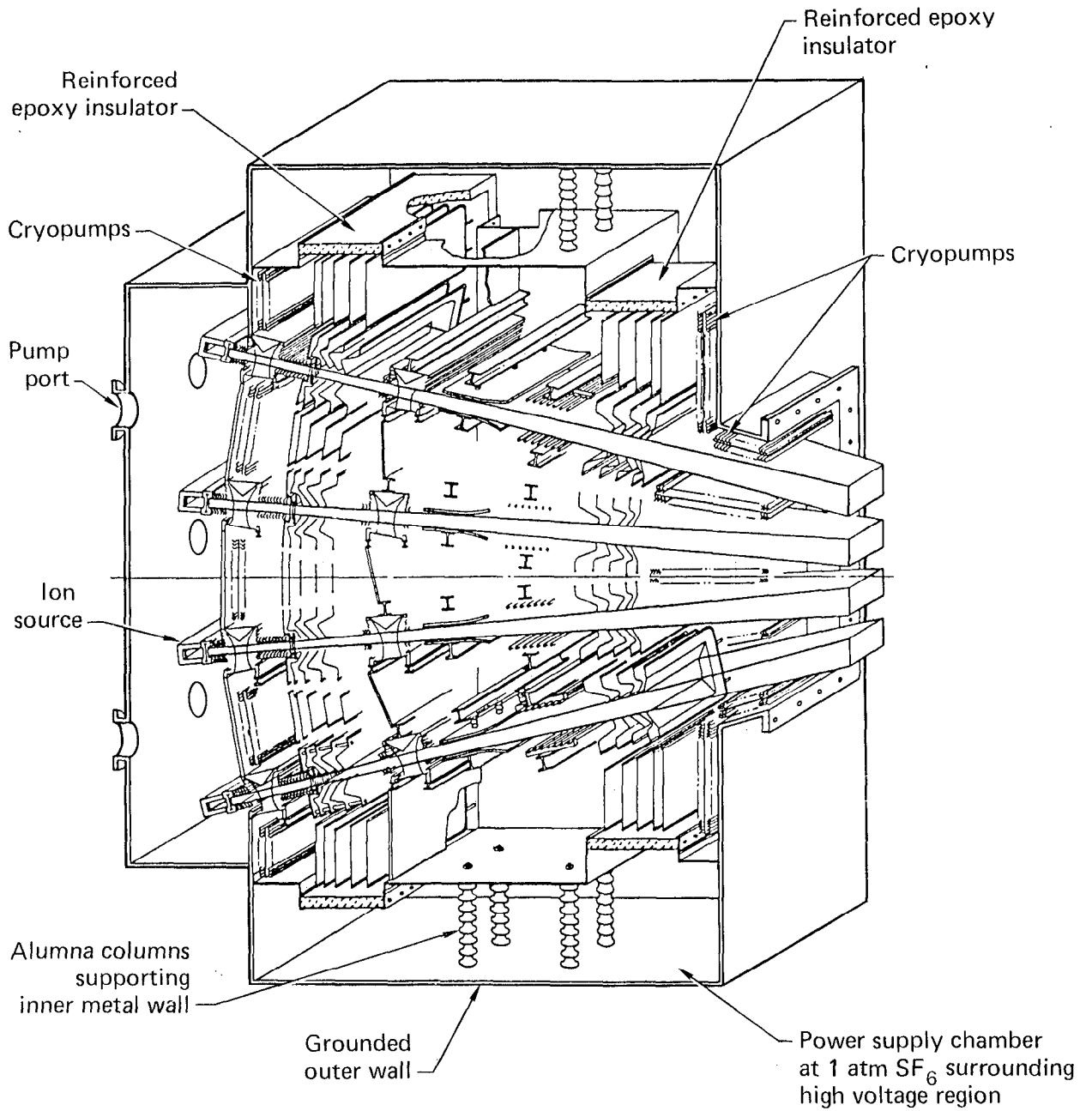


Fig. 4-1. TMHR neutral beam injector design (24 MW).

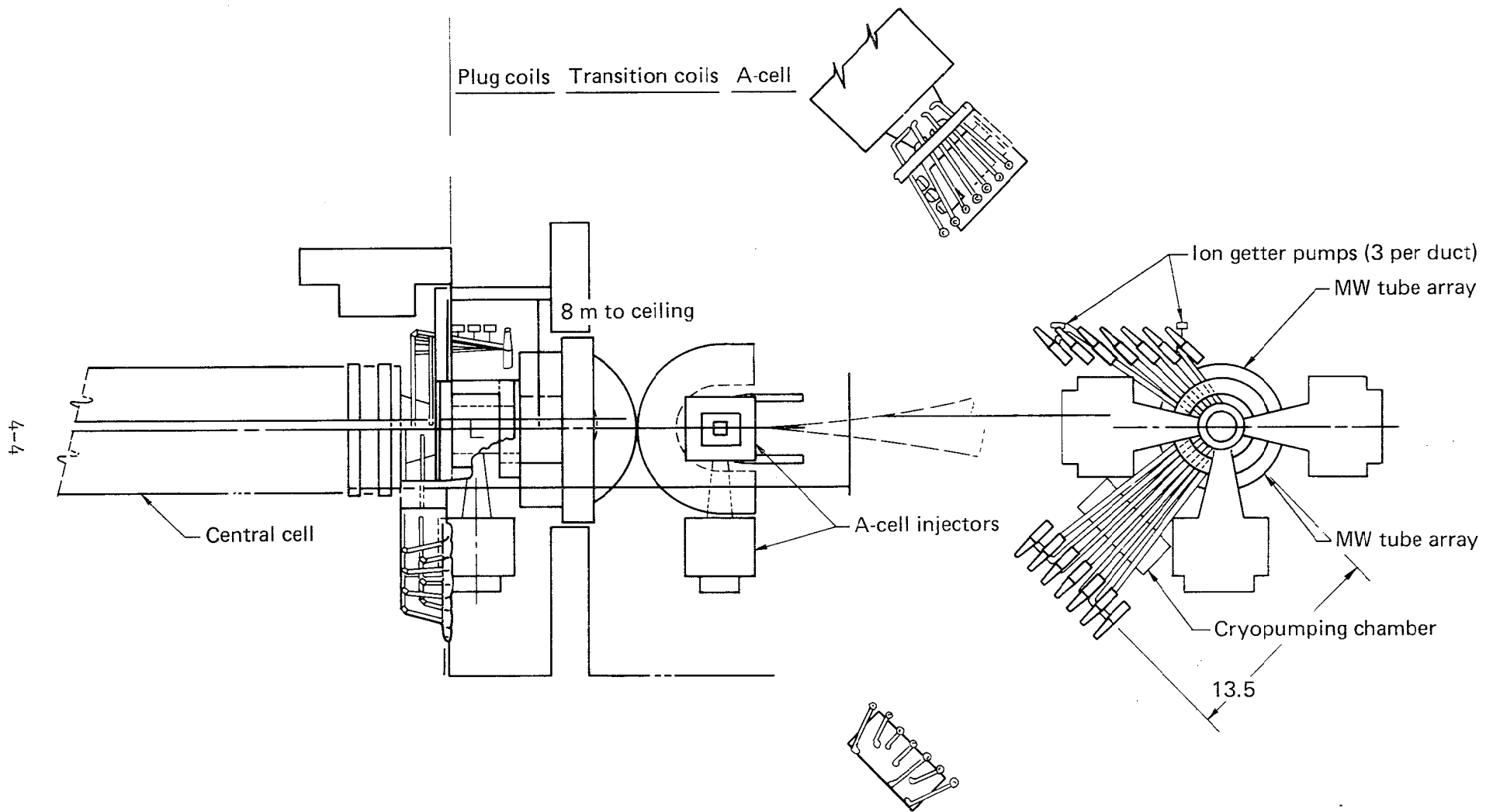


Fig. 4-2. TMHR end plug configuration.

reactor through a drift duct maintained at low pressure of 10^{-5} Torr to limit reionization. Unneutralized ions emerging from the stripping cell are deflected onto beam dumps from which energy is thermally recovered.

The stripping cells, residual ion deflectors, and ion pumps are located in a large region of the injector maintained at 400 kV. Electrostatic shields grade the voltage to ground up and down the beamline. A chamber of sulfur hexafluoride (SF_6) at 1 atm surrounds the high voltage region. Power supplies are located in the SF_6 . The electrostatic shields are supported and powered by rods passing through insulating epoxy walls and into the SF_6 chamber.

DEVELOPMENT REQUIREMENTS

Construction and reliable operation of neutral beam injectors, such as those for the TMHR plugs and A-cells, require a long list of development activities. The high energy level involved and the requirement for continuous operation are the most important reasons for this. Five of these necessary developments have been highlighted by previous work:¹

- A continuously operating low voltage source of positive ions with a high atomic fraction.
- A continuously operating metal vapor cell that can virtually eliminate metal vapor loss.
- A three-dimensional computer code to predict particle paths (a result of CW operation at high power).
- Reliable high voltage insulators obtained by using a coating to bleed charges from the surface.
- Methods for preventing damage from occasional arcs in the system, such as reducing stored energy and using arc suppressors (snubbers).

These injectors are not unique in this list of development requirements. The positive ion-based pulsed machines used today are already pressing the technology in directions that will greatly simplify the design of high voltage negative ion beamlines.

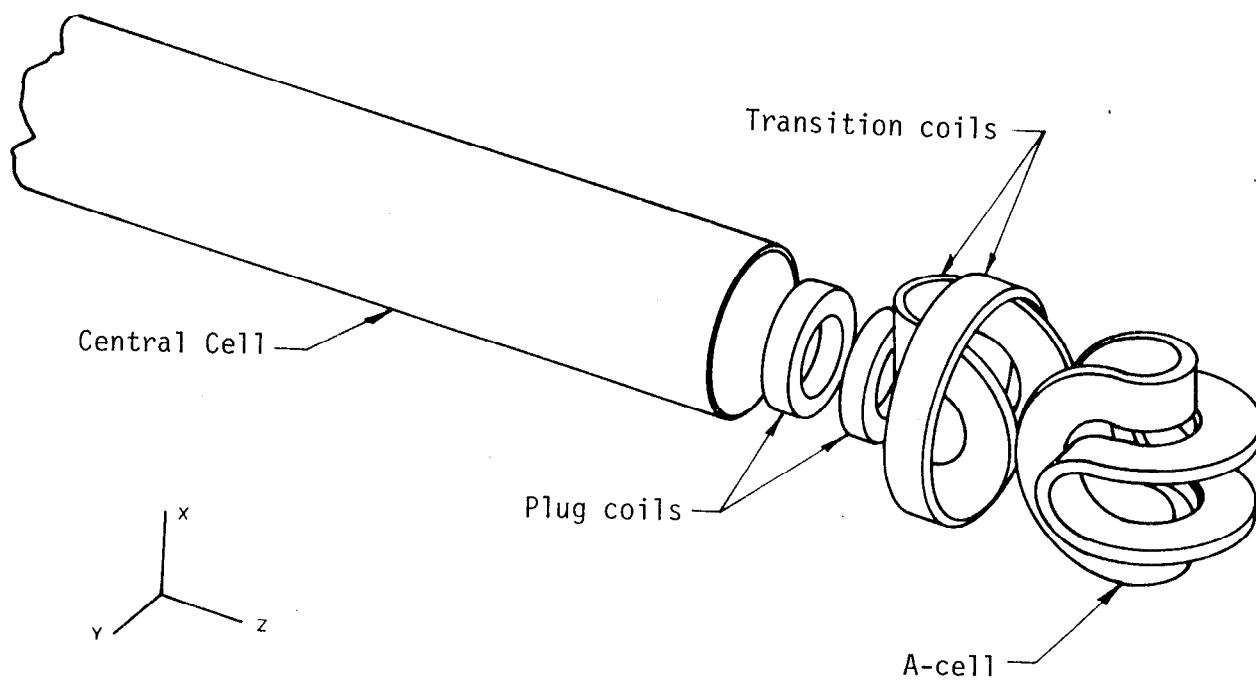


Fig. 4-3. Magnet arrangement for the 2500-MW hybrid reactor.

The A-cell is an auxiliary plasma cell that reduces the outward potential drop of the plug plasma, improving plasma confinement. Plasma within the central cell and plug is circular; if it entered the A-cell yin yang directly, it would distort to an elongated, elliptical shape. The transition coil elongates the plasma in the opposite (perpendicular) direction, opposing the subsequent effect of the yin yang and enabling the plasma to return to an approximately circular section at the center.

We designed the magnets using the Electromagnetic Field, Force, and Inductance (EFFI) computer code,⁴ which gives the peak field values indicated in Fig. 4-4. Also shown is the variation in field magnitude on the machine axis. The design is preliminary in that conductor fields have not been reduced to their optimum values.

An advantage of the chosen arrangement is that the highest on-axis field, the plug field, is produced by circular coils. With further refinement of the design, we could limit the maximum conductor field of these coils to 14 T. The lower coil efficiency typical of yin yangs would result in a maximum field of

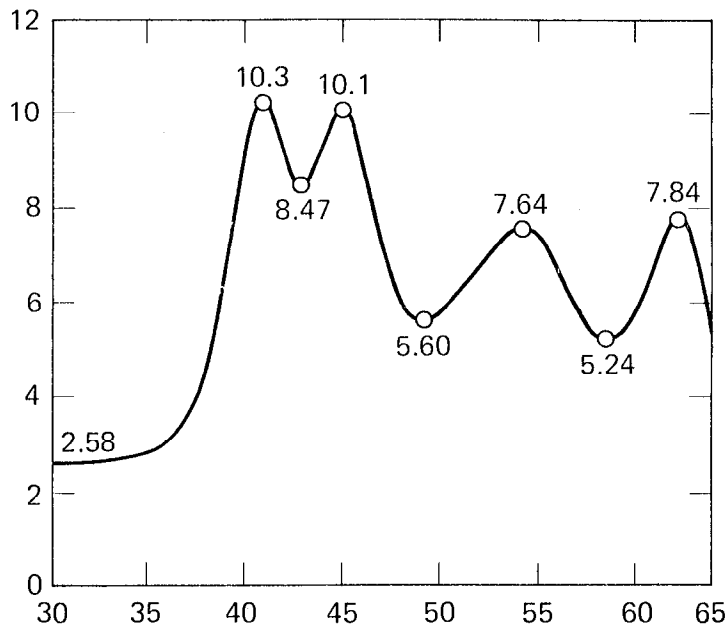


Fig. 4-4. Hybrid-field magnitude $|B|$ on machine axis.

about 17 T for the same on-axis field. The use of simple mirror plugs is permissible in this design, if the minimum-B A-cells provide MHD stabilization for the entire tandem mirror system. Although the plasma pressure is lower in the A-cell than in the plug (bad for stability), the radial well depth or "good curvature" is large. Stability calculations have not yet been performed, but will be a significant factor in later designs.

Future work will probably involve a change to the thermal barrier concept. The magnet arrangement will be very similar to that shown in Fig. 4-3, except that the two plug solenoids will be replaced by a single, high-field barrier solenoid and the A-cell will become the plug.

CENTRAL CELL

Figure 4-3 shows the central-cell magnet represented as a continuous solenoid of 75.4 m, and has discrete short solenoids occupying about 30% of the total cylindrical surface. The inside radius of this magnet model is 4 m, and the centerline field is 2.52 T.

PLUG COILS

The plug coil pair is required to have a field on center of 8.4 T and a vacuum mirror ratio of 1.2; the mirror field is thus 10.1 T. Each coil is a solenoid with an inside radius of 2.10 m, a radial thickness of 1 m, and a length of 1.38 m. The spacing between the coil centers is 4.2 m. The current densities are 25 MA/m^2 for the inner coil and 18.3 MA/m^2 for the outer coil; the difference is due to the close proximity of the transition coil, which contributes significantly to the field at the outer mirror point.

For this preliminary design, the maximum conductor field is 16.3 T and occurs at the inside surface of the inner coil. This could easily be reduced to less than 14 T by modifying the proportions of the coils; i.e., by approximately doubling the length and halving the radial thickness of each coil (also adjusting the spacing between them). Niobium-tin superconductor would be required in the high field portions of the coils.

TRANSITION COILS

The plasma within the central cell and plug is circular in cross section; the function of the transition coil is to distort the plasma to an elongated shape, so that the similar effect in the A-cell yin yang is cancelled, and the plasma returns to a circular section at the center of the A-cell. The transition coil is a full 180° c-coil with the following dimensions:

- Major arc mean radius: 3.80 m
- Minor arc mean radius: 2.57 m
- Cross section: 2.80 x 0.40 m
- Current density: 25.0 MA/m^2

The large minor arc radius is required because the coil overlaps the A-cell yin yang. Maximum conductor field in the c-coil is about 13.5 T.

A requirement of the A-cell concept is that the field on centerline in the region between the plug and the A-cell must be greater than that in the A-cell (see Fig. 4-4). A simple solenoid coil is therefore provided surrounding the center of the transition c-coil. The coil dimensions are:

- Inside radius: 5.53 m
- Radial thickness: 0.22 m
- Length: 2.00 m
- Current density: 25.0 MA/m²

Niobium-tin conductor would be required.

A-CELL

The A-cell is required to have a central field of 5.25 T and a mirror field of 7.9 T (hence, a vacuum mirror ratio of 1.5). It must also have a radial magnetic well. The latter requirement together with the need for MHD stability dictate the choice of full 180° yin yang.

Each half of the yin yang consists of three layers of equal thickness, separated in the minor arc portion of the coils. The separation is to reduce the average current density and thereby the magnitude of the field within the conductor (the maximum normally occurs on the inside of the minor arc). The conductor section is relatively deep and narrow for the same reason. We calculated a maximum conductor field of 13.7 T, giving a magnetic efficiency of 58%. Further refinement of the design (by using still deeper and narrower sections and further separating the minor arcs) should permit the maximum conductor field to be reduced to 12 T or less. Niobium-tin semiconductor will be used. The coil dimensions are:

- Mean radius of major arc: 4.0 m
- Mean radii of minor arcs: 1.80 m, 2.02 m, and 2.24 m
- Depth of conductor section: 2.5 m
- Thickness of conductor section:
 - Inner half of yin yang: 3 layers of 0.13 m
 - Outer half of yin yang: 3 layers of 0.22 m

The center and outer layers have short, straight sections between the major and minor arcs to give the required 0.07-m separation between layers.

The current density is 25.0 MA/m² for each half of the yin yang.

COMPARISON WITH MFTFB

MFTFB utilizes the thermal barrier concept that was previously mentioned as a probable configuration for future hybrid designs. Because of this difference in concept, the two machines cannot be directly compared. However, similar magnet types are used for the two cases, although they perform different functions. So, the A-cell for the hybrid and the plug for the MFTFB use yin yang coil sets and are compared in Table 4-2.

Table 4-2. Comparison of hybrid with MFTFB.

Item	Hybrid	MFTFB
Mirror field, T	7.9	4.0
Well field, T	5.25	2.0
Mirror ratio	1.5	2.0
Mirror-to-mirror length, m (one yin yang)	7.8	3.6
Overall length between centers of two yin yangs, m	117.0	40.0
Major arc radius, m	4.0	2.5
Minor arc radii, m (hybrid has 3 layers)	1.80, 2.02, 2.24	0.75
Major radius, half-angle	90°	75°
Conductor cross-sectional area, m ² (yin yangs have different thickness)	0.975 and 1.650	0.27
Current density, MA/m ²	25	26.5 and 29.8
Conductor volume, m ³ (one full yin yang)	102.7	9.62

DIRECT CONVERTER - MECHANICAL CONSIDERATIONS

(W. S. Neef, Jr.)

INTRODUCTION

We have spent a short time on the mechanical design of direct converters for the TMHR. A magnet design for the end plugs had to be completed first, so we defined the flux line geometry. Also, a new physics concept evolved for the tandem mirror plugs, which strongly influenced the direct converter. The new barrier cell provides ambipolar potential adjustments that allow all ions to escape at one end of the machine and all electrons to escape to a dump at the other end. This electron dump, since it can be completely opaque, has sufficient area to be easily cooled convectively. The power flux into the ion direct converter can be $200 \text{ W} \cdot \text{cm}^{-2}$ or higher. If electrons are present, the cooling problem of the electron ground grid limits acceptable power density to about $100 \text{ W} \cdot \text{cm}^{-2}$. A much more compact and economical direct converter structure should be possible than previously presented. It is the detail of that design we intend to pursue in the continuation of this work.

END TANK GEOMETRY

The flux plot from the end plug magnet set is plotted in Fig. 4-5. Due to the high mirror ratio of the yin yang plug coils, the ellipticity of the flux bundle is quite large. At the mirror plane near the mouth of the outboard coil, the aspect ratio is 18:1. It is easily seen that a large, flat, fan-shaped vacuum tank is necessary to enclose such a field line pattern. The cost of such a vacuum structure is very high and a secondary containment structure, either integrated with the vacuum tank structural needs, or as a separate unit, requires expenditures out of proportion to the rest of the plant cost. The reason for the cost penalty is that this vacuum tank can have no internal supports. Such internal structure would intercept ions, drastically reducing the efficiency of the direct converter and presenting very complex structural cooling problems.

A second objection to the fan-shaped flux bundle is the requirement that the two exit fans be oriented at 90° (i.e., twisted about the solenoid axis). This perpendicularity is necessary to maintain MHD stability of the entire

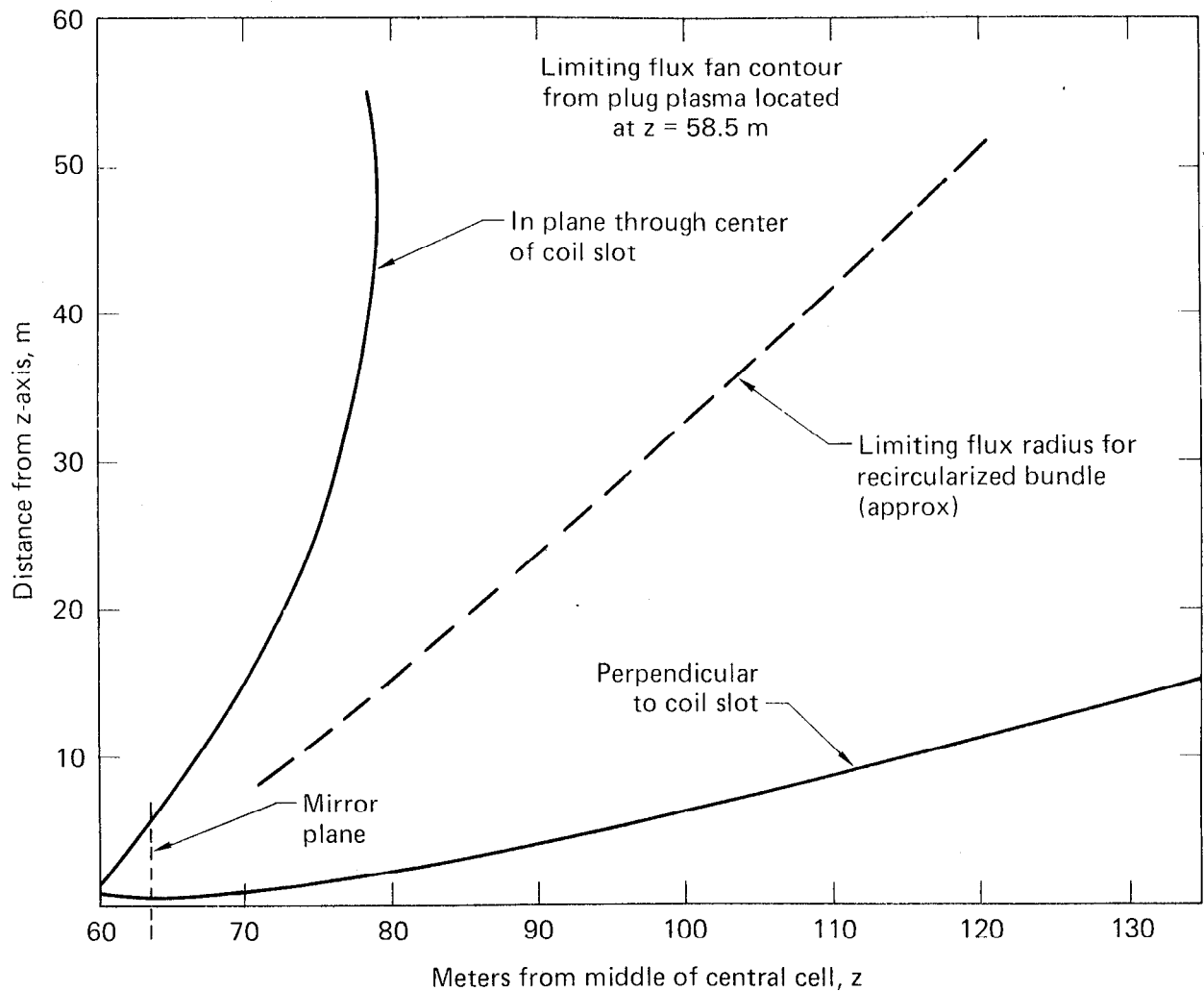


Fig. 4-5. TMHR yin yang plug flux fan.

plasma system. The cost of a fan-shaped vacuum structure and secondary containment of this size whose major dimensions are vertical will present an enormous cost penalty.

Our new design circumvents these problems by adding--at one end of the machine only--a circularizing magnet. This coil can be nearly identical to the transition coil, whose purpose is reshaping the inboard flux fan to form the circular flux bundle required by the central cell. This additional C magnet recircularizes the outboard flux fan from the yin yang plug coil set and permits the direct converter tank to be cylindrical and the direct converter

collector array to be circular. This affords a much more economical vacuum vessel to manufacture and house in a containment shell.

The power of escaping ions in the thorium-U₂₃₃ reactor is 1919 MW, requiring an ion collector array 35 m in diam if the average power density is $200 \text{ W} \cdot \text{cm}^{-2}$. (Or, if $300 \text{ W} \cdot \text{cm}^{-2}$ proves feasible, only 28.5 m in diam.) Containment vessels for systems of this diameter are common in the fission power industry; however, with vertical axis of symmetry.

A much smaller power dump is required at the other end of the machine. The electron energy is only about 15% that of the ions. Since an opaque-cooled plate can serve as a collector instead of transparent grid wires, the power density can approach $1000 \text{ W} \cdot \text{cm}^{-2}$. This converts to a dump area requirement of less than 30 m^2 . An elliptical plate less than 10 m beyond the yin yang mirror plane can perform this function. The plate would be about 20 m on its long axis and 2 m across. Helium flow in pipes parallel to the plate's short dimension can cool such an energy dump at a high enough temperature to be useful in the main thermal cycle for electricity generation. Since internal bracing members would be permitted if they are cooled, the design and manufacture of that small flat vessel would be relatively simple and inexpensive.

VACUUM PUMPING

Again considering the molten salt reactor because its injected power is largest, we calculate that particle injection amounts to $162 \text{ Torr} \cdot \text{s}^{-1}$. We assume the pumping speed for a well-baffled cryopanel is $4 \text{ l} \cdot \text{s}^{-1} \text{ cm}^{-2}$ (in an isolated location so it can be easily valved off for periodic degassing). The active pumping area required is 811 m^2 . Some fraction of the pump surface will be inactive, being degassed, at any given moment. Assume that fraction is 1/2. We then require about 1600 m^2 of vacuum tank surface dedicated to the cryopanel. Their present design is such that only about half the assembly area is actually cryosurface--but both sides of the surface pump.

The perimeter of the tank is 110 m at one end of the machine. If the panels form a cylindrical array 15 m long and 36 m in diam, the required area will be provided. The vacuum tank will be slightly over 15 m long as controlled by the path of the outer flux lines from the recircularized bundle (see Fig. 4-6). No cryopanel can be on the end of the tank--at least not near its center--due to heating of the cryosurfaces by neutrons beaming from the plasma.

The electron dump in the other end tank necessitates a much smaller end tank. Probably not over 10% of the total cryopump area can be located in that tank.

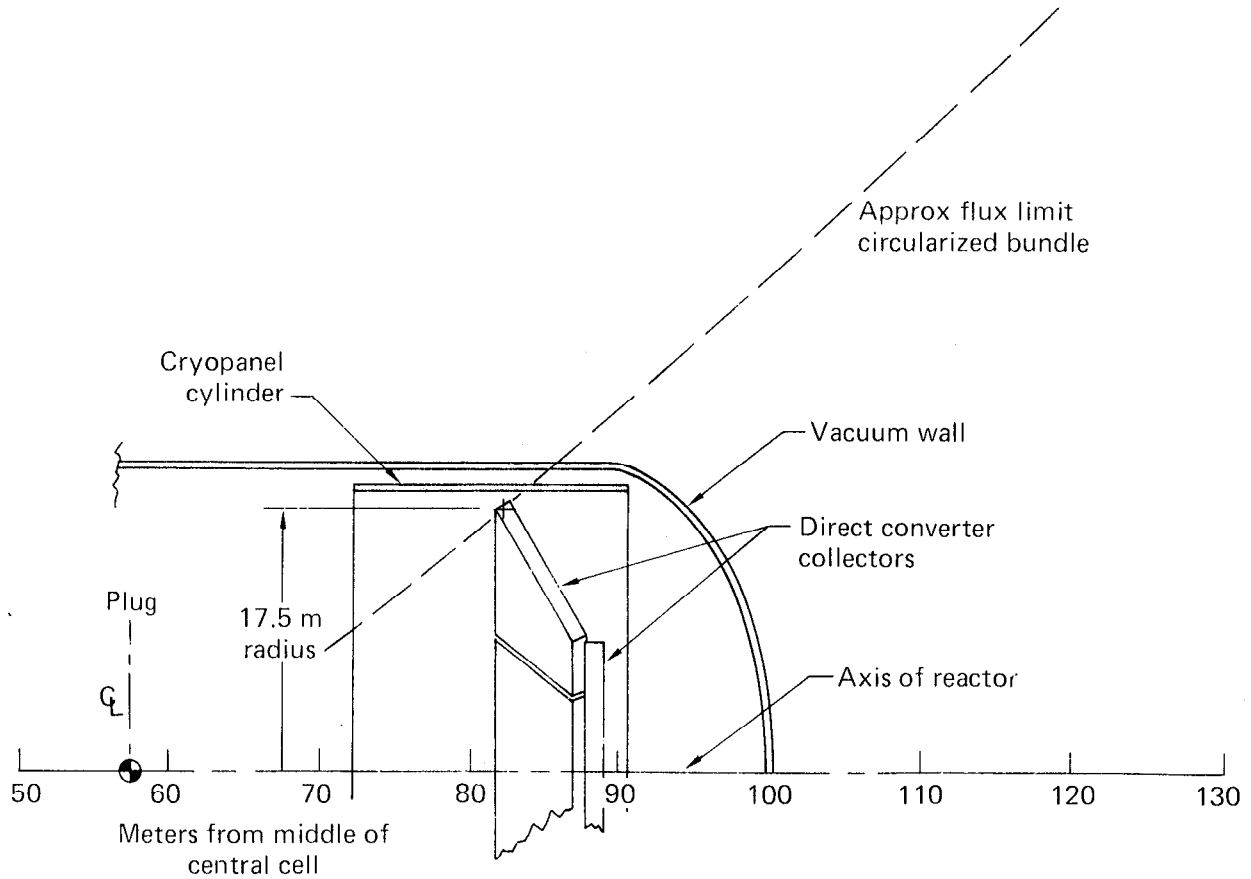


Fig. 4-6. TMHR cryopump panel location.

REFERENCES

1. Fink, Hamilton, Erickson, "A 24 MW Neutral Beam Injector of 400 keV H⁰ for the End Plugs of a Tandem Mirror Reactor," Eng. Probs. in S.F. (Nov. 1979).
2. Carlson et al., "Tandem Mirror Reactor with Thermal Barrier," UCRL-52836 (1979).
3. V. V. Alikaev et al., "Gyrotrons for the Electron Cyclotron Plasma Heating in Large Tokamaks," presented at the Joint Varenna-Grenoble Int'l Symposium on Heating in Toroidal Plasmas, Grenoble, France (1978).
4. S. J. Sackett, "EFFI--A Code for Calculating the Electromagnetic Field, Force, and Inductance in Coil Systems of Arbitrary Geometry," Lawrence Livermore Laboratory, UCRL-52402 (1978).

SECTION 5

ALTERNATE BLANKET COOLANT STUDIES

INTRODUCTION

During the initial scoping phase of the Tandem Mirror Hybrid Reactor (TMHR) design study, we made a preliminary investigation of blanket concepts based on four reactor coolant technologies. Preconceptual designs were developed for several of these concepts. General Atomic Company investigated gas-cooled blanket designs. Bechtel National, Inc. studied liquid metal-cooled concepts. General Electric Company pursued water-cooled options, including pressurized water, boiling water and steam. Lawrence Livermore Laboratory developed molten salt-based blanket concepts. The results of these scoping studies and preconceptual designs are discussed at length in Ref. 1.

The results of the scoping phase evaluation are summarized in this section. On the basis of the preliminary scoping evaluations, we made choices to narrow the list of candidates for Phase two, the preliminary conceptual design of the TMHR. The thorium/uranium-233 fuel cycle was chosen. With this fuel cycle, the helium-cooled blanket option and the molten salt-based blanket designs appeared to be the most attractive and were selected to be studied further. Preliminary conceptual design work was performed on these TMHR blanket concepts; this is discussed in Sections 6 and 7 of this report.

HELIUM

The approach used in the scoping study evaluations was to take a broad look at the possible blanket options rather than focus closely on the technical details of any one option. The intent was to ensure that the wide variety of gas-cooled blanket options available was considered and that the choice of one concept for more detailed design and investigation was made on a rational and informed basis. This study is summarized here as it formed the basis for the helium-cooled designs developed during the second phase of the study discussed in Section 6 of this report.¹

Gas-cooled reactor technology has been pursued since the very early days of the nuclear program. It is one of two technologies (the other being water cooling) that has successfully been developed to commercial status. Gas cooling was originally pursued most vigorously in Europe with the development of the French and British CO₂-cooled, graphite-moderated, natural uranium-fueled MAGNOX reactors. These led to the CO₂-cooled Advanced Gas Reactor (AGR) program in Great Britain and the helium-cooled High Temperature Gas-Cooled Reactor (HTGR) programs in Britain, France, and Germany. A brief summary list of the world gas-cooled nuclear reactor technology programs is shown in Table 5-1.

In the U.S., interest in gas-cooled reactor technology is led by General Atomic Company with its helium-cooled HTGR and Gas-Cooled Fast Reactor (GCFR) development programs. General Atomic designed and built the 40-MW_e prototype Peach Bottom HTGR, which operated successfully for over 5 years on the Philadelphia Electric Company grid. General Atomic designed and built the 330-MW_e demonstration Fort St. Vrain HTGR, which is now in operation (70% derated) on the Public Service of Colorado grid.

A wide variety of gases has been proposed for use in gas-cooled reactors including CO₂, helium, dry steam, nitrogen, and nitrogen oxide. The technical aspects of gas-cooling are reviewed in Refs. 2 and 3, and the application of gas-cooled technology to fusion power systems is discussed in Refs. 4 and 5. Because of its high heat capacity, high sonic speed, and chemical inertness, helium has generally been the first choice of coolant for gas-cooled systems and will be used as a basis for the design of a gas-cooled blanket and power conversion system for the TMHR.

ADVANTAGES OF HELIUM

The principle advantages of helium cooling are summarized on Table 5-2. Helium is the most inert of all proposed coolants. It has very small nuclear interaction cross sections and at the densities found in reactor systems is virtually transparent to neutrons. This allows excellent neutron economy to be achieved, and helium-cooled reactors, as a consequence, have the highest fuel breeding performance capability.

TABLE 5-1. Gas-cooled reactor programs.

United Kingdom

MAGNOX:	CO ₂ /graphite/U metal/MgO 9 GW _e in operation
AGR:	CO ₂ /graphite/UO ₂ /steel 3 GWe in operation 6 GWe under construction

France

MAGNOX:	3 GWe in operation
HTGR:	\$20M/yr research & development

Germany

HTGR:	He/Graphite/U-ThO ₂ /PyC-SiC 15 GWe in operation 300 MWe under construction \$100M/yr research and development and design
-------	---

Japan

HTGR:	\$5M/yr research
-------	------------------

United States

HTGR:	230 MWe in operation \$50M/yr research and development and design
GCFR:	\$20M/yr research and development and design

<u>Total experience:</u>	550 reactor yr of operation
--------------------------	-----------------------------

TABLE 5-2. Advantages of helium-cooling.

- Helium is inert:
 - Chemically inert
 - Neutronically benign
 - No phase changes
 - Negligible gravity effects
 - Nonmagnetic
 - Nonconductive

 - Developed technology:
 - Heat transfer
 - Power conversion
 - Purification (including tritium recovery)

 - Maintenance advantages:
 - No activation
 - No isolation
 - Transparent
-

Helium is a noble gas and is chemically inert. Reactions with the fuel, cladding, and environment during both normal and accident conditions are not of concern. Because helium is a gas, no phase changes are possible; thus, the heat transfer regime is stable in both normal, pressurized operation, and in the event of depressurization. Because of this, a loss-of-coolant accident (LOCA) cannot occur for a gas-cooled system, although loss-of-coolant pressure and loss-of-coolant flow accidents are, of course, a possibility that must be protected against.

For magnetically-confined fusion systems the fact that helium is non-magnetic and nonconductive is of advantage. Even with a high level of impurities, helium will not support electromagnetic effects. Because of the low density of helium coolant, gravitational effects are quite small compared to normal flow forces. As a consequence, the heat transfer in a helium system is not greatly affected by gravitational orientation. This can allow

axisymmetric blanket designs that can be quite compact and can allow full coverage of the plasma chamber surface.

Because of the large world gas-cooled reactor program and commercial deployment, gas cooling enjoys a developed technology. The heat transfer and thermal-hydraulic correlations are understood and power conversion equipment (steam generators, circulators, etc.) is developed. Helium purification systems have been successfully developed and include the capability for tritium recovery from the helium stream.

Helium cooling has several advantages from a reactor maintenance point of view. It is transparent, so visual observation is possible. Since helium does not activate, only impurities are of concern with regard to coolant radioactivity. The helium circuits do not need to be isolated from ambient conditions during maintenance operations. Air can be allowed into the helium system ducting. Air could be used for residual heat removal during fuel changeout and transport operations, making use of the circulators and heat exchangers used for normal operation.

DISADVANTAGES OF HELIUM

The principle disadvantage of all gas coolants is their low volumetric heat capacity. To achieve adequate heat removal capacity with acceptable coolant pumping power requirements, pressures in the range of 40 to 80 atm appear to be needed. The heat transfer coefficient that may be obtained at reasonable flow velocities in a helium-cooled system is generally smaller than that found in liquid-cooled systems; hence, the temperature differential is larger, leading to higher fuel and clad temperatures.

Because of the compressible nature of helium, the power required to operate the helium circulator can be high. With the pressure drops encountered with steam cycle power conversion system, the pumping power is on the order of 2 to 5% of the reactor thermal power. Most of this power is returned to the helium as it is compressed, and by using steam driven circulators, the electrical conversion losses can be avoided.

Because of the low volumetric heat capacity of helium, natural convection cooling is difficult to achieve. Although natural convection can provide some shutdown afterheat cooling when the coolant loop is pressurized, it cannot be counted on in the depressurized state.

Despite the fact that gas-cooled reactor technology has been deployed commercially, experience is less extensive than that enjoyed by water-cooled technology, particularly in the U.S. A potential concern for helium-cooled systems in the mid 21st century is the possibility of resource limitation. Helium is presently extracted from natural gas, which will be in increasingly limited supply in the future. Helium can be extracted from the atmosphere but at higher cost. The helium produced in the fusion reactions of a fusion hybrid reactor would amount to about 1% of the power conversion system helium inventory each year.

GAS-COOLED BLANKET OPTIONS

Within the general category of helium-cooled hybrid blankets there is a number of further choices that must be made. The fuel cycle may be the uranium/plutonium cycle or the thorium/uranium cycle, or both may be used. The fuel structural material may be metal cladding (GCFR technology) or coated particles in graphite (HTGR technology). A set of nine helium-cooled blanket concepts was developed for consideration for the TMHR. This set is shown on Table 5-3 along with estimated blanket performance parameters (Table 5-4); each concept is discussed in the following paragraphs.

Uranium, Metal (U, M)

This blanket would be similar to that developed for the Standard Mirror Hybrid Reactor.⁶ It is a high performance, fast fission blanket that shows both a large energy multiplication and large plutonium production rate because of fast fission of the ^{238}U by fusion neutrons. Because of its high performance, we selected this blanket for further study.

Uranium, Graphite (U,G)

This concept was briefly investigated for the small tandem mirror reactor as part of the EPRI Small Reactor Study.⁷ Because of the low uranium content in this blanket, its energy production and fuel breeding performance is quite low. Because of this low performance, it was not pursued in any depth.

TABLE 5-3. Helium-cooled blanket concepts.

Concept	Fuel material	Structural material
Uranium, metal (U,M)	U ₃ Si	Stainless steel
Uranium, graphite (U,G)	UC ₂	Graphite
Uranium/thorium, metal (U/Th,M)	U ₃ Si Th	Stainless steel Stainless steel
Uranium/thorium, metal/graphite (U/Th,M/G)	U ₃ Si ThO ₂	Stainless steel Graphite
Uranium/thorium, graphite (U/Th,G)	UC ₂ ThO ₂	Graphite Graphite
Thorium, metal (Th,M)	Th	Stainless steel
Thorium, graphite (Th,G)	ThO ₂	Graphite
Beryllium/thorium, metal (Be/Th,M)	Be Th	Stainless steel Stainless steel
Beryllium/thorium, graphite (Be/Th,G)	Be ThO ₂	Stainless steel Graphite

Uranium/Thorium, Metal (U/Th,M)

This blanket was suggested by work of Maniscalco⁸ and was selected for the small TMHR in the EPRI Small Reactor Study.⁷ It was not pursued far in that study, as the field-reversed mirror concept appeared more attractive as a small reactor than the tandem. This concept combines the high energy production of a fast fission ²³⁸U zone with the desirable ²³³U bred fuel from the thorium zone. It combines excellent fuel production with moderate energy multiplication and was selected for further study.

Uranium/Thorium, Metal/Graphite (U,Th,M/G)

This blanket concept was developed in some detail for the Refresh Cycle Hybrid Reactor evaluation.⁹ Although that study showed that this concept is technically viable, its performance is modest and its design complicated. It was developed to meet the unusual requirement to provide fissile fuel for

burner reactors without allowing reprocessing because of concern about nuclear proliferation and diversion. The refresh cycle is not specifically of interest for this study. The (U/Th,M/G) blanket with reprocessing is inferior in performance to the (U/Th,M) option and was not pursued further.

Uranium/Thorium, Graphite (U/Th,G)

This concept was an attempt to obtain the advantages of using HTGR technology fuel (established technology, safety), while getting improved performance compared to the (U,G) or (Th,G) options. The attempt was unsuccessful, as the performance of this option is quite poor; consequently it was dropped.

Thorium, Metal (Th,M)

This blanket is the thorium cycle analog to the (U,M) fast spectrum blanket. It enjoys good fuel production performance with moderate energy multiplication.¹⁰ The lower fuel production rate of a thorium blanket compared to uranium is balanced by the higher value of ²³³U as a fuel for thermal spectrum burner reactors than plutonium.¹¹ This blanket is attractive for the TMHR because of its relatively high fuel production rate and because the TMHR can operate at a high enough Q_p value to not require a large blanket energy multiplication. This concept was kept for further evaluation.

Thorium, Graphite (Th,G)

This blanket would be a direct application of HTGR technology to the TMHR. Conventional HTGR fuel made of ThO₂ particles coated with pyrocarbon coatings loaded into graphite blocks would make up the blanket region. This fuel could be fabricated today in General Atomic's fuel fabrication facility in San Diego. It could be reprocessed and refabricated in HTGR recycle facilities that are expected to be available shortly after the year 2000. The low power density and large mass of graphite result in very slow heating due to fission product afterheat. Thus, this blanket would be quite tolerant of loss-of-coolant flow accidents, unlike the very high-power density, metal-clad uranium blanket options. The nuclear performance of this blanket, however, is

very poor. The net breeding rate of ^{233}U and tritium is only 0.8. A tritium breeding ratio of greater than 1 can only be obtained if 70% of the reactor length contains tritium breeding modules ($T/N = 1.5$ assumed), leaving 30% of the length available for (Th,G) modules for a net ^{233}U breeding rate of only 0.2. Because of this low performance, this option was modified by inclusion of a lead or beryllium zone for neutron multiplication through (n,2n) reactions.

Beryllium/Thorium, Metal (Be/Th,M)

This concept was an attempt to improve upon the breeding performance of the (Th,M) blanket by getting (n,2n) reactions in beryllium. The low blanket multiplication gives reduced concern about afterheat. Since the TMHR needs a higher blanket multiplication to break even on electrical power and since the (Th,M) blanket appears to be reasonably tolerant of loss-of-coolant flow, the (Be/Th,M) blanket does not exhibit any unique advantage and was dropped.

Beryllium/Thorium, Graphite (Be/Th,G)

This blanket concept grew out of interest in improved performance for the (Th,G) option with the desire to retain the use of present-day HTGR technology and a very low level of afterheat. This option was given further evaluation.

SCOPING STUDYING EVALUATIONS

On the basis of very simple performance estimates and system energy balance and economic evaluations, we narrowed the nine gas-cooled blanket options in Table 5-3 to four blanket candidates:

- A metal-clad uranium blanket.
- A metal-clad blanket with a uranium fast fission zone and a thorium breeding zone.
- A metal-clad thorium design.
- A graphite-base blanket using ThO_2 fuel (HTGR) technology and lead or beryllium for neutron multiplication by (n,2n) reactions.

We performed preliminary scoping studies on these four blanket options including consideration of the blanket mechanical design, thermal hydraulic aspects, fuel reprocessing concerns, and neutronic performance. The neutronic evaluation included consideration of the blanket fuel production, energy multiplication, materials damage effects, and fission product afterheat for safety and residual heat removal system evaluations. Using the results of these scoping calculations, the energy balance characteristics of tandem mirror hybrid reactors using these blanket concepts were compared. The relationship between blanket multiplication, plasma energy amplification (Q_p), and reactor energy handling efficiencies was explored. Finally, a simple system economics models were used to compare the four options.

The system electrical cost in mills/kWh for a system composed of a TMHR and the thermal burner reactors it could support was estimated. To get a more direct and distinct comparison between the four blanket options, we also made an estimate of the cost of the bred fuel as a function of the price of electricity. The results of these preliminary evaluations of the four blanket options are summarized in the following paragraphs, and some of the performance characteristics of these blankets are shown in Table 5-4.

Uranium, Metal Blanket

The uranium blanket is a high-performance, plutonium-producing design that also produces significant amounts of blanket thermal power similar to that developed for the standard Mirror Hybrid Reactor.⁵ Because of the large thermal output, the fuel production per unit thermal power is less (1.0 kg/yr per MW_t) than that of the thorium blanket (1.5 kg/yr per MW_t). This, plus the lower nuclear value of plutonium for thermal burner reactors compared to ^{233}U , results in a high fuel production cost when the price of electricity is low. With increasing electricity price the fuel cost falls rapidly, and for high electricity price can be quite low. Because of the large energy production, this blanket can be used with a low plasma amplification Q_p and low energy handling efficiencies and still attain net power production. The high blanket power results in a high level of blanket afterheat. If this afterheat is not removed from the blanket, the fuel will heat up quite quickly. Assuming no afterheat removal (adiabatic heating) after shutdown and that the reactor has operated for 1 yr at a wall load of 1 MW/m^2 , the heatup rate will result in fuel melting in approximately 1 min.

TABLE 5-4. Blanket characteristics.

Blanket	Uranium metal	Uranium/ thorium metal	Thorium metal	Beryllium/ ThO ₂ graphite	
Breeding ratio ^a (atoms/fusion neutron) (with T/n = 1.1)	Pu 233U	1.8 --	0.81	-- 0.74	-- 0.49
Energy multiplication ^a		10	5.6	2.6	1.6
Fuel production ^a (kg/MW _t -yr)	Pu 233U	0.97 --	0.78 0.75	-- 1.54	-- 1.65
Adiabatic time to melting		1 min	1 min	1.5 hr	26 hr
Approximate fuel lifetime (MW·yr/m ²)		6	9	9	2
Fuel cost ^b - (\$/gm) (at 15 mills/kWh electricity)		93	77	84	98

^aBeginning of blanket life values.

^bAdjusted for relative value of plutonium vs ²³³U, MHR efficiency set used, 15% capital charge rate.

This rapid thermal response will require use of a highly reliable, fast-acting residual heat removal system to prevent fuel damage.

Uranium/Thorium, Metal Blanket

The metal-clad uranium fission plate/thorium breeding zone design has many characteristics similar to those of the uranium blanket but enjoys the benefit of producing ^{233}U , which is a more valuable fuel for thermal burner reactors than is plutonium. It produces 0.8 kg of plutonium and 0.8 kg of ^{233}U per $\text{MW}_t\text{-yr}$. The uranium fast-fission zone has the same rapid thermal response time and sensitivity to loss of cooling as does the all-uranium blanket. The use of two blanket fertile materials will complicate reprocessing somewhat, with an approximate 20% reprocessing cost penalty.

Thorium, Metal Blanket

The metal-clad thorium blanket has sufficient energy production to be able to break even electrically with even low Q_p and low energy handling efficiencies. It produces only ^{233}U (at 1.5 kg/ $\text{MW}_t\text{-yr}$); thus, reprocessing is simpler than for the U/Th design. Because of the lower blanket power density and higher fuel melting temperature, the thorium blanket is much more tolerant of loss of cooling than are those containing uranium. With totally adiabatic heatup after plasma shutdown, fuel damage would not occur for over an hour, thus relaxing the requirements for residual heat removal safety systems.

Beryllium, ThO_2 , Graphite Blanket

The graphite-base Be/ ThO_2 is a relatively low performance design. Due to the small energy production, it requires fairly high energy handling efficiencies and a Q_p approaching 2 to be able to break even electrically. Because of the low energy production, the amount of fuel produced per unit thermal power is quite high (1.7 kg/ $\text{MW}_t\text{-yr}$). The low power density, high specific heat, and high allowable temperatures of this blanket make it quite tolerant of loss of cooling. Adiabatic heating for about 24 hr could be allowed before fuel damage would occur.

The cylindrical geometry of the tandem mirror plasma and solenoid coils lead naturally to a cylindrical module configuration. An axisymmetric cylinder gives the best nuclear and thermal/hydraulic design as well as a mechanical design that is structurally simple and compact. Because of the aspect ratio of the cylinder, a horizontal attitude was chosen, giving easy access and minimum building structure penalties.

Two components of the machine require regular service: the first wall and the blanket immediately behind it where fuel is bred. It was considered best to cut the long cylinder into modules to give access to the central regions of the reactor. The problem of breaking this high pressure shell and remaking it during reactor downtime has been dealt with by clamping the string of modules into a longitudinal frame incorporated into the prestressed concrete reactor vault. The clamping force is applied by inflatable all-metal cushions between the cylindrical modules. When pressure in the system is released, modules can be quickly changed. No welding or cutting is required to remove or replace the module. The module is removed to an offline hot shop for removal and replacement of its center. The spent module is quickly replaced with a fresh one so that the reactor can be put back online as quickly as possible. The time-consuming remote maintenance on the module thus does not impact plant availability.

This central area is to be made as a cartridge with its principal components the first wall and blanket. The cartridge is a self-contained pressure vessel, which enables it to be simply slid out from the reusable shield. This shield receives a new cartridge and is reinstalled at the next changeout.

The intermodular pressure exerted by the inflatable cushion is used to make the major online seal in the central vacuum chamber, using double-knife seals with interspace evacuation. The projected downtime for change of one module is 444 h, with an increment of 134 h for each additional module changed during the downtime.

Application of this cylindrical blanket module concept to the four blanket options was studied. It was determined that the concept is well-suited to all four and that the blanket material choice has little impact on this design concept. The metal-clad thorium blanket option appears especially well suited in that first wall life and best breeding times are of the same

order, and the afterheat level is relatively low. The low afterhead minimizes the ancilliary mechanical penalty and offers the possibility for design simplicity and potential safety advantages.

RECOMMENDATION

On the basis of the considerations discussed above, we chose the metal-clad thorium blanket as the gas-cooled blanket candidate for the TMHR. This choice offers the simplest design, good economics, and assured positive net electric power while being reasonably tolerant of loss of cooling. The approximate characteristics expected for this blanket are shown in Table 5-5, and the characteristics of a 4000 MW_t TMHR using this blanket are shown in Table 5-6.

It should be noted that the characteristics shown here are for the preliminary design as estimated during the initial scoping phase of this study.¹ The characteristics of the reference design presented in Section 6 of this report differ considerably from these original estimates.

With an assumed thermal power of 4000 MW_t, the TMHR is physically large and produces 930 MW_e. It could be described as a fuel factory in that it produces sufficient ²³³U to support 16 GW_e of LWR burner reactors or 35 GW_e of HTGRs. Because of the large power requirement of the neutral beam injectors (913 MW_e) needed to sustain the relatively low Q_p plasma, the net station efficiency is a modest 23%. The plasma energy from the mirror end plug leakage fans is recovered using direct converters and a bottoming steam cycle thermal power conversion system. If this leakage fan energy were not recovered, the TMHR could still produce enough electricity using just thermal conversion of the blanket thermal power to break even but would have a net electrical output of less than 50 MW_e.

The selection of the metal-clad thorium blanket for the leading TMHR gas-cooled blanket candidate should not be construed to indicate that the other three blanket options are not desirable. In fact, all four options appear to be attractive hybrid blanket alternatives, and all four show similar economic estimates of fuel cost and system electricity cost. The metal-clad thorium design selected, however, appears to offer a combination of attributes that is particularly attractive for the TMHR. It produces a large amount (~1.1 kg/MW_t·yr) of ²³³U, which is the most attractive fuel for thermal burner reactors and that could be denatured with ²³⁸U or possibly spiked

TABLE 5-5. Helium-cooled blanket characteristics.

Axisymmetric cylindrical module configuration.

Inconel-718 first wall.

~60 atm coolant pressure.

Metal-clad thorium fuel elements ~20-cm-thick containing metal, alloy, or oxide pellets.

Metal-clad elements of solid lithium compound for tritium breeding, ~50-cm-thick.

Helium conditions: $T_{\text{inlet}} \approx 300^{\circ}\text{C}$
 $T_{\text{outlet}} \approx 550^{\circ}\text{C}$

Thermal power conversion efficiency ~36%

Blanket energy multiplication,^a $M = 3.4$

^{233}U production^a $U/n = 0.74,$
(at $T/n = 1.1$) $1.1 \text{ kg/MW}_t \cdot \text{yr}$

^aApproximate blanket lifetime average values.

TABLE 5-6. Helium-cooled TMHR characteristics.

Assume:

Nuclear power	=	4000 MW _t
Q _p	=	1.5
Neutron wall loading	=	2 MW/m ²
First wall radius	=	1 m
Efficiencies:		
th	=	0.36
DC	=	0.50
inj	=	0.75

Then:

Fusion power	=	1370 MW
Reactor length	=	109 m
Blanket power	=	3726 MW _t
Injected power	=	913 MW _t
Direct converter power	=	593 MW _e
Total thermal power	=	4319 MW _t
Gross electric power	=	2148 MW _e
Net electric power	=	930 MW _e
Net station efficiency	=	23%
Fuel production	=	4380 kg/yr
Burners supported:		
LWR (270 kg/GW _e ·yr)	=	16.2 GW _e
HTGR (126 kg/GW _e ·yr)	=	34.8

with ^{232}U to resolve concerns about nuclear proliferation and diversion. It enjoys sufficient energy multiplication to allow the TMHR to easily produce net electrical power with a net efficiency of about 25% despite the tandem mirror's relatively low plasma energy amplification ($Q_p = 1.5$). Use of metal-clad thorium elements in the cylindrical blanket cartridge in the TMHR module promises to offer a simple, straight-forward design. The relatively low fission power density in the thorium fuel results in afterheat levels a factor of 7 less than those of a uranium blanket. The slower fuel heatup rate in the event of loss of cooling makes the thorium blanket fairly tolerant of loss-of-cooling events. More than 1 h would be available for action to restore cooling before the fuel would be damaged.

The uranium blanket option is a very attractive design for production of plutonium. The uranium/thorium blanket would allow ^{233}U production while achieving a high energy multiplication, which is important for low Q_p fusion drivers. The thorium/graphite blanket is a very attractive concept that has potential safety advantages that may be significant but that requires a high Q_p fusion driver to break even electrically because of its low energy multiplication. Each of these blanket concepts has advantages, and there are situations where each could be chosen as the best design for that situation. For application on the TMHR, the metal-clad thorium blanket appears to be the optimum choice and has been selected for the reference helium-cooled blanket design. The preconceptual design for a helium-cooled TMHR blanket developed during the scoping phase of the TMHR study that was summarized above is discussed in more detail in Ref. 1. It served as the basis for the preliminary conceptual design work that is presented in Section 6 of this report.

LIQUID METAL-COOLED BLANKET DESIGN

INTRODUCTION AND SUMMARY

Bechtel National has been working with LLL since 1975 on laser fusion-fission hybrid blanket designs. The fission blanket is composed of sodium-bonded, depleted uranium metal fuel pins, arrayed in process tubes and sodium-cooled. This array is backed by a fusion blanket composed of lithium and graphite. To assess the feasibility of using a liquid metal blanket in the TMHR, this blanket was modified to the new geometry, and magnetic field

constraints were incorporated. No new neutronics calculations were performed, and the blanket thermal performance was estimated from the previous laser fusion hybrid results.

A reference tandem mirror module with a length of 3 m, a plasma radius of 1 m, and a fusion neutron power of 18.8 MW (1 MW/m^2) was selected. The fuel rods were oriented horizontally so that the coolant flow in the fission blanket would be parallel to the magnetic field. Uranium metal fuel rods require gas plena to accommodate fuel swelling and fission gas release. These plena cannot be simply included in horizontal, sodium-bonded rods, so that gas bonding between the fuel rod and the clad was selected. Fuel temperature limits and swelling considerations then led to the selection of uranium carbide as the fuel rod material. The maximum energy multiplication in a uranium carbide blanket designed for a tritium breeding ratio of 1 is about 7, or 30% less than that possible in a uranium metal blanket. (The uranium is assumed to be depleted uranium with a ^{235}U fraction of 0.25%).

A conservative flow design, allowing space for flow turning and fuel process tube plena, resulted in a reference blanket design with an active length of 1.6 m, or 53% of the module length. The effective energy multiplication of the reference design module is 3.8.

In the flow calculations, it was assumed that the magnetic Reynolds number in the coolant supply pipes must be less than 0.1. This restricts the thermal power of the module blanket to 120 MW under the reference conditions. The pressure drop through the reactor, excluding turns, is 50 psi for the reference design module and 80 psi at the thermal power limit of 120 MW. Therefore, if the fuel elements can be lengthened to 2.7 m, with acceptable turning pressure loss, the blanket multiplication in the reference design can be 6.4, which corresponds to the coolant design limit of 120 MW. Energy multiplications greater than 7 can be realized by using natural or enriched uranium fuel or using a ceramic fuel with greater uranium density than the carbide, and by reducing the design fusion neutron flux.

It is concluded that liquid metal cooling can be used in the TMHR. The advantages of liquid metal cooling are its excellent heat transfer characteristics, its well developed technology, and the ability to breed tritium in the coolant. The free convection cooling capability of liquid metals is reduced by the horizontal fuel element arrangement.

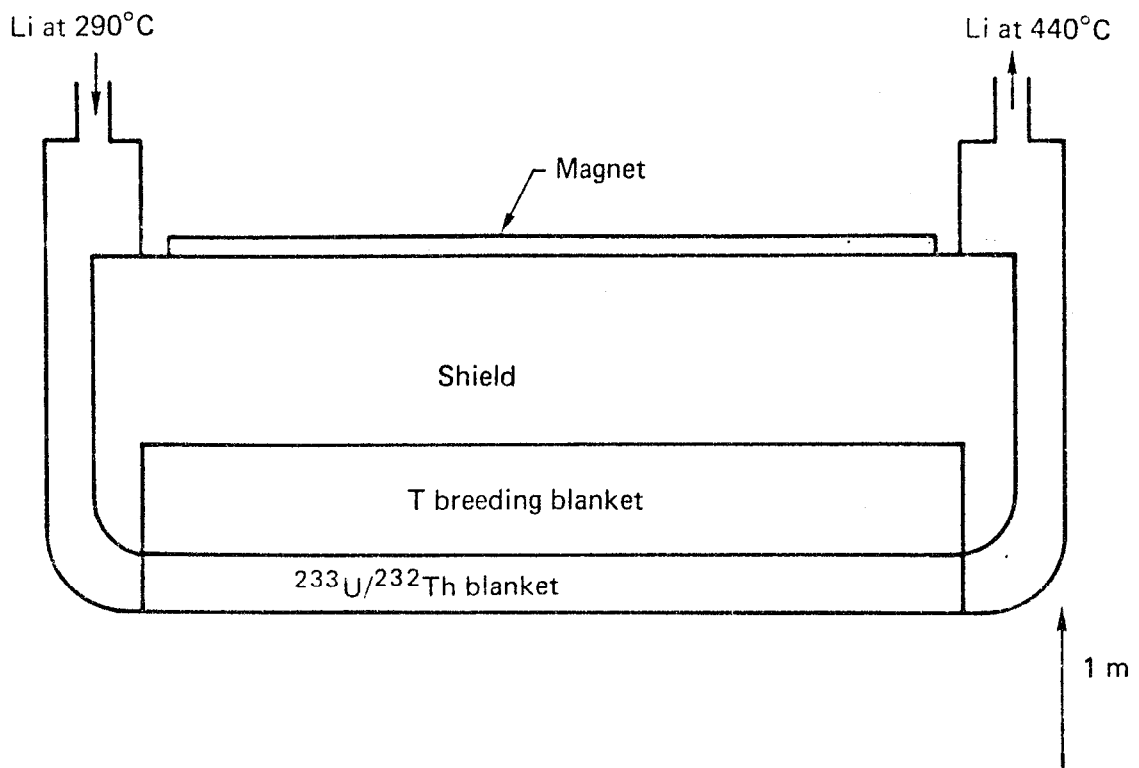
The disadvantages of the liquid metal blanket is that the total power that can be removed from a single module is limited by magnetic field effects. This limitation may undesirably constrain the module design. Further analysis of the coolant flow, including sharp turns and large induced magnetic fields, is required to establish the thermal hydraulic limitation of a liquid metal-cooled module.

BLANKET CONFIGURATION

A schematic diagram of the lithium-cooled blanket design for one module of the TMHR is shown in Fig. 5-1. The reference module is a 3-m-long section with a first wall radius of 1 m. The neutron flux at the first wall is 1 MW/m^2 , and the fusion power delivered to the module blanket is 18.8 MW. The fission fuel elements are oriented axially, with an active length of 1.6 m in the reference design. The estimated thermal power generated in the fission blanket is 71 MW, so that the fission energy multiplication for the total module is 3.8. Each blanket module will also produce approximately 60 kg of fissile Pu per full power year. The performance of the reference blanket design and a less conservative hydraulic design (High Power Design) with a 2.7-m-long active length is summarized in Table 5-7.

The fuel elements are arrayed axially in two rows of hexagonal process tubes, containing 19 fuel rods per tube. The lithium coolant is supplied to a ring header by two 80-inch lines. The header feeds 20 lines of 12-in.-diam each, which penetrate the reactor radially to supply the process tubes. The lithium temperature rise is 150 K, and the total pressure drop through the reactor is 0.34 MPa (50 psi) in the reference design and about 0.55 MPa (80 psi) in the High Power Design. The total mass of uranium in the blanket is $1.51 \times 10^4 \text{ kg}$ ($2.54 \times 10^4 \text{ kg}$ in the High Power Design), giving an effective surface density in the fuel region of 1500 kg/m^2 .

The above blanket performance is based on the neutronics calculations of Maniscalco (UCRL-76763) as extended for the Bechtel laser fusion hybrid studies (UCRL-13720 and UCRL-13796). The fission zone is backed by a lithium and graphite zone, and the uranium content is limited by the requirement of having a tritium breeding ratio greater than 1. The fuel rods in the laser fusion hybrid designs were depleted uranium metal, sodium-bonded and steel-clad. The fuel elements were vertical and included a plenum at the top to allow for fuel swelling and fission gas generation. This plenum cannot be



Major features:

- Li (or Na) coolant.
- MHD limitations.
- Close reliance on LMFBR materials technology.

Fig. 5-1. Liquid metal-cooled blanket configuration for TMHR.

TABLE 5-7. Lithium blanket performance.^a

Parameters	Reference design	High power design
Active length/solenoid length	0.53	0.9
Energy multiplication	3.8	6.4
Fissile breeding ratio	0.71	1.2
Nuclear power, MWt	4,000	4,000
Fusion power, MWt	1,235	752
Blanket power, MWt	3,754	3,850
Length of solenoid, m	157	96
Total mass heavy metal, kg	15,100	25,400
Total fissile prod./FPY, kg Pu	3,890	4,000
Number of modules	53	32
Blanket power/module, MWt	71	120
Module pressure drop, psi	50	80

^aBasis: 1 MW/m² (neutron loading)

1 m (wall radius)

UC fuel (depleted - 0.25% ²³⁵U)

Tritium breeding ratio = 1

satisfactorily incorporated in a sodium-bonded horizontal fuel element, so gas bonding was chosen for the tandem mirror elements. Uranium carbide fuel rods, at 90% of theoretical density, were chosen to operate with a helium gas bond, since uranium carbide can operate at much higher temperatures than the metal (as required by the lower bond heat conductance), and because swelling can be accommodated internally.

The fuel rods are 26-mm-diameter slugs of depleted uranium carbide, bonded with helium and clad with 0.5 mm of ferritic steel. The fuel rod outside diameter is 28 mm, and the fuel rod pitch is 30 mm. The maximum power generation in the fuel is estimated to be 94 W/cc, and the average power generation in the blanket is 55 W/cc. The flow through the process tubes is laminar in all cases, because of the effect of the high magnetic field. The average power generation in the first row is about 75 W/cc, so that an element peak to average temperature factor of 94/75, or 1.25, was used. The temperature of the steel cladding exposed to lithium was limited to 500°C, which limits the lithium-mixed mean outlet temperature to 440°C. The maximum temperature in the uranium carbide fuel is 750°C, which is well below its limit. The fuel slug diameter was limited to 26 mm because of fabrication uncertainties, not because of temperature limits.

Active cooling must be maintained to remove decay heat from the fuel elements during fuel handling. It is desirable to remove the fuel elements without removing the module from the solenoid. However, this does not appear to be feasible with long horizontal fuel elements. Therefore, provision must be made to cool the module while it is being removed. This might be done by cooling the lithium in the blanket by an auxiliary cooling system, or by gas circulation through the fusion core or through a gas blanket surrounding the fission blanket. Decay heat calculations and licensing considerations are required to determine feasible fuel handling approaches.

MAGNETIC FIELD CONSIDERATIONS

When a conducting fluid flows perpendicularly to a magnetic field, a current is induced perpendicular to the flow and to the field. This induced current in the magnetic field produces a body force opposing the fluid motion, which is the dominant cause of pressure drop in the flow. The induced current also induces a magnetic field perpendicular to the applied field. The induced magnetic field is assumed to be small in this analysis. The magnetic field

also modifies the flow profile and suppresses turbulence in conducting fluid flows, regardless of flow orientation.

The magnitude of the net induced current in the fluid depends on the degree to which the current paths are closed in the fluid. This is expressed by the conductance ratio

$$C = \frac{\sigma_w t_w}{\sigma r} ,$$

where t_w is the wall thickness, r is the pipe radius, σ_w is the wall conductivity, and σ is the fluid conductivity. The magnetic pressure drop due to the induced current is given by

$$\Delta P = \sigma v L B^2 C / (1 + C) ,$$

where v is the fluid velocity, and L is the distance the fluid flows perpendicularly to the magnetic field of strength B .

The magnetic Reynolds number, which is the ratio of the strength of the induced magnetic field to the applied magnetic field, is

$$R_m = \mu_0 \sigma v r ,$$

where μ_0 is the permeability.

If the induced magnetic field is not allowed to exceed 10% of the applied field of 2 T, then the velocity and radius of a pipe crossing the magnetic field are constrained by

$$vr = 0.04 \text{ m}^2/\text{s} ,$$

and the maximum lithium flow in the pipe, \dot{m} , is

$$\dot{m} = 61 r \text{ kg/s} ,$$

where r is the radius of the circular pipe in m. If the induced field exceed 10% of the applied field, then the induced field and its effect on the lithium flow must be explicitly included in the analysis. Allowing a higher magnetic

Reynolds number would permit higher thermal power generation in an individual module.

The number of pipes that can supply the blanket at 1-m, first-wall radius is equal to π/r by geometry, so that the total allowable flow to a module is 190 kg/s. If the allowable lithium temperature rise is 150 K, the total power that can be removed in one lithium circuit is 120 MW.

No attempt was made to design vertical fuel assemblies for the tandem mirror, because the pressure drop due to the magnetic field appears to be excessive. Four vertical assemblies, each 0.75 m in the magnetic field direction and 2-m-high, could be accommodated in the 3-m tandem mirror module. Each of these assemblies would receive 1.18 MW of fusion neutron power, and could generate 11.8 MW with depleted uranium metal fuel rods, giving a net multiplication for the module of 2.5. The coolant could be supplied in a 24-in. lines at 0.13 m/s with a magnetic Reynolds number of 0.1.

The lithium must be accelerated in the blanket through closely-packed fuel rods to achieve effective cooling. For a uranium volume fraction of 60%, the coolant velocity must be 0.8 m/s, and the pressure drop due to the body force through the reactor for a nominal conductance ratio of 0.05 is about 100 psi. However, it is unlikely that an effective conductance ratio of 0.05 can be achieved in a packed-rod geometry, and wall velocity gradient steepening due to the magnetic field may make the frictional losses unacceptable.

THERMAL-HYDRAULIC ANALYSIS

The coolant flow between the ring header and the fission process tube plenum is transverse to the magnetic field lines. The required lithium flow for the 71-MW blanket is 113 kg/s. If this flow is carried in twenty, 12-in. o.d. lines with a 0.5-in. wall thickness, then the flow velocity is 0.19 m/s, and the magnetic Reynolds number is 0.07. The conductance ratio is 0.054, the magnetic field strength is 2 T, and the flow distance across the field lines is 2 m, so that the pressure drop in the line is 0.16 MPa (23 psi). The Hartman number is 40,000 and the Reynolds number is 65,000. Turbulence is fully suppressed by the magnetic field. If the fission blanket is designed for 120 MW, the pipe flow velocity is 0.32 m/s, the magnetic Reynolds number is 0.22, and the pressure drop is 0.26 MPa (38 psi).

The outside diameter of the fuel rods is 28 mm, and the pitch is 30 mm. The maximum lithium velocity in the 19-rod cluster is 1.1 m/s for the 71-MW blanket. The Hartman number is 520 and the Reynolds number is 7800, so that turbulence is fully suppressed. The laminar heat transfer coefficient (Nusselt number of 5) was used in the fuel rod thermal calculations, and the pressure drop was calculated to be negligible.

No detailed thermal-hydraulic analysis of the high power density design was performed; its performance was extrapolated from the reference design.

WATER-COOLED BLANKET DESIGN CONCEPTS

Five conceptual designs of TMHR blankets utilizing water cooling are proposed as potential candidates for detailed evaluations:

- Mirror Hybrid Reactor (MHR) blanket module
- Oblong tube concept
- Cartridge concept
- Linked assembly concept
- Pool concept

The first four concepts are intended to contain the water (any phase) at temperatures and pressures amenable to the production of electricity in a balance-of-plant similar to light-water reactors. In the pool concept fissile fuel is the only useable product; the heat from the blanket is discarded as waste in low temperature water.

For practical coolant temperatures and pressures the blanket coolant water can be used as liquid, steam, or a two-phase mixture. At high temperatures and pressures the liquid-cooled blanket can utilize pressurized water reactor (PWR), balance-of-plant technology, so little extra development is required. However, at high coolant temperatures blanket performance and reactor cost are adversely affected by shortened structure life and frequent replacement of all the blanket inner structure, not just the blanket fuel. In liquid form the high coolant density in the blanket will result in a sizable neutronics degradation. Preliminary physics cases indicate that liquid-cooled blankets achieving a unity tritium breeding ratio have exceedingly poor fissile fuel producing capabilities unless the structure and coolant to fuel atom ratio are very low (such as the ratio achieved in the pool design). If the temperature of the blanket structure is lowered to around 400°C or less,

the material life can increase dramatically, and only the blanket fuel (not structures) would need replacement at each refueling.

A blanket with steam cooling would experience very little neutronic performance degradation due to the coolant. The degradation is comparable to helium-cooled blankets. The heat capacity of steam is lower than helium by a factor of about 2, while its density is greater by a factor of about 10. This results in a circulator power requirement for steam cooling that is about 23% less than for helium at the same reactor power, pressure, and temperature. Offsetting the improvement in pumping power provided by using steam instead of helium in a gas-cooled blanket is the increased corrosion caused by the steam. Helium is inert to most structural materials while steam is not and will limit the choice of materials available for use in the blanket. For high-temperature, steam-cooled designs, the structure life is short, and a large amount of structure must be replaced with each refueling. As with the liquid-cooled blankets, the solution to the problem is to use cool steam against the structure and limit permanent structure temperatures to 400°C.

A mixed coolant phase blanket design offers a potential balancing of the coolant neutronics effects with the blanket local neutronics needs. Liquid in the tritium breeding (lithium) region and steam in the fissile fuel breeding region are such a match; however, the heat released in the lithium blanket is insufficient to vaporize the quantity of steam required in the fissile blanket. Uncertainties in the area of boiling become important and would make larger design margins necessary in the blanket. Offsetting the negative effects of the increased design uncertainties is the potential for nearly isothermal blanket operation (due to the nature of a boiling water system) and the potential for keeping the structural temperatures low enough to permit permanent blanket structure.

The MHR module conceptual design is shown in Fig. 5-2. Because there is a large coolant volume between the plasma and the breeding fuel, only steam is considered as the coolant phase. The module is refueled and the first wall (module nose hemisphere) is replaced by removing "break slice" sections of the blanket and fusion system vacuum boundary. The entire module and a large amount of blanket structure are discarded with each refueling.

The oblong tube concept presents a design that permits refueling without disassembly of any central region structures. The conceptual design is based on these premises:

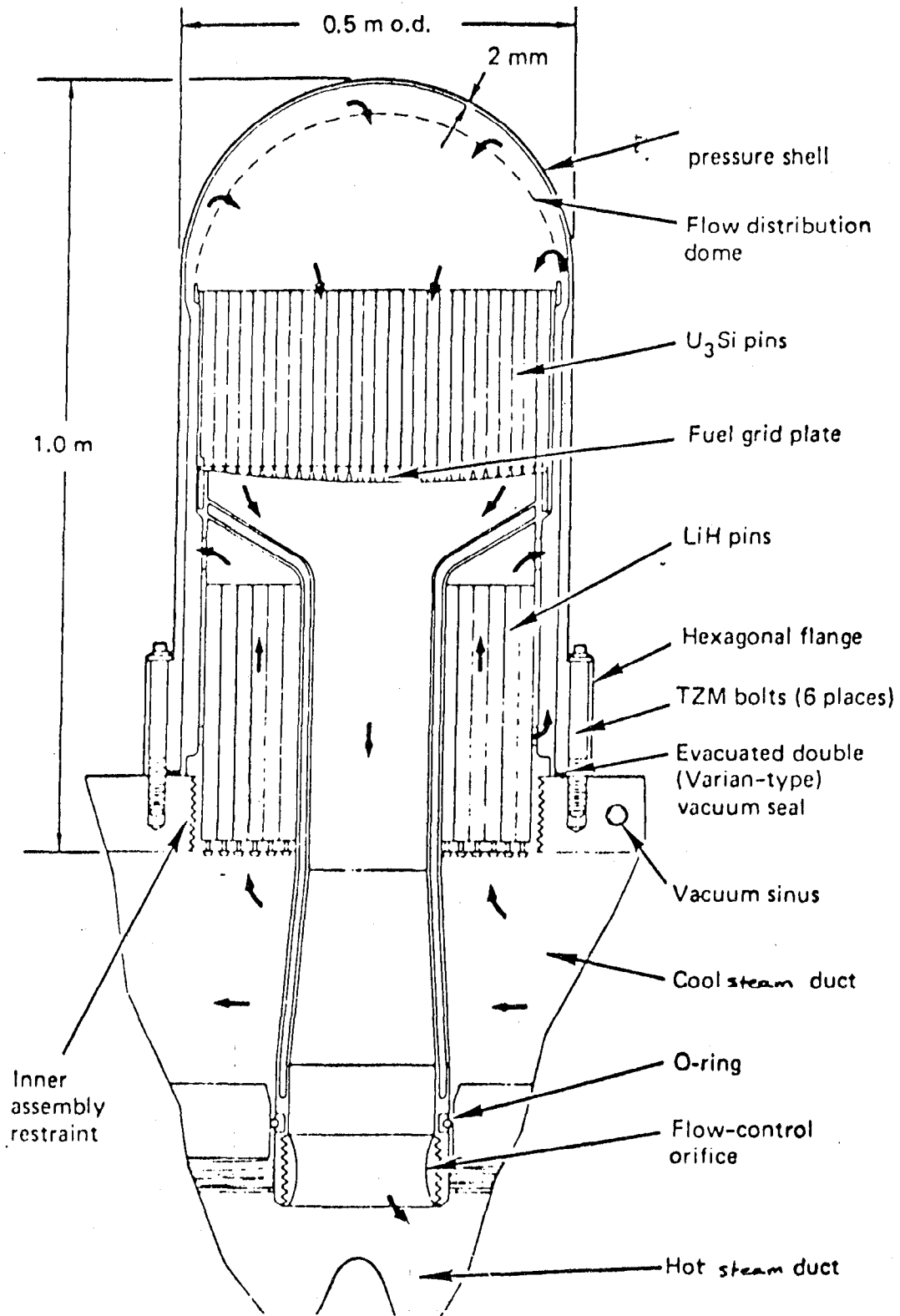


Fig. 5-2. Pool design--one-dimensional analytical model.

- With adequate cooling, and perhaps periodic annealing, the first wall and other blanket structure can be made long-lived, i.e., two decades or more.
- Refueling without disassembly will increase reactor availability.
- Longevity for the central region structure significantly reduces costs.

OBLONG TUBE CONCEPT

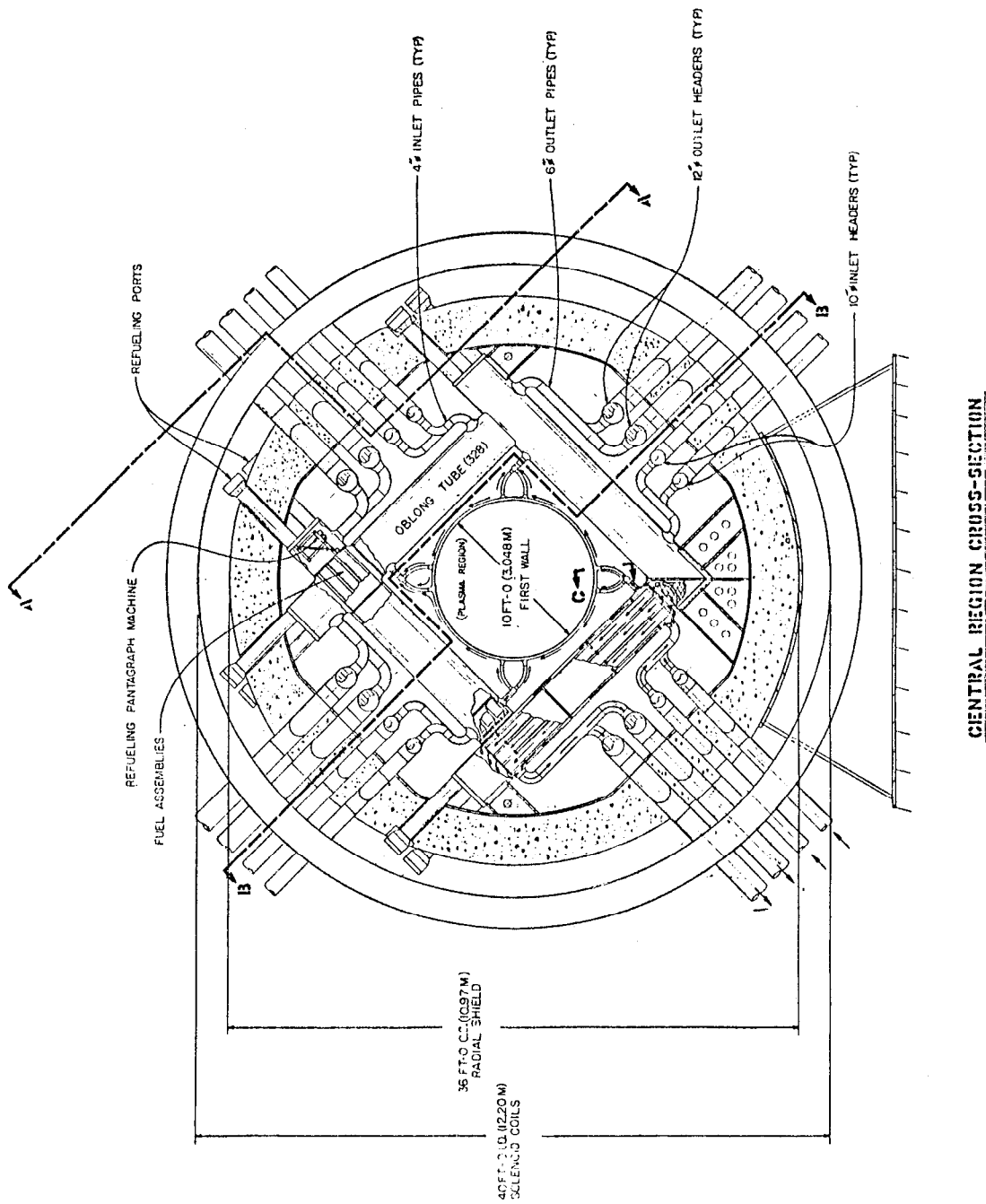
The general arrangement of the oblong tube concept is illustrated in Figs. 5-3 and 5-4, which show a cross section of the central region and views taken along the axis of the central region.

This concept assumes permanent installation of all components of the central region except the fuel assemblies. Refueling operations are performed without any structural disassembly. The first wall/plasma region vacuum boundary is separate from the fuel containers in this concept. As can be seen in Fig. 5-3, the first wall is circular. It is made from integrally connected tubular rings through which steam flows for cooling. The fuel containers are oblong tubes arranged in a square array around the first wall. Longitudinally, the squares of oblong tubes are nested against each other, as shown in Fig. 5-4. Around the squares of oblong tubes is the cylindrical radial shield, and beyond the shield are the magnet coils of the central region solenoid. Between the oblong tube squares and the radial shield are the coolant pipes to and from each oblong tube and the headers for the pipes.

Each oblong tube on each side of each square contains three cylindrical fuel assemblies. The innermost assembly contains fissile breeding fuel, the other two contain tritium breeding fuel. For refueling the fuel assemblies are withdrawn and inserted through a port in the upper end of each oblong tube. The refueling ports on the oblong tubes project through the radial shield for access of the refueling machine. Access to two-thirds of the ports will require movement of the solenoid coils in the direction of the axis of the central region.

CARTRIDGE CONCEPT

The cartridge concept is based on the same premise as the oblong tube concept: cool structure, refueling without structural disassembly, and long



CENTRAL REGION CROSS-SECTION

Fig. 5-3. Oblong tube concept.

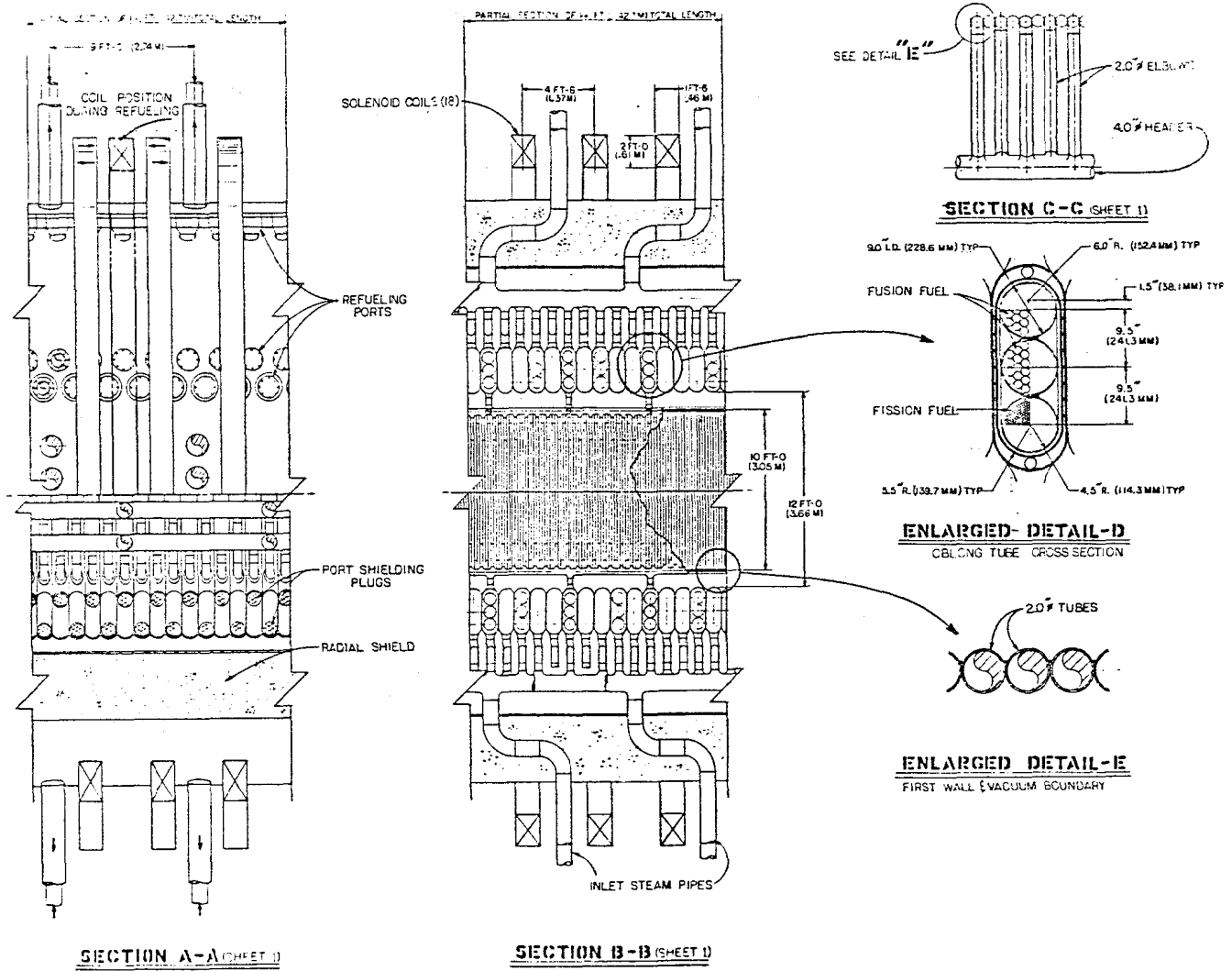


Fig. 5-4. Oblong tube concept details.

structure life. It is a configuration in which blanket elements are contained within cylindrical cartridges cantilevered into the plasma vacuum chamber. The unique geometry shown in Fig. 5-5 provides a close packing of the cartridges around the central cell plasma region, while allowing spacing between cartridges where they penetrate the vacuum boundary. The boundary of the vacuum chamber also serves as the shield and as the basic structural member for supporting the cartridges. Each cartridge comprises a cylindrical vessel designed to accommodate the coolant pressure on its inside surface, the fuel elements, a shield section, piping to accommodate inlet and outlet flow and to direct flow along the fuel elements, and means for mounting and sealing to the shield-vacuum chamber wall.

Two possible cartridge refueling approaches are proposed. In the first approach refueling consists of replacing the entire cartridge, including a disconnect of coolant pipes. This requires the vacuum chamber to be vented to the atmosphere. Concentric inlet and outlet pipes are used in order to minimize the number of joints that must be sealed. A J-shaped pipe, as shown in Fig. 5-5, permits straight withdrawal of a cartridge after disconnecting the piping flange and the vacuum chamber seal. In an alternative refueling approach the cartridge pressure vessel remains in place while fuel is removed and replaced. This allows the vacuum to be maintained during a normal refueling outage. The pressure vessel can be replaced when required, and in this case the vacuum must be broken. Pipes can be located where they will not interfere with withdrawal of fuel.

The two rows of cartridges shown will contain different fuels and possibly different coolants. The inner row contains the fissile breeder and generates most of the system power. The outer row contains lithium for tritium production and generates much less heat. Since these two rows are independently cooled, the outer lithium cartridges can be cooled and the tritium purged by helium or lithium, while the inner cartridges are cooled by steam or boiling water. In this way there appears to be no problem of water contamination with tritium. The outer lithium cartridges would probably not require frequent replacement if the tritium can be continuously purged. Since they have essentially no residual heat generation, replacement of these lithium cartridges can be done after completely disconnecting their coolant pipes. It is suggested that very infrequent replacement of the entire cartridge could be adequate.

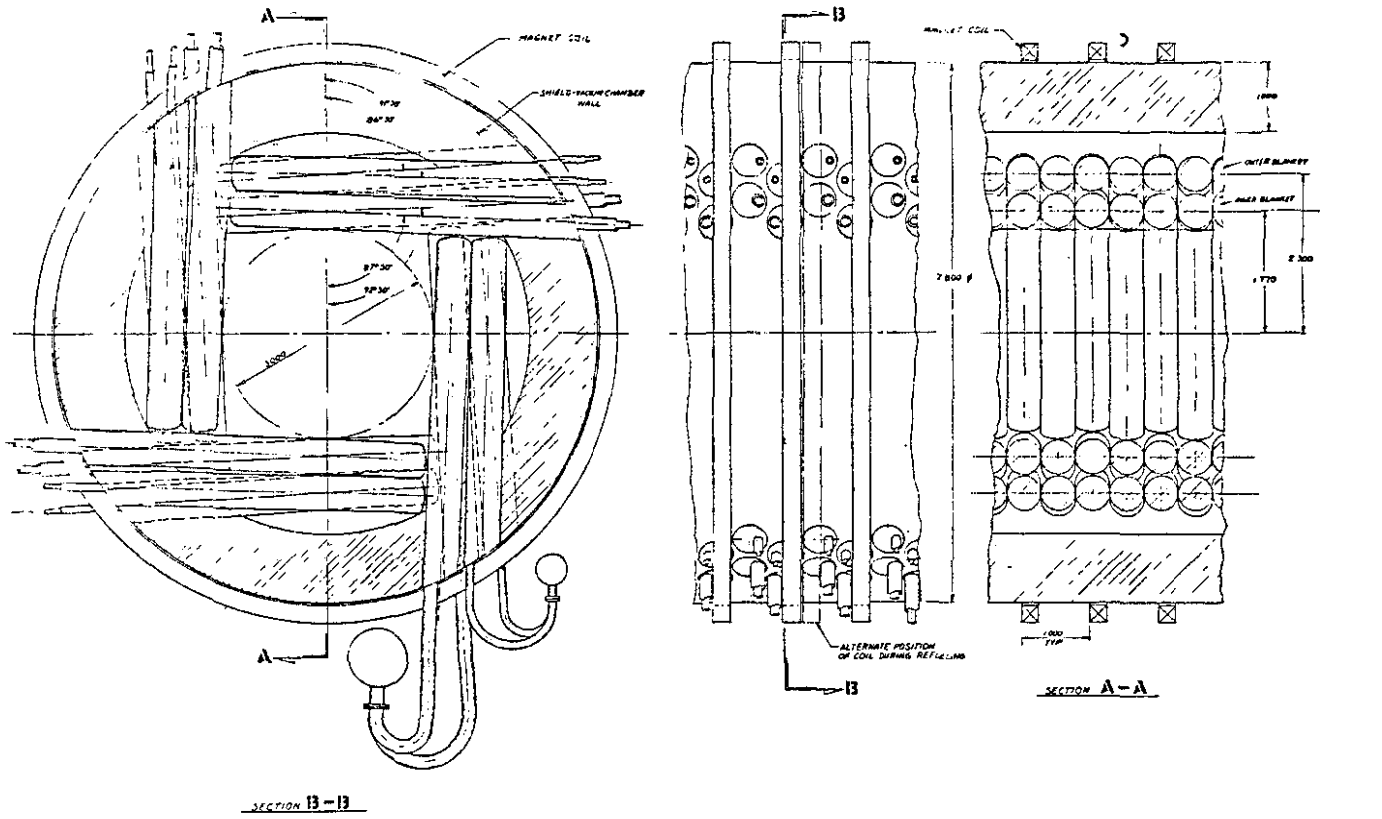


Fig. 5-5. Original cartridge concept--two rows.

LINKED ASSEMBLY

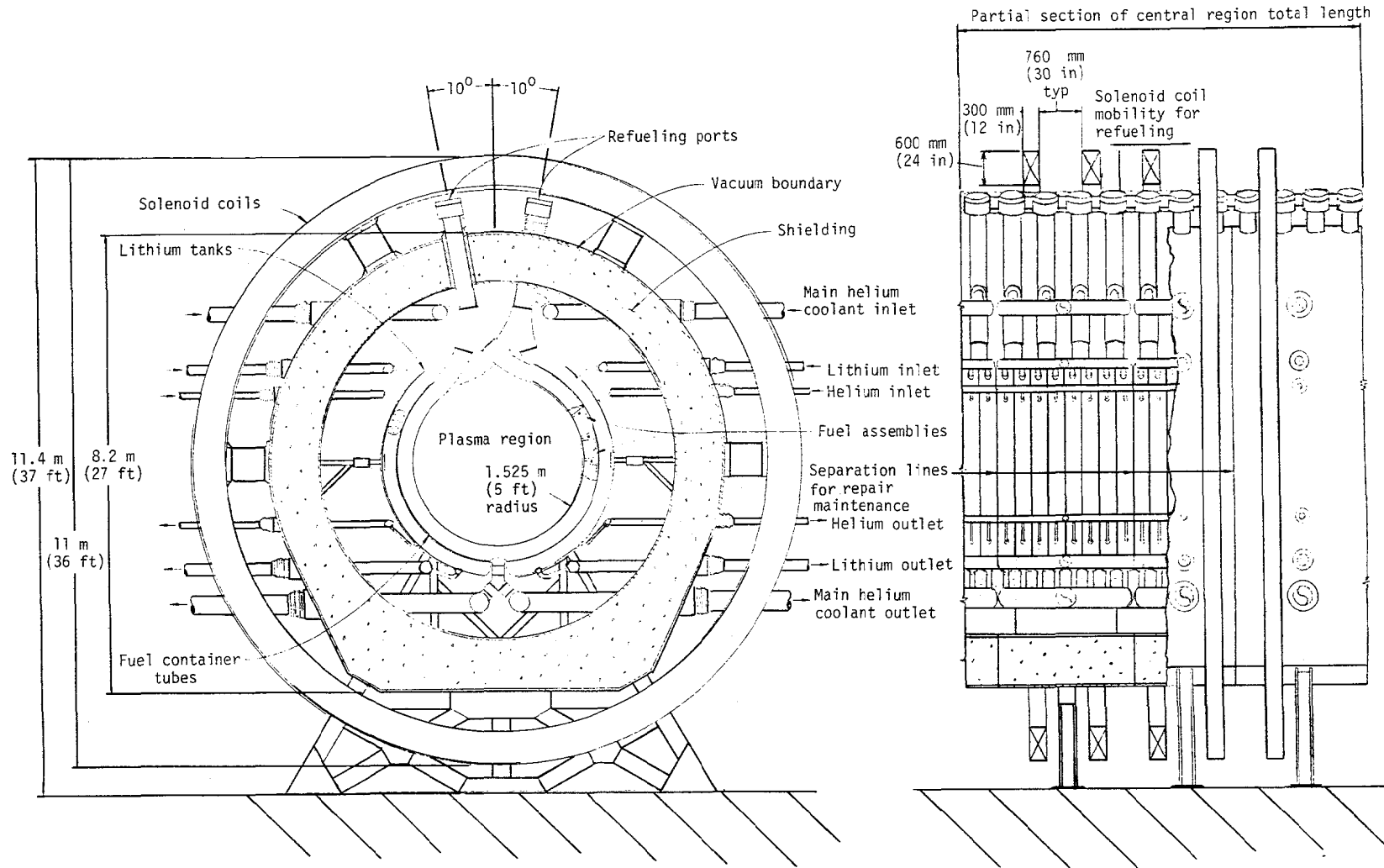
The general arrangement of the linked assembly concept is illustrated in Figs. 5-6 and 5-7, which show a cross section of the central region and a side view of part of the total length. The concept is based on the premise that the central region structures are to be long-lived and permanently installed, and refueling is to be performed without disassembly of central region structures. Either superheated steam or boiling water cooling can be used; however, boiling is preferred for lower structure temperatures.

The vacuum boundary is at the encased surfaces of the primary shield. The first wall is at the layered noose-shaped tubes, which are the coolant pressure boundary and the fissile fuel containers. Coolant pipes penetrate each noose-shaped tube at top and bottom. Radially beyond the noose-shaped tubes are lithium filled tanks with their connected piping for circulation of the lithium and helium. All of the piping is manifolded within the shield to larger pipes that penetrate the shield and pass between the solenoid magnet coils outside the shield. The blanket, shield, and piping are segmented along the axis of the central region. Figure 5-7 illustrates how an entire segment of the central region is withdrawn sideways to give access to the inside of the segment for unexpected maintenance. Adjacent segments are withdrawn to opposite sides.

The fissile fuel in the linked assembly concept is contained within tubes of circular cross section immediately adjacent to the plasma region. Each tube is shaped somewhat like a noose, with the noose intersection being a Y-forging above the plasma region. The stem of the Y is the refueling access port.

The noose-shaped tubes are arranged in layers along the entire axial length of the reactor. Each tube is identical with the others except for the opposite hand location of the coolant outlet nozzles on adjacent tubes. The refueling ports of adjacent tubes are shown offset 20° from each other and 10° from the vertical centerline. The separation gives room for the necessarily thickened Y-forging in each tube, prevents interference between refueling port penetrations and flanges, and improves access to the refueling ports.

Each side of each noose-shaped tube contains 16 short, cylindrical fuel assemblies linked together in a chain. For refueling the spent fuel assembly chains are withdrawn through the Y and out the port over the Y, and new chains



Central region cross section

Fig. 5-6. Boiling water-cooled linked fuel assembly blanket.

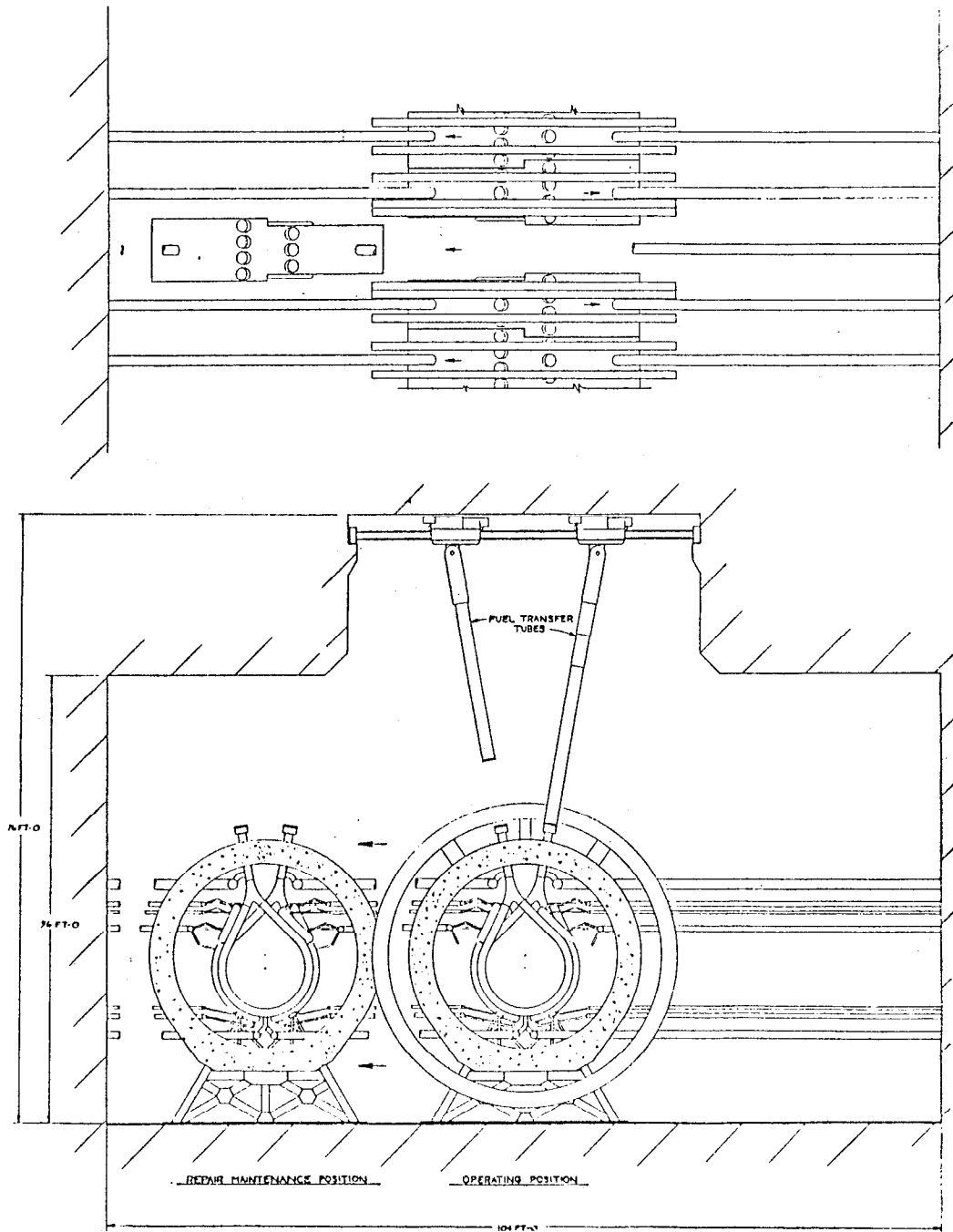


Fig. 5-7. Refueling and servicing layout--linked assembly concept.

are lowered into place. The port on each noose-shaped tube projects through the shield for easy access of the refueling machines. The entire central region is supported at the bottom, all external piping extends out from the sides, and all refueling operations are from the top.

The angularity of the Y in each noose provides for saturated steam flow direction not less than 45° from horizontal. Maintenance of this angle is necessary to prevent phase separation in the coolant flow. Coolant is piped into each tube at the bottom of the noose and is piped out at the top above the stem of the Y. For coolant other than boiling water, the flow direction would probably be reversed.

The method of separation of flow for cooling the fuel and for cooling the pressure boundary/first wall has not been defined. The inlet water and outlet steam for boiling water cooling or the inlet steam for single phase cooling will be about 572°F (300°C). Operation at this low temperature allows longevity of the structure to be assumed provided that periodic annealing is performed. The structure for the linked assembly concept seems particularly adaptable to annealing. After removal of the fuel, hot gas can be circulated through the pressure boundary components.

Tritium production occurs in closed tanks filled with liquid lithium. The tanks are located outside the fuel tubes and follow the contour of the fuel tubes. At the curved portion of the contour, the lithium tanks' centerlines are tangent with the fuel tubes to minimize neutron streaming between the tubes. At the straight portions of the contour, the fuel tube and lithium tank centerlines are in the same radial plane. The diameters of the lithium tanks are the same as the diameters of the fuel tubes. Within each lithium tank a coil of helium filled piping provides the means for cooling the lithium and removing the tritium. Separate inlet and outlet piping connections are made at each tank for circulation of the helium and lithium.

POOL CONCEPT

When fission reactors are built only for isotope production or for test purposes, they are often designed to be totally immersed in a pool of water. The water pool serves both for shielding and for cooling during normal operation as well as during refueling. This, along with cool permanent structure, is the basis of the pool design concept for the TMHR. This concept is for fuel production only and produces no electric power. Such a low temperature

blanket would cause difficulties in the balance-of-plant if the blanket thermal output is to be converted to electricity. The minimum pool (and containment building) pressure, in that case, would be about 14-17 atm, and a limited redesign of the low pressure ends of conventional light-water reactor turbines would be required along with increased building strength. The net plant generating efficiency would be about 20% at such a low pressure and temperature. This power producing alternative is not evaluated--only the nonpower producer, as shown in Fig. 5-8.

A central pipe containing the vacuum and the fusion plasma is located below the surface of the pool, and its outer surface is kept cool by the water. The central pipe is surrounded by a blanket and shield with magnet coils surrounding the shield. The design includes means for forced cooling of the blanket as well as means for replacement of the blanket. The shield and fuel are divided into split modules, each having an axial length of about 2 m.

Fuel in each module is made up of two close-packed bundles of horizontal rods about 1 m long and clad with steel. Grid spacers hold these rods parallel to the central first-wall pipe. Water enters both ends of the fuel assembly from the small gaps separating the modules. The heated water leaves at the middle of the assembly between the two rod bundles where it enters pipes to the primary heat transfer system. The fuel bundle is attached to the inner surface of the 1-m-thick radiation shield and can be removed and replaced after the shield is pivoted into a horizontal position.

Refueling must be preceded by moving the magnet coils axially to a position where they will not interfere with pivoting the shield. During reactor operation, the magnet coils are locked in position to resist magnetic forces. The two half modules are pivoted at separate axes, permitting support of the coils on a bottom rack. A lower water outlet manifold automatically connects to the modules at their operating positions, eliminating the need to remove pipes before pivoting these modules. Special-purpose fuel transporters mounted on each side of the pool wall are used to transfer fuel assemblies from the pivoted modules to a fuel receiving station.

Table 5-8 summarizes blanket performance parameters for the five design options, all at beginning-of-life and operated at 1 mw/m^2 neutron flux at a 3-m diam. The designs presented are representative of the outcome of pursuing different decisions in the major design tradeoffs--reactor concept, coolant phase, and fuel type.

5-28

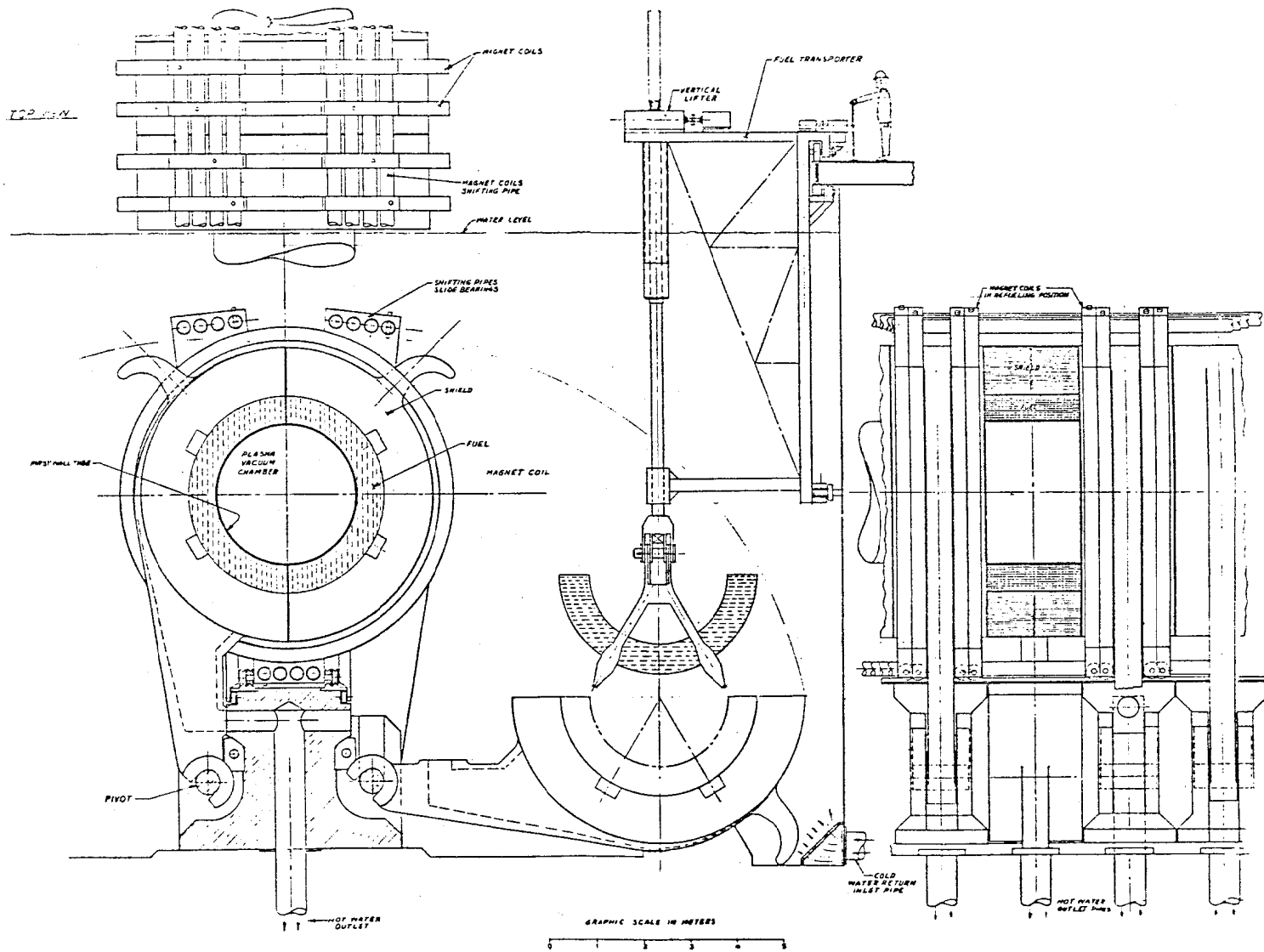


Fig. 5-8. Pool Concept No. 2.

The pool design opts for the simplest reactor and balance-of-plant but forfeits power generation. The oblong tube and linked assembly designs characterize blanket systems with permanent, difficult-to-replace pressure boundaries (tubes) but simple refueling. The cartridge blanket design combines replaceable internal structure and simple refueling, but requires a sizable containment building. The module blanket characterizes designs with removable reactor segments to allow refueling. Except for the MHR module, the internal structural temperatures are limited to 400°C or less to allow long material life.

Since the MHR module is only amenable to steam cooling, and since steam has the same neutronic effects as helium, no nuclear analysis of the module was performed--only thermal-hydraulic calculations. Thus, no MHR module performance results are presented in Table 5-8 because the performance is the same as for the helium-cooled cases.

The cartridge and oblong tube designs have nearly identical performance and are grouped together. To facilitate nuclear analysis of boiling water coolant effects in these designs, blanket coolant atom volume functions are estimated based on a Russian design,¹⁴ boiling-water TMHR blanket, rather than on detailed thermodynamic analyses.

Due to the limited volume fraction of fuel in all blanket concepts except the pool design, liquid cooling will not permit tritium breakeven and fissile fuel production simultaneously. For this reason only the pool concept is presented in Table 5-8 with liquid phase cooling.

A comparative evaluation of these five blanket concepts shows the linked assembly arrangement to be superior over all within the guidelines of this study. Each concept has its advantageous features relative to the others, but the linked assembly best satisfies the major concerns involved in bringing a realistic product to market:

- Ease and speed of refueling.
- Repair and maintenance accessibility.
- Structural simplicity.
- Minimal unique development needs.
- Versatility in coolant type and phase.
- Tritium production and isolation.
- Fissile fuel production.
- Power production.
- Capital cost.
- Fuel cost.

TABLE 5-8. Water-cooled TMHR blanket performance.

Design concept	MHR module		Oblong tube and cartridge				Linked assembly		Pool
Coolant phase	Steam		Steam		Boiling		Boiling		Liquid
Fertile fuel form	U ₃ Si	Th Metal	U ₃ Si	Th Metal	U ₃ Si	Th Metal	U ₃ Si	Th Metal	Th Metal
Fissile product form			²³⁹ Pu	²³³ U	²³⁹ Pu	²³³ U	²³⁹ Pu	²³³ U	²³³ U
Breeding ratio									
- Fissile fuel			1.06		1.2	0.36	~1.2	~0.36	0.84
- Tritium			1.0		1.06	1.0	1.0	1.0	1.0
Energy multiplication			6.97		9.07	1.09	8.48	1.01	2.11
Blanket length, m			58.8		38.6	224.1	41.2	239.3	180.3
Power, MWt									
- Nuclear			4000		4000	4000	4000	4000	4000
- Fusion			692		537	3731	573	3968	2123
- Blanket			3862		3893	3254	3886	3206	3575
Fissile production, kg/yr			3262		3552	5993	3530	5836	7724
Burner support ratio, GWe									
- LWR, 270 kg ²³³ U/GWe-yr			--		--	22.2	--	21.6	28.6
- ACR, 126 kg ²³³ U/GWe/yr			--		--	47.6	--	46.3	61.3
- LWR, 400 kg ²³⁹ Pu/GWe/yr			8.16		8.88		8.83	--	--

For more detailed information on the five water cooled blanket concepts, the TMHR Interim Report should be consulted.¹³

BERYLLIUM/MOLTEN SALT-COOLED DESIGN

CONCEPT AND JUSTIFICATION

Fissile breeding blankets can be characterized neutronically by the kind and amount of fissile material produced and energy multiplication that occurs in the blanket. The nuclear performance of four blanket types is listed in Table 5-9. The uranium performance is from the standard mirror hybrid study and is a good estimate.¹⁶ The thorium performance estimate is also reasonably good.¹⁷ Performance estimations for the last two blanket types are educated guesses based on our (and others') work. How should we compare various blanket types? One obvious way is by cost of the ultimate product (mills/kWh). Another important way is by support and capacity expansion ratios. Here, support ratio is the ratio of nuclear powers of fission reactors and fissile breeding fusion reactors (hybrid) supplying makeup fissile material to these fission reactors. The capacity expansion ratio is similar except the hybrid is now supplying initial fissile inventories to the fission reactors.

TABLE 5-9. Blanket neutronics--representative types and performance.

Blanket type	Nuclear performance ^a (anticipated)			Multiplication, M
	Breeding ratio ²³⁹ Pu	energy ²³³ U	T	
Uranium	1.5	--	1.0	11
Thorium	--	0.6	1.0	3.4
Uranium/thorium	0.6	0.7	1.0	7.6
Be + Thorium ^b	--	0.8	1.0	1.6

^aTime- and spatially-averaged.

^bThorium containing molten salt.

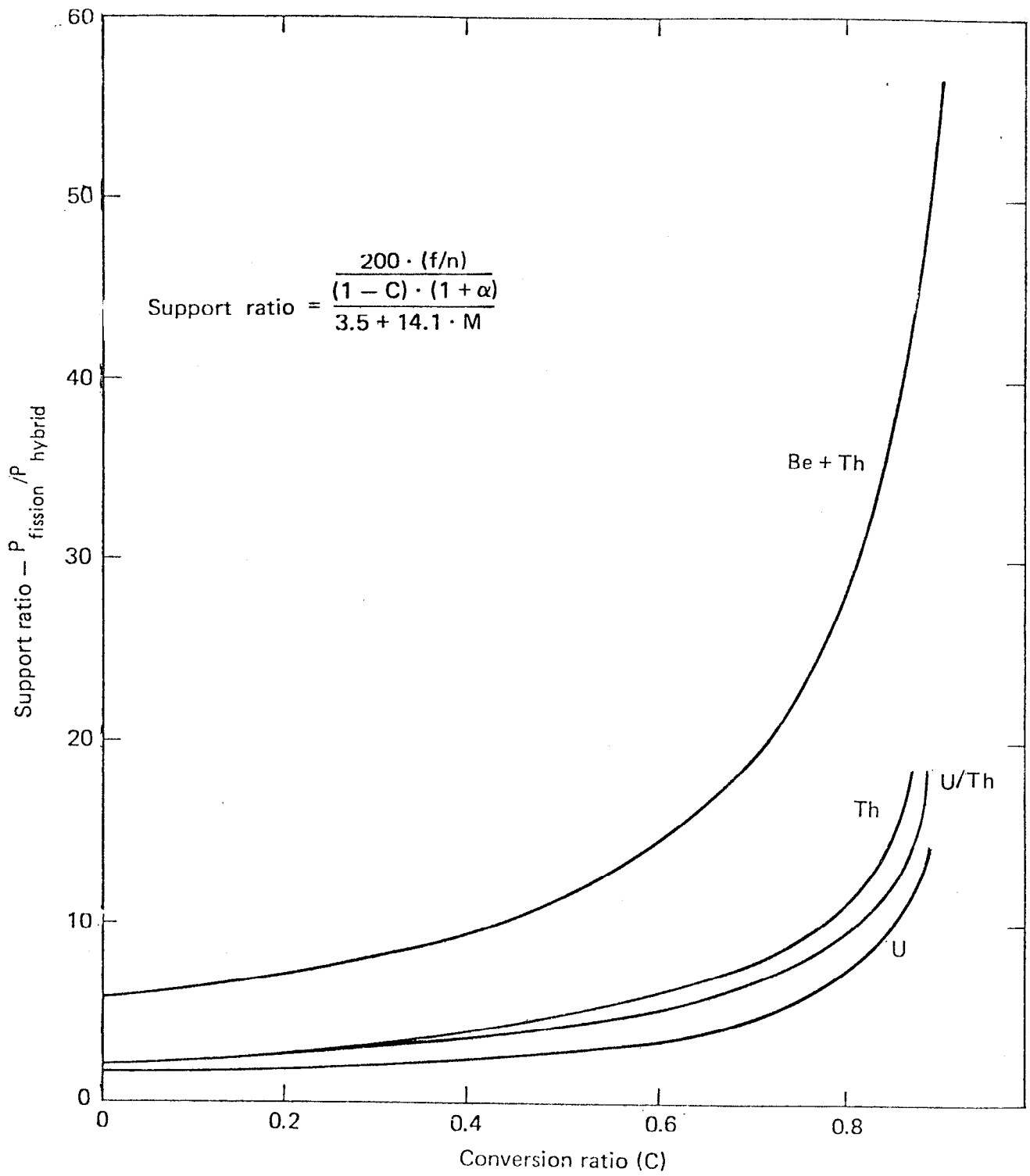


Fig. 5-9. Support ratios for blanket types. $(P_{\text{fission}}/P_{\text{hybrid}})$.

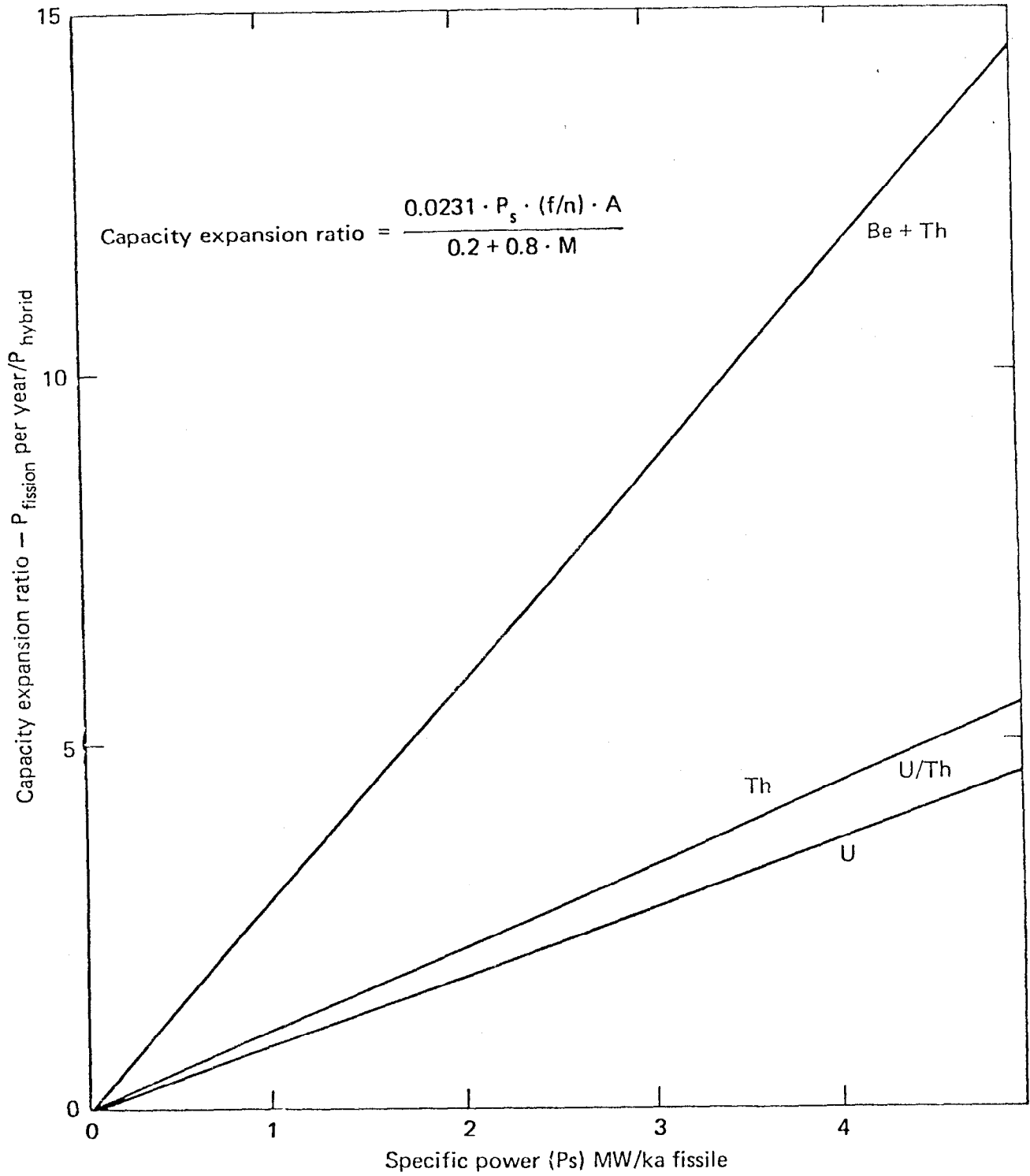


Fig. 5-10. Capacity expansion ratios for blanket types. (P_{fusion} per year/P_{hybrid}).

Support and capacity expansion ratios for the four blankets in Table 5-9 are compared in Figs. 5-9 and 5-10. The term (f/n) stands for fissile breeding ratio of the hybrid, and α is the fissile capture-to-fission ratio in the fission reactors ($\alpha = 0.1$ for ^{233}U , 0.3 for ^{239}Pu).

High support (and capacity expansion) ratios are perceived to be advantageous. Examples of possible reasons are:

- Relatively little or no net electricity will be produced or consumed by the hybrid, therefore integration with electric power grids would not be a major concern. Hybrid capacity could be built rapidly to meet fissile fuel requirements.

- Utility companies will not have to build high-technology fusion systems. They can buy fuel for the simpler fission systems with which they are already familiar. The hybrids would be built by a few private companies or the Government (like enrichment plants).

- If proliferation or diversion problems are real, the smaller the number of secured sites in which fissile production, reprocessing, and fuel fabrication occurs, the more acceptable a fusion/fission economy should be.

- Minimizing relative energy generation in the hybrids may result in lower system electricity costs because of the fusion reactor's less-compact geometry relative to fission reactors. This effect should be dependent on plasma performance, increasing as plasma performance increases. In short, we may not have to pay an economic penalty for a high-support ratio if a high enough plasma performance is achieved.

Assuming that the advantages of high support and capacity expansion ratios are real, we need to find a blanket in which fission is suppressed but still has good fissile breeding.¹⁸ Neutron multiplication without fission and quick removal of bred fissile material are required. A beryllium neutron multiplier and a fertile containing molten salt seem a likely candidate. Such a blanket should contain a large atom fraction of Be and just enough Th and ^6Li in the proper ratio to capture nearly all of the neutrons. Scattering as well as capture by the structure should be minimized by judicious choice of materials and their spartan use. An appraisal of the theoretical nuclear potential of a Be blanket was made by calculating breeding (T and ^{233}U) in a thick Be assembly containing 5-atom percent $^6\text{Li} + \text{Th}$. At a $^6\text{Li}(n,T)$ rate of 1.0 per 14 MeV neutron, 1.7 Th (n,γ) reactions occurred. The tradeoff between $^6\text{Li}(n,T)$ and $^{232}\text{Th}(n,\gamma)$ reactions is displayed in Fig. 5-11.

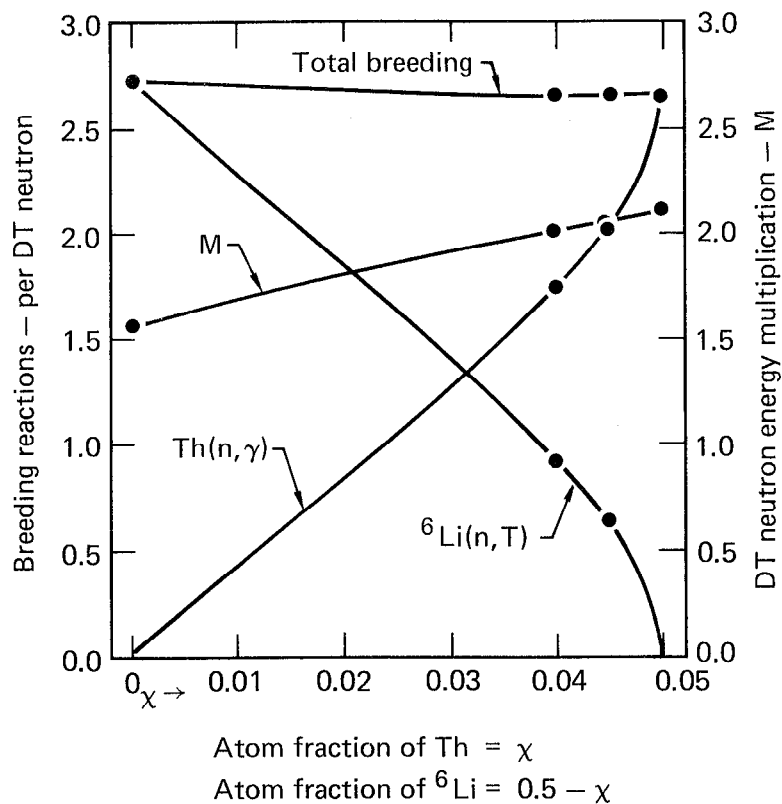


Fig. 5-11. Nuclear potential of Be blanket. [95% Be + 5% (${}^6\text{Li}$ + Th)].

The estimate of nuclear performance of a Be blanket given in Table 5-9 (0.8 ${}^{233}\text{U}$ + 1.0 T) is based on a conceptual Be blanket developed for the standard mirror fusion reactor.²⁰ It remains to be seen if we can achieve similar performance in the proposed molten salt + Be blanket.

Perceived advantages of the molten salt/Be blanket are outlined below:

- Safety (real and perceived).
 - Loss-of-coolant accident (LOCA) problems virtually eliminated by virtue of suppressed fission and the continuous online removal of fission products, as well as the fissile and fusile materials produced.
 - No plutonium produced.
- High-support ratio (implications already discussed).
- Online refueling and reprocessing should result in higher capacity factors and continuous sale of ${}^{233}\text{U}$. Both should improve hybrid economics.

- Low-pressure coolant should simplify mechanical design.

The technology base for molten salt systems is summarized below:

- Aircraft Nuclear Propulsion (ANP) Program 1947-1957; approximately 60M\$ invested in molten salt technology.
- Molten Salt Reactor Experiment (MSRE) (7MW) was built and operated successfully for two and one-half years.
- Demonstrated fuel reprocessing on laboratory scale.
- Developed conceptual design of a 1000-WEe molten salt breeder reactor.

Schematic diagrams of a conceptual molten salt breeder reactor (MSBR) and its reprocessing plant are shown in Figs. 5-12 and 5-13. For our application, the blanket would replace the reactor. The blanket would contain Be as well as graphite. The Be probably cannot stand up to flowing molten salt, so the Be must likely be clad. Metal, graphite, and possibly SiC cladding could be considered. The Be could be in powder form and the clad end caps porous so helium produced in the $^9\text{Be} (n,2n)2 \text{He}$ reaction can escape without causing unacceptable swelling or clad failure.

The reprocessing flow sheet for molten salt blanket could be similar to that shown in Fig. 5-13, except fission produce generation would be very small and all the ^{233}U removed would be sole; none of it would be returned to the salt.

Material selection will be a crucial element of molten salt blanket design. Materials used in the Molten Salt Reactor Experiment (MSRE) and chosen for the MSRE are listed in Table 5-10.

The Russians are also looking at Molten Salt Fusion-Fission (MSFF) systems. Material combinations they are looking at are also listed in Table 5-10. Figure 5-14 shows the blanket layout and some nuclear performance estimates from the Russian work.²² Note there is little or no tritium breeding in their blanket. They propose to breed tritium in the fission reactors.

While much of the Molten Salt Reactor Program technology is applicable, there are important differences in the fusion blanket environment. Low-blanket fission rate should reduce the fission product corrosion problem encountered in the MSRE. On the other hand, high neutron fluxes in structural components (first-wall, etc.), magnetic fields, and much larger tritium production rates will be more demanding of materials. Magnetic fields will induce electric current in flowing molten salt, which could enhance corrosion as could larger concentrations of T or TF.

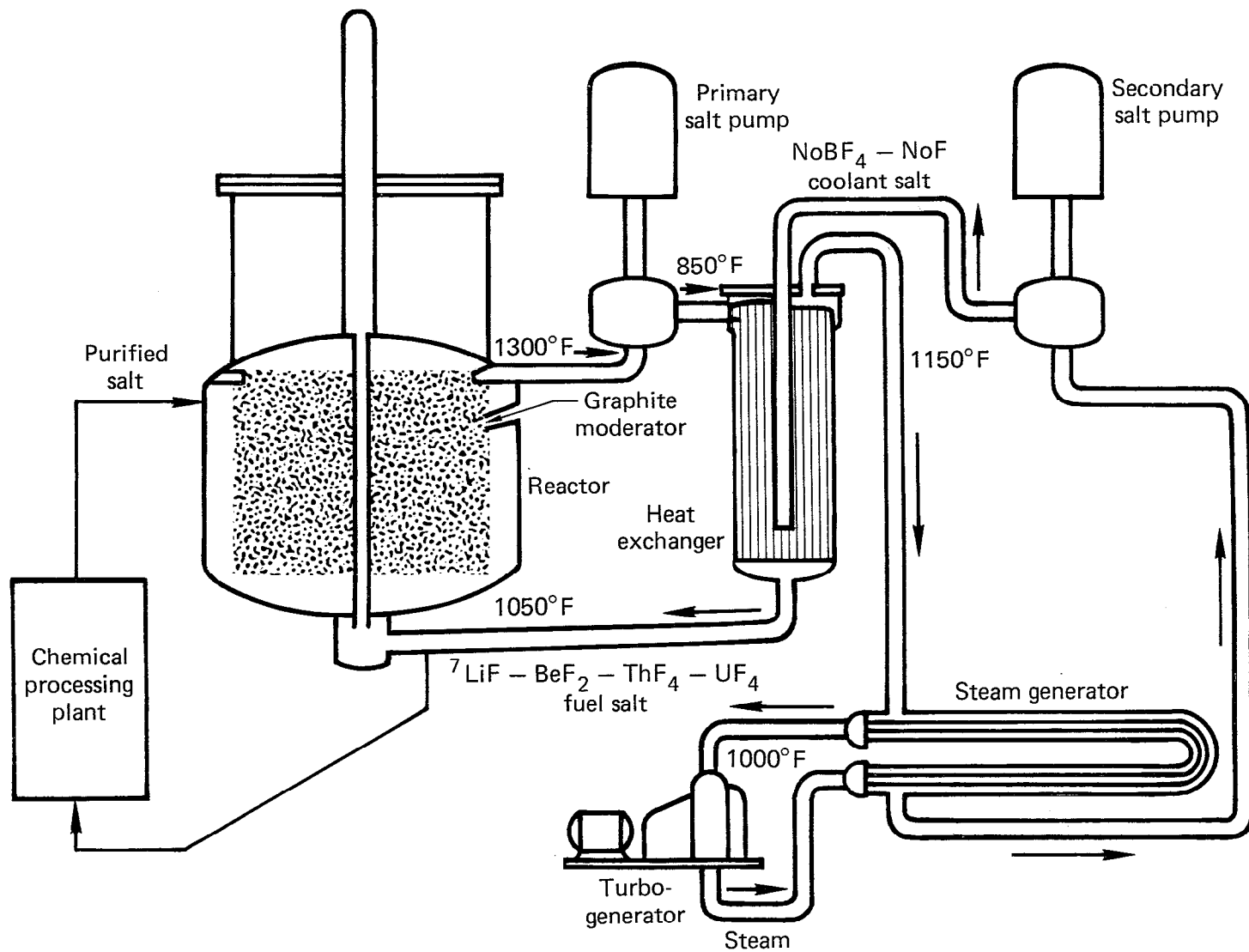


Fig. 5-12. Single-fluid, two-region, molten salt breeder reactor. For 1000 MW(e), the fuel salt flow rate through the core is 55,000 gpm, but less than 1 gpm passes through the processing plant. Electricity is produced from supercritical steam with an overall efficiency of 44% (from ORNL 4812).

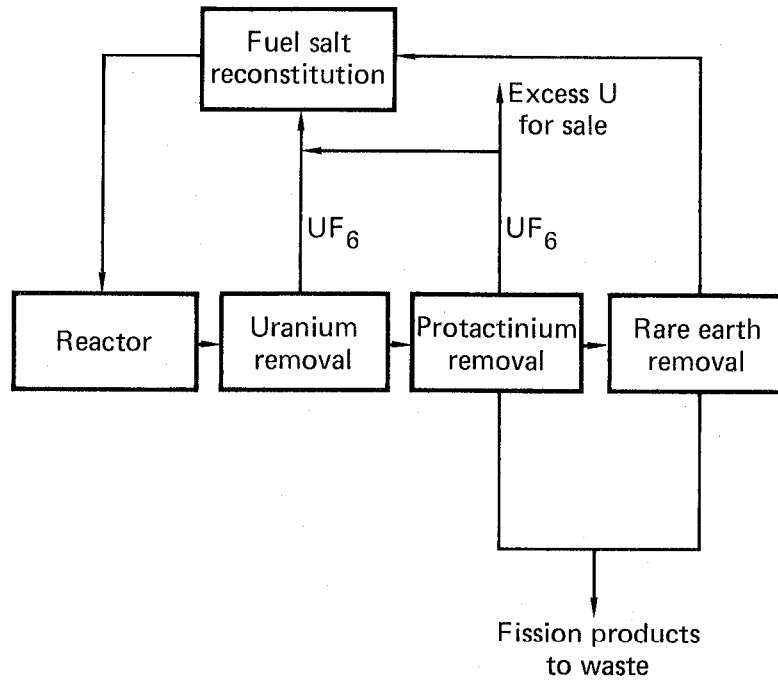
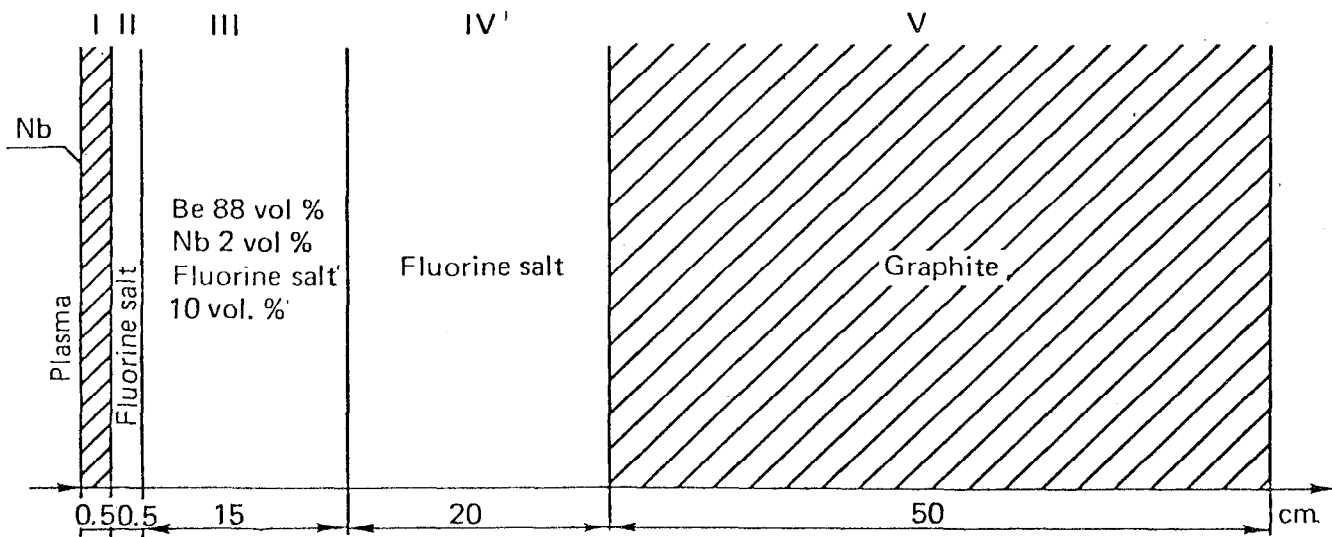


Fig. 5-13. Simplified flow diagram for processing a molten salt breeder reactor (from ORNL 4812).

TABLE 5-10. Materials used in the Molten Salt Reactor Experiment (MSRE) and the Molten Salt Fusion-Fission (MSFF) Systems.

Characteristic	MSRE	MSBR	MSFF (Russian)
Molten salt			
Fuels	LiF (65)	LiF (71.7)	LiF (71)
(Mole %)	BeF ₂ (29)	BeF ₂ (16)	BeF ₂ (2)
	ZrF ₄ (1)	ThF ₄ (12)	ThF ₄ (27)
	UF ₄ (1)	UF ₄ (0.3)	
Liquidus, °C	434	500	560
Structure	Hastelloy N	Modified Hastelloy N	Niobium
Moderator	Graphite	Graphite	Be/graphite
Coolant salts	LiF (66)	NaBF ₄ (92)	
	BeF ₄ (34)	NaF (8)	
Liquidus, °C		385	



Alternative no.	Salt composition, mol. %	Number of Th(n, γ) reactions*	Number of reactions Li (n, n', α) T*	Number of fissions of Th nuclei*
1	${}^7\text{LiF} - 71$ $\text{BeF}_2 - 2.0$ $\text{ThF}_4 - 27$	1.59	0.035	0.0085
2	$\text{NaF} - 71$ $\text{BeF}_2 - 2.0$ $\text{ThF}_4 - 27$	1.51	0.00	0.0110

*Normalized to 1 thermonuclear neutron.

Fig. 5-14. Russian molten salt (fusion reactor) blanket.

An initial attempt to lay out a mechanical design for the molten salt/Be blanket is now described. Our objective is a simple design that can be easily maintained. Partial unassembled as well as assembled views are shown in Figs. 5-15 and 5-16. Close-packed Be and C rods are contained in an annular-cylindrical fuel bundle of some length limited by heat transfer or module handling size limits. The module shown is about 6 m long. One end of the bundle has an orifice plate-to-meter salt flow to match heat transfer requirements. The first-wall is a cylindrical sleeve that fits inside the fuel bundle. The thin, annular gap (~ 1 cm) formed between the first-wall, and the inner fuel bundle jacket allows for first-wall cooling. Annular disks welded to the first-wall sleeve and to the outer jacket of the fuel bundle form the inlet and outlet plena.

The first-wall sleeve and annular disks should be the critical components with respect to radiation damage. Assuming a neutron fluence limit of 2×10^{23} nvt ($E > 0.1$ MeV), we estimate the first-wall and disks would need replacing after an exposure of 21 MW-yr/m^2 . The same fluence limit is reached after $\sim 8 \text{ MW-yr/m}^2$ in fast-fission uranium blankets like the U_3Si blanket used for the standard mirror hybrid. The Be fuel rods are envisioned to consist of Be powder ($\sim 80\% p_{\text{th}}$) contained in graphite (or possibly SiC) cladding. Be powder is assumed to facilitate release of He, and cladding is assumed necessary to protect the Be from flowing molten salt. The rods would have porous end caps for helium release. Conceivably, the Be and C fuel bundle would last much longer than the critical first-wall and end disks. First-wall replacement would require draining molten salt from the blanket and removal of the individual blanket modules followed by disassembly and replacement.

An objective of the mechanical design of this blanket is to minimize the amount of structural materials (first-wall, cladding, etc.) that will compete with the fuels for the neutron's favor. Another objective is no leaks. If first-wall leaks are inevitable, then a guard vacuum sleeve might be needed to protect the plasma from molten salt vapors. We hope that the simple cylindrical design of this blanket would result in a leak-tight first-wall.

A preliminary neutronics appraisal of the conceptual blanket just described is encouraging; calculated reactions per source DT neutron are tritium breeding = 1.35, $^{232}\text{Th}(n,\gamma)$ reactions = 0.82, $^{232}\text{Th}(n, \text{fiss.}) = 0.008$, energy multiplication, $M = 1.53$. This blanket has a 0.5-cm nickel first-wall followed by 100 cm of fuel consisting of (by volume) 10% molten salt, 10%

5-52

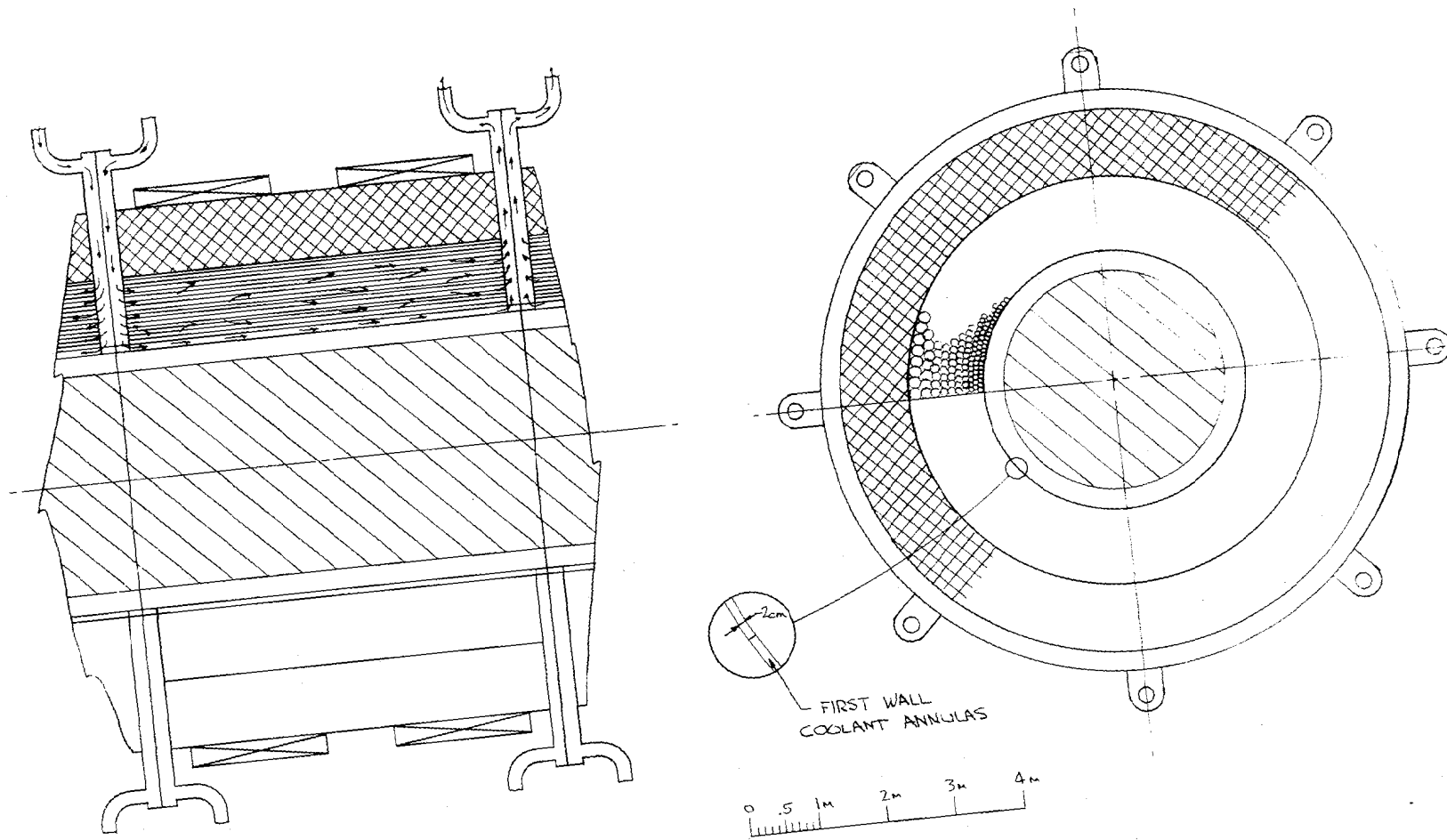


Fig. 5-15. Molten salt blanket concept--partial unassembled view.

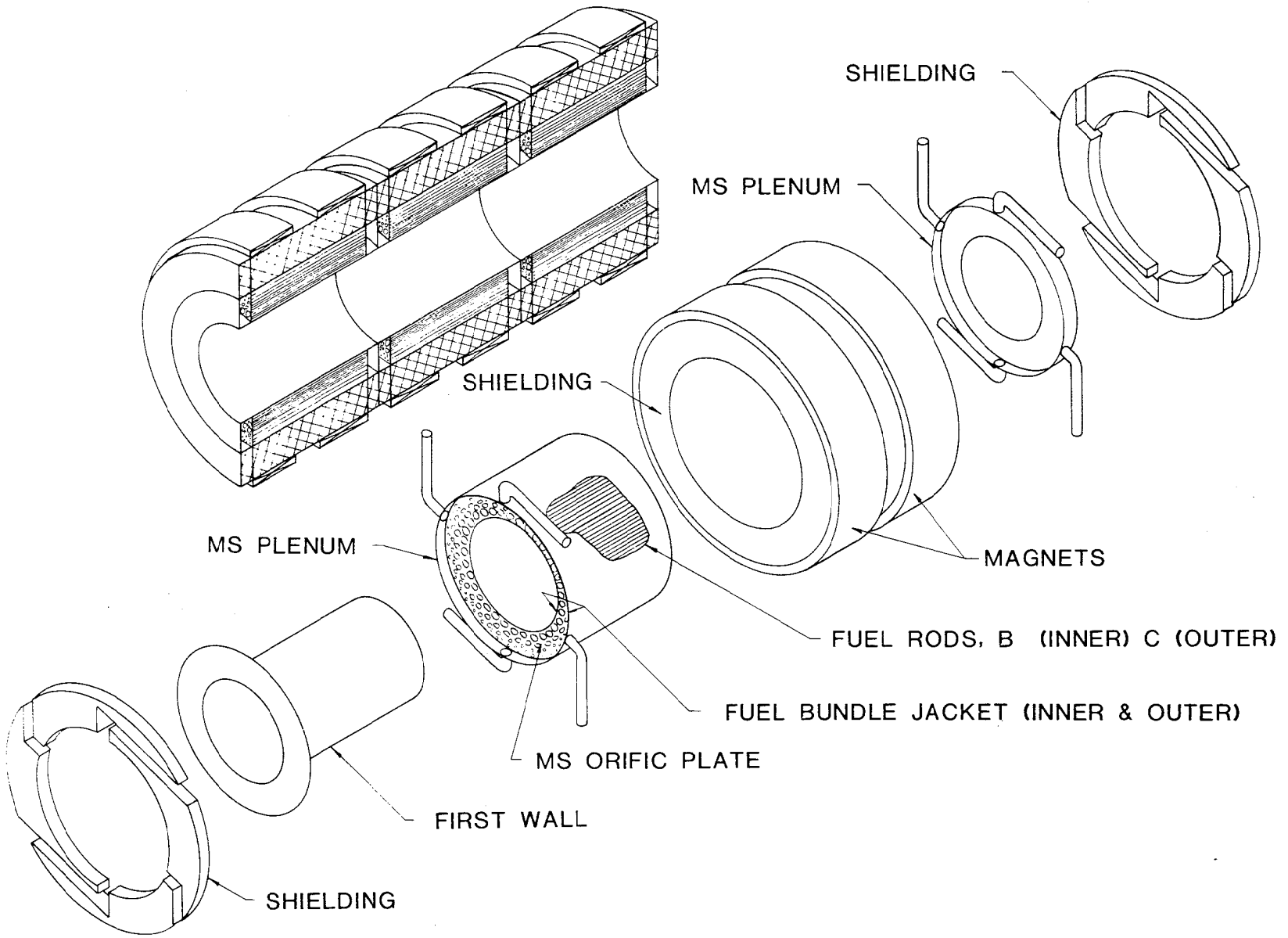


Fig. 5-16. Molten salt blanket concept--exploded view.

graphite cladding, plus 80% beryllium. The molten salt composition is (in mole %) LiF (71), BeF₂ (2), ThF₄ (27); its density is 4.5 g/cc. The Li is depleted to 1% ⁶Li. The liquidus temperature vs composition of the molten salt is shown in Fig. 5-17. For the composition chosen, the melting point is ~550°C.

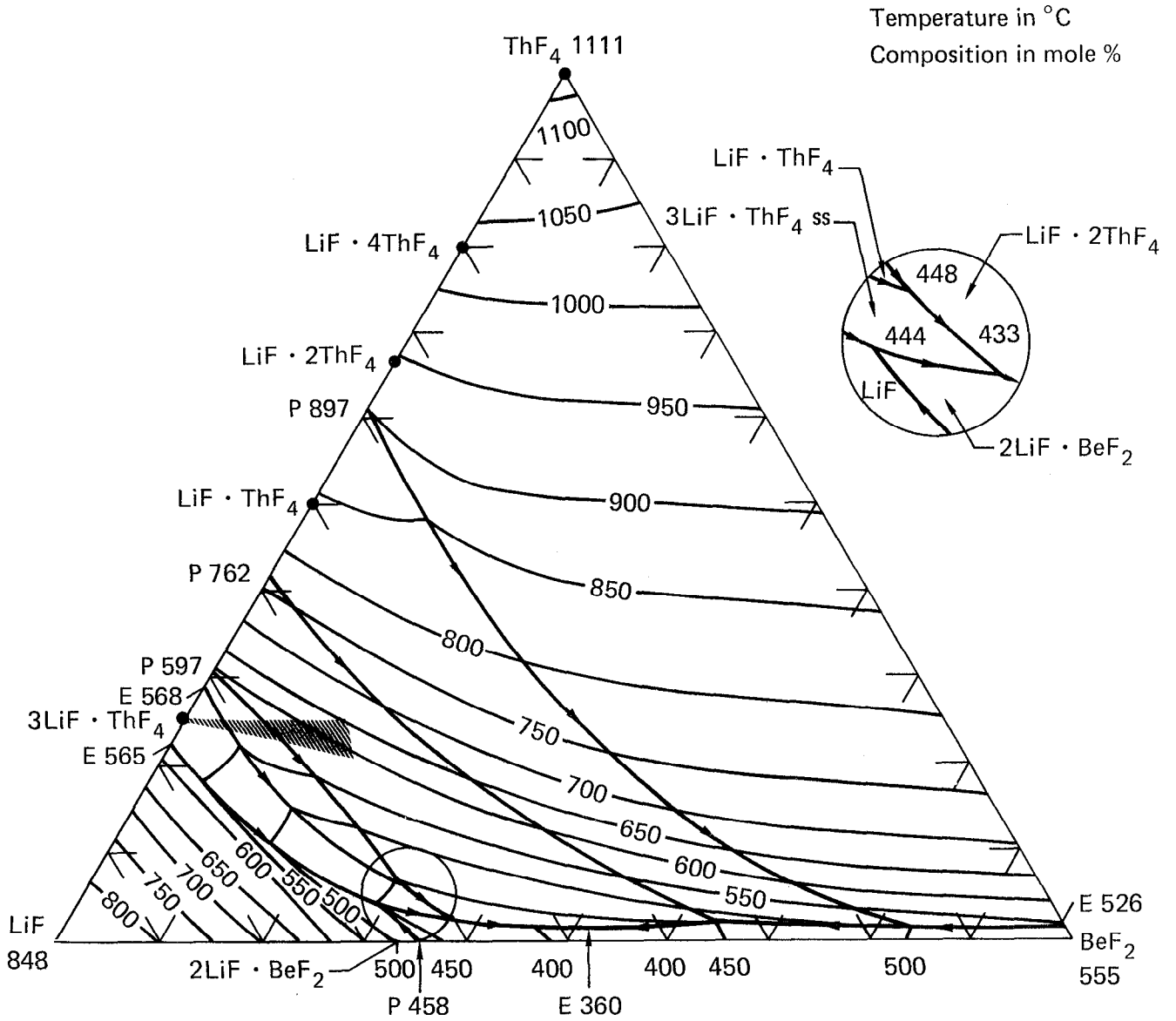


Fig. 5-17. The system LiF-BeF₂-ThF₄.

In summary the Be/molten salt blanket concept has some very attractive features. There is no economic penalty to such a fission-suppressed ^{233}U breeding blanket when compared to the other blanket types considered. There is a technology base for molten salt systems, stemming from the Aircraft Nuclear Propulsion (ANP) and Molten Salt Reactor Programs. However, there are environmental differences in a hybrid blanket that could be important, such as magnetic fields, high tritium generation rate, high neutron fluxes in structural components, and large amounts of beryllium. Materials compatibility will be a major aspect of Be/molten salt hybrid blanket design.

MOLTEN SALT TECHNOLOGY ASSESSMENT

Summary

A summary process description for a molten salt blanket has been made based on the work reported by ORNL for the Molten Salt Reactor Experiment (MSRE)²³ and the Molten Salt Breeder Reactor (MSBR)²⁴ conceptual design.

Fluoride salt discharged from the blanket is processed to separate Pa for decay to ^{233}U , recover the product fissile U, and remove fission products and contaminants from the fertile salt. High temperature (about 600 to 700°C) reductive extraction, fluorination, and metal transfer processes similar to those used for the molten salt fission reactors are used.

Initially, Pa, U, and fission products (excepting Kr and Xe removed as off-gas by sparging) are removed from the blanket salt by reductive extraction. The molten salt is contacted in a counter-current packed extraction column with Bi metal containing Li and Th reductants. The Pa, U, and fission products are extracted into the Bi metal. The fertile molten salt, essentially free of Pa and U, is circulated to a second reductive extraction step.

The Bi metal stream from the extraction step is routed to a hydrofluorination column and contacted with hydrogen fluoride gas in the presence of the Li-Th fluoride recirculating salt stream for the Pa decay system. Pa, U, fission products, and Li in the Bi metal stream are oxidized to fluorides with the hydrogen fluoride gas and are transferred to the Li-Th fluoride salt. The clean Bi stream from the hydrofluorinator is recycled to the reduction extraction steps. The Pa containing salt is transferred to a holdup storage tank for decay to ^{233}U .

After a suitable decay period (about 100 days), the captive salt (with grown-in ^{233}U) is recycled to the hydrofluorinator for use in the oxidation transfer from the Bi metal stream. The salt from the hydrofluorinator is routed to a fluorination column and contacted with F gas. The fissile product UF_6 stream from the fluorinator is recovered for transport to fission reactor fuel fabricators. The recirculating Li-Th fluoride salt is routed back to the holdup storage tank for decay of the Pa transferred from the Bi metal stream at the hydrofluorination step.

The fertile molten salt from the first reduction extraction step, free of U and Pa, is routed to a second reduction extraction column. The salt is contacted with molten Bi-Li-Th alloy to extract the rare earths, alkaline earths, and alkali metals. The metal alloy stream is routed to the cleanup system to remove the rare earths and fission products. As a final step, the blanket molten salt is routed to a gas/liquid contactor and treated with H gas to reduce any remaining corrosion products to metals. The treated blanket salt is passed through a Ni wool bed to react and remove any residual Bi. The blanket salt is passed through final filters to remove reduced metal particulates and is recycled back into the fusion reactor blanket.

The extracted rare earths and fission products in the Bi metal alloy stream from the second reduction extraction step are transferred to molten Li chloride salt. The metal alloy stream is contacted with Li chloride in a packed column. Cleaned Bi metal alloy is combined with the bismuth stream from the Pa system hydrofluorination step and is recycled to the blanket salt reduction extraction columns.

The rare earths and fission products are removed from the recirculating Li chloride carrier salt by extraction into a captive Bi metal alloy stream containing high Li concentrations. Two countercurrent packed extraction columns are used. Trivalent fission products and rare earths are extracted in the first column with a Bi-5 and a Li alloy. The Bi alloy, downstream of the extraction column, is hydrofluorinated in the presence of waste blanket salt. The trivalent nuclides are oxidized and transferred to the waste salt, which is held up in an intermediate term storage vault prior to final waste disposition.

Separation

Chemistry and process technology for the separation of bred Pa/U from the Li fluoride-Th fluoride molten salt is available from the MSRE²³ and MSBR²⁴ work. Engineering scale work,²⁵ using batch processes and nonradioactive simulated nuclides, demonstrated the Bi molten metal reductive extraction process. Mass transfer and process chemistry data were obtained for the separation process. The downstream separation of the fission products and rare earths from the Bi alloy into the recirculating Li chloride salt has also been demonstrated in the nonradioactive engineering scale tests.

No continuous pilot plant or process scale equipment has been operated. Conceptual designs of extraction columns were worked on in conjunction with the MSRE and MSBR tasks.

Cold pilot plant and hot engineering testing will be required for the design and development of separation process and equipment for continuous processing.

Fluorination and Hydrofluorination

Under the MSRE effort batch fluorination and hydrofluorination operations were carried out using the radioactive MSRE fuel salt and the reactor flush salt. Uranium hexafluoride was produced as the product. Engineering studies and tests have been done by ORNL on continuous fluorination equipment using a frozen salt, wall equipment concept.^{26,27}

Blanket Salt Cleanup

Molten salt recycled to the blanket requires thorough cleanup of residual Bi, corrosion products, and metals. The recycle salt cleanup system is conceptual only and will require design, development, and demonstration.

Waste Handling

The primary and intermediate extraction systems for the fission products, rare earths, alkaline earths, and alkali metals are conceptual only. Mass transfer data and process chemistries are applicable from molten salt and liquid metal work. Process and equipment design, development, and

demonstration will be required to obtain a waste byproduct compatible to indicated government policies for final waste treatment and disposition.

Materials

Equipment and process materials selection are basic problems for the molten salt and the Bi metal alloy systems. Molybdenum has been demonstrated to have excellent corrosion resistance to Bi; however, it is very difficult to fabricate. Graphite has been considered as an alternate material. Coating, cladding, or plating of graphite, Mo, or W onto Ni-base alloys may be a satisfactory alternate material system.

Hastelloy N, Ni-base alloy was used for the MSRE salt processing work and was considered for the MSBR salt circuit. However, modified alloys with additives such as Ti, Hf, and Nb were thought to be required to provide satisfactory resistance to neutron irradiation embrittlement for process temperatures of 600 to 700°C.²⁸

For fluorination and hydrofluorination process equipment, Ni-base alloys and Mo do not have satisfactory corrosion resistance. Graphite and graphite clad equipment have been considered²⁹; however, size and complexity are thought to be beyond current manufacturing capabilities. A frozen salt wall concept for continuous fluorination columns has been investigated by ORNL^{26,27} with encouraging results.

Materials and fabrication development and demonstration work will be required for the molten salt and metal alloy process systems and equipment.

CONCLUSIONS

WATER-COOLED BLANKETS

We examined a variety of blankets using liquid, steam and two-phase water. The great advantage of water coolant systems is the vast amount of knowledge available on such systems. Several designs appeared to be feasible. However, each design suffered a reduction in fuel breeding because of the moderation of the neutrons by the water. This reduction is significantly greater for ²³³U production than for Pu production. Another problem with water cooling is the difficulty of tritium decontamination. Steam was considered, but was found to be only marginally better than halium.

Corrosion was also a problem. For these reasons, further work on water cooling was discontinued.

LIQUID METAL COOLING

Liquid metal cooling was not considered at an early stage because of the increased hazard relative to helium and because of MHD-related design problems, such as loss of wall coverage due to inlet and outlet manifolds. If sodium was the primary coolant, a great deal of technology from the liquid metal fast breeder program could be used directly. We felt feasible design solutions existed for liquid metal cooling, and further work is appropriate if other coolants having greater safety prove unfeasible or less desirable.

MOLTEN SALT

Molten salt was a case study of an example of a broad class of blanket options having the following characteristics:

- Fission suppression by an order of magnitude over fast-fission blankets resulting in less hazard from fission products. Loss-of-coolant accident hazards are virtually eliminated.
- The large number of fission reactors (>20) supported by one such fuel producer leads to desirable deployment scenarios and favorable economics compared to fast-fission blankets.
- Online processing allows removal of certain fission products and bred-fissile fuel.

We saw great virtue in the class of fission-suppressed blanket concepts, and further work was done and is presented in Section 7. A comparison between molten salt and helium cooling is discussed in Section 10.

HELIUM COOLING

The helium-cooled thorium metal blanket was found to perform as well as expected. As predicted earlier, the study continued to show the feasibility of this method. The helium-cooled design can take advantage of the rather large world-wide development work in that field. The fission rate is such that with no cooling, fuel damage would occur in about 10 min after shutdown, requiring a reliable emergency cooling system. The power density is such,

however, that ^{238}U fast-fission blankets would have fuel damage under similar conditions in about one minute.

Further work was carried out on helium cooling (Section 6) and the method is compared to molten salt (Section 10).

REFERENCES

1. R. W. Moir, Editor, "Interim Report on the Tandem Mirror Hybrid Reactor Design Study," Lawrence Livermore Laboratory, Rept. UCID-18078 (1979).
2. G. M. d'Hospital and P. Fortescue, "On the Choice of Gas Coolant for Nuclear Reactors," General Atomic Co., Rept. GA-7344 (1966).
3. G. M. d'Hospital and M. Simnad, "Status of Helium-Cooled Nuclear Power Systems," General Atomic Co., Rept. GA-A14067 (1976).
4. G. M. d'Hospital and G. R. Hopkins, "Gas Cooling for Fusion Reactor Blankets," General Atomic Co., Rept. GA-10004 (1970).
5. P. H. Sager, "Thermal Power Conversion Systems for Fusion Power Plants," General Atomic Co., Rept. GA-A13405 (1975).
6. D. J. Bender, et al., "Reference Design for the Standard Mirror Hybrid Reactor," joint Lawrence Livermore Laboratory and General Atomic Co. report, UCRL-52478/GA-A19796 (1978).
7. G. A. Carlson, et al., "Definition and Conceptual Design of a Small Fusion Reactor," EPRI report to be published.
8. J. A. Maniscalco, "Fusion-Fission Hybrid Concepts for Laser Induced Fusion," Nucl. Tech. 28, 98 (1976).
9. K. R. Schultz, et al., "Evaluation of the ^{233}U Refresh Cycle Fusion-Fission Power System Concept," General Atomic Co., Rept. GA-A15108, to be published.
10. D. J. Bender and J. D. Lee, "The Potential for Fissile Breeding with the Fusion-Fission Hybrid Reactor," Lawrence Livermore Laboratory, Rept. UCRL-77887 (1976).
11. K. R. Schultz, "A Review of Hybrid Reactor Fuel Cycle Considerations," General Atomic Co., Rept. GA-A14475 (1977).
12. D. J. Bender, Editor, "Reference Design for the Standard Mirror Hybrid Reactor," joint Lawrence Livermore Laboratory and General Atomic Co. report, UCRL-52478/GA-A14796 (1978).
13. Tandem Mirror Hybrid Reactor Interim Report

14. N. N. Vasiliev, M. G. Kuznetsov, G. E. Shatalov, and A. A. Borkov, "A Hybrid Reactor Blanket Based on an Open Trap with Double Plugs (TROL)," presented at the U.S.-U.S.S.R. Workshop on Hybrids, Jan. 22-26, 1979, Princeton, New Jersey, Translation Lawrence Livermore Laboratory, Rept. UCIR-1286 (1979).
15. R. W. Moir, et al., "Preliminary Design Study of the Tandem Mirror Reactor (TMR)," Lawrence Livermore Laboratory, Rept. UCRL-52302 (1977).
16. D. J. Bender, et al., Reference Design for the Standard Mirror Hybrid Reactor, joint Lawrence Livermore Laboratory and General Atomic Co. report, UCRL-52478/GA-A14796 (1978).
17. D. J. Bender and J. D. Lee, The Potential for Fissile Breeding with the Fusion-Fission Hybrid Reactor, Lawrence Livermore Laboratory, Rept. UCRL-77887 (1976).
18. D. J. Bender, "The 'Best' ²³³U Producing Blanket for the Tandem Mirror Hybrid," Lawrence Livermore Laboratory, Rept. UCID-17823 (1978).
19. J. D. Lee, "The Beryllium/Molten Salt Blanket--A New Blanket Concept," Third U.S.-U.S.S.R. Symposium on Fusion Fission, January 1979; Lawrence Livermore Laboratory, Rept. UCRL-82663 (1979).
20. R. W. Moir, et al., "Standard Mirror Fusion Reactor Design Study," Lawrence Livermore Laboratory, Rept. UCID-17644 (1978).
21. M. W. Rosenthal, P. N. Haubenreich, and R. B. Briggs, Molten-Salt Reactor Program, The Development Status of Molten-Salt Breeder Reactors, Oak Ridge National Laboratory, Rept. ORNL-4812 (1972).
22. V. L. Blinkin, V. M. Norikov, Optimal Symbiotic Molten-Salt Fission-Fusion System, Kurchatov, IAE 2119 (1977).
23. Lindauer, R. B., "Processing of the MSRE Flush and Fuel Salts," Oak Ridge National Laboratory, Rept. ORNL-TM-2578 (1969).
24. W. L. Carter and E. L. Nicholson, "Design and Cost Study of a Fluorination--Reduction Extraction--Metal Transfer Processing Plant for the MSBR," Oak Ridge National Laboratory, Rept. ORNL-TM-3579 (1972).
25. J. R. Hightower, Jr. and H. C. Savage, "Engineering Tests of the Metal Transfer Process for Extraction of Rare-Earth Fission Products from a Molten-Salt Breeder Reactor Fuel Salt," Oak Ridge National Laboratory, Rept. ORNL-5176 (1977).
26. "Engineering Development Studies for Molten-Salt Breeder Reactor Processing," report series. See Oak Ridge National Laboratory, Rept. ORNL-TM-5041 (1976).

27. "Molten Salt Reactor Program Semi-Annual Progress Report," report series. See Oak Ridge National Laboratory, Rept. ORNL-5132 (1976).
28. H. E. McCoy Jr., "Status of Materials Development for Molten Salt Reactors," Oak Ridge National Laboratory, Rept. ORNL-TM-5920 (1978).

SECTION 6.
HELIUM-COOLED SYSTEM DESIGN

(K. Schultz)

During the scoping phase of the Tandem Mirror Hybrid Reactor (TMHR) design effort, various He-cooled blanket options were considered and a metal-clad, Th-based fuel design was chosen for further study. This scoping phase work is described in Section 5 of this report. The preliminary conceptual designs presented in this section were developed from the initial concepts considered during the scoping phase. Two distinct approaches emerged for the blanket design. General Atomic Co. (GA) proposed a large module approach, based on segmenting the reactor into large axial slices, removed as a unit for offline maintenance, and developed the preliminary conceptual design described in Section 6. General Electric Co. (GE) developed the linked fuel option based on moveable fuel with minimum disassembly of the reactor and developed the preliminary conceptual design also described in Section 6. Bechtel National Inc. developed the He-cooled, balance-of-plant (BOP) design discussed in Section 6 that should be applicable to either blanket design option.

INTRODUCTION TO BLANKET DESIGN

The tandem mirror reactor is characterized by low plasma power amplification but can operate in a steady state mode. The low Q_p capability implies the need for a significant neutron interaction rate in the blanket to provide blanket energy multiplication if energy production is a major design goal. In a fuel- and energy-producing hybrid, fissile fuel is the primary product although significant amounts of energy may be produced by neutron interaction with the blanket internals. The He-cooled design is a good example of this situation. A fuel-producing hybrid would attempt to minimize the energy and fission product production in the blanket by suppressing fission. Neutron multiplication through (n, 2n) reactions is used to improve breeding performance. The intent in suppressing fission is to simplify blanket design and handling by operating at a low power density with low after heat and very small quantities of fission product waste. The molten salt blanket typifies these design considerations.

Both U and Th fuel blankets can produce significant amounts of fissile fuel. If this fuel is burned in a thermal spectrum fission reactor, a large number of burner reactors could be supported by each hybrid reactor. The lower breeding performance of the Th blanket is offset by the higher value of the bred ²³³U as a fuel for thermal burner reactors. In addition to bred fissile fuel, the hybrid blanket can also produce significant energy multiplication of the fusion neutron energy. This can produce very high power densities in the blanket fuel material. The high performance potential of hybrid systems results in a challenging design environment. Structural concerns will play an important role in the tradeoff between high performance and design simplicity for hybrid reactor systems.

Interaction of the 14 MeV D-T fusion neutrons with the fertile materials in the blanket of a hybrid reactor can result in significant neutron and energy multiplication. Both U and Th exhibit significant (n, 2n), (n, 3n), and (n, fission) reactions with 14 MeV neutrons. Since the fertile blanket of the hybrid reactor is highly subcritical, the power density gradient in the blanket can be quite steep, which can lead to differential thermal expansion and radiation-induced swelling with resulting stress in the blanket materials. The energy multiplication of the hybrid blanket also worsens the thermal cycling problems associated with the transient response of the blanket.

Because the hybrid blanket can experience a significant fission power density, it can build up a fission product inventory with its associated after-heat and radiological hazard potential. As a consequence, it is expected that some hybrid blanket structures will have to be treated as fission reactor primary containment structures under design rules such as the ASME Section III, Class 1 design code. This requirement may ultimately result in stringent design conditions because loss of ductility appears to be one of the primary limitations to the lifetime of structural materials located in areas of significant fusion neutron fluence, and this effect is strongly temperature-dependent. This could lead to the possibility of brittle failure of the primary coolant pressure boundary.

As fissile material is bred into a hybrid blanket, the energy multiplication increases. To minimize the reactor-average power variation, it is advantageous to refuel the blanket continuously or in staggered increments rather than all at one time. This, plus the low exposure, results in the desire for fairly frequent, perhaps annual, refueling. The need to refuel frequently

implies the need for blanket structural design that can be readily disassembled and reassembled. Since the blanket pressure boundary may also have to serve as the plasma vacuum chamber wall, the need for easy disassembly will require a careful structural design.

Despite the severe design environment, the structural design of a hybrid blanket must be quite efficient because the blanket performance is quite sensitive to the amount of structural material located in the fuel zone. It is clearly important to minimize the amount of structure in the blanket, the thickness of the wall between plasma and blanket, and the amount of other materials (such as coolant) used in the blanket. In a molten salt-cooled blanket, the volume fraction of coolant becomes even more critical than for other coolants because the coolant is also the breeding fuel. Too little coolant degrades breeding performance due to excessive neutron absorption by other blanket materials, while too much coolant degrades breeding by displacing the neutron multiplying medium in the blanket.

Although the fuel production capacity of the fission-suppressed blankets appears modest compared to gas-cooled fission blankets, the much lower energy production allows the fuel production per unit of hybrid reactor power to be quite high. This allows a large number of fission burner reactors to be supported by one hybrid reactor. The relative advantages of high performance, high support ratio, design simplicity, and potential safety concerns are still uncertain. In the final analysis, the fission suppressed hybrid may prove to be very desirable.

Plasma-wall interactions are a concern for all fusion reactors, and there appears to be no significant difference between pure fusion and fusion-fission systems.

$$P_{\text{fusion}} \propto \bar{\sigma}_{DT} E_F \frac{n^2}{4} ;$$

$$Q = P_{\text{fusion}} / P_{\text{injection}}$$

Low Q implies high $P_{\text{injection}}$, but P_{fusion} is independent of Q.

As in all nuclear systems, materials behavior is vital to the success of fusion-fission reactors. The reactor structure, fuel, and cladding materials must exhibit adequate lifetime under irradiation and must show predictable behavior during this lifetime.

Radiation damage is, of course, of prime concern for fusion-fission reactors. Gas production and atom displacement damage are a concern in the structural materials and also in the nuclear fuel and cladding. Fission burnup is also a concern.

Materials compatibility for fusion-fission blankets may be more of a concern than for pure fusion reactors. Since the blanket must accommodate more materials, the possibility for interactions is increased. Reactions between fuel and cladding, cladding and coolant, and fuel and coolant in both the fertile zone and Li compound zone are possible. In addition, the possibility of reactions between the fertile material, the coolant, and the Li compound must be considered under possible accident conditions.

The materials concerns associated with hybrid reactors do not appear to be unique. Rather they are an overlapping of the concerns held for fission reactors and those of fusion reactors. The principal fission fuel material concerns associated with the structural materials (first-wall and cladding) are related to the high fluence of very high energy neutrons. Except for the possibility of increased plasma-wall interaction for low Q_p systems described above, the first-wall problems are not significantly affected by the hybrid blanket.

Fuel cycle economics appear to dictate the removal of the fuel at fairly low exposures. Further, there is no economic incentive to push to higher fluence limits. It should be noted, however, that the structure does not have to be replaced at the economic optimum fuel removal time. Clever design may allow fuel replacement without structure replacement. In addition, further optimization studies may show that higher reprocessing costs encourage a longer fuel life. The low exposure expected in the hybrid blanket has prompted interest in metallic fuels. The higher density of fertile atoms and lower density of nonfuel atoms in metallic fuels offer an improvement in the neutronic performance of hybrid blankets; however, continuous reprocessing benefits will favor molten salt blanket designs.

Hybrid blankets, like pure fusion blankets, are generally annular regions about one-meter-thick and wrapped around plasma vacuum chambers with characteristic dimensions on the order of a few to tens of meters. The blanket components are typically thin shell structures. Due to the large surface to volume ratio of these blankets, they tend to contain a lot of structure and may be composed of many small parts to accommodate the awkward geometry of the plasma chamber. Because of this, fabrication cost for hybrid reactor blankets

may be quite high. Solution to materials concerns for fission reactors frequently involved very precisely made fuels, materials, and components. For hybrid systems, innovative and economic fuel materials and fuel designs are very important. The fuel material and design must be capable of withstanding the environment and yet must be easy to fabricate, refuel, and maintain.

LARGE MODULE APPROACH

The TMHR gas-cooled blanket concept developed by GA is a direct extension of the preliminary work done originally to help select the blanket coolant. A large module configuration was proposed for the He-cooled design. This approach segments the reactor into large axial slices, which are moved laterally to a remote service area for offline maintenance. The reactor blanket consists of 16 of these large modules, two of which are replaced every calendar year. The design philosophy that led to this large module approach is discussed in this section, and the performance characteristics of the resulting design are presented.

DESIGN PHILOSOPHY AND CONCEPT

There are four basic requirements that must be considered in the design of a hybrid reactor blanket. First, it must show good nuclear performance. The reactor average tritium breeding ratio must be greater than 1.1 T/n. The net fuel breeding ratio must be as large as possible. If energy production is a major goal, the blanket energy multiplication must be high without consuming the bred fissile fuel. The requirement for good nuclear performance implies the need to minimize the amount of extraneous structural materials in the blanket zone.

Second, the blanket design must exhibit good thermal-hydraulic performance. A large fraction of the blanket energy must be captured at high temperature to allow high efficiency power conversion from thermal energy to electricity. The pressure drop through the blanket and around the primary coolant loop must be kept to acceptable levels while still allowing adequate flow velocity for good heat transfer. An upper bound of about 4% $\Delta p/p$ is allowed for conventional single-stage He circulators. In addition, the

pumping power requirement should not exceed a few percent of the total thermal power.

Third, the mechanical design must be sound. The blanket must be mechanically feasible and easily fabricated. The structural design must accommodate a wide variety of environmental constraints including coolant pressure loads, thermal stress, radiation-induced swelling and creep, and seismic forces. Of prime importance is the requirement for easy maintenance. The severe fusion thermal and radiation environment implies the need for regular maintenance, repair, and replacement. The mechanical design must facilitate this expected maintenance while allowing for minimum reactor downtime.

Finally, the blanket must exhibit acceptable safety and economic characteristics. The design features must not compromise safety considerations and should enhance the safety aspects of the design as much as possible. Since the purpose of this design work is a commercial reactor, it is important that economics be given serious consideration.

The performance requirements led us to minimize the structural to solid fraction in our blanket design. Since the neutron flux decreases exponentially from the first-wall towards the shielding region of the reactor, efforts were made to design the blanket to fit the neutron flux such that minimum structural to solid fraction was maintained at the first-wall region, the fertile material zone, and the tritium breeding region of the hybrid reactor blanket. Because of this, the design of a modularized first-wall was developed. Instead of a simple tubular first-wall with a thickness of 3-4 cm, the first-wall is composed of 40 submodules, each with a semicircular first-wall 0.5-cm thick, which forms the plasma chamber and high pressure He pressure boundary. The plate geometry blanket fuel design was also evolved from the same basic requirement in order to avoid the geometric restrictions of cladding fraction and packing fraction limits of other geometries, e.g., rods or balls. With the selection of a plate design for the fuel, the plate cladding thickness is then restricted by manufacturing and mechanical design limits.

The maintenance requirement led us to our maintenance design philosophy, which is to avoid remote maintenance and repair work on the reactor if at all possible. This is attempted by making components modular and as large as practical and by removing the entire component to an offline repair area for maintenance. Welded joints that require cutting and rewelding appear to be

particularly time consuming and are to be avoided if at all possible. Accomplishing this goal requires special design for all components to maximize maintainability. That is, each component must specifically be designed to operate remotely. We have found that using conventional design approaches and then trying to maintain this equipment using remote manipulations are extraordinarily time consuming. For example, fastening a conventional nut and bolt using a general purpose remote manipulator takes about 100 times as long as it would manually. On the other hand, a special purpose fastening device that accomplishes the same function as the nut and bolt can be operated in 1/100 the time as manual fastening of the nut and bolt. This special purpose fastening device costs considerably more than a nut and bolt, but we feel that it can pay for itself in reduced downtime.

To realize the potential advantages of trying to do all maintenance offline, it is important that we try to make all the components of the reactor modular and fairly easily removable. This includes not only anticipated maintenance but also unexpected repairs. Given the severity of the fusion blanket design environment and the uncertainties about materials and technology performance in this environment, we must anticipate replacement and repair of all parts of the reactor system. To this end we have proposed that the entire reactor--first-wall, blanket, shield, magnets, coolant piping and support components--be easily and routinely removable.

The maintenance philosophy described above developed as a result of our tokamak design studies. In a tokamak application of this philosophy has proven to be a difficult task. The good plasma confinement characteristics of the tokamak are purchased at the expense of awkward reactor topology. The tandem mirror appears to offer unique advantages in the maintenance area. There are no interlinked coils; there is no axial current path at all. Thus, the reactor can be broken into axial modules that are virtually not connected to each other. No coolant paths, current path or structural path need run between the modules. The only connection between modules is for vacuum sealing and, if a vacuum vault is used, even this connection need have only minimal characteristics.

To summarize our maintenance design philosophy, we offer three major points. First, we want to be able to disassemble the entire reactor in as large pieces as practical and to perform maintenance in an offline maintenance area. Second, we believe that to accomplish rapid maintenance, we must have and be able to economically justify special purpose maintenance equipment,

such as remote operating pipe joints. And, finally, we must take maximum advantage of the natural maintenance advantages that the tandem mirror reactor has.

MECHANICAL DESIGN

A major concern of fusion reactor design is the time required for remote maintenance of the reactor blanket. Since the first-wall/blanket region must operate in a hostile environment, contain high pressures at high temperatures, and maintain the plasma chamber vacuum, the design of a blanket/ first-wall that will satisfy these requirements and allow rapid maintenance is a difficult task. The tandem mirror reactor concept enjoys a simple cylindrical geometry with relatively unobstructed lateral access. The design of the gas-cooled TMHR module concept has emphasized utilization of this geometry to allow rapid maintenance and changeout of the blanket/first-wall zone.

The objective at this stage is to produce a soft design that is tolerant of change of input numbers by perhaps 50% without requiring change of principal or configurations. As the connecting link between physics and materials, the mechanical design should provide a good buffer between excursion by either discipline.

Reactor Orientation

The first mechanical factor considered in this design was reactor orientation. While some advantages were seen for a vertical machine, it was not really practical to build it above ground because of the earthquake resistance requirements, and the alternate below ground machine carried not so much reactor penalties as direct converter problems at the lower end. These required difficult shaft bottom excavation that would negate the normal advantages experienced in foundation design for deep silos. The ease of surface access to all major components led us to settle for the horizontal configuration and tolerate the large foundation necessary.

Reactor Modularity

A reactor this size must essentially be broken down into modules, to be maintainable with acceptable downtime. Options considered were:

- Transverse slices. This was selected and is discussed below.
- End access. This is cumbersome since removal of any element involves breaking into the end magnet area as the element is withdrawn. The requirement for fine manipulation in restricted spaces ruled this out.
- Separate pieces pulled radially off the first-wall. Complex pressure containment made this unacceptable.
- Radially pulled rods. These handled very badly, had a poor packing fraction, and required many seals.

Subgroups of the above were also considered. The approach finally emerged where a large piece of the machine could be rapidly changed (i.e., replaced with a fresh one) and taken to an offline area for a less intensive service schedule not connected to reactor working time. Sixteen such large modules of total length 39 m were finally chosen.

The reactor layout for the long, cylindrical TMHR is based upon use of a hot vault with lateral access to a maintenance area that could be entered when the vault is closed. Figure 6-1 shows how the large module might be installed in a hot vault from which it could be rolled out, having had its probes that carry the module services disconnected behind the main biological shield. The door shown could be rolled clear in any convenient direction giving access from the vault to the maintenance areas. No problems of principal were found with the concept of rolling the modules out on a wheeled truck. Foundation pressures would be conventional. Standard journal bearings also are feasible, although six rails are required with perhaps eight wheels of 60 cm diam per rail for each 3.5-m module. The truck chassis is shown in Fig. 6-2. This could be made of nonmagnetic material if necessary and appears to be designable. It would, however, require some suspension softness to ensure that the load was properly shared with the many supporting elements.

When the decision was made to cut the reactor transversely, the ability to get geometric access to the ends of a slice, once pulled offline, gave us the freedom to design the shield and blanket radially symmetric, which leads to the most efficient neutronics. Neutronics considerations indicate that only 1% of the heat deposition takes place in the shield volume; hence it is possible to either water-cool, or low-pressure gas-cool, the shield. As a

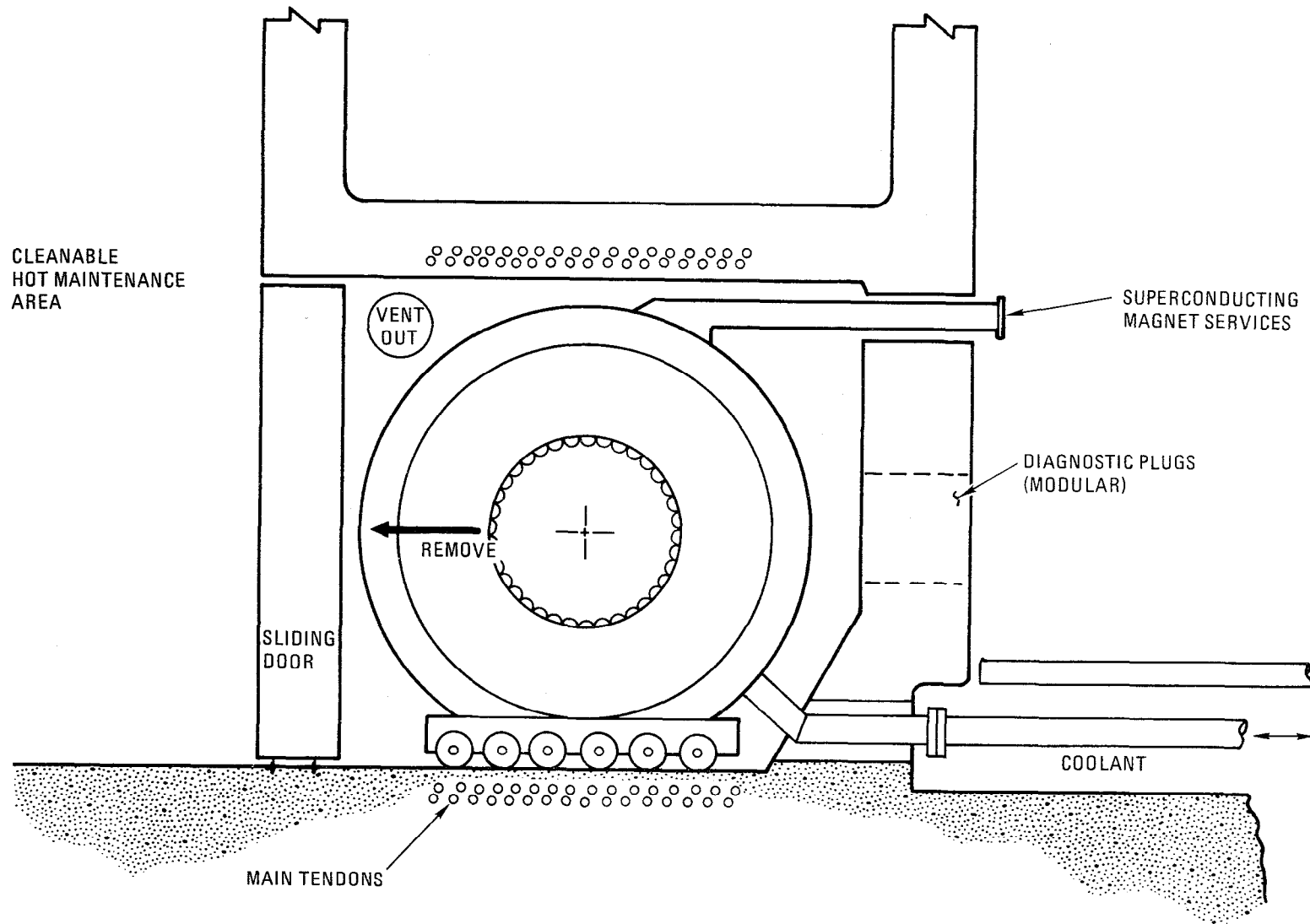


Fig. 6-1. Large module maintenance concept.

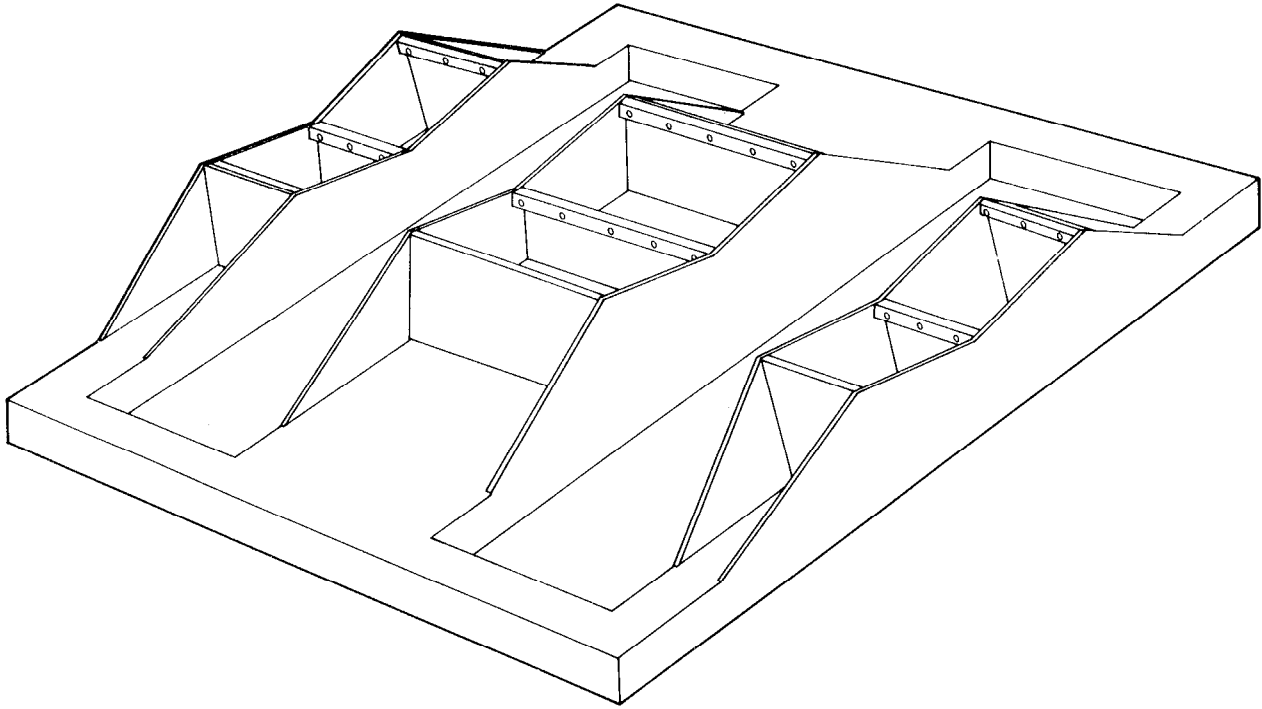


Fig. 6-2. Module truck chassis.

result, the shield can be fairly easily broken transversely. The blanket requires a hard end to resist the high coolant pressure at the break. It appears probable that such a hard end of an inside radius of 2 m and an outside radius of approximately 2.5 m can be configured to be coolable. This leads us to make the blanket and shield separable. Gaps for thermal expansion are necessary, particularly on the blanket cylinders. Each module is therefore structurally self-sufficient and easily mobile. Figure 6-3 shows the proposed movement paths.

Vacuum Seal Configuration

To close the vacuum in the plasma chamber, it is necessary to seal between the modules. This is achieved with a seal driven by an inflatable, all-metal cushion between the shields. Deflation of this cushion provides maneuvering from between the shields.

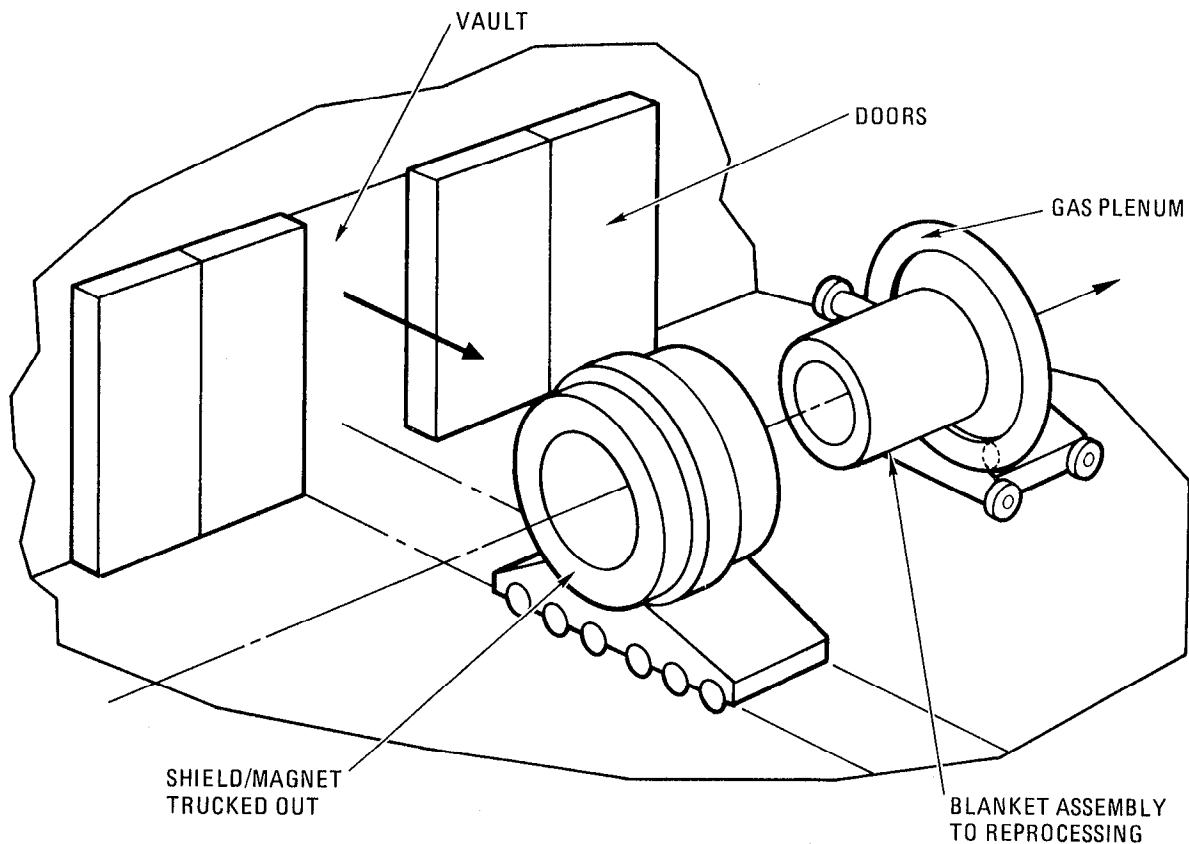


Fig. 6-3. Blanket changeout movement paths.

Inflatable Cushion

Various alternates for achieving the extensible shells of the inflatable cushion were considered. Simple bellows suffered severely from pressure-generated bending stress and coning plates, and being extremely compact, they required large supporting structures and were very bulky. The omega joint (Fig. 6-4) was selected because at large ratios of diameters it becomes very efficient in deflection generation. With proper design it can be arranged to have a low and uniform stress pattern while the machine operates.

Vacuum Seals

Only those seals related to running and maintenance operation are here considered, while others are considered conventional. The factors presented above removed any pressure seals from online environment. The available

alternates for vacuum sealing were online skate welding and mechanical knife seals.

The existence of very large forces at the module ends led to the proposal that these forces could be brought to bear on knife type vacuum seals (Fig. 6-5). These would be of the double-type with evacuated interspace. The achievement of required loads per unit length according to existing practice for these seals is easily demonstrated, and considerable insensitivity to installation inaccuracy can be shown. To preserve seals that are not to be broken during changeout of a given module, a small residual pressure must be kept in the modules not moved since there is no assurance that a seal can be made twice.

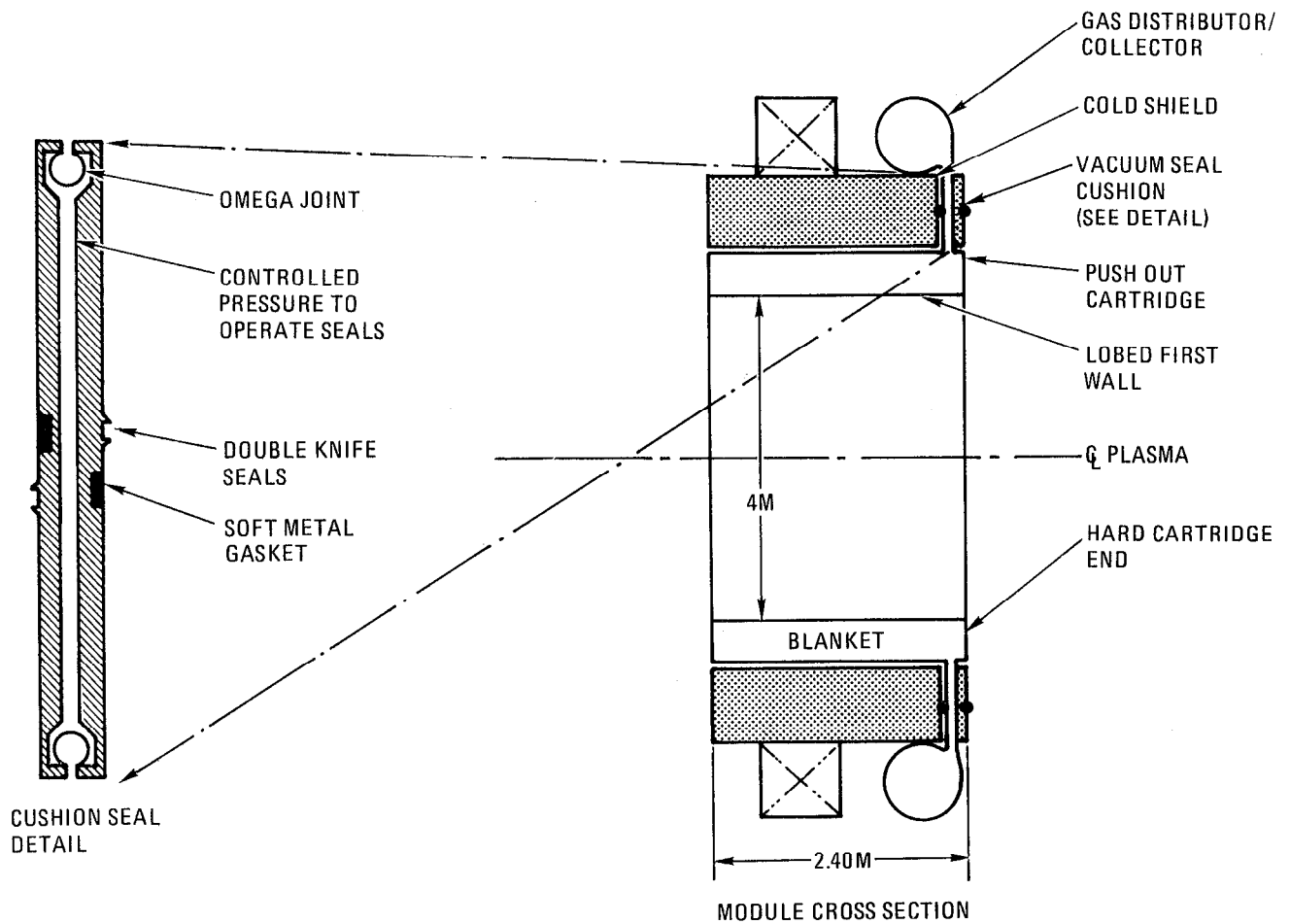


Fig. 6-4. Omega point.

Fig. 6-5. Module cross section.

Table 6-1 shows the outline and costs for a seal development program that would almost automatically test other features. The use of the pressure operated knife seal has useful developmental characteristics. Should the seal prove impractical, it would be fairly easy without configurative change to fall back to a skate weld technique, which is known to be further developed but slower in operation.

Table 6-1. Automatic cushion seal development program.

-
- Consult with present suppliers and establish present technology base.
 - Detail design of test module:
 - Seal
 - Membrane
 - Omega joint
 - Construct test.
 - Run test and feed back to design (and designers):
 - Estimated cost \$300,000
 - Time 1 yr
-

Also considered is the possibility of the entire reactor vault being a vacuum chamber. Should this proposal mature, we calculate that by reasonably careful finishing of the contacting cushion faces, a satisfactory differential between the coarse and fine vacuums could be maintained by merely pressing the cushion faces together, simplifying the system by omission of both knife- and soft-sealing pads.

Summary of Vacuum Seal Systems

- Module services disconnected by hands-on operations with probes into cold areas.
 - No online welding operations.
 - Fast modular separation.
 - Fast modular replacement.
 - No online servicing.
 - No major structural make/break joints.

Shield Design

The shield design is dominated by the requirement to cool a large block of material. We initially intended to build this block of stainless steel plates (Fig. 6-6) with their thickness determined by the cooling requirement as is the space between them. This has as one advantage: the ease with which fractions of other required materials such as boron compounds can be incorporated in these plates. The plates would be very large diameter washers (4.5 m). Temperature stresses in these washers are comparatively easily controlled by slitting the washer through on lines radially out from its center hole. The slit length governs the temperature stress. By merely seal-welding the cooling gaps around the washer assembly periphery, no pressure vessel shell was required, and the washers holds the pressure at very low stress levels. The shield could be within the primary coolant loop and would not require separate cooling. Alternately, the shield could be a separate, water-cooled structure. A further advantage of the washer shield concept is that complex plena and coolant passages are easily cut into the individual plates before assembly.

A problem with the washer shield concept is cost. Because of the low level of energy deposition, the shield could be water-cooled at low temperature, and the possibility for use of cheaper materials, such as concrete, appears attractive.

Blanket Changeout and Fuel Handling

The procedure involved with the changeout of the TMHR blanket structure has received preliminary study. The major system operations are described in Table 6-2. The changeout procedure of the TMHR blanket module follows. When the plasma power supply is shut off, the main coolant stream is left in action on all modules to cool the modules down, controlling differences in temperature between incoming and remaining units for purposes of seal matching. Work on service disconnections then starts. The principal vacuum is vented with a clean gas, the magnet electrically runs down, and the vacuum interseal sinus breaks.

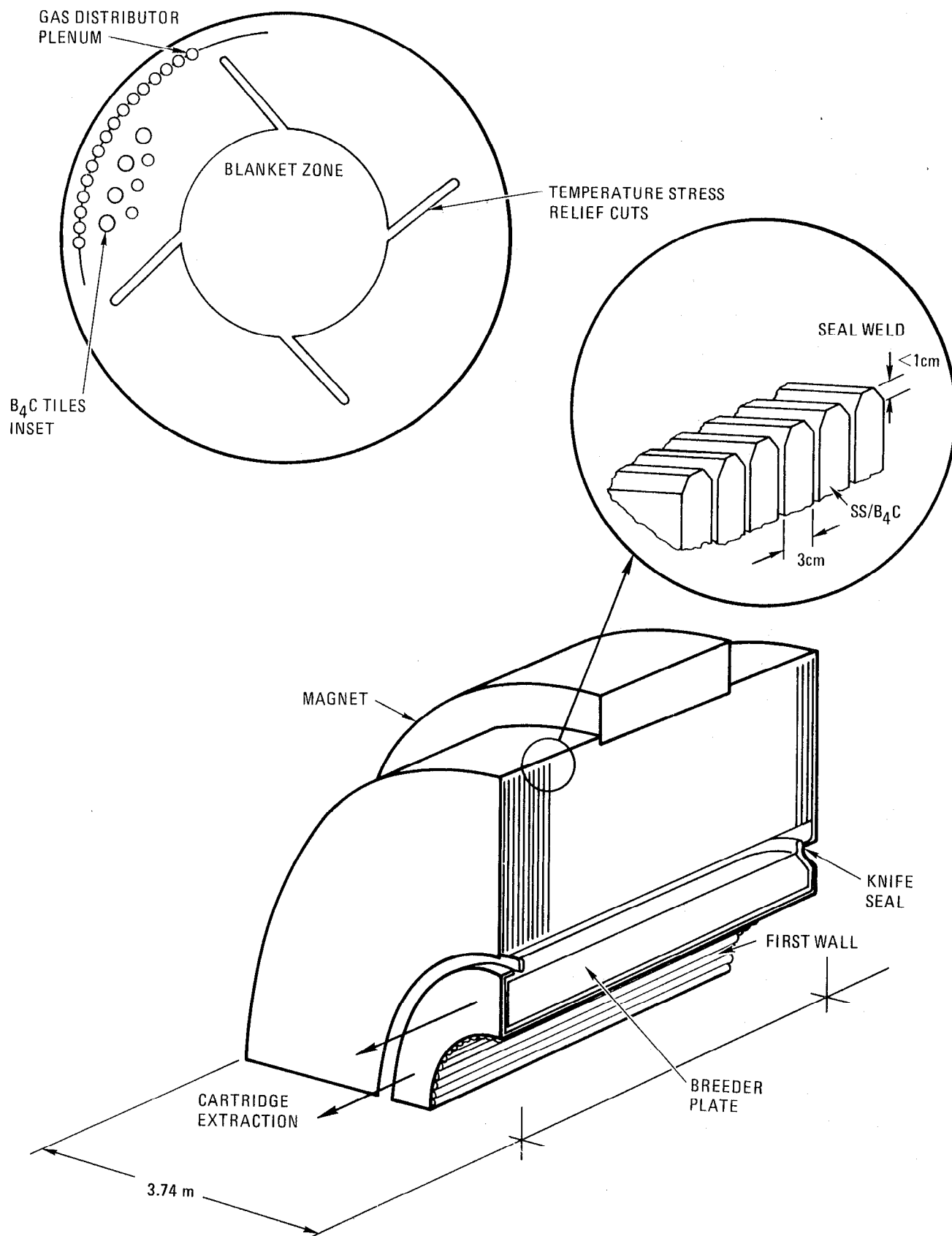


Fig. 6-6. Washer-shield concept.

Table 6-2. Changeout affected equipment and conditions list.

- Plasma
The trip out and normal stop functions for the plasma are expected to receive considerable attention elsewhere, and the desirability of a sudden stop is questionable. The changeout start point is defined as where the plasma input power ceases. A cooldown period has been inserted, although a normal plasma stop may already include one.
- Main coolant
Two lines of about 1 m diam must be made and broken remotely.
- Cushion pressure line
Sized to allow fast depressurization should a module line break, this single line should not be contaminated. It is hoped to avoid circulation through the cushion.
- Vacuum sinus
This sinus is sized to evacuate the double-knife seal interspace and not expected to require remote work.
- Main vacuum
This is neither made nor vented at the module. The intermodular joint and seal are required to maintain it. When it is vented, we would expect to take precautions to preserve the cleanliness of the vacuum surfaces exposed.
- Tritium purge
The inclusion of this line is speculative. Depending on tritium inventory requirements, it may be possible to gather tritium from the main coolant.
- Water lines
These lines have been included for assessment on the assumption that a water-cooled shield is used.
- Auxiliary cooling lines
A pair of 15-cm lines that allow control of module pressure and cooling while the main lines are valved into isolation for work. These lines carry the changeout critical path rather than the large ones.
- Door
This is considered to be opened and closed by simple mechanical push devices (pulling or ball screws are not acceptable in remote areas).
- Blanket transportation
Carries the blanket from the shield. This device must carry cooling capability for afterheat and have the capacity to make the connections.

Table 6-2. (continued)

-
- Dowels
Large pins (15 cm diam) inserted into the top and bottom of each shield. They align the module and hold it during operation and are only withdrawn for module removal. They can hold the module against a small intermodular ΔP and are hydraulically operated.
 - Module truck
Unpowered and pushed on a journey of about 7 m each way. Retains the magnets and shield.
 - Module
Only the afterheat coolant system that this may have to carry is of interest in this mode. This must not interfere with the module rollout from the vault or magnets.
 - Magnet
Services have been defined as off the shelf and are cold, consisting only of electrical and cryogenic elements. The probe to carry them has been defined as noncritical.
 - Instrumentation and diagnostics
Information carriers, not yet defined, but should not intrude on power-carrying critical path.
-

The main coolant joints are valved into isolation and the interspace vented so that work to break them can be started. The auxiliary coolant line is used for depressurization and flushing of the system, and the entire reactor is drawn down prior to applying subatmospheric pressure to the cushion to break the main vacuum seal on the units to be moved and to give mechanical clearance. The door is moved, and the blanket carrier is set up in this period, the magnet vacuum isolated and disconnected, and the magnet cryogenic bayonets withdrawn. The main coolant lines are disconnected, and the auxiliary coolant lines are broken after starting the transfer cooling system on the module. Until experience is gained, most lines, with the exception of magnet services, will be designed as radioactive although they may not all be so.

The next phase of the change is the railroad procedure. The railroad layout is shown in Fig. 6-7. Since the blanket module connections prevent two-way entry into the shield, the old-out and new-in journeys must be consecutive. Hence, the sequential journey averages 100 m. Ten cm/s is proposed as the travel speed.

The rebuild phase is largely dominated by the establishment of the vacuum since the drawdown and bakeout times are very long. Thus, cushion pressurization operations are on the critical path. The assumption is made that small lines are easier to connect than large ones, and use of the separate cushion drivers seal leaves a long period to make the large coolant connections.

Throughout these operations, verification and inspection of the details are essential. We expect that this will be more time consuming than actual operations.

There are obvious areas of concern in the preceding scenario. The remote pressure-operated main vacuum seal has received attention, and the first and second order effects appear to be tractable design problems. Similarly, the major gas joints on circulating lines have been examined. We would expect these joints to be developed to a high standard of reliability by the time the reactor is built; in fact, many areas for improvement over present techniques have been clearly identified.

We expect that the annual change of two of the 16 modules for reprocessing will not in total take more than 1 month. Some appreciable fraction of this time will be used in preparation and restart of the machine. Table 6-3 illustrates details of the expected changeout time required for the proposed scenario.

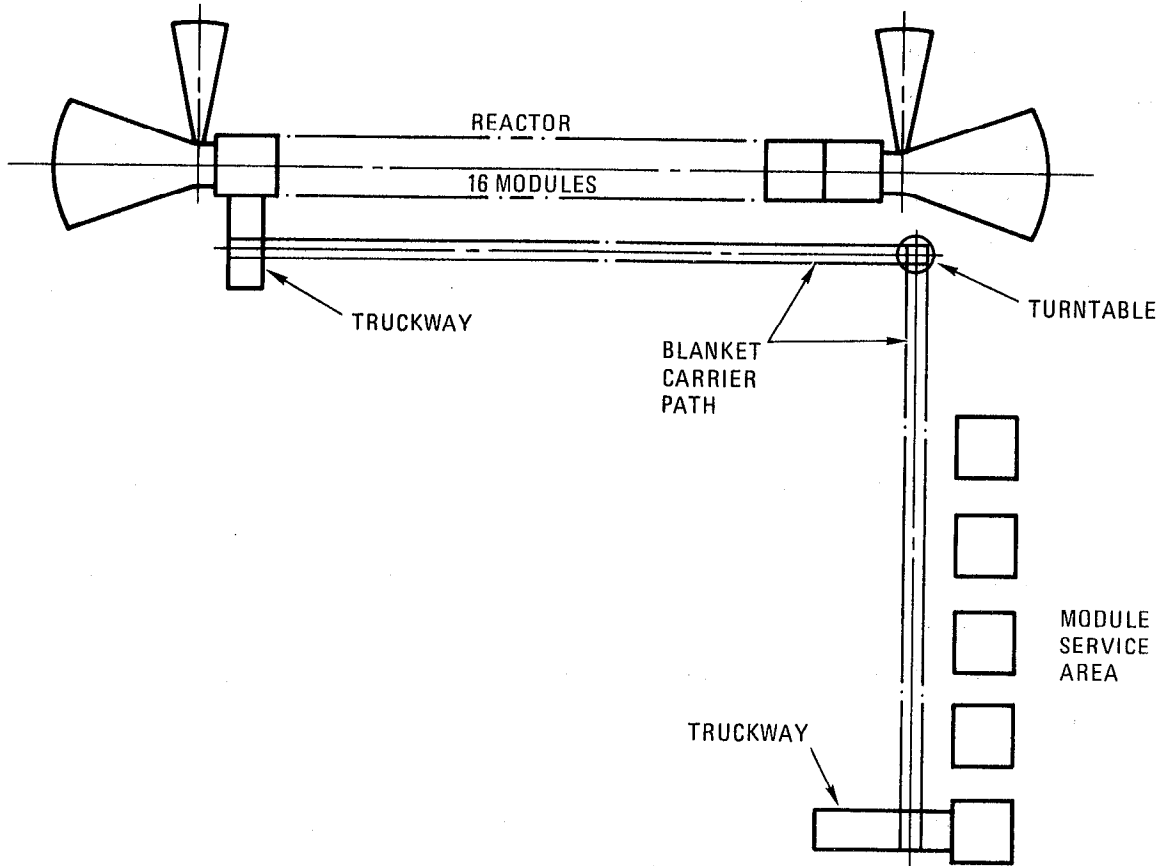


Fig. 6-7. Module service layout.

Table 6-3. Module changeout.

Preparation:	Power reduction Disconnection and tagout (minor) Vault checkout Unlocking Door opening Final inspection	1 day
Operation:	Making temporary connections Magnet disconnect Major disconnections Cushion deflation Dowel removal Changeout Inspect Reseal and drawdown Major reconnections Dowel insertion Remove temporary connections Inspection	11.5 days (1 cell)
Restart:	Recheck seals Clean up cell Close cell Test Restart Bring to power	6 days

Note: For annual 2-cell changeout, operation time would be 1.5 x single-cell time:

1 cell total = 18.5 days

2 cell total = 24.1 days

The afterheat problem has also been given preliminary attention. It is probable that this system will not constitute a major portion of the changeout procedure and design, at least with the relatively low power Th/metal blanket, although it is clear that reliable auxiliary cooling system and transport cooling systems will be required.

Materials Considerations

In a He-cooled, fusion reactor blanket design, it is important to select suitable materials for different regions of the blanket in order to optimize the overall design. We selected Inconel 718 (50-55% Ni, 17-21% Cr, 5% Nb + Ta, 3% Mo, 1% Ti, 0.5% Al, remainder Fe) to be the structural material because of its high strength at elevated temperature for the first-wall, which is the high pressure boundary between the high pressure He and near vacuum of the plasma chamber. HT-9 was selected as the cladding material for fuel region because the material is relatively inexpensive and has excellent swelling resistance under high fluence. HT-9 is one of a class of ferritic materials having 12% Cr, 1% Mo, and 0.3% V by weight. Thorium was selected as the fertile material because of its excellent breeding performance. The other physical properties of Th were also considered. The tritium breeding material is Li_2O because of its favorable neutronics performance and the possibility that it may exhibit safety advantages compared to the alternative considered, Li_7Pb_2 . The present design shows a stainless steel shield with B_4C inserts. Borated concrete may prove to be a more cost-effective choice for the low power density/low temperature outer shield region. More details of the above selections are presented in the following subsections.

Structural Material Requirements

The TMHR blanket will be exposed to a severe thermal and nuclear radiation environment in performing the multiple functions of converting fertile materials to fissile materials and neutron and gamma ray energy into heat, transferring the heat to the system coolant, containing the breeding material, and shielding the superconducting coils from both heat and nuclear radiation. The blanket module assembly will be required to maintain its structural integrity and perform these functions reliably while exposed to conditions of high temperature and high neutron flux.

The materials selected for the modules must be machinable and weldable, and the alloys must be commercially available in the quantities and forms required for construction of the TMHR. The selection of materials with reasonable property data bases and significant application histories would also be desirable, although not technically required. Another desirable characteristic would be a relatively low rate of induced activation to alleviate radwaste problems and to reduce the complexity of plant maintenance, although this appears to be difficult to obtain in a high-temperature alloy. Because of different requirements for the structural material of the blanket first-wall and the breeder plates, Inconel 718 was selected for the first-wall, and HT-9 was selected for the fuel clad.

First-Wall Structural Material

A wide range of possible blanket structural materials has been reviewed in the TMHR Interim Report.¹

Inconel 718 is recommended as the baseline gas-cooled TMHR blanket module material on the basis of its high allowable stresses at the 550°C operating temperature and its excellent potential swelling resistance in the TMHR neutron environment. The allowable design stresses of solution treated and aged Inconel 718 are compared to those for 316 stainless steel and Mo TZM in Fig. 6-8. The allowable curve for 316 stainless steel was taken from Section III of the ASME code (Class 1 components), while the values for Inconel 718 and Mo TZM were calculated from available data.^{2,3} The allowable stresses for these two alloys were determined at each temperature as two-thirds of the minimum creep-rupture strength or one-third of the minimum ultimate tensile strength, whichever was lower. This criterion is consistent with current ASME Section III procedures for determining allowable design stresses. Notice in Fig. 6-8 that at 550°C the allowable stress of Inconel 718 is about four times greater than 316 SS. Figure 6-8 indicates that the refractory alloys such as Mo TZM do not offer advantages in design stresses over Inconel 718 at or below 650°C, due to the lower short-term tensile properties of the refractories. Figure 6-8 also indicates that the design stress of Inconel 718 decreases rapidly above 600°C, to about one-half of its 550°C value at 700°C. For operating temperatures above 700°C, other materials (i.e., the refractory metals Mo, Nb, V or ceramics) would become increasingly strong candidates.

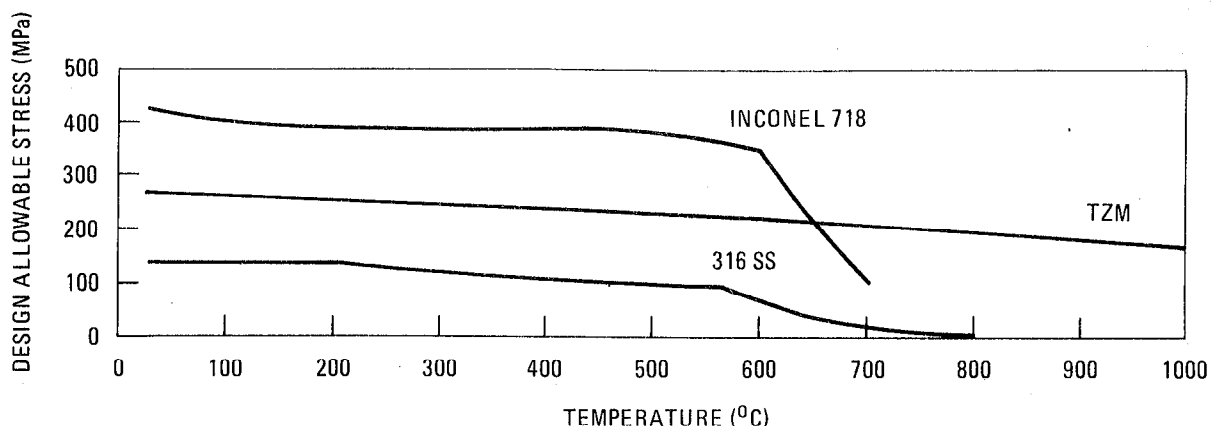


Fig. 6-8. Allowable stresses for TMHR blanket module candidate materials.

Some pertinent properties and characteristics of Inconel 718, relevant to its application in the TMHR blanket, are shown in Table 6-4. Published data⁴ indicate that void swelling at a fluence of 5.6×10^{22} n/cm² and 36 DPA (displacement per atom) at 550°C should not exceed 0.2%. This fluence level would correspond to 3.5 MW-yr/m² in the TMHR with Th blankets.

Table 6-4. Properties of Inconel 718 relevant to its application in TMHR blanket modules.

Design allowable stress ² at 550°C and 25,000 h	350 MPa (50 ksi)
Minimum yield strength at ² 550°C	870 MPa (126 ksi)
Minimum ultimate strength at ² 550°C	1065 MPa (155 ksi)
Young's modulus at 550°C ²	170 GPa
Helium generation at 1 MW/m ² for 1-yr service, with the Th blanket	140 appm
Hydrogen generation at 1 MW/m ² for 1-yr service, with the Th blanket	1480 appm
Thermal expansion (mean to 550°C) ²	14.5 micros/°C
Thermal conductivity ²	20 W/m-°C
Approximate cost (forging stock)	\$10/Kg

Approximately 140 appm He will be produced in Inconel 718 TMHR blanket modules after 1-yr service. Although there are no current data on the effects of this He production on the residual ductility of the alloy, test data on austenitic stainless steel alloys⁵ indicate that there will be a significant reduction in ductility. For Inconel 718 at temperatures above 500°C, there is growing concern about radiation embrittlement of these precipitation-strengthened nickel alloys.⁶ The reduction of uniform elongation to 0.5% would control the design lifetimes of the modules. Fast reactor irradiation test on Inconel 718, resulting in large DPA levels combined with sufficient He generation, (such as obtained in the HFIR), must be performed to obtain the necessary data on He embrittlement. There is some possibility that the presence of Nb carbides at the grain boundaries of Inconel 718 may be effective in inhibiting grain boundary sliding and might reduce the rate of He embrittlement.

The compatibility of Inconel 718 with impure He is being investigated in the current GT-HTGR Materials Screening Program, and current results to 5000 h at 650°C indicate little or no corrosion or creep property degradation from impurity-metal interactions. Metallurgical stability of the alloy at 650°C also appears acceptable. Detailed analyses of Inconel 718 specimens aged in controlled impurity He at 650°C are in progress.

Although fabrication (machining and welding) of Inconel 718 is inherently more difficult than austenitic stainless steels, the construction of blanket modules from the former alloy appears very feasible. Inconel 718 is conventionally solution-treated at from 927 to 1010°C for 1 h, air-cooled, and then aged at 718°C for 8 h, furnace-cooled to 621°C, held for a total of 18 h, and air-cooled. The module bodies could be either forged, roll-formed, or perhaps vacuum shell-cast.

Machining of Inconel 718 is about four times more difficult than 316 stainless steel, so the selected fabrication procedure should minimize final machining. Welding properties of Inconel 718 in section thickness of up to 1 cm using Tungsten Inert Gas (TIG) methods is good, and no post-weld heat treatment would be required if the welds do not exceed 540°C in service.

Cladding Material for Fuel

From the properties given in the previous subsection, Inconel 718 can be used as the cladding material for the fuel plates, yet from the general class

of ferritic steels considered by the current U.S. program, HT-9 may be a better choice because of lower cost, easier fabrication, and reduced radiation-induced swelling.

The commercial 12 Cr-1 Mo-0.3V Sandvik alloy HT-9 (DINX20 CrMoV) has been used in Europe for steam pipe lines and for tubes/headers in fossil-fired boilers for over 10 yrs and is currently being considered for a number of thermal and fast reactor components including steam generators, recuperators, auxiliary heat exchangers, and steam piping.

The minimum ultimate tensile strength of HT-9 compared to that for several other candidate first-wall/blanket alloys is shown in Fig. 6-9. Above 550°C, HT-9 short-term strength decreases rapidly. Since the cladding of the fuel plate would not require very high strength, a possible operating temperature limit extended to 650°C might be feasible.

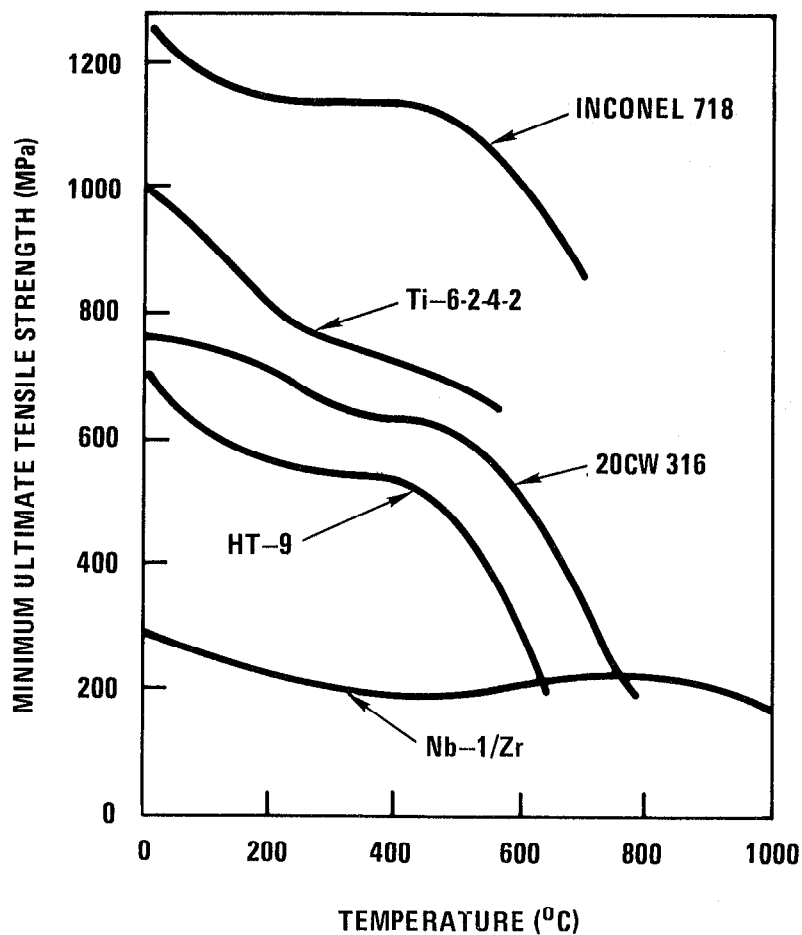


Fig. 6-9. Structural material strength.

Recent work⁶ indicates that magnetic effects should not be a serious concern since the HT-9 will saturate at less than 1 T field, and magnetic field permeability will then approach unity. There is so little material in the blanket that the perturbation of the magnetic field at the plasma should be only about 1% or less whereas the field perturbation in the blanket material itself can be greater than 10%.

The primary reason for investigating the application of HT-9 is, of course, its apparent resistance to neutron radiation damage. Most of the pertinent information with respect to void swelling, in-reactor creep, and embrittlement has been developed in the Experimental Breeder Reactor (EBR) program and has not yet been released for general dissemination. Although discussion of the radiation damage resistance of HT-9 must therefore be qualitative, a number of relevant observations can be made on the basis of EBR II data to greater than 1×10^{23} n/cm² ($E > 0.1$ MeV).

Figure 6-10 illustrates the expected irradiation induced swelling and feasible structural material as a function of temperature.¹ It shows that the maximum swelling ($\Delta V/V$) of HT-9 is less than 1% which is less than half of the swelling of Inconel-706. This would ease some of the mechanical design requirements for the fuel plates.

A concern that is presently unresolved is that of increase in the ductile-to-brittle transition temperature of HT-9 with irradiation. This effect could result in very low fracture toughness values for irradiated HT-9. Research programs presently underway should resolve this concern.

Tritium Breeding Material

We selected Li₂O as the tritium breeding material for the TMHR. When compared to Li₇Pb₂, the higher melting point of Li₂O allows the reactor to operate at a higher thermal cycle efficiency; and because of its lower release of energy from exothermic reaction with H₂O, Li₂O is apparently a better choice than Li₇Pb₂ from reactor safety considerations.

The three most widely considered tritium breeding materials are Li, Li₇Pb₂, and Li₂O. These three were again identified after a review of twenty lithium containing materials.⁷ The following summarizes the results from this review for Li, Li₇Pb₂, and Li₂O.

Lithium metal has been selected as the tritium breeding material in many fusion blanket design concepts. The use of Li raises several design

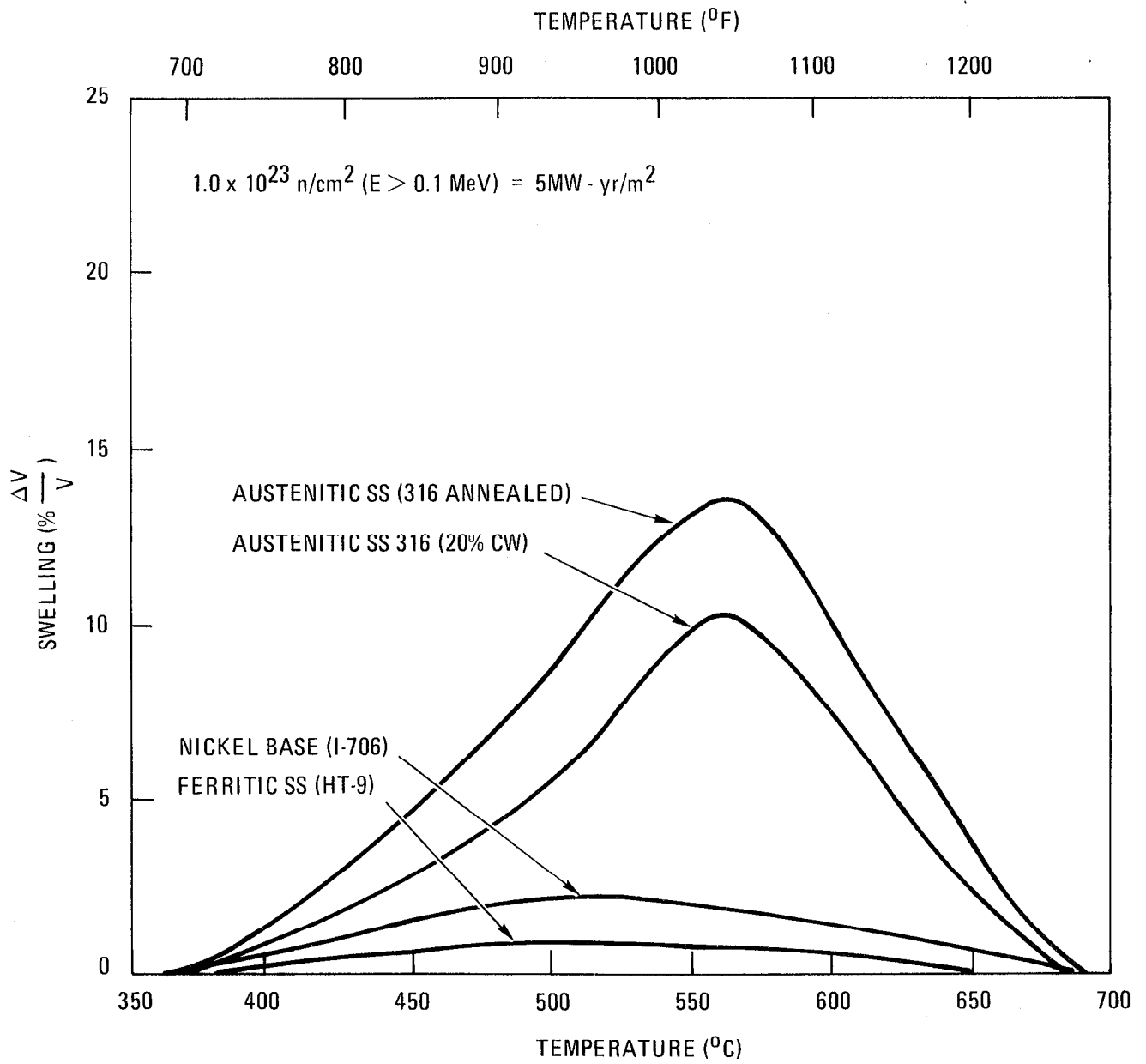


Fig. 6-10. Expected irradiation-induced swelling in candidate structural materials.

questions, however. Because of its affinity for H, an Li blanket will accumulate a large tritium inventory. Methods for tritium recovery from Li are being developed but will probably require that the Li be circulated out of the blanket for processing. Because of the MHD pumping losses and other effects associated with pumping a liquid metal across magnetic field lines, the circulation rate may have to be small. With a separate coolant flow, the Li circulation rate required for tritium recovery would be small.

A major concern with the use of Li is safety. Lithium reacts with C or water violently and reacts slowly with dry air and oxidizes rapidly to form hydroxide in moist air. In the event of a Li spill, the energy released by reaction of Li with air, water, or concrete could contribute to failure of the containment and release of the tritium inventory.

Another concern about use of Li metal is corrosion. At temperatures above its melting point (180°C), corrosion of most structural materials may be a serious problem; yet use of Li as a solid is totally impractical due to the very low blanket and coolant temperature limits this would impose. The high degree of chemical activity of liquid Li makes its application to a near-term fusion blanket difficult. Because of this, material selection for the TMHR has focused on solid Li breeding compounds.

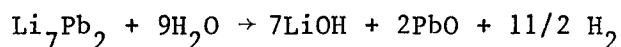
In the Li-Pb binary system containing 20 to 30 at.% Pb, there are four intermetallic compounds with melting points (T_m) varying from 915 to 999 K. As Li_7Pb_2 possesses the highest melting point, the melting temperature of such a system would decrease as the composition changed during neutron irradiation. At the very small fractional Li burnup expected in a fusion blanket (0.1% per $\text{MW}\text{-yr}/\text{m}^2$), this should not significantly lower the melting point. Due to the low melting point of Li-Pb alloys, sintering of Li_7Pb_2 granules is of concern. Sintering is expected to occur at temperatures as low as 500 K. This would increase the effective grain size and decrease the tritium release rate. One experiment, however, showed that prolonged annealing at $0.83 T_m$ (830 K) actually improved the tritium extraction even though this temperature exceeds the expected sintering temperature.⁸ Further studies are certainly required to explain this phenomenon. Assuming this tritium release behavior⁸ is representative, the Li_7Pb_2 blanket material would exhibit a tritium inventory of only about 30 g. Li_7Pb_2 has the advantage of built-in neutron multiplication through $(n,2n)$ reactions in the lead.

Among different Li containing material, Li_2O has the highest Li atomic density, which makes it a favorite selection. It has a high melting point (1700°C), which allows it to operate at high temperature; this allows high coolant temperature, which leads to relatively high thermal cycle efficiency depending on the particular design. It releases the bred tritium in the form of T_2O , which allows relative ease in tritium control by using a purged flow design. The drawback of Li_2O is that it is extremely hygroscopic and forms LiOH or LiOT , which are very corrosive to cladding material. Purity control to reduce the impurities of LiOH and Li_2CO_3 can be expensive. Impurity control in the purging stream can also be important.

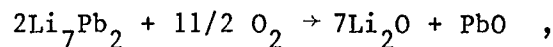
Safety Aspects of Lithium Materials

The corrosive properties and the high reactivity of liquid Li as well as the risks involved in the use of some solid Li compounds were presented in the previous subsection. From both the neutronics and thermal standpoints, Li_2O and Li_7Pb_2 have advantages as tritium breeders over other compounds. To assess the plant safety when either of these two compounds is used, it is of interest to compare the enthalpy change or free energy change for oxidation and for the reaction with moisture.

While Li_2O is itself an oxide, and thus immune from any further oxidation reaction, it does react with water vapor. The reaction $\text{Li}_2\text{O} + \text{H}_2\text{O} \rightarrow 2\text{LiOH}$ carries a free energy change of -27.2 kcal/mole at 298 K and an enthalpy change of -32.9 ± 2.1 kcal/mole at 298 K. The corresponding reaction for Li_7Pb_2 ,



has an enthalpy change of -324.8 ± 7.5 kcal/mole at 298 K; at the melting point of Li_7Pb_2 the enthalpy change of this reaction was estimated to be -277 kcal/mole. The oxidation reaction of Li_7Pb_2 is



which has an enthalpy change of -527.6 ± 5.6 kcal/mole of Li_7Pb_2 at 298 K. The negative sign of the enthalpy change implies that heat is evolved. The effect of heat evolution during oxidation and reaction with H_2O can be visualized by calculating the quantity of the remaining solid Li compound, which would be melted under adiabatic situation.

With an enthalpy change of -32.9 kcal/mole for Li_2O , a mole of Li_2O will be heated from room temperature to 1600°C , which is approximately 100°C below its melting point. While recognizing the energy needed to heat the Li_7Pb_2 to its melting point is only 44 kcal/mole, the heat evolved in its oxidation reaction and the reaction with H_2O are more than 500 kcal/mole and 270 kcal/mole, respectively. With each unit weight of Li_7Pb_2 reacted, more than 11 units would melt with oxidation; six units would melt in its reaction with H_2O . The actual temperature profile in the Li compound depends upon the granule size and the heat transfer characteristics in the blanket area; but because of the magnitude of the enthalpy change involved in the reaction, it is probably much less safe to use Li_7Pb_2 unless appropriate design accommodations can be incorporated. Moreover, the use of Li_7Pb_2 would also complicate the design as the molten Li_7Pb_2 should not be in contact with concrete. It is therefore apparent that for reactor safety considerations Li_2O is a better choice.

Thorium Metal Fuel

From the surveying study of the TMHR interim report,¹ Th metal was selected as the fertile fuel for the TMHR. The following discusses some of its pertinent properties applicable to this study. Metal fuel has a relatively higher breeding potential based upon heavy atom density compared to the alternate fuel types: oxide, carbide, or nitride fuels. The use of Th metal mitigates the limitations of melting temperature, phase stability, and thermal cycle and irradiation damage that are of concern in the use of metallic U and Pu. Thorium metal has a reasonably high melting point (1755°C and bcc above 1400°C), high thermal conductivity, and good irradiation stability to the burnup levels required in the TMHR.

Production. Reactor grade Th metal has been produced commercially for a number of years, and Th fuel element manufacturing processes have been developed on a relatively large scale. Thorium metal is readily worked by both hot and cold forming. It is claimed that Th fuel fabrication costs can be substantially reduced by using metallic rather than ceramic fuel because metallic fuel can be produced by a once-through fabrication process such as casting or extrusion, which is much cheaper than a conventional fuel-pelletizing and canning procedure.

Properties. The physical and mechanical properties of Th metal are given in the attached Table 6-5. The density of the metal is 11.7 g/cc compared to 10 g/cc for ThO₂ and 10.96 for ThC.

Table 6-5. Physical properties of thorium metal.

Property	Characteristic
Melting point, °C	1755°
Structure	fcc(to 1400°C) bcc (1400-mp)
Density, g/cc	11.7
Thermal conductivity, w/m°K	42
Thermal expansion, x 10 ⁻⁶ /°C	12.5
SS-clad compatibility	OK
Irradiation	Acceptable to 1000°C 1-2% ΔV/V/bu

Irradiation Effects. The isotropic cubic structure of Th limits irradiation growth. The swelling is limited to solid fission product swelling below about 650°C (1 to 2% volume swelling per at.% burnup). The much superior irradiation stability of Th and Th/U alloys over U-alloys has been demonstrated by the extensive studies at Argonne National Laboratory (ANL). The ANL investigations were carried out at irradiation temperatures of up to 1000°C and to burnups of up to 10 at. %. Between 650 and 800°C the swelling rate was about 2.5% per at. % burnup. Above 800°C the swelling rate increased to about 8% per at. % burnup and appeared to level off.

Operating Limits in TMHR. The burnup level to which the Th metal fuel will be exposed in the TMHR blanket is about 1 to 1.5%. With nominal operating fuel center-line temperature 850°C and hot-spot temperature 1000°C, the average swelling behavior of the fuel would be 2%, which should be acceptable with proper fuel design.

Cartridge Design

The mechanical design of the fuel zone has to couple with other design considerations. One major consideration is the frequency with which the blanket fuel material must be changed, compared to the expected lifetime of the blanket structural material. Short cycle materials favor mobile blankets with their attendant complications or greater reactor downtime. Long cycle materials, while giving an infrequent yield from one module, can be arranged to give a steady flow from a series of modules. The Th-metal choice appears most favorable. The expected optimum fuel lifetime is around 9 MW-yr/m^2 , based upon neutronic calculations to reach 1% burnup and upon previous economic optimization studies.¹⁰ This exposure is comparable to estimates of first wall material lifetimes being made for various structural materials.⁶ It is of obvious benefit if the breeding time is of the same order as the first-wall life since the change operations can be unified. It is expected that the metal-clad Th blanket selection will allow this.

The blanket cartridge is shown in Fig. 6-11. The outer shell fits into the shield and is 4.5 cm thick to contain the coolant pressure at 5 m in diam. From one end a radial double passageway connects to an outer torus, which serves (by being internally divided) to deliver and collect the coolant gas.

The body of the blanket cartridge is made nominally about 1% short to allow thermal and neutronic growth. The module ends, having about 0.5-m radial span, will be built up structures to allow cooling.

The first-wall could not at this diameter be made as a simple cylinder since its thickness would cause a considerable neutronic penalty, and it could not easily be cooled. Accordingly, after some exploration, a lobed design (Fig. 6-12) was adopted in which the lobes are suspended from the outer shell. The suspension webs serve as part of the gas distribution system, but they must be broken at intervals to prevent the development of neutron swelling stresses. Materials nearest the plasma are Inconel 718, with the first-wall being 5 mm thick.

Several alternative designs were investigated in an attempt to combine the neutronic advantage of a thin, lobed first-wall with a structural design that would allow the outer zones of the cartridge to be reused without extensive remote cutting and welding. It is expected that the Li zone could survive several blanket life cycles, and that the pressure vessel itself could

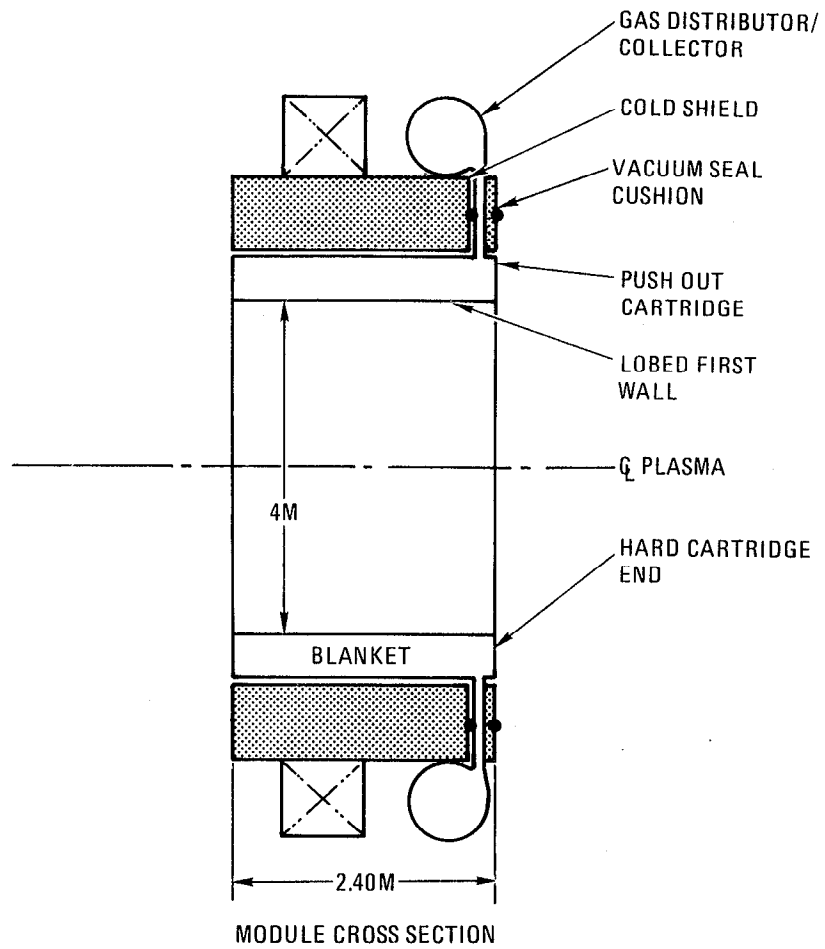


Fig. 6-11. Module cross section.

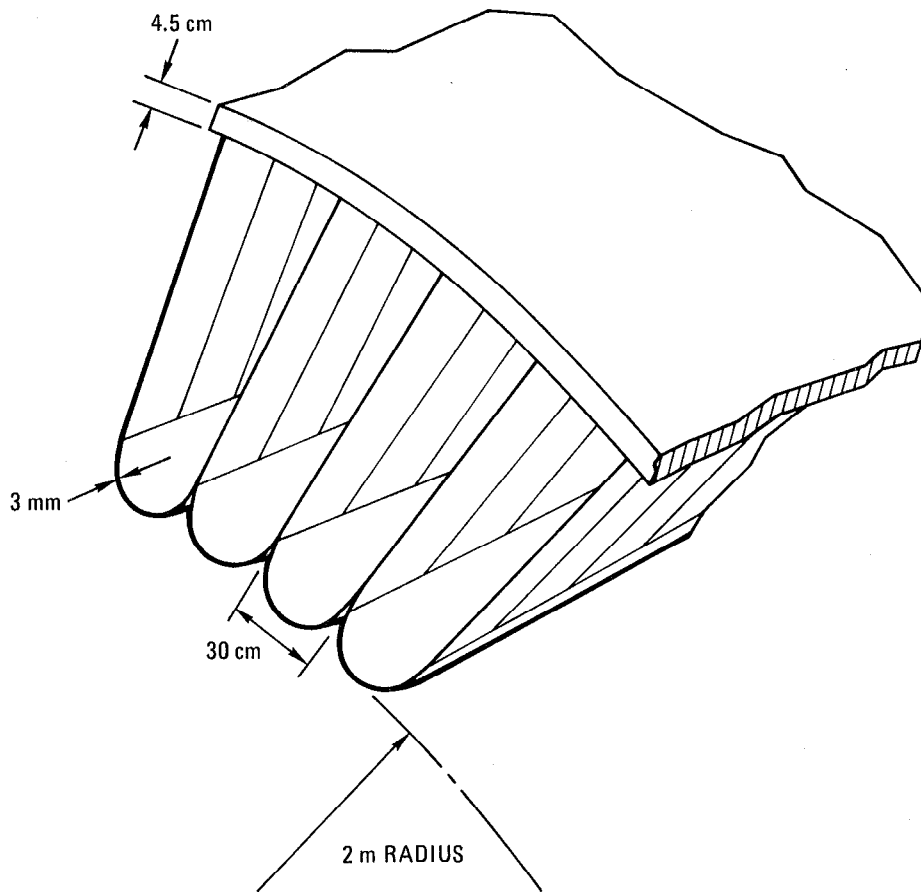


Fig. 6-12. Blanket pressure vessel and first wall.

last the entire 40-yr life of the reactor. The radial load paths of the lobed first-wall design, however, made this goal impossible to achieve in the present design.

Submodule Configuration

The configuration chosen for the TMHR blanket module is that of a large, axisymmetric cylindrical segment about 3.5 m long with a cusp-shaped first-wall. Each of the cusp-shaped azimuthal sectors of the module may be considered a submodule, although they would not be separable from one another. The flow configuration and fuel configuration within these submodules have several possible options.

Submodule Flow Configuration

Coolant flow through the submodule can be either radially or axially oriented. The general characteristics of gas cooling, described in Section 5, generally result in designs that have a high temperature differential from coolant inlet to coolant outlet in order to minimize pumping power requirements. The heat transfer characteristics of gas-cooled systems, together with the fairly high power densities generally found in hybrid blankets, result in a large temperature differential between the fuel and the coolant. These two facts act to make axial coolant flow unattractive. The limiting fuel design conditions would occur at the coolant outlet end of the submodule, and the rest of the submodule fuel would be operating substantially below its design capabilities. Due to the steep radial power density gradient in the blanket, use of axial flow would also necessitate use of radial flow orificing.

Use of radial coolant flow allows the temperature characteristics of the gas coolant to be matched to the very steep radial power density gradient found in a hybrid blanket. By introducing the inlet coolant at the plasma side of the blanket, the coolest coolant is applied at the point of highest power density. This results in fuel centerline and cladding temperatures that are fairly uniform along the flow path and thus yields an efficient design. The radial outward flow path matches well with the submodule cusp geometry. The coolant is distributed axially along the module through an inlet plenum at the back of the module. It flows radially inward along the cusp radial tie plates to the first-wall region, turns, cooling the first-wall, and flows radially outward through the fuel zone. In this manner the entire module structure is maintained near the coolant inlet temperature. This submodule flow path is shown in Fig. 6-13.

Submodule Fuel Configuration

The fuel configuration within the submodule can take the form of balls, rods, or plates. Rods may be radially or axially oriented. Plates may be axially or azimuthally oriented but with the cusp geometry azimuthal orientation would not be structurally efficient. Four fuel configurations were considered, each within the cusp geometry/radial flow configuration chosen for the submodule. These are balls, radially oriented rods, axially oriented rods, and axially oriented plates. We feel that the blanket cartridge concept and

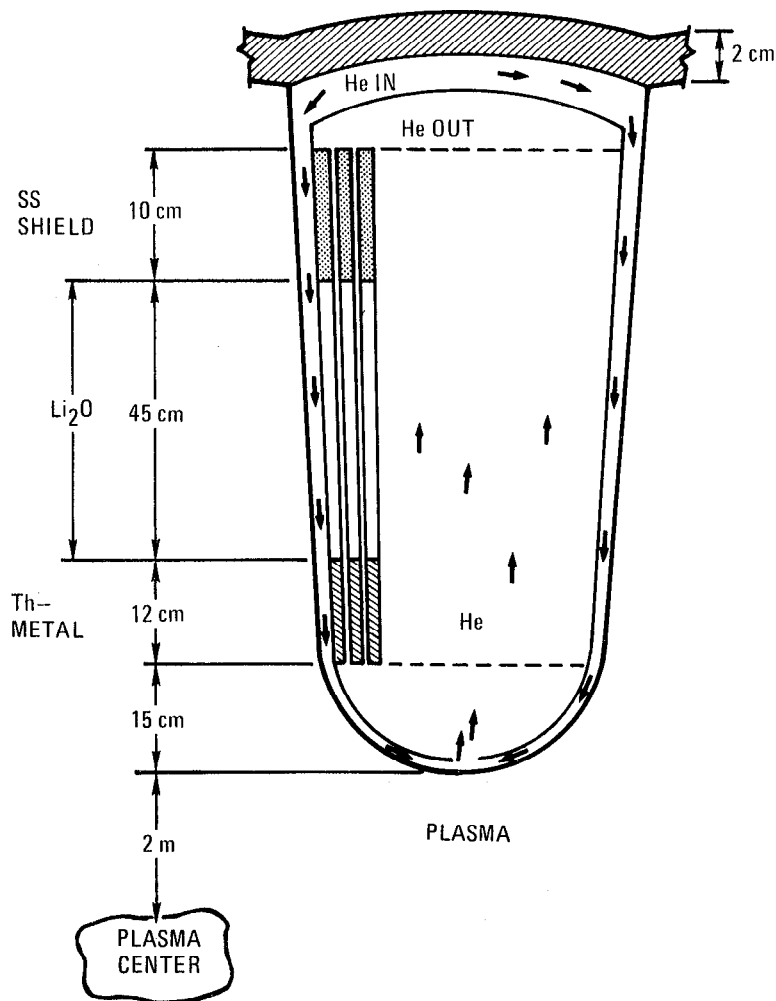


Fig. 6-13. TMHR He-cooled submodule.

submodule design are not too sensitive to this choice and could accommodate any one of the four. Secondary changeout systems for the fuel, not part of the major first-wall changeout system, were also considered. These essentially involve mobile blankets, and since the Th and first-wall best irradiation life times are of the same order, this was rejected. Both rods and balls were examined and it was readily apparent that a mobile blanket would intrude detrimentally into many other design areas.

Past experience indicates that any of these fuel configurations can be developed into a design that is structurally feasible and has acceptable thermal-hydraulic characteristics. The ball configuration appears to have a

poor fuel-to-structure ratio and was not pursued in any depth. The radial rod configuration is very similar to conventional fission reactor geometry and has been studied for many hybrid reactor designs, including the Standard Mirror Hybrid Reactor¹¹. This configuration appears quite feasible. Radial rods must be short and can result in high blanket fabrication costs. In addition, grid plates and other necessary support structure can interfere with blanket neutronic performance.

Use of axially oriented rods would allow longer rods and thus lower cost. This configuration has apparently not been previously explored for hybrid systems. It appears to be mechanically quite straightforward. Different radial blanket zones are easily accommodated as are different rod sizes to match the heat transfer characteristics to the heat deposition rates in the various blanket zones. The axially oriented plate configuration appears to be well suited to gas cooling and has been applied to both hybrid¹² and pure fusion¹³) designs in the past. This configuration is mechanically very efficient and offers the potential for a compact, structurally rigid design.

For both axially oriented configurations, bowing of the fuel elements due to differential thermal and radiation-induced swelling is a concern. Based on previous detailed design and analysis¹³, this concern appears to be manageable.

The thermal-hydraulic designs of radial rods, axial rods, and plates were studied for use in the TMHR gas-cooled blanket and are discussed in the next subsection of this report.

Thermal-Hydraulics Design

The thermal-hydraulic design of a gas-cooled reactor system should have high thermal efficiency and low pressure losses. The high efficiency requirement dictates a high coolant outlet temperature, restricted by the maximum operating temperature limits of the reactor materials. The low pressure loss requirement leads to high system operating pressure to obtain high coolant density, a large coolant inlet-to-outlet temperature differential, and velocity restrictions of the coolant in various sections of the coolant loop. On the other hand, the restrictions on material operating temperature limits leads to high coolant velocities to maintain high heat transfer coefficients.

During the course of the TMHR thermal-hydraulics design, close interaction was maintained with the mechanical design, neutronics analysis, and material selection efforts.

In considering the thermal hydraulics of the TMHR, the location and magnitude of the heat sources must be known. For magnetically confined fusion reactors different concepts have different locations where the most severe heat transfer problems are expected to occur. In the tokamak concept essentially all the fusion energy goes through the first-wall of the reactor and nearly 20% of the total energy, in the form of charged particles, is deposited onto the first-wall, thus severely restricting the allowable wall loading from a thermal hydraulics point of view. For the mirror confinement concept, where all the charged particles are guided by the axial magnetic field to the direct converters, there is assumed to be no charged particle or radiation heating deposited onto the first-wall. The neutrons deposit only a fraction of their energy (about 5%) as they pass through the first-wall. The rest of the fusion energy is captured in the blanket where the fusion neutron heating is attenuated exponentially. Because of the cylindrical geometry of the TMHR plasma, the neutron wall loading is assumed to have no axial distribution. The maximum material temperatures calculated in this report are modeled by an infinite cylinder which is a conservative estimate.

Temperature and Pressure Drop Limits

The temperature limits of different materials crucial to the design of the blanket must be established. At the same time the pressure drop limits for different regions of the blanket will need to be defined to establish a basis for the thermal-hydraulic design and analysis. In the blanket region the crucial materials are the structural material and the fuel materials. At the first-wall, where the material strength is important and radiation levels are high, Inconel 718 is recommended to be the structural material. Inconel 718 has a maximum nominal temperature limit of 550°C, above which the loss of ductility due to radiation induced embrittlement can be severe⁶.

Typically, the reactor first-wall would experience the highest flux of high energy neutrons, thus this temperature limit would be applicable to the heat transfer analysis of the first-wall. Beyond the first-wall region, where the neutron flux would be lower and high strength capability not crucial, a hot spot temperature limit of 700°C and a maximum nominal temperature limit

of 650°C can be applied. This limit is proposed for the fuel-cladding materials, which can also be Inconel 718; or, alternately, HT-9 could be used. The centerline temperature limits (with inclusion of hot spot factors) for the breeding materials Li_2O and Li_7Pb_2 are 1700°C and 726°C, corresponding to their respective melting temperatures. These melting temperature limits are considered acceptable because the effects would be local and the nominal maximum temperature is expected to be much lower. Sintering of Li_2O and Li_7Pb_2 under irradiation at these temperatures may be a concern because this could reduce tritium release.

Low coolant pressure drop in a power-producing machine is important in reducing the power necessary to circulate the He coolant. The acceptable pressure-drop depends on the overall optimization of the reactor economics. At this stage of the conceptual design two pressure drop limits can be used. A value of 5% of the thermal power can be used for the pumping power for the complete coolant circuit, which includes the heat exchangers, the blanket, pumps, and piping. The second limit is imposed by the pressure differential capability of the Helium circulator. Using a single-stage circulator, a value of $\Delta P/P \sim 4.3\%$ can be used for the entire coolant loop. The acceptable pressure in the reactor section of the loop (blanket and flow ducts) can be about 50% of the above value. Thus, a value of P equal to 1.2 atm (124 kPa or 18 psi) can be used for the reactor section of the He loop, operating with a He pressure of 55 atm (5.6 MPa).

Experience with He-cooled nuclear power systems indicates that a He pressure of 40 to 80 atm will be needed for a good thermal/hydraulic design. Steam generator design conditions dictate a minimum coolant inlet temperature of about 280°C and a minimum coolant temperature rise of about 100°C. Based on this information, a He operating pressure of 5.6 MPa (55 atm) and an inlet temperature of 285°C were selected. For the Th metal- Li_2O blanket an outlet temperature of 515°C was determined from detailed calculations to give a thermal cycle efficiency of about 38%. For the Li_7Pb_2 blanket, because of its lower melting point, the coolant outlet temperature was set at 435°C, giving a thermal cycle efficiency of about 35%. The selection of coolant outlet temperatures of 515°C was based on detailed design of the plate configuration. To satisfy the design constraints of coolant pressure drop (≤ 20.7 kPa), maximum fuel centerline temperature ($\leq 1000^\circ\text{C}$ in the Th zone), and fuel cladding temperature ($\leq 700^\circ\text{C}$) while maintaining a minimum plate thickness of at least 1 cm for mechanical design considerations, the

coolant outlet temperature was forced to be limited to 515°C. This coolant temperature is lower than the earlier estimate of 585°C, which was used in the BOP calculation. The lower outlet temperature would reduce the thermal cycle efficiency by approximately 1% and would increase the blanket pressure drop by ~70%, which is still within the acceptable pressure drop limit. It is expected that higher outlet temperature could be achieved if thinner fuel plates were used. This would raise concern about increased void and cladding fractions and possible mechanical design constraints. This temperature limit should be examined further during detailed fuel design.

For the Li_7Pb_2 blanket, because of its lower melting point, the coolant outlet temperature was set at 435°C by similarly considering the pressure drop, temperature, and fabrication limits, giving a thermal cycle efficiency of about 35%. On the basis of thermal-hydraulics considerations and potential safety advantages Li_2O was selected as the tritium breeding material for the TMHR. Thus, all thermal-hydraulic calculations in this report are based on the properties of Li_2O .

Analysis

Thermal-hydraulics analysis of the TMHR was performed to establish the temperature and pressure drop characteristics of the first-wall and the breeder sections. The approaches to the problems and the key equations used in these calculations are presented here.

The first-wall design for the TMHR is a simple lobed cylinder. Thermal-hydraulic calculations for this wall were performed with flat-plate geometry. To calculate the temperature distribution in the first-wall and in the breeder zone, a one-dimensional heat transfer model was established.

The energy balance equation was used to calculate the coolant temperature at positions of interest from the local volumetric heat generation rates. Knowing the thickness of the plate, the heat flux was calculated. The convective and conductive heat transfer equations were then used to calculate cladding and material temperatures. Hot-spot factors were included to account for manufacturing defects and material inhomogeneity. In calculating the pressure drops, the energy balance equation was used to calculate the coolant velocity, knowing the power generated, the geometry of the flow channel, and the inlet-outlet coolant temperature differential. Knowing the fluid velocity, the friction factor was calculated, which was then used to calculate the pressure

drops. Care was taken to distinguish between the laminar regime with $Re < 3000$ and the turbulent regime with $Re > 6000$ and to avoid operating in the transitional unstable regime whenever possible. Due to difference in blanket energy multiplication at the beginning and at the end of life, the coolant in the plate design would have to be operating in the transition regime, which is an approach that was adapted to calculate the heat-transfer coefficient in this regime.

First-Wall Cooling

Thermal-hydraulics calculations were performed on the first-wall, which is that section of the reactor closest to the plasma with the highest structural volumetric heat generation. The maximum temperature criterion of the first-wall was set at 500°C . To keep the blanket pressure drops within the limit of 124 kPa (18 psi), a limit of 13.8 kPa (2 psi) was set for the pressure drop through the first-wall. These criteria are not absolute, but they represent reasonable limits from what we presently know.

Based upon the material temperature and coolant pressure drop criteria, the temperature of the coolant at the midplane of the blanket module next to the first-wall may be estimated from the amount of energy absorbed by the coolant as it passes through the blanket. With reference to Fig. 6-13, Fig. 6-14 shows schematically the coolant temperatures at different locations. The He, which enters at 285°C , flows axially along the cold plenum, reaching the module side plenum at 288°C . The coolant temperature increases by about 6°C to 294°C as it flows through the module side plenum. It then flows along the first-wall and is heated to about 300°C before it enters the first-wall plenum and is distributed to the breeder plates. The coolant temperature exiting the module is set at 515°C to give a coolant inlet-outlet temperature differential of 230°C . At the operating pressure of 5.6 MPa (55 atm), this ΔT yields a potential thermal efficiency of 38%. Utilizing this coolant temperature distribution along with the first-wall volumetric heat generation rate of 14 MW/m^3 from the neutronics results, the temperatures of the first-wall were calculated.

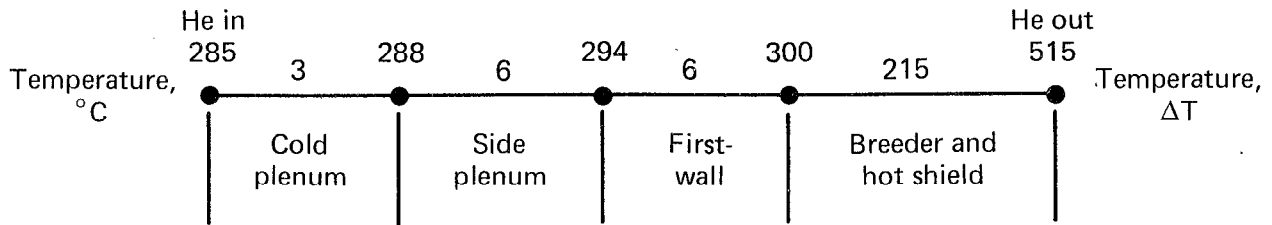


Fig. 6-14. Schematic of the He coolant temperature distribution in the blanket.

The simplest approach is a flat coolant channel immediately adjacent to the first-wall. This design was analyzed and was found to be acceptable. The flat-plate, first-wall cooling approach is shown in Fig. 6-15, where the coolant is distributed through the inlet-coolant gap of the flow distributor to the fuel plates after cooling the first-wall. The wall thickness of 0.5 cm is defined by mechanical design considerations, and the variable x is the coolant channel height. As the gap width decreases, the wall temperature decreases while the pressure drop increases.

With a first-wall thickness of 0.5 cm and a gap width of 0.5 cm the maximum wall temperature is 330°C , and the pressure drop along the wall is 1.4 kPa (0.2 psi); both are within the limits of 550°C and 3.4 kPa (0.5 psi), respectively. These numbers show the feasibility of the design and should be optimized in future studies.

Fuel-Plate Thermal-Hydraulic Design

Thermal-hydraulics calculations were performed for the plate design of the TMHR blankets. Results indicate that the design with an average plate thickness of 1.36 cm is acceptable and must have performance characteristics that meet the operating temperature and pressure drop criteria.

Plate Design and Mechanical Design Limits

Figure 6-16 shows a schematic of the tapered fuel-plates. Each plate has three sections: a 12-cm Th-metal section, a 45-cm Li_2O section, and a 10-cm section of stainless-steel hot shield. The plate is tapered from a thickness of 1.15 cm at the narrow end to 1.58 cm at the wider end. Helium

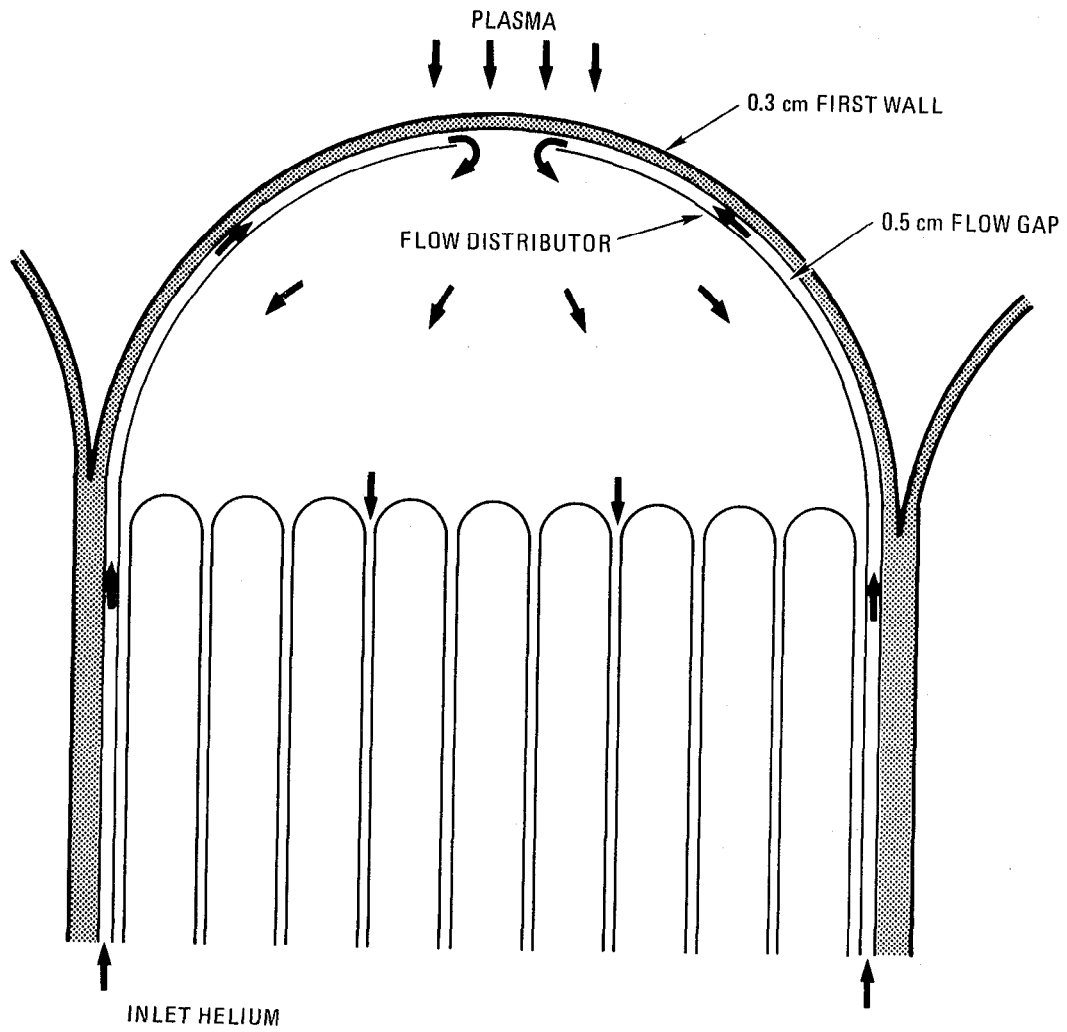


Fig. 6-15. First-wall cooling flow path.

coolant leaving the first-wall area flows in from the narrow edge toward the thicker edge through the wire-wrap gaps between the plates. The plates, each 50 cm long, are supported from the ends by a grid structure that also contains the piping for the Th plate pressure equalization system and the Li_2O plate tritium purge system. The plate assemblies are stacked to cover the length of the reactor. This coverage of the reactor central area would capture more than 95% of the fusion neutron energy. The slits at the narrow ends of the plates accommodate the change in plate dimensions and relieve the strain due to neutron induced swelling.

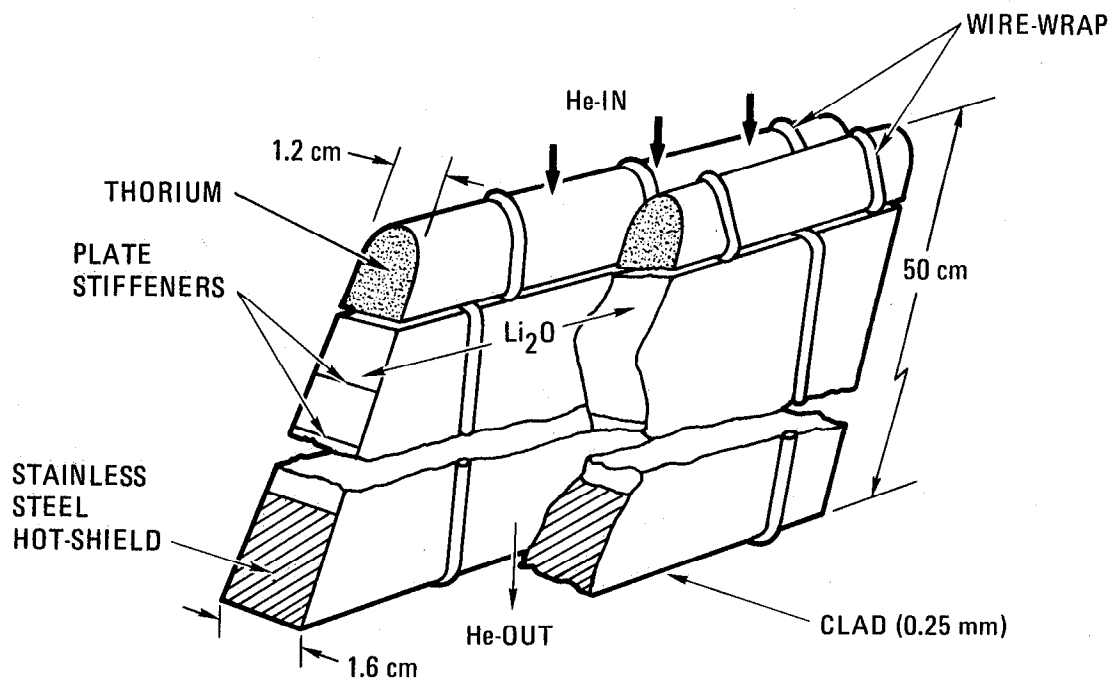


Fig. 6-16. Schematic of the wire-wrap fuel plates.

The primary functions of the clad are to separate the plates, to support the Th and Li_2O fuel materials, to contain the Li_2O , and to confine the T_2O that is produced from the tritium breeding reaction. Because the vented clad does not have to carry much load, mainly the weight of Th and Li_2O , a higher temperature limit of 665°C was used, whereas the temperature limit of the first-wall is 550°C . The centerline temperature limit of the plate was taken as the melting point of Li_2O at about 1700°C . The clad thickness was taken to be as thin as reasonable, from a manufacturing standpoint, about 0.25 mm. The He gap width was fixed at 1 mm to keep the convective heat

transfer coefficient high without exceeding the fuel zone coolant pressure drop limit of 20.7 kPa (3 psi). The coolant gaps are small, and tight tolerances are needed for the wire-wrap plate design in order to minimize hot spots from flow nonuniformities. Because of its favorable swelling properties under irradiation and lower cost than Inconel 718, HT-9 is recommended as the cladding material.

Input from Neutronics Results

Since more than 99% of the total thermal energy from nuclear interactions is deposited in the plate blanket section and the first-wall, it is crucial to know the spatial distribution of the energy deposition and to design the blanket thermal-hydraulics accordingly. Figure 6-17 gives the volumetric nuclear heating (MW/m^3) in the blanket as a function of distance from the first-wall. The energy deposition decreases roughly exponentially from the first-wall. For this reason the design is such that the coolant is first routed to the first-wall and then passes radially outward through the breeder plate section, putting the lowest He temperature in the region of highest power density. Figure 6-17 also shows the energy output at the highest energy multiplication, which is found at the end of life.

Flat Plate Fuel Design

The equations used were those applicable to flat plates which can adequately represent the geometry of flat-plate-type first-wall and breeder plates.

The following key equations were used in calculating the temperature distributions:

Heat transfer coefficient,

$$g = 8.23 k/D_e \quad \text{for } Re < 3000$$

$$h = 0.021 Re^{0.8} Pr^{0.6} k/D_e \quad \text{for } Re > 6000,$$

(1)

where Re and Pr are the Reynolds and Prandtl numbers, k and ϵ are coolant thermal conductivity and roughness factor, and D_e is the equivalent diameter.

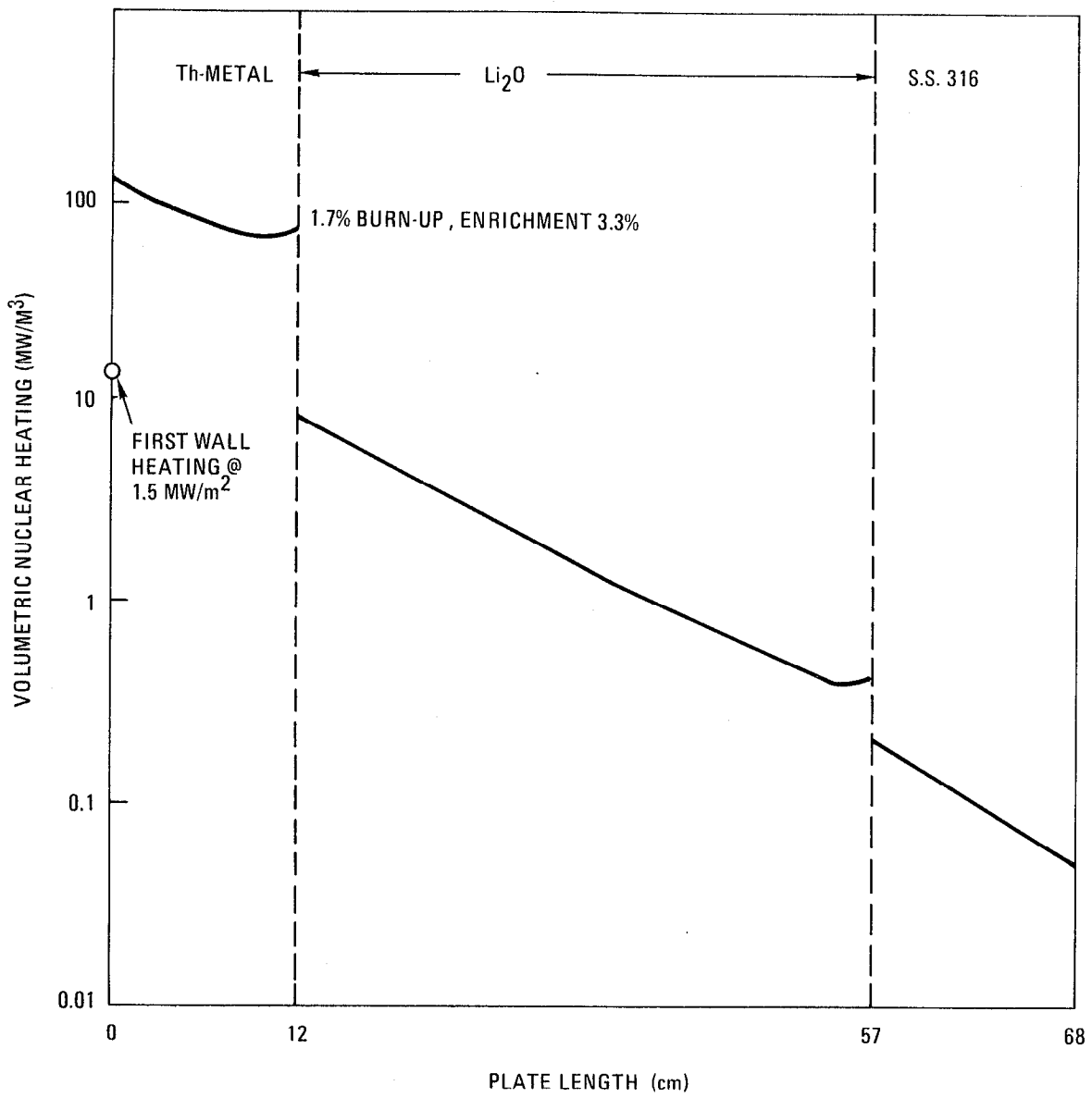


Fig. 6-17. Blanket end-of-life power density.

Coolant thermal conductivity,

$$k = \mu C_p / Pr \quad , \quad (2)$$

where μ and C_p are the coolant viscosity and specific heat.

Coolant viscosity,

$$\mu = 3.953 \times 10^{-7} (T_c)^{0.687} \quad , \quad (3)$$

where T_c is the coolant temperature in degree K.

Coolant density,

$$\rho = P / (RT_c) \quad , \quad (4)$$

where P is the He pressure, and R is the constant (2077 J/kg⁰ K).

Hot spot cladding and fuel temperatures,

$$T_{WHSF} = T_o + F_b \Delta T_b + F_{cf} \Delta T_f + F_c \Delta T_c$$

$$T_{CHSF} = T_o + F_b \Delta T_b + F_{ff} \Delta T_f + 2F_c \Delta T_c + F_g \Delta T_g + F_F \Delta T_F \quad .$$

The respective symbols and values used in the calculations are listed in Table 6-6. The volumetric heating rates in the blanket (\dot{q}''') were obtained from neutronics calculations. The various temperature differentials were calculated by one-dimensional heat transfer conduction and convection equations.

One major difficulty in analyzing the thermal hydraulics of the plate design was caused by the varying energy multiplication of the blanket during the lifetime (6.4 full power yrs) of the plate from 2.8 to 8.5, as shown in Fig. 6-18. To maintain a constant coolant outlet temperature the coolant mass flow rate has to be changed; thus, the Reynolds number would vary for a fixed-plate geometry during the submodule lifetime, as shown in Fig. 6-19. Since the Reynolds numbers indicate the coolant would be operating in the transition regime at some time during blanket life, an appropriate method must be developed for the calculation of heat transfer coefficients operating in this regime.

Table 6-6. Hot spot factor variables, coefficients, and their values.

Parameter	Symbol (units)	Values
Inlet temperature	T_o (C)	285
Bulk coolant temperature rise	T_b	-
Film temperature rise	T_f	-
Cladding temperature rise through half the cladding thickness	T_c	-
Fuel-cladding gap temperature rise	T_g	-
Fuel temperature rise	T_F	-
Bulk coolant hot spot factor	F_b	1.3
Film hot spot factor for coolant	F_{cf}	1.25
Cladding hot spot factor	F_c	1.25
Fuel-cladding gap hot spot factor	F_g	1.5
Fuel hot spot factor	F_F	1.2

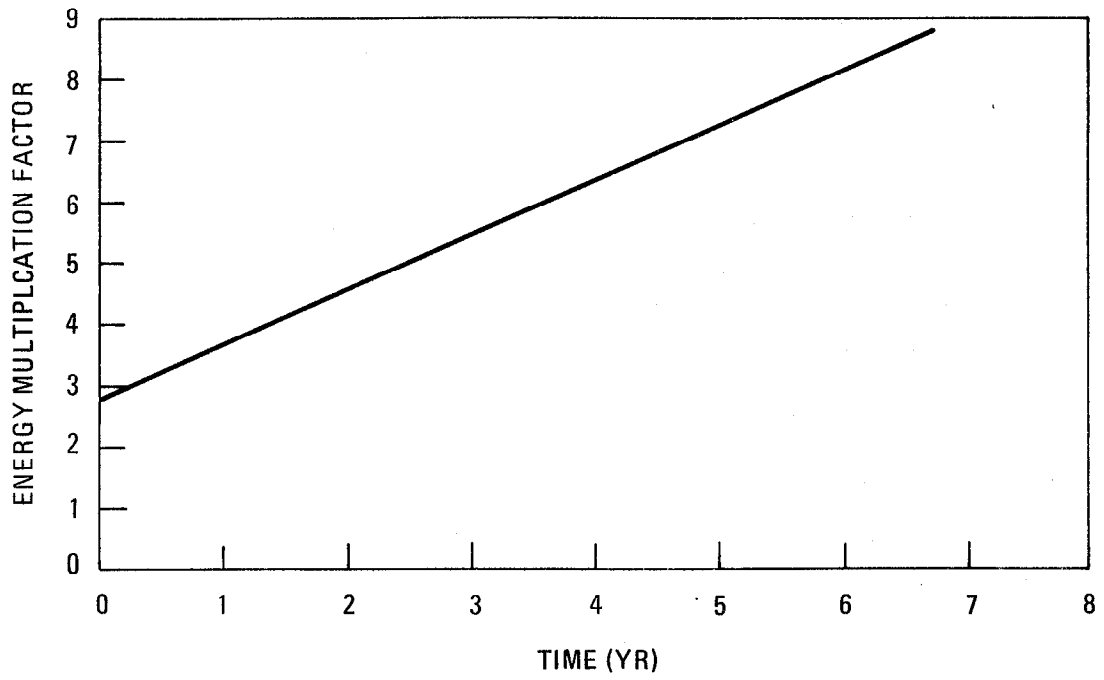


Fig. 6-18. Energy multiplication factor vs time.

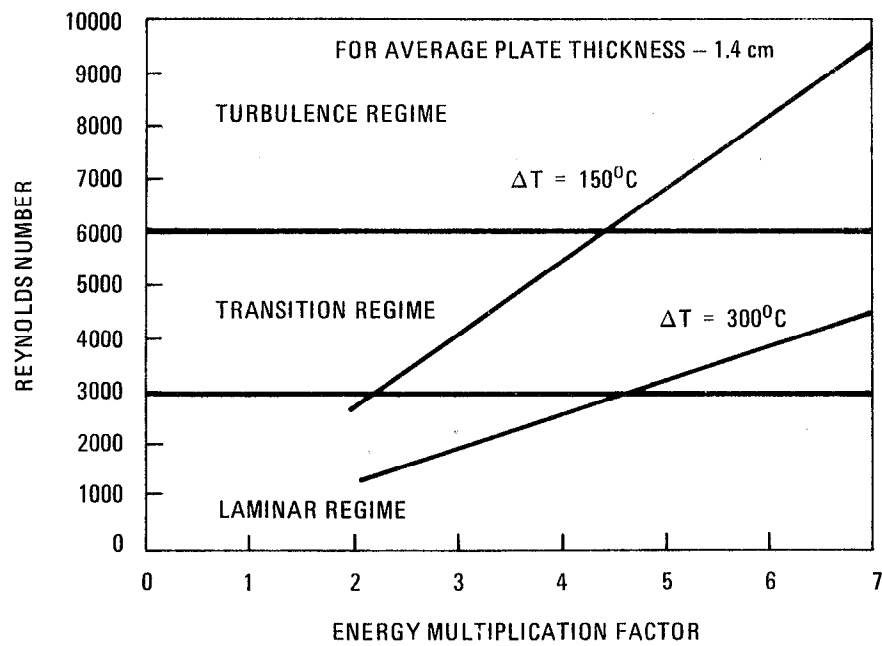


Fig. 6-19. Reynolds number versus multiplication factor (for plate thickness - 1.4 cm ave.).

From the experience of GCFR the heat transfer coefficient for transitional flow was obtained by first comparing the friction factors for laminar and turbulent flow at the given Reynolds number; then the higher friction factor, f , was selected for the pressure drop calculation, and the corresponding heat transfer coefficient was used for the film drop calculation. Calculations for the beginning and the end-of-life of the blanket were calculated to bracket the thermal hydraulics performance. The key equations used in the calculation of pressure drop are the following: In the laminar regime, $Re < 3000$, the friction factor f is equal to

$$f = 16/Re \quad , \quad (5)$$

and in the turbulent regime, $Re > 6,000$

$$f = 0.0791 Re^{-0.25} \quad (6)$$

The pressure drop is given by

$$\Delta P = 4 \frac{L}{D_e} f \frac{1}{2} V^2 \quad , \quad (7)$$

where L and V are the coolant path length and average velocity, respectively.

Plate Design Thermal Hydraulics Results

Figure 6-20 shows the variations of coolant mass flow rate, pressure drop, and blanket energy multiplication during reactor life. It shows that the coolant pressure drop is within the criterion of 20.7 kPa (3 psi).

Figure 6-21 shows the temperature distributions of the plate and coolant at the beginning and the end-of-life. The thermal conductivity used in the Li_2O zone was calculated as that of a mixture of Li_2O powder and static He and would be a conservative estimate. Figure 6-21 also shows the satisfaction of design criteria for centerline and cladding temperatures.

Table 6-7 summarizes the plate design parameters of the TMHR. These parameters are the results of simple one-dimensional model calculations, principally showing the feasibility of the proposed design. Further detailed calculations and analyses will be needed during the advanced phases of the design.

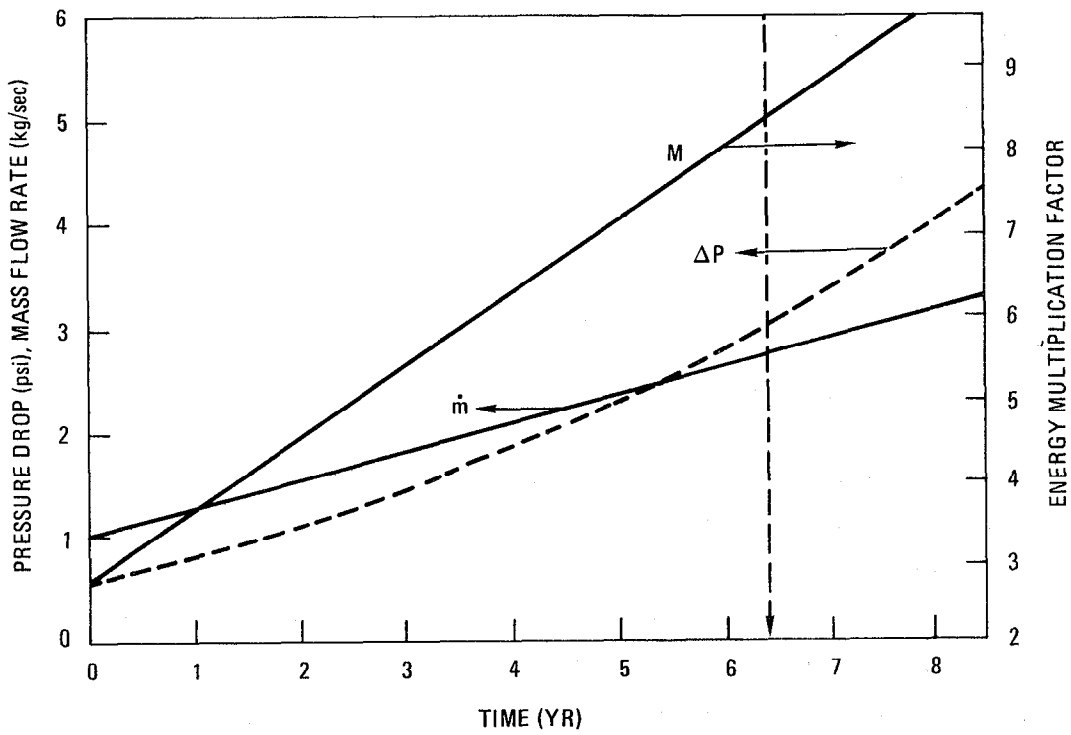


Fig. 6-20. Energy multiplication factor - pressure drop (mass flow rate vs time).

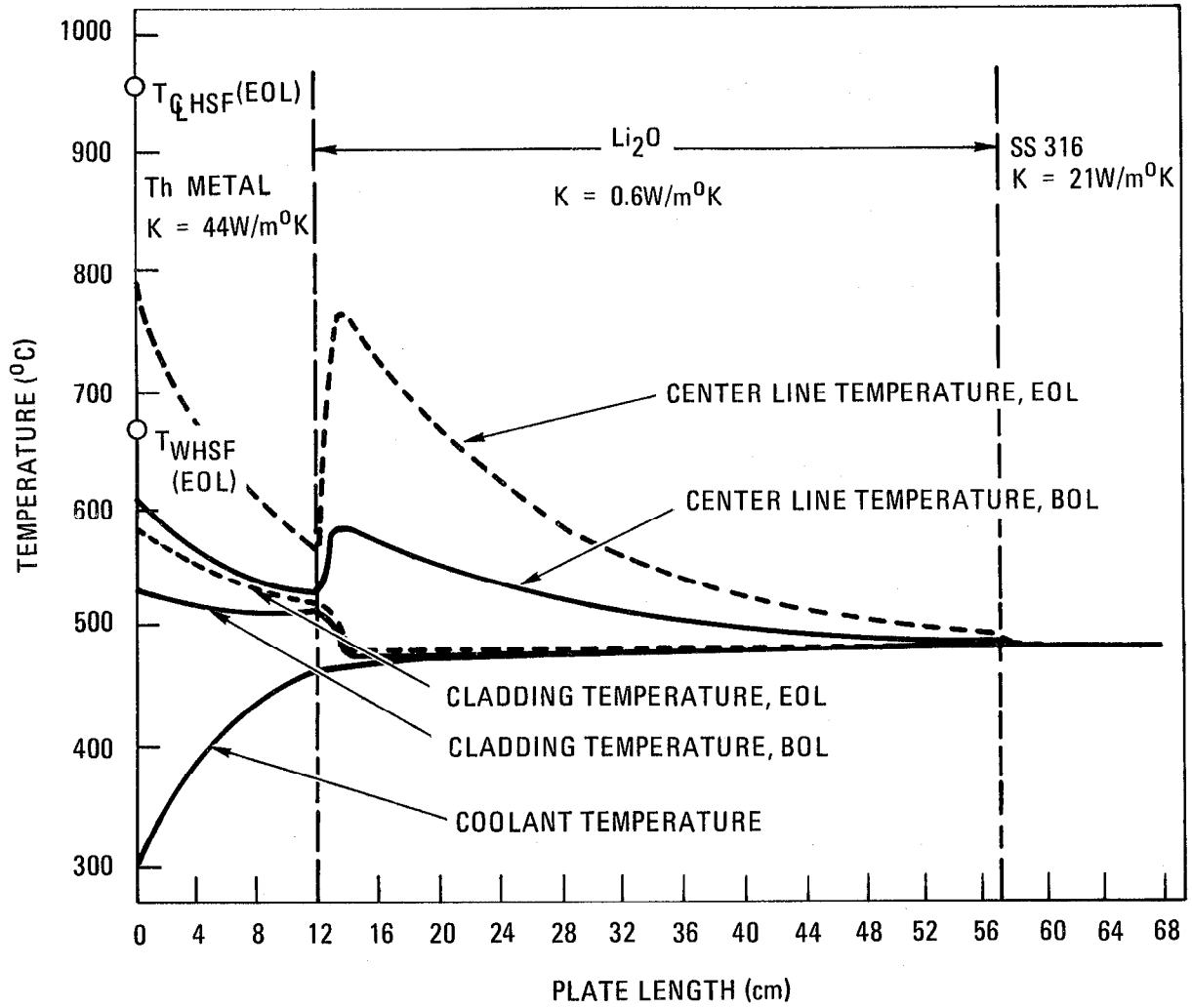


Fig. 6-21. Nominal temperatures in the blanket.

Table 6-7. Breeder plate design parameters.

Fertile material	Th
Tritium breeding material	Li ₂ O
Thermal power output	4000 MW _t
Maximum volumetric nuclear heating	120 MW/m ³
Maximum wall loading	1.5 MW/m ²
Number of plates/submodule	24
Dimensions:	
Width of plate (narrow side)	1.15 cm
Width of plate (wide side)	1.58 cm
Length of plate	68 cm
Height of plate	50 cm
Cladding thickness	0.25 mm
Width of coolant gap	1 mm
Helium parameters:	
Pressure	5.6 MPa (55 atm)
Inlet temperature to fuel zone	300°C
Outlet temperature	515°C
Reynolds number	2162 → 6562
Pressure drop	3.4 → 20.7 kPa (0.5 → 3.0 psi)
Mass flow rate/module (3.5 m long)	140 → 385 kg/s
Thermal cycle efficiency	~38%

Axially Oriented Rods With Cross Flow

Design calculations were made for axially oriented rods with cross flow in the blanket of TMHR in order to compare this option with the plate configuration. The rods can be fairly long (~1 m) by putting them in the axial direction in the blanket module, which may reduce the blanket cost. Further, the rods would be easier to manufacture than plates. A preliminary analysis was done to determine the optimized design within the allowable thermal and mechanical constraints. A comparison between plates and tangential rods design was also made.

To compare the plate design with the axial rod design the coolant inlet-outlet differential was set at 230° C, and the coolant pressure drop was set at 20.7 kPa (3 psi). An analysis based on the coolant operating conditions at the blanket end-of-life was made. Because of the exponentially decreasing distribution of the nuclear volumetric heating from the first-wall outward, the heat source for the axial rod calculation is that from the rod next to the first-wall, which gives an indication of the worst situation. The inlet temperature of He to the fuel region is 300° C, and the volumetric heat generation rate is 120 MW/m³ at the end-of-life. The axial rod was designed with annular pellets to allow swelling from neutron irradiation. By a conservative evaluation maximum volumetric swelling of Th metal is about 2%, which corresponds to a linear expansion of 1.4%.

The temperature differentials for cylindrical rods can be calculated by the following expressions:

$$\Delta T_f = \frac{1}{h_f} q''' \frac{(r_p^2 - r_h^2)}{2r_r}, \quad (8)$$

$$\Delta T_c = \frac{t}{k_c} q''' \frac{(r_p^2 - r_h^2)}{4(r_r - t)}, \quad (9)$$

$$\Delta T_g = \frac{1}{h_g} q''' \frac{(r_p^2 - r_h^2)}{2r_p}, \quad (10)$$

$$T_F = \dot{q}''' \frac{r_p^2}{4k_f} \left(1 - \frac{r_h^2}{r_p^2} - \frac{r_h^2}{r_p^2} \ln \frac{r_p}{r_h} \right), \quad (11)$$

where

t = cladding thickness.

r_p = radius of fuel pellet.

r_h = radius of central fuel hole.

r_r = radius of fuel rod (including clad).

The hot-spot temperatures were calculated by using Eq. (9) and Eq. (11) with coefficients defined in Table 6-8.

Table 6-8. Fuel configuration thermal-hydraulic characteristics.

Parameter	Plate	Axial rod, cross-flow	Radial rod, radial flow
Characteristic:	Plate thickness: 1.15 - 1.58 cm	Outer diam: 1.19 cm	Outer diam: 1.67 cm
Dimension:	Coolant channel: 1 mm	Pitch/diameter: 1.18	Pitch/diam: 1.05
$\Delta T = T_{out} - T_{in}$	230°C	230°C	230°C
ΔP (kPa)	20.7	20.7	7.2
h (W/m ² °K)	2434	2174 (minimum 1087)	1122
$T_{max,CLAD}$	666°C	663°C	662
T_{maxmcl}	939°C	775°C	765°C
Reynolds number	6562	18212	4170
Void fraction	7.3%	35%	17.8%
Clad/solid	3.6%	8.2%	5.9%

The radial rods in the blanket submodule were designed in a staggered arrangement in order to reduce neutron streaming and to enhance heat transfer. Correlations for heat transfer coefficient, friction factor, and pressure drop in staggered tube banks in the turbulent-flow regime, $G_{\max} d_H / \mu_n > 6000$, are as follows¹³:

$$\bar{h}_c = \frac{k_f}{r_r} \times 0.33 \cdot \left(\frac{B_{\max} r_r}{\mu_f} \right)^{0.6} \cdot Pr_f^{0.3},$$

where

G_{\max} = mass velocity at the minimum area.

μ_f = viscosity at film temperature.

The friction factor f can be calculated by

$$f = 0.25 + \frac{0.1175}{(P/D - 1)^{1.08}} \frac{T_{\max} r_r}{\mu_b}^{-0.16}$$

for $Re > 6000$, where

P/D = pitch to diam ratio.

μ_b = viscosity at bulk temperature.

The Reynolds number in this staggered rod bank design is usually very high; therefore the coolant is operated in turbulent regime. The frictional pressure drop for flow over a bank of rods can be calculated by

$$\Delta p = \frac{2f G_{\max}^2 N}{\rho} \left(\frac{\mu_s}{\mu_b} \right)^{0.14},$$

where

N = number of transverse rows of rods.

μ_s = viscosity at rod surface temperature.

Thermal-Hydraulic Results for Axial Rod, Radial Flow Design

The clad temperature is a function of both rod size and pitch-to-diameter ratio: the larger the rod size, the higher the clad temperature. The clad temperature is also an increasing function of pitch-to-diameter ratio.

Figure 6-22 shows the relation between clad temperature, rod size, and pitch-to-diameter ratio. Acceptable ranges for rod diameters and pitch-to-diameter are also indicated for clad temperature less than 665°C .

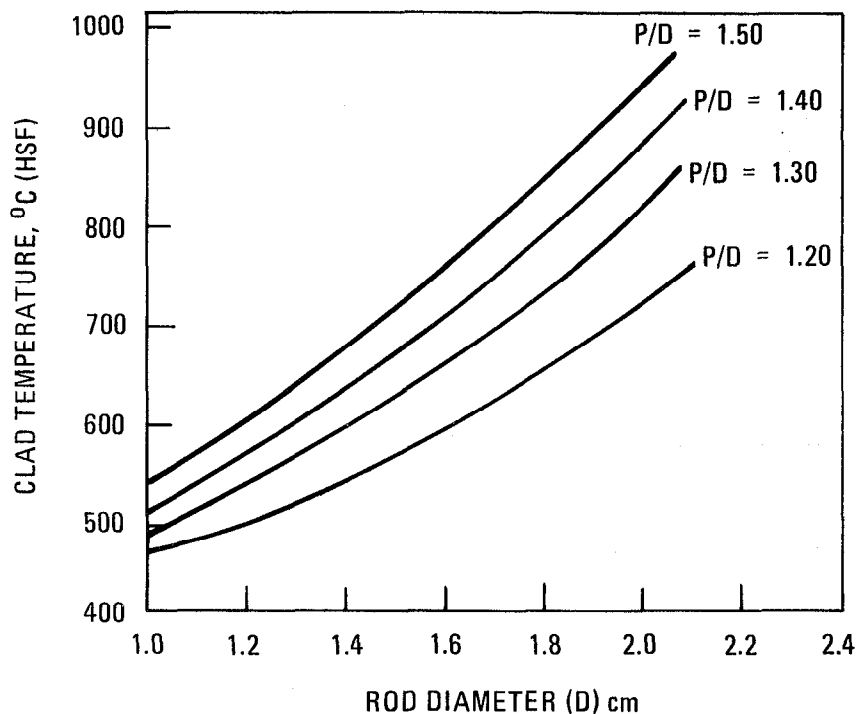


Fig. 6-22. Hot spot cladding temperature vs rod diameter for cross flow rods (average h).

The frictional pressure drop is also a function of rod size and pitch-to-diameter ratio, as shown in Fig. 6-23. For close packed arrangement (pitch-to-diameter ratio = 1.15), the pressure drop exceeds the design limit of 20.7 kPa (3 psi). Figure 6-23 also indicates the acceptable operating regime when the temperature limit is also taken into consideration. The analysis so far is based on the average heat transfer coefficient. However, with cross flow rods there would be a circumferential variation in the heat transfer coefficient around the individual rod. A conservative approximation for the minimum local heat transfer coefficient may be obtained by considering an isolated rod. Reference 14 indicates that the minimum value of h is half of the value of the average heat transfer coefficient. As a result, the acceptable operation regime has been reduced as shown in Fig. 6-24.

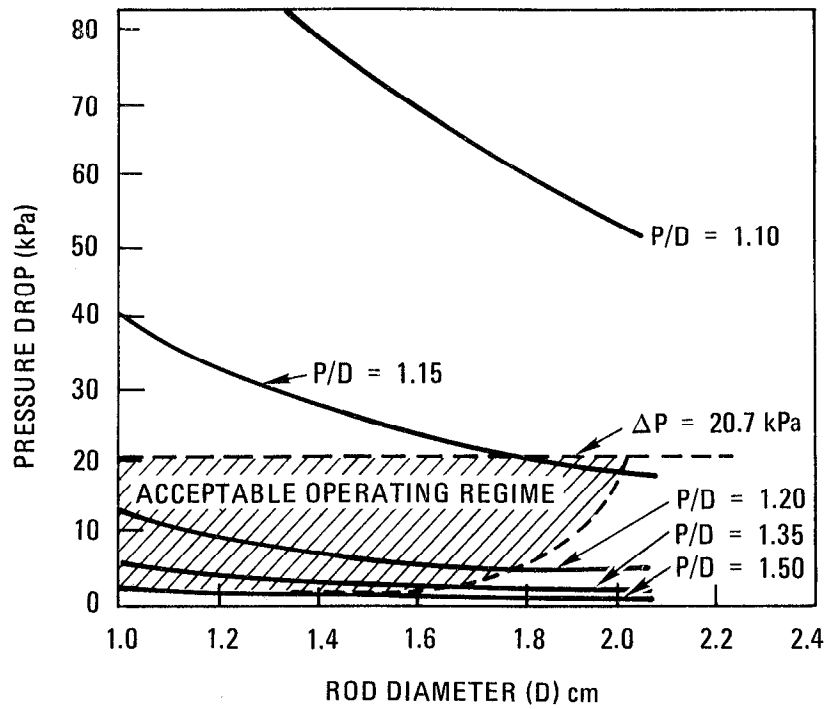


Fig. 6-23. Pressure drop vs rod diameter for cross flow rods.

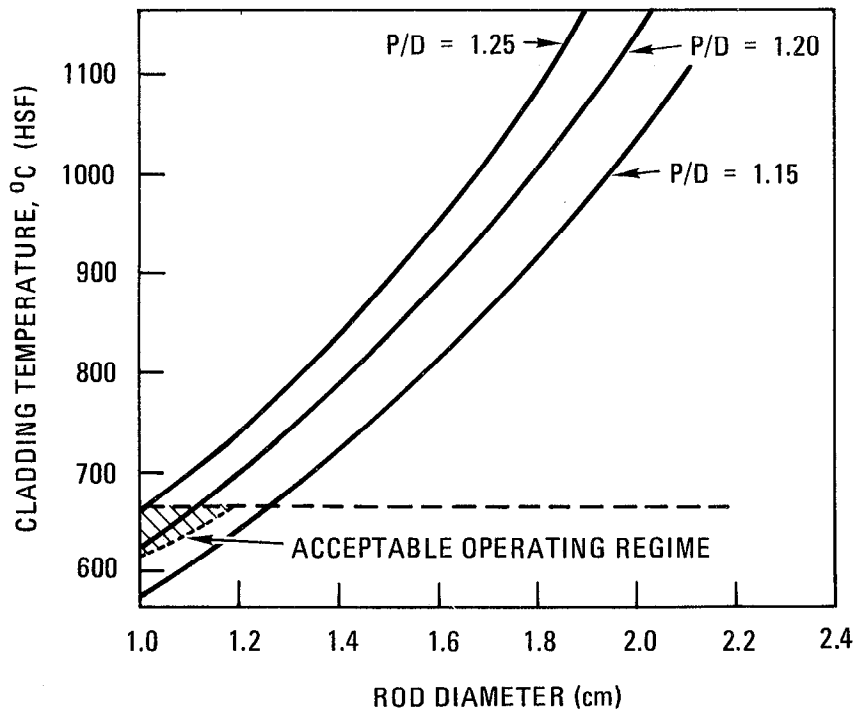


Fig. 6-24. Peak cladding hot spot temperature vs rod diameter for cross flow rods.

Radial Rod, Radial Flow Design

The third fuel configuration considered is that of radially oriented rods with radial coolant flow. Use of this configuration for gas-cooled hybrid blankets under the same flow conditions and with the same fuel geometry has been studied by Rao and Baxi with U_3Si as fertile material for the Standard Mirror Hybrid Reactor design¹¹. The basic strategy and calculation method are the same as in the previous studies.

The fuel rod in the blanket is made of three different zones. Thorium is placed in the first zone as fertile material, followed by Li_2O in the center part of the rod as the tritium breeding zone. The end part of the blanket is composed of a 10-cm, stainless steel 316 reflector/shield. Since the limiting rod diameter occurs in the Th zone, future studies should investigate use of larger rods in the Li and reflector/shield zones.

The thermal-hydraulic correlations for the wire-wrapped radial blanket assemblies are obtained from experimental data done by the GCFR group for a pitch-to-diameter ratio of 1.05.¹⁵

The friction factor correlations are listed below:

$$f = 25.72 Re^{-0.835} \quad \text{in laminar region}$$
$$f = 0.436 Re^{-0.263} \quad \text{in turbulent regime}$$

The heat transfer coefficient can be calculated by

$$Nu = 2.82 \quad \text{in laminar flow}$$
$$Nu = 0.0203 Re^{0.79} \quad \text{in turbulent flow}$$

Entrance effects have also been considered during the calculation. Again, for consistency of comparison between the three fuel configurations, the inlet and outlet temperature difference is set at 230° C. Because of the relatively large flow area between even close-packed rods, the pressure drop is not a limiting consideration with radially oriented rods. The hot spot cladding temperature limit of 665° C limits the fuel rod diameter to 1.67 cm. The characteristics of this design are shown in Table 6-8.

Thermal Hydraulic Comparison

The comparison between plate, axial rod, and radial rod results is tabulated in Table 6-8. Due to the entrance effect, the maximum cladding temperature in the radial rod and plate design occurs at a few centimeters away from the front face of the fuel zone. This is where the volumetric heat source

strength is lower than that in axial rod, and where the maximum cladding temperature is found at the first rod in the module. This results in a higher maximum center line temperature in the axial rod case, even though it has a smaller rod diameter than the radial rod design.

Table 6-8 compares the thermal-hydraulic characteristics of the three fuel configuration options under equal design conditions. All three configurations result in different amounts of coolant void fraction and different clad/structure fractions in the three designs. The higher clad fraction in the two rod designs means that these blankets will have to be thicker than the plate design blanket in order to achieve the same level nuclear interactions.

Further, the higher structural content of the rod design blankets will degrade the nuclear performance of these concepts compared to the plate design. The additional structural fractions shown in Table 6-8 will degrade the U breeding ratio and energy multiplication factor of the axial rod design by about 7% and the radial rod design by about 4% compared to the performance expected from the plate design blanket.

Because of the superior nuclear performance, the acceptable thermal hydraulic characteristics, and the mechanical design feasibility, the plate geometry concept has been chosen for the reference gas-cooled TMHR blanket design. More detailed design and analysis of the blanket is required to fully assess the performance and feasibility concerns of the blanket. On the basis of the preliminary analysis presented above, however, the plate design appears quite feasible.

Blanket Coolant Pressure Drops

Simple but reasonable system pressure drop calculations were performed. The total blanket pressure drop from He inlet to outlet is estimated to be 59 kPa (8.5 psi), which is well within the limit of 124 kPa (18 psi). In this phase of the study efforts were concentrated on the dominant features of the FRM blanket design, namely the first-wall and blanket plate. The coolant channels in the blanket along the rest of the coolant route were not considered in significant detail. The approach taken was to use reasonable rule-of-thumb calculations to estimate these pressure drops.

For the coolant plena the mass flow rates were determined from energy balances, and the flow velocities and ducting dimensions were then found by assuming velocity heads of 0.5 psi (3.49 kPa). Knowing the coolant velocity

and channel dimensional characteristics, pressure drops for the various sections were then calculated. Turning losses were estimated as half a velocity head each, while contraction and expansion losses were assumed to be 0.5 psi (3.49 kPa) each. The number of channels in the different sections were selected based on the local geometries.

Figure 6-25 is a schematic of the coolant routing in the blanket. The numerals represent different sections of the blanket, the letters represent expansions or contractions, and the turns are indicated by the right angles.

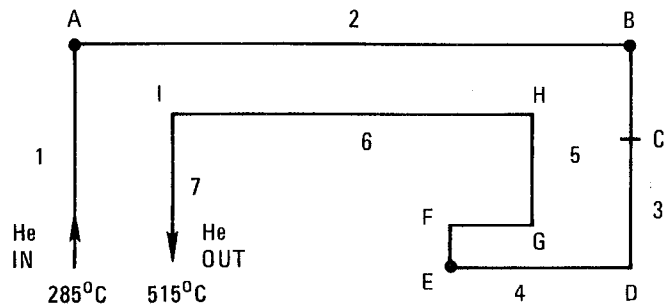


Fig. 6-25. He coolant routing in the FRM blanket.

The identifications of the sections are given in Table 6-9. Table 6-10 shows the flow and pressure drop characteristics of the reactor blanket.

Turning losses from coolant inlet to outlet add up to about 11.9 kPa (1.72 psi), while expansion and contraction losses total about 27.6 kPa (4 psi). Therefore, the total pressure drop in the blanket is $25.4 + 11.9 + 27.6 = 65$ kPa (9.4 psi), well within the pressure drop limit of 124 kPa (18 psi).

With the inclusion of estimated pressure losses from the steam generator and external ducting ~ 110 kPa (16 psi), the total system pressure loss is 170 kPa (24.5 psi). Thus, the system $\Delta P/P$ is 3.0%, which is quite acceptable and less than 4.3%, the stated $\Delta P/P$ limit.

Table 6-9. Identification of blanket coolant channels (ref. Fig. 6-25).^a

Section	Description
1	Coolant inlet piping.
2	Cold He annular plena coolant flowing along reactor axis.
3	Cold He flowing through the module side plena radially inward.
4	First-wall channels.
5	Gaps between fuel zone, Li ₂ O, and hot shield plates.
6	Hot He plena outside the hot shield, coolant flowing axially.
7	Coolant outlet piping.

^aThe respective turns, expansions and contractions are between the sections. Turns F, G, and H are for the coolant going through the first-wall flow distributor to the plenum and into the channels between the breeder plates.

Table 6.10. Pressure drops through different blanket sections.

Section	Characteristic dimension, m	Number of channels	Mass flow rate, ^a kg/s	Flow velocity, m/s	Pressure drop, kPa	psi
1	1.25	1	209	41.0	1.54	0.22
2	0.07	1	209	41.0	0.012	0.002
3	0.007	80	2.6	26.0	0.88	0.13
4	0.005	80	2.6	36.0	0.5	0.073
5	0.001	Plates	5.2	25.0	21.0	3.00
6	0.08	1	209	50.0	0.015	0.002
7	1.38	1	209	50.0	<u>1.42</u>	<u>0.2</u>
TOTAL					25.4	3.6

^aThese numbers are for a reactor thermal power of 250 MW per module and a coolant ΔT of 230°C.

Nucleonics

The nucleonic design of the blanket and shield for the TMHR reported here is a continuation of the interim design study.¹ In the interim design study the nucleonics investigation was concentrating on obtaining the confidence in the calculational results and providing the nuclear performance evaluations of several hybrid blanket concepts, such as Th metal and U₃Si-Th at the beginning of life of the power plant. After this evaluation, the He-cooled, Th-fueled blanket concept was chosen for the follow-up design. The choice was made based on the comparisons on the quality of the bred fuel (²³³U vs ²³⁹Pu), blanket design simplicity, economics, assured net energy production, and tolerance to loss-of-coolant flow accidents. The tolerance to the loss-of-coolant flow accident is inversely proportional to the blanket thermal energy multiplication and the temperature difference between the melting point of the fuel material and the blanket operating temperature.

The exploration of the nucleonic performance capabilities of the Th materials (namely Th metal, ThC, ThC₂, and ThO₂) is given in more depth. To fully utilize the neutron multiplication of the Th zone, different blanket zone arrangements were investigated. The reference Th-metal fuel design selected was based on the comparisons of nucleonic performance, physical material properties, thermal-hydraulic performance, and mechanical design considerations.

The final nucleonic results calculated for the reference He-cooled TMHR blanket design are presented and discussed, and the conclusions from the nucleonic studies are presented.

Method of Calculations and Nuclear Data

The one-dimensional discrete-ordinates transport code, ANISN, was employed for all neutronics calculations with the P₃S₆ approximation in cylindrical geometry.¹⁶ All the nuclear data used except Th were from the DLC-37¹⁷ library and were collapsed into a coupled 25 neutron and 21 gamma-ray group structure. The new group structure is given in Table 6-11 and 6-12 for neutrons and gamma rays, respectively. The Th nuclear data were from the DLC-41¹⁸ library and were also collapsed into the same group structure.

Table 6-11. Neutron 25 energy group structure (in eV).

Group	Group limits			Corresponding fine groups in 100 group structure ^a
	E(Top)	E (low)	E (midpoint)	
1	1.4918 (+7)	1.3499 (+7)	1.4208 (+7)	1
2	1.3499 (+7)	1.2214 (+7)	1.2856 (+7)	2
3	1.2214 (+7)	1.1052 (+7)	1.1633 (+7)	3
4	1.1052 (+7)	1.0000 (+7)	1.0526 (+7)	4
5	1.0000 (+7)	9.0484 (+6)	9.5242 (+6)	5
6	9.0484 (+6)	8.1873 (+6)	8.6178 (+6)	6
7	8.1873 (+6)	7.4082 (+6)	7.7979 (+6)	7
8	7.4082 (+6)	6.7032 (+6)	7.0557 (+6)	8
9	6.7032 (+6)	6.0653 (+6)	6.3843 (+6)	9
10	6.0653 (+6)	5.4881 (+6)	5.7787 (+6)	10
11	5.4881 (+6)	4.4933 (+6)	4.9907 (+6)	11 - 12
12	4.4933 (+6)	3.6788 (+6)	4.0860 (+6)	13 - 14
13	3.6788 (+6)	3.0119 (+6)	3.3453 (+6)	15 - 16
14	3.0119 (+6)	2.4660 (+6)	2.7390 (+6)	17 - 18
15	2.4660 (+6)	1.3534 (+6)	1.9097 (+6)	19 - 24
16	1.3534 (+6)	7.4274 (+5)	1.0481 (+6)	25 - 30
17	7.4274 (+5)	4.0762 (+5)	5.7518 (+5)	31 - 36
18	4.0762 (+5)	1.6573 (+5)	2.8667 (+5)	37 - 45
19	1.6573 (+5)	3.1828 (+4)	9.8779 (+4)	46 - 54
20	3.1828 (+4)	3.3546 (+3)	1.7591 (+4)	55 - 63
21	3.3546 (+3)	3.5358 (+2)	1.8541 (+3)	64 - 72
22	3.5358 (+2)	3.7267 (+1)	1.9542 (+2)	73 - 81
23	3.7267 (+1)	3.9279 (+0)	2.0597 (+1)	82 - 90
24	3.9279 (+0)	4.1399 (-1)	2.1718 (+0)	91 - 99
25	4.1399 (-1)	2.2000 (-2)	2.1800 (-1)	100

^aThe original Experimental Power Reactor (EPR) library group structure.¹⁷

Table 6-12. Gamma 21 multigroup structure (in MeV).

Group	Group boundaries		
	E (top)	E (low)	E (midpoint)
1	1.4E01	1.2E01	1.30E01
2	1.2E01	1.0E01	1.10E01
3	1.0E01	8.0E00	9.00E00
4	8.0E00	7.5E00	7.75E00
5	7.5E00	7.0E00	7.25E00
6	7.0E00	6.5E00	6.75E00
7	6.5E00	6.0E00	6.25E00
8	6.0E00	5.5E00	5.75E00
9	5.5E00	5.0E00	5.25E00
10	5.0E00	4.5E00	4.75E00
11	4.5E00	4.0E00	4.25E00
12	4.0E00	3.5E00	3.75E00
13	3.5E00	3.0E00	3.25E00
14	3.0E00	2.5E00	2.75E00
15	2.5E00	2.0E00	2.25E00
16	2.0E00	1.5E00	1.75E00
17	1.5E00	1.0E00	1.25E00
18	1.0E00	4.0E-01	7.00E-1
19	4.0E-01	2.0E-01	3.00E-1
20	2.0E-01	1.0E-01	1.50E-1
21	1.0E-01	1.0E-02	5.00E-2

Note here that the Th nuclear data derived from ENDF/B-IV do not include the gamma production cross sections; the gamma rays generated from the neutron interaction with the Th could not be handled by the coupled neutron and gamma-ray transport scheme. The portion of the energy generated from the Th is calculated using the Q value (or mass-energy balance) released from each neutron interaction. We also made the assumption that the secondary gamma ray is deposited at the site of the production. This assumption may over estimate the heating in the fuel. However, the contribution of the secondary gamma-ray heating to the total heating in the fertile material is only about 10% and 5% at the beginning of blanket life and the end-of-life, respectively. Thus, the effect of this simplified assumption on the blanket heat transfer analysis would be small.

Nucleonic Performance Comparisons of the Th Materials

The Th materials considered as candidates for the blanket fertile material are Th metal, ThC, ThC₂, and ThO₂. The nucleonic performances of the blanket employing these materials are explored in this subsection. The parameters to be revealed in this attempt are the maximum number of neutrons available for breeding per fusion neutron and maximum blanket energy multiplication as functions of both percent structure in the blanket and blanket thickness. For these purposes the blanket model used consists of a 10-mm first-wall and a varying thickness of Th material and structure. The first-wall and blanket structure used here is Inconel 718. The available neutrons are either those neutrons absorbed by the Th element in the blanket or those leaked out of the Th zone and thus available for tritium production.

The results for the blanket at the beginning-of-life with Th metal, ThC, ThC₂, and ThO₂ materials at 7% structure by volume are given in Figs. 6-26 and 6-27. In Fig. 6-26 the available neutrons per fusion neutron are displayed as a function of fertile blanket thickness. The blankets reach their full capabilities at a thickness of about 0.3 m for all Th materials considered here. The maximum available neutrons (at 7% structure by volume) for Th metal ThC, ThC₂, and ThO₂ blankets are 1.95, 1.75, 1.65, and 1.60 per fusion neutron, respectively. The blanket energy multiplications are displayed in Fig. 6-27, and the maximum values of them are 3.5, 2.80, 2.55, and 2.50 for Th metal, ThC, ThC₂, and ThO₂ blanket, respectively. In these two figures it is clear that from the neutronics performance point of view, the Th metal is the best material to be employed as the fertile material.

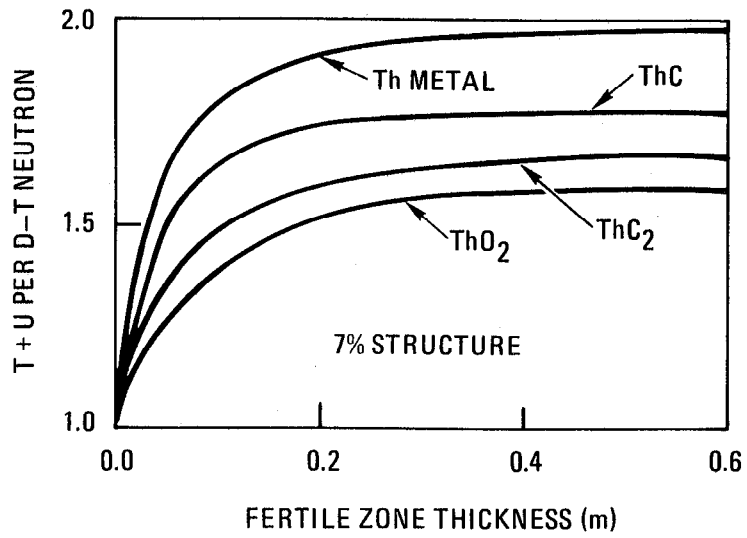


Fig. 6-26. Breeding ratios vs fertile zone thickness at time = 0.

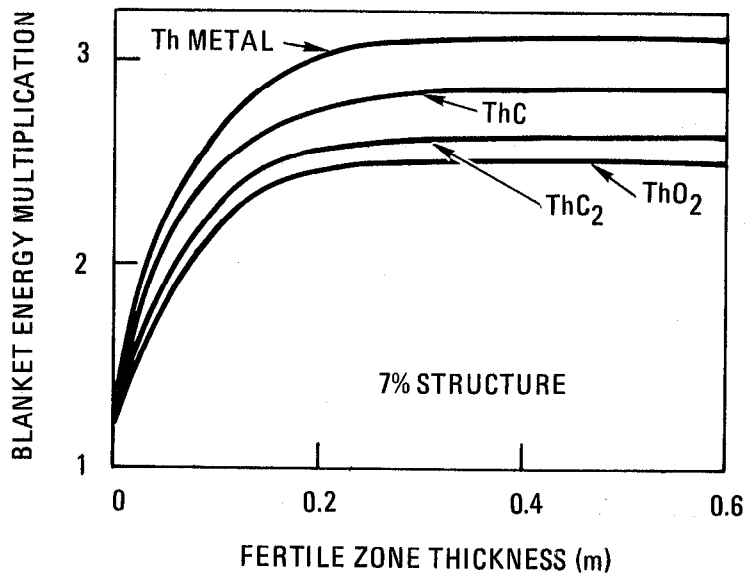


Fig. 6-27. Blanket energy multiplication vs fertile zone thickness at time = 0.

The structural effect on the available neutrons and blanket energy multiplications are presented in Fig. 6-28 for the Th metal, ThC, ThC₂, and ThO₂ blankets of 0.3-m thickness. The presence of more structure in the blanket would compete with the neutron multiplication of the Th material and decrease the total available neutrons per fusion neutron and blanket energy multiplication. From Fig. 6-28 the available neutrons per fusion neutron and blanket energy multiplication for the Th metal blanket decrease to 1.90 and 3.00, respectively, at 12% structure by volume. As compared to the performance, it is relatively small; however, in a more complete blanket design model with distinct ²³³U and tritium production regions, the structural effect will cause the tritium production rate to fall. In an optimized design with just adequate tritium production and maximum ²³³U production, this will mean that the Th zone thickness will have to be reduced to again achieve adequate tritium breeding. This reduction will reduce the total number of neutrons available for breeding. Thus, the simple model used here is expected to underestimate the impact of blanket structure upon net breeding performance.

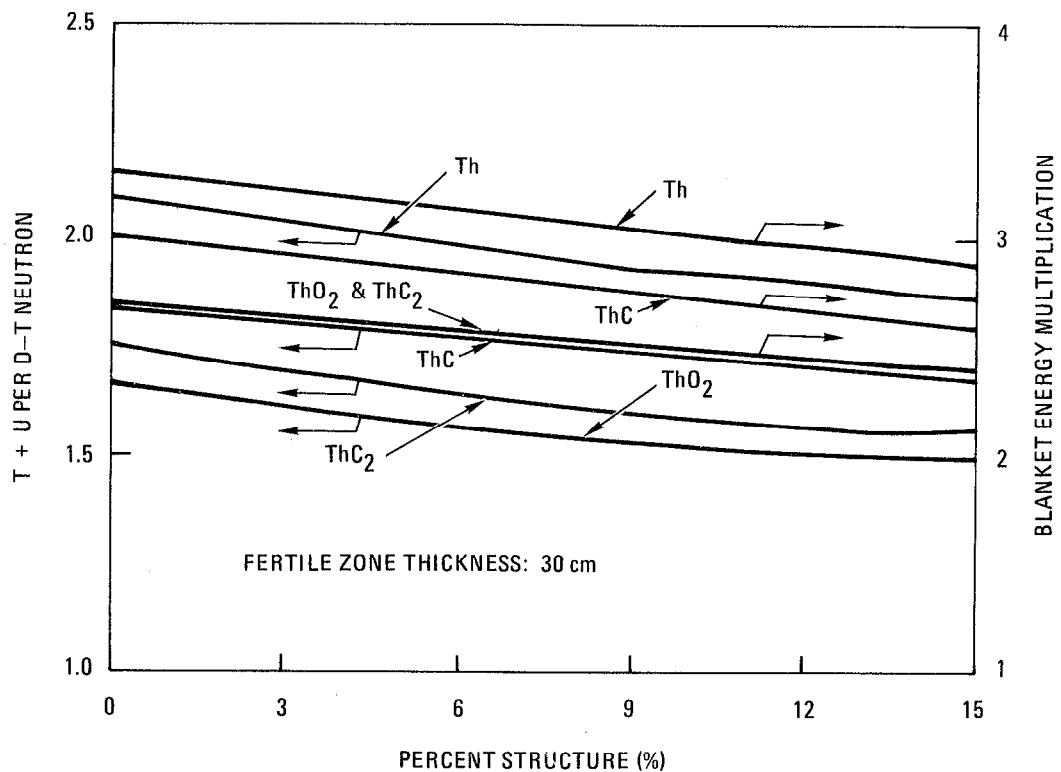


Fig. 6-28. Breeding ratio and blanket energy multiplication vs structural percent at time = 0.

The first-wall thickness is another important consideration for the blanket nucleonic performance because the first-wall is the first material with which the 14.1 MeV fusion neutron is going to interact, and attenuation or softening of the 14.1 MeV spectrum will reduce the neutrons produced by (n,2n), (n,3n), and (n,f) reactions in Th.

Blanket Nucleonic Design Concepts

Four blanket concepts are considered for the purpose of the nucleonic capability exploration. These are identified in Table 6-13, which shows results for blankets optimized to have $T/n = 1.1$ and maximum U/n . All blankets presented here have a structure made of Inconel-718. The first-wall thickness for all blankets is 10 mm. The tritium breeding material is Li_2O compound for Design I and II blankets. For the Design IV blanket it is Li_7Pb_2 . Design III has no Li zone. The first-wall thickness and structural content in the blanket may vary with each design. The structure content of 7% by volume for all blankets is used. The volume fraction of He coolant and void is taken as 20%. The results of this investigation are given in Table 6-13. Note that these results are obtained at the beginning-of-life.

Design I is a typical fusion-fission hybrid blanket that consists of a fertile zone immediately behind the first-wall followed by a tritium breeding zone. The tritium breeding zone thickness was varied to investigate its effect on the ^{233}U and tritium production in the blanket. The results show that the ^{233}U production rate is not sensitive to the Li_2O zone thickness behind the Th zone, and that when the Th zone is less than 0.1 m, the Li_2O zone thickness must be no less than 0.3 m in order to reduce the neutron leakage into the hot shield (316 SS) to less than 1% of the fusion neutrons. When the Th zone is more than 0.15-m thick, the Li_2O zone could be 0.2-m thick to obtain the maximum tritium production potential. Note, however, that in order to breed 1.1 T/n, the Th zone cannot be more than about 0.1-m thick. To include the ^{233}U buildup effect at the end of blanket life, which enhances the fission neutrons leaking into the shield, a 0.5-m Li_2O zone thickness is used in this blanket design study. To produce a tritium breeding ratio of about 1.1 T/n, the thickness of the fertile zone in this design is restricted to no more than 95 mm, which then limits the neutron multiplication and energy multiplication in the fertile zone, as shown in Table 6.13. The ^{233}U production rate and blanket energy multiplication range from 0.32 to 0.63 U/n and from 1.75 to 2.45, respectively, for these candidate Th materials.

Table 6-13. Optimized fertile zone thicknesses and corresponding neutronic performance characteristics for Th fusion-fission blanket designs.^a

Th fuel	Design I				Design II			
	Th	ThC	ThC ₂	ThO ₂	Th	ThC	ThC ₂	ThO ₂
Fertile zone thickness, mm	95	70	50	50	144	120	95	75
²³³ U production, U/fusion neutron	0.63	0.47	0.34	0.32	0.62	0.48	0.34	0.27
Blanket energy multiplication, M	2.45	2.10	1.85	1.75	2.50	2.25	1.95	1.90
Th (n,2n), reactions/ fusion neutron	0.291	0.210	0.161	0.131	0.399	0.240	0.181	0.166
Th (n,3n), reactions/ fusion neutron	0.097	0.064	0.045	0.041	0.095	0.069	0.051	0.048
Th (n,fission), reactions/fusion neutron	0.089	0.064	0.046	0.039	0.093	0.075	0.054	0.050

Th fuel	Design III			Design IV
	Th	Th	Th ^b	Th
Fertile plate thickness, mm	95	380	380	125
²³³ U production, U/fusion neutron	0.96	1.80	0.56	0.40
Blanket energy multiplication, M	2.75	3.50	2.00	1.30
Th (n,2n), reactions/ fusion neutron	0.29	0.40	0.12	0.0163
Th (n,3n), reactions/ fusion neutron	0.10	0.14	0.04	0.0031
Th (n,fission), reactions/fusion neutron	0.09	0.13	0.04	0.0058

^aA tritium breeding ratio of 1.1 T/fusion neutron is obtained for all blankets except as noted for III.

^bReactor average performance with 69% tritium breeding modules with T/n = 1.6 and 31% Th modules.

Design II blankets were intended to overcome this thickness and performance restriction by inserting a 10-mm Li_2O zone between the first-wall and the fertile zone to absorb backscattered neutrons. Lithium in the Li_2O compound in this zone is 90% enriched in Li-6. Table 6-13 reveals the optimized designs for this Design II concept give no appreciable nucleonic performance advantage over that of the Design I concept. The increased fertile material and Li compound inventories and increased design complexity limit further interest in this blanket concept.

To utilize the full neutron multiplication capability of the Th materials, Design III is proposed here for consideration. In this concept the blanket does not produce tritium. Tritium may be supplied by a completely independent fusion or fission tritium producer. The Li_2O zone is replaced by a graphite reflector to enhance U production in the Th zone. As shown in Table 6-13, the ^{233}U production rate could be increased from 0.96 to 1.80 U/n if the Th plate goes from 95 mm to 0.38 m. The blanket energy multiplication varies from 2.75 to 3.50 for this design. If this blanket is used with separate tritium breeding modules with $T/n = 1.6$ and $M = 1.15$, the reactor average performance at $T/n = 1.1$ is $U/n = 0.56$ and $M = 2.0$. These average performance parameters are inferior to those of Design I. Thus, there appears to be no performance incentive to consider separate U and tritium breeding modules.

The Design IV blanket concept is basically a pure fusion blanket followed by a Th fertile zone. The thickness of the Li_7Pb_2 zone is 0.5 m in this design to have a tritium breeding ratio of 1.10. The ^{233}U production rate is 0.40 U/n as shown in Table 6-13. The blanket energy multiplication is similar to that of a pure fusion reactor, 1.30. As discussed in the interim report¹, this low multiplication raises concerns that the low Q_p tandem mirror may have difficulty breaking even on electrical production. This blanket suppresses the current of fast neutrons into the Th zone. Due to the appreciable reduction of Th (n,2n), Th (n,3n), and Th (n,fission) reactions, it produces fissile material with the highest quality and lowest fission product and actinide (such as Pa^{231}) inventories among the blanket concepts discussed above. The ^{233}U production performance of this fission-suppressed blanket is only 65% of that of the fast-fission Design I concept. This performance difference increases with exposure as the fast-fission-suppressed blanket is only 65% of that of the fast-fission Design I concept. This performance difference increases with exposure as fast-fission of some of

the bred ^{233}U further enhances the neutron and fuel production of the Design I blanket. The Design IV blanket is of interest mainly because of its potential safety advantages. By suppressing fission of both the bred fissile material (^{233}U) and the fertile ^{232}Th , the fission product inventory can be kept very low, and the afterheat problems of the blanket are expected to be no more than those for pure fusion designs. Although this concept has not been extensively studied, it appears that the fission-suppressed Th blanket design could offer attractive safety advantages. With increased concern about nuclear safety being evident in the fusion community, this concept appears to deserve further attention in the future.

Based on the preceding discussions, the Design I blanket with Th metal as fuel material has been chosen. This design offers the blanket energy multiplication needed by the relatively low plasma amplification (Q_p) performance of the TMHR to break even on electrical power and produces a significant amount of bred ^{233}U fuel. The use of Th metal maximizes both the fuel and energy production capabilities of this blanket design.

Because of its potential safety advantages and despite the lower breeding and energy production performance, the fission-suppressed Design IV blanket should be kept in mind for possible future study.

Final Blanket Design Calculations

From the neutronics and thermal design iterations the plate design option, which was chosen as the reference version of the blanket module design, gives He coolant volume fractions of about 11% and 10% in the Th and Li_2O zones, respectively. The structural content in the Th zone varies radially from about 8 to 7% by volume from the first-wall to the Li_2O zone. For simplicity in the calculation an average value of 7.5% by volume was used to account for the structure in the Th zone. In the Li_2O zone the structure was averaged to be about 6% by volume. The first-wall thickness was also found to be about 5 mm. For purpose of comparison the results of the 10-mm first-wall blankets are also presented in this subsection.

The blanket calculational model is shown in Fig. 6-29, and consists of either a 5-mm (or a 10-mm) first-wall, a variable thickness Th zone, a 0.4-m Li_2O zone, and a 0.3-m 316 SS reflector/shield. An albedo of 0.3 is assumed for all neutron and gamma-ray groups to account for the effect of the rest of

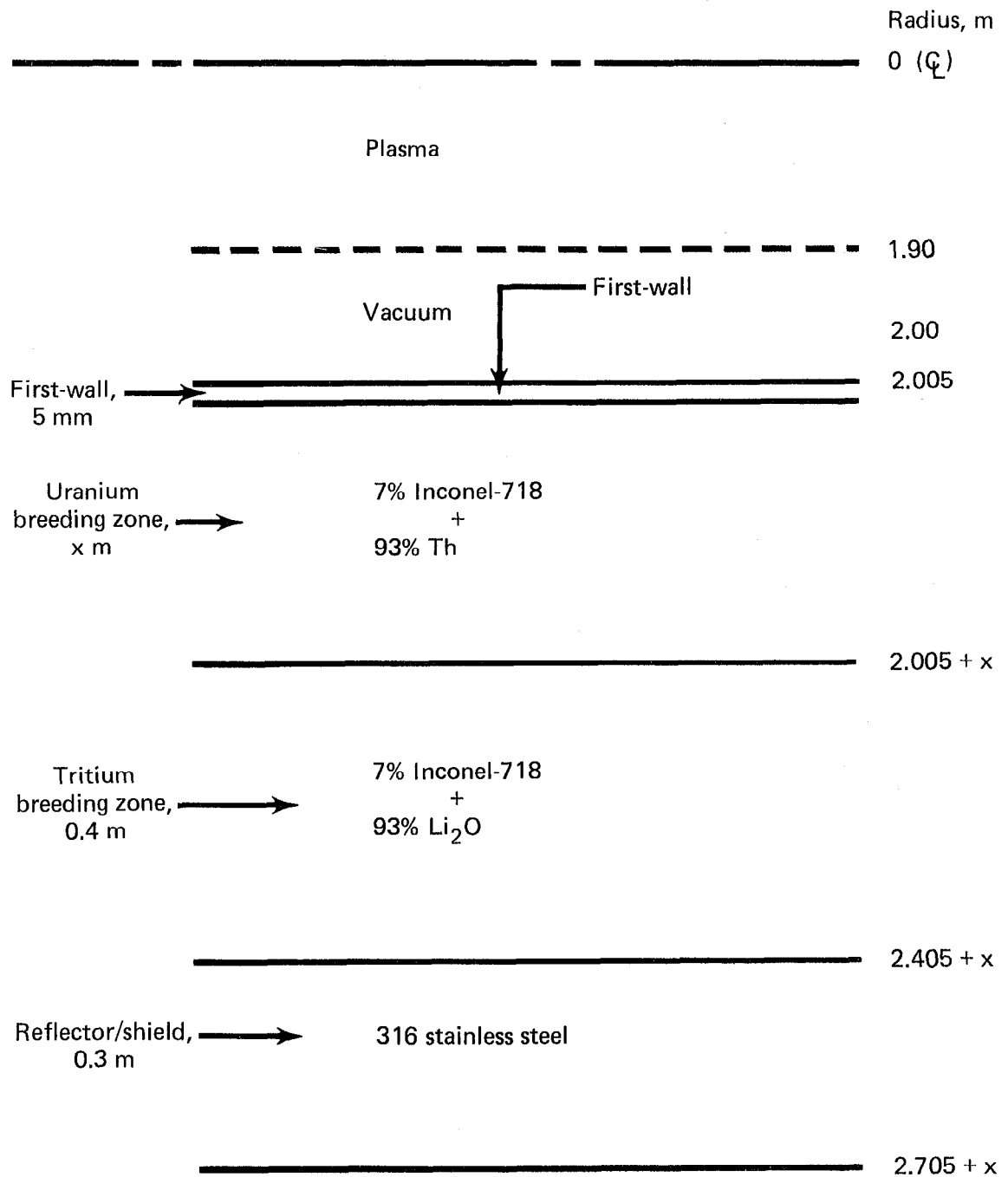


Fig. 6-29. One-dimensional schematic of the fusion-fission hybrid blanket neutronics calculational model.

the shield not included in the calculation. The first-wall and blanket zone thicknesses used here are the net solid material thickness (He volume neglected) despite the fact that the He coolant content is now available for inclusion in the calculations. However, the extrapolation of the results (particularly the nuclear heat rate) from the net solid material blanket models to the actual blanket configurations is easily done by simply increasing the effective blanket thickness with no change in nuclear performance since the geometrical effect involved in the neutron and gamma ray flux distributions is negligible.

The results of the tritium and ^{233}U production as a function of the Th zone thickness are summarized in Fig. 6-30. As expected, the tritium breeding ratio decreases while the ^{233}U production rate increases when the Th zone becomes thicker. At the beginning-of-life the blanket shows tritium breeding ratios of 1.14, 1.06, and 0.98 tritons per fusion neutron are obtained at Th zone thicknesses of 80, 100, and 120 mm, respectively, when the first-wall is 5-mm thick. The corresponding ^{233}U production rates are 0.69, 0.84, and 0.96 ^{233}U per fusion neutron, respectively. However, when the first-wall is 10-mm thick, the tritium breeding ratios decrease slightly and are 1.07, 0.99, and 0.91 triton per fusion neutron for the above Th zone thicknesses, respectively. Note here a value of 0.07 tritons per fusion neutron decrease is observed when the first-wall thickness increases from 5 to 10 mm. This is primarily due to the competing effects between the first-wall material and ^7Li (n,n' α) reaction for the high energy neutrons. A difference of about 0.03 ^{233}U per fusion neutron is observed in the ^{233}U production rate when the first-wall thickness increases from 5 to 10 mm. This is primarily due to the neutron flux decrease in the low energy range as a result of the increase of the first-wall thickness.

A very important consideration in the blanket design is the blanket life time, which is governed by the structural material damage, the fissile material burnup in the Th fertile fuel, and the blanket energy multiplication. The structural material life time is defined by the life time of the first-wall. In our design this is not a major concern, since the selected structural material (Inconel 718) is expected to be able to survive a fluence of about 20 MW-yr/m^2 , which is probably longer than the blanket module fuel cycle time.

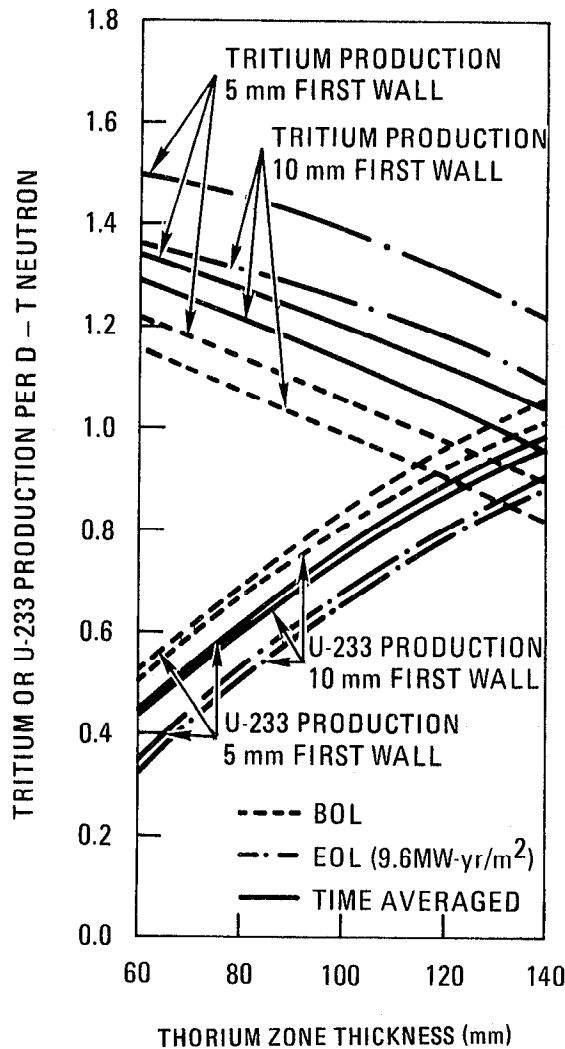


Fig. 6-30. Production of tritium or ^{233}U breeding ratio.

The burnup in the Th fuel is perhaps the dominant factor of the blanket lifetime. The Th metal fuel with a ^{233}U enrichment of about 3-4% would probably be swelling-resistant when the fission burnup is no more than 2% (1.15% is equivalent to 10,000 MW-d/T burnup.) The blanket thermal design is indeed limited by the maximum blanket temperature and the pressure drop; however, these might be so designed once the peak blanket energy multiplication at the end-of-life is specified. Based on the preliminary study of a 10-mm-thick first-wall with a wall loading of $1.5 \text{ MW}\cdot\text{m}^2$ and a scenario of an 8-yr fuel cycle scheme and a plant factor of 0.8, the blanket lifetime was found to be equivalent to $9.6 \text{ MW}\cdot\text{yr}/\text{m}^2$. At the end of the $9.6 \text{ MW}\cdot\text{yr}/\text{m}^2$ lifetime the fission burnup in the Th metal is 1.7% and 1.3% for the blanket with 5-mm and 10-mm first-wall, respectively, as given in Fig. 6-31.

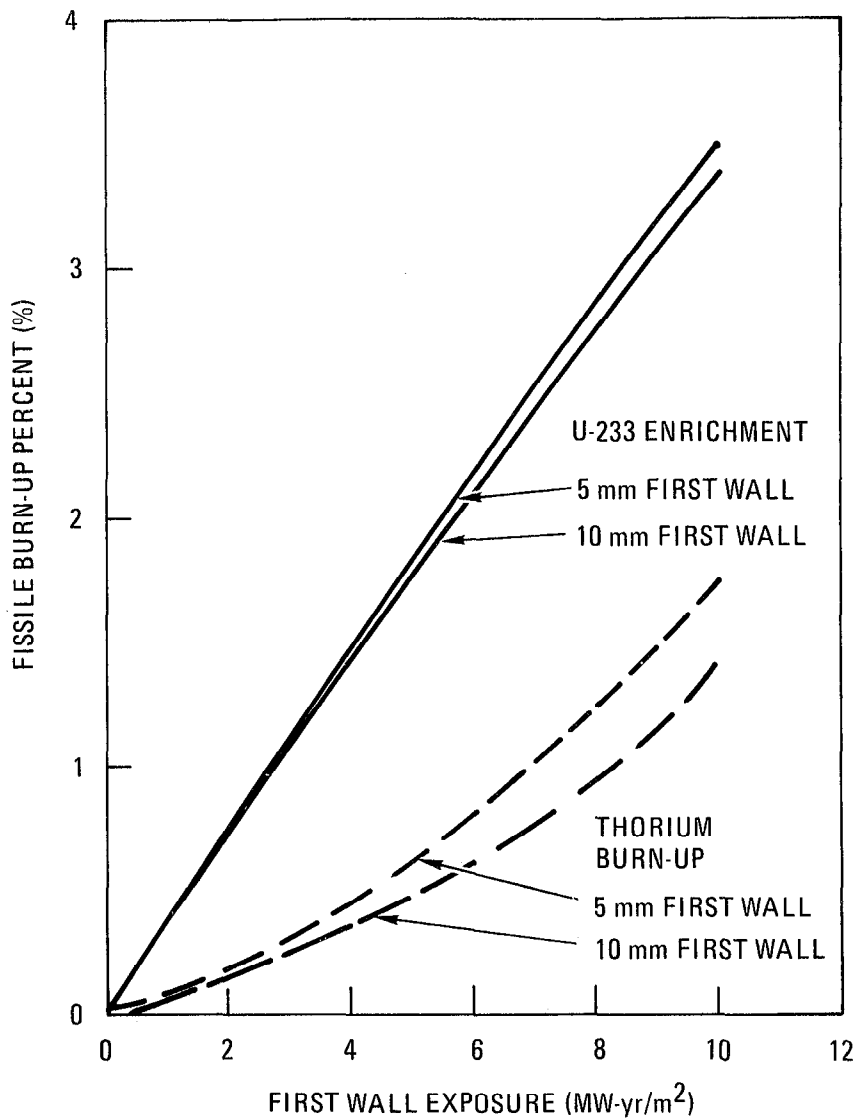


Fig. 6-31. Burnup and fissile concentration vs exposure.

At the above estimated 9.6 MW-yr/m^2 blanket end-of-life exposure, the tritium and ^{233}U production rates are displayed as a function of the Th zone thickness in Fig. 6-30. Due to the increased fission rates because of the buildup of U in the Th zone, the Li (n,α) and Th (n,γ) reaction rates are enhanced. This results in the net increase of the tritium breeding ratio. However, the net ^{233}U production rate decreases. The time-averaged tritium breeding ratios and ^{233}U production rates are also shown in Fig. 6-30. For an average tritium breeding ratio of 1.1 tritons per fusion neutron, the Th thicknesses are optimized to be about 109 mm and 126 mm for the blanket with 10-mm and 5-mm first-wall. The corresponding average ^{233}U production rates

are 0.79 and 0.92 U per fusion neutron, respectively, as shown in Fig. 6-30. Due to the linear relations of the ^{233}U production rate with the Th zone thickness in the range of interest, 80-120 mm, we may expect that the U enrichment at the end-of-life would be roughly constant in this particular range. For the blanket with 5-mm and 10-mm first-wall, the U enrichments are given in Fig. 6-31 as a function of neutron exposure in units of MW-yr/m^2 . Note that at the end-of-life the U enrichments for the above blankets are about 3.4 and 3.3%, which differ only slightly.

The blanket energy multiplication shows the same trend as the tritium breeding ratios. They are shown in Fig. 6-32 for the two cases of first-wall thickness as a function of the Th zone thickness. The first-wall variation gives about 7% difference in the blanket energy multiplication. For the optimized (average tritium breeding ratio 1.1) blankets with a 5-mm and 10-mm first-wall the blanket energy multiplications are 2.85, 2.65, and 8.75, 7.65 at the beginning and end-of-life, respectively. The average blanket energy multiplications, however, are 5.8 and 5.1, respectively.

From the nucleonic design observations we selected the blanket that consists of a 5-mm first-wall, a 0.12-m Th metal zone, and a 0.4-m Li_2O zone for final design evaluation. Including allowance for coolant volume, the physical dimensions of these zones are 0.135 m and 0.44 m, respectively. A series of more detailed neutronic calculations was performed to reveal the ^{233}U enrichment and volumetric nuclear heating spatial distributions in the Th zone. In these calculations the 0.12-m Th zone was divided into seven regions. During the blanket life, the regions are enriched with different amounts of U, and this effect was taken into account in each time step calculation. The initial time step is 2 MW-yr/m^2 exposure; after 4 MW-yr/m^2 the time step becomes 1 MW-yr/m^2 until it reaches $9 \text{ MW-yr}^2/\text{m}^2$. The final step is only 0.6 MW-yr/m^2 . The nucleonic parameters of this blanket design at the beginning and end-of-life are tabulated in Table 6-14. The average tritium breeding ratio, ^{233}U production rate, and blanket energy multiplication are 1.13, 0.881, and 5.5, respectively. At the end-of-life of the blanket the ^{233}U enrichment is about 3.4%, which is equivalent to a U production of 0.57 metric tons per meter of reactor axial length. The tritium breeding ratio and ^{233}U production rate as a function of the neutron irradiation in units of MW-yr/m^2 are displayed in Fig. 6-33.

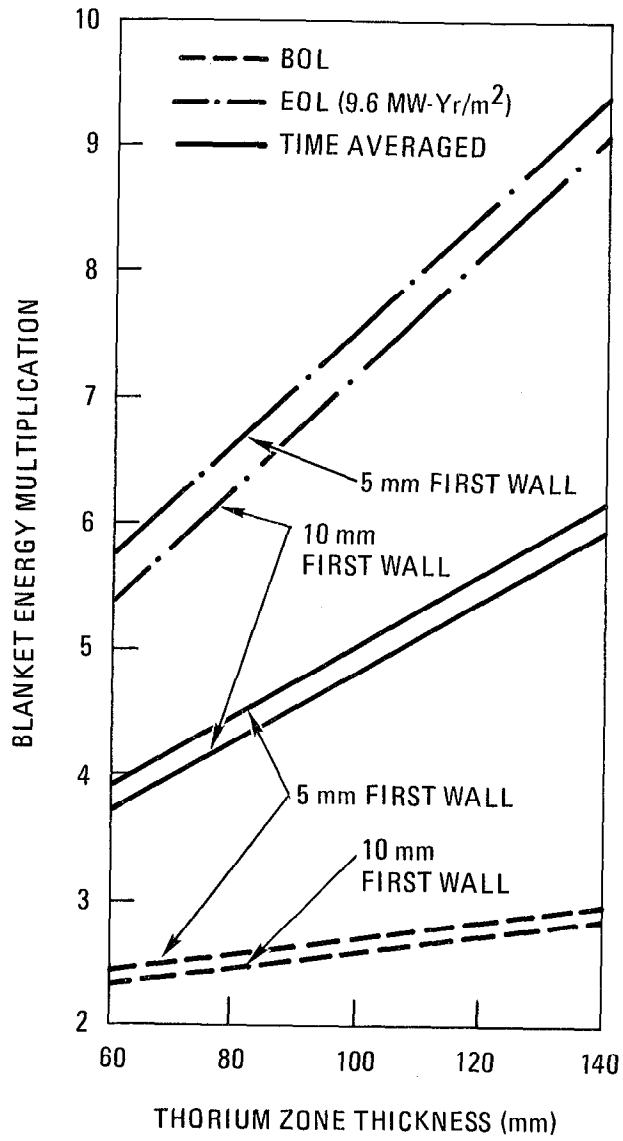


Fig. 6-32. Blanket energy multiplication as a function of the Th zone thickness.

Table 6-14. Helium cooled blanket performance at beginning and end-of-life (9.6 MW-yr/m² exposure).^a

Parameter	BOL	EOL	Average
⁶ Li (n,α)	0.8925	1.2208	
⁷ Li (n,n'α)	0.0852	0.0872	
Tritium breeding ratio	0.9777	1.3080	1.13
²³³ U production	0.9644	1.2055	
U (n,f)	--	0.3869	
Th (n,f)	0.1184	0.1351	
Net ²³³ U production	0.9644	0.7883	0.881
Blanket energy multiplication	2.8	8.5	5.5
First-wall heating, W/cc	13.4	14.3	
Peak nuclear heating in the			
Th zone, W/cc	42	120	
²³³ enrichment, %	0	3.35	
²³³ U, MT/m	0	5.74 x 10 ⁻¹	

^aLocal blanket values multiplied by 0.95 to get reactor average values.

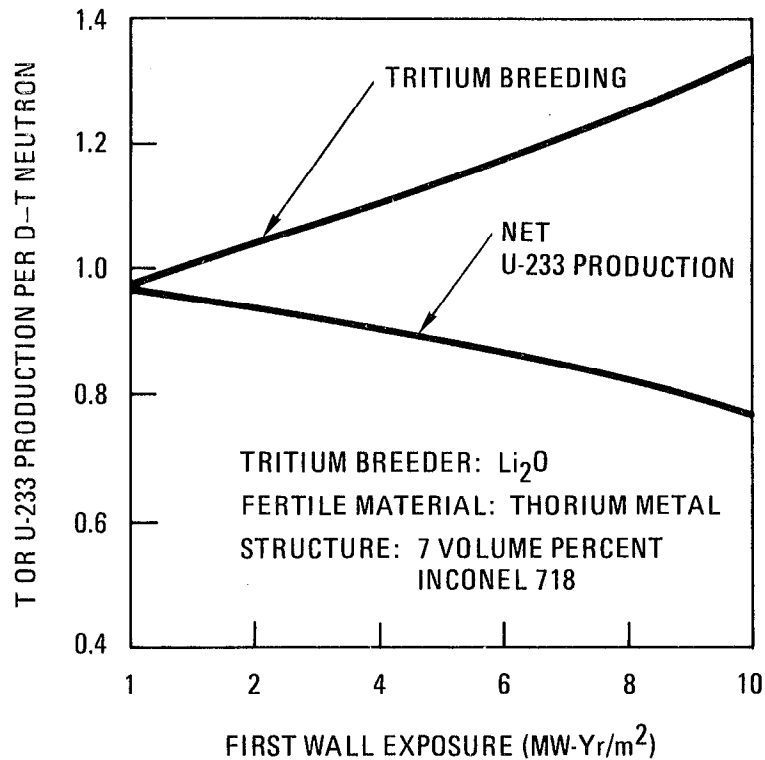


Fig. 6-33. Tritium and ²³³U breeding ratio as a function of first-wall exposure.

The spatial distributions of the volumetric nuclear heating at a neutron wall loading of 1.5 MW/m² are given in Fig. 6-34 for the blanket at the beginning and end-of-life. Note that the peak nuclear heating occurring in the Th zone near the first-wall are 42 and 120 MW/m³ at the beginning and end-of-life, respectively, of which about 88 and 96% are contributed from the fission reactions at the beginning and end-of-life, respectively. In the Th zone the peak ratio of the highest to the lowest nuclear heating is about a factor of 4 at the beginning-of-life, and it drops to less than a factor of 2 at the end-of-life. The nuclear heating fractions due to the fission energy are important factors for the nuclear afterheat estimation. By integrating the standard fission product decay heat curve, dividing by the specific heat of Th and comparing to the Th melting point, the adiabatic after-heat meltdown time for the fuel is estimated to be about 1 h at the beginning-of-life. However, it is reduced to a time interval of about 11 min at the end-of-life. For the fuel cladding material the meltdown time is about a factor of 1.3 less than that of the Th metal, due to its lower melting point.

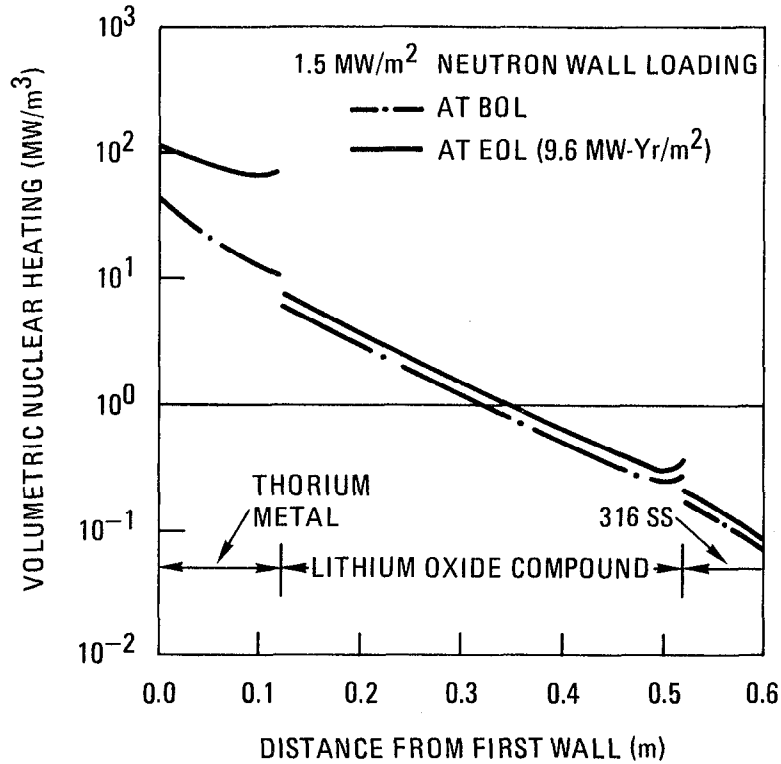


Fig. 6-34. Blanket spatial distribution of volumetric nuclear heating.

The spatial distribution of the ^{233}U enrichment at the end-of-life is shown in Fig. 6-35. The enrichment of ^{233}U is fairly uniform spatially with the lowest value of about 3.2% and highest of about 3.9%. Note that the highest enrichment occurs at the back of the fertile zone primarily due to the moderation and reflection of slow neutrons in the tritium breeding zone.

Shield Design

At the steady-state condition, changeout of two of the 16 blanket modules is expected to occur once every year. During the blanket replacement, the reactor is to be shut down for maintenance and the module removed from the reactor. The superconducting magnet could be annealed at this time. Hence, the shield design criteria could follow the fuel cycle scenario. The maximum atomic displacement in the copper stabilizing material is about 5×10^{-5} dpa, which is based on a maximum 20% resistivity increase due to the neutron

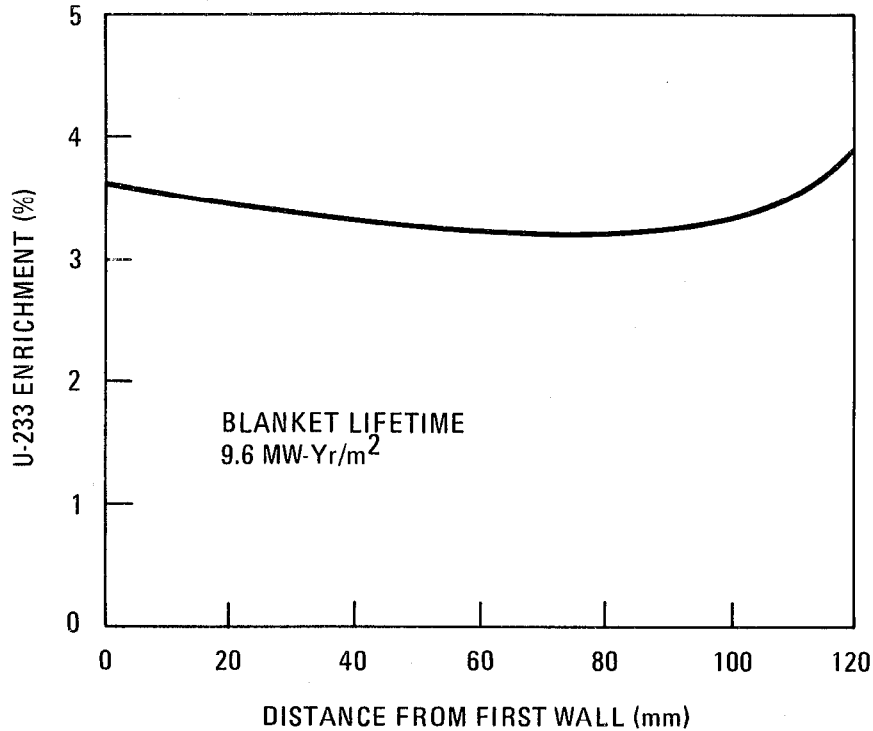


Fig. 6-35. Spatial distribution of ^{233}U enrichment as the end-of-life ($t = 9.6 \text{ MW-yr/m}^2$).

irradiation damage. The neutron fluence limit in the superconductors is about $1 \times 10^{21} \text{ n/m}^2$, and the maximum limit for radiation dose deposited in the super-insulating materials is about $5 \times 10^7 \text{ G}$.

From the final blanket design calculation we found that the neutron flux and atomic displacement rate in copper material immediately behind the tritium breeding zone would be about $4.5 \times 10^{24} \text{ n/m}^2/\text{yr}$ and $7.3 \times 10^{-2} \text{ dpa/yr}$, respectively, at the beginning-of-life. They increase to $5.4 \times 10^{24} \text{ n/m}^2/\text{yr}$ and $8.6 \times 10^{-2} \text{ dpa/yr}$, respectively, at the end-of-life. The increments are about 30 and 20% for neutron flux and atomic displacement rate, respectively. The volumetric nuclear heating in the magnets if they are immediately behind the tritium breeding zone increased from 0.17 MW/m^3 at the beginning of life to 0.20 MW/m^3 at the end of life. The increase is also about 20%. The dose rate to the epoxy insulation material in the same location was found to be 8.3×10^8 and $9.8 \times 10^8 \text{ G/yr}$ at the beginning and end-of-life, respectively. To reduce the radiation damage effects below the desired limit for the superconducting magnet assuming an 8-yr anneal life, a shield capable of

attenuating the neutron and gamma radiation by about four orders of magnitude must be provided between the blanket and the magnet.

An optimized combination of 316 SS and B_4C has been studied for the Small Fusion Reactor.⁷ The attenuation coefficient for neutron flux, atomic displacement, nuclear heating, and dose rate is listed below:

<u>Attenuation Coefficients</u> ⁷	
Neutron flux	$1.49 \times 10^1 \text{ m}^{-1}$
Atomic displacement	$1.34 \times 10^1 \text{ m}^{-1}$
Nuclear heating	$1.16 \times 10^1 \text{ m}^{-1}$
Dose rate	9.17 m^{-1}

Using the attenuation coefficients, the 316 SS + B_4C shield thickness required for the atomic displacement in the copper stabilizer to reach an accumulating value of 5×10^{-5} dpa in 8 yr (6.4 continuous operating yr) is estimated to be about 0.7 m. Note that the average radiation damage rates were used for the estimation of accumulated effects. At this 316 SS + B_4C thickness the accumulated neutron flux after 6.4 yr of continuous operation in the magnet is about $9 \times 10^{20} \text{ n/m}^2$, which is approaching the limit of $1 \times 10^{21} \text{ n/m}^2$. The dose on the epoxy insulation material is about $4.4 \times 10^7 \text{ G}$ for a continuous plant operating lifetime of 30 yr, which is below the limit of $5 \times 10^7 \text{ G}$. At the end-of-life the maximum nuclear heating rate in the magnet is about $6 \times 10^{-5} \text{ MW/m}^3$, which is considerably lower than the manageable limit. The 316 SS + B_4C shield of 0.7 m is adequate for the protection of the superconducting magnet. Also from Fig. 4-6 of Ref. 7 this shield composition corresponds to about 0.36-m and 0.34-m thick 316 SS and B_4C , respectively.

In light of the relatively thin (0.7 m) 316 SS + B_4C shield needed to protect the superconducting magnet and because of the fairly high cost anticipated with this shield design, it may be advantageous to consider alternate shield concepts. Since the shield is now separate from the blanket and can be water-cooled at low temperature, boronated concrete may be a cost-effective substitute and should be investigated in the future.

Conclusions

The nucleonic design of the blanket and shield for the TMHR was performed to achieve the goals of breeding adequate tritium, producing a maximum amount of U and producing enough thermal heat to allow electrical breakeven. Based on the chosen blanket concept, which consists of a Th metal zone placed between the plasma first-wall and the Li_2O tritium breeding zone, the time averaged (over the blanket lifetime of 9.6 MW-yr/m^2) tritium breeding ratio and U production rate are 1.13 and 0.88 atoms per fusion neutron, and the blanket energy multiplication is 5.5. The end-of-life U enrichment is about 3.35%, which corresponds to a quantity of about 0.57 metric tons of U per meter of reactor length. The U enrichment in the Th metal zone is quite uniform with, at most, 10% variation around the average value of 3.35%. The nuclear heating in the Th zone differs spatially by about a factor of 2, with the peak heating of $\sim 120 \text{ MW/m}^3$ (at a neutron wall loading of 1.5 MW/m^2) occurring at the end-of-life near the first-wall. Due to the nuclear heating increase at the end-of-life, the adiabatic afterheat meltdown time of the Th fuel will be reduced from a beginning-of-life estimate of about 1 h to about 11 min. However, this is still about one order of magnitude longer than the U_3Si -fueled hybrid blanket alternatives considered during the interim study. Use of the fission-suppressed Th blanket option could further increase the adiabatic meltdown time by a factor of 50 or more and could make possible the design of a blanket that could be completely passively cooled for after-heat removal.

Power Conversion System

To complete the thermal hydraulic considerations of the TMHR study this subsection discusses the required power conversion equipment for the He-cooled blanket concept. The preliminary BOP design, performed by Bechtel National, Inc., also contains more detailed information on the power conversion system.¹

The power conversion system consists of a primary coolant loop, a secondary coolant loop, and an auxiliary cooling system. The primary coolant loop consists of 16 blanket modules that are interconnected by ducts and the hot and cold He manifolds at one side of the reactor. There are eight monotube, helical-coil design steam generators and eight He turbocirculators.

Based on previous experience, the He loop pressure drop through the steam generators is about 40 kPa (6 psi) in the economizer-evaporator-superheater section and 14 kPa (2 psi) in the resuperheater. The He ducts experience about 55 kPa (8 psi) pressure drop. The pressure rise through the He circulator is about 170 kPa (25 psi).

The secondary coolant loop consists of eight once-through steam generators, including re-superheating sections, the turbine generator, steam-turbine drives for the He circulators, condensers, feed pumps, feedwater heaters, and associated piping. The auxiliary cooling system is designed to provide an independent means of cooling the shutdown reactor and removing the decay heat produced by the blanket. This loop consists of two heat exchangers and two circulators.

More detailed design criteria, functional requirements, and description of the equipments for the power conversion system will be needed for the next phase of this study. The requirements expected for the gas-cooled TMHR power conversion system appear to be very similar to those developed for the Standard Mirror Hybrid Reactor design¹¹. As a consequence, we expect that the design of this system and the characteristics of the components of this system will be very similar to those discussed in some detail in Ref. 11, and no original power conversion system design work specifically for the TMHR has yet been done.

Blanket Cost Estimates

A cost estimate for the He-cooled large blanket module was performed to evaluate the direct cost and the annual blanket replacement cost of the blanket. This estimate is subject to many uncertainties inherent in an estimate of costs at this early conceptual design stage. The results obtained, however, should be useful for comparison with other blanket options and for identification of the major cost components of the He-cooled TMHR blanket design.

The blanket costs were determined from the amount of materials present in the various zones and components and multiplied by the installed unit costs of these materials. The installed unit costs for different materials were taken from Ref. 14, which used July 1979 price levels. Only direct costs are shown. Construction indirects, contingency, project engineering, and development costs are not included.

Blanket Direct Cost

Table 6-15 summarizes the direct costs of different materials in different zones and components of the He-cooled TMHR blanket. The complete TMHR blanket was considered. It was 39 m long, had a 2-m first-wall radius, with 16 axially separable modules. Each module has 42 submodules with 24 fuel plates in each submodule. The fuel plates are separated by annular support rings spaced 0.5 m apart.

Annual Replacement Cost

With the scenario of changing two modules annually during equilibrium operation of the reactor, the annual replacement cost can be estimated by identifying replaceable components of the blanket and calculating the cost for shipping (@ \$20/kg), reprocessing (@ \$ 380/kg), and disposal (@ \$ 95/kg) of the Th heavy metal.

The replaceable parts of the blanket are the first-wall, the Th zone, the Li_2O zone, the SS reflector/shield zone, the plena, the pressure vessel, and the tritium purging system. The direct cost of these for two modules is 25 million dollars. The amount of heavy metal in two modules is 80.8×10^3 kg. Thus, including shipping, reprocessing and disposal charges, the total annual replacement cost for the reactor is 51.5 million dollars.

With a production of 2.7 metric tons of ^{233}U annually, the cost component of the bred ^{233}U due to blanket replacement is $57.5 \times 10^6 / 2.7 \times 10^6 = \$ 21.0/\text{gm}$. The blanket replacement cost of the ^{233}U could be reduced by the following considerations:

- Recycling of the Th fuel, since the heavy metal contains only 3.4% of ^{233}U ; similarly, the Li_2O could be reused.
- Optimize the lifetime of different radial zones of the blanket and reduce the material to be replaced; reuse those components that still have useful irradiation life.

The latter suggestion would need improvement of the mechanical design of the blanket to allow extraction of selected radial zones from the blanket.

Table 6-15. Direct cost of He-cooled TMHR blanket.

Blanket zone or component	Material	Mass, 10 ³ kg	Installed		Subtotal, \$10 ⁶
			cost, \$/kg	Cost, \$10 ⁶	
First-wall	Inconel 718	34.6	60	2.1	2.1
Th zone	Th	646	120	77.5	-
	HT-9 ^a	36	32 ^b	1.2	78.7
Li ₂ O zone	Li ₂ O	388	33	12.8	-
	HT-9	130.6	32	4.2	17
SS reflector/shield	SS	484.9	32	15.5	-
	HT-9	12.7	32	0.4	15.9
Plena	HT-9	48.3	32	1.5	1.5
Pressure vessel	HT-9	574	25 ^c	14.4	14.4
Cold/shield	SS	4648.3	5 ^d	23.2	-
	B ₄ C	360	13	4.7	27.9
Concrete/shield ^e	Concrete	2646	0.15	0.4	-
	Borated H ₂ O	69	10	0.7	-
Omega joints ^f	HT-9	181.0	25	4.5	-
	Omega joints	-	-	9.0	13.5
He ^g					
Piping	HT-9	40.9	14 ^h	0.6	-
	Connections	-	-	3.6	2.2
T ₂ O purging ⁱ	Th zone	-	-	8.7	-
Systems	Li ₂ O-zone	-	-	10.0	12.1
Cart ^j	HT-9	75.6	15 ^k	1.1	<u>1.1</u>
TOTAL					186.4

Table 6-15. (continued)

^aThe installed cost of HT-9 was estimated to be the same as SS-316.

^b\$32/kg is for complicated fabrication, thin wall with rigid quality control, and testing.

^c\$25/kg is for highly machined components, forgings, and castings.

^d\$5/kg is for the sample plate construction used in the shield.

^eThe reference shield is SS and B₄C at 70 cm thick. An alternate shield is 95% concrete with 5% borated water. From previous experience the concrete shield is estimated to be 140 cm thick. With the use of a concrete shield the total direct cost would be reduced from 186.4 to 159.6 million dollars.

^fThe omega joint cost was estimated to be twice the cost of the structural material of the annular plates.

^gThe piping remote quick connections were estimated to cost \$50,000 each.

^h\$14/kg is for tubular structure thin wall.

ⁱFrom GCFR experience the purging system estimates used the following costs:

Manifold*	=	\$15/plate
Valves	=	\$500/submodule
External piping	=	\$500,000/reactor
Plate length	=	0.5 m

*Multiply by 1 for the Th plate venting system outlet. Multiply by 2 for the Li₂O plate inlet-outlet purging system.

^jIf the blanket transporter cart is not used in the TMHR design, this cost component should be omitted.

^k\$15/kg is for structure fabricated from heavy plates.

Conclusions and Recommendations

This subsection summarizes our conclusions and recommendations from the design of a He-cooled TMHR blanket. The areas of discussion are mechanical design, neutronics design, and material selections.

We have designed a He-cooled TMHR blanket using Th metal as the fertile material with an average thermal power of ~4000 MW and a production of 2.7 metric tons of ^{233}U per year. The characteristics of this blanket are shown in Table 6-16. This design is within the temperature and pressure drop limits imposed with close coupling between the mechanical, neutronics, and thermal-hydraulics designs.

The design uses fairly conventional gas-cooled reactor technology to minimize the need for extensive development programs. The fuel mechanical design and thermal hydraulic performance are quite similar to gas-cooled fission reactor concepts. The blanket materials require extrapolation of the current state-of-the-art because there is presently only limited experience with use of metallic Th, Inconel-718, and HT-9 in nuclear power systems. The materials irradiation behavior uncertainty associated with a fusion neutron spectrum, of course, is a concern with this design as with all fusion system studies. The Th fuel cycle is intended to interface with a Th/ ^{233}U fuel cycle economy that is expected to be available in the early part of the 21st century. Although new head-end facilities will be needed for TMHR fuel, the reprocessing and recycle facilities expected to be in existence can be used directly. Thus, fuel cycle development will not be needed to implement the TMHR.

Gas-cooled power conversion system technology has been developed to the commercial stage and the gas-cooled TMHR utilizes this technology. No new component development programs are expected to be needed. The blanket tritium systems will require new development as there is presently little experience in this area. By using a separate tritium purge flow system, tritium concerns in the fission zone and primary loop are minimized.

The mechanical design of the blanket system attempts to maximize the topological advantages of the simple cylindrical tandem mirror geometry. The ease of lateral access is utilized to provide the capability for rapid change-out of entire reactor modules. The entire blanket and solenoid section of the reactor is thus replaceable. By using spare modules, the reactor can be rapidly put back into operation while refurbishment or repair of spent modules is accomplished offline in the hot shop.

Table 6-16. Helium-cooled blanket characteristics--large module design.

Axisymmetric cylindrical module configuration:

- Sixteen modules, each 2.4 m long, total length 39 m.
- Eight-yr module lifetime (6.4 full power yr at 80% capacity factor), two replaced each yr.

Helium coolant at 55 atm pressure, radial flow direction.

Inconel-718 first-wall.

Metallic Th fuel plates, clad in Ht-9, each ~1.2 cm thick, 12 cm deep.

Purged plates of Li₂O clad in HT-9 for tritium breeding, each ~1.5 cm thick, 45 cm deep.

Reflector/hot shield of SS-316, 10 cm deep.

Cold shield of SS-316/B₄C, 70 cm thick.

Blanket energy multiplication,^a $M = 5.2$

- Reactor power = 4000 MW_t
- Blanket power = 3817 MW_t

Thermal cycle efficiency ≈ 38%

²³³U production,^a $^{233}\text{U}/n = 0.84$

Annual production = 0.83 kg/MW_t·yr
= 2647 kg/yr^b

^aReactor time and space averaged values.

^b80% capacity factor has been assumed.

Areas of technical uncertainty exist in the present design, where further analysis, design, and optimization are needed; however, the design appears technically feasible. The basic design requirements have been satisfied, and we believe the design could be developed into a practical fusion hybrid reactor, producing about 1000 MW_e of net electricity and about 3000 kg/yr of high quality ²³³U fissile fuel for use in a fission burner reactor economy.

Mechanical Design

The advantages and disadvantage of the large module design follow:

Advantages:

- It is a relatively compact design with a first-wall radius of 2 m and a total axial length of 39 m separated into 16 replaceable modules. The total blanket thickness including the cold shield is 1.72 m for a stainless steel-B₄C shield and ~2.42 m for a concrete-borated-water shield.
- Individual modules can be completely replaced in a short time (18.5 days). Online maintenance of the modules is avoided to reduce downtime.
- The cylindrical geometry of the tandem mirror has been taken advantage of by segmenting the modules axially and using lateral access path for easy maintenance.

Disadvantages and development programs:

- With the equilibrium operating scenario of replacing two modules per year, the replacement cost is quite high at 56.4 million dollars per year. This cost could be reduced by replacing only the first-wall and Th fuel zone at 4-yr intervals and replacing other blanket components less frequently instead of replacing the entire blanket within and including the pressure vessel. This would require extensive redesign of the blanket cartridge mechanical configuration.
- Because of the movement of large blanket modules weighing 600-700 metric tons, more development would be needed to study the module carrying cart design and the tracking system of the cart. Alternate transport systems should also be considered.
- To facilitate the changeout of the modules quick piping connect and disconnect devices and blanket cartridge extraction devices would need to be developed.
- Development of the omega joints operating under the TMHR condition would also be needed.

Neutronics Design

Early in this study the choice was made to use a fast-fission Th blanket. This decision was due to the requirement for a blanket multiplication of about 2.5 to break even on electrical power with the low plasma Q_p of about 1.5 that was projected at that time. Since then, the plasma Q_p of the tandem mirror has risen to about 2.5. The change of plasma Q_p reduces the requirement of blanket energy multiplication M from 2.5 to about 1.

This reduction in required blanket multiplication opens the possibility for use of alternate blanket concepts. The low multiplication Be/Th-graphite blanket considered during the scoping phase may now be more attractive (see Section 5). The fission-suppressed Design IV blanket (discussed in Section 6) may be a very attractive alternative to the reference fast-fission Th blanket. This concept uses essentially the same blanket technology and materials as the reference design; only the arrangement of the blanket zones is altered. In the fission-suppressed design the Li zone is located between the plasma and the Th zone instead of outside the Th zone. This alternative arrangement could help alleviate the neutronic design concerns of the fast-fission Th blanket:

- The reference fast-fission Th blanket has excellent neutronic performance, producing significant amounts of bred fuel and blanket energy. The cycle average, blanket average, ^{233}U breeding ratio is 0.84, ^{233}U atoms per DT neutron, and the average blanket multiplication is 5.2.

- The local blanket energy multiplication varies from 2.8 at BOL to 8.3 at EOL. By changing out 1/8 of the blanket (two modules) per year the power swing of the entire reactor can be kept to a tolerable $\pm 6\%$. The power swing for an individual module, however, is more than a factor of 3 from BOL to EOL, which complicates the thermal-hydraulic design.

- The peak blanket fuel power density at EOL is 120 W/cc, 96% of which is due to fission power. This results in a high level of afterheat and an adiabatic meltdown time of only 11 min, which necessitates the provision of highly reliable auxiliary cooling and decay heat removal systems.

- The neutronics performance of the blanket is quite sensitive to the details of the design. The average blanket multiplication is a strong function of blanket lifetime, first-wall thickness and Th zone design. The reactor power for a given length (or length for a given power) is directly

proportional to average multiplication. Thus, the blanket design, reactor length, and fuel lifetime must be carefully coordinated to achieve the simultaneous design goals of a given reactor power level, adequate tritium breeding, acceptable fuel irradiation lifetime, and favorable fuel handling economics. This sensitivity will make final design specifications important and difficult.

Because of these concerns about the neutronic design and performance of the reference fast-fission Th blanket, a closer look should be taken at the relative merits of the fission-suppressed blanket concept, and the economic tradeoffs inherent with use of a relatively low performance hybrid blanket of this type should be evaluated.

Materials Selection

The material selections for use in the gas-cooled TMHR blanket are fairly conventional and are based on previous fission reactor experience or fusion reactor design study selection. The first-wall is made of Inconel-718 because of its high strength at elevated temperature and projected good fusion irradiation lifetime. The balance of the module structural material, including the cladding, was chosen to be the martensitic alloy HT-9, because of lower cost and projected very low radiation-induced swelling. The fuel material is metallic Th because of superior neutronic performance and the acceptable swelling behavior expected at the low TMHR burnup levels. Li_2O was chosen as the tritium breeding compound, used as a packed powder in metal-clad plates with a He purge flow to recover tritium.

All of these choices still appear to be reasonable, but several areas of concern are mentioned below:

- The use of HT-9 for cladding in both the Th and Li zones is attractive because of its low induced swelling under neutron irradiation, low thermal expansion, and high thermal conductivity. Concern about reduction of the ductile-to-brittle transition temperature, however, may restrict the allowable operating temperature to 500°C or less. Since both Th and Li_2O plate designs are cladding temperature-limited, this will impact the design, and the HT-9 choice should be reevaluated.

- The choice of Th metal for the fuel material still appears best, but the 1.7% peak burnup in the fuel, with peak temperatures approaching 800°C , may result in excessive swelling. This needs to be assessed. Possible

solutions to this potential problem include reduction in blanket exposure lifetime and burnup or reduction in fuel temperature.

- At the temperatures found in the Li_2O zone excellent tritium extraction is expected, but the fraction of tritium given off in the form of LiOT may approach 10%. This raises concerns about corrosion of the cladding and purge system. Since the excellent breeding performance of Li_2O is not needed in a hybrid system, consideration should be given to alternative breeding materials such as LiAlO_2 and Li_2SiO_3 .

- The expected lifetimes of the various blanket materials differ widely: Inconel-718 first-wall, >13 yr; Th fuel, <8 yr; Li_2O breeding zone, ≈ 20 yr; and HT-9 pressure vessel, 40 yr. The difficulty of implementing different zone lifetimes was discussed on page 6-33. In light of the large cost associated with replacement of the entire blanket cartridge every 9 yr, this should be reassessed.

As stated above, these areas of technical uncertainty require further analysis and optimization. They do not, however, contradict the basic assessment that the gas-cooled TMHR blanket concept is technically feasible.

AN ALTERNATE APPROACH - THE LINKED ASSEMBLY CONCEPT

Introduction - Philosophy and Concept

An economically feasible TMHR design includes reasonable assurance that its operational availability compares with the availability of other types of power plants. The principal limiter to availability in current nuclear power reactors is the time needed for refueling and normal shutdown maintenance. Availability of the TMHR is expected to be limited in the same way.

A second concept for a He-cooled blanket region is presented herein. It is different from the design described in Section 6, primarily because the philosophy of refueling and maintenance used in its preparation was different. In this concept all blanket structures are designed to be long-lived, and refueling is performed without disassembly and removal of any central region structures.

This philosophy coincides with the approach taken in earlier design study work on steam cooled TMHR.¹ Advocates of this approach believe that better assurance of availability exists for designs in which the first-wall and blanket structures remain intact during refueling operations. The designs

must make possible the disassembly and reassembly of central region structures but only as a repair and recovery procedure from an unexpected event requiring abnormal maintenance operations. This position imposes the long-life requirement on structures subjected to severe environmental conditions. Long life (20 yr or more) is believed attainable with two very important provisions:

- The selected structural material must be able to be fabricated and also functional at high temperature (300 to 600°C, depending on design).
- Capability must exist for periodic in-place annealing of the structure. (Annealing temperature will depend on the material but will exceed 700°C.)

Several advantages accrue if blanket and first-wall structures can be made permanent. Directly and indirectly, the advantages relate to refueling operations, and therefore, to availability:

- Refueling equipment is single-purpose, smaller, simpler, and state-of-the-art. As a result, automation is made easier, operations are fast, and costs of handling equipment are greatly reduced.

- The plasma region vacuum boundary need not be broken. Pressurization and reevacuation of the region is not a necessary refueling operation.

- Replacement blanket structure modules and their attendant large hot cells are not required.

- Normal and seismic support structures are not disturbed during refueling outages.

- Coolant system piping, instrumentation lines, and electrical leads need not be broken during refueling outages.

- In transit decay heat removal is required for fuel assemblies only, (i.e., not for structural modules whose normal cooling circuits have been disconnected).

- Fewer disassembly and simpler refueling operations improve the reliability of the operations.

Disadvantages also are produced by designing with the philosophy of long-lasting structures. The following list shows them to be significant. With operational availability being the goal the advantages of refueling without disassembly outweigh the disadvantages:

- Unplanned repair maintenance will require abnormal procedures, special and extra equipment, and long shutdown periods.

- In place periodic annealing could be the source of design conditions more severe than reactor operating conditions.
- Long life requirements might restrict material selection more than if the blanket structures were replaced after short term exposures.
- Inspection access to the first-wall and blanket structures is not as available as it is with removable modules.

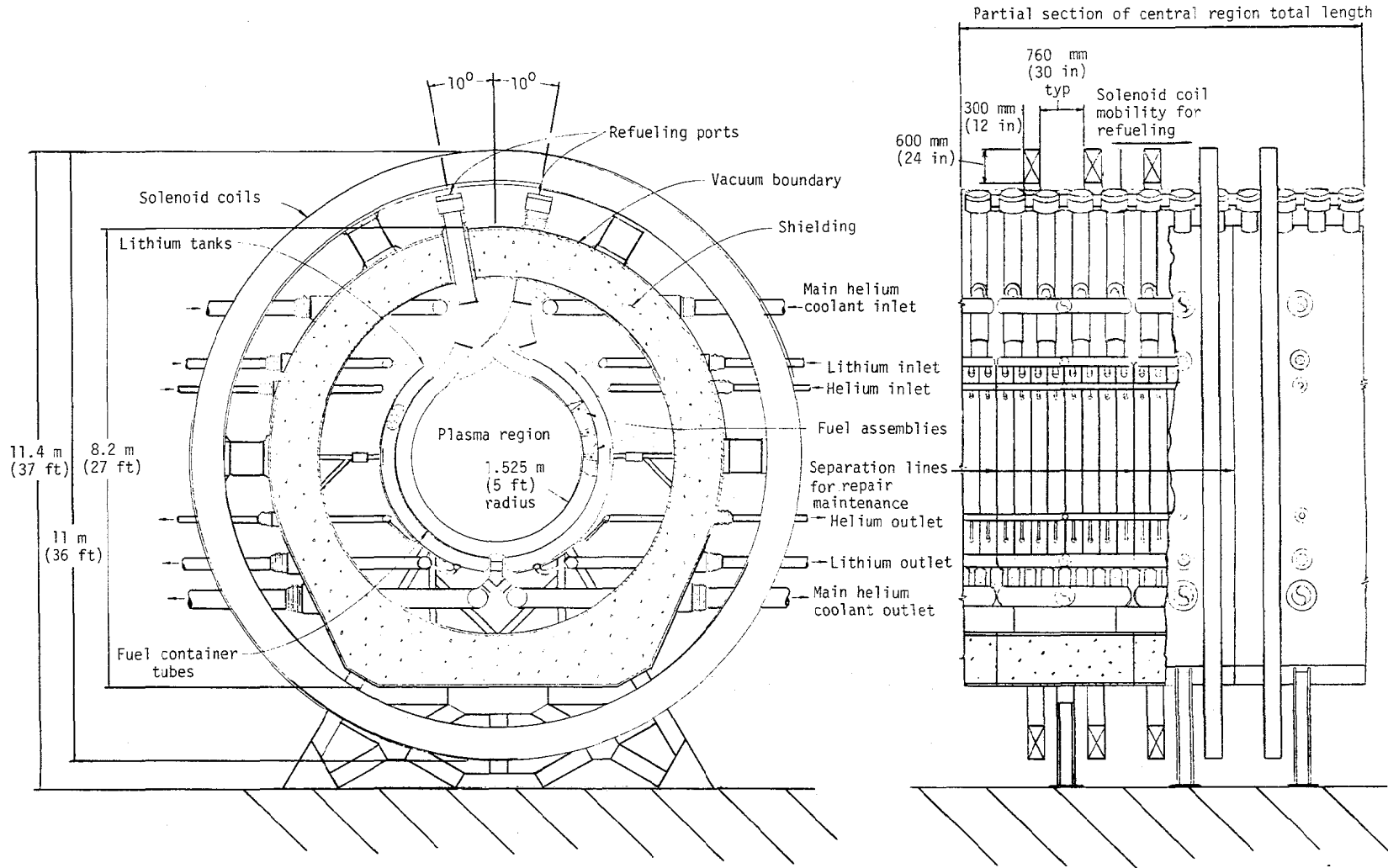
The linked assembly concept is a carryover from a steam-cooled blanket design concept prepared earlier in the TMHR design study. As reported in the interim report for this study, the linked assembly concept is the currently preferred design of several steam-cooled designs.¹ It is also the choice for a conceptual design, whereby to illustrate the alternate approach of providing for refueling without disassembly of structures.

The configuration of a blanket region designed to be cooled with superheated steam will not change significantly if the coolant becomes He. The neutronics are essentially the same, and the mechanical design is affected to the extent of differences in pressures and temperatures. Thermal-hydraulic and neutronic analyses with He as the coolant have not been performed for the linked assembly concept, but the descriptions and illustrations that follow are believed to be valid representations of the concept. Only mechanical and structural design features are included. Their description suffices for the intent of presenting a design based on the philosophy of long-lived, central region structure.

General Description

The general arrangement of the linked assembly concept is illustrated in Fig. 6-36. The figure shows a cross section of the central region and a side view of part of the total length.

The vacuum boundary is at the encased surfaces of the primary shield. The first-wall is at the layered, noose-shaped tubes with inverted Y's at the tops. The tubes are the coolant pressure boundary and the fissile fuel containers. Coolant pipes penetrate each noose-shaped tube at top and bottom. Radially beyond the noose shaped tubes are Li-filled tanks with their connected piping for circulation of the Li and He. All of the piping is manifolded within the shield to larger pipes that penetrate the shield and pass between the solenoid magnet coils outside the shield.



Central region cross section

Fig. 6-36. Linked assembly concept.

Each side of each noose-shaped tube contains 11 or 12 short cylindrical fuel assemblies linked in a chain. For refueling the spent fuel assembly chains are withdrawn through the Y and out the port over the Y, and new chains are lowered into place. The port on each noose-shaped tube projects through the shield for easy access of the refueling machines. The entire central region is supported at the bottom; all external piping extends out from the sides; and all refueling operations are from the top.

Fusion Reactor Requirements

Figure 6-36 takes into account these preliminary dimensional requirements of the fusion reactor:

● Plasma radius, cm (in.)	120 (47)
● First-wall diam, cm (in.)	305 (120)
Solenoid magnet:	
Number of separate coils	As required
Spacing	Uniform
Coil-to-coil diam variation	0
Minimum axial coverage by coils (including supports), %	25
● Minimum magnet shielding thickness in high density concrete, cm (in.)	91 (36)

Fuel Container Tubes

The fissile fuel in the linked assembly concept is contained within tubes of circular cross section immediately adjacent to the plasma region. Each tube is nose shaped, with the noose intersection being a Y forging above the plasma region. The stem of the Y is the refueling access port. The noose-shaped tubes are arranged in layers along the entire axial length of the reactor. Each tube is identical with the others, except for the opposite hand location of the coolant inlet nozzles on adjacent tubes; and the orientation of adjacent tubes. In Fig. 6-36 the refueling ports of adjacent tubes are shown offset 20 deg from each other and 10 deg from the vertical centerline. The separation gives room for the necessarily thickened Y forging in each tube, prevents interference between adjacent refueling port penetrations and flanges, and improves access to the refueling ports.

Inlet He coolant flow enters each tube through a nozzle in the stem of the Y. The Y separates the downflow to the two semicircular portions of the fuel tubes. The coolant flow rejoins at the bottom and exits through a nozzle.

Because a thermal hydraulic analyses have not yet been performed for the use of He in this concept, it is not known whether the first-wall and the fuel will need separated coolant flow paths. The conceptual design includes a second concentric tube within each noose-shaped tube. The inner tube extends from the branches of the Y to the outlet nozzle. If first-wall and fuel coolant separation is necessary, the inner tube is the separator. The inner tube also functions as the travel surface upon which the fuel assembly chains ride.

In Fig. 6-36 the diam used for each fuel tube is 305 mm (12 in.). The dimension is somewhat arbitrary and can be adjusted to optimize the neutronics. In so doing the design conditions and material selection become the important factors as the determinants of the tube's thickness and diam combination. Should an inner tube for flow separation and travel surface be necessary, its diam is estimated to be about 25 mm (1 in.) less than that of the pressure tube.

The inside diam of curvature of the fuel tubes is the specified first-wall diam of 3.05 m. Support for the tubes has not been given design attention but is given in Fig. 6-36. The fuel tubes are supported on the Li tanks, which are, in turn, supported by the shield structure.

Lithium Tanks

In this concept tritium production takes place in closed tanks filled with liquid Li. The tanks are located outside the fuel tubes and follow the contour of the fuel tubes. To eliminate gaps through which neutron and gamma streaming could occur, the Li tanks are nested with the tubes (i.e., the radial centerlines of the tanks are tangent with outside of the fuel tubes, and vice versa).

Within each Li tank is a piping coil through which He is circulated for cooling the Li and removing the tritium. Each tank has inlet and outlet piping connections for both He and Li.

The nested tank to fuel tube configuration requires that the diam of each tank be the same as that of the tubes. In Fig. 6-36, the tank diam is therefore 305 mm (12 in.). Design conditions and material specifications for the tanks and coils have not been established.

Coolant Piping

The He inlet and outlet piping for each seven adjacent fuel tubes connect to two inlet manifolds and two outlet manifolds; one of each on each side of the blanket region. On one side the manifolds connect to four tubes and on the other side to three tubes. The four/three manifolding alternates along the length of the blanket. From each manifold a single header extends through the shield and between the coils.

The Li tank piping for both the He and the Li is also manifolded on both sides of the blanket. These manifolds connect eight sets of tanks on one side and six on the other. The eight/six combination also alternates along the length of the blanket. Headers from the Li and He manifolds extend outward through the shield in the same plane as the main He coolant headers.

The described manifolding of the piping is a part of a method for separating the central region structures into modules, which can be moved for repair maintenance access, if necessary.

The size requirement for pipes and headers are not now known but are believed adequately represented in Fig. 6-36.

Primary Shield

The primary shield is a steel-encased, reinforced and cooled, high-density concrete cylinder with an inner diam of 6.4 m (21 ft). The steel casing on the shield is the vacuum boundary and must, therefore, be a sealed boundary.

The shield is segmented in the axial direction of the central region, with the segment lengths matching those of the blanket region modules. To form the segments radial joints with steel liners are provided; thus, only the outer casing of the shield is continuous for the entire length. Segmenting of the shield has the same purpose as modularizing the blanket region; i.e., providing the means for repair maintenance access.

Each segment of the shield has penetrations for seven refueling ports and for 12 He and Li headers. Each penetration is insulated from its process pipe and provided with a bellows expansion joint to maintain the vacuum boundary seal while allowing differential thermal displacements.

The shield supports all central region components including the solenoid coils and it is supported by structure extending to the building foundation.

Solenoid Coils

We require that the solenoid coils and their support structure cover at least 25% of the central-cell length with uniform spacing. As shown on the side elevation of Fig. 6-36, coils 305 mm wide are spaced 1070 mm to give better than 25% coverage. They have an i.d. of 9.75 m (32 ft). The coverage requirement was derived from a more fundamental criterion on the magnetic field ripple allowed at the plasma edge caused by lumped coils. This criterion is discussed in Section 3.

Fuel Assemblies

The linked assembly concept derives its name from the type of fuel assembly proposed. The curvature of the noose-shaped fuel container tubes necessitates short length assemblies. For refueling removal the assemblies must be linked. In this concept chains of 11 and 12 assemblies occupy the two semi-circular sides of each fuel tube.

Designs of the fuel assemblies and the chains require extensive development. Factors in the design are the method of linkage, the arrangement and maintenance of flow paths, the minimization of gaps in the fuel, and the method for assuring smooth and easy travel of the assemblies and chains within the tubes. Figure 6-37 shows an early conceptual design of a fuel assembly that can be linked with others to form a chain. Linkage is at the ends of a tube held in position by circular support frames at the ends of the assembly. On the outside of each frame are four equally spaced ball casters that allow easy movement of the assembly within the tube around it.

The inner flow separator tube can also function as the bearing surface during movement of fuel assembly chains. Some possibility exists that the bearing surface function may be the primary or only function of an inner tube.

The ends of the assembly shown in Fig. 6-37 are perpendicular to the axis of the assembly. As a result, circular wedge-shaped gaps will occur in the fuel of the blanket region between each pair of assemblies. Future design efforts should attempt to reduce these gaps.

Each assembly is estimated to weigh about 150 kg (330 lb), and each chain of assemblies about 1800 kg (4000 lb).

6-103

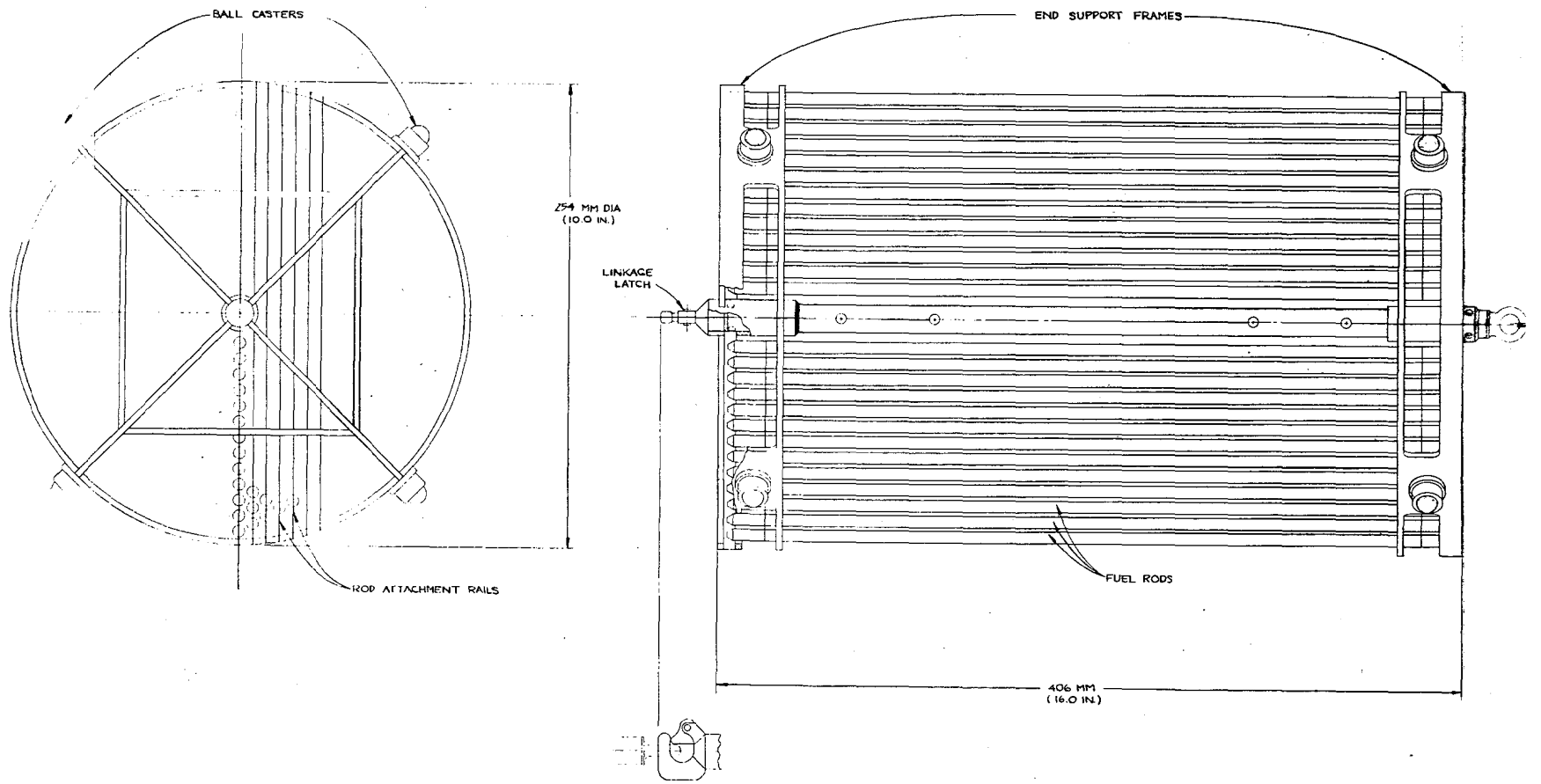


Fig. 6-37. Conceptual design--linked fuel assembly.

Refueling and Maintenance

Figure 6-38 illustrates in simple fashion how the linked assembly concept of the TMHR would be refueled and how the central region structures could be separated to provide access for repair maintenance. The figure does not intend to convey that the structural separation is a part of the refueling procedure. The fuel transfer tubes are used with the entire central region in the location labeled Operating Position.

Refueling. Fast and simple refueling is the prominent feature of this concept. The refueling ports outside the shield give easy overhead access without any disassembly of structures other than those which permit axial movement of the magnet coils. Between one-half and two-thirds of the refueling operations will require magnet coil movement to give access to the refueling ports.

After opening the ports the fuel assembly chains are pulled up through the Y forgings, out the ports, and into straight cannisters. New fuel assembly chains are then lowered into the fuel tubes. Tapered bottom guides on the chains direct them to the proper side of each tube. All fuel handling equipment is believed to be current state-of-the-art equipment. In-blanket residual heat removal during refueling can be readily accomplished by continued low level circulation of coolant through the coolant circuits.

In a refueling time analyses performed on several TMHR concepts,¹ it was estimated that the entire blanket region of the linked assembly concept could be refueled in 12 days. That time could be reduced by using more overhead refueling machines spaced along the length of the TMHR central region.

Maintenance. The important design considerations relative to maintenance are capability to periodically anneal the fuel tubes and capability to provide access for repair from abnormal occurrences. Capability to anneal is necessary to be in accord with the initial premise that refueling without disassembly is also necessary for adequate reactor availability. Annealing in the linked assembly concept is envisioned as being accomplished by the circulation of hot gas through the fuel tube cooling circuits after removal of the fuel.

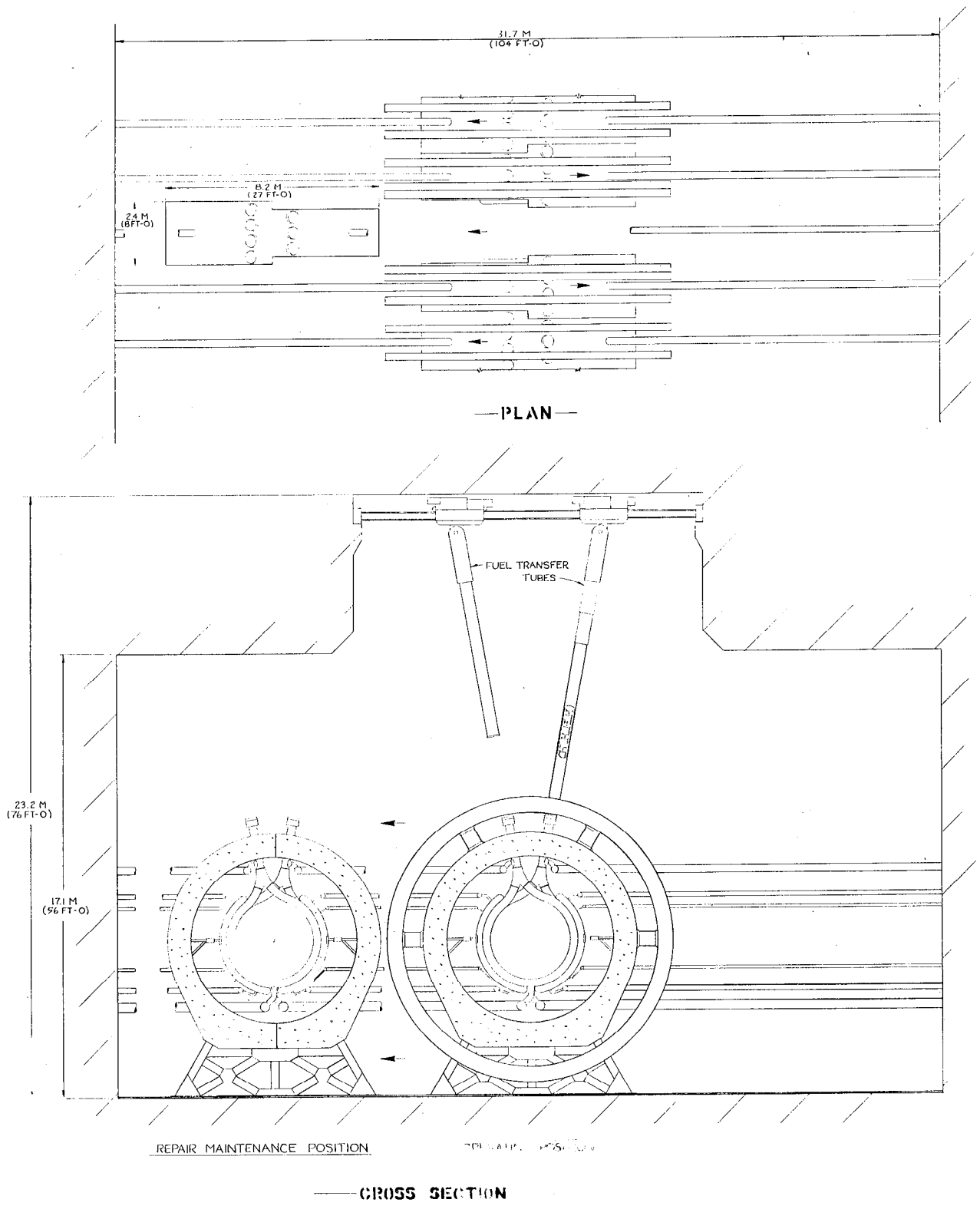


Fig. 6-38. Linked assembly concept refueling and servicing layout.

Access for repair maintenance is mentioned in previous paragraphs describing the blanket region and shield. Both were designed to be segmented along the axis of the central region. Figure 6-38 illustrates how an entire segment of the central region is withdrawn sideways to give access to the inside of the segment. Adjacent segments are withdrawn to opposite sides. For segment movement the outer liner of the shield must be cut at its two radial joints, and the external piping headers for the segment to be moved must be cut. The manifold arrangement previously described, and the offsets in the shield joints, shown in Fig. 6-38, allow the segment being withdrawn to clear the adjacent central region structures, which remain in place.

The method of transport for moving a segment is indefinite. Each segment is estimated to weigh about 220 tons when the blanket region is empty.

Design Development Requirements

The central region structures are relatively simple and conventional. The neutronic and thermal-hydraulic analyses must be performed, however, before material selections can be made and the pictured simplicity substantiated. Several obvious features require design development:

- Fuel assembly linkage.
- Fuel chain travel freedom requirements.
- Coolant flow channeling within the fuel tubes.
- Reduction of blanket region radial gaps.
- Support of the fuel tubes and Li tanks.

Blanket Cost Estimate

A cost estimate was made for the original linked assembly concept in which steam was the coolant. That estimate is presented in the interim report.¹ A new estimate for this concept with He as the coolant has not been made.

Introduction

A conceptual balance-of-plant (BOP) design and an order of magnitude cost estimate were developed for the He-cooled TMHR and are described in this subsection. In any nuclear power plant reactor design and performance are the major determining factors of the plant economic and technical viability. However, the BOP, which includes heat transport and energy conversion systems, plant auxiliary systems, plant electrical system, and structures and facilities, has a major effect on the plant economics. In fact, the BOP can account for as much as 75 to 80% of the total plant cost and therefore has a significant impact upon the economic viability of the plant. Further, decisions made in the reactor design have significant impact on the BOP design and costs.

The BOP design was based on the reactor operating characteristics and design information provided by General Atomic Co. (GA) for the He-cooled TMHR. Bechtel National, Inc. used this information to calculate plant performance and develop a preconceptual reactor mechanical arrangement and integrated plant design.

There were two major alternatives to consider in developing the BOP design. One was the choice between using a module or nonmodule solenoid design. For the module approach the reactor solenoid region is divided into many identical units (modules). The modules would be periodically removed and taken to a hot cell where the fuel pins would be removed and the module renovated. For the nonmodule approach the entire solenoid is essentially a single unit; fuel pin removal and reactor repair are performed in place. The module approach was chosen for this design.

The second alternative was the use of a prestressed concrete vessel for piping, circulators, and steam generators vs the use of a standard piping loop. The prestressed concrete reactor vessel is used for gas-cooled fission reactors because it eliminates the possibility of a double-ended piping failure, and it contains the He better in a smaller space-efficient package. The standard piping layout was chosen because the TMHR liner design is not conducive to the prestressed concrete vessel configuration.

The TMHR design base parameters are given in Table 6-17. The table shows that the blanket multiplication factor M changes from a low of 2.48 at the BOL to a high of 6.65 at the EOL. This results in a blanket power 2.7 times higher at the EOL. This large power swing is reduced by operating the modules at different M values by suitably staggering the fuel pin changeout scheme.

Table 6-17. TMHR design base parameters.

M values for each module	BOL 2.48
	EOL 6.65
	AVE 4.56
Q	2.23
P_F (fusion power)	1040 MW _t
Γ	1.5 MW/m ²
Reactor length	56 m
Number of modules	16
Module length	3.5 m
Helium conditions for blanket cooling	$T_{hot} = 585^\circ \text{C}$
	$T_{cold} = 285^\circ \text{C}$
	$Press_{av} = 5.5 \text{ MPa}$
Maintenance frequency	2 modules/yr
Yearly power swing after first 8 years of operation	3660 - 4110 MW _t

For the He-cooled TMHR with 16 modules and a maximum module repair interval of 8 yr, two modules are replaced each yr. The conditions can be established to produce a smaller power swing for the entire reactor. This swing is 3660 to 4100 MW_t. Even though the power swing for the entire reactor is only 11% of the peak power, the modules still undergo power change between 129 MW_t at BOL to 745 MW_t at EOL. The BOP was designed to accommodate the 11% power swing.

Heat Transport System

A significant amount of heat must be removed from the first-wall/blanket sections, the direct converter, plasma dump, cold shield, neutral beam injectors, rf plasma heating system, and magnet loads. Helium is to be used for cooling the first-wall/blanket sections, the direct converter, and the plasma dump. The other components are cooled by low pressure, low temperature water systems.

Only the heat from the He circuits is used to generate electricity. The heat in the water systems is of low grade and is rejected by cooling towers.

Figure 6-39 shows the heat transport system for the He cooling circuits. Helium is circulated through the blanket such that the He cools the first-wall, passes through the layers of fuel, Li, and hot shielding, and leaves the blanket at 585°C . The nominal He pressure is 5.5 MPa.

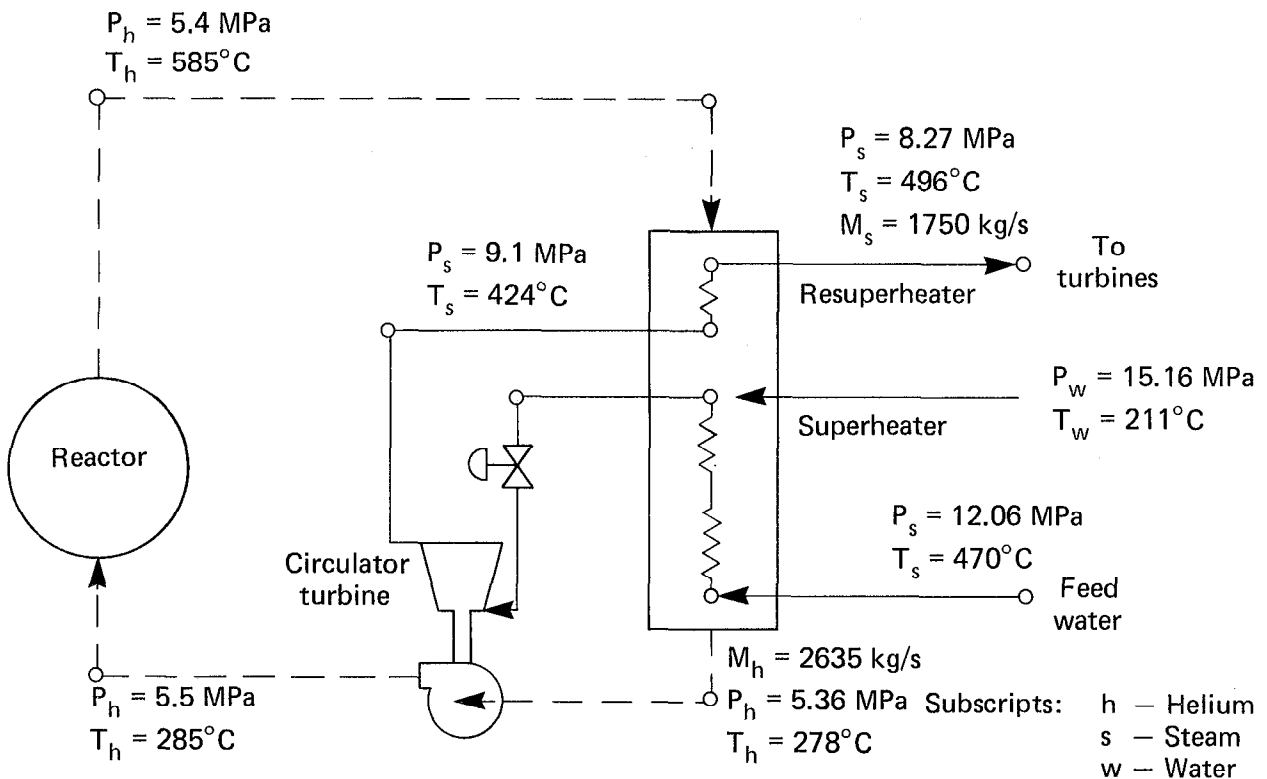


Fig. 6-39. TMHR He-cooled heat transport system heat balance.

The He goes directly to a steam generator; no intermediate loop is used. The assumption is that the concentration of tritium can be kept low enough in the He coolant so that the amounts that diffuse into the steam and be released in the turbine building is acceptably small.

There are eight 550-MWt steam generators in the blanket cooling circuit and eight He circulator/steam turbine drive sets. The direct converter/plasma dump cooling circuit has two 500-MWt steam generators, and each has a He circulator/steam turbine drive set.

The He used for direct converter cooling operates at the same pressures and temperatures as the He cooling the blanket. The heat transport system and energy conversion system is based on peak blanket power output of the 4110 MWt and 337 MWt from direct converter. The He circuit for cooling the direct converter is shown in Fig. 6-40, and is normally operated separately from the blanket cooling circuit; the circuit is cross-connected in emergencies. The He mass flow rate, 26345 kg/s, shown in Fig. 6-39, is the total for the blanket and direct converter cooling.

The heat transport systems used in the blanket cooling loops and the direct converter cooling loops are identical except for thermal rating. The steam conditions for steam from both the blanket cooling steam generators and direct converter steam generators are the same and are combined in two large steam piping headers, which are cross-connected. The steam conditions at the turbine inlet are 496° C and 8.27 MPa.

The steam cycle used is the same as that used for the gas-cooled fast reactor (GCFR); except for thermal rating, the steam generators are the same. Each steam generator has three sections: evaporator, superheater, and re-superheater. The incoming He enters the shell side and heats the resuperheater bundle first, then the superheater bundle, and finally the evaporator section.

The feedwater enters the tube side of the steam generator where it is heated, and steam is generated in the evaporator section. The steam is then superheated in the superheater section. The superheated steam is expanded through a turbine, which drives a He circulator. The exhausted steam is re-superheated and then expanded in the main turbines.

The direct converter steam generators are sized so that they can be used as backups for the blanket cooling circuit steam generators. The blanket cooling circuit can be cross-connected with the direct converter cooling circuit, as shown in Fig. 6-40.

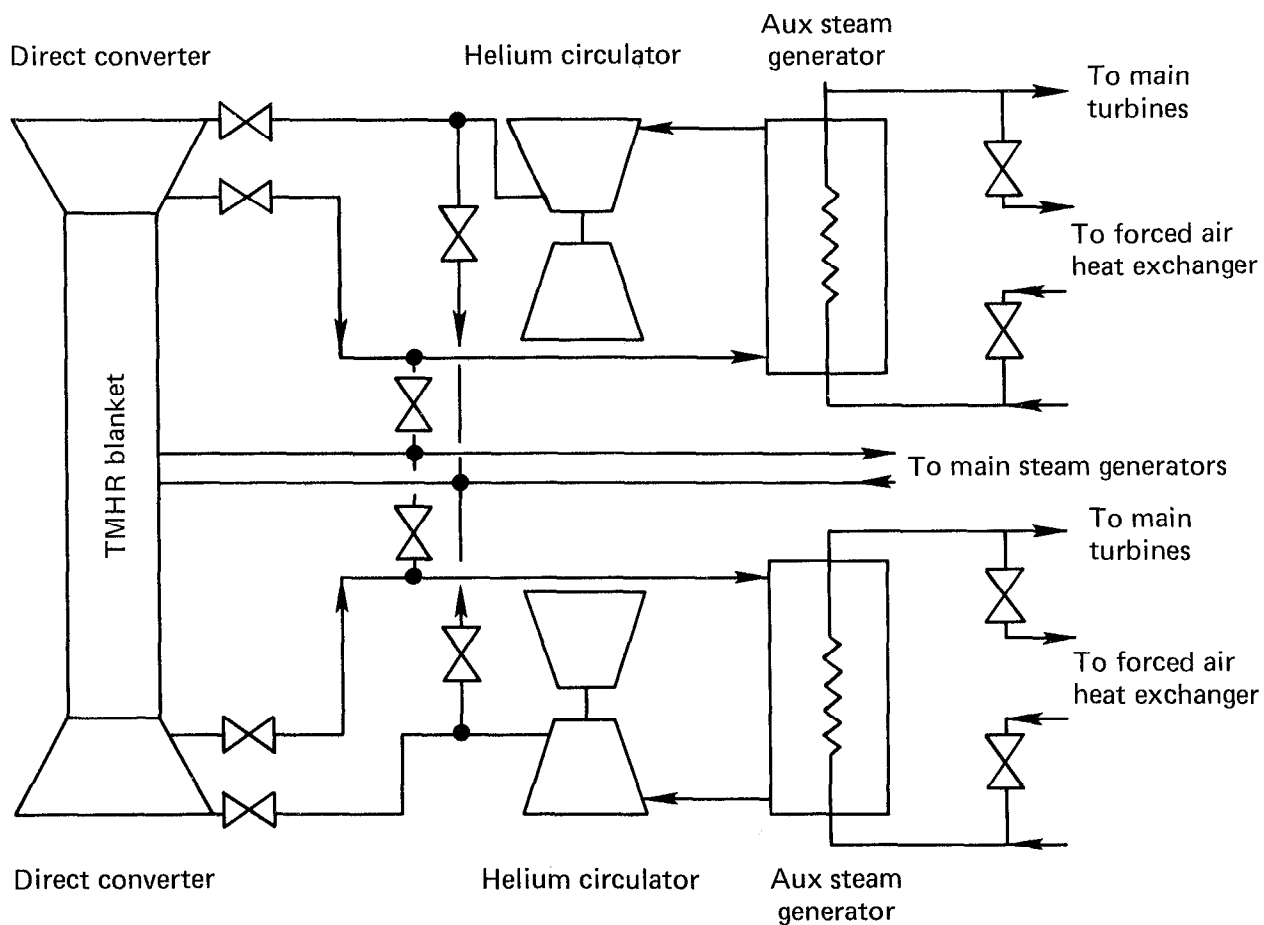


Fig. 6-40. Direct converter cooling and auxiliary blanket cooling system.

The inlets and outlets of eight of the 16 reactor modules are connected to hot and cold leg-mixing plena. Even though the power produced by each module varies with time, the combined power of the eight modules remains constant. By using the mixing plena, the power handled by all the steam generators of the blanket circuit is the same.

The mixing plena also provides reactor protection for loss of circulator or steam generator. With eight steam generators there is a very low probability of a complete loss of cooling. Using the direct converter steam generators, it is possible to isolate a blanket steam generator and its respective He circulator and still operate at full power.

Energy Conversion System

Figure 6-41 shows a heat balance diagram for the energy conversion system. Mass flow rates and power outputs listed are the total for the plant. The present concept uses two identical, tandem-compound, 1800-rpm turbine generators.

The superheated steam enters the throttle control valve at 496° C and 8.27 MPa. The turbine generator sets are rated for 840,000 kW each. The turbine consists of a high pressure and two low pressure sections.

Three extraction points are taken from the high pressure section for three high pressure feedwater heaters. Steam is directed from the crossover pipe between the high pressure and low pressure sections to the two feedwater pump turbines. There are three extraction points from the low pressure turbines, which are used for feedwater heating in the three low pressure feedwater heaters.

Three condensate pumps pump water from the condenser hot well to the two feedwater pumps. The generator is rated for 900,000 kVa.

Heat Rejection System

A large amount of heat is rejected from the energy conversion system while condensing the turbine exhaust steam in the steam condenser. This rejected heat amounts to approximately 60 to 65% of the total heat generated in the reactor. This is due to the thermodynamic inefficiency of the Rankine cycle used in the conversion system.

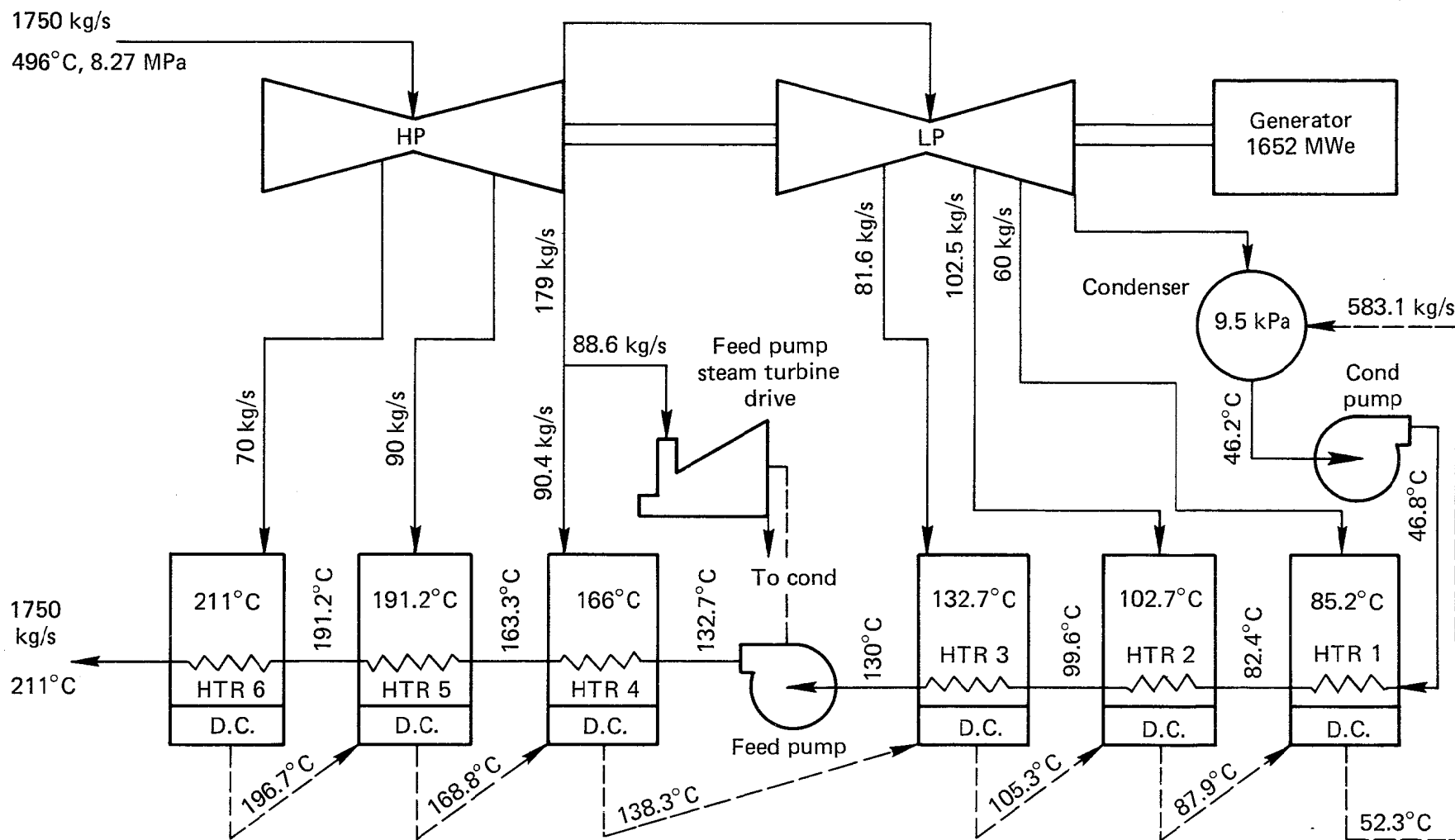


Fig. 6-41. Energy conversion system heat balance.

The function of the heat rejection system is to reject this waste heat to an ultimate heat sink. The function is accomplished by transporting the heat rejected in the condenser to cooling towers, where it is exhausted to the atmosphere. The system schematically consists of a circulating water pump and a cooling tower. The circulating water pump draws cold water from the cooling tower and delivers it to the condenser to cool the condensing steam. The effluent hot water from the condenser then flows back to the cooling tower and exchanges heat with air. The heat rejection system is shown in Fig. 6-42. Four wet cooling towers with 15 cells each are used. Cooling water flow is 49,000 l/s.

An integrated schematic of the main BOP system is shown in Fig. 6-43.

Plant Performance

The overall plant performance was calculated based on the parameters listed in Table 6-17. The plant performance is shown in the power flow diagram in Fig. 6-44 and is summarized below:

Thermal converter output	=	1615 MWe
Direct converter output	=	337 MWe
Gross electric output	=	1952 MWe
Recirculating power		
Neutral beam injector	=	172 MWe
RF heating	=	605 MWe
Miscellaneous plant loads	=	91 MWe
Total recirculating power	=	868 MWe
Net plant output	=	(+) 1084 MWe

Integrated Plant Design

Reactor Mechanical Arrangement. Several considerations influenced the development of the conceptual reactor containment design. The first is that the solenoid region is divided into several identical sections. Maintenance of the reactor will be accomplished by removing one or more of the modules and performing the module maintenance work in a hot shop area.

To accomplish this the design must accommodate isolating, moving, and reinstalling the module, besides the normal function of providing services and reactor support. The design should limit the placement of equipment in areas

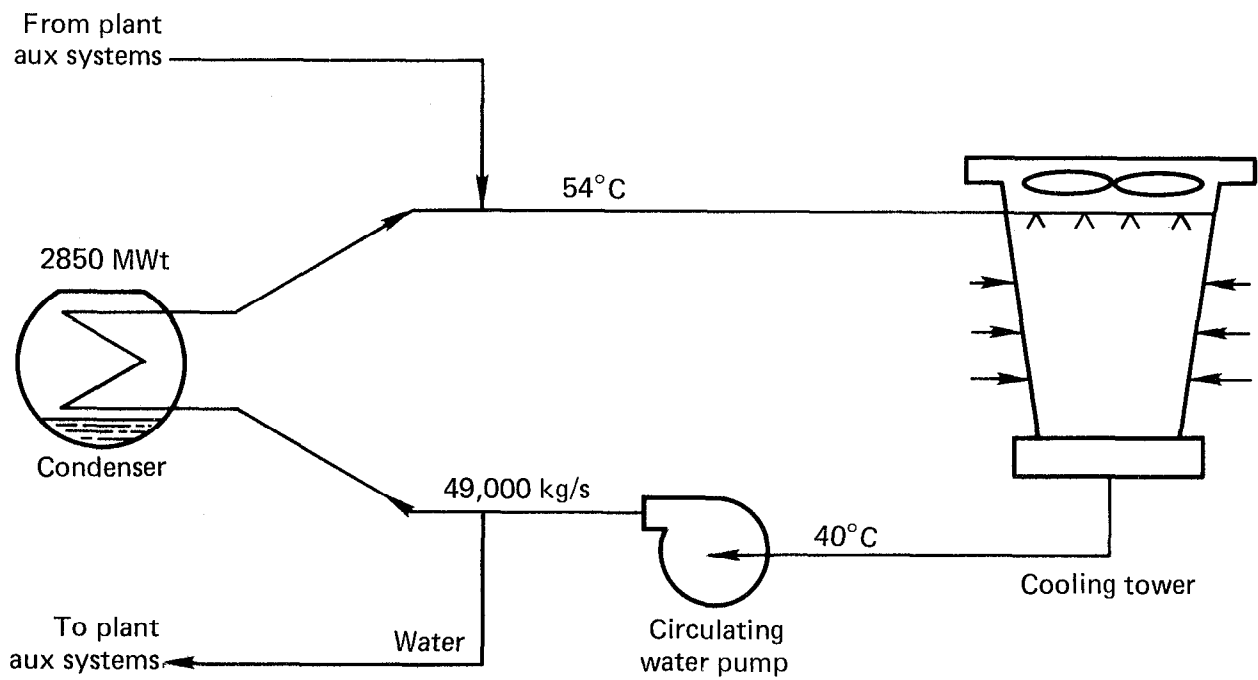


Fig. 6-42. Heat rejection system.

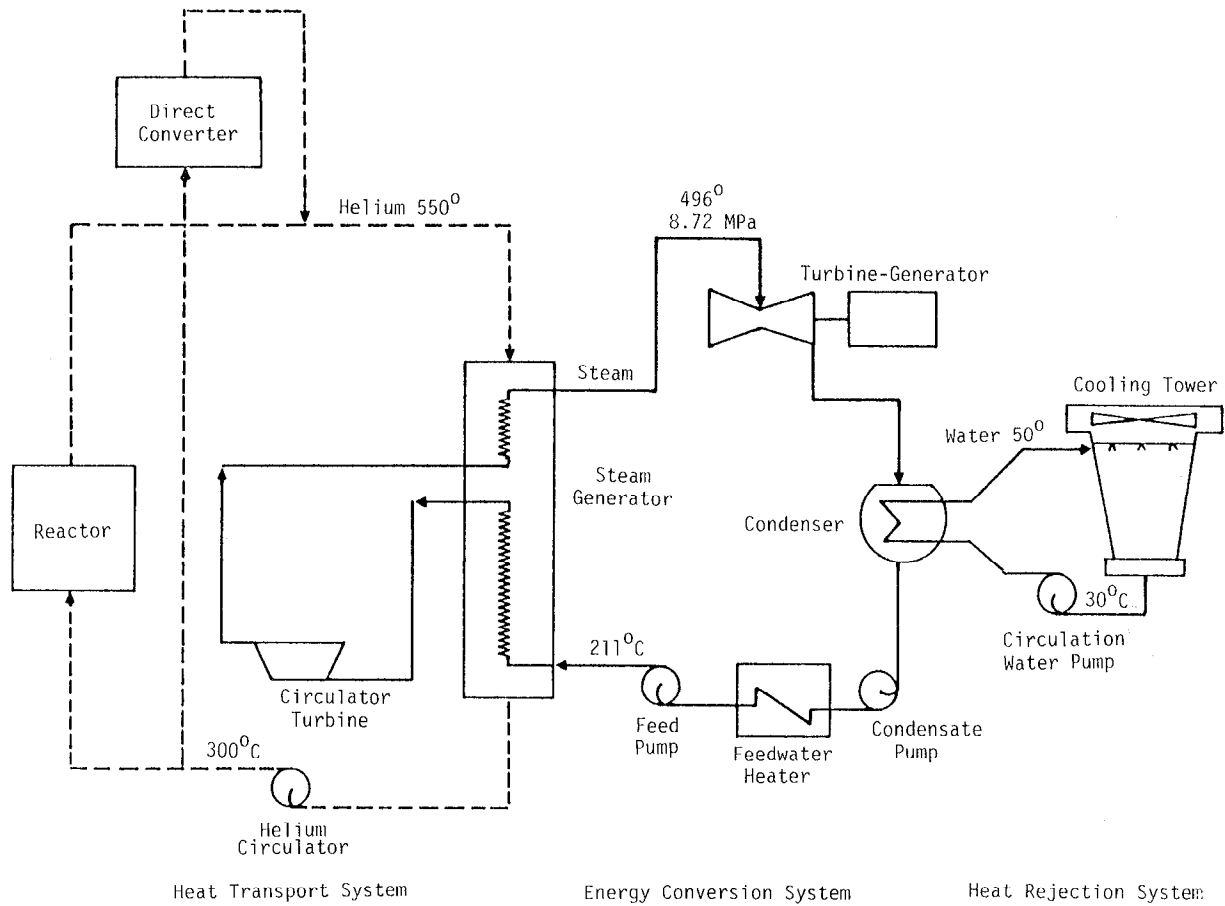


Fig. 6-43. Integrated main BOP systems for He-cooled concept.

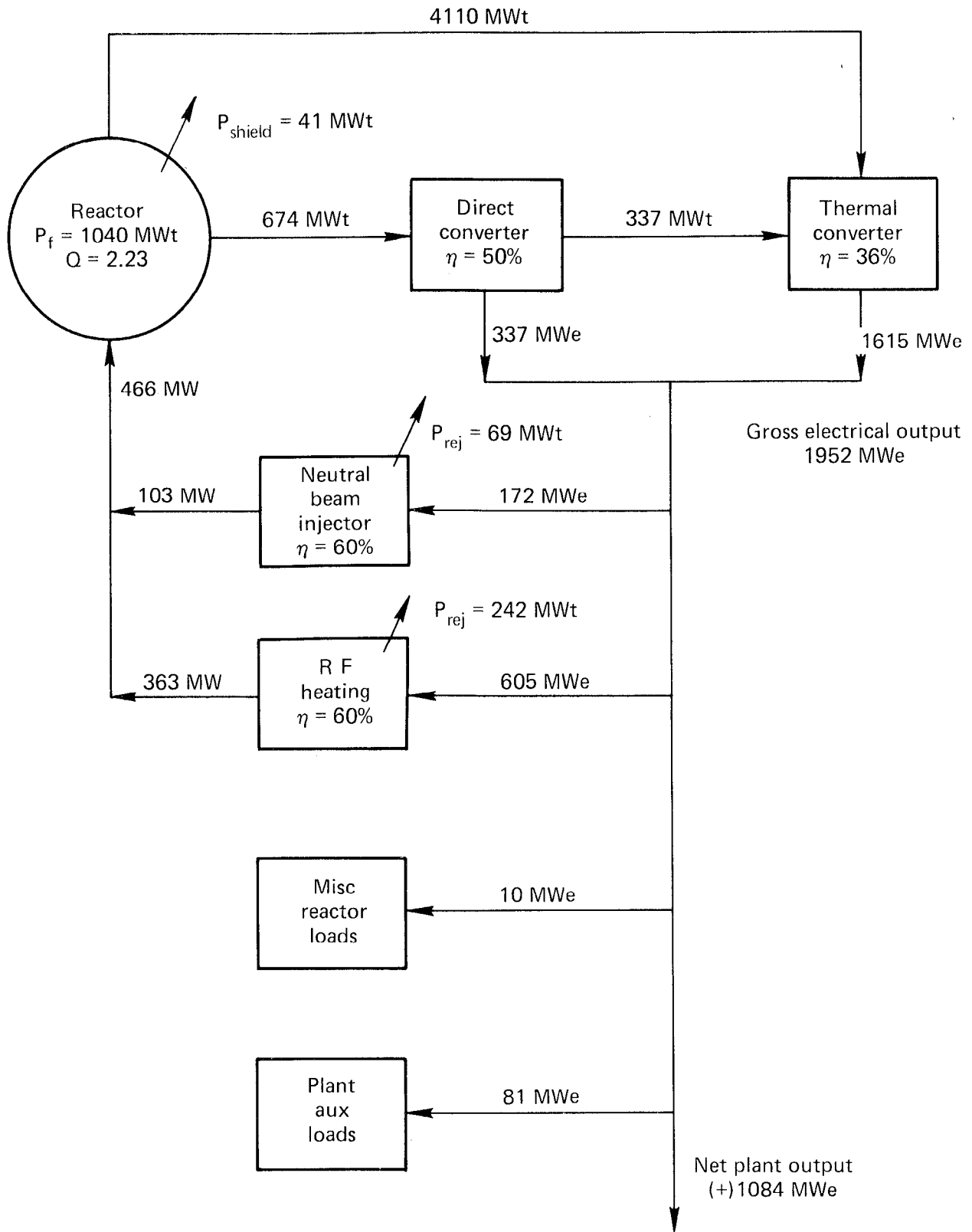


Fig. 6-44. TMHR power flow diagram--He-cooled.

where personnel cannot enter. Manual maintenance should be permitted whenever possible.

The design must incorporate provisions for the power swing that occurs during plant operation. The blanket multiplication factor increases over life and can be accommodated by one of the following:

- Controlling fusion power.
- Controlling fission fuel programming.
- Varying plant output by oversizing equipment.
- Combination of the above.

The choice was to accommodate the power swing in the BOP, and is considered the simplest approach. The design must also provide decay heat removal for the fuel pins. The assumption is that the pins will have to be continuously cooled. Cooling will not be interrupted even during module removal, and a closed system should be used at all times.

The plasma must be placed in a high vacuum. Establishing the vacuum boundary is another major consideration. The boundary can be established at the following:

- First-wall.
- Outside the shield.
- Reactor chamber.

For this design the reactor chamber was designed as the vacuum boundary. This greatly simplifies the problems of making and breaking an intermodule vacuum seal. This approach does increase the volume, which must be evacuated, but the volume associated with direct converters greatly exceeds the increased volume of the solenoid vacuum region. The percentage increase to the total volume evacuated is very small.

The following are some important additional considerations in the containment design:

- Access to valves and valve actuators.
- Provide backup cooling systems, redundancy, and flexibility.
- Restrain the magnet and modules and provide adequate support.
- Limit He pipe size and length of runs.
- Limit size of steam generators.
- Limit piping penetrations through walls and floors.
- Provide a layout that will minimize material and equipment that will be activated.

The reactor mechanical arrangement was developed based on the preceding considerations. An isometric view of this arrangement is shown in Fig. 6-45.

6-119

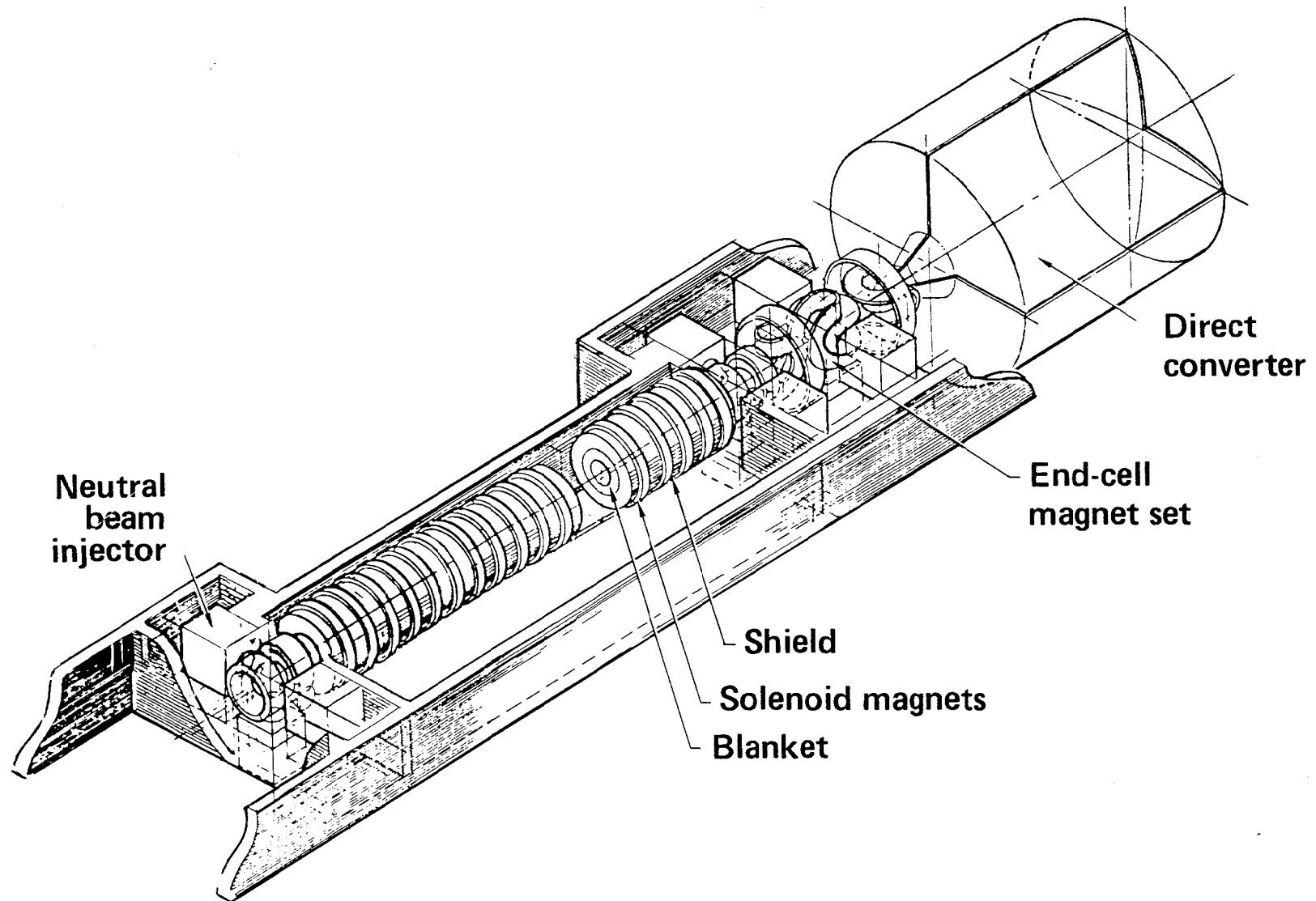


Fig. 6-45. Artist's drawing of the Tandem Mirror Hybrid Reactor (TMHR).

Plant Arrangement. A preliminary conceptual plant arrangement was developed for the He-cooled TMHR. A primary objective of this effort was to develop a containment concept that would allow remote maintenance of the reactor in addition to the normal function of providing services and support to the reactor systems and equipment. Another major objective was to develop a concept for the heat transport systems and equipment and piping arrangement to gain an understanding of the requirements imposed by them on the building design. Because of the high temperature (550° C) and large pipe sizes (150 cm in. diam) required for the He coolant, the thermal expansion and support requirements for the coolant pipes affect the building size and its cost significantly. Thus, primary emphasis was placed on developing a plant arrangement concept for the reactor and the heat transport systems equipment containment. Approximate building volumes required for the plant auxiliary systems were also identified.

Plan and cross section views of the plant are shown in Figs. 6-46 through 6-49. Figure 6-46 is a plan view of the He-cooled TMHR plant. This shows the layout of the reactor containment building, the reactor service building, the steam generator building, and the two direct converter buildings. In addition, it shows the location of the control building and two auxiliary buildings.

The reactor solenoid is enclosed in a long chamber called the reactor chamber. The solenoid is 56 m long and is divided into sixteen 3.5-m long sections. Each section is referred to as a module.

Each module consists of a blanket, shield, solenoid magnet, a base foundation, a double square main frame, and associated distribution piping and instrumentation. The blanket contains the fuel pins and tritium breeding Li and is cooled by He.

The square main frame encases the two magnets and restrains the magnet during operation. The magnets can be freed for removal by disassembling the frame. The frame also contains the four lifting pads for the module.

The module base supports the module, accurately locates its position, and contains locking devices for securely fastening the module in position. The base also contains the valves and actuators for isolating the two inlet and two outlet He pipes for the module. Seals are provided on the bottom around the inlet and outlet piping and around the electrical cable penetrations to provide a vacuum tight seal with the base foundation.

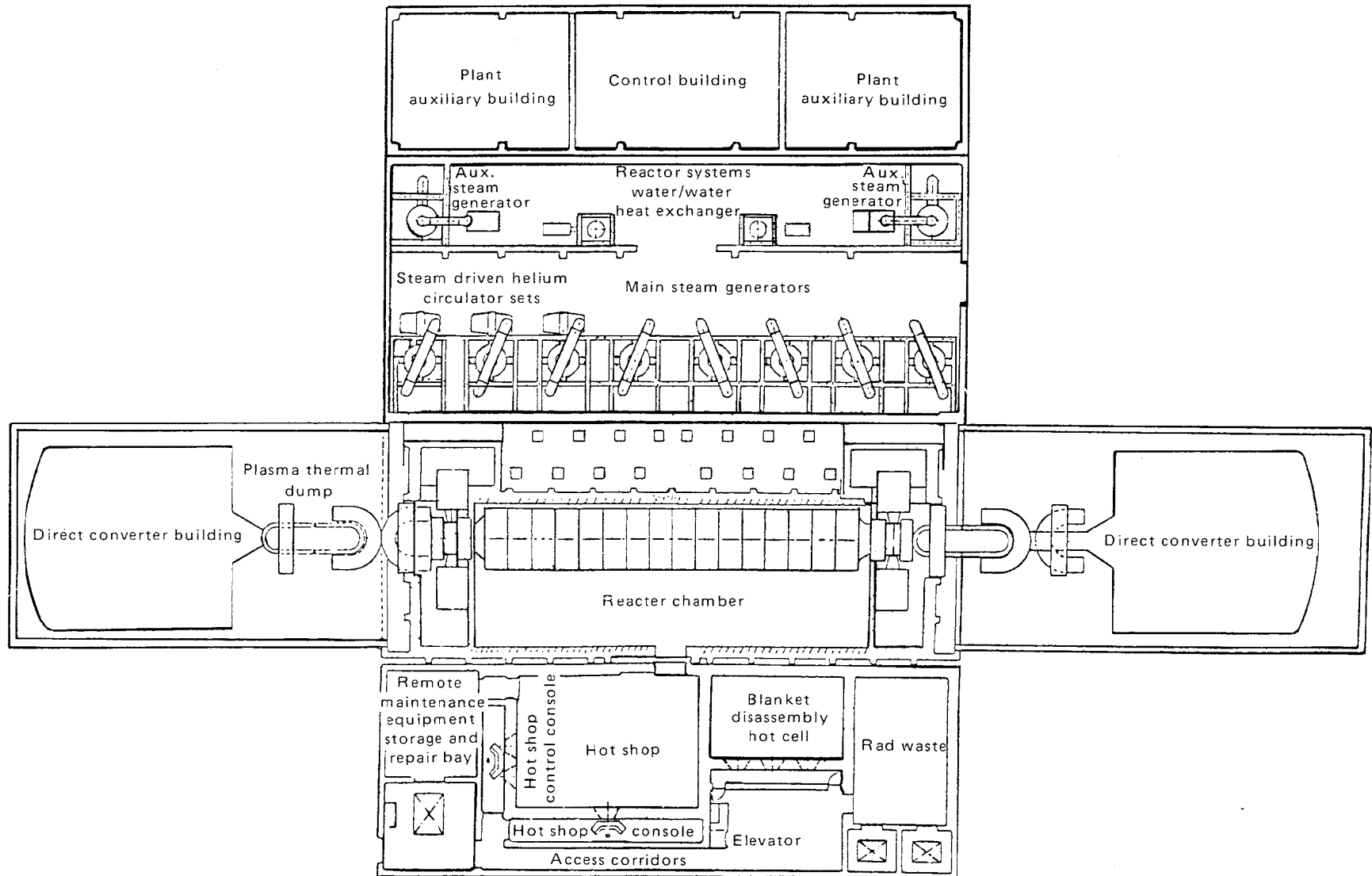


Fig. 6-46. General arrangement of reactor and support buildings (He-cooled).

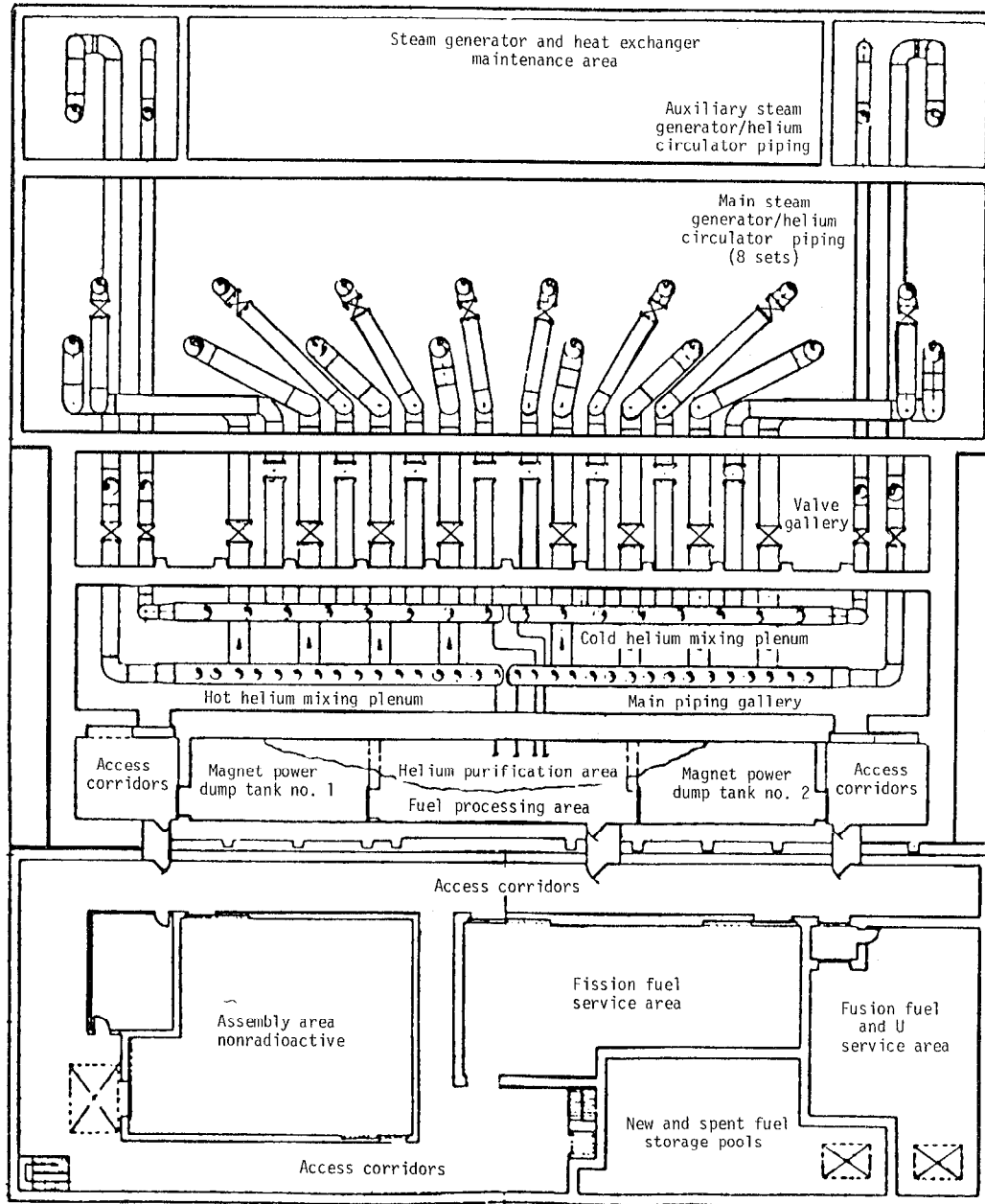


Fig. 6-47. Reactor and support buildings (He-cooled).

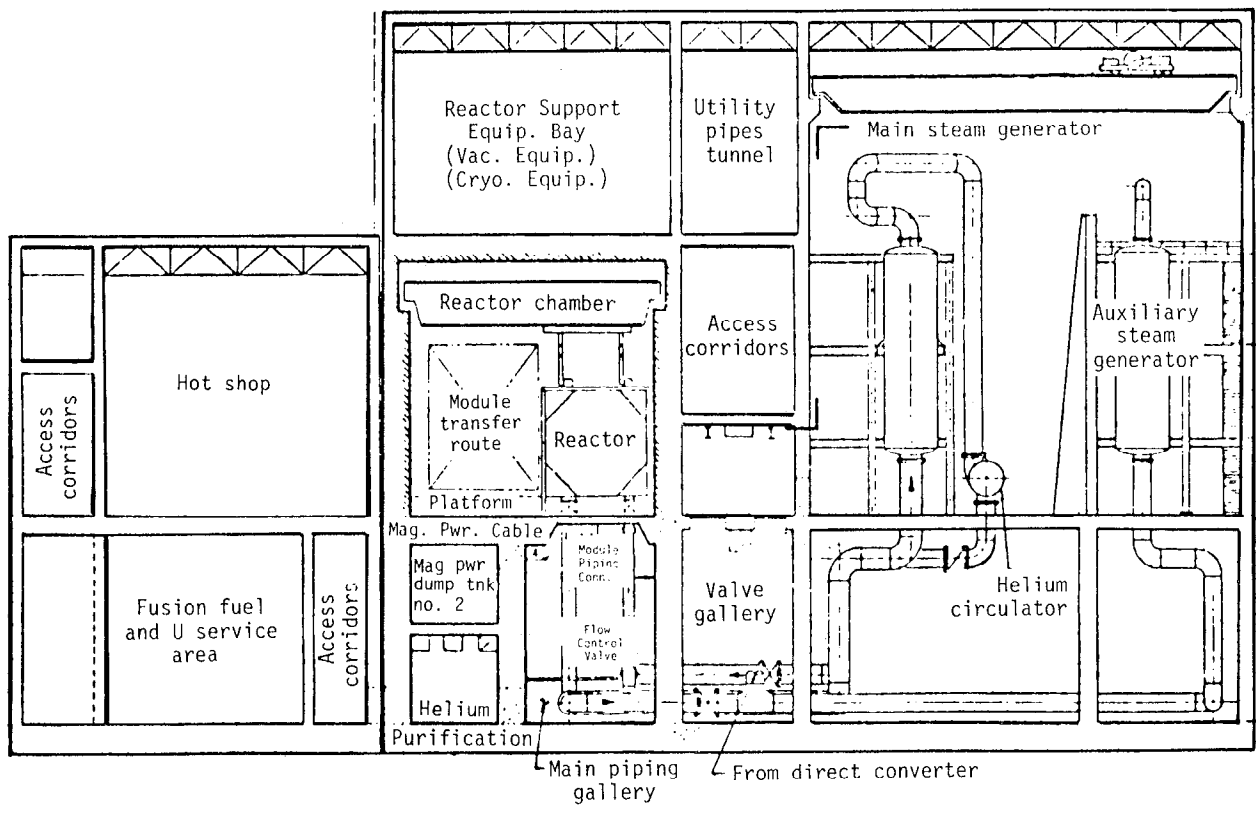


Fig. 6-48. General Arrangement of reactor and support buildings--Section A-A (He-cooled).

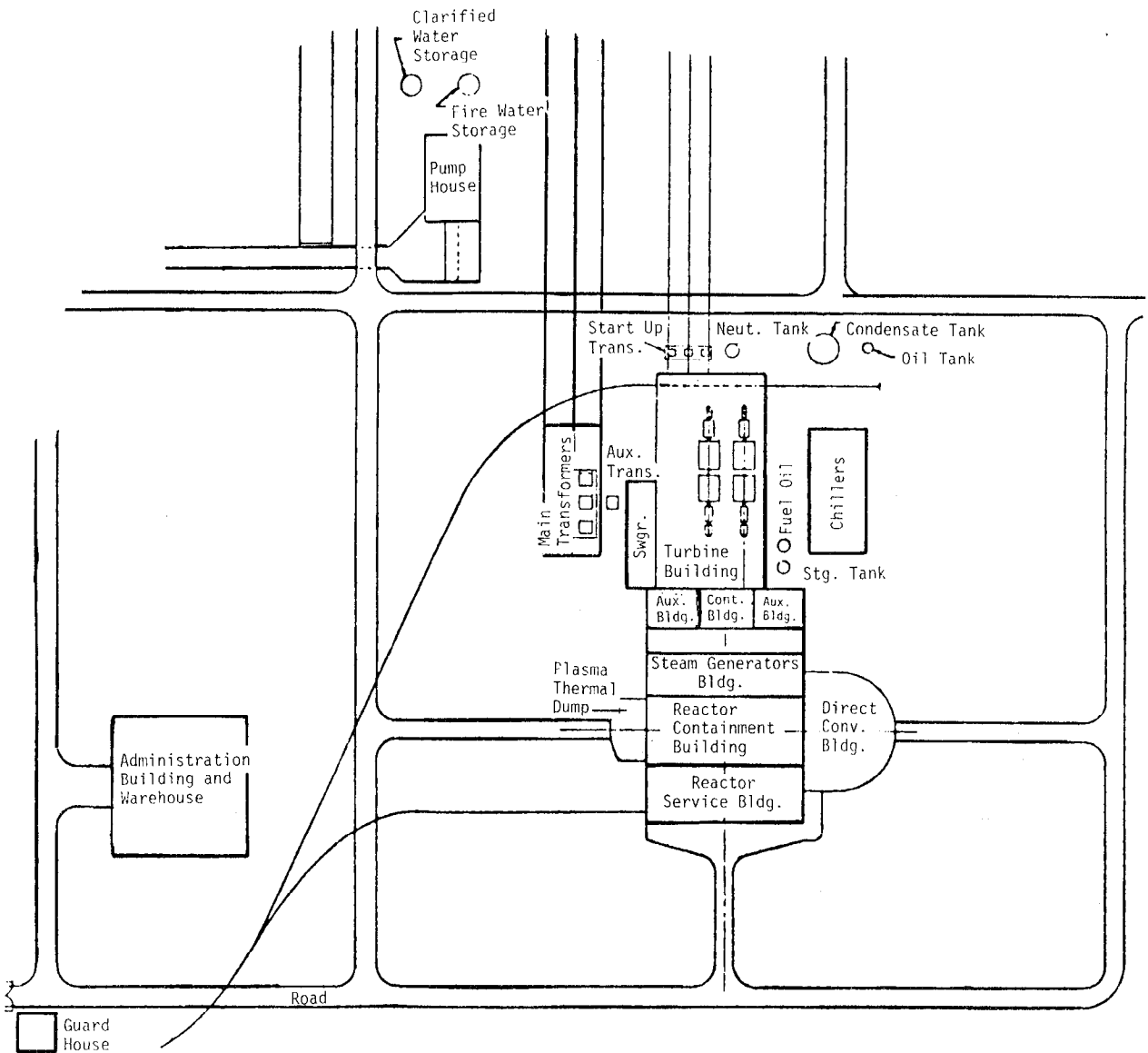


Fig. 6-49. Helium-cooled TMHR plot plan.

On the side of the base facing away from the near wall is an auxiliary service connection panel. Cryogenics, shield cooling, and instrumentation are examples of auxiliary services that are attached here.

The module is free-standing and is not connected to adjoining modules. The intermodule magnet forces are transferred into the square mainframe and the base, which are securely attached to the floor and near wall.

Each module has two inlet and two outlet pipes. Each pipe has an outside diam of about 100 cm.

Since the power of a module varies from BOL to EOL, the mass flow rate of He coolant needs to be controlled. This is done by providing a flow control valve on the inlet (cold leg) pipe to the module. To reduce the number of valves and improve the flow control, one pipe branches off of the cold leg mixing plenum and then Y's above the flow control valve.

The hot and cold mixing plena are shown in Fig. 6-47. These pipes are about 180 cm in diam. There are two hot and two cold mixing plena, and they are cross-connected.

There are eight main steam generators, and each has a He circulator, steam-drive turbine. The piping from and to the mixing plena can be isolated in case of a problem with a steam generator or a He circulator.

The reactor auxiliary systems water/water heat exchangers shown in Fig. 6-46 are for the waste heat rejected from the neutral beam injectors, rf heaters, magnet power cables, and any other low grade heat from reactor support systems.

The auxiliary steam generators are used primarily for removing heat from the direct converter He cooling circuits and also used as a backup for the main steam generator system. Pipes connect to the ends of the hot and cold mixing plena, which connect into the He pipes coming from the direct converter. The valves in the pipes coming from the mixing plena are normally closed.

Figure 6-49 shows the plot plan. The major buildings are:

- Reactor containment building.
- Reactor service building.
- Steam generator building.
- Direct converter buildings.
- Control building.
- Auxiliary building.
- Turbine building.

The reactor containment building and the steam generator building are on a common base mat. This reduces the potential for a He pipe break due to differential base mat movement during a seismic event. The base mats for the direct converters need to be separated because if they were joined, a potential thermal expansion problem would exist.

Reactor Containment Building

The reactor containment building contains the following major equipment:

- Reactor solenoid.
- Neutral beam injectors.
- RF heaters.
- Magnet.
- Helium piping and valves.
- Magnet power dump tanks.
- Fuel processing.
- Vacuum pumping.
- Cryogenic.
- Helium purification.

The major areas and location of equipment inside the reactor containment building are discussed below.

Reactor Chamber. The reactor chamber contains the reactor solenoid region and is a vacuum chamber. The walls are 2.5 m thick and are lined with stainless steel. Figure 6-48 shows a cross section of the chamber. The chamber width was established by the space needed to move a module out plus enough room for reactor service piping and cables.

The reactor modules sit on a stainless steel foundation and high density neutron and gamma shielding that is heavily enforced, which is needed to provide the necessary shielding and strength with the minimum thickness. When the module is disconnected, the module pipe that extends below the base should be as short as possible. If the pipe has to pass through a large thickness foundation, the pipe ends will be too long. Heavy shielding was desired to limit activation of material below and possibly permit personnel access to the piping gallery when all the modules are in place.

A bridge-type lifting device is used in the reactor chamber for lifting and transporting modules in and out. The lifting device has four arms that can be locked in the raised position. Four-point-positive-lift is used to prevent sway during movement and to eliminate the alignment problem that a typical crane has.

Reactor Support Equipment Bay. The mechanical vacuum pumping equipment (HVAC) and cryogenic equipment are located in this bay. We chose this location because it reduces the ducting length for vacuum systems and pipe length for cryogenics. Since their functions are interrelated, it was beneficial to place them relatively close together. This bay has limited access during operation.

Main Piping Gallery. This gallery contains the large mixing plena, module connection piping, magnet power cables, and flow control valves. A platform is provided for workers, plus rigging fixtures for disconnecting the module piping and electrical cables. This area has limited accessibility during operation. Access is not permitted if a module is removed because of radiation streaming from above.

Other Areas. Helium purification equipment, magnet power dump tanks, fuel processing system, and valve gallery are located such as to reduce the distance from the reactor solenoid and efficiently use the adjacent spaces.

Steam Generator Building

The steam generator building contains the following major equipment:

- Eight main steam generators, eight He circulator and steam turbine drive sets, and associated piping.
- Two reactor system water/water heat exchangers, motor driven pumps for circulating water, and associated piping.
- Two auxiliary steam generators, two He circulator and steam turbine drive sets, and associated piping.

The building also contains a maintenance bay where the steam generators, heat exchangers, and circulators can be repaired.

Reactor Service Building

The reactor service building contains the following major equipment:

- Fission fuel storage and handling.
- Fusion fuel storage and handling.
- Module disassembly.
- Blanket disassembly.
- Remote maintenance.
- Radwaste storage and handling.

The reactor service building can be best described by describing a module renovation. The module is disconnected and carried to the door of the hot shop, which is centrally located. The module is placed on a transporter, which transports the module through the hot shop works and storage stations. The hot shop has enough space to store two modules and space to work on two more.

Specially designed equipment that is remotely controlled from consoles outside the hot shop removes the blanket sections, which are then transferred to the blanket disassembly hot cell. New blanket sections are installed, and the module is tested and placed into storage.

The fuel pins and Li are removed and transferred into the radwaste area and down to the level below for further processing. Other disposable material is processed in the radwaste area.

In the level below the Li is processed by removing tritium and impurities and is then placed into new blankets. The fuel pins are processed and placed into spent fuel storage pools, which also store new fuel pins. (This is where new blankets are loaded with fuel pins.)

Control Building

The control building contains the following:

- Central control room.
- Cable spreading room.
- Switchgear.
- Auxiliary panels.
- M-G sets.
- HVAC.

Auxiliary Building

The auxiliary building contains the following:

- Diesel engine generators.
- Batteries.
- Gas engine generators.
- Switchgear.

Turbine Building

The turbine building contains the following major equipment:

- Two 900,000-kVa generators.
- Two 845,000-kW turbine sets that consist of one high pressure and two low pressure turbines each.
- Two condensers.
- Feed systems consisting of:
 - Motor driven condensate pumps.
 - Feedwater heaters.
 - Steam turbine driven feedwater pumps.

Conclusions and Recommendations

The present design allows an initial assessment of the problems associated with the plant design for fusion reactor plants in general and the TMHR plant in particular. The design and analyses are relatively superficial and conceptual in nature. Many of the systems and associated equipment are not identified. We have made allowances to accommodate these unknown and uncertainties; but until further design and analysis are done, many uncertainties remain. On the basis of the present study, the following comments are in order:

- The plant layout including equipment and piping arrangement is conceptual. Further study is needed to detail and improve the arrangements. The primary piping arrangement is a critical aspect of the plant layout and can have a large impact on the building costs. The layout is based on the use of expansion joints in the primary piping. This will require development and testing to gain ASME Code acceptance.

- The design and layout of high temperature piping is critical. Stress analysis has not been performed to substantiate the piping arrangement. The stress analysis will likely rely heavily on inelastic analysis and other sophisticated techniques leading to high design costs. Special design configurations, such as concentric and externally-cooled pipe, might be required.

- The structures in this plant are significantly larger than those in fission power plants. All the structures are very massive because of shielding and other safety requirements. The conceptual design is considered to be a feasible design consistent with current technology and industry practice. However, some aspects of the design/analysis of the structures have to be investigated further before a method for their design can be established. As an example:

- In the reactor containment building special vehicles, possibly running on tracks, have to be built for removing blankets, which will subject the floor slab to moving dynamic loads. A thorough analysis of the floor slab, subjected to moving loads, is needed.

In addition to the preceding general comments the following are potential problems associated with the He cooled TMHR systems and some possible recommendations.

- Helium piping - The pipes are very large and present a seismic restraining, a fabrication, and a thermal expansion problem. The use of flexible joints could decrease the thermal expansion problem. Methods for connecting the He piping to the modules have to be examined.

- Valves - There are many large valves in the He piping. Fabrication and reliability have to be examined. The accurate control of He flow rate may be a problem, and a large penalty may be paid for the pressure drop across such a control valve.

- Emergency cooling - The ability to adequately cool the fuel pins in the case of a double-ended piping failure should be examined further.

- Vacuum chamber - A detailed study should be made into all the potential ramifications of using a vacuum chamber.

- Tritium removal and handling equipment - This equipment should be defined so it can be integrated into the plant design. The systems could significantly affect the design because of size and service requirements.

- Thermal transient - The operating and accident transients associated with either the cold leg temperature going to hot leg temperature or vice versa should be examined in detail. Reduced lifetime or damage to the reactor module piping and blanket may result from transients.

Preconceptual Cost Estimate

The results of the preconceptual cost estimate, its basis, qualifications, and exclusions are presented in this subsection. This estimate is an order-of-magnitude evaluation of the direct-level BOP costs. A summary and detail presentation of this estimate are presented in Tables 6-18 and 6-19, respectively. The format of these presentations is in conformity with the May 1978 Battelle Report PNL-2648, "Fusion Reactor Design Studies - Standard Accounts for Cost Estimates."

Table 6-18. Direct level capital cost summary (3Q 1979 pricing).

Account	Description	Cost in \$
21	Structures and site facilities	212
22	Reactor plant equipment (excludes reactor)	450
23	Turbine plant equipment	280
24	Electric plant equipment	140
25	Miscellaneous plant equipment	<u>20</u>
	Total direct level cost	1102

Costs are stated at third-quarter 1979 pricing levels with no allowance for future escalation.

The process under discussion in the study is taken to be a first generation model designed in a time when the major equipment functions have been successfully demonstrated. At that time industry will have developed the capability to produce the equipment--a capability which does not necessarily exist today. Development and first-of-a-kind costs are therefore not considered.

Table 6-19. Direct level capital cost detail (3Q 1979 pricing).

Account	Description	Cost in \$ millions	
21	Structures and site facilities:		212
.01	Site improvements and facilities	15	
.02	Reactor building	82	
.03	Turbine building	30	
.04	Cooling system structures	5	
.06	Miscellaneous buildings	<u>80</u>	
22	Reactor plant equipment:		450
.02	Main heat transfer and transport system	355	
.03	Auxiliary cooling system	20	
.04	Radioactive waste treatment and disposal	10	
.06	Other reactor plant equipment	<u>65</u>	
23	Turbine plant equipment:		280
.01	Turbine generators	105	
.02	Main steam system	15	
.03	Heat rejection systems	40	
.04	Condensing systems	15	
.05	Feed heating system	35	
.06	Other turbine plant equipment	30	
.07	Instrumentation and control	<u>40</u>	
24	Electric plant equipment:		140
.01	Switchgear	10	
.02	Station service equipment	15	
.04	Protective equipment	2	
.05	Electrical structures and wiring containers	60	
.06	Power and control wiring	50	
.07	Electrical lighting	<u>3</u>	
25	Miscellaneous plant equipment	<u>20</u>	
	Total direct level cost		1102

Basis and Scope Definition

The estimate is based on the conceptual design and engineering information prepared for the study; this includes system descriptions, flowsheets, block diagrams, system schematics, plot plans, and general arrangement drawings.

With respect to the actual estimating procedure, it is normal practice when engineering is well defined to derive the cost estimate by building up the cost item by item. In a less well defined study, where perhaps only 60% of the equipment is identified, this method can still be used, but a large portion of the cost must be based on allowances and factors. However, in a preconceptual study, such as the TMHR where less definition is available, a different approach is necessary. The plant must be viewed as a series of systems that are similar in content (but not necessarily in function) to systems in existing analogous plants, or to systems in well defined studies. The costs are then developed by inductive reasoning using the costs of the analogous systems.

This particular estimate is thus derived by a macro approach rather than a micro approach, based on comparisons with the design and cost estimate of the prototype large breeder reactor (PLBR) study, prepared by Bechtel and GE in May 1977. The major categories of the PLBR estimate (escalated to third-quarter 1979) were adjusted by cost-design parameters to derive the major categories of the TMHR estimate. These costs were then further refined and adjusted, as required, to correspond to the TMHR conceptual design.

The following paragraphs briefly address each of the major cost categories, describing the project scope and the methods employed to develop the estimate.

Civil/Structural. This includes site clearing, earthwork, roads, fences, fire and sewer systems, and all building foundations and structures. Each of the major buildings and miscellaneous civil items was compared with the corresponding portions of the PLBR estimate. The PLBR costs were then adjusted for size differences, based on building volumes, land area, etc., and adjusted for structural complexity based on appropriate scaling exponents.

Mechanical Equipment. This includes heat transfer equipment, turbine generator, surface condenser, feedwater heaters and pumps, and all other mechanical equipment throughout the BOP. This equipment was categorized into the following major groups:

- Turbine generator and condenser.
- Other turbine mechanical equipment.
- Balance of mechanical equipment.
- Main heat transfer equipment.

Each group (except for the main heat transfer equipment) was compared with the corresponding PLBR mechanical equipment. The PLBR costs were adjusted for size differences, based on the gross electrical capacity of the respective plants and appropriate scaling exponents. The cost of the main heat transfer equipment was estimated based on information provided by GA.

Piping. This includes both process and nonprocess pipe throughout the entire plant. The cost of the primary heat transport piping was estimated based on developing quantities from conceptual layout drawings, estimating installation labor, and obtaining telephone quotes for material. All other process and nonprocess piping costs were estimated by comparing with the PLBR estimate. The PLBR costs were adjusted for the differences in overall plant capacity based on building volumes, the thermal MW rating of the respective plants, and appropriate scaling exponents.

Instrumentation. This includes control valves on process piping systems, all gauges, indicators, transmitters, recorders, piping and tubing for hydraulic control systems, control boards and panels, computerized data processing hardware/software, and all other control room equipment for monitoring and controlling plant operations. Costs were developed by comparing with the PLBR estimate. The PLBR costs were adjusted for the differences in overall plant capacity based on building volumes, the thermal MW rating of the respective plants, and appropriate scaling exponents.

Electrical. This includes all electrical equipment and bulks to serve in plant loads and the main power transformers. This does not include reactor power rectification or storage and switching equipment for the electrical bulks between such equipment. The electric equipment was compared with the corresponding portions of the PLBR estimate. The PLBR costs were then

adjusted for quantity and load differences, based on building sizes, the electrical MW requirements of the respective plants, and appropriate scaling exponents.

Exclusions. The following items are excluded from the estimate:

- The TMHR, direct converter, related equipment, and installation.
- Field distributables, engineering and home office costs, contingency, future escalation, and fees.
- Owner's costs, such as land acquisition, costs of financing, owner's licensing and engineering, royalties, etc.
- Initial charges, stocks of operating supplies, and spares.
- Assistance to the owner in obtaining EPA clearances, permits and authorizations from DOE, or any other governmental agencies.
- Ecological and environmental considerations other than those incorporated in the present conceptual design.
- Startup, training, and operating costs.
- State and local taxes.
- Switchyard and transmission facilities.
- All facilities beyond the hypothetical site boundary.

Cost Scaling Algorithms

In addition to the base BOP cost estimates, cost scaling algorithms were developed for each of the four BOP cost categories (civil and structural, mechanical equipment, piping and instrumentation, and electrical equipment and bulks). These cost scaling algorithms are listed in Table 6-20 and are intended for scaling the BOP costs for parameters other than those used in this study (see Table 6-17). To arrive at these algorithms, an approximate curve-fitting-type approach was used.

Caution needs to be exercised in using the algorithms. For the cost algorithms to be valid, the variation of parameters (Q, wall loading, wall radius, blanket multiplication, injection efficiency, direct converter efficiency, etc.) should not result in a variation of the parameters in this study exceeding an approximate +20% from the base values assumed (see Table 6-17). These parameters are thermal energy from the blanket, thermal exhaust from the direct converter, and the length of the reactor solenoid.

Table 6-20. Cost scaling algorithms--He-cooled case (in million \$).

Civil and structure	$140.5 + 0.293 \sqrt{P} + (31 + L_{cc})^{0.85}$.
Mechanical	$0.263 (MW_{tt} \cdot \eta_{th})^{0.9} + 0.062 MW_{tb}$.
Piping and Instr.	$186.8 + 0.00123 (487.3 + L_{cc})^{0.7} (MW_{tt})^{0.85}$ $+ 1.076 (L_{cc} - 39) + 0.269 (0.4 \sqrt{P} - 10.4)$.
Electrical	$3 + 1.75 (P_{aux})^{0.65} + 0.044 (627.4 + L_{cc})$ $+ 0.319 P_{aux}$.

where

- L_{cc} = Length of central cell, m.
- P = Power input to dc, MW = $P_f/Q + 0.2 P_f$.
- MW_{tt} = Thermal MW from blanket + thermal MW from dc.
 $= MW_{tb} + P(1 - \eta_{dc})$.
- η_{th} = Thermal conversion efficiency (turbine cycle efficiency).
- P_{aux} = $10 + 0.05 MW_{tt} \cdot \eta_{th} + 0.1 P_f/Q \cdot N_{inj}$.
-

REFERENCES

1. R. W. Moir, et al., "Interim Report on the Tandem Mirror Hybrid Design Study," UCID-18078, August 1979.
2. Nuclear Systems Materials Handbook, Vol. 1, Design Data, Section 5, TID 26666 Hanford Engineering Development Laboratory, Richland, Washington.
3. Briggs, J. Z., and Barr, R. Q., "Air Cast Molybdenum Base TZM Alloy: Properties and Applications," High Temperature-High Pressures, 1971, Vol. 3, p 363.
4. Pard, A. G., and Garr, K. R., "Some Observations on the Damage Structure of Neutron Irradiated Inconel 718," National Alloy Development Program Information Meeting, May 22, 1975, TC291, HEDL.
5. Bloom, E. E., and Wiffen, F. W., "The Effects of Large Concentrations of Helium on the Mechanical Properties of Neutron Irradiated Stainless Steel," ORNL Report ORN-TM-4861, May 1975.
6. Rosenwasser, S. N., et al., "The Application of Martensitic Stainless Steels in Long Lifetime Fusion First Wall/Blankets," First Topical Meeting on Fusion Reactor Materials, Miami Beach, Florida, January 1979.
7. Schultz, K. R., et al., "Blanket, Shield and Power Conversion System for a Small Field Reversed Mirror Fusion Reactor," General Atomic Co. report GA-A15533, July 1979.
8. Wiswall, R., and Wirsing, E., "The Removal of Tritium from Fusion Reactor Blankets," Brookhaven National Laboratory report BNL 50748, 1977.
9. Kittel, J. H. et al., "Effect of Irradiation on Thorium and Thorium-Uranium Alloys," ANL-5674 (1963).
10. Bender, D. J. and Lee, J. D., "The Potential for Fissile Breeding with the Fusion-Fission Hybrid Reactor," Lawrence Livermore Laboratory report UCRL-77887, June 1976.
11. Bender, D. J., et al., "Reference Design for the Standard Mirror Hybrid Reactor," joint Lawrence Livermore Laboratory/General Atomic Co. Report UCRL-52478/GA-A14796, May 1978.
12. Schultz, K. R., et al., "Evaluation of the ^{233}U Refresh Cycle Fusion-Fission Power System Concept," General Atomic Co., Report GA-A15108, to be published.
13. McAdams, W. H., "Heat Transmission," Third Edition, McGraw-Hill, New York, 1954.

14. Kays, W. M., "Convective Heat and Mass Transfer," McGraw-Hill, New York, 1966.
15. Bennett, F. and Baxi, C., "Convection to Nusselt Number Correlation for GCFR Radial Blanket," General Atomic Company Internal Memo, July 1979.
16. Engle, W. W., Jr., "A User's Manual for ANISN," K-1693, Oak Ridge Gaseous Diffusion Plant (1967).
17. Plaster, D. M., et al., "Coupled 100 Group Neutron and 21 Group Gamma-Ray Cross Sections for EPR Calculations," ORNL-TM-4873, Oak Ridge National Laboratory, 1975.
18. "Vitamin-C - 171 Neutron, 36 Gamma-Ray Group Cross Section for Fusion and LBFBR Calculations," DLC-41, Radiation Shielding Information Center, Oak Ridge National Laboratory, 1978.

SECTION 7
MOLTEN SALT-COOLED SYSTEM DESIGN

INTRODUCTION

The Tandem Mirror Hybrid Reactor/Molten Salt (TMHR/MS) system would utilize the 14 MeV neutrons produced by a deuterium/tritium-fueled tandem mirror fusion driver to breed tritium and fissile nuclear fuel in a blanket region located around the fusion zone. The purpose of this breeding is twofold: 1) to breed enough tritium to sustain the fusion reaction, and 2) to convert fertile ^{232}Th into fissile ^{233}U . This bred ^{233}U would then be used in a fission reactor.

From a neutronics point of view, it is mandatory to breed neutrons in the blanket zone, because without neutron breeding the one neutron produced by the D-T fusion reaction would be used in the production of the replacement tritium, leaving no excess neutrons to breed the ^{233}U . Fortunately, there are several nuclear reactions that will breed neutrons. In the TMHR/MS design the neutron breeding will come primarily from the (n, 2n) reaction of beryllium.

The study reported on here carries on from the preliminary study of Section 5. The idea of using molten salt as a fuel breeding media was previously discussed by Lidsky. The breeding was rather low in that design, a situation remedied by Lee in a design using metallic Be as a neutron multiplier. The present discussion is an assessment of the Beryllium/Molten Salt design.

The TMHR/MS system is composed of four main sections: 1) the tandem mirror fusion driver, 2) the blanket region, 3) the chemical processing system, and 4) the balance-of-plant (BOP). The fusion driver design was covered in Section 4; the blanket region, chemical processing system, and BOP designs will be described in this section. Figure 7-1 is a block diagram of the TMHR/MS concept showing the main functions and their interconnections.

The molten salt blanket concept has several unique features when compared to more conventional approaches. The most significant difference is that the system operates on a continuous basis and includes a close-coupled, fuel processing step. This mode of operation is possible because the lithium and thorium breeding materials are in the molten salt that is pumped through the

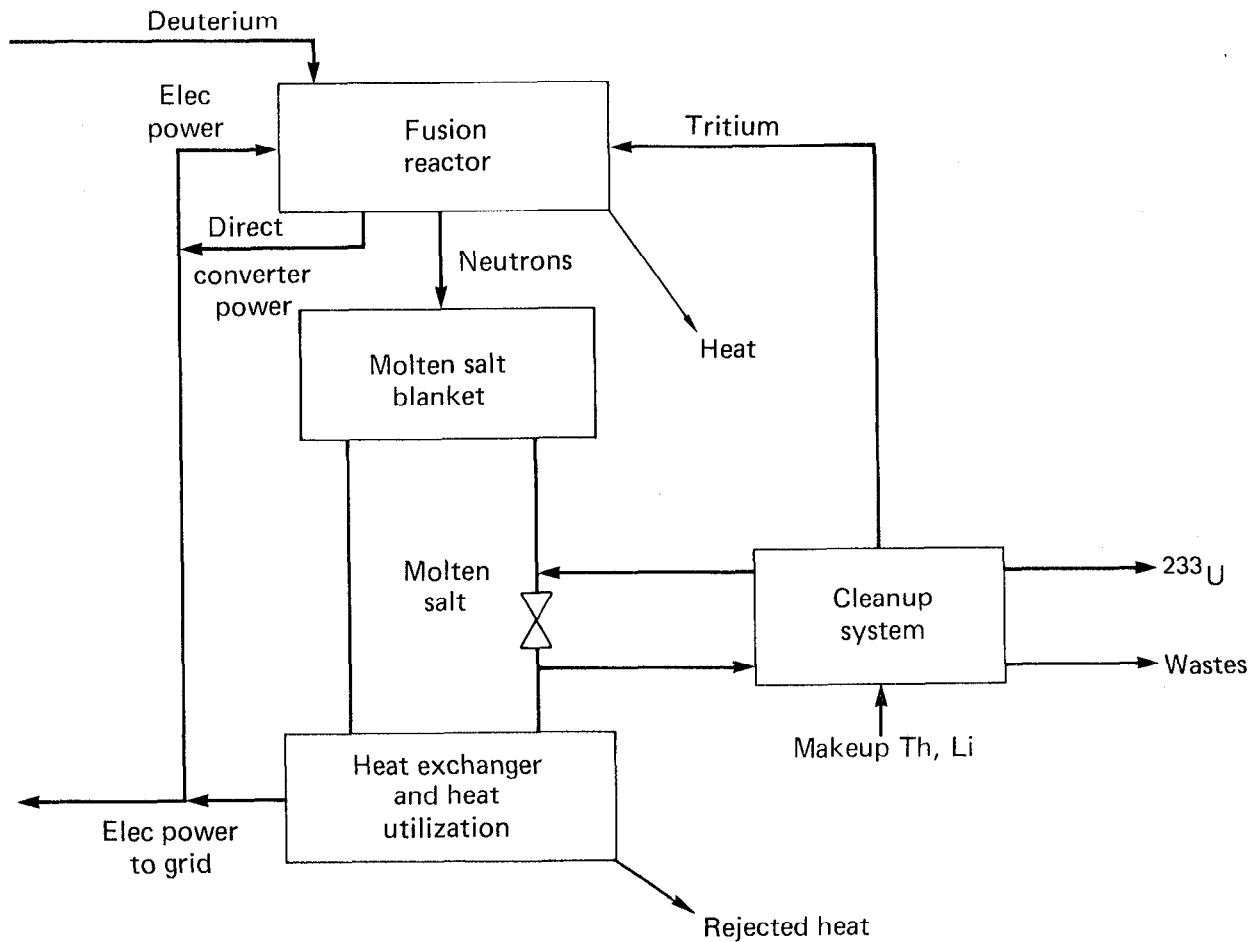


Fig. 7-1. Block diagram of TMHR/molten salt concept.

blanket. In the conventional approaches the thorium and lithium are contained in pins as a fixed part of the blanket. This geometry requires a batch-type operation with fresh fuel loading and product removal on a periodic shutdown and maintenance schedule. An additional benefit of the molten-salt blanket concept is the possibility of suppression of ^{233}U fissioning by its continuous removal. This yields two benefits: 1) it maximizes the production of ^{233}U for use by fission-type reactors, and 2) it greatly reduces the fission product generation rate and thus the after shutdown decay heat removal problems.

STUDY OBJECTIVES AND METHODOLOGY

The culmination of the alternate blanket/coolant evaluation phase selected two systems for further evaluation. The helium-cooled design using metal clad thorium and lithium oxide fuels was selected as the most promising conventional approach, while the molten salt blanket was chosen for further consideration because of its attractive preliminary economics (see Sec. 5) and its inherent ability to multiply neutrons without fissioning.

Based on this decision, the remainder of this year's effort was concentrated on these two blanket/coolant systems. Specifically, a molten salt evaluation team was organized to "...investigate the molten salt case to access its feasibility with particular considerations to materials, corrosion, and process requirements"...¹. To perform this assessment it was decided to pursue a preliminary design of a molten salt-cooled blanket system. The intent was to use the design type discipline as a tool to look at the molten salt technology; the underlying philosophy is "that following the design discipline route will systematically evaluate the technology from a relevant point of view."

From a logistical point of view the design effort was broken into several stages as shown in Fig. 7-2. The starting point for this design effort was the nuclear feasibility and general economic considerations generated during the previous blanket coolant studies stage (see Sec. 5). The first step of this assessment effort was to verify these nuclear performance calculations and then develop a reference case from which the various design activities could proceed.

The numerical results of this reference case was then used as a starting point for parallel design efforts in the blanket, chemical processing, and BOP areas.

This technical assessment was concluded by an independent design review and critique. Specifically, we contacted the Oak Ridge National Laboratory (ORNL) and asked them to critique our design. They responded by assembling a review staff headed by J.R. Engel, which represented a sizeable portion of the MSRE/MSBR engineering talent. A summary of their review and comments is included at the end of this section.

When considering the following design and technical evaluation, bear in mind the following points:

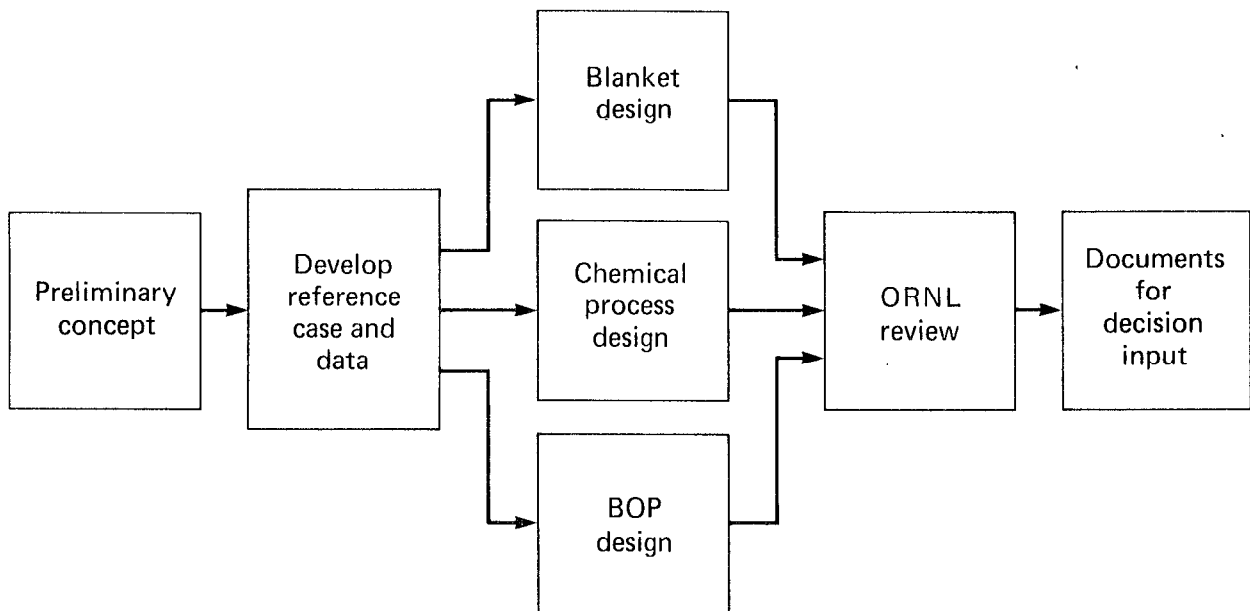


Fig. 7-2. TMHR/molten salt design effort logistics.

- The main objective was to determine if there are any unique problems with the TMHR/MS concept which make further evaluation, design, and development impractical.
- The approach was to develop this design as an analysis tool for evaluation of the technical feasibility.
- In order to expedite the design procedures, a decision was made to rely heavily on established technology whenever possible (i.e., the MSBR molten salt composition was chosen even though this was not necessarily an optimum choice).

BLANKET DESIGN

The blanket design portion of this work was broken down into four areas: 1) materials considerations, 2) neutronics considerations, 3) mechanical design, 4) thermal hydraulics considerations. The blanket design efforts were based on the following design philosophy:

- Use beryllium metal as a neutron multiplier.

- Minimize metallic structure in the blanket, especially thermal neutron absorbing materials.
- Use He-cooled first-wall separate from the blanket. Design for long first-wall life.
- Design blanket for natural drainability, handle after shutdown decay heat removal problems in the dump tanks.
- Design blanket for a minimum magnet coverage of 20%.
- Suppress ^{233}U fission to minimize fission products handling problems, and maximize ^{233}U production for use in fission reactors.
- Breed a minimum of 1 tritium atom per fusion neutron.

The starting point for the blanket design was the previous molten salt case nuclear evaluations and economics work.^{2,3} Table 7-1 lists the fusion reactor parameters that were assumed for this design work.

Table 7-1. Fusion driver performance assumptions

Fusion energy multiplication, Q	= 2.12
Neutron wall loading,	= 2.0 MW/m ²
First-wall radius, R wall	= 2.1 m
Total nuclear power, P _{NUC}	= 4000 MW
Fusion power, P _{FUS}	= 33.20 MW/m
Total blanket energy multiplication, M	= 1.5

As previously mentioned, the molten salt was assumed to be similar in composition to the one chosen for the Molten Salt Breeder Reactor (MSBR) program⁴, except that the uranium composition would be kept much lower so as to suppress uranium fissions; Table 7-2 gives the TMHR/MS assumed molten salt compositions and properties.

Table 7-2. Properties of TMHR/MS case molten salt

Composition, mole %	LiF 72
	BeF ₂ 16
	ThF ₄ 12
Liquidus:	
°C	500
°F	932
Properties at 600°C (1112°F) :	
Density, g/cm ³	3.35
Heat capacity, cal/(g°C) or Btu/(lb °F)	0.33
Viscosity, cP	12
Vapor pressure, Torr	<0.1
Thermal conductivity, W/°C cm)	0.011

Figure 7-3 shows a cross sectional view of TMHR/MS reactor concept. The plasma region is contained by a separately-cooled first wall. Moving radially outward, there is next a blanket zone that contains the Be metal neutron multiplier in rods cooled by axially oriented molten salt flow. Again, moving out radially, the next zone is high density concrete shielding followed by the solenoidal magnets.

MATERIALS

The materials considered will be used to construct the first wall, contain the molten salt, act as neutron multipliers, and form any structure that sees a significant neutron fluence. Because of the unique characteristics

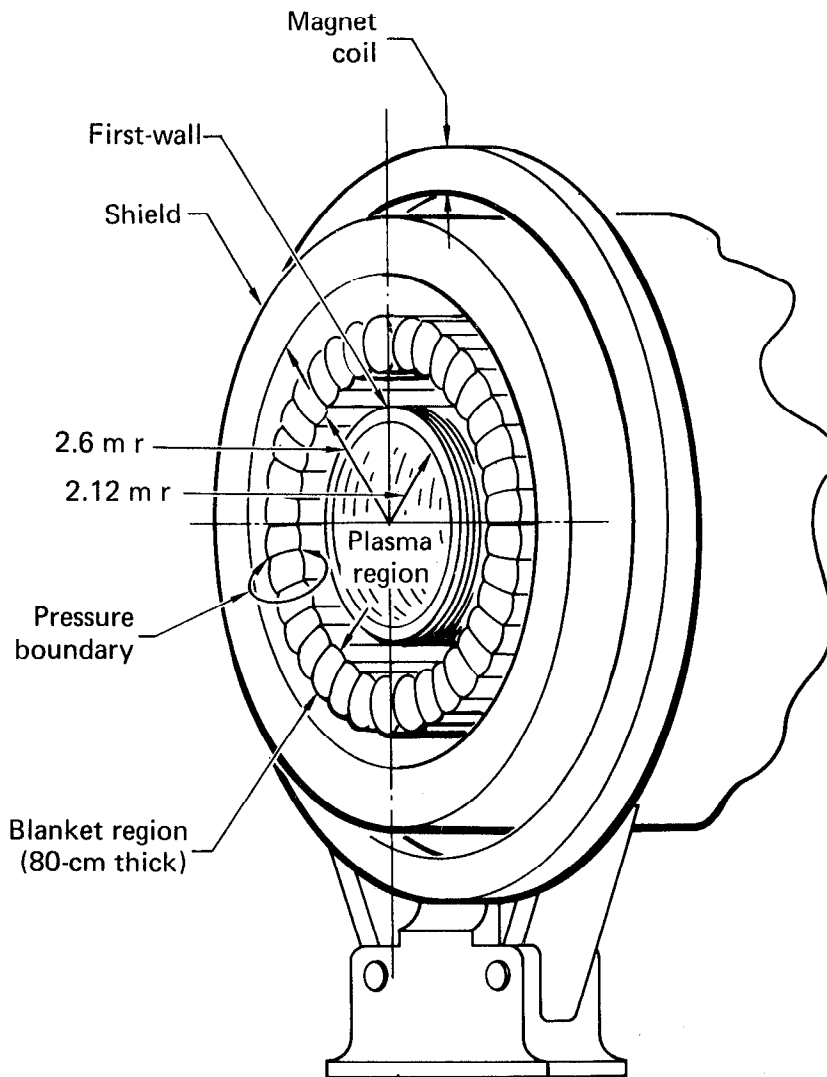


Fig. 7-3. Cross-sectional view of TMHR/molten salt concept (central region).

necessary for each of the above components, it is quite likely that different materials will be used. However, care must be taken to assure that if different materials are used, they are compatible with each other. The factors that should be considered in choosing materials include:

- Mechanical properties: Structural materials should have sufficient strength and ductility at the temperatures of interest after they have been exposed to the expected environment. Possible degradation of these mechanical

properties due to radiation damage, thermal aging, or chemical changes due to interactions with coolants or fission products should be considered.

- Compatibility: The materials should be compatible with structural materials as well as the fuel, cladding, and coolants. The compatibility does not have to be absolute, but any reaction must be sufficiently small to allow functional adequacy. Considerations should also be given to minimize mass transfer, which is quite likely to occur for carbon and nitrogen if large ΔT 's are present for the coolant and if different materials are used in the coolant loop.

- Fabrication and welding technology: Materials should be chosen for which fabrication and welding technology is sufficiently developed. Since the designed reactor is scheduled to be the fifth of the series, allowance for improvement in fabrication and welding technology during the next 30 years can be made.

- Availability and cost: The materials considered should be available in adequate amounts and at reasonable cost in the amounts needed for the fusion reactors. Consideration should be given to the strategic availability of the materials; e.g., if they are commercially mined in the U.S.

- Neutronics: In choosing a specific material, note that some neutrons are lost to parasitic captures in the material. The optimum alloy is the one that introduces the lowest neutron loss and still fulfills other design needs.

- Physical properties: The main physical properties of interest are irradiation induced swelling, thermal expansion, and thermal conductivity. The optimum material is that which had minimum swelling and thermal expansion while the thermal conductivity was quite high. Both swelling and thermal expansion can generate secondary stresses, which are undesirable.

- Tritium permeability: Tritium permeability is important because of the difficulty in cleaning the system of the radioactive tritium. If possible, a material with the lowest tritium permeability should be used.

Table 7-3 provides the material choices and their operating conditions. The rationale for these choices and any possible concerns will be discussed below.

Table 7-3. Material choices for the TMHR/MS.

Structure	Material	Max. Temp. (°C)	Environment
First wall	316SS	425	Helium
Container Vessel	TZM	900	Molten salt
Neutron multiplier	Beryllium	720	Graphite
Multiplier cladding	Graphite	750	Molten salt

First Wall

A unique design feature for the TMHR/MS is a first wall that is expected to stay in place for the whole life of the reactor. This will be accomplished by reducing the temperature during irradiation to levels less damaging and periodically annealing the first wall, removing the radiation damage. The two materials considered for the first wall were the molybdenum alloy TZM (Mo-0.5Ti-0.08Zr) and 316 austenitic stainless steel.

TZM has the advantages of better neutronics and higher strength; however, it has some serious shortcomings. The main disadvantage is that neutron irradiation increases the ductile-to-brittle transition temperature⁵ as shown in Fig. 7-4. This means that at the first wall operating temperature of 425°C, the TZM would be ductile but would become brittle when the reactor was shut down for maintenance. A possible method for alleviating this problem would be to anneal the first wall before shutdown. Another drawback with TZM is that the present day state of fabrication and welding technology needs significant improvements. However, it is reasonable to assume that improvements in those technologies would take place during the next 30 yrs.

Although the neutronics performance of the austenitic stainless steels like 316SS is inferior to that of TZM, the radiation damage at 425°C is less severe. At irradiation temperatures of less than ~500°C radiation causes displacement damage in the stainless steel, which results in increases in strength and decreases in ductility.⁶ At temperatures above ~500°C the displacement type of damage is annealed out and the strength remains at its

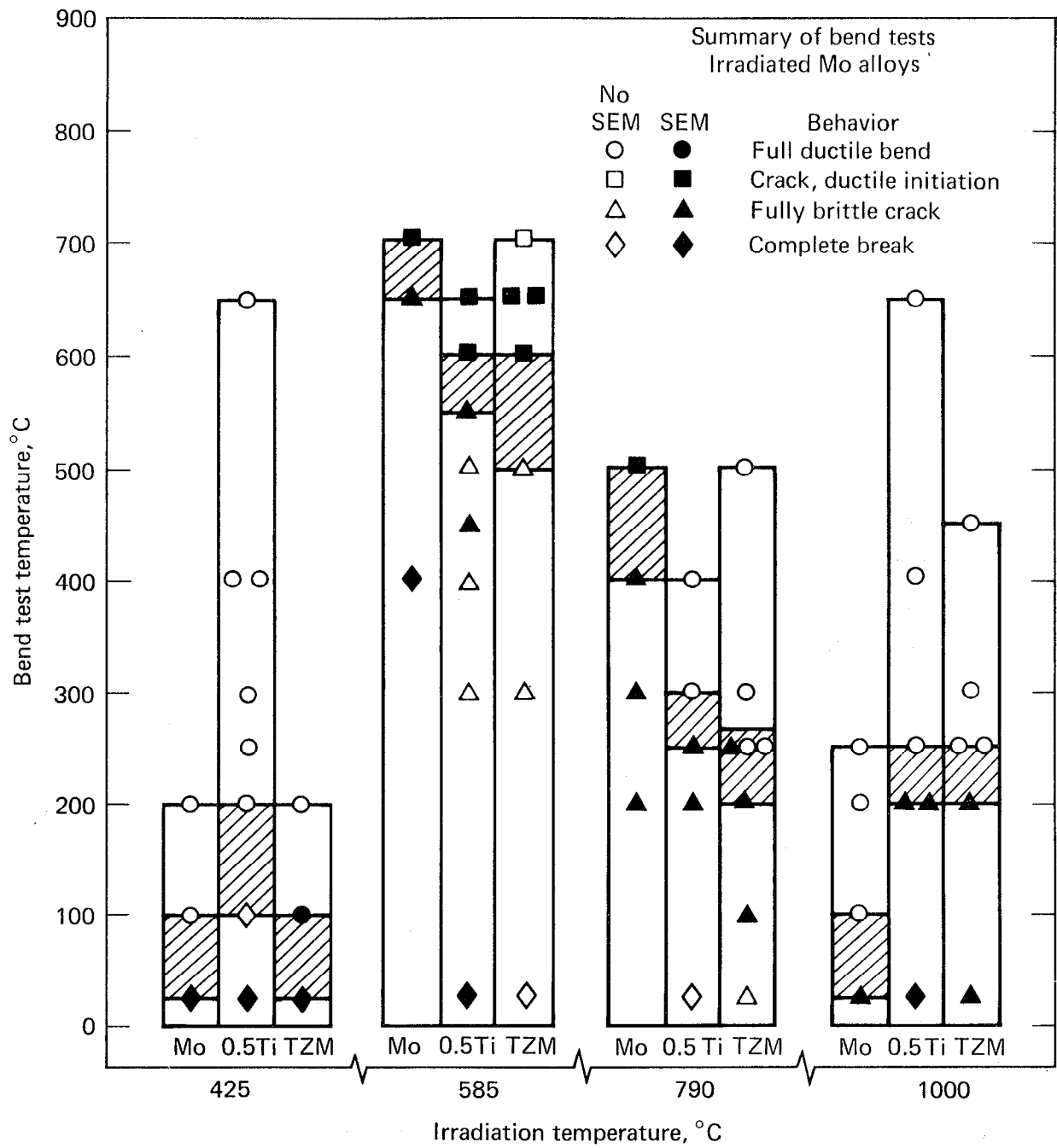


Fig. 7-4. Effect of irradiation temperatures of molybdenum alloys irradiated to $2.5 \times 10^{22} \text{m/cm}^2.5$

preirradiation level. However, at test temperatures above $\sim 500^{\circ}\text{C}$ helium-induced embrittlement starts to operate. Considerable amounts of helium are produced by (n,α) reactions, especially by 14-MeV neutrons in stainless steels. This helium does not play a role at temperatures below $\sim 500^{\circ}\text{C}$, where fracture occurs transgranularly. However, at higher temperatures where intergranular fracture occurs, the helium migrates to grain boundaries and accelerates the intergranular fracture, thereby causing extreme embrittlement. Figure 7-5 illustrates that preirradiation ductility can be restored by annealing if the testing temperature is below 525°C . Thus, the displacement type of radiation damage can be removed, while the helium embrittlement cannot be removed by postirradiation annealing.

Figure 7-6 illustrates the irradiation-induced swelling characteristics of various structural materials. Since the projected irradiation temperature is about 425°C , only minimal swelling is expected in the austenitic stainless steel.^{8,9}

Since the first wall will be separately cooled with flowing helium at about 400°C , compatibility problems between the 316 stainless steel and helium will not occur.

We therefore propose that the vacuum-tight first wall should be made of 316 stainless steel, and it should be periodically (~ 2 years) annealed to restore its preirradiation mechanical properties and ensure its long life.

Blanket Structural Material

To utilize as much of the ORNL experience with molten salts as possible, we considered modified Hastelloy N (Ni-12Mo-7Cr-2Ti) as a structural material since it was used in the Molten Salt Reactor Experiment (MSRE) and proposed for the Molten Salt Breeder Reactor (MSBR).¹⁰ However, the expected fluences in the TMHR/MS are in the order of 4×10^{22} n/cm²/year, while the Hastelloy N vessel in MSBR was expected to receive a fluence of 4×10^{21} n/cm² over its 20-year lifetime. With severe radiation-induced helium embrittlement expected in Hastelloy N at the projected temperatures, we estimated the elongation would be reduced to about 0.2% after two years. Also, the temperatures would exceed 800°C in some locations, and this would exceed the strength

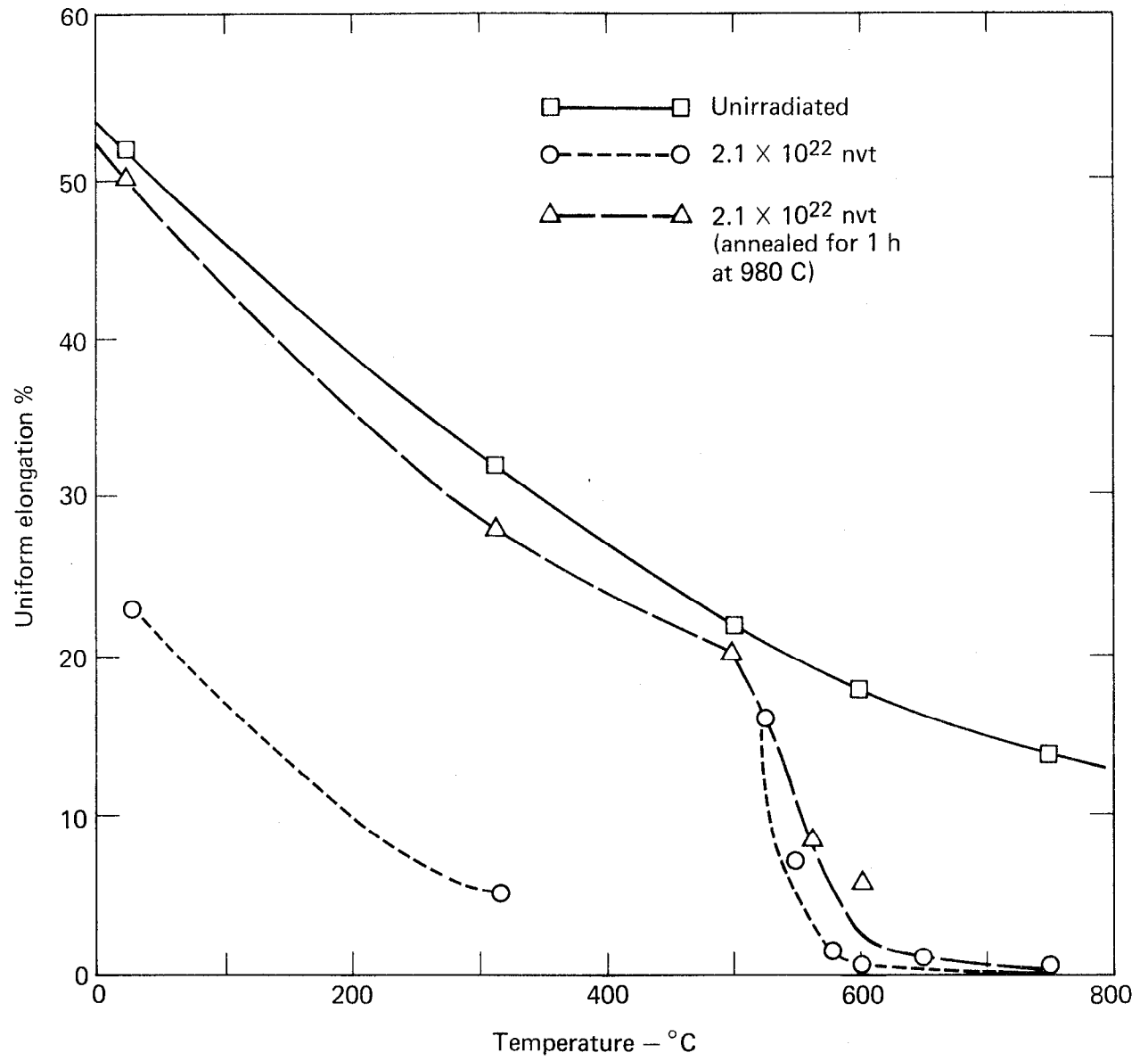


Fig. 7-5. Effect of postirradiation annealing on the ductility of irradiated austenitic stainless steel.⁷

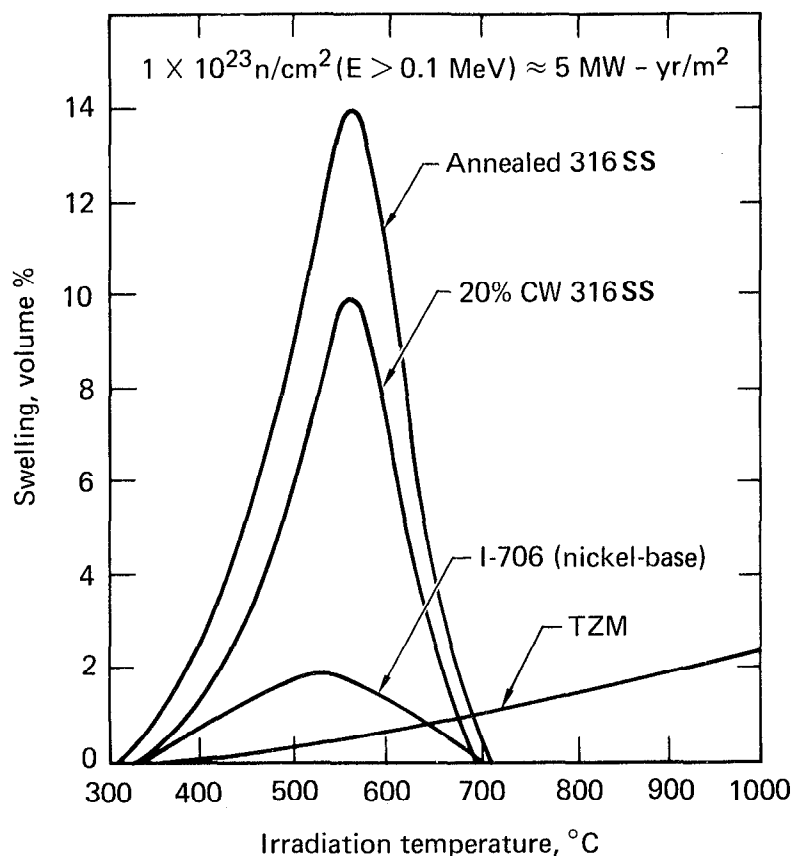


Fig. 7-6. Estimated irradiation induced swelling in different structural alloys.^{8,9}

limits as shown in Fig. 7-7. Stainless steels would even be weaker and would not be resistant to molten salt corrosion at these temperatures. Consequently, TZM and Nb-1Zr were the only available alloys at the expected conditions.

We chose TZM because of its significantly higher strength and better known irradiation performance. Irradiation of TZM results in increases in strength and decreases of ductility due to displacement type of damage, as illustrated in Figs. 7-8 and 7-9.¹¹ The existence of irradiation-induced helium embrittlement in TZM has not been established since only low amounts of helium are produced by (n,α) reactions in TZM, which has been irradiated in a fast neutron environment. Significantly higher amounts of helium will be produced by a flux that contains a high fraction of 14 MeV neutrons. Figure 7-9

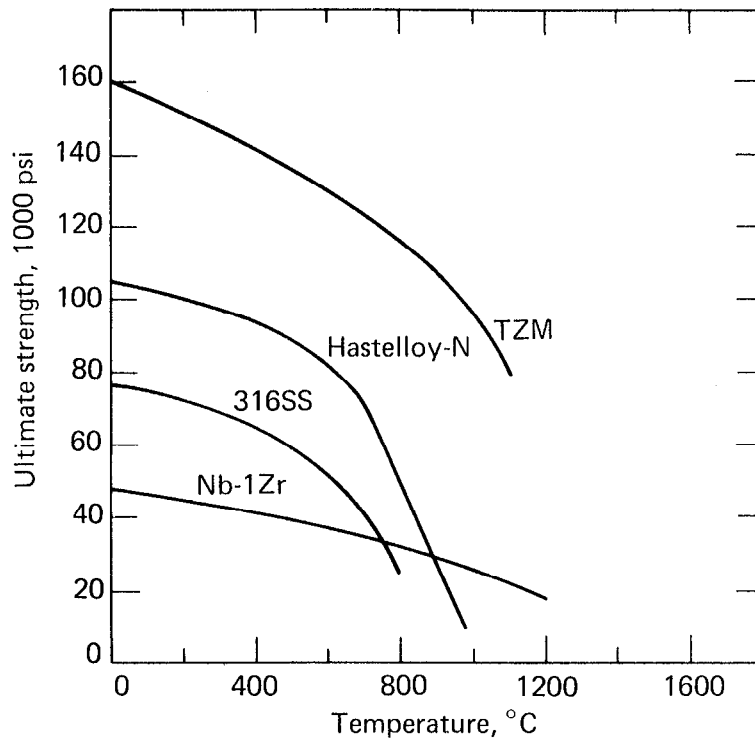


Fig. 7-7. Ultimate strength of selected alloys as a temperature function.

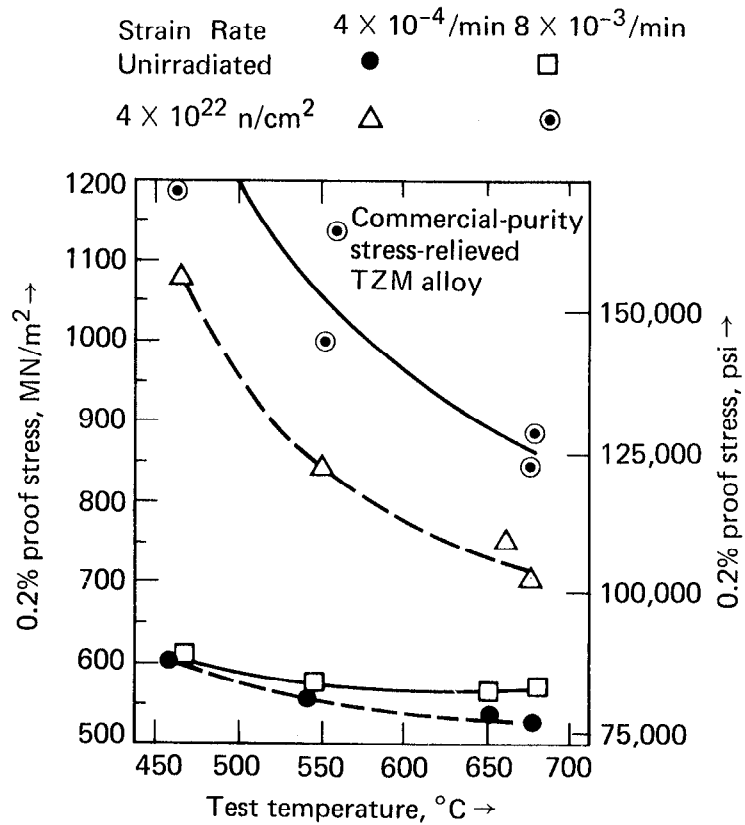


Fig. 7-8. Effect of irradiation temperature on the ultimate strength of TzM.¹¹

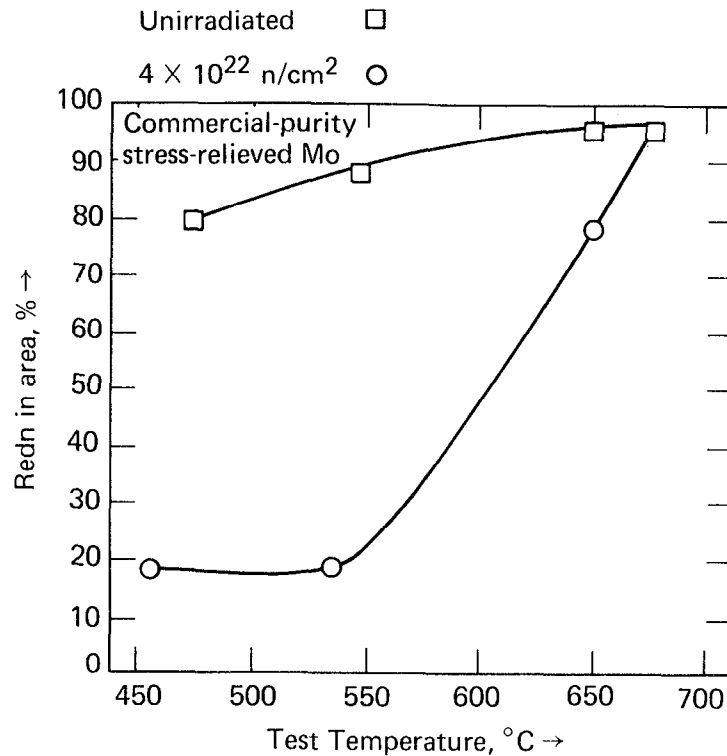


Fig. 7-9. Effect of irradiation temperature on the ductility of Mo.¹¹

illustrates that the loss of ductility caused by displacement type of radiation damage is almost removed at an irradiation temperature of 680°C.

Irradiation-induced swelling has not been thoroughly investigated in TZM. Preliminary studies show that TZM swells about 0.5% when irradiated at 800°C to a fluence of 3×10^{22} n/cm² ($E > 0.1$ MeV).⁹

TZM has been shown to be corrosion-resistant to molten salts at temperatures up to 1100°C. Although TZM appears to be the best choice as a structural material for containing molten salts at 800°C, there are several reservations:

- The fabrication and welding technology has to be significantly developed before the proposed blanket structure can be produced.
- Irradiation performance of TZM is presently available for only 4×10^{22} n/cm², which represents the expected fluence for only one year. Of concern is the effect of the large amounts of helium, which will be generated by 14 MeV neutrons, on the ductility.

- The molten salt may act as a carrier of carbon from the graphite cladding and carburize the TZM, which may deteriorate its properties.

Neutron Multiplier and Cladding

To increase the number of neutrons for breeding purposes, large amounts of beryllium will be placed in the molten salt. Since the beryllium would be rapidly dissolved into the molten salt at operating temperatures, it is necessary to clad the beryllium. Graphite was chosen as the cladding material, and the proposed pin design is shown in Fig. 7-10. Since large amounts of helium are produced in the beryllium during irradiation, the beryllium is expected to swell. Swelling of the beryllium would result in hoop stresses on the graphite. To minimize the hoop stresses on the graphite cladding, we propose

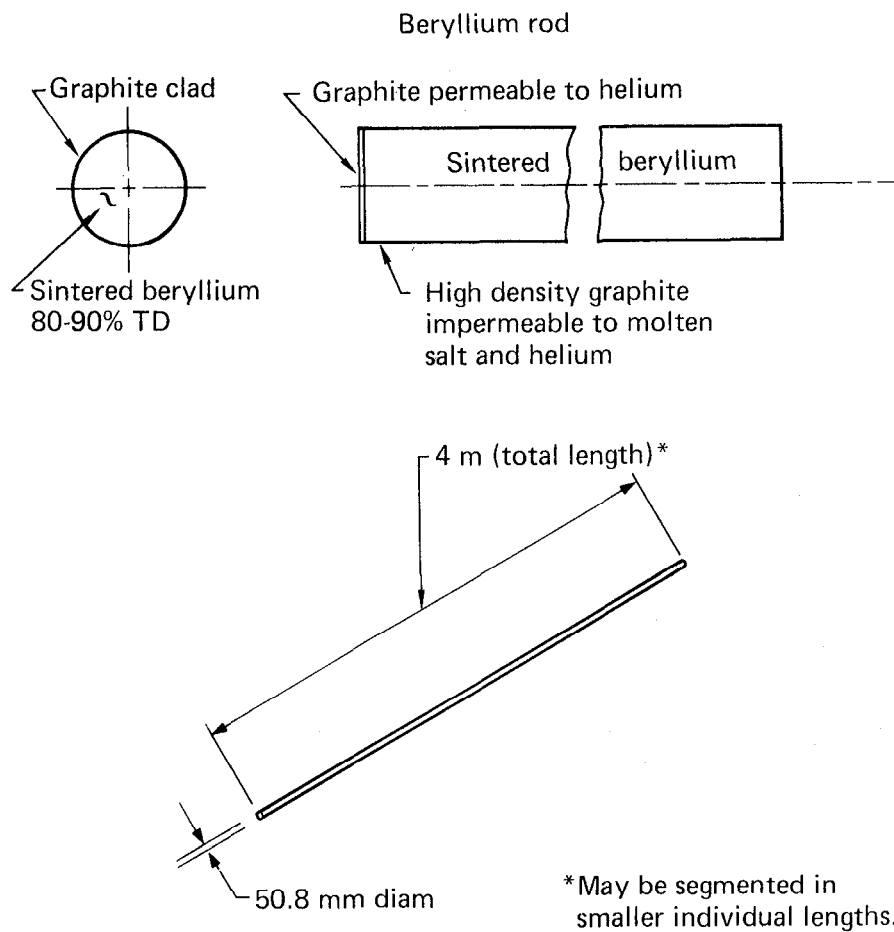


Fig. 7-10. Pin design for graphite-clad beryllium rod.

to vent the helium gas from the beryllium pins. Venting is achieved by using graphite that is permeable to helium but not to molten salt. To assure total release of helium from the beryllium, we propose to sinter the beryllium to 80-90% of theoretical density. Figure 7-11 illustrates the particle size necessary to obtain 100% helium release for a given beryllium temperature.

Graphite was chosen as a cladding material because it is compatible with the molten salt, is neutronically acceptable, and is permeable to helium. The main drawback for using graphite is the irradiation-induced densification at low fluences, which is followed by swelling at higher fluences as shown in Fig. 7-12. Different types of graphite exhibit significantly different swelling behavior. However, the high density graphites do not exhibit significant swelling, as shown in Fig. 7-13. A possible alternate may be the replacement of the graphite clad with a metallic clad (TZM or Nb-1Zr).

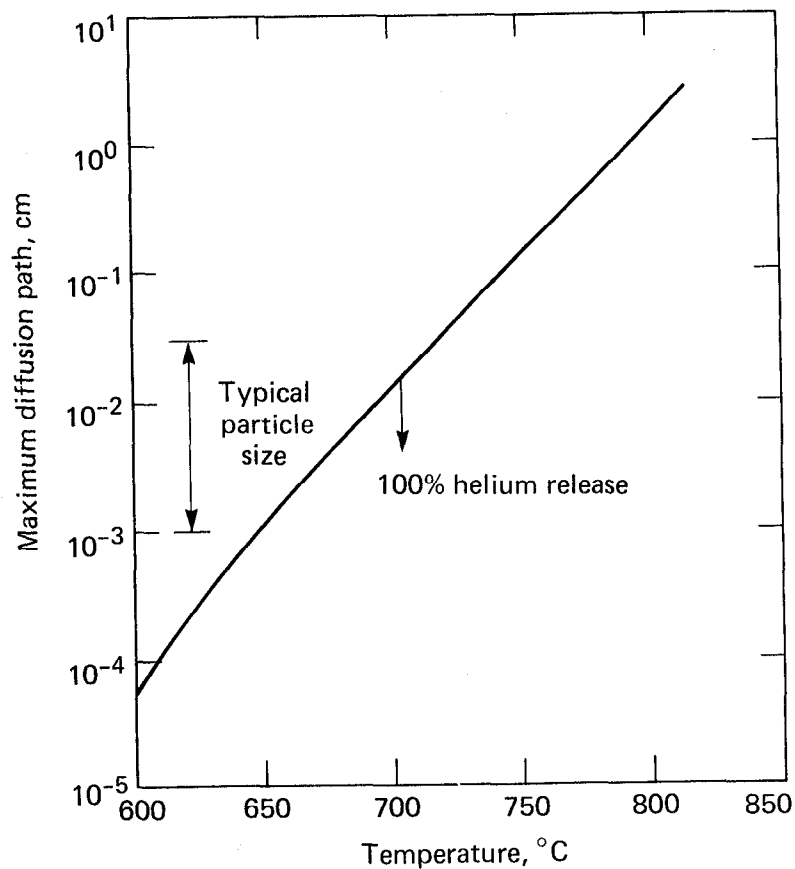


Fig. 7-11. Helium release from beryllium as a function of irradiation temperature.

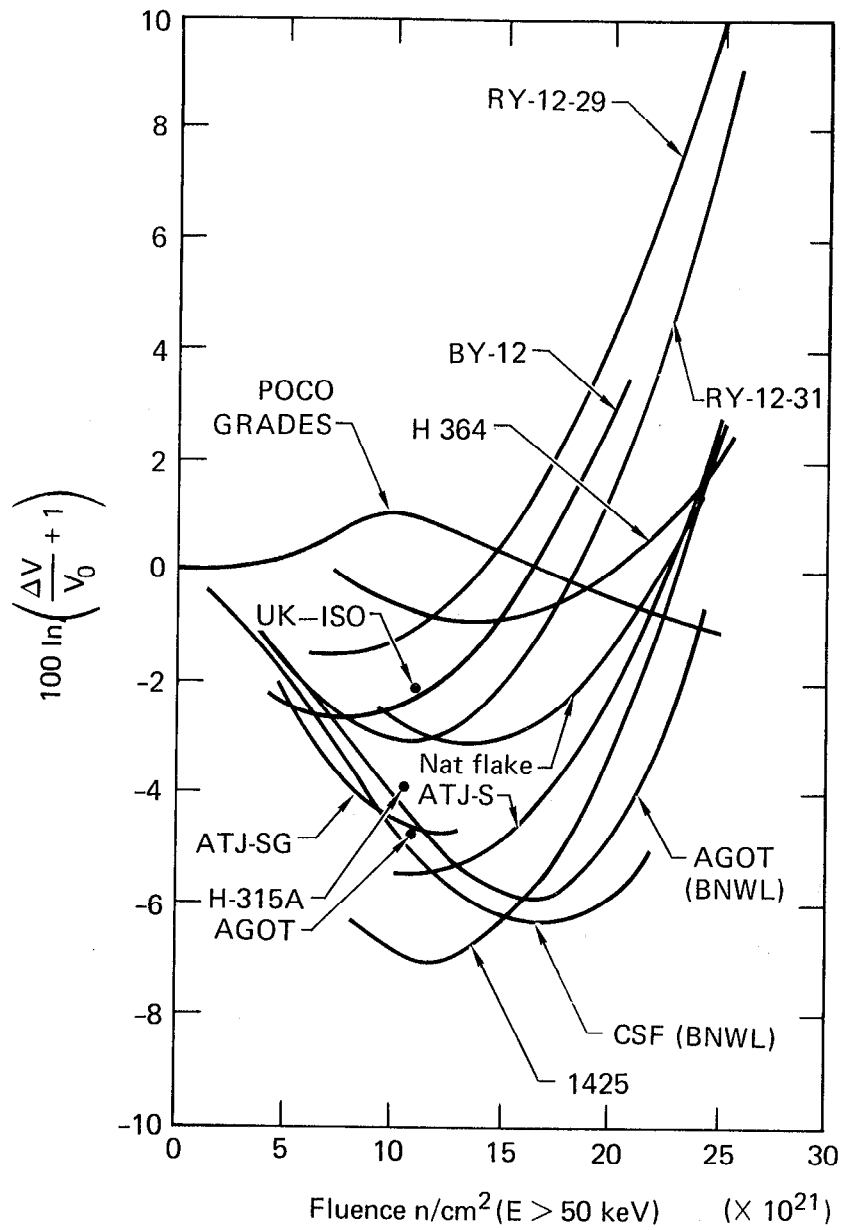


Fig. 7-12. Irradiation-induced volume changes in different grades of graphite; irradiated at 705°C.¹²

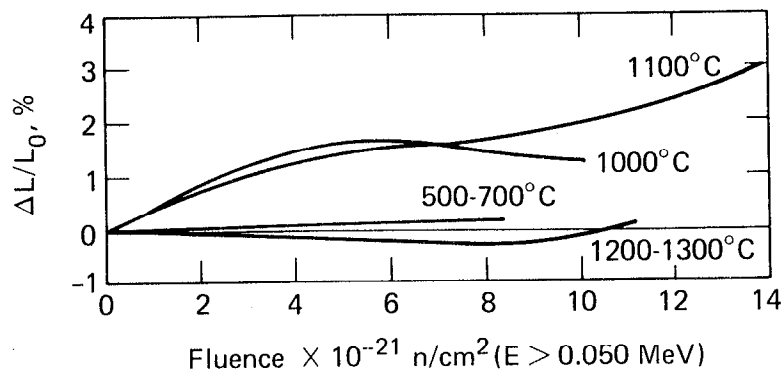


Fig. 7-13. Dimensional changes vs fluence of high-density, five-grained isotropic graphites.¹³

A further concern for using beryllium is the large amounts of beryllium that are needed for each TMHR/MS relative to the present production of beryllium. Beryllium consumption in the U. S. has decreased from 350 tons in 1973 to 70 tons in 1978 due to more stringent Environmental Protection Agency rules and subsequent substitutions by users.^{14,15} We estimate that more than 1000 tons of beryllium would be required for one TMHR/MS. This represents about 15 times the present yearly production. The cost of setting up a beryllium refining plant would be about \$10M for a capacity of 60 tons per year. The known beryllium deposits in the U. S. are also somewhat limited with the identified resources being 80,000 tons, while the economically recoverable reserves (based on processes that yield beryllium at \$16,000/ton) are 28,000 tons.¹⁵ The estimated world identified resources are 400,000 tons.¹⁶ Consequently, the beryllium mining and processing facilities would have to be greatly expanded to furnish enough beryllium for TMHR/MS.

Tritium Permeability

Tritium has an extremely high permeation rate through most alloys, as shown in Fig. 7-14.¹⁷ The exceptions to this are materials that react with tritium to form stable compounds. Molybdenum alloys show significantly lower permeability to tritium than most alloys, with only tungsten and beryllium being better. Therefore, molybdenum-based alloys (e.g., TZM) would be preferred to niobium-based alloys for any tritium handling system.

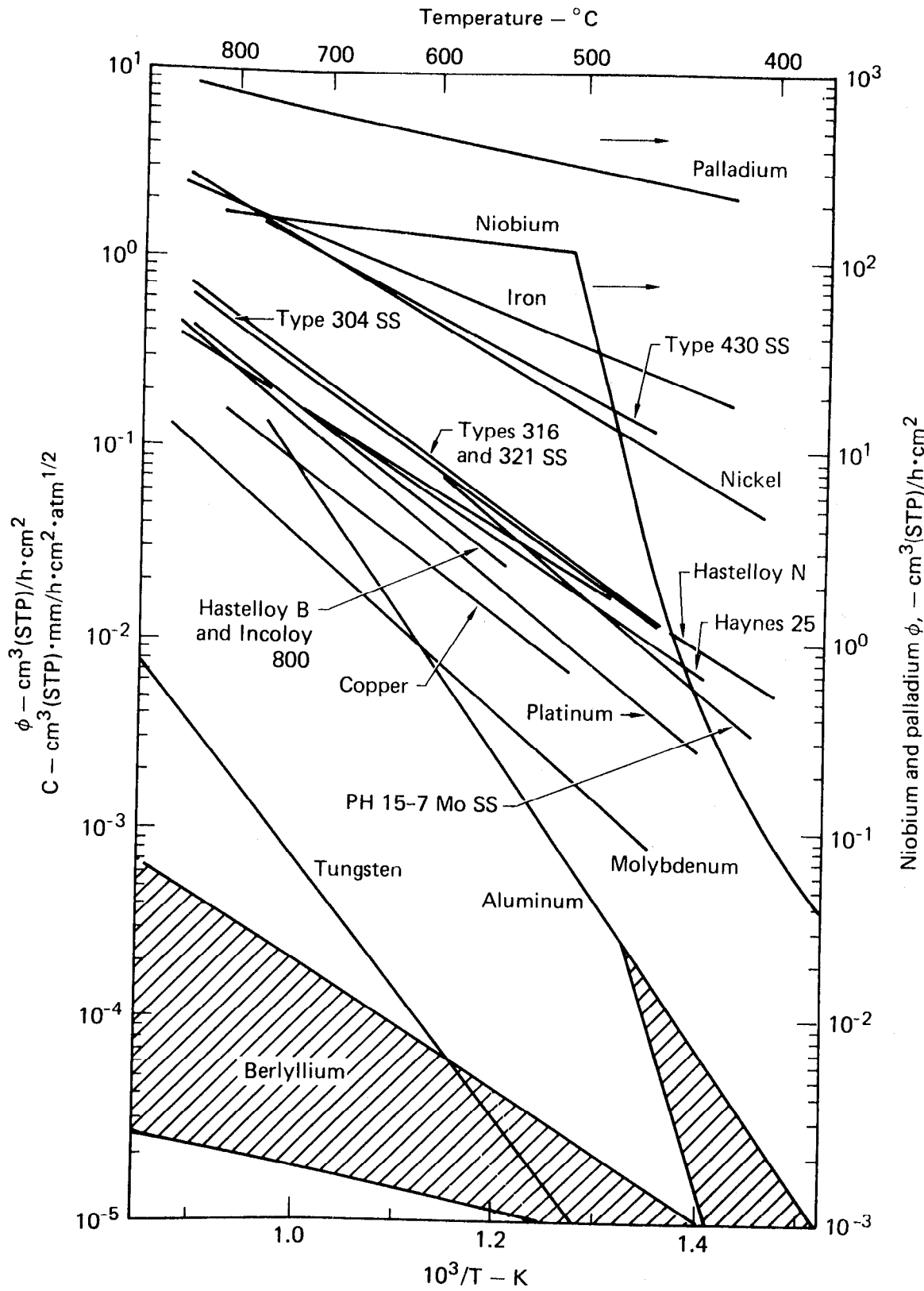


Fig. 7-14. Permeation of tritium through various alloys. ¹⁷

Corrosion Due to MHD Effects

Corrosion is the degradation of a metal by chemical reaction(s) between the metal and its environment. In the TMHR/MS blankets the normal corrosion reactions may be accelerated by MHD-induced voltages that are generated when the molten salt flows across the magnetic field lines. This section further covers the MHD voltage generation phenomenon; Appendix A discusses corrosion effects resulting from these voltages. The main conclusions are:

- MHD-induced voltages can either cause or accelerate galvanic cell-type corrosion reactions.
- Induced voltages of 1 V or less appear to be tolerable.

NEUTRONICS

In the present design concept beryllium is used for neutron multiplication, and a molten salt containing lithium and thorium is used for online removal of bred fusile tritium (T) and fissile (^{233}U) fuels. This subsection describes the results of calculations that examine the sensitivity of the nuclear performance of a Be/MS blanket to parameters representing practical design considerations. Although some deterioration in performance is introduced by these considerations, it appears that this deterioration can be accommodated by the design approach.

Discussion

The preliminary phase of this analysis consisted of performing a quick parametric survey in order to establish an acceptable reference design that could be used to generate information needed for thermal hydraulics and balance-of-plant studies. This reference design represents the initial choice following the parametric survey and does not represent the final design discussed in subsequent subsections. The specifically examined relationships include the effects of: 1) material heterogeneity introduced by the mechanical design, 2) varying the Li-6 enrichment in Li, and 3) a tradeoff between beryllium and molten salt volume fractions. The base case used for these parameter studies consisted of blanket volume fractions (80/10/10 vol% Be/graphite/MS) and a molten salt composition (72/16/12 mole %

LiF/BeF₂/ThF₄).¹⁸ The first wall and pressure boundary were assumed to each have an effective thickness of 3 mm of nickel. A schematic diagram of the geometry corresponding to this base case is shown in Fig. 7-3.

It was required for the reference design that the tritium breeding ratio be slightly greater than 1 to provide for replenishing the fusion plasma. This requirement introduces a need to balance the ²³³U breeding against the tritium breeding to meet the tritium breeding ratio requirement and simultaneously maximize the ²³³U breeding ratio. (A breeding ratio in this context is defined as the number of bred atoms produced per fusion neutron incident on the first wall.) In addition to this requirement thermal hydraulic considerations dictate that the lowest practical limit for the molten salt volume fraction is 0.15. Also, there are design constraints arising from the need to accommodate material strength, thermal hydraulic, magnetohydrodynamic, and chemical considerations.

The calculations were performed in one-dimensional and three-dimensional cylindrical geometry, respectively, with the SNID discrete ordinates computer code¹⁹ and the TARTNP Monte Carlo code.²⁰ The use of two different methods provided a cross-check on the calculational results. Since the values obtained from the two methods are in reasonably close agreement even though different neutron cross section data bases were used, confidence in the results is enhanced.

For the discrete ordinates calculations a 50-group, neutron cross section library based on ENDF/B-IV data was used, and all calculations were performed in the S₄P₁ mode. The Monte Carlo calculations used a 175-group, neutron cross section library based on ENDL data. The analytical model consists of a central plasma region of 2-m radius. This region is surrounded by cylindrical zones representing the first wall, pressure boundary, molten salt blanket, and shield. The molten salt blanket region is assumed to be 80 cm thick, which provides essentially infinite blanket results for all calculations.

The reference case analytical model and calculated performance parameters are shown in Table 7-4. For the SNID calculations a shell source was placed in the interval 159.5 to 160.5 cm, with the angular distribution chosen such that an isotropic 14.06-MeV neutron source was approximated for the plasma region. In the Monte Carlo model the isotropic source was uniformly distributed in the cylindrical plasma volume.

Table 7-4. Analytical model and computed performance parameter values for TMHR molten salt reference design

Region	Region thickness, cm (region radial boundaries measured from plasma center, cm)		Region compositions and volume fractions
1 Plasma	160.50	(0.00 - 160.50)	Plasma
2 Void	49.50	(160.50 - 210.00)	Void
3 First wall	5.08	(210.00 - 215.08)	0.06 Ni, 0.94 void
4 Void	5.08	(215.08 - 220.16)	Void
5 Pressure boundary	5.08	(220.16 - 225.24)	0.06 Ni, 0.94 void
6 Blanket zone 1	2.00	(225.24 - 227.24)	0.65 Be, ^a 0.25 MS, ^b 0.1 graphite
7 Blanket zone 2	19.00	(227.24 - 246.24)	0.65 Be, ^a 0.25 MS, ^b 0.1 graphite
8 Blanket zone 3	19.00	(246.24 - 265.24)	0.65 Be, ^a 0.25 MS, ^b 0.1 graphite
9 Blanket zone 4	19.00	(265.24 - 284.24)	0.65 Be, ^a 0.25 MS, ^b 0.1 graphite
10 Blanket zone 5	19.00	(284.24 - 303.24)	0.65 Be, ^a 0.25 MS, ^b 0.1 graphite
11 Blanket zone 6	2.00	(303.24 - 305.24)	0.65 Be, ^a 0.25 MS, ^b 0.1 graphite
12 Shield liner	10.00	(305.24 - 315.24)	Steel
13 Shield	90.00	(315.24 - 405.24)	Concrete

Performance Parameter Values

²³³ U breeding ratio ^c	= 0.64
Tritium breeding ratio ^c	= 1.08
Total breeding ratio ^d	= 1.72
Energy multiplication ^d	= 1.47

^a 80% theoretical density

^b 72 mole % LiF, 16 mole % BeF₂, 12 mole % ThF₄

^c Defined as the number of atoms produced per fusion neutron incident on the first wall

^d Defined as the ratio of the total energy deposited in the blanket to the total fusion neutron energy incident on the first wall.

The results of the preliminary phase of the analysis are summarized in Tables 7-5 through 7-7. Table 7-5 shows the performance sensitivity to various heterogeneous arrangements of the molten salt and beryllium in the blanket. The heterogeneous arrangements which were treated in this study are illustrated in Fig. 7-15. The study shows the impact of some practical engineering considerations on the blanket concept. The first numerical column in the table gives the absolute values of the parameters for the base case. It is clear from the table that some molten salt is required between the first wall and beryllium zone to absorb the backscattered and moderated neutrons. One also observes little deterioration in performance if only a modest degree of material heterogeneity is introduced.

The results of varying the Li-6 enrichment in the lithium are shown in Table 7-6. Reducing the Li-6 enrichment changes the relationship between ^{233}U and tritium breeding with the net effect of lowering the total breeding ratio. It is noted that decreasing the Li-6 enrichment to 1% is still not sufficient to decrease the neutron capture in lithium such that the tritium breeding ratio is close to 1.0. Table 7-6 also shows an absolute value of 1.8 corresponding to a 1% enrichment. It is also interesting to note that the first wall neutron absorption ratio increases by a factor of 2.54 as the Li-6 enrichment is decreased from natural enrichment (7.5%) to 1%. (The first wall neutron absorption ratio is defined as the ratio of the total number of neutron absorptions in the first wall to the total number of incident 14.06 MeV fusion neutrons.) It is noted that, for the base case, the total number of neutrons of all energies absorbed in the first wall is 10% of the number of incident fast neutrons. It should be made clear that due to neutron multiplication, the total number of neutrons absorbed in the blanket is greater than the number of incident fusion neutrons; and therefore, compared to the total number of blanket neutron absorptions, the number of first wall absorptions is less than 10% of this total. Nevertheless, the impact on blanket performance of first wall parasitic neutron capture is emphasized by this study.

Table 7-7 illustrates the impact of a tradeoff between beryllium and molten salt volume fractions. Starting with the base case molten salt composition and material volume fractions described previously, the molten salt volume fraction was increased to 25%. Table 7-7 also shows a decrease in the total breeding ratio of 9%. However, the ^{233}U breeding ratio increases from 0.36 to 0.64, and the tritium breeding ratio decreases from 1.52 to 1.08,

Table 7-5. TMHR molten salt blanket heterogeneity study

Performance parameter	Performance relative to base case, % ^f				
	Base case ^a	10-cm zones Be 1st ^b	10-cm zones MS 1st ^c	20-cm zones MS 1st, 2cm ^d	20-cm zones MS 1st, 1 cm ^e
²³³ U breeding ratio	0.36	78	100	89	78
Tritium breeding ratio	1.55	95	99	96	103
Total breeding ratio	1.91	92	99	95	98
Energy multiplication	1.56	105	99	99	101

^a Homogeneous model with 80 vol% beryllium, 10 vol% molten salt, and 10 vol% graphite cladding.

All cases use natural lithium.

^b Repeating sequence of: 0.5 cm graphite/8.0 cm Be/0.5 cm graphite/1.0 cm MS.

^c Repeating sequence of: 1.0 cm MS/0.5 cm graphite/8.0 cm Be/0.5 cm graphite.

^d Repeating sequence of: 2.0 cm MS/1.0 cm graphite/16.0 cm Be/1.0 cm graphite.

^e Repeating sequence of: 1.0 cm MS/1.0 cm graphite/16.0 cm Be/1.0 cm graphite.

^f See Fig. 7-15.

Table 7-6. TMHR molten salt blanket Li-6 enrichment study

Performance parameter	Li-6 enrichment → 7.5% Base case ^a	Performance relative to base case, %		
		4%	2%	1%
²³³ U breeding ratio	0.36	111	125	147
Tritium breeding ratio	1.55	95	87	76 ^b
Total breeding ratio	1.91	98	94	90
First-wall neutron absorption ratio	0.10	131	181	254
Energy multiplication	1.56	101	103	104

^a Absolute values (for this study the base case blanket composition was: 80 vol% Be, 10 vol% graphite, 10 vol% MS, natural Li).

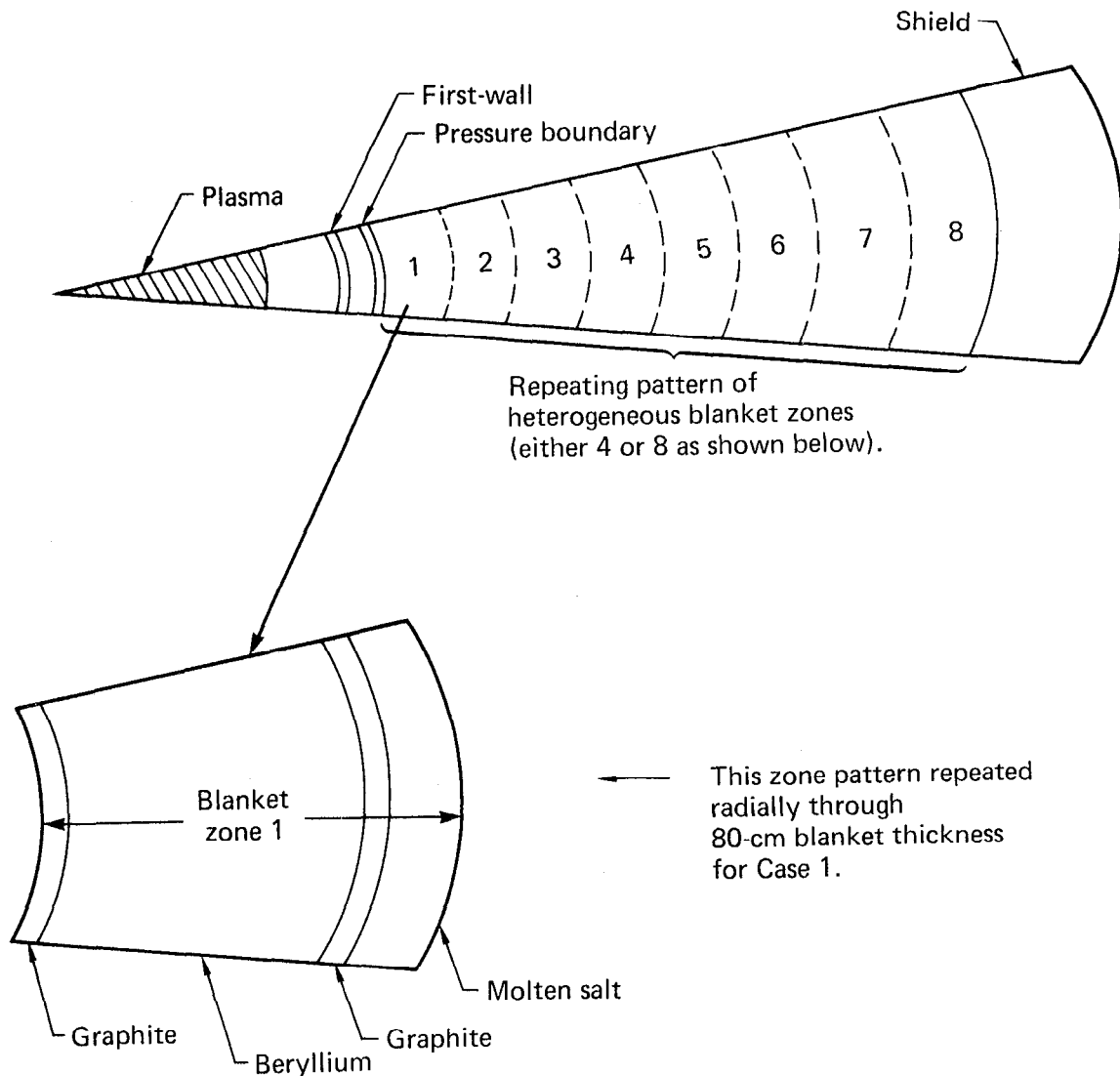
^b Absolute value - 1.18

Table 7-7. TMHR molten salt blanket MS/Be volume % tradeoff study

Performance parameter	MS volume %		
	10 ^a	20	25 ^b
²³³ U breeding ratio	0.36	0.57	0.64
Tritium breeding ratio	1.52	1.21	1.08
Total breeding ratio	1.88	1.78	1.72
Energy multiplication	1.56	1.50	1.47

^a Base case (80 vol% Be, 10 vol% graphite, 10 vol% MS, natural Li).

^b Reference case selected as a result of parameter studies.



Case*	No. Zones	Zone pattern
1	8	0.5 cm graphite/8.0 cm Be/0.5 cm graphite/1.0 cm MS
2	8	1.0 cm MS/0.5 cm graphite/8.0 cm Be/0.5 cm graphite
3	4	2.0 cm MS/1.0 cm graphite/16.0 cm Be/1.0 cm graphite
4	4	1.0 cm MS/1.0 cm graphite/16.0 cm Be/1.0 cm graphite

*See TABLE 7-5.

Fig. 7-15. Schematic diagram of repeating zone geometry for blanket heterogeneity study.

which is in the desired range. Consequently, the reference composition was chosen to be 65/10/25 vol% Be/graphite/MS. The reference design selected as a result of these parameter studies was therefore exactly the same as the base case discussed in the first paragraph of this subsection, except for the difference Be/graphite/MS composition.

Subsequent to the parameter studies that resulted in the reference design already described, some additional parametric effects were examined. These studies were performed to search for further improvements in the blanket neutronic performance. Table 7-8 summarizes the results of these miscellaneous parametric effects. The absolute values of the performance parameters are given for the reference design and the performance of three cases of particular interest are given relative to this design. In the first case the graphite clad (10 vol% of the blanket) was replaced by nickel. A 27% decrease in the total breeding ratio is indicative of the high thermal neutron cross section and consequent parasitic neutron capture in nickel. If nickel (or Hastelloy N) must be used as cladding in the design, it must be limited to small cladding thickness -- as thin as is structurally feasible.

The second case in Table 7-8 illustrates the effect of changing the first wall and pressure boundary composition from nickel to an equivalent thickness of the refractory metal TZM (99.4/0.5/0.1 wt% Mo/Ti/Zr). This modification results in a 5% increase in ^{233}U breeding ratio and a slight increase in the other performance parameters also. Clearly, TZM offers advantages over Ni from a neutronics viewpoint. In addition to TZM another refractory metal was examined although the results are not given in Table 7-8. The case was exactly the same as the one just described, except that niobium was used instead of TZM for the first wall and pressure boundary. The performance parameters for this case showed a few percent improvement over the TZM case, so Nb or Nb-1Zr offer good alternatives to TZM as far as neutronics performance is concerned.

The use of refractory metals for structural materials in the blanket introduces the possibility of using a molten salt composition having a higher operating temperature. Therefore, a case was studied that used the alternate salt composition shown in Table 7-8.¹⁸ The superior neutronic performance of this salt compared to our current reference is clearly evident. A 75/10/15 vol% Be/graphite/MS blanket composition was used.

Table 7-8. TMHR molten salt blanket miscellaneous parametric studies

Performance parameter	Reference ^a Design		Performance relative to reference design, %		
	Perturbed case	→	C → Ni clad	Ni → TZM FW and PB	Alternate ^c MS
	d	e	d	e	e
²³³ U breeding ratio	0.64	(.76)	89	105	129
Tritium breeding ratio	1.08	(1.01)	70	101	96
Total breeding ratio	1.72	(1.77)	73	103	110
Energy multiplication	1.47	(1.44)	103	107	110

^a Absolute values for reference design.

^b Nickel replaced by TZM in first wall and pressure boundary.

^c Composition, salt $\left. \begin{array}{l} 71 \text{ mole \% LiF} \\ 2 \text{ mole \% BeF}_2 \\ 27 \text{ mole \% ThF}_4 \end{array} \right\} \begin{array}{l} 75/10/15 \text{ vol\% Be/C/MS} \\ \text{blanket composition} \end{array}$

used TZM first wall and pressure boundary.

^d SN1D calculation.

^e TARTNP calculation.

Conclusions

The parameter studies described in this subsection have provided some general design guidelines. The primary conclusions are summarized as follows:

- Blanket heterogeneity study: It is desirable that some molten salt be present between the first wall and the beryllium zone to absorb the back-scattered and moderated neutrons. Also, little degradation in performance is caused if only a modest degree of material heterogeneity is introduced.

- Li-6 enrichment study: Reduction of the Li-6 enrichment in order to increase the ²³³U breeding ratio decreases the total breeding ratio due to increased neutron absorption in the first wall and other structural material. Therefore, a penalty against the blanket neutron economy is introduced by this approach.

- Be/MS volume fraction tradeoff study: The MS volume fraction can be adjusted to provide the tritium breeding ratio goal. However, there is a penalty associated with reducing the amount of Be and hence the neutron multiplication.

- Miscellaneous parametric studies: TZM or Nb-1Zr offers a significant neutronic advantage over nickel alloys for use as a blanket internal structure. This is due to the relatively high thermal neutron absorption cross section of nickel and the high temperature strength properties of these refractory metals. The refractory metals TZM and Nb-1Zr also offer some advantage over nickel or steel for use in the first wall and pressure boundary.

It was also found that a blanket design that changes the molten salt composition to 71/2/27 mole % LiF/BeF₂/ThF₄ provides a marked improvement in performance compared to the base case 72/16/12 mole % composition.

In general, designs that contain larger amounts of beryllium exhibit enhanced breeding characteristics.

It is clear from these neutronics studies that some deterioration in blanket performance occurs as practical design and engineering considerations are introduced into the Be/MS blanket concept. However, it is encouraging to observe that the analysis indicates that this degradation in performance can be limited to acceptable values with proper design approaches.

MECHANICAL DESIGN

This report states (in Sec. 6) the philosophy that the TMHR design should permit refueling and normal maintenance without disassembly and removal of central region structures. The molten salt concept inherently agrees with this philosophy through its feature of online refueling by salt circulation. The design concept presented herein furthers this philosophy by:

- Including a method for opening the central region structures to provide access for maintenance.

- Allowing the first wall to remain intact when the other structures are opened.

To provide these design features the first wall is a structure separate from the blanket region and is separately cooled. Both separations lessen the severity of the first wall operating conditions and thereby extend its operational lifetime.

Design Input

The fusion reactor imposes design requirements on the components of the central region. To these are added the design conditions determined by preliminary thermal hydraulic and blanket neutronics analyses. Table 7-9 contains the design input used in the preparation of the conceptual design for the molten salt TMHR.

Table 7-9. Input to mechanical design

First wall:

Minimum diameter, m	4.2
Neutron energy loading (14 MeV neutrons, Mw/m ²)	2
Coolant	Helium
Coolant design conditions, °C	430 (58 atm)

Blanket region:

Blanket composition (not including structure) in volume fractions:	
Beryllium (80 to 90% dense)	0.65
Molten salt	0.25
Graphite	0.10
Boundary structure design conditions, °C	800 (13.5 atm)
Primary flow direction of molten salt	Parallel to reactor axis

Primary shield

Material	High density concrete
Thickness, m	1
Design temperature, °C	80

Solenoid magnet coils

Number of separate coils	As required
Spacing	Uniform
Diameter	Uniform
Minimum axial coverage, %	20

Conceptual Design Description

A conceptual design for the central region of a TMHR using molten salt as coolant is shown in the oblique view of Fig. 7-16. The view pictures only a small portion (approximately 20%) of the total length of the central region. Subsequent paragraphs provide a general description of the concept and descriptive information about the major components of the central region. The descriptions are of mechanical design and configuration.

Overall General Description. The central region comprises several layers of horizontal and concentric cylindrical structures that encircle the fusion plasma. From inside out the principal structural layers are the first wall, the blanket region, the primary shield, and the solenoid coils. The first wall is separate from the blanket region and is separately cooled with helium. It is also the vacuum boundary for the plasma region.

The blanket region is made from connected segments of cylinders whose axes are parallel to the axis of the central region. The cylindrical segments are arranged in semicircles around the first wall. Within the segments the molten salt flows through bundles of graphite-clad beryllium rods. The blanket structures and internals are supported by the shield, as are the magnet coils that encircle the shield.

As Fig. 7-16 shows, the design concept includes a method for opening the shield for maintenance access to the blanket region and first wall. The shield and blanket are sectioned along the axis of the central region. Halves of each section are on pivoted supports, which allow lowering of the halves after axial displacement of magnet coils.

The central region is 88-m (289 ft) long. The outer diameter of the primary shield is 11 m (36 ft).

First Wall. Because the first wall is the vacuum boundary and is separate from the blanket region, it must have sufficient strength to prevent buckling and must be separately cooled. In the concept shown in Fig. 7-16 the first wall is constructed from tubular rings. The tubular cross section of each ring provides both a coolant flow passage and the necessary moment of inertia to withstand the external pressure load.

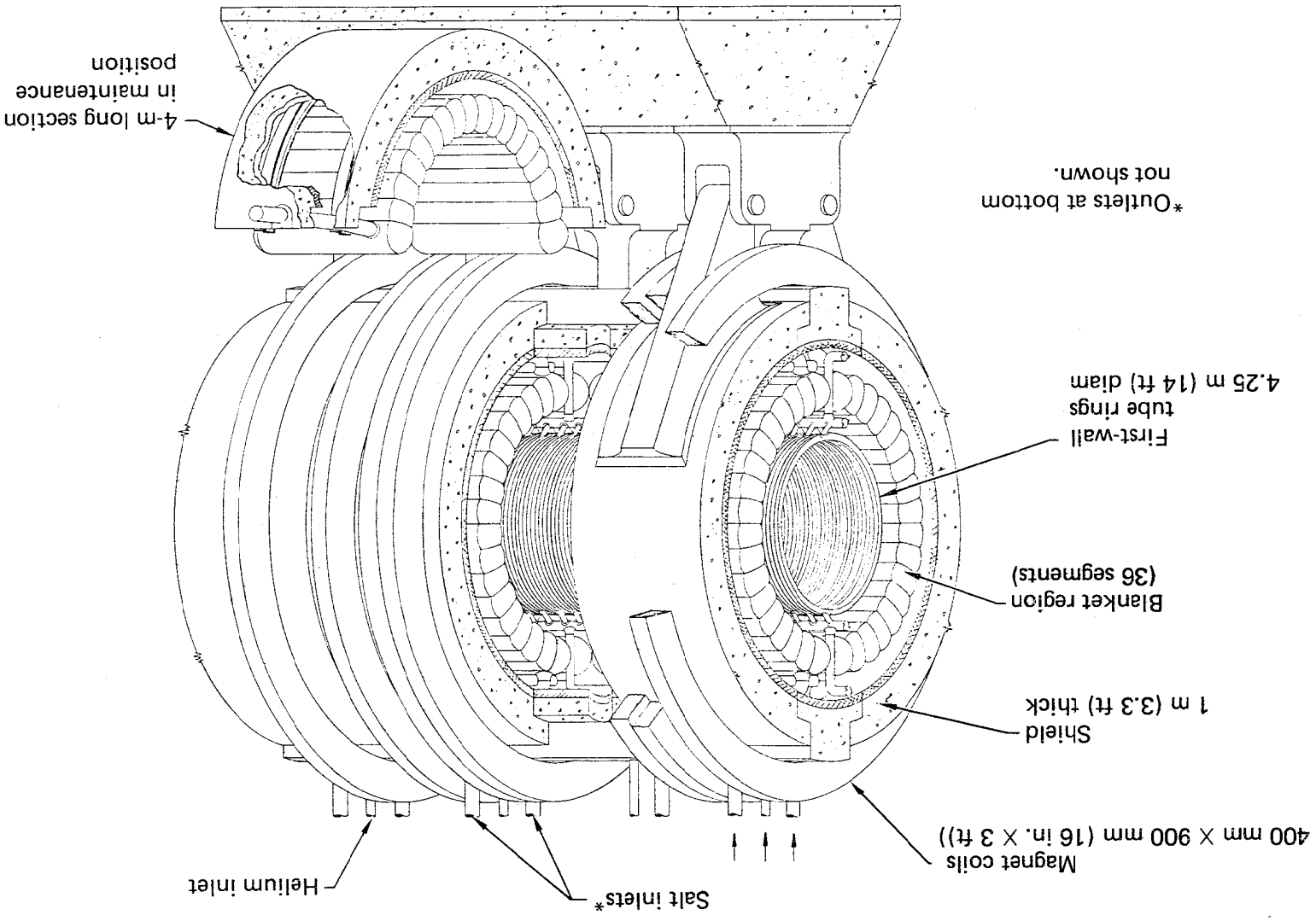


Fig. 7-16. Portion of TMHR central region - molten salt concept.

The first wall is made continuous along the reactor axis by horizontally stacking the rings and welding one to the other with circular strips at their outside surfaces.* Each tubular ring has a coolant inlet at the top and a coolant outlet at the bottom. The inlets and outlets are manifolded inside the blanket region. Pipes from the manifolds pass between the ends of the blanket segments and penetrate the shield between magnet coils. The manifolds and pipes that penetrate the movable parts of the shield provide support for the first wall.

A more detailed design of the first wall would include special circumferential joints spaced at about 2 m along the axis of the central region. The special joints would allow the first wall to be cut without cutting a coolant tube. Cutting two joints (and some piping) would make it possible to remove and repair or replace a section of the first wall, if such procedures were ever necessary. The special joints might be designed to also function as expansion joints for the first wall.

Table 7-10 summarizes descriptive data for the first wall. Dimensional data are given for tubes made of the molybdenum alloy, TZM, and of type 316 stainless steel. The TZM is the preferable material for neutronics performance and strength reasons but is difficult to seal weld and becomes brittle at the first wall operating temperature. Currently, therefore, the first wall is assumed to be constructed of stainless steel.

Blanket Region. The configuration of cylindrical segments for the blanket region shown in Fig. 7-16 results from application of several criteria for optimizing the design:

1. Minimize structure that will introduce parasitic neutron capture in the blanket.
2. Minimize potential neutron leakage paths.
3. Direct the molten salt flow parallel to the reactor axis wherever possible so that the corrosion and hydrodynamic effects caused by the magnetic field are minimized.

* A first wall made from layers of tubular rings was first proposed for a steam-cooled TMHR concept called the Oblong Tube Concept. A picture of the tubular rings and their connecting strips is on Fig. 5D-4.2

Table 7-10. Descriptive data - first wall

<u>Structure</u> - Consecutive tubular rings welded together with circular strips.		
Overall length, m (ft)	88 (289)	
Centerline diameter of rings, m (ft)	4.25 (14)	
Material	TZM	316SS
Number of rings	1386	1156
Outside thickness of tubes, mm (in)	65 (2.5)	76 (3)
Thickness of tubes, mm (in)	1.5 (0.06)	2 (0.08)

4. Provide for capability to drain the molten salt.
5. Provide the capability to repair or replace blanket region components.

The natural inclination in designing to meet this criteria would be to make the blanket structure from large concentric cylinders around the first wall. In that type design, however, the innermost cylinder is subjected to a significant molten salt pressure as an external pressure. Calculations show that a 4.8-m-diam TZM cylinder supported by rings and at 1-m intervals would require a thickness of 20 to 25 mm for a pressure in range of 13.5 atm. That thickness is excessive for criterion 1; for the ring supports at 1-m intervals hinder compliance with criterion 3; and with a separate first wall criterion 5 cannot be met.

Similar designs with a corrugated inner cylinder were also investigated. Marked reductions in pressure boundary thickness were obtained, but the total structure fraction was still too much, and the inability to meet criteria 3 and 5 remained.

The structure of the blanket region must contain the molten salt and is thus a boundary. Shells of revolution are the thinnest pressure containers, and cylinders are the shells most adaptable to the TMHR central region. The

concept shown in Fig. 7-16 was founded on this logic applied to the five previous criteria.

The pressure boundary of the pictured blanket region comprises semicircular arrays of 18 cylindrical segments. Adjacent segments are connected for their entire length between end caps. Bulkhead type plates span between the connection lines of the segments. Although not intended to illustrate the structure, Fig. 7-17 may help in understanding this description. Cylindrical segments are used to reduce the number of gaps in the blanket to meet criterion 2. Gaps do exist, however, at the top and bottom between the two semicircular arrays and at the ends of the 4-m-long segments.

Table 7-11 gives dimensional data for the cylindrical segments. The plates which separate the segments have been calculated to be 6.5 mm (0.25 in) thick when constructed of TZM. The molybdenum alloy is used for the entire blanket region because its high strength at high temperature minimizes structural thicknesses.

Within each cylindrical segment are 166 graphite-clad beryllium rods. The rods are 50.8 mm (2 in.) in diam and are spaced on a 55.9-mm (2.2 in.) triangular pitch.

Figures 7-16 and 7-17 show the molten salt entrances to the blanket region at the top. Flow is downward, but it makes 18 horizontal passes about 4 m long in its travel through the blanket region to the bottom. From top to bottom of each semicircle of segments, the salt flow reverses direction at each successive segment. It enters one end of each cylindrical segment, flows through the contained bundle of graphite-clad beryllium rods, and exits the other end of that segment into the next one. The described flow pattern is shown in Fig. 7-17. Also shown in that figure is flow crossing at the ends of the segments. The crossing flow paths provide for mixing, which prevents thermal stratification. The method for forcing the flow to mix has not yet been designed.

We chose the top-to-bottom molten salt flow direction in the blanket because it coincided with draining flow. To aid in the purging of gases from the blanket, however, flow from bottom-to-top would be better. The concept can accommodate either flow direction.

The blanket and its contents are supported on strongbacks (curved beams) between the blanket region and shield. Each semicircle of cylindrical segments has two strongbacks for each 4-m-long section. The strongbacks are supported on the primary shield.

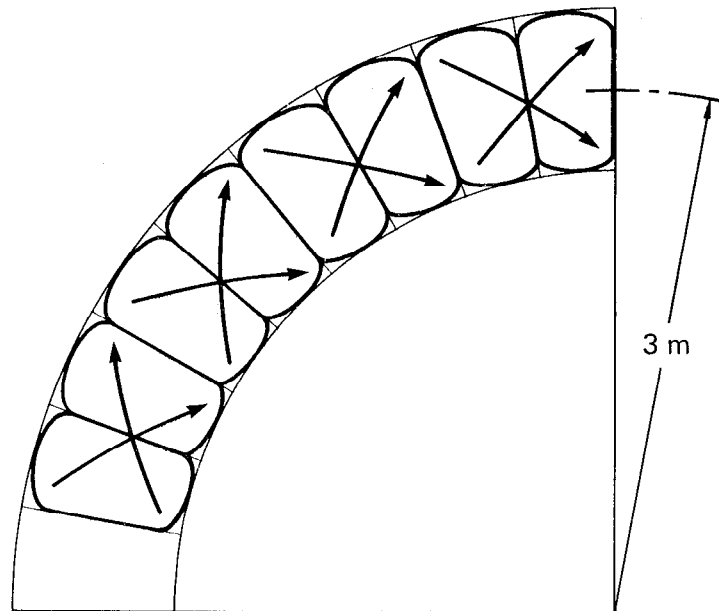
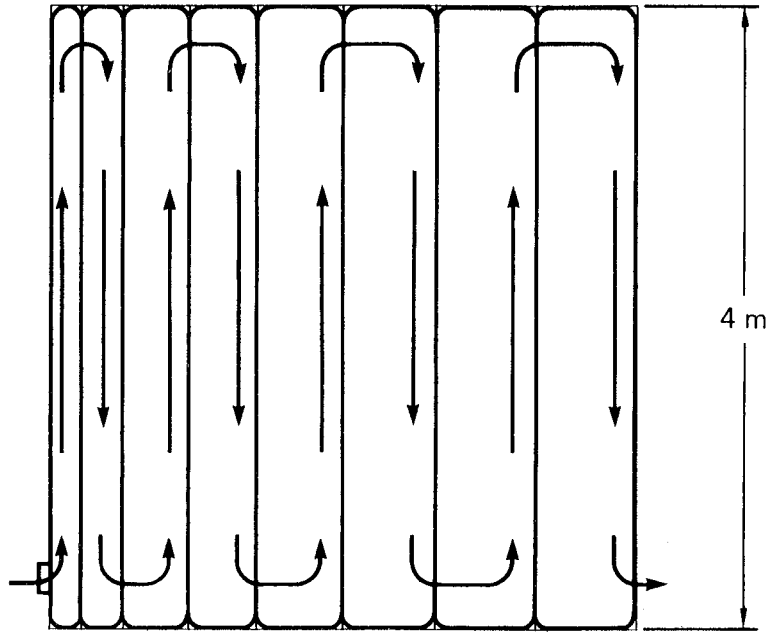


Fig. 7-17. Molten salt flow pattern in blanket segments.

Table 7-11. Descriptive data - blanket pressure boundary.

Structure - Cylindrical segments arrayed in semicircles.

Segments:

Length, m (ft)	4 (13)
Diameter, mm (in)	914 (36)
Average width, mm (in)	533 (21)
Wall thickness, mm (in)	2.5 (0.1)
Material	TZM
Number/semicircle	18
Total number	792
Semicircle radius to segment centerline, m (in)	3 (10)

Primary Shield. The primary shield is conceived to be a steel-encased, reinforced, gas-cooled, high-density concrete structure with a thick layer of insulation on its inside surface to protect it from the high temperature environment of the blanket region. During reactor operation, the shield is a closed cylinder, but the cylinder is made from 46 separable parts; 44 half sections of the cylinder, each 4-m long and two girders that run the length of the central region. The girders are at the top and bottom of the shield.

Primary support for the shield is at the bottom. As Fig. 7-16 shows, each of the half sections is mounted on a large pivot on its side of the centerline. The pivots provide the means for opening up the shield for maintenance. The top and bottom girders are stationary, and they provide the structure to which the cylinder halves can be locked in place during operation. Figure 7-16 does not include lateral support structure outside the shield. Supports extending from the shield to adjacent building structure are expected to be necessary to withstand seismic loads.

The inner diameter of the shield is 9 m, and its nominal thickness is 1 m. Each of the 4-m-long half sections of shield and blanket is estimated to weigh about 350 metric tons, including its structure to the pivot.

Solenoid Magnet Coils. The magnet coils shown in Fig. 7-16 are 400 mm (16 in.) wide, 900 mm (36 in.) deep, and are spaced at 2 m (78.7 in.), center-

to-center. The width and spacing dimensions give an axial coverage of 20.3%. Forty-four coils with an inner diameter of 12.2 m (40 ft.) are required.

Maintenance Access

The environmental conditions to which the blanket region is exposed in the molten salt concept create uncertainty about the operating life of the blanket constituents. The conceptual design therefore shows a method for opening the shield to gain access to the blanket region. Other methods should be investigated and compared.

To open a half section of the shield and attached blanket structures, it is necessary to move two magnet coils. The two coils are moved axially, one in each direction, to positions over the next adjacent sections of the shield. Each coil is moved about 1.5 m to clear the 4-m-long section to be lowered. It is not known whether or not magnet leads and magnet coolant conduits need be disconnected for this motion. The inlet and outlet pipes for the molten salt will have to be cut, however, and external seismic support structures (not shown on Fig. 7-16) must be disassembled.

From a lowered half section an entire semicircle of blanket segments can be removed by lifting attachment to the four ends of the two strongbacks. When emptied of salt, one semicircle of segments weighs approximately 53 metric tons.

Prior to the "opening up" operations to acquire maintenance access, molten salt must be drained from the blanket. Consideration of this fact brings to attention other items which must be factored into the design:

- Salt drainage from the blanket will sometimes be required at times other than when opening the central region for maintenance.
- Drained molten salt must be stored. Storage facilities must be heated to keep the salt liquid.
- The drained blanket will be refilled. The design must include capability to preheat the blanket region structures prior to refilling. (The design must also consider the preheating and filling problems of preoperational testing and initial startup.)

Opening the shield and blanket also gives access to the first wall for unplanned repair maintenance. The previous description of the first wall noted that a more detailed design would include special circumferential joints

at 2-m intervals. With a 4-m shield and blanket section open, a 2-m-long section of the first wall could be cut and removed. Removal of a section of the first wall gives some potential to the possibility of removing and replacing a magnet coil. Replacing a whole circle coil could not be done without the added difficulty of separating the top and bottom girders of the primary shield, but such separation might be made feasible if anticipated in the design.

The uncertainties in the design life of the blanket structural material were previously discussed in this section. Because those uncertainties exist, consideration must be given to a design that has planned replacement of blanket structures every few years; although such consideration disagrees with the philosophy of long-lived structures. The operations for periodic molten salt blanket structure changeout are analogous to the refueling operations for the pool concept briefly discussed in Sec. 5.² A refueling time study² performed for several water and steam-cooled concepts showed the pool concept to have the shortest refueling time of those compared. The operation for opening and closing the molten salt concept will take longer than the refueling operations of the pool concept, but the intervals between operations should also be longer. The longer operating intervals may compensate for the longer shutdowns. If so, reactor availability should be comparable.

Alternate Concept

Figure 7-18 shows an alternate and similar concept for the molten salt TMHR. Plan B in that figure pictures a method of access in which the shield and blanket halves are rolled out horizontally instead of pivoted. After rolling a half section out, the top quarter of the shield is lifted to give access for lifting the blanket semicircle. The blanket structural arrangement shown was less acceptable because of the difficulties of draining the uppermost vessels and of fabricating end heads that would fit the shape of the vessels.

Cost Estimate

The central region of the molten salt TMHR concept is estimated to cost $\$2.3 \times 10^6$ per m. This cost does not include:

7-41

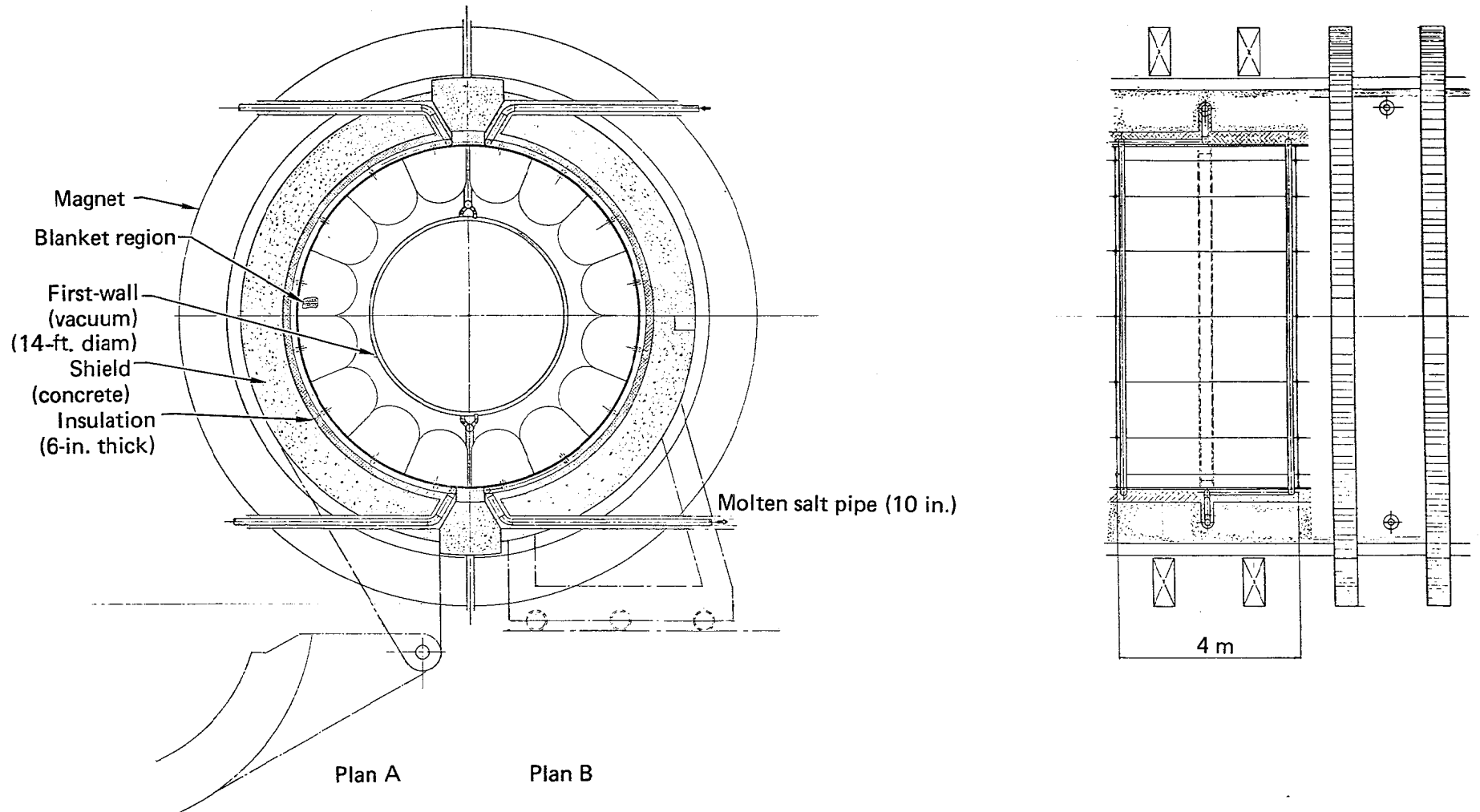


Fig. 7-18. Alternate concept - TMHR/molten salt central region.

- Blanket internals (molten salt, beryllium, and graphite).
- Magnet coils, coil restraints, and coil services.
- Blanket maintenance equipment.
- Spare blanket sections.
- Instrumentation.
- Piping beyond the shield.
- Building structures and foundations.

The estimate includes the structural components of the central region out to the outside of the shield and the support structures for the central region. The components and structures are itemized and priced in Table 7-12.

Table 7-12. Central region cost estimates.

Quantity per m of axial length	\$/m
<u>First wall:</u>	
850-kg type SS-316 tubes and manifolds @ \$41/kg	11,900
350 m of seal welding and seal weld inspection @ \$4/m	1,400
<u>Blanket region:</u>	
3,000 kg TZM pressure boundary components @ \$190/kg	570,000
1,500 kg TZM structural parts @ \$169/kg	253,500
<u>Shield:</u>	
940 kg thermal insulation @ \$5/kg	4,700
110,000 kg high density concrete @ \$0.15/kg	16,500
Reinforcing steel @ \$0.40/kg of concrete	44,000
5,500 kg SS-316 cooling coils @ \$16/kg	88,000
6,000 kg SS-316 liner plate @ \$20/kg	120,000
400 kg SS-316 anchors and penetrations @ \$25/kg	10,000
<u>Support structures:</u>	
36,000 kg SS-316 bottom support structure @ \$20/kg	720,000
18,000 kg SS-316 lateral support structure @ \$25/kg	450,000
Miscellaneous hardware for latching, locking, sealing, etc.	<u>10,000</u>
TOTAL	2,300,000

The items listed are consistent with those included for previous cost estimates on steam and water-cooled concepts,² but the unit costs are not. The unit costs in this estimate come from the same source as those used in Sec. 6 to estimate the cost of the helium-cooled modular blanket concept.

To determine a total capital cost per m of length of the central region, the actual cost for several "not included" items in the first line must be added. The costs of the blanket region's internal constituents are of particular importance. The quantities of those constituents are estimated to be about 17,000 kg/m of beryllium, about 4000 kg/m of graphite, and about 13,000 kg/m of molten salt.

THERMOHYDRAULIC AND PERFORMANCE EVALUATION

The evaluation of the blanket performance ties together the nuclear, mechanical design, and thermohydraulic analyses. Overall plant performance along with the performance of the two independent cooling systems, helium for the first wall, and molten salt for the breeding blanket are presented. Since the molten salt is an electrically conducting fluid moving in a magnetic field, the MHD effects in that coolant loop are also discussed.

Internal Description

Table 7-13 lists the overall description of the blanket modules. Each module is a semicircular group of 18 segments, and each contains a multiplier rod bundle cooled by molten salt. The salt enters at the top and flows in a serpentine path sequentially through the 18 segments, exiting at the module bottom. The axial length of each module is 4 m and 73.8 MWt power is removed from each module. The molten salt bulk average temperature rise is 100°C. There are 44 modules in the 88-m-long blanket.

Within each of the segments are approximately 166 multiplier rods, or a total of about 132,000 rods in the blanket. Table 7-14 describes the multiplier rods. The rods are approximately 4 m long (possibly segmented), 5 cm diam, and oriented axially with respect to the fusion system. They are sintered beryllium rods with a 1.75-mm-thick graphite cladding. The cladding isolates the beryllium metal from the molten salt. Contact between the salt and beryllium will cause the salt to precipitate U, Pa, and Th and dissolve

Table 7-13. Blanket module description.

Semicircular layout (module)	
18 Multiplier rod bundles (segments)	
Interconnected pressure shells	
Serpentine coolant flow path	
Length, m	4.0
Centerline radius of module, m	2.7
Arc subtended by segments, °	10.0
Module (radial) thickness, m	0.91
Centerline width of segment, m	0.47
Power, MW _t	73.8
Coolant, ΔT, °C	100.0

Table 7-14. Multiplier Rod Description

Rods axially oriented, grid-spaced	
Helium removed by venting and diffusion	
Length, m	4.0
Pitch/diameter	1.10
Outer dimension, cm	5.08
Graphite cladding thickness, mm	1.75
Beryllium metal neutron multiplier:	
Sintered powder	
80-90% theoretical density	
Voids for helium escape	

the beryllium into the salt in their place. Such an occurrence also upsets the reduction--oxidation balance that must be maintained in the fluoride salt to reduce its corrosive potential. The helium generated in the beryllium as a result of the desired neutron multiplication reactions is bled from the rod by: 1) diffusion from the beryllium grains into the voids left in the rod (Be at 80-90% of theoretical density), 2) passage through the voids to the cladding, and 3) diffusion through the porous graphite and into the molten salt.

Table 7-15 shows the energy deposition rates in the blanket and the model geometry used in the nuclear analysis. The powers are zone-average over the annuli indicated. The calculated powers are for beginning-of-plant life and have no buildup of fissile materials in the blanket. Since continuous salt cleanup is expected to keep the fissile inventory very low in the salt, these powers are representative of all times in life. There is no significant swing in blanket power through life because there is no batching.

From the zone power deposition data and the study ground rules, the overall blanket size and power splits can be determined. Table 7-16 summarizes these results based on a total nuclear power (including the fusion system) of 4,000 MWt. The molten salt blanket design suppresses fissioning to a great

Table 7-15. Blanket geometry and power model (2 MW/m² first wall neutron loading).

Zone description	Zone outer radius, m	Zone average power density, w/cc	Peak to average
Fusion system	2.10	-	
Vacuum boundary first wall	2.15	2.33	
Void	2.20	-	
Blanket pressure boundary	2.25	2.21	
Blanket:	3.05	2.64	5.39
25% molten salt		6.38	4.46
65% beryllium		1.39	6.73
10% graphite		1.50	7.25
Steel liner	3.15	0.02	1.37
Concrete shield	4.14	(Negligible)	

Table 7-16. Power split (MW)

Fusion power (alphas)	570
Fusion power (neutrons)	2285
Fission power	240
(n, α) reaction power	<u>905</u>
TOTAL	4000

extent. Only about 6% of the total nuclear power comes from fission. The blanket is also quite effective in fuel formation--producing over 8,000 kg of ^{233}U per year. This quantity of fuel is enough to support from about 20,000 to 40,000 MW of electric power from the burner reactor power grid, depending on the average burner conversion ratio assumed.

Helium Coolant Performance

The blanket surrounds a separately-cooled first wall. Helium is used to cool this structure, which is the vacuum boundary that prevents contamination of the fusion plasma due to blanket leaks or the building environment. Table 7-17 describes the helium cooling system performance. The first wall receives 139 MWt power from nuclear heating and 30 MWt power from radiant heat transfer to its outside from the high temperature molten salt blanket modules. The peak temperature of the first wall structure is limited to about 400°C, so that radiation damage may be annealed out of the structure. By this approach, a first wall life similar to the plant design life is hopefully possible. As shown in Table 7-17, the central cell region of the TMHR has little effect on the overall size of the helium cooling system, since only about 10% of the total heat handled by the system comes from the first wall. The remaining 90% comes from the fusion system components.

Table 7-17. Helium cooling system performance.

Temperature, °C	In	288
	Out	343
	First wall	417
Loop pressure, atm		58
Pressure drop, atm	First wall	0.14
<u>Component</u>	<u>Heat Load, MWt</u>	<u>He flow, kg/s</u>
Injectors	913	3140
Direct converters	964	3355
First wall	169	581
Shielding	3	12

Magnetohydrodynamic (MHD) Effects

As the molten salt flows through the blanket, it encounters the solenoidal magnetic field that contains the central-cell plasma. Since molten salt is electrically conductive, there will be MHD effects to be considered in blanket design. These MHD effects may influence the blanket coolant performance by: 1) changes in the molten salt flow regimes and pressure drops, 2) changes in the heat transfer characteristics, and 3) changes in the corrosion processes. All of these effects are related to MHD-induced voltages (and subsequent electric currents), which are generated by the flow of molten salt within the blanket region's magnetic fields.

These MHD-induced voltages are related to the fluid velocity and magnetic field strength by Faraday's law of electromagnetic induction:

$$\vec{E} = \vec{U} \times \vec{B} \quad ,$$

where

\vec{E} is the electric field strength vector in V/m.

\vec{U} is the fluid velocity vector in m/s.

\vec{B} is the magnetic field strength vector in V-s/m²(T).

From a geometric point of view, Faraday's law can be visualized by three perpendicular vectors. The vector cross product of the fluid velocity and the magnetic field determines the magnitude and direction of the induced voltage. This induced voltage by itself can significantly increase the corrosion in the system, as previously discussed in this subsection and in Appendix A.

As well as effects on corrosion, there are MHD-induced fluid dynamics effects that may become important. If the MHD-induced voltage generates a significant electrical current through the molten salt, a force develops because of the interaction of the magnetic field with this induced current. The magnitude and direction of the force is given by the vector equation

$$\vec{F} = \ell (\vec{I} \times \vec{B}) \quad ,$$

where

\vec{F} is the force vector (N) applied to the fluid.

\vec{I} is the current vector (A) flowing through the fluid.

ℓ is the length (m) of the electrical field through the molten salt.

The implications of these MHD-induced forces on the coolant pressure drops are:

- For flow transverse to a magnetic field electrical eddy currents flow in the fluid in a plane perpendicular to the fluid velocity, causing a thinning effect in the side wall boundary layers and an increase in the wall friction.

- For flow transverse to a magnetic field in a channel with electrically conducting (metal) walls eddy currents generated across the flowing fluid and perpendicular to the magnetic field return through these conducting walls, resulting in a net electromagnetic body force in the fluid that opposes its flow.

- For flow transverse to a magnetic field of changing strength electrical eddy currents circulate perpendicular to the magnetic field but in the direction of the fluid velocity. These eddy currents result in a net retarding electromagnetic body force.

- For flow either parallel to or transverse to a magnetic field there is a tendency for the magnetic field to resist the turbulence in the fluid (turbulent suppression). This effect generally tends to laminarize the flow, and for a flow parallel to the magnetic field, reduces the pressure drop.

Since the coolant flow has reduced turbulence, its heat transfer capabilities are reduced, and both structural and multiplier rod temperatures are increased.

The magnitude of these effects is controlled by the current flow through the current paths. This limiting effect can be clearly seen by combining Ohm's law ($\vec{V} = I\vec{R}$) with Faraday's law and then substituting the result into the force equation. Then,

$$\vec{F} = \frac{\rho^2}{R} * [(\vec{U} \times \vec{B}) \times B] .$$

The magnitude of the induced forces are inversely proportional to the current path resistance. For molten salt in a metal piping system the main resistance factor is the high electrical resistivity of the molten salt itself (2.12 Ω -cm for Be,Li-F). Thus, the fluid dynamics effects are negligible compared to the voltage limitations imposed by corrosion considerations.

Molten Salt Coolant Performance

The molten salt enters and leaves each module through one or more radially-oriented pipes. As it enters or leaves the solenoidal magnetic field, it encounters a region of changing field strength. Since the field strength is changing, the generated potential also varies along the pipe axis. This variation leads to circulating currents in the V, E plane as shown by the vector diagram on the left side of Fig. 7-19. Once the salt is within the solenoid, the magnetic field strength is constant, and the resultant circulating currents are in the B, E plane. They are caused by the coolant velocity distribution perpendicular to the magnetic field. At the pipe walls the coolant velocity drops, and thus, the electric potential drops. The differences in potential cause the circulating currents, as shown on the right side of Fig. 7-19.

Once the molten salt enters the module, its flow is predominantly parallel to the magnetic field through the multiplier rod bundles. However, at each bundle end the coolant must flow tangentially around the blanket a short distance to reach the next rod bundle. During this tangential flow, the velocity and magnetic field vectors are again not parallel, and a potential can be generated. Due to the complex flow field at the bundle ends and cross-overs, the circulating current paths are not obvious; however, the generated

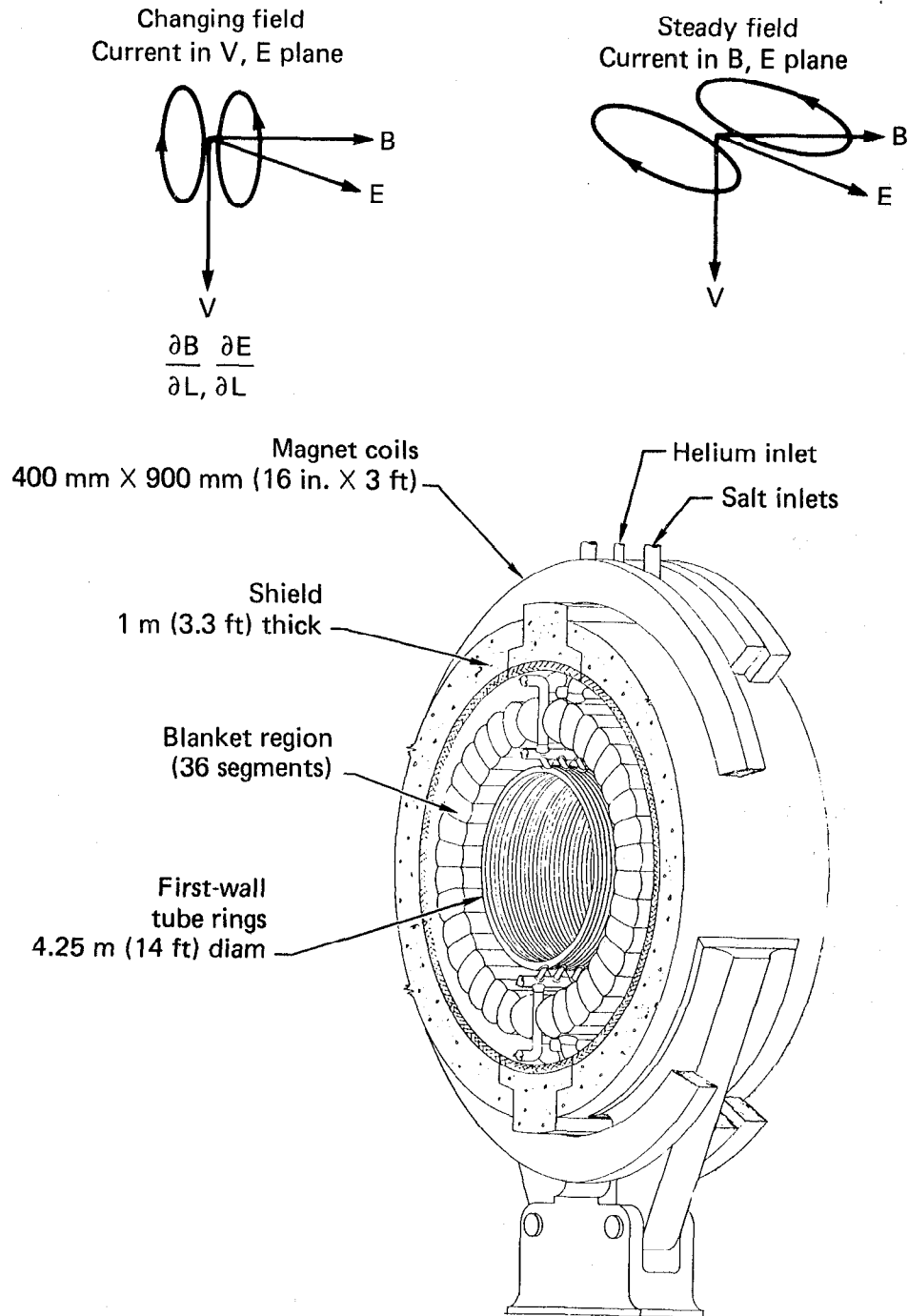


Fig. 7-19. Piping MHD effects.

potential is predominantly oriented in the radial direction. This will be complicated by the future design of the crossover region to either force complete flow mixing at each crossover or force the flow exiting the inner radius of one bundle (the highest power region) to enter the next bundle at the outer radius (the lowest power region). Such an arrangement is necessary to limit structural temperatures. Figure 7-20 illustrates this crossover region MHD effect without addressing the flow mixing considerations.

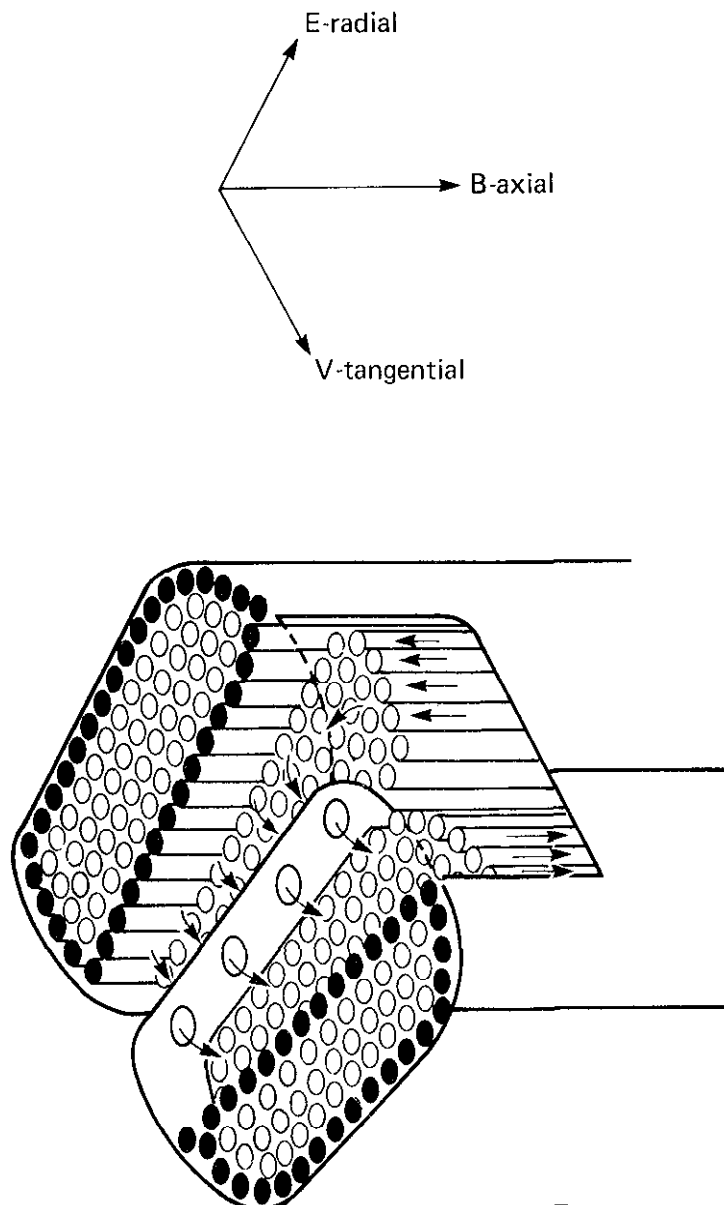


Fig. 7-20. Crossover MHD effects.

Tentatively, the MHD electric potential is limited to about 1 V to prevent salt dissociation and increased structural corrosion. This limit is applied to both the piping flows and the blanket crossovers and provides limits to coolant velocities and blanket geometries. The molten salt properties assumed are given in Table 7-2.

Table 7-18 summarizes the overall performance of the molten salt cooling system in the blanket. The salt carries 3,247 MWt power from the blanket with a 23,500-kg/s flow rate. The flow rate for each semicircular module is 534 kg/s. In the bundle region this results in an average velocity of 1.6 m/s. The peak beryllium and module shell temperatures, including radial power peaking but not including uncertainties, are about 720°C and 780°C, respectively. These temperatures are limited by assuming efficient mixing of the hot and cold coolant streams in the crossover region between rod bundles. Without mixing, both peak temperatures approach 1200 to 1300°C.

The frictional pressure loss in the 18 rod bundles, including entrance and exit losses, is 5.8 atm (85.3 psi). The inlet and outlet piping pressure losses are determined by the number of parallel inlet and outlet pipes used for each module. The number and size of pipes is governed by the 1-V MHD potential limit. If one pipe is used, it is 0.512 m (20 in.) in diam and has a 0.157-atm (2.31 psi) flow pressure loss per meter of pipe. The MHD pressure loss is 0.002 atm/m. If our parallel pipes are used, they have a 0.128-m (5.04-in.) diam and a 2.520-atm/m (37.04-psi/m) flow pressure loss. The MHD pressure loss is 0.009 atm/m. As shown in these pressure losses, the high resistivity of the molten salt limits the currents caused by the MHD potential and thus limits the induced MHD pressure loss.

Conclusions

From this very limited blanket performance evaluation three conclusions are drawn:

- The conceptual design appears feasible.
- MHD effects may limit or govern design.
- Flow mixing between bundles is necessary.

Table 7-18. Molten salt cooling system performance.

Temperature, °C	In	550
	Out	650
Breeding zone heating, MWt		3,247
Total flow rate, kg/s		23,496
Module flow rate, kg/sec		534
Bundle region velocity, m/s		1.58
Pressure losses:		
Piping, atm/m	MHD	0.002 ^a -0.009 ^b
	Flow	0.157 ^a -2.520 ^b
Bundle, atm	MHD	~ 0
	Flow	5.80
MHD potential, V:		
Piping		1.0
Crossovers		1.5
Bundle		~ 0
Maximum beryllium temperature, ^c °C		720
Maximum shell temperature, ^c °C		780

^a One inlet or outlet pipe with an 0.512-m inner diam.

^b Four inlet or outlet pipes in parallel with an 0.128-m inner diam.

^c Without uncertainties, but with radial peaking effects and flow mixing at mixing at crossovers.

MOLTEN SALT CHEMICAL PROCESSING

INTRODUCTION AND OBJECTIVES

The evaluation of molten salt processing requirements for removal of bred tritium, fissile material, and impurities is described in this subsection. Because of the preliminary scoping nature of the study, only the major processes required are identified and simplified process diagrams developed based on proposed technology for the MSBR.

The main objectives of the molten salt processing are the isolation of ^{233}Pa from the region of high neutron flux during its decay to ^{233}U and the removal of fission products from the salt. The system also recovers the bred ^{233}U and tritium from the salt and removes corrosion product impurities (e.g., Ni). The salt is processed to keep the neutron losses by absorption to Pa and fission products to a very low level, thus enhancing breeding of the fissile ^{233}U from the fertile ^{232}Th and tritium from Li contained in the salt. Continuous processing of a small salt stream in an onsite processing system limits the concentrations of Pa and fission products to acceptable limits.

The approach taken in this study to evaluate the TMHR salt processing requirements includes the following steps:

- Review the chemical processes proposed in the MSBR design for removal of gaseous products, U, Pa, fission products, and impurities.
- Determine if these processes are applicable to the TMHR salt and satisfy the TMHR objectives.
- Determine the adequacy of these processes and identify any additional processing needs.

As a result of this evaluation, we found that the proposed MSBR salt processing scheme is generally applicable to the TMHR salt. However, due to the need for tritium as a TMHR fusion fuel, we identified additional processing requirements to isolate tritium from the mixture of gaseous products. As suggested by the MSBR design group at ORNL, some simplification of these processing requirements is feasible. (This is discussed at the end of this subsection.)

EVALUATION OF MOLTEN SALT PROCESSING SYSTEM

It is believed that a molten salt chemical processing system similar to that proposed for the MSBR satisfies the chemical processing objectives of the TMHR for the following reasons:

- The two reactor systems (MSBR and TMHR) utilize the same salt composition -- LiF 71.7 mole %, BeF_2 16 mole %, ThF_4 12 mole %, and UF_4 0.3 mole % (for the MSBR only).

- The same processes take place in the two reactors -- fission of ^{233}U (suppressed in the TMHR) and ^{232}Th , breeding of tritium and ^{233}U , generation of Pa and fission products, and generation of corrosion product Ni.

Due to the fact that fission is suppressed in the TMHR while it is enhanced in the MSBR and the need to breed tritium, and due to the difference in the reactor neutron flux and its energy spectra, the generation rates of the different materials to be handled by the chemical processing systems for the two reactor systems are different. This mainly affects sizing of the different components of the system and not the applicability of the MSBR salt processing technology to the TMHR fuel salt. An additional complexity is introduced by the very small uranium content of the salt, which limits the oxidation/reduction control capability.

The chemical processing system consists of two subsystems: a gaseous system and a nongaseous processing system. A brief description of each system follows. A simplified flowsheet for processing the molten salt is shown in Fig. 7-21.

Processing of Gaseous Products

A small percentage of the discharge flow of the fuel-salt circulation pump is bypassed back to the pump (see Fig. 7-22). This bypass loop contains a gas bubble injection section, where a sparging gas (principally He) is introduced as small bubbles. These bubbles, generated by a bubble generator, have diameters of 15 to 20 mils. The bypass also contains a gas separator, upstream of the bubble generator, that removes the inert gas and its burden of fission product gases and tritium with nearly 100% stripping efficiency. The stripped gases consist principally of Xe, Kr, tritium, and exceedingly small amounts of noble metals. The removed gas, along with a small amount of

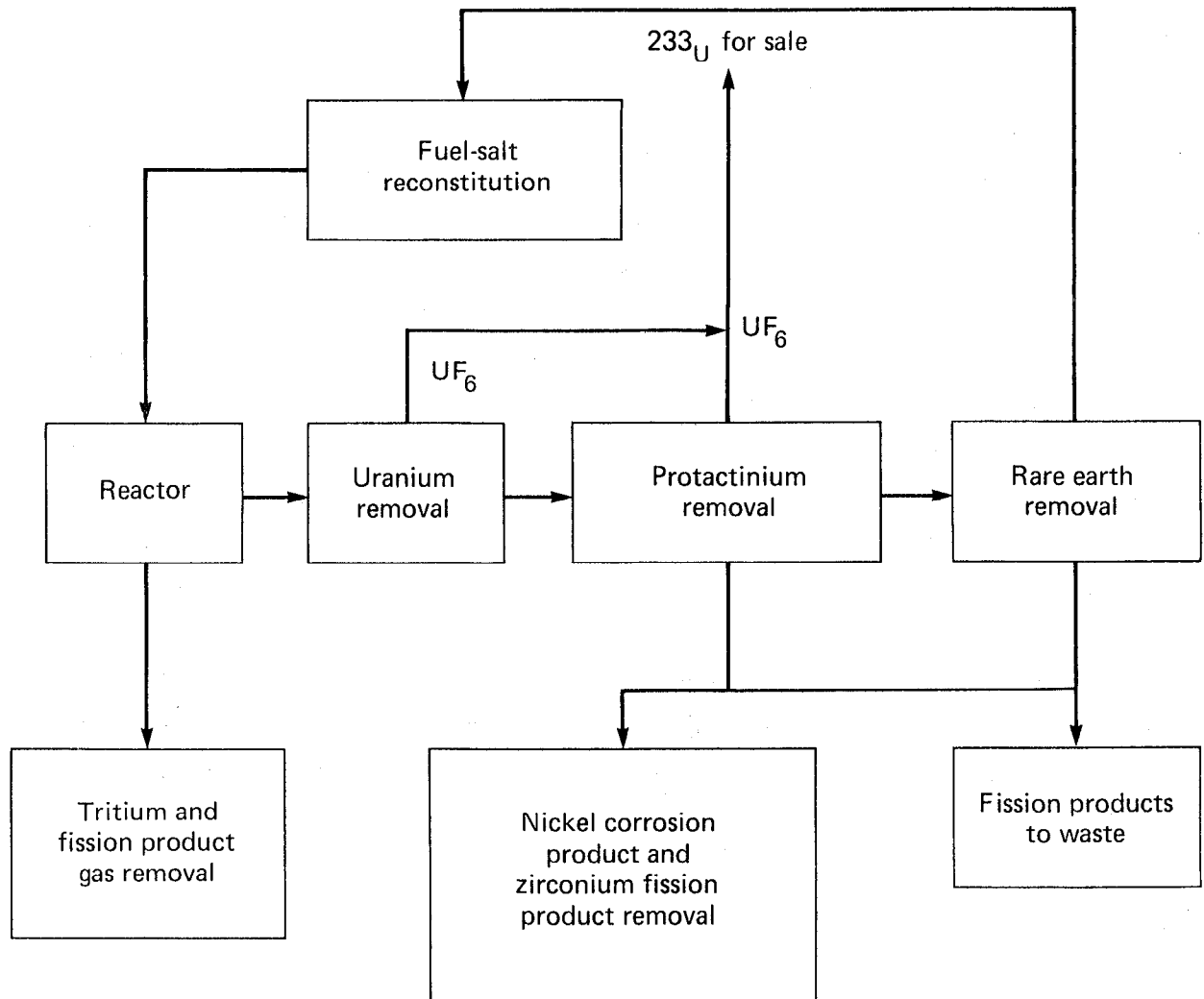


Fig. 7-21. Simplified flow sheet for molten salt processing.

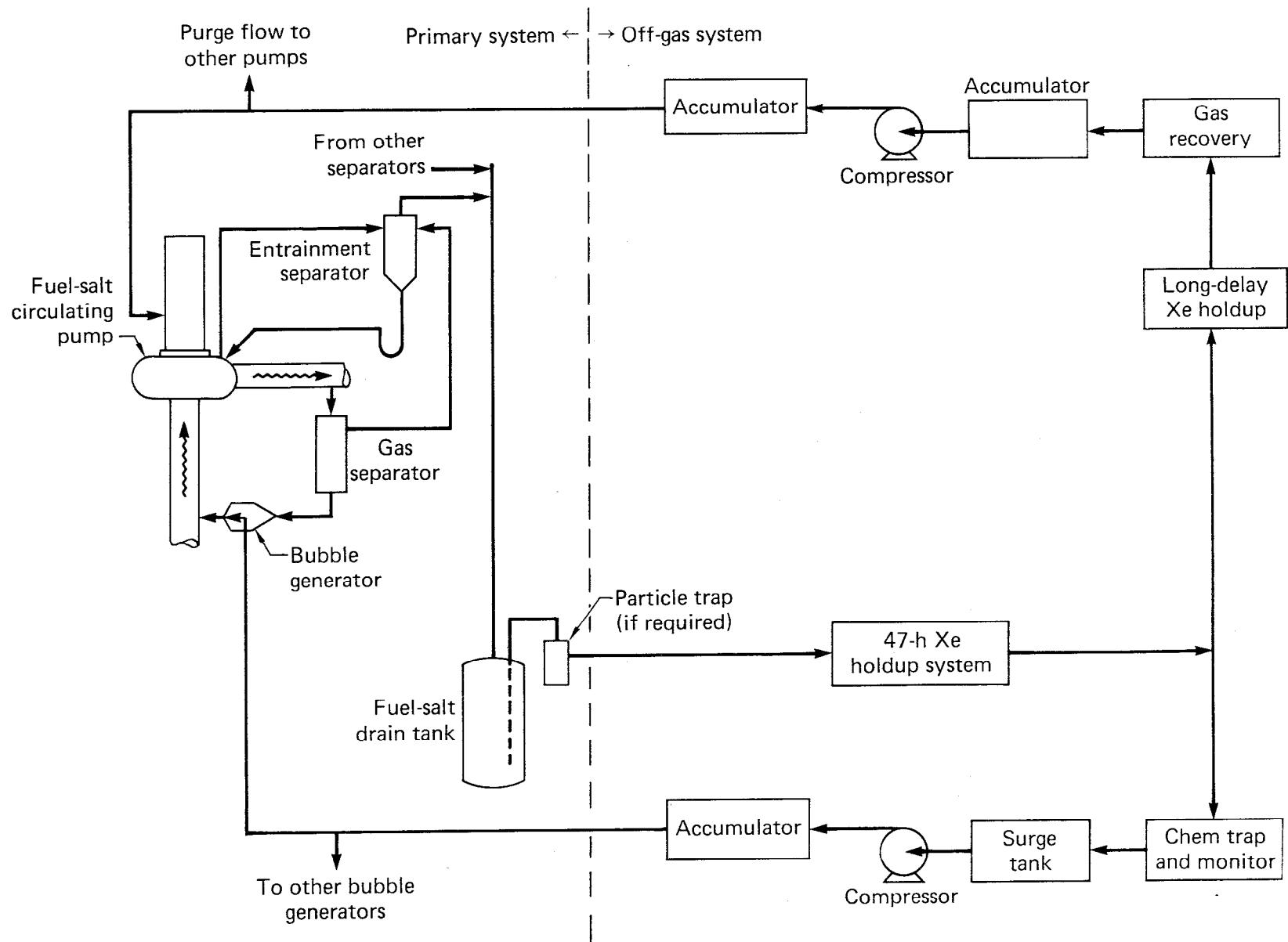


Fig. 7-22. Schematic flow diagram of off-gas treatment system.

entrained salt, is taken to a small tank, where the off-gas is combined with that purged from the pump bowls.

A two-hour holdup of the off-gases in the fuel-salt drain tank permits deposit of a portion of the noble metals on the internal surfaces. The off-gases are then passed through particle traps, where the remaining particulates are removed before the gases are introduced into the charcoal beds for absorption and 47-hour holdup of the Xe, permitting decay of 97% of the ^{135}Xe . A small portion of the gas leaving the 47-hour charcoal bed enters the long-delay charcoal bed (about 90-day Xe holdup), and then the gas flowing out of this bed passes through tritium and Kr traps before entering a gas storage tank. The gas entering this tank is augmented by makeup He and used wherever clean He is needed. Tritium, Kr, and the remaining Xe would then be purged off the traps and stored in bottles for future disposal. Most of the gas leaving the long-delay charcoal bed is compressed for reintroduction into the salt circulation system at the bubble generators.

Due to the use of tritium as a TMHR fusion fuel, it needs to be separated from the Kr-Xe-tritium mixture. Two tritium isolation processes are shown in Figs. 7-23 and 7-24. The first process, Fig. 7-23, utilizes a Palladium Diffusion Separation process to isolate ^3H and ^1H from the gaseous stream. This process had been applied successfully to H isolation and should theoretically be applicable to tritium isolation as well. In this process H (and tritium) are first absorbed by Pa and then diffused through the Pa media, where it is collected at high H (and tritium) purity. The remainder of the Xe-Kr isolation train follow the same process previously described for the MSBR.

Although the tritium generation rate in the case of the TMHR is about 2000 times higher than the MSBR, the fraction of gases to be removed from the He gas increases only from 0.1 to 0.6, which represents no process applicability problems from the MSBR to the TMHR.

The proposed Pa separation process assumes that tritium would diffuse through Pa in a manner similar to that of H. A second tritium isolation process shown in Fig. 7-24 may also be used. In this process, tritium is first converted into tritiated water, absorbed in zeolite beds, desorbed from the beds, and then recovered by electrolysis. Any H present in the tritium stream is then removed before tritium is used as TMHR fuel.

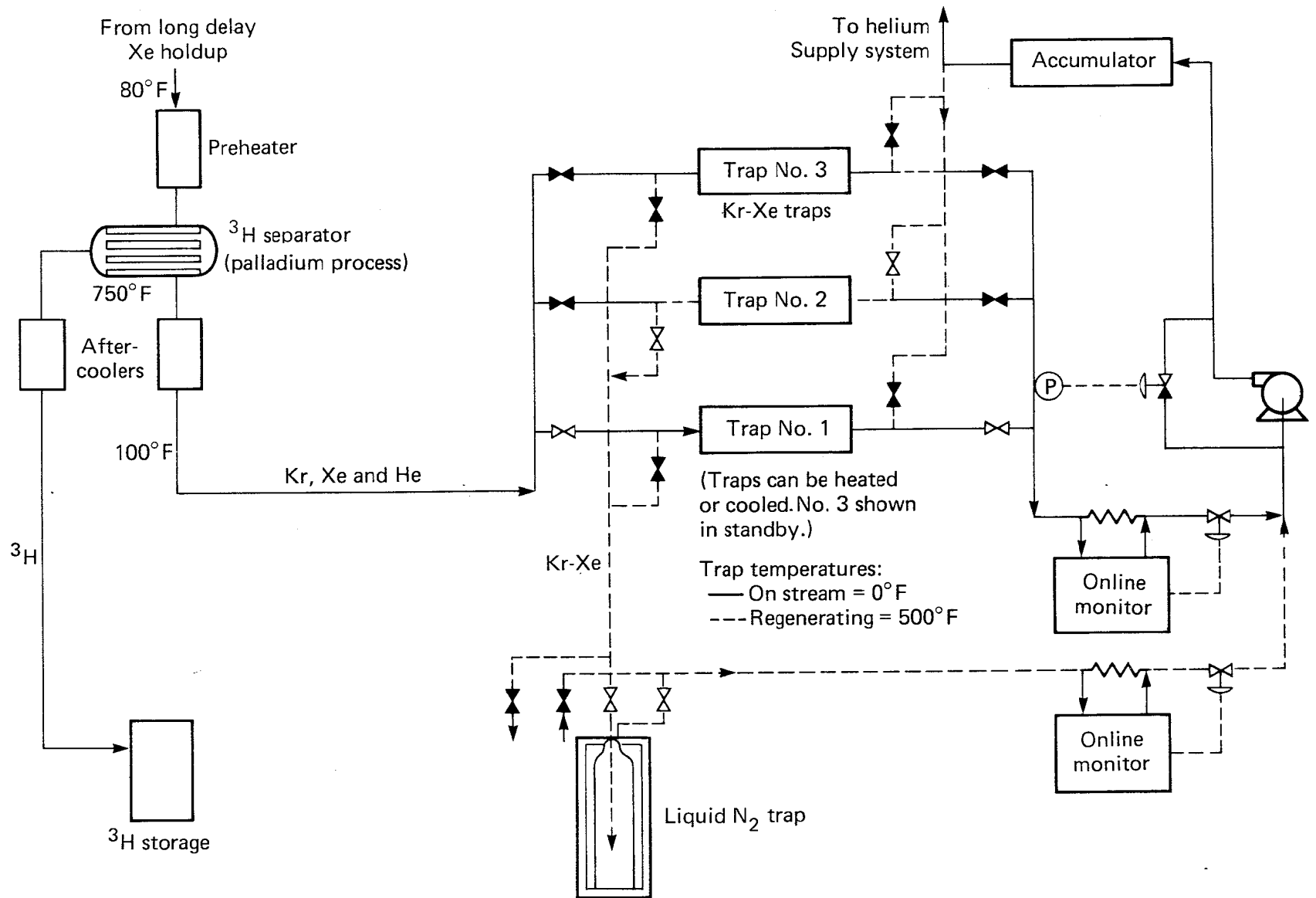


Fig. 7-23. Gas recovery, if ^3H and H pass through Pd separator.

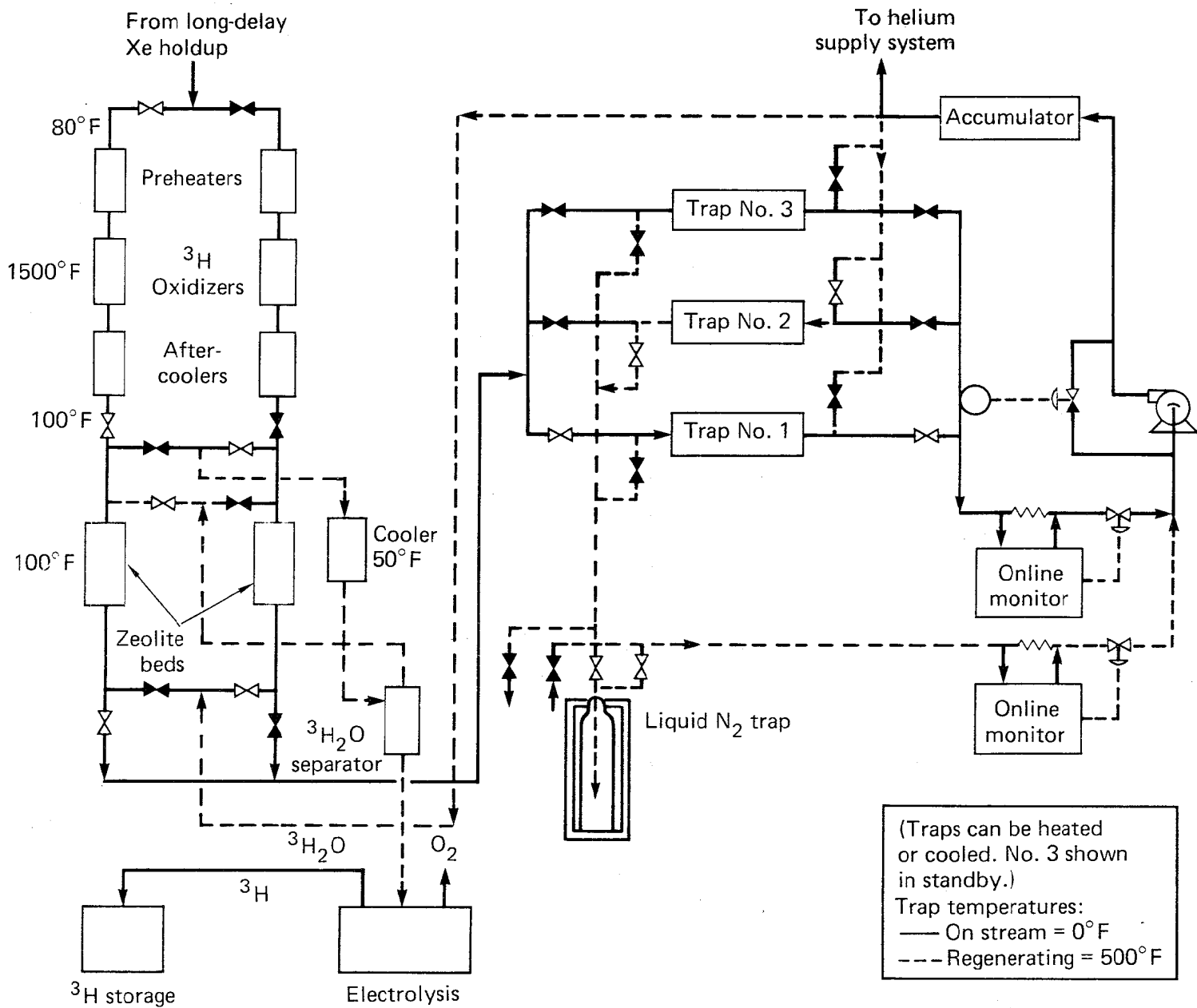


Fig. 7-24. Tritium recovery without Pd separator.

Processing of Nongaseous Products

A small stream of the fuel-salt is continuously processed in a fluorination-reductive, extraction-metal transfer process (Fig. 7-25). This process consists of two parts: 1) removal of U and Pa from the salt leaving the reactor, and 2) removal of rare-earth fission products from the salt. This side stream of salt, taken from the reactor drain tank, flows through a fluorinator, where about 95% of the U is removed as gaseous UF_6 . The salt then flows to a reductive extraction column, where Pa and the remaining U are chemically reduced and extracted into liquid Bi flowing countercurrent to the salt. The reducing agent, Li and Th dissolved in Bi, is introduced at the top of the extraction column.

The Bi stream leaving the column contains the extracted U and Pa as well as Li, Th, and fission product Zr. The extracted materials are removed from the Bi stream by contacting the stream with an $HF-H_2$ mixture in the presence of a waste salt, which is circulated through the hydrofluorinator from the Pa decay tank.

The salt stream leaving the hydrofluorinator, which contains UF_4 and PaF_4 , passes through a fluorinator where about 95% of the U is removed. The resulting salt stream then flows through a tank where most of the Pa decay heat is removed. Uranium produced in the tank by Pa decay is removed by circulation of the salt through a fluorinator.

Materials that do not form volatile fluorides during fluorination will also accumulate in the decay tank; these include fission product Zr and corrosion product Ni. These materials are subsequently removed from the tank by periodic discard of salt. Hence, the effluent salt from the extraction column carries fission products but no U or Pa.

The rare earths are removed from the salt stream leaving the top of the Pa extractor by contacting it with a stream of Bi that is practically saturated with Th metal. This Bi stream, with the extracted rare earths, is contacted with an acceptor salt -- LiCl. Because the distribution coefficient (metal/salt) is several orders of magnitude higher for Th than for the rare earths, a large fraction of the rare earths transfers to the LiCl in this contactor, while the Th remains with the Bi.

Finally, the rare earths are removed from the recirculating LiCl by contacting it with Bi streams containing high concentrations of Li (5 and 50 mole %). These materials, containing the rare earths, are removed from the process. The fully processed salt is returned back to the reactor. To maintain the U and Pa concentrations acceptably low, the molten salt chemical processing loop flow rate was set at 60 litre/min (approximately 16.0 gpm). This flow rate would keep the rate of fission product generation due to ^{233}U fission less than 1% of the total fission product generation rate.

Discussions with some of the MSBR team members at ORNL indicated that potential criticality of ^{233}U in the salt chemical processing system was not considered as it was not viewed as a potential physics or engineering problem. The concentration of ^{233}U in the salt is very low, and it would be an easy task to preclude criticality by proper choice of equipment size and configurations.

We believe that besides the removal of ^{233}U , ^{233}Pa should also be isolated to avoid its return to the blanket, whereby through neutron absorption, it will form ^{234}Pa and reduce the breeding potential of the reactor. This would also suppress the ^{233}Pa (n, 2N) reaction, which is a major contributor to the formation of ^{232}U , an undesirable strong gamma emitter. Also corrosion products should be removed to reduce the potential of depositing activated corrosion products on the different components in the molten salt loop.

The impact that the buildup of fission products in the molten salt has on the blanket's breeding potential needs to be evaluated in more detail. The effect that a batch chemical processing system for the molten salt would have on the size of the processing components also needs to be evaluated further. Batch processing may require larger components because of the need for handling higher flow in a shorter time.

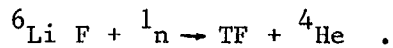
EVALUATION OF R&D NEEDS

A preliminary assessment of the present status of development and further R&D needs was made and is outlined below.

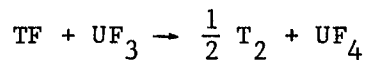
- A complete, full-scale fuel-salt chemical processing loop has not, to date, been operated to demonstrate the technical feasibility of the total system. The chemical processes proposed for the MSBR fuel-salt processing

system include fluorination, hydrofluorination, and various exchange reactions between fuel-salt and liquid Bi and between Bi and other salts, such as LiCl. There are sufficient data at hand to assure these processes are chemically sound. Most of the operations involved in the continuous processing system described previously have, to date, been carried out only in small-scale laboratory experiments.

- Large quantities of tritium fluoride (TF) are produced in the TMHR blanket according to the following reaction:



Due to the corrosive nature of TF, it should be almost completely reduced to T to avoid its corrosive effect on components and piping. This may be accomplished in the following chemical reaction:



Hence, enough UF_3 should be supplied in the salt mixture to transform all of the TF present to T. Work done by the MSBR team (ORNL/TM-6415) indicates that the TF content of the salt would be almost completely reduced to T_2 if a UF_3/UF_4 fraction of 0.01 was maintained and would be more completely eliminated at a UF_3/UF_4 fraction of 0.1. If this valence adjustment of UF_3/UF_4 is performed in a separate bypass loop, the loop transformation efficiency of UF_4 to UF_3 is 100%, and if overall equilibrium UF_3/UF_4 ratio in the main salt loop was to be 0.01, preliminary calculations show a bypass loop flow of about 269 gpm. The feasibility of such valence adjustment in the salt main loop should be considered. In the TMHR, however, the U concentration is too low for these controls. If adequate U is not present in the salt, the $\text{Ce}_3^+/\text{Ce}_4^+$ couple may possibly serve the function.

- The MSRE experience indicates that the presence of Te fission product in the molten salt caused embrittlement and cracking of Hastelloy-N used to contain the salt in the system. Further testing by the Oak Ridge MSBR team (ORNL/TM-6415) indicated that at UF_4/UF_3 ratios of 60 or less, Te bearing salt caused very little cracking of even standard Hastelloy-N. It was also observed that for ratios of UF_4/UF_3 above 80, the cracking was very extensive. It is important to note that due to the fact that U concentrations in the MSBR were expected to be much higher than that in the TMHR, the optimum

equilibrium of UF_4/UF_3 in the TMHR salt needs to be further investigated. Excessively reductive molten salt can lead to a plating-out of U or Th. Thus, the molten salt chemistry must be controlled within a band.

- One basic engineering problem facing the chemical processing system is the use of material that can contain Bi and Bi-salt mixtures. Iron and nickel-based alloys are susceptible to dissolution and mass transfer in Bi. Although fluorination of a flowing salt stream has been demonstrated, establishing and maintaining a protective layer of frozen salt on the fluorinator walls has not been demonstrated except in a fluorination simulation. Complete removal of entrained Bi from molten salt and satisfactory high temperature instrumentation for process control are yet to be developed and demonstrated.

BALANCE-OF-PLANT DESIGN AND PRECONCEPTUAL COST ESTIMATE

INTRODUCTION AND OVERALL DESCRIPTION

A preliminary conceptual balance-of-plant (BOP) design and an order-of-magnitude cost estimate were developed for the molten salt-cooled TMHR and are described in this subsection. The main objective of the BOP design study was to develop a preliminary understanding of the requirements of plant design. Of particular importance are the requirements imposed by the high temperature reactor molten salt coolant and the intermediate He coolant on the heat transport system; and the requirements imposed by the reactor and its auxiliaries on buildings and structures. These requirements have a significant impact on the economic viability of the plant. Thus, the primary BOP systems addressed in this study include:

- Heat transport system.
- Energy conversion system.
- Plant arrangement.

The BOP design and cost estimates developed here were based on the following set of parameters:

- Reactor thermal output = 4000 MWt = Pf (0.2 + 0.8M) where Pf = fusion power = 2904 MW and M = blanket multiplication factor = 1.4716
- Plasma Q = 2.12
- Wall loading = 2.0 MW/m²
- Direct converter efficiency - 50%

- Neutral beam injector and RF heater efficiency = 60%
- Coolant temperature, cold/hot = 550°C/650°C
- Reactor length = 88 m
- Number of modules = 22
- Average coolant pressure = 1.5 MPa

Although the TMHR plant has a large number of BOP systems, only the main BOP systems are described here. The main systems are:

- Heat transport system.
- Energy conversion system.
- Heat rejection system.

The other systems, not described here, are the plant electrical systems and the plant auxiliary systems. The plant auxiliary systems typically include:

- Helium storage and handling system.
- Helium purification system.
- Primary molten salt handling systems.
- Primary molten salt purification systems.
- Inert gas receiving and processing system.
- Radiation monitoring system.
- Tritium monitoring system.
- Tritium processing and handling system.
- Plant fire protection system.
- Recirculating gas cooling system.
- Atmospheric gas cleanup system.
- Radioactive waste system.
- Heating, ventilating, and air-conditioning system.
- Remote maintenance system.
- Leak detection system.
- BOP instrumentation system.
- Heat tracing system.
- Plant control system.

HEAT TRANSPORT SYSTEM

The TMHR thermal heat is produced in three components of the reactor: 3247 MWt in the molten salt-cooled blanket, 169 MWt in the first wall, and 976

MWt in the direct converter. The blanket heat output is carried by a molten salt that has the following composition:

- LIF 72 mole %
- BeF 16 mole %
- ThF 12 mole %

Because of the high tritium concentrations and corrosion products in the molten salt, an intermediate loop is used to isolate the molten salt loop from the steam system. Helium coolant was chosen for this intermediate loop because of its chemical and neutronic inactivity in the case of its leaking into the fuel salt. Tritium permeating from the fuel salt into the He secondary coolant can be combined with O and/or water added to the He loop for that purpose to form tritiated water, which can be removed in the cleanup system.

The schematic diagram of the heat transport system is shown in Fig. 7-26. The salt leaving the blanket has a temperature of 650°C, a pressure of 1.5 MPa, and flow rate of 23.5×10^3 kg/s. The salt then transfers its heat to a He secondary coolant loop in an intermediate heat exchanger (IHX) and is pumped back to the blanket at 550°C. The molten salt pressure drop in the blanket is 0.69 MPa. Hot He leaves the IHX at 550°C temperature, 5.5 MPa pressure, and flows (3.12×10^3 kg/s) to the steam generator. Helium discharged from the steam generator is pumped back to the IHX at a temperature of 350°C. Steam is generated in the steam generator at a temperature of 495°C, pressure of 8.13 MPa, and flows to the energy conversion system. After utilization of the steam in the energy conversion system for the generation of electricity, feedwater is returned to the steam generator at 211°C.

The direct converter thermal exhaust is carried by He at 550°C temperature, 5.5 MPa pressure, which flows to a steam generator and pumped back to the direct converter at 350°C. The He heat is exchanged with water in the steam generator to generate steam at 495°C temperature, 8.13 MPa pressure. Steam flows to the energy conversion system, and feedwater is returned to the steam generator at 211°C. The TMHR first wall cooling heat is carried by He at 343°C temperature, 6.87 MPa pressure, and 590 kg/s flow. This heat is introduced into the energy conversion system for feedwater heating.

The heat generated in the shield, neutral beam injectors and the RF plasma heating system are removed by low pressure, low temperature water systems, and rejected to the atmosphere by cooling towers.

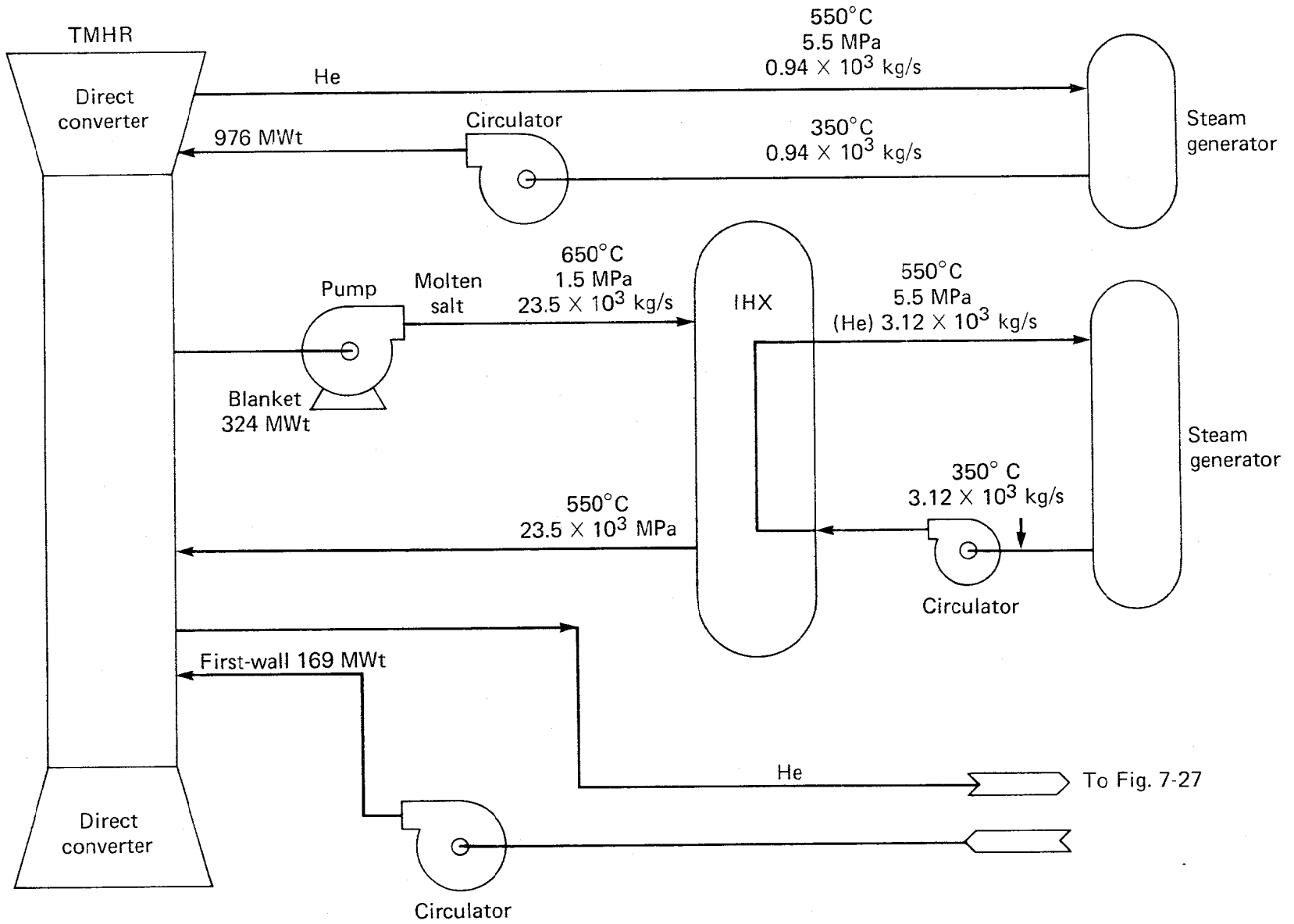


Fig. 7-26. Heat transport system schematic.

ENERGY CONVERSION SYSTEM

A schematic diagram of the conversion system is shown in Fig. 7-27. The steam cycle selected for energy conversion is similar to that considered in the gas-cooled fast reactor (GCFR) designs. Steam conditions at the turbine inlet are 8.13 MPa and 495°C.

The turbine-generators selected are two identical tandem compound 1800-rpm units operating with a superheat cycle. Each unit typically consists of one high pressure cylinder, three low pressure cylinders, and one generator.

The conversion system also includes a condensate system and a feedwater heating system. The function of the condensate system is to condense the steam exhausted from the low pressure cylinders of the turbine-generator unit. The condensate system schematically consists of a steam condenser and a condensate pump that delivers the condensate to the feedwater heating system.

The condensation is accomplished by circulating cold water through the condenser. The function of the feedwater heating system is to preheat and pressurize the condensate and deliver it to the steam generator at the required temperature and pressure conditions. The system schematically consists of a feedwater pump and a feedwater heater. The pump is driven by a steam turbine. The heating of feedwater is accomplished by extracting steam from the turbine and passing it through the feedwater heater.

HEAT REJECTION SYSTEM

A large amount of heat is rejected from the energy conversion system while condensing the turbine exhaust steam in the steam condenser. This rejected heat amounts to approximately 60 to 65% of the total heat generated in the reactor, and is caused by the thermodynamic inefficiency of the Rankine cycle used in the conversion system.

The function of the heat rejection system is to reject this waste heat to an ultimate heat sink. The function is accomplished by transporting the heat rejected in the condenser to cooling towers, where it is ultimately exhausted to the atmosphere. The system schematically consists of a circulating water pump and a cooling tower. The circulating water pump draws cold water from the cooling tower and delivers it to the condenser to cool the condensing steam. The effluent hot water from the condenser then flows back to the cooling tower

7-70

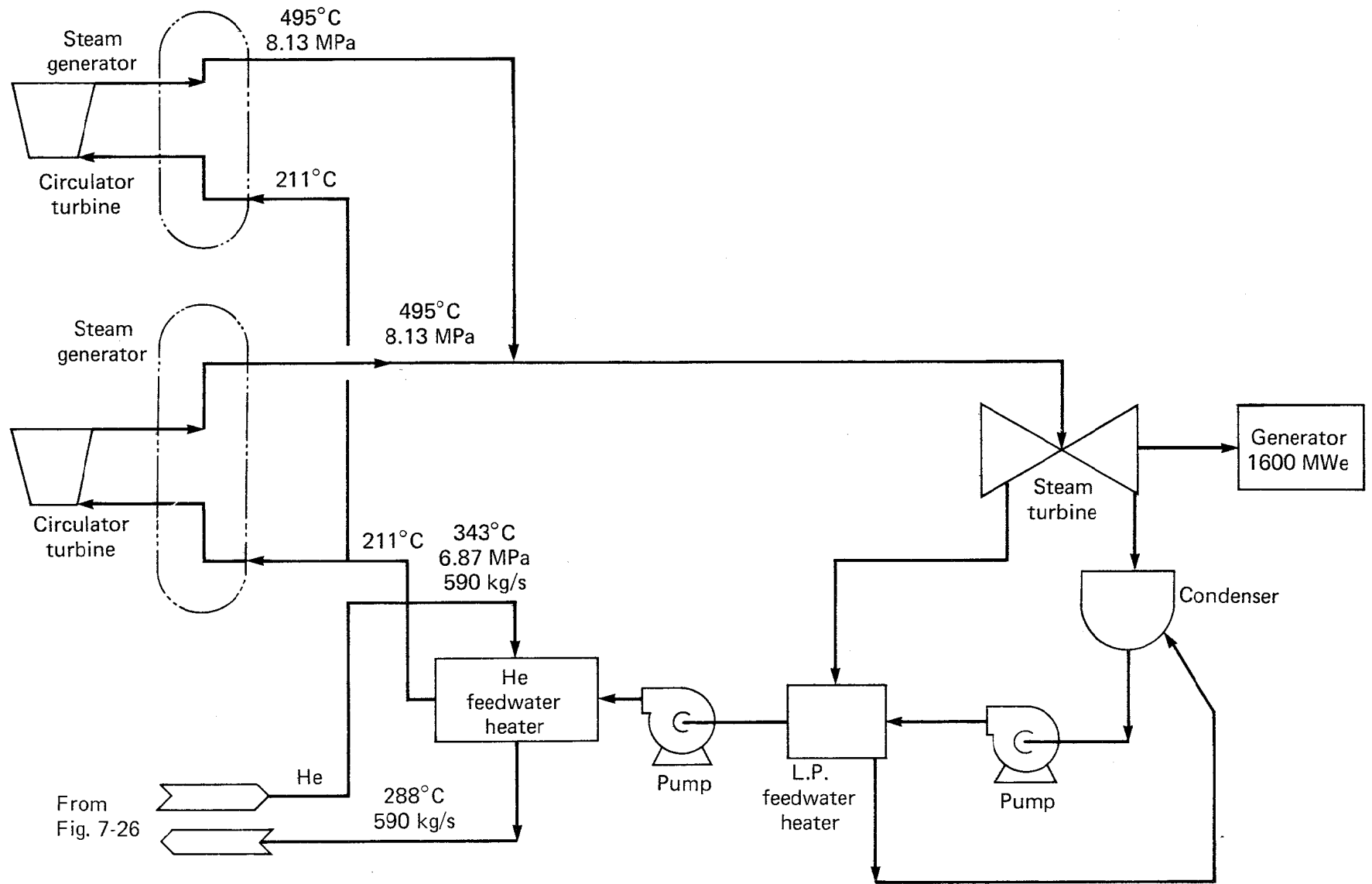


Fig. 7-27. Energy conversion system schematic.

and exchanges heat with air. A schematic diagram of the heat rejection system is shown in Fig. 7-28. The integrated major BOP systems previously presented are shown in Fig. 7-29.

EMERGENCY COOLING AND AFTERHEAT REMOVAL

In the molten salt-cooled TMHR concept the fuel salt plays the dual role of being the medium in which heat is generated within the reactor and the medium that transfers heat from the reactor to the primary heat exchanger.

Due to the fact that the heat source is in the coolant and not in solid-fueled core requiring continuous cooling to avoid melting, the safety philosophy is very different than solid-fueled reactors. In the case of any credible accident conditions involving loss of flow or loss of coolant in the primary loop, the fuel salt is drained to the drain tank. In the drain tank the decay heat (17.5 MWt at $t = 0$) would be removed through redundant cooling systems. The drain tank and its cooling systems would represent the systems emergency core cooling system (ECCS).

PLANT PERFORMANCE

The overall plant performance was calculated based on the parameters indicated in the previous subsection. The plant performance is presented as the power flow diagram in Fig. 7-30 and is summarized below:

Thermal converter output	= 1600 MWe
Direct converter output	= 975 MWe
Gross electric power	= 2575 MWe
Recirculating power	
Neutral beam injector	= 505 MWe
RF heating	= 1778 MWe
Miscellaneous plant loads	= 90 MWe
Total recirculating power	= 2373 MWe
Net plant output	= (+) 202 MWe

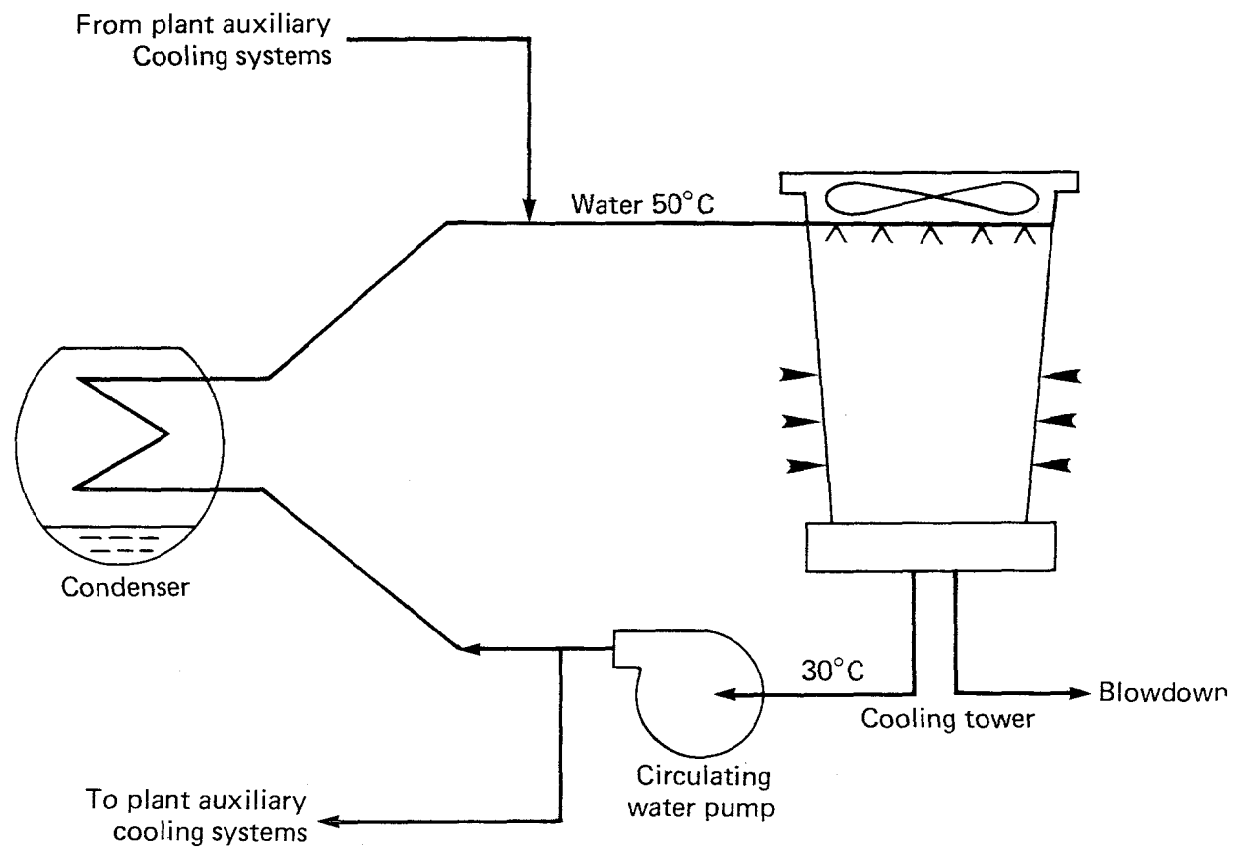


Fig. 7-28. Heat rejection system.

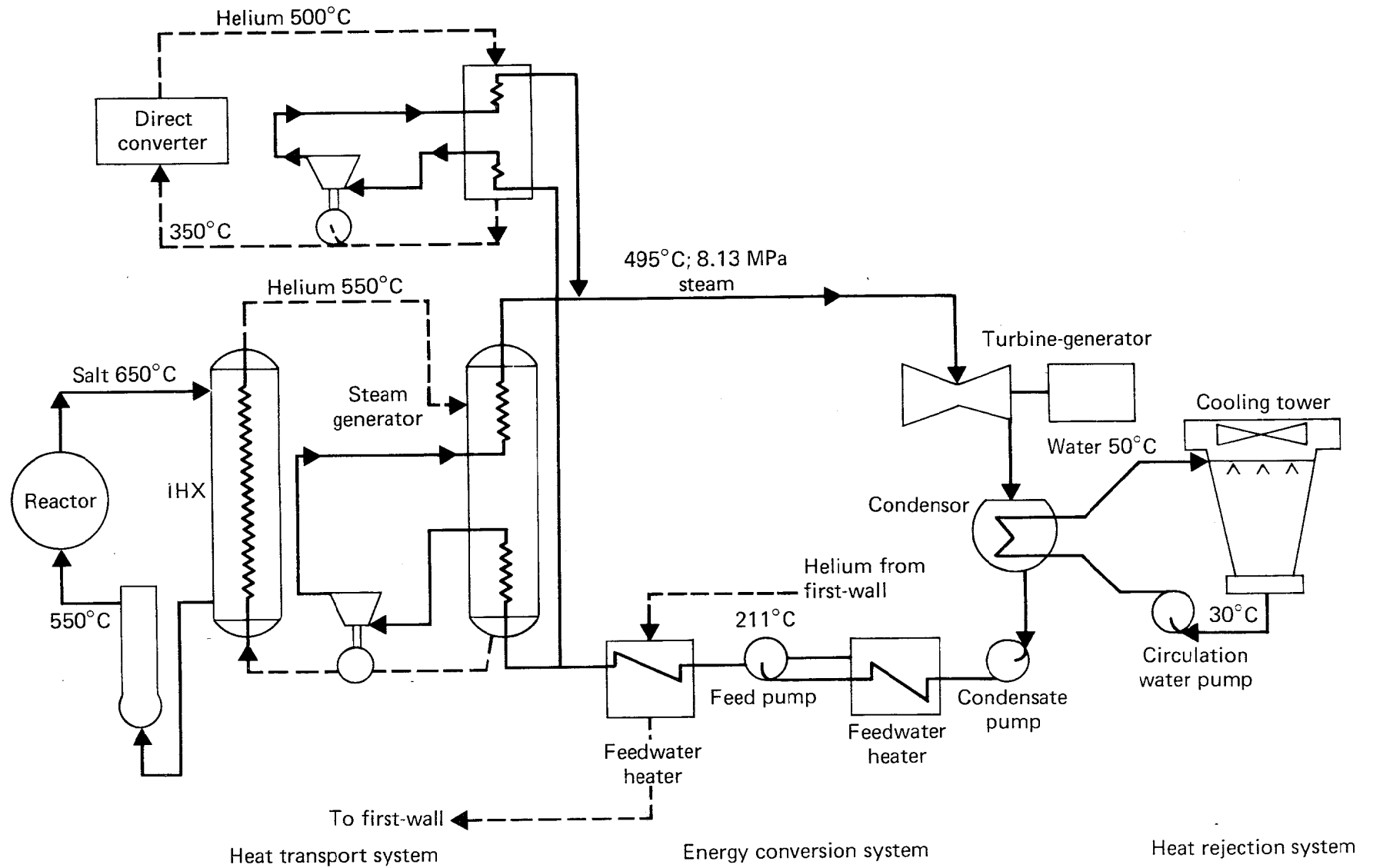


Fig. 7-29. Integrated main BOP system for molten salt-cooled concept.

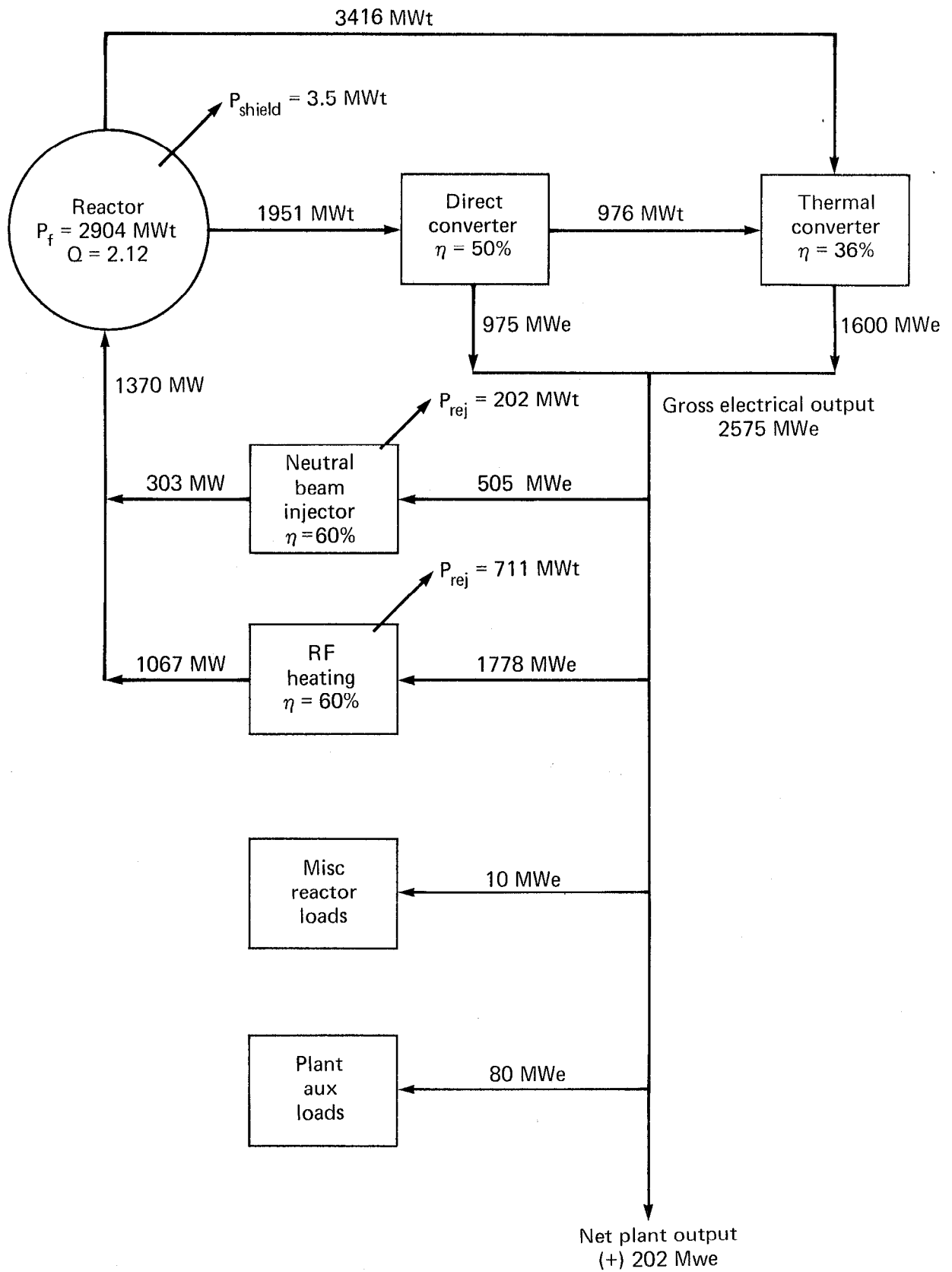


Fig. 7-30. TMHR power flow diagram (molten salt-cooled concept).

PLANT ARRANGEMENT

A preliminary conceptual plant arrangement was developed for the molten salt-cooled TMHR. A primary objective of this effort was to develop a containment concept that would allow remote maintenance of the reactor in addition to the normal function of providing services and support to the reactor systems and equipment. Another major objective was to develop a concept for the heat transport systems equipment and piping arrangement to gain an understanding of the requirements imposed by them on the building design. Because of the high temperature (650°C) of the molten salt, and due to the large pipe sizes (150-cm-diam) required for the intermediate helium coolant, the thermal expansion and support requirements for the coolant pipes affect the building size and its cost significantly. Thus, primary emphasis was placed on developing a plant arrangement concept for the reactor and the heat transport systems equipment containment. Approximate building volumes required for the molten salt processing system and other plant auxiliary systems were also identified.

Figures 7-31 and 7-32 show plan and cross section views of the major plant buildings. The molten salt system is comprised of four loops, each includes one molten salt pump and two intermediate heat exchangers (IHX). The molten salt pipe size is 75 cm in diam. Each IHX is connected to a steam generator via the He cooling lines of 150 cm in diam. There is a total of eight He secondary loops.

Considerations affecting the equipment locations in the system are:

- The pumps are located in the hot legs to reduce the pressure load on the blanket.
- Upward flow of the molten salt through the blanket is chosen to ease collection of gases at the pump-free surface.
- Molten salt pumps are located at highest level in the loop in order to have only one molten salt gas interface in the system at the top of the pump bowls.

The layout of the reactor modules, blanket, and related equipment shown is preliminary. More in-depth study needs to be done to investigate the removal and replacement of such components and possible interferences uncovered.

7-76

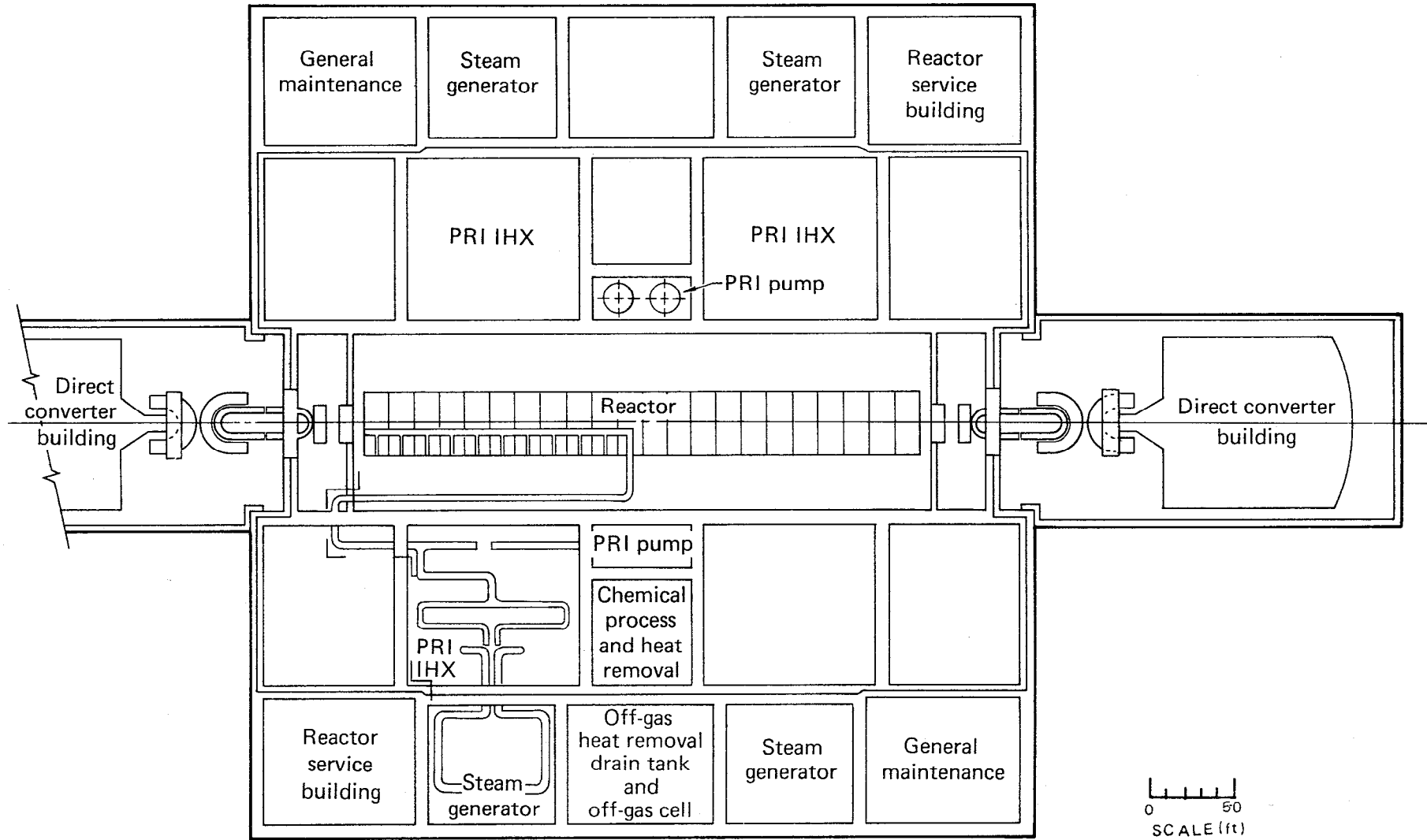


Fig. 7-31. Reactor and support building -- general arrangement plan -- molten salt-cooled concept.

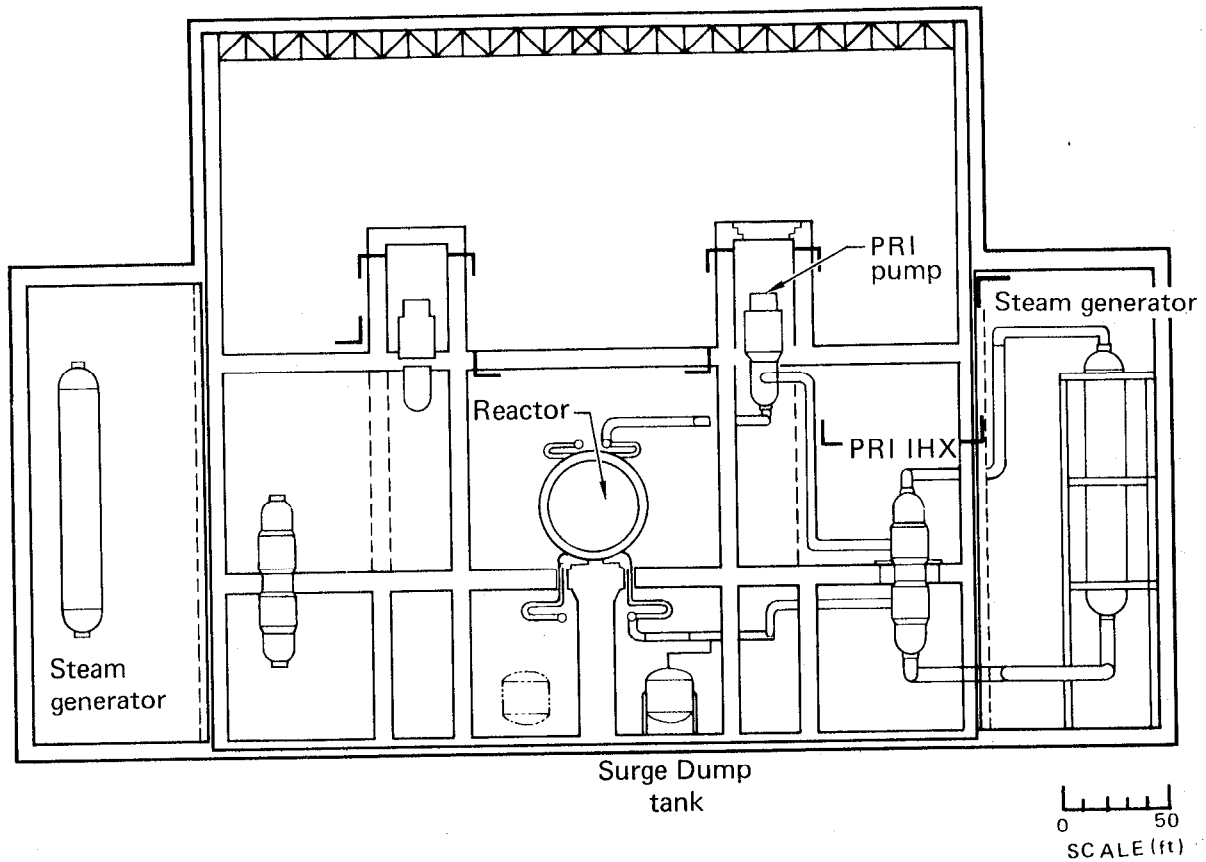


Fig. 7-32. Reactor and support building - section A-A.

CONCLUSIONS AND RECOMMENDATIONS

As a result of this preconceptual study, we identified problem areas and areas of uncertainty, which are discussed in the following paragraphs as preliminary conclusions and recommendations.

The present design allows an initial assessment of the problems associated with the plant design for fusion reactor plants in general and the TMHR plant in particular. The design is relatively superficial and conceptual in nature. Many of the systems and associated equipment are not defined in detail, and some of them probably have not yet been identified. Allowances have been made to accommodate these unknowns and uncertainties; but until further design and analysis are done, many uncertainties remain. On the basis of the present study consider the following comments:

- The plant layout including equipment and piping arrangement is conceptual. Further study is needed to detail and improve the arrangements. The primary piping arrangement is a critical aspect of the plant layout and can have a large impact on building costs.

- The design and layout of high temperature piping are critical. No stress analysis has been performed to substantiate the piping arrangement. The stress analysis will likely rely heavily on inelastic analysis and other sophisticated techniques leading to high design costs. Special design configurations, such as concentric and externally-cooled pipe might be required.

- The operating temperatures of the molten salt heat transfer systems are beyond the present state-of-the-art, and there is no experience in designing and operating large systems at these temperatures. The following are some factors that must be considered in developing the system design:

Section III of the ASME Boiler and Pressure Vessel Code and other applicable codes will likely require modification to provide a basis to determine the structural adequacy of piping and components.

Basic data is needed on the behavior of materials and structures at the anticipated operating conditions. These should include long-term behavior and properties, interaction with coolant and other system materials, corrosion, compatibility, mass transfer, creep ratcheting, and creep-fatigue evaluation.

- Design and fabrication of heat exchangers to handle the molten salt primary loop on one side and helium in the secondary side have not to date been done, adding uncertainties requiring further investigation.

- Modified Hastelloy-N has been experimented with and does not seem to exhibit cracking under simulated MSBR operating conditions (ORNL/TM-6415). Although these results are encouraging, uncertainties still exist about its long-term behavior in an actual loop under high temperature and thermal transient conditions.

- Although helium appears to be an adequate secondary coolant for the TMHR, more detailed comparisons should be performed to evaluate its advantages and disadvantages as it compares to other coolants; e.g., sodium fluoroborate (NaBF - NaF).

- The structures in this plant are significantly larger than those in fission power plants. All the structures are very massive because of shielding and other safety requirements. The conceptual design is considered

to be a feasible design consistent with current technology and industry practice. However, the design analysis aspects of the structures have to be investigated further before a method for their design can be established.

PRECONCEPTUAL COST ESTIMATE

The results of the preconceptual cost estimate, its basis qualifications, and exclusions are presented in this subsection. This estimate is an order-of-magnitude evaluation of the direct level BOP costs. A summary and detail presentation of this estimate are exhibited in Tables 7-19 and 7-20, respectively. The format of these presentations is in conformity with the May 1978 Battelle Report PNL-2648, "Fusion Reactor Design Studies - Standard Accounts for Cost Estimates." Costs are stated at third quarter 1979 pricing levels with no allowance for future escalation.

Table 7-19. Direct level capital cost summary (3Q 1979 pricing).

Account	Description	Cost in Millions
21	Structure and site facilities	418
22	Reactor plant equipment (excludes reactor and molten salt processing)	700
23	Turbine plant equipment	340
24	Electric plant equipment	250
25	Miscellaneous plant equipment	<u>30</u>
TOTAL DIRECT LEVEL COST		1738

Table 7-20. Direct level capital cost detail (3Q 1979 pricing).

Account	Description	Cost in Millions
21	<u>Structures and Site Facilities</u>	418.
.01	Site improvements and facilities	15
.02	Reactor building	248
.03	Turbine building	30
.04	Cooling system structures	5
.06	Miscellaneous buildings	<u>120</u>
22	<u>Reactor Plant Equipment</u>	700
.02	Main heat transfer and transport system	555
.03	Auxiliary cooling system	30
.04	Radioactive waste treatment and disposal	10
.06	Other reactor plant equipment (excludes molten salt processing)	105
23	<u>Turbine Plant Equipment</u>	340
.01	Turbine generators	105
.02	Main steam system	20
.03	Heat rejection systems	60
.04	Condensing systems	15
.05	Feed heating system	50
.06	Other turbine plant equipment	50
.07	Instrumentation and control	<u>40</u>
24	<u>Electric Plant Equipment</u>	250
.01	Switchgear	18
.02	Station service equipment	25
.04	Protective equipment	3
.05	Electrical structures and wiring containers	110
.06	Power and control wiring	90
.07	Electrical lighting	<u>4</u>
24	<u>Miscellaneous Plant Equipment</u>	<u>30</u>
	TOTAL DIRECT LEVEL COST	1738

The process under discussion in the study is taken to be a first generation model designed in a time when the major equipment functions have been successfully demonstrated. At that time industry will have developed the capability to produce the equipment, a capability that does not necessarily exist today. Development and first-of-a-kind costs are therefore not considered.

Basis and Scope Definition

This subsection addresses only those areas where the basis and methods employed to develop the estimate differ from the He-cooled TMHR.

Mechanical Equipment

This includes an intermediate heat exchanger. The cost of this heat exchanger was based on developing the heat exchanger area from engineering design parameters, estimating installation labor, and obtaining telephone quotes for material.

Piping

This includes Hastelloy-N piping between the reactor and the IHX. The cost of this piping was estimated based on developing quantities from conceptual layout drawings, estimating installation labor, and obtaining telephone quotes for materials.

Electrical

This includes the heat tracing equipment and bulk materials required for the molten salt piping. The cost estimate was developed by comparing with the PLBR estimate, which was adjusted for the difference in heating requirements and the capacity of the handling and initial salt melting facilities.

Exclusions

The following items are excluded from the estimate:

- The TMHR, direct converter, related equipment and installation.

- Field distributables, engineering and home office costs, contingency, future escalation, and fees.
- Owner's costs, such as land acquisition, costs of financing, owner's licensing and engineering, royalties, etc.
- Initial charges, stocks of operating supplies and spares.
- Assistance to the owner in obtaining EPA clearances, permits and authorizations from DOE or any other governmental agencies.
- Ecological and environmental considerations other than those incorporated in the present conceptual design.
- Startup, training, and operating costs.
- State and local taxes.
- Switchyard and transmission facilities.
- All facilities beyond the hypothetical site boundary.

The molten salt processing system is also excluded from the estimate. The primary reason is that no engineering information is available for the system design even to allow a preconceptual order-of-magnitude estimate. However, if the design developed for the MSBR chemical processing system can be assumed to represent the TMHR molten salt processing system, an initial indication of the trend of cost of the system may be obtained. Thus, based on the MSBR salt processing system design and cost estimate (ORNL-TM-3579, May 1972), the direct level cost of the TMHR salt processing system is projected to be approximately \$40 million at third quarter 1979.

COST SCALING ALGORITHMS

In addition to the base BOP cost estimates, cost scaling algorithms were developed for each of the four BOP cost categories (civil and structural, mechanical equipment, piping and instrumentation, electrical equipment, and bulks). These cost scaling algorithms are listed in Table 7-21. These algorithms are intended for scaling the BOP costs for parameters other than those used in this study. To arrive at these algorithms an approximate curve-fitting-type approach was used.

Exercise caution in using these algorithms. For the cost algorithms to be valid the variation of parameters (Q, wall loading, wall radius, blanket multiplication, injection efficiency, direct converter efficiency, etc.) should not result in a variation of the parameters in this study exceeding

approximately $\pm 20\%$ from the base values assumed. These parameters are thermal energy from the blanket, thermal exhaust from the direct converter, and the length of the reactor solenoid.

TABLE 7-21. Cost scaling algorithms molten salt-cooled case
(in million \$)

Civil and structure:	$282.1 + 0.293 \sqrt{P} + 1.19 (33 + L_{cc})^{0.85}$
Mechanical:	$0.284 (MW_{tt} \cdot \eta_{th})^{0.9} + 0.05 (MW_{tt} + MW_{tb})$
Piping and instr.:	$330 + 0.0015 (703.4 + L_{cc})^{0.7} (MW_{tt})^{0.85}$ $+ 1.183 (L_{cc} - 88) + 0.296 (0.4 \sqrt{P} - 17.6)$
Electrical:	$23 + 1.73 (P_{aux})^{0.65} + 0.0508 (841 + L_{cc})$ $+ 0.316 P_{aux}$
L_{cc}	= Length of central cell, m
P	= Power input to DC, MW = $P_f/Q + 0.2 P_f$
MW_{tt}	= Thermal megawatt from blanket + thermal megawatt from DC = $MW_{tb} + P(1 - \eta_{DC})$
η_{th}	= Thermal conversion efficiency (turbine cycle efficiency)
P_{aux}	= $10 + 0.08 MW_{tt} \cdot \eta_{th} + 0.1 P_f/Q \cdot \eta_{inj}$

DESIGN REVIEW AND CRITIQUE*

This subsection of the report summarizes the comments and opinions expressed by the ORNL review team. The efforts of J. R. Engel to organize the team are appreciated. Table 7-22 lists the ORNL contingent. Some of the reviewers are now retired, but still participate as part of this review effort. The thoughtful evaluation of these individuals and their openness has added significantly to the understanding of molten salt technology as applied to a TMHR.

*Review comments from R. McGrath, Exxon Corp., are appreciated.

TABLE 7-22. ORNL review team.

E. S. Bettis (Ed)	SAI
R. B. Briggs (Beecher) ^a	Consultant
S. Cantor (Stan)	ORNL
W. P. Eatherly (Walt)	ORNL
J. R. Engel (Dick)	ORNL
W. R. Grimes (Warren)	ORNL
P. N. Haubenreich (Paul) ^a	ORNL
H. E. McCoy (Herb)	ORNL
L. E. McNeese (Gene) ^a	ORNL
M. W. Rosenthal (Murray) ^a	ORNL
R. T. Santoro (Bob)	ORNL
R. E. Thoma (Roy)	ORNL

^aFormer MSR program director

The review comments and critique are broken down into five subsections: 1) general comments, 2) materials considerations, 3) neutronics considerations, 4) mechanical, maintenance, and safety considerations, and 5) molten salt chemistry/chemical processing and BOP considerations.

GENERAL COMMENTS

About 30 years of work are needed to make fission molten salt technology viable. The technology development will cost about \$1 billion and to that must be added two to four test reactors at \$1-2 billion each with extensive blanket testing. A molten salt-cooled TMHR would also require a significant development program. Some critical molten salt components (steam generators, mechanical valves, and several instruments) have yet to be developed. Fully remote maintenance for a molten salt system has not yet been demonstrated.

MATERIALS COMMENTS

To make use of common fluoride salts it is necessary that operating temperatures be above those thought acceptable for iron and nickel-base alloys. Molybdenum is a candidate structural material that logically must be considered because of its high melting point, good corrosion resistance in salts, and its excellent high-temperature strength.

Molybdenum is presently used in very selected applications requiring small diameter tubes and thin sheets. ORNL attempted to build a small processing facility utilizing molybdenum vessels about 4 in. diam x 12 in. long and found that they were pressing the technology. The facility was partially completed before funding for the entire project was terminated, but a good understanding was obtained of the fabrication problems associated with molybdenum. Many of the problems with molybdenum are associated with scale-up and can be solved as production demand increases. However, the inherent brittleness of recrystallized molybdenum is a fact of nature and will likely never be changed. Interstitial elements such as oxygen, nitrogen, and carbon have very low solubilities in molybdenum and are concentrated in the grain boundaries during recrystallization. Welding not only leads to recrystallization but has the further detrimental effect of adding more interstitial elements as contaminants. Thus, it is not likely that a massive welded molybdenum structure can ever be fabricated. This would not simply require an advancement of technology but a change of basic property of molybdenum. Cox and Wiffen of ORNL have observed that the displacements caused by irradiation raise the ductile-to-brittle transition temperature (DBTT) of molybdenum. This means that even the unrecrystallized base metal may be brittle after irradiation. Thus, molybdenum and its alloys are not reasonable candidates for structural components of a fusion device. (This is not to say that molybdenum could not be used as a limiter or other low-- stressed, unwelded components.)

Niobium and tantalum (and their dilute alloys) have attractive high temperature properties and are more ductile than molybdenum. Their main shortcoming stems from embrittlement due to the absorption of oxygen, nitrogen, carbon, and hydrogen. Although niobium and tantalum weld deposits can be ductile, it is necessary that they be protected from contamination while molten. The necessary degree of protection can only be obtained by welding in a vacuum enclosure, and this limitation is very serious for an engineering system. It is further necessary that these materials be protected during operation at temperatures above 400°C, and a vacuum of about 10^{-7} Torr would be required. Thus, niobium and tantalum (and their alloys) are usable engineering materials, but it will be very expensive to fabricate and operate a large system without embrittlement by environmental contamination.

Expected Difficulties with Graphite

Eatherly pointed out that it would be difficult to have a graphite that was both nonswelling and nonpermeable to helium. Although bulk graphite (porous) and pyrolytic graphite (nonporous) have reasonable irradiation stability individually, they should not be used together (a pyrolytic sealing layer on bulk graphite) because their irradiation deformation occurs at different rates. The graphite layers would separate or damage one another during irradiation. He also indicated that specialty graphites like low temperature isotropic graphite (LTIG), which may possibly work, were expensive.

Eatherly did state that a high density graphite (like Poco grade) would be low swelling and impermeable to molten salt, but that helium and tritium would easily pass through it. This would allow tritium to be trapped in the multiplier rods and decay away to helium. The high graphite creep rate will allow the cladding to follow slow, steady state growth of the beryllium rod.

Rod failure may be a serious problem. Contact between the molten salt and the beryllium will cause the precipitation of uranium or thorium in that area. Hot spots could develop. Beryllium is currently produced as a side product of other chemical processes. Availability and cost probably need not be major concerns for this design.

Reactions Between Tritium and Beryllium

It was pointed out that tritium would diffuse through the graphite cladding and react with the beryllium, thus tying up the tritium and preventing its reprocessing. However, this fear is unfounded since tritium does not react with beryllium at temperatures up to 1000°C (R. P. Elliot, Constitution of Binary Alloys, McGraw-Hill, 1965, p. 162). Tritium may be held up extensively in the graphite.

NEUTRONICS CONSIDERATIONS

The ORNL nuclear physics staff made a few general comments for which Harless has developed responses. For these situations, the comment (C) is presented first, then the response (R).

- C. Neutron cross sections should be temperature corrected.

R. Our neutron cross sections for SN1D calculations were corrected to a molten salt temperature of 560°C. The LLL cross sections used in our Monte Carlo calculations are not temperature corrected. An evaluation of this difference in treatment has not yet been made.

C. There will be a significant amount of tritium generated due to neutron reactions with beryllium.

R. For the reference case our Monte Carlo results indicate that the total amount of tritium generated from beryllium in the neutron multiplier rods and in the molten salt is about 1.5% of the amount generated in the Li-6; i.e., the contribution due to neutron reactions with beryllium would be about 2.7 kg/yr.

C. Molybdenum (TZM is 99.4% Mo) will be subject to significant radiation damage if used as a structural material. ORNL suggests Nb-1 Zr or Ta as alternates.

R. From a neutronics standpoint, Nb-1 Zr would be the best choice. The thermal neutron capture cross sections of Ta, Nb, and Zr are 21.5, 1.13, and 0.184 b/atom, respectively. Therefore, the parasitic neutron capture in Ta would be proportionately higher than for Nb and Zr. Also, natural Ta is 99.988% Ta-181, which transmutes into the highly radioactive isotope Ta-182 after neutron capture. The Ta-182 nucleus has a half-life of 115 days and, following decay, usually emits a high energy gamma approximately in the range 1.0 to 1.5 MeV.

C. How do you calculate the energy deposition from secondary gammas?

R. For our SN1D and TARTNP scoping analyses the gamma energy is deposited at the site of creation. This is the standard procedure used in all our preliminary LMFBR studies. However, for a refined design, we must treat the neutron-generated gamma source separately and perform the photon transport analysis.

Balance of Plant Comments

A complete MSBR-type processing system is not needed. Only generated ²³³U should be isolated by a fluorination process. Buildup of fission and corrosion products in the plant lifetime will not be significant; hence no need to remove them via a processing system.

The gaseous treatment part of the molten salt processing system is adequate as shown in Figs. 7-23 and 7-24.

The following are information comments by ORNL:

- The neutron cross section for the reaction $^{19}\text{F} (n, \alpha) ^{16}\text{N}$ is high enough to cause some concern about the generation of ^{16}N gamma emission. This should be investigated.

- Breeding ratios may be overpredicted due to the assumption of blanket homogeneity. Also, some of Santoro's experiments have shown that in a heterogeneous geometry neutron source "hot spots" may appear such that for some blanket or shield locations, the primary neutron source appears to be spatially shifted.

- The neutron cross sections related to tritium and ^{233}U breeding are fairly well known. (ENDF/B-IV and ENDF/B-V evaluations are available.) However, it might be worthwhile to perform a sensitivity study to see how blanket performance is affected if an important cross section is varied by a few percent. Also, the effect of density and temperature uncertainties could be examined in this way.

- Xenon and krypton fission products will leak into the voids between the beryllium granules and provide undesired radioactive sources. Xenon will introduce the most severe gamma source.

- If we use Hastelloy-N as a first wall and/or pressure boundary, we will have to be concerned with radiation damage; i.e., the (n, α) reaction in nickel will be a problem.

MECHANICAL, MAINTENANCE, AND SAFETY CONSIDERATIONS

Several questions in this area were prepared ahead of time for ORNL to review and respond to. The following are our questions and the ORNL answers:

Q. Are there flow problems unique to molten salt?

A. It was recommended that the design change the flow pattern to the inlet at the bottom and exit at the top. This method eliminates gas entrapment during fill and operation. MSRE had success with this flow pattern. The transition from laminar to turbulent flow occurs in molten salt at a Reynolds number 2 to 3 times higher than for other liquids. There is as yet no explanation for this phenomenon.

Q. Are mechanical joints allowed with molten salt?

A. MSRE did use mechanical joints at some locations. However, the pipes being joined were small in diameter. The maximum size was for a 5-in. diam pipe, which had a flange diameter of 18 in. that included a cold salt seal backed up by an O-ring seal. It appears ORNL may consider using mechanical joints on 1- to 2-in. size pipes. We recommend having welded joints for large size pipes and certainly for the 30-in. pipes under consideration.

Q. Does freezing and thawing of the molten salt cause hidden problems?

A. Freezing and thawing should not be a problem if it is done slowly so that the melting takes place from the outer portion of the salts to the center, eliminating any possibility of over-stressing the component. Because the salt is a multicomponent chemical mixture, the frozen salt will be of a different composition than the molten salt phase, and the frozen salt will thaw at a temperature determined by its composition. In the case of the MSBR salt the melting temperature has been observed to be up to 60°C above the freezing temperature. Because of this effect, freezing and thawing of localized areas should be done with care because a frozen plug of salt could be released and move downstream to create a temporary flow blockage.

Q. Will frozen salt seal a conduit for downstream maintenance?

A. The salt has a large heat capacity and may take a long time to freeze, but it could be done. However, there is no reason to consider having a seal since a sodium/air problem does not exist with the salt. To repair an area simply drain the salt and remove and replace the component in an air atmosphere. After a reactor operation this is required to be done remotely.

Q. How and where would large quantities of salts be manufactured? How transported?

A. Large quantities of molten salt were not a requirement for the MSRE project. Thus, ORNL formulated the salts themselves. To prepare salt mixtures BeF_2 and LiF , in the proper proportions, were heated to 600°C and treated with HF and H in a copper vessel. Most impurities could be removed in this way. The resulting salt had only 3-4 appm impurities. To prepare the molten salt to be used in TMHR Th would then be dissolved in the purified salt to the desired concentration. For transfer, the molten salt was simply placed in drums and allowed to solidify, then heated when necessary for transfer into the system tanks.

Q. What is the cost of the molten salt?

A. The true cost of the molten salt for the MSRE could not be determined because ORNL did most of the salt preparation and cleaning work themselves. Purification costs are expected to be something much less than \$100/lb of product. Some current price estimates are: BeF_2 - \$15/lb, Be powder - \$80/lb, Li (natural) - \$20/lb, and ^7Li (at 50 appm ^6Li) \$120/kg. The large quantities of salt required for the proposed TMHR/MS system would probably be sufficient to justify an on-site plant operated by a normal salt supplier.

Several questions were raised concerning the flow of molten salt in the presence of a magnetic field. While every effort is made to avoid flows across the field lines, the issues listed below remain unsolved:

- Can adequate mixing of the salt, necessary to sufficiently cool the portion of the blanket closest to the plasma, be achieved?
- Is the molten salt chemically stable in induced fields of 0.5 to 1.5 V?
- Will the induced fields result in enhanced corrosion? These problems are specific to the TMHR design. Consequently, the ORNL staff had no experience with them.

The following are a few additional comments:

- Startup of a molten salt reactor, both initial and following a maintenance outage, could present some unique design problems. It is believed the initial startup will require the salt to be flow checked through the system before the reactor is activated to ensure a leak-proof system. How the molten salt temperature is obtained and maintained could have an impact on the design. ORNL designed their conceptual reactor in a furnace for heating. Preheating time in the blanket may limit the plant availability.
- Additional design requirements could be necessary for startup following a maintenance outage.
- Molten salt does not easily wet steels or graphite so 1/4- to 1/2-in. holes are the minimum size the salt will drain through.
- Molten salt cleans metals so that self welding (galling) at very low contact pressures is to be expected. Due to this problem, there have been no mechanical molten salt valves at ORNL. The molten salt must also be isolated from pump bearings and any other moving interfaces. The MSRE did use "freeze valves," flattened sections of loop piping that can be cooled by an external coolant (air) to freeze a plug of salt in the pipe as a valve.

- Even though the vapor pressure of the molten salt is very small, offgassing or venting the molten salt can cause misting and dusting that can damage or plug hardware.
- Molten salt does not release a lot of active gas while freezing (as in a spill).
- The large tritium production rate and large quantities used in the fusion driver may make containment cleanup much more complex than currently anticipated. The blanket and primary loop must be designed to avoid pockets that can trap free gases.
- There is a question of ever being able to license a commercial facility with beryllium in it due to the toxic nature of beryllium in any form.
- All parts of the loop (pipes, valves, pumps, seals, welds, etc.) must be designed for fully remote maintenance.
- All hardware and buildings must be designed to allow salt spills to drain off to tanks before freezing.

Salt Flow and Recovery Systems

The following comments and recommendations were made concerning pumping of the molten salt in the blanket:

- Top to bottom flow of the molten salt, thought necessary to ensure that the salt could be quickly drained into a holding tank in an accident situation, is not advisable. Bottom to top flow would help to avoid formation of bubbles in the blanket modules. The salt has a very large heat capacity. It can easily be drained to a holding tank before it freezes if an accident occurs.
- It was noted that it would be necessary to preheat the entire blanket structure prior to salt fill. It was not clear that this could be done using helium gas. Providing electrical heaters to the blanket structure may be necessary. These would take up room complicating the design considerably, since shielding for the magnet coils already limits the available space.
- Remote maintenance for the TMHR system was viewed as a difficult and complicated task. As mentioned earlier, since mechanical joints cannot be used on molten salt feed pipes, even routine maintenance may involve a substantial amount of welding.

Concerning recovery and removal systems, the following comments were recorded:

- Uranium removal of a fluoride precipitate is easily accomplished.
- Protactinium and rare earth removal may not be necessary for such low fission rates. The cycle time for the molten salt in the TMHR is 30 days. Since the half-life of Pa is only 27 days and the removal process is only about 50% efficient, it may not be worth the trouble and expense to incorporate a Pa removal system into the reactor design.

MOLTEN SALT CHEMISTRY/CHEMICAL PROCESSING AND BOP CONSIDERATIONS

Grimes of the ORNL Chemical Technology Division presented a tutorial on molten salt chemical considerations, and a summary is included in Appendix B. The following are general comments on the molten salt chemistry and chemical processing that were offered by various ONRL reviewers:

- Major chemical treatment of the salt has not yet been demonstrated. Prior tests used batch processing.
- Due to the low fission rate, fission product buildup in the blanket is very slow. It seems likely that cleanout of the fission products from the salt is not needed for the life of the plant (about 30 years). In any case the salt reprocessing chemistry worked out for fission systems will only remove some products, not all; thus, the molten salt is always "dirty" after its first use.
- The salt reprocessing can be even more simplified by letting the Pa decay to ^{233}U and then cleaning the uranium from the system. Uranium cleanup of the salt is easily done by fluorination to 10^{-4} molar fraction. Cleanups to 10^{-6} to 10^{-9} molar fraction have been done.
- If the molten salt contacts the beryllium, U, Pa, and Th will precipitate from the salt at the contact location as Be is taken up. One-half to 1% of the rods with simultaneous cladding failures may swamp the loop with Be and decompose the salt. Gradual cladding failures (excess Be) may be tolerable if the number at any one time is small.
- Control of the salt chemistry (reduction/oxidation) will be difficult. The tritium production from Li and the Be (n, 2n) reactions both increase the fluoride ion concentration (oxidative nature) in the salt. There

is not enough uranium in the salt to use as the redox buffer and other methods may not be as good.

- The data on Ce is too limited to allow a numerical analysis of using Ce as the redox buffer in the salt, although qualitatively it looks reasonable.

- There is not substantive data on the electric potential corrosion of the blanket structure in molten salt, so the I-V design limit may not be conservative enough.

The following comments concern the tritium handling and the secondary loop:

- A He secondary loop to isolate the thermally sensitive molten salt primary loop from BOP transients is useful. This will significantly reduce the possibility of an IHX freezeup due to the low heat capacity of the He.

- Due to the surface area and thin tubes of the IHX, about 80% of the gaseous tritium in the salt will diffuse into the secondary loop (He), where cleanup will be easy.

- Centrifugal separators ahead of the IHX for the full primary loop salt flow may be able to separate a large portion of the bred tritium before it reaches the secondary coolant.

- Tritium recovery is expected to be a complicated task. Tritium will certainly find its way into the secondary coolant loop. For this reason and because of accidental mixing of the secondary coolant with the molten salt, it was noted that the use of He as the secondary coolant was an excellent choice.

REFERENCES

1. J. W. Feldmann to J. F. Cage, Jr., "Trip Report on LLL Hybrid Project Meeting," YL-886-JWF9056, 9 May 1976.
2. R. W. Moir, Editor, "Interim Report on the Tandem Mirror Hybrid Design Study," Lawrence Livermore Laboratory Report UCID-18078 (1979).
3. J. D. Lee, "The Beryllium/Molten Salt Blanket - A New Blanket Concept," Lawrence Livermore Laboratory Report UCRL-82663 (1979).
4. W. R. Grimes, "Molten Salt Reactor Chemistry," Nuclear Applications & Technology, Volume 8, No. 2, February 1970, pp. 137-155.
5. Alloy Development for Irradiation Performance, Quarterly Progress Report, Oct-Dec 1978, DOE/ET-0058/4 May 1979, p. 93.
6. J. J. Holmes, R. E. Robbins, and A. J. Lovell, "Postirradiation Tensile Behavior of 300 Series Stainless Steels," Irradiation Effects in Structural Alloys for Thermal and Fast Reactors, ASTM-STP-457 (December 1969).
7. M. Kangilaski, J. S. Perrin, and R. A. Wullaert, "Irradiation Induced Embrittlement in Stainless Steel at Elevated Temperatures," Irradiation Effects in Structural Alloys for Thermal and Fast Reactors, ASTM-STP-457.
8. J. J. Laidler, "Alloy Properties Datebook," TC-293 (Rev. 2), June 30, 1976.
9. F. W. Wiffen (ORNL), personal communication.
10. H. E. McCoy, Jr., "Status of Material Development for Molten-Salt Reactors," ORNL/TM-5920, October 1977.
11. T. H. Webster, B. L. Eyre, and E. A. Terry, "The Effects of Fast Neutron Irradiation on the Structure and Tensile Properties of Molybdenum and TZM," Irradiation Embrittlement and Creep in Fuel Cladding and Core Components, British Nuclear Energy Society, London (1973), p. 61-80.
12. H. E. McCoy, Jr., et al., "New Development in Materials for Molten-Salt Reactors," Nucl. Appl. & Tech., Vol. 8 (Feb. 1970), p. 156-167.
13. S. R. Engle and W. P. Eatherly, "Irradiation Behavior of Graphite at High Temperature," High Temperatures - High Pressures, Vol. 4, p. 119-158.
14. R. A. Wood, "Beryllium - Utilization/Availability," July 1975, MCIC SR-75-02.
15. Mineral Commodity Summaries 1979, Bureau of Mines, U. S. Department of the Interior.

16. Mineral Facts and Problems, 1975 Edition, Bureau of Mines Bulletin 667, p. 139.
17. P. J. Bender, "Reference Design for the Standard Mirror Hybrid Reactor," UCRL-52478, May 22, 1978.
18. J. D. Lee, "The Beryllium/Molten Salt Blanket - A New Blanket Concept," Preprint UCRL-82663, April 25, 1979.
19. R. Protsik, "SN1D - A One-Dimensional Discrete Ordinates Transport Code with General Anisotropic Scattering," GE-FBRD, FBRD-00074 (IR), February 1978.
20. J. Kimlinger and E. Plechaty, "TARTNP User's Manual," UCID-17026, February 9, 1976.

jbs/1771t

SECTION 8
SYSTEMS ANALYSIS

SYSTEM MODELING AND ANALYSIS

(J. D. Lee)

This subsection covers the objectives, modeling, and results of the system analysis work done in support of the initial (scoping) phase of the Tandem Mirror Hybrid Reactor (TMHR) project.

OBJECTIVES

The principle objective is to compare the various blanket options being considered vs tandem mirror driver performance. The intent is to quantify gross differences in the blanket options to aid us in choosing the most appropriate type blankets to pursue. A second objective is to examine the effects of different plasma physics and fusion technology regimes to aid in choosing those as well.

SYSTEM MODEL

To compare hybrid performance with different blankets and plasma regimes in a reasonably consistent manner, we developed a minisystem model. The model calculates power level and cost of the hybrid components, net hybrid output (electricity and fissile material), fissile material cost information, support ratios, system capital cost, capital cost ratio, and fission burner electricity cost information.

A power flow diagram of the system model is shown in Fig. 8-1. The power levels of the hybrid reactor's subsystems are calculated to result in a desired nuclear power level (fusion power plus fusion neutron induced energy amplification). Hybrid net electric power is determined based on P_f , Q , and component efficiencies. The production rate of net fissile material is calculated based on fusion power (as calculated above) and the net average breeding ratio in the blanket.

Hybrid

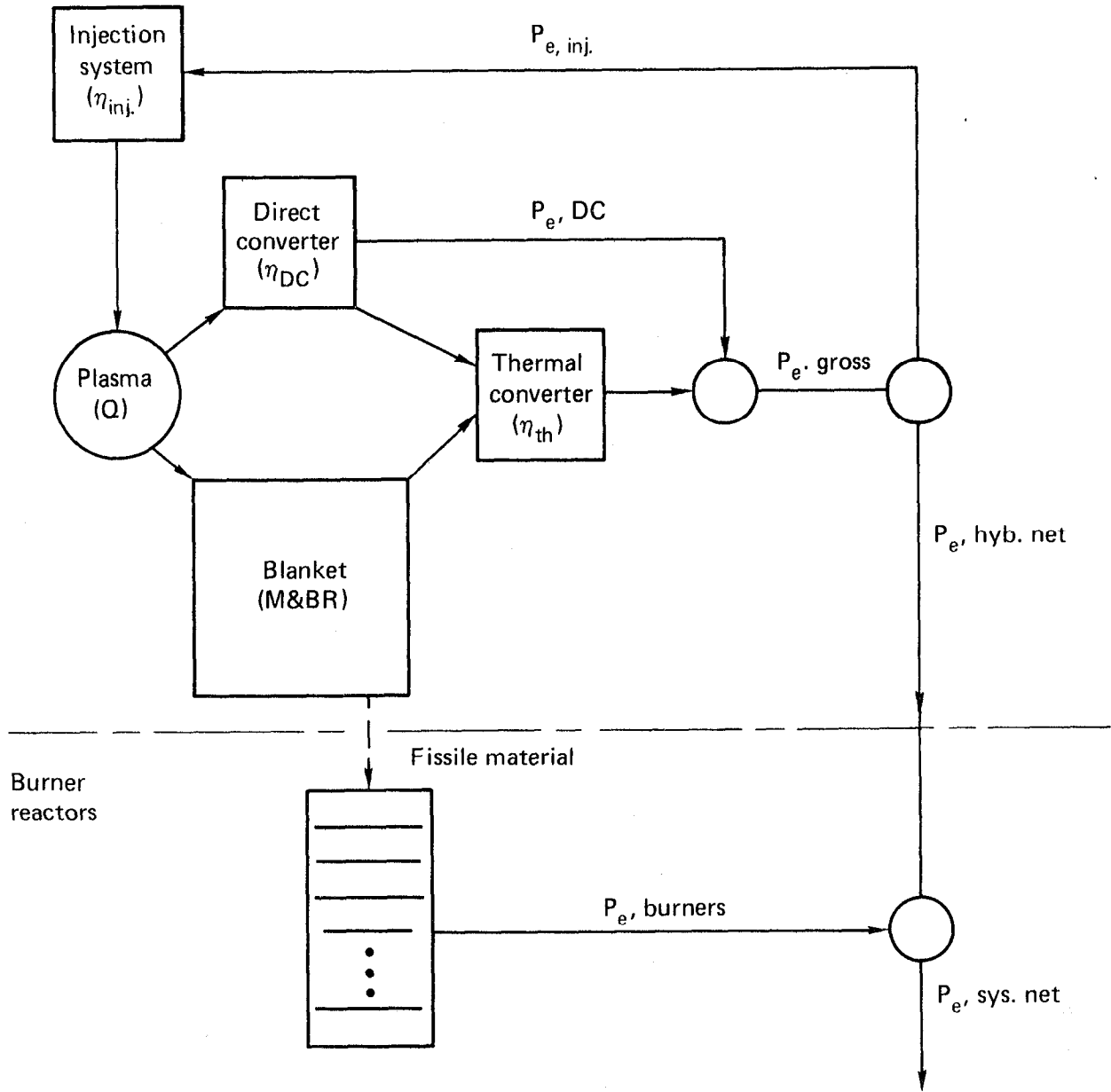


Fig. 8-1. System power flows.

Costs of the tandem mirror driver components are scaled with central-cell length and component power levels based on unit costs reported in the Tandem Mirror Reactor (TMR) report.¹ In the early phase of this work blanket and balance of plant (BOP) costs were also based on Ref. 1. For later phases water and He-cooled blanket costs (and performance) and BOP cost estimates were provided by our subcontractors (General Electric, General Atomic, Bechtel, respectively). Central-cell shielding and magnetic coil costs, like all the other fusion component costs, are based on Ref. 1. Total direct capital cost of the hybrid is determined by summing the component direct costs. Capital cost of fissile material produced (\$/g) is determined by multiplying hybrid direct capital cost by 1 + an indirect cost factor, and by a capital (or fixed) annual charge rate, then dividing by the average annual net fissile production rate and by the hybrid's capacity factor. Total fissile material cost (\$/g) is the sum of capital cost, fuel cycle + O&M, and power. Fuel cycle + O&M cost is an input quantity. Hybrid power cost is based on burner power cost (mills/kWhe), which is dependent on fissile material costs. Since fissile material cost and burner power cost are dependent variables, two linear simultaneous equations are solved to find the unique set of fissile and power costs.

The model then determines electric power level of the burners fueled by the hybrid (hybrid fissile production rate/burner consumption rate), the electric support ratio ($P_{e, burners}/P_{e, hybrid}$), the nuclear support ratio ($P_{nuclear, burners}/P_{nuclear, hybrid}$), and the system power ($P_{e, burner} + P_{e, hybrid}$); assuming equal capacity factors for hybrids and supported burners. Finally, system direct cost (mills/kWhe) and direct cost ratio (C'_{system}/C'_{burner}) are determined.

Fusion driver performance is integrated into the following input variables:

$$\begin{aligned}
 Q_f &\equiv P_{fusion}/P_{injection, trapped} \\
 P_f &\equiv P_{fusion}/\text{central-cell length (MW/m)} \\
 \text{Eff.}_{inj} &\equiv P_{injection, trapped}/P_{e, injection} \\
 \text{Eff.}_{dc} &\equiv \text{Direct conversion efficiency} = P_{e, dc}/P_{leakage}
 \end{aligned}$$

SYSTEM MODEL DETAILED DESCRIPTION

A detailed description of the system model is given in this subsection. All variables are identified and defined.

- Fusion power (P_f)

$$P_f = P_{\text{nuclear}} / (0.2 + 0.8 M) ,$$

where

P_{nuclear} = desired nuclear power level of the hybrid reactor (input).

M = blanket 14 MeV neutron energy multiplication (input).

- Central-cell cost (C_{cc})

$$C_{cc} = (P_f / P'_f) \cdot C'_{cc} ,$$

where

P'_f = fusion power per meter of central cell (input).

C'_{cc} = central cell cost per meter (input).

- Plasma leakage power (P_l)

$$P_l = (1/Q + 0.2) P_f ,$$

where

Q = fusion power/injected power (input).

- Electrical power generated in direct converter ($P_{e,dc}$)

$$P_{e,dc} = P_l \cdot \text{Eff.}_{dc} ,$$

where

Eff._{dc} = direct conversion efficiency (input).

- Direct converter cost (C_{dc})

$$C_{dc} = (0.13 + 0.035) \cdot P ,$$

where the coefficient 0.13 M\$/MW is taken from the TMR report,¹ and 0.035 is for direct converter related BOP.

- Electric power generated by thermal converter ($P_{e,th}$)

$$P_{e,th} = (P_{\text{nuclear}} + P_f/Q - P_{e,dc}) \text{Eff.}_{th} ,$$

where Eff._{th} = thermal to electric conversion efficiency (input)

(Note: This efficiency is assumed to reflect mechanical power used to run refrigeration system and the other auxiliary systems.)

Thermal conversion system plus thermal energy related BOP costs

(C_{th}) is $C_{th} = 0.11 \cdot P_{e,th} / \text{Eff.}_{th} ,$

where the coefficient 0.11 M\$/MW_{th} was provided by Bechtel

(molten salt case).

- Electrical equipment cost ($C_{el. eq.}$)

$$C_{el. eq.} = 0.054 \cdot P_{e \text{ gross}}$$
 where the coefficient 0.054 M\$/MWe gross was provided by Bechtel (molten salt case).
- Electric power to injector ($P_{e, inj}$)

$$P_{e, inj} = P_f / Q / \text{Eff.}_{inj}$$
 where Eff._{inj} = injector efficiency (input).
- Recirculating electric power fraction (R_{el})

$$R_{el} = P_{e, inj} / P_{e \text{ gross}}$$
- Net electric power from hybrid ($P_{e, hyb}$)

$$P_{e, hyb} = P_{e \text{ gross}} - P_{e, inj}$$
- Net electrical efficiency of the hybrid (Eff._{hyb})

$$\text{Eff.}_{hyb} = P_{e, hyb} / P_{\text{nuclear}}$$
- Cost of injection system (C_{inj})

$$C_{inj} = 0.320 \cdot P_{e, inj}$$
 where the coefficient is 0.320 M\$/MWe.¹
- Total direct cost of hybrid ($C_{hyb. dir.}$)

$$C_{hyb. dir.} = 758 + \text{sum of previous costs}$$
 where 758 M\$ are fixed costs consisting of:

- Plugs	171 M\$
- Crawler-transporter ¹	22
- Other	<u>140</u>
	333 ⁽¹⁾ + 425 (BOP costs from Bechtel)
- Unit direct cost of hybrid [$C'_{hyb. dir.}$ (M\$/MWe)]

$$C'_{hyb. dir.} = C_{hyb. dir.} / P_{e, hyb.}$$
- Fissile production rate [FP (kg/y)]

$$FP = 4.32 \cdot P_f \cdot BR$$
 The coefficient is for ²³³U; for ²³⁹Pu it is 2.6% higher.

$$BR = \text{fissile breeding ratio (atoms/DT neutron) (input)}$$
- Capital cost of fissile material ($C'_{fiss. cap.}$ \$/g) calculated and printed

$$C'_{fiss. cap.} = 1580 \cdot C_{hyb. dir.} \cdot \text{fixed charge rate/FP/Hyb. cap. factor}$$
 where coefficient = (1 + indirect cost factor) x \$/m\$/g/kg

$$= (1 + 0.58) \cdot 1000.$$

- The indirect cost factor (0.58) provided by Bechtel.

- A fixed charge rate was of 0.0674 was recommended by T. Osborne of GE.

- Hybrid capacity factor is input.

- Power cost of fissile material ($C'_{\text{fiss. power}}$ (\$/g) at cost of power from burner, C'_{burn} (mills/kWhe)

$$C'_{\text{fiss. power}} = 88 \cdot (-P_{e,\text{hyb.}})/FP \cdot C'_{\text{burner}}$$

where coefficient = $8760 \text{ (h/y)} \cdot 0.001 \text{ (\$/mill)} \cdot 1000 \text{ (kW/MW)} \cdot 0.001 \text{ (kg/g)}$.

- Cost of electric power from burner [C'_{burner} (mills/kWhe)]
Since this model assumes the cost of hybrid power (+ or -) is equal to the cost of fission burner power in the hybrid-burner system,

C'_{burner} and $C'_{\text{fiss tot}}$ (\$/g) are dependent variables.

$$\text{Let } C'_{\text{fiss tot}} = X$$

$$C'_{\text{burner}} = Y$$

$$X = C + DY$$

$$Y = A + BX$$

where

$$C = C'_{\text{fiss. cap.}} \text{ (\$/g)} + (\text{fuel cycle} + \text{O\&M})_{\text{hyb.}} \text{ (\$/g)}$$

$$D = 8.8 \cdot (-P_{e,\text{hyb}})/FP \text{ (\$/g/mills/kWhe)}$$

$$A = 245 \cdot C'_{\text{burner, cap., direct}} \cdot \text{Capital charge rate} + (\text{fuel cycle} + \text{O\&M})_{\text{burner}} \text{ (mills/kWhe)}$$

where coefficient

$$245 = \frac{(1 + \text{indirect cost factor})}{8760 \text{ (h/y)} \text{ Cap. factor}} \cdot 10^9 \text{ (mills/M\$)} \cdot 10^{-3} \frac{\text{kW}}{\text{MW}}$$

$$\text{Indirect cost factor} = 0.5$$

$$\text{Capacity factor} = 0.7$$

$C'_{\text{burner, cap., direct}}$, capital charge rate, and fuel cycle + O&M are input.

B = fissile depletion and inventory charge rate to burner (mills/kWhe/\$-fiss.) input.

$$Y = \frac{A + B \cdot C}{1 - B \cdot D}$$

A graphical solution of the burner electric cost and hybrid fissile cost equations is shown in Fig. 8-2.

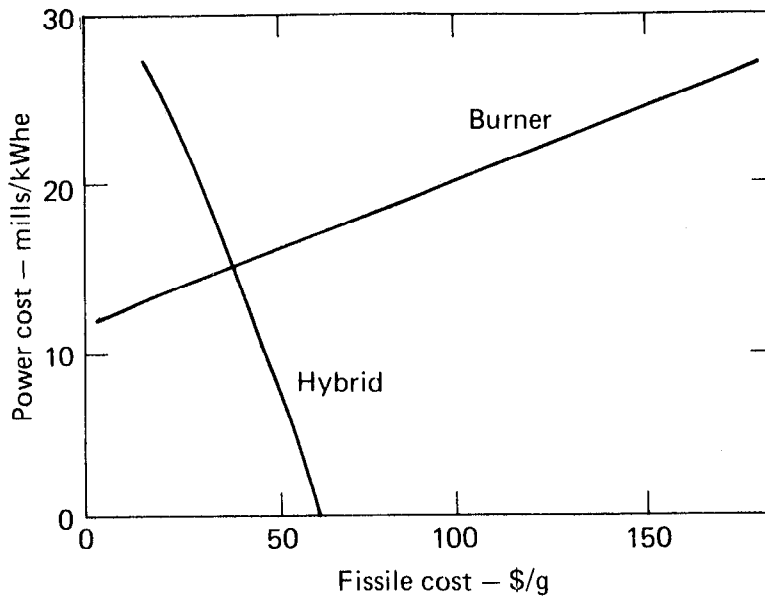


Fig. 8-2. Graphical solution of burner electric cost and hybrid fissile cost.

- Total cost of fissile material ($C'_{\text{fiss. tot.}} \text{ \$/g}$)

$$C'_{\text{fiss. tot.}} = (C'_{\text{fiss. cap.}} + C'_{\text{fuel cycle}} + \text{O\&M}) + C'_{\text{fiss. power}} = C + DY$$

where

fuel cycle + O&M are input.

- Power of fission burners supported ($P_{e, \text{burn.}}$)

$$P_{e, \text{burn.}} = FP/FM \text{ ,}$$

where

FM = fissile make-up (kg/MWe-Y) (input).

- Support ratio, electric (SR_{e1})

$$SR_{e1} = P_{e, \text{burn.}} / P_{e, \text{hyb}}$$

- Support ratio, nuclear (SR_n)

$$SR_n = P_{e, \text{burn.}} / P_{\text{nuclear}} / \text{Eff.}_{\text{th, burn.}} \text{ ,}$$

where

$\text{Eff.}_{\text{th, burn.}}$ = thermal efficiency of burners (input).

- Electric power of hybrids plus burners ($P_{e, \text{tot}}$) calculated and printed

$$P_{e, \text{tot}} = P_{e, \text{hyb}} + P_{e, \text{burn.}}$$

- System direct capital cost ($C'_{\text{sys,dir}}$) calculated and printed

$$C'_{\text{sys,dir}} \text{ (M\$/MWe)} = (P_{\text{e,burn.dir.}} \cdot C'_{\text{burn.}} + C_{\text{hyb.dir.}}) / P_{\text{e,tot}}$$

where

$C'_{\text{burn.dir.}}$ = unit direct cost of burner (M\$/MWe) (input).

- System direct capital cost ratio ($R_{\text{dir. cost}}$) calculated and printed

$$R_{\text{dir. cost}} = C'_{\text{sys. dir.}} / C'_{\text{burn}}$$

- Burner power cost [C'_{burner} (mills/kWe)]

$$\text{Total} = Y$$

$$\text{Less fissile} = A$$

$$\text{Fissile} = Y - A$$

SYSTEM MODELING RESULTS

System modeling results are reported in four phases.

Phase I Results

For the first phase of the scoping study four generic blanket types are coupled with two perceived extremes in fusion driver performance. Performance estimates of the four blanket types used in the analysis are listed in Table 8-1.^{2,3} The U and Th blankets rely on fast fission (n,2n) and (n,3n) reactions in the fertile materials for neutron multiplication. The Be + Th (molten salt) blanket uses Be (n,2n) reactions for neutron multiplication. Performance parameters for the two fusion drivers used are given in Table 8-2. The high performance driver case is modeled after the TMR, while the low performance driver case is taken to represent two-component operation. The low performance case is given lower efficiency injection and direct conversion as well.

Hybrid reactor costs are scaled directly from costs reported for TMR. The central-cell cost per meter is 4.73 M\$. Neutral beam injector costs scale directly with electric power input (320 \$/kW), direct convertor (or beam dumps) scale with plasma leakage power (130 \$/kW), thermal system scales with thermal power (70 \$/kW), and electrical equipment cost scales with gross electric power (74 \$/kWe). In addition, there are fixed costs of 353 M\$ consisting of plugs

Table 8-1. Blanket neutronics - representative types and performance.

Blanket type	Nuclear performance (anticipated) ^a			
	Breeding ratios			Energy multiplication, M
	²³⁹ Pu	²³³ U	T	
U	1.5	0	1.0	11
Th	-	0.6	1.0	3.4
BE + Th	-	0.8	1.0	1.6
U/Th	0.6	0.7	1.0	7.6

^aTime and spatially averaged.

Table 8-2. Driver performance parameters.

Parameter	High (TMR)	Low (two-component)
Q	4.8	1.0
Fusion power ^a	2500	500
First-wall radius, m	1.6	Same
Wall loading, Γ_n	2.1	1.0
P' _f , MW/m	25	12
Injection efficiency	0.72	0.60
Direct conversion efficiency	0.60	0.50

^aPower at which plasma parameters were calculated.

(171 M\$), plus buildings (20 M\$), crawler transportation (22 M\$), and other (140 M\$). Total capital cost is taken to be 2.5 times direct cost. Thermal conversion efficiency (net) is taken to be 35%.³ Capacity factors of 0.74 for the U and Th blanket cases and 0.80 for the Be/molten salt blanket cases are used. A fuel cycle + O&M cost of 30 \$/g fissile is used for all cases.

Burner fission reactor data is listed in Table 8-3.

Table 8-3. Burner related input data.

Fissile makeup	0.4 kg ²³⁹ Pu/MWe-yr 0.2 kg ²³³ U/MWe-yr
Thermal conversion efficiency	0.32 (used only to calculate nuclear support ratio)
Direct cost	450 \$/kWe
Capital cost _{tot}	900 \$/kWe
Fixed charge rate	0.0674 (same as for hybrid)
Capacity factor	0.7
Fuel cycle without fissile makeup	1.7 mills/kWe
O&M	1.0 mills/kWe

Burner fissile cost consists of only depletion cost $C'_{\text{depletion}}$ (mills/kWe) = $0.114 \cdot \text{fissile makeup (kg/MWe-yr)} \cdot \text{fissile cost (\$/g)}$.

The results of the eight cases (four blankets x 2 drivers) are summarized in Table 8-4. The table lists hybrid fissile production costs in (\$/g) composed of capital, fuel cycle plus O&M, and power cost. Support ratios (burner power/hybrid power) and system direct capital cost ratio (\$ per kWe system/\$ per kWe burner) are also listed. Finally burner costs in mills/kWe composed of capital, fuel cycle (less makeup) plus O&M, and fissile makeup (from hybrid) are listed. Nuclear power of all cases is 4000 MW.

Comparing the results summarized in Table 8-4 shows that there is an economic advantage of the ²³³U producing Be blanket for high fusion driver performance when fissile makeup or total electricity costs are compared. With low driver performance, the Be and U/Th blankets are the same, but the Be blanket results in a negative hybrid power balance. When straight fissile costs (\$/g) are compared, the ²³⁹Pu-producing U blanket is best. When support ratios are compared, the Be blanket is the clear winner.

Table 8-4. Summary of Phase I results.

Fusion driver performance	High (Q=4.8,Γ=2)				Low (Q=1,Γ=1)			
	444	1370	2703	637	444	1370	2703	637
Fusion power, MW	U	Th	Be	U/Th	U	Th	Be	U/Th
Blanket type								
Hybrid output rates:								
Fissile, kg/yr	2880	3255	9341	3577	2880	3255	9341	3577
Electricity, MW	1375	1322	1246	1364	988	131	-1106	810
Fissile cost, \$/g:								
Capital	71	85	38	61	99	163	88	94
Fuel cycle + O&M	30	30	30	30	30	30	30	30
Power cost, at fission								
burner total mills/kWH	- 61	- 50	- 18	- 48	- 48	- 6	17	-31
TOTAL	40	65	50	43	81	187	135	93
Support ratio:								
Nuclear	5.6	12.7	36.5	9.56	5.6	12.7	36.5	9.56
Electric	5.2	12.3	37.5	8.97	7.3	125	-42.3	15.1
System direct cost ratio	1.07	1.08	1.05	1.06	1.22	1.31	1.21	1.19
Fission burner, Mills/kWhe:								
Capital	9.9	9.9	9.9	9.9	9.9	9.9	9.9	9.9
Fuel cycle (less								
makeup) + O&M	2.7	2.7	2.7	2.7	2.7	2.7	2.7	2.7
Fissile makeup	1.7	1.4	1.2	1.5	3.5	4.3	3.1	3.1
TOTAL	14.3	14.0	13.8	14.1	16.1	16.9	15.7	15.7

These initial results suggest that the most attractive blanket is one that produces a respectable amount of ^{233}U (breeding ratio ≈ 0.8) with little energy multiplication via nonfission neutron multiplication. Such a blanket (the Be case) has the technical advantages of the highest support ratios, produces no Pu, and minimizes after heat by suppressing fission; and, these advantages are achieved with no economic penalties. However, additional R&D might be necessary to produce a fusion device that is six times larger than for the U cases.

The Th blanket and low performance driver was then used to examine the effects of a number of input variations.

- Thermal conversion of hybrid heat was eliminated by setting $\Gamma_{th} = 0$ and reducing cost of the thermal handling equipment from 70 $\$/kW_{th}$ to 30 $\$/kW_{th}$. Fissile cost increased 30%, and system power cost increased 8%.

- Fixed charge rate was increased 123%--from 0.0674 to 0.14. Fissile cost increased 103%, and system power cost increased 98%. (Note: The reference cases assume a fixed charge rate of 0.0674. This is appropriate, because the model calculates all costs in constant dollars, inflation removed.)

- This case was then used to examine sensitivity to independent variations of Q and wall loading (Γ). Results are displayed in Fig. 8-3. It appears for this case at least, there is little incentive to increase Q much above 2 or wall loading much above 1 MW/m^2 .

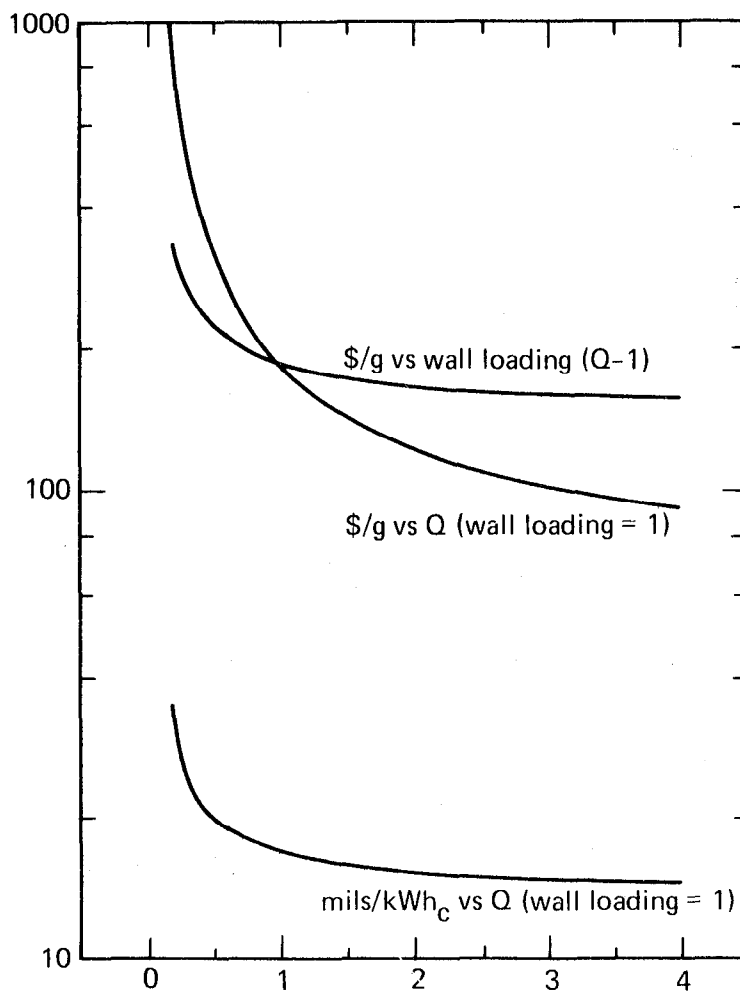


Fig. 8-3. System economics vs Q and wall loading (Γ) (base case is Th blanket and low technology driver).

• Bear in mind the minisystem model does not account for fissile material being removed and reprocessed in patches (must use cash flow techniques for that). Also the capacity factor was not varied with wall loading.

Since Q and wall loading are not independent, another series of cases was calculated to examine the tradeoff between these two important plasma physics parameters.

Results of this tradeoff for a modest technology TMR driver ($E_{inj} = 200$ keV, $B_{coil\ max} = 12$ T) and the Be + Th molten salt blanket is displayed in Fig. 8-4. The Q vs wall loading dependence used is for a $2500\ MW_f$ plasma, where electron/cyclotron heating is 4 times the neutral beam heating. Note that this series optimizes at a wall loading of ~ 1.0 and a $Q \sim 1.8$ with a ^{233}U cost of 93 $\$/g$ and an electric power cost of 14.7 mills/kWhe.

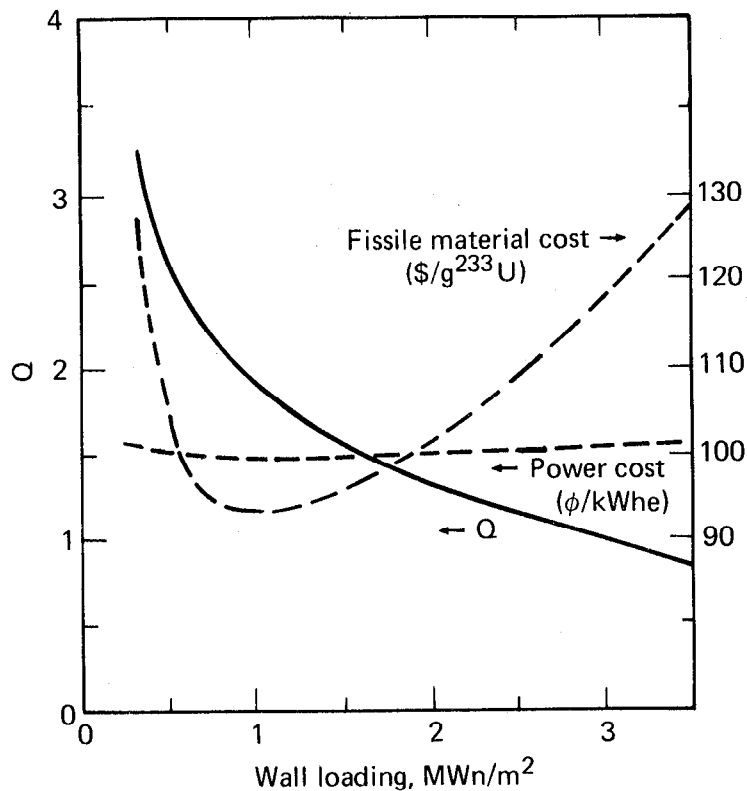


Fig. 8-4. Q vs wall loading trade off. The tandem driver was low technology (i.e., $B_{max} = 12$ T, $E_{inj} = 200$ keV, with "A" cell). The blanket used Be and Th (molten salt).

The plasma variables used in this tradeoff study are listed in Table 8-5. The first-wall radius is used to set central-cell cost per meter. Central-cell cost is scaled directly with first-wall radius from the base TMR case of 4.73 M\$/m at a 1.56-m first-wall. Central-cell length (L_{cc}) is used to set fusion power per meter. Fusion power for all of these physics cases is 2500 MW.

Table 8-5. Plasma variables for Q vs wall loading tradeoff.

Wall loading, Γ	Q	$R_{\text{first-wall}}$	Length, L_{cc}
0.311	3.23	3.09	331
0.516	2.58	2.89	213
1.13	1.79	2.70	104
1.60	1.49	2.61	76.1
2.66	1.09	2.52	47.4
3.74	0.839	2.51	33.9

($E_{\text{ing}} = 200$ keV, $B_{\text{max}} = 12$ T, with A cells and ECRH heating in CC, $P_f = 2500$ MW)

Phase II Results

For the Phase II series of system performance calculation, the following improvements are made in the modeling:

- Improved physics models are used.
- More realistic indirect cost factors are used--0.58 for the hybrid and 0.5 for the burners.
- Preliminary performance and cost data for the Th/He blanket is provided by the subcontractor (GA).
- Molten salt reprocessing cost based on ORNL work.⁴
- Fission burner performance and cost data provided by subcontractors; LWR by GE and HTGR by GA.
- Balance-of-plant (BOP) costs provided by Bechtel.
- Hybrid capacity factor model is included.

Two tandem mirror plasma physics modes are treated: one is a thermal mode (one-component) and uses central-cell ECRH heating, and second is the two-component mode. Technology limitations of 12-T conductor fields, 400-keV neutral beams, and 110 GHz ECRH are imposed for both modes. Wall loading, plasma Q, first-wall radius and length of central-cell tradeoffs for two fusion power levels (2500 MW and 1500 MW) are listed in Tables 8-6 and 8-7 and displayed in Figs. 8-5 through 8-8. The two-component mode Q is independent of wall loading to a wall loading of 5, so the wall loading = 5 case is used.

The performance and cost parameters provided by GA for the Th/He blanket are listed in Table 8-8.

Central-cell unit cost (M\$/m) includes cost for the blanket (plus 25% spares), shield, coil and coil structure, vacuum vessel, main structure, blanket handling equipment, and BOP. Since first-wall radius varies ($r_{fw} = 2 \pm 0.5$ M) with plasma parameters, the blanket and shield, unit costs are scaled with cross-sectional area. The coil and coil structure are scaled with circumference. The other costs are taken to be independent of r_{fw} . For scaling purposes the blanket and shield are taken each to be 1-m thick.

The base costs used to develop the central-cell unit cost scaling were taken from the TMR report,¹ except for the Th/He blanket that GA provided and the BOP that Bechtel provided. From the TMR report: $r_{fw} = 1.56$ m, $C'(\$/m)$ Be Blk. = 2.74, $C'(\$/m)$ shield = 0.62, $C'(\$/m)$ coils + structure = 0.56, $C'(\$/m)$ vac. vessel + main structure + blk. handling equip. = 0.84. The Th/He blanket cost is based on GA's 2.82 M\$/m for a 1-m radius first-wall. Based on this scaling, unit cost (M\$/m) of the central cell is:

$$2.12 r_{fw} + 3.20 \text{ for Be/MS blanket cases}$$

$$2.81 r_{fw} + 3.73 \text{ for Th/He blanket cases}$$

Burner reactor performance and cost parameters used for this phase of the system analysis is listed in Table 8-9.

Another improvement in this series of system performance calculations is the use of BOP costs dependent on coolant (He or molten salt) provided by Bechtel. These costs are for a plant handling 4000 MW_{th} and are shown in Table 8-10.

Combining the BOP with the fusion components and blanket cost results in the complete set of cost coefficients listed in Table 8-11.

Table 8-6. Thermal plasma central-cell ECRH cases--2500 MW_f.

Wall loading	Q	R fw	Length	P , MW/m f	C , \$/m cc	Capacity factor ^a
0.5	4.36	2.30	275	9.09	7.88	0.796
1.0	3.15	2.19	147	17.0	7.66	0.792
1.5	2.54	2.13	100	25.0	7.53	0.788
2.0	2.12	2.10	75.4	33.2	7.47	0.784
Extrapolation						
2.5	1.82	2.1	60.3	41.5	7.47	0.781
3.0	1.58	2.1	50.3	49.7	7.47	0.777
<u>Two-component case:</u>						
5	1.1	1.91	33.1	75.1	7.07	0.761

^aWith Be/molten salt blanket.

Table 8-7. Thermal plasma central-cell ECRH cases--1500 MW_f.

Wall loading	Q	R fw	L cc	P , MW /m f f	C , \$/m cc	Capacity factor ^a
0.50	3.72	2.21	174	8.62	9.74	0.792
1.01	2.71	2.05	92.2	16.3	9.31	0.784
1.50	2.23	2.00	64.3	23.3	9.17	0.776
Extrapolation						
2.0	1.95	2.00	48.2	31.1	9.17	0.768
2.5	1.67	2.00	38.6	38.9	9.17	0.762
<u>Two-component case:</u>						
5	1.0	1.91	20.0	75.1	8.92	0.723

^aWith Th/He blanket.

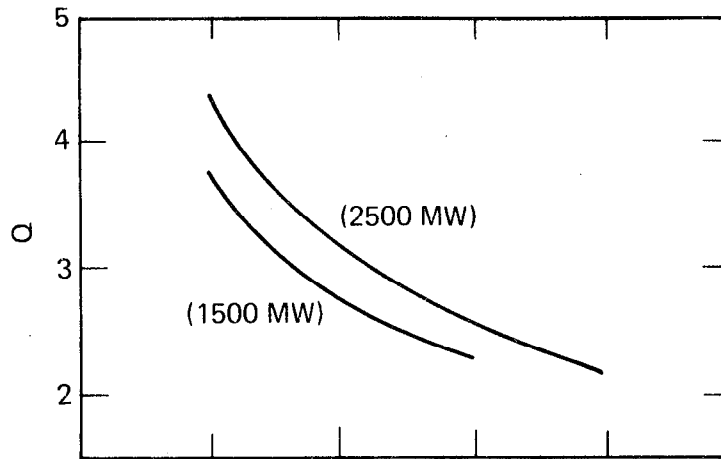


Fig. 8-5. Plasma Q vs first wall loading, Γ .

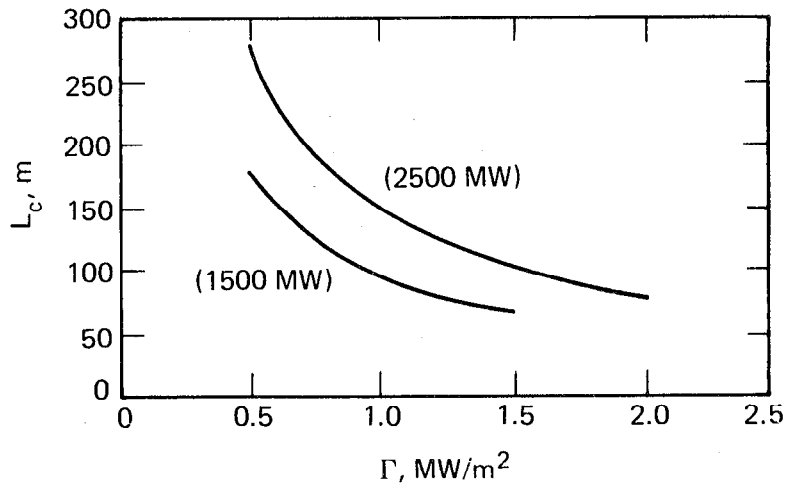


Fig. 8-6. Central cell length vs Γ .

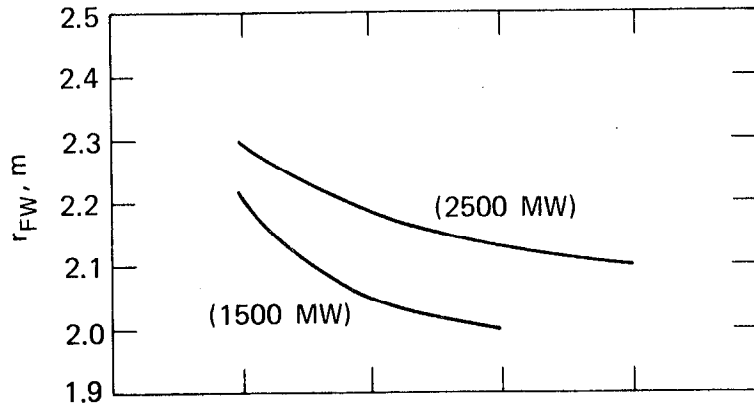


Fig. 8-7. First wall radius vs Γ .

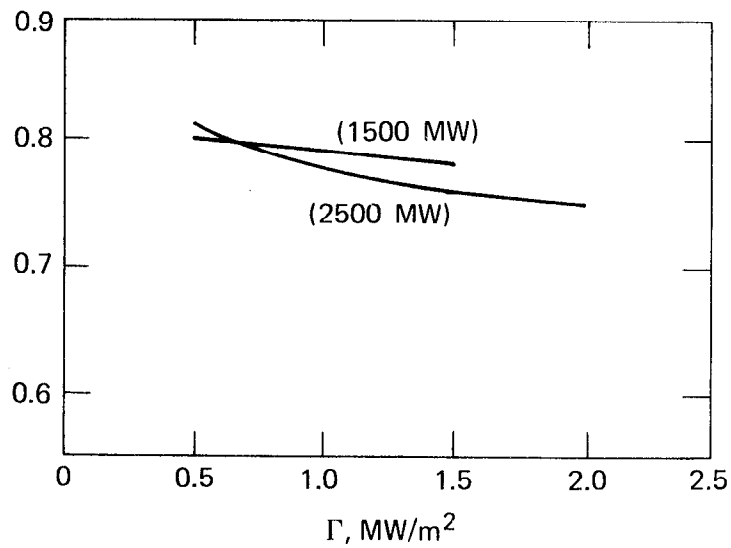


Fig. 8-8. Fraction of input power in the form of direct electron heating vs Γ .

Table 8-8. Th/He blanket performance and cost.

First-wall radius:	1 m, 2 MW/m ² , 8 MW	yr/m ² life	
	M = 3.5	U/n = 0.60	
Blanket cost: \$/m	Li ₂ at \$73/lb	Blanket \$2.82 M/m	
	Th at \$20/lb		
	SS at \$10/lb	Shield \$1.11 M/m	
		<u>\$3.93 M/m</u>	
Replacement cost, \$/g:			
	(Assume Li ₂ O recycle, shield reuse)		
	\$0.14 M/m yr	<u>\$4.60/gm</u>	
Time for replacement:	200 h/yr		
Fuel cycle costs: \$/g			
		<u>Direct</u>	
		<u>Capital (6.4% W. C. rate)</u>	
Fab.	\$120/kg	4.44	1.61
Shipping	\$ 20/kg	0.74	0.05
Repro.	\$380/kg	14.07	0.44
Disposal	\$ 95/kg	3.52	<u>0</u>
		22.77 \$/g	2.1 \$/g = 24.87
Average enrichment:	2.7%		

Table 8-9. Burner reactor performance and cost parameters.

Parameter	Burner reactor type		
	Current LWR ^a	LWR ^a	Advanced HTGR ^a
Fuel cycle	U/Pu	Th/U	Th/U
Capital cost, total \$/kWe	900	900	900
Fabrication and reprocessing, mills/kWe	3.33	4.11	2.59
O&M	2.5	2.5	
Inventory and depletion, mills/kWe/\$/g-fissile	0.083	0.056	0.040
Fissile makeup, kg/yr for 1 GWe at 75% capacity factor	0.333	0.227 ^b	0.125
Thermal efficiency, %	0.32	0.32	0.38

^aThe LWR and HTGR parameters are based on information provided by GE and GA, respectively.

^bDenatured with Pu recycle; 0.333, denatured without Pu cycle; 0.24, not denatured.

Table 8-10. BOP costs (in millions of dollars unless indicated otherwise).

	Helium case	Molten salt case
Buildings:		
Containment	180 + 0.68/m _{cc} ^a	200 + 0.50/m _{cc}
HX		
Steam generator		
Auxiliary		
Hot cell		
End plug (including injectors)		
DC building, \$/kW	35	35
Mechanical equipment (Blk. + DC thermal Heat exchanger Turbine generator and condensor Other auxiliary BOP equipment	90 + 0.087/MW _{th}	145 + 0.087/MW _{th}
Electrical equipment, MW _e gross	0.050 + 0.2/m _{cc}	0.054 + 0.2/m _{cc}
Piping and instrumentationm MW _{th}	117 + 0.023/MW _{th} + 0.21/m _{cc}	80 + 0.023/MW _{th} + 0.21/m _{cc}
Thermal efficiency, %	36	39

^aCost per linear meter in central cell.

The BOP costs reduce to:

Parameter	Molten salt coolant ^a	He coolant
Fixed costs, M\$	425	387
Central cell, M\$/m	0.91	1.09
M\$/MW _{th}	0.11	0.11
Gross, M\$/MW _e	0.054	0.050
M\$/MW direct converter	0.035	0.035

^aMolten salt processing plant not included.

Table 8-11. Cost coefficients.

Coefficient	Be/molten salt case	Th/He case
Fixed ^a		
Plugs	171	171
Crawler transporter	22	22
Other	140	140
	<u>333</u>	<u>333</u>
BOP ^b	425	387
	<u>758</u>	<u>720</u>
Direct converter, M\$/MW	0.13 ^a	0.13 ^a
BOP ^b	0.035	0.035
	<u>0.165</u>	<u>0.165</u>
Thermal conversion system, M\$/MW _{th}		
BOP ^b	0.110	0.110
Electrical system, M\$/MW _e -gross	0.054	0.050 ^b
Injection system, M\$/MW _e -input	0.320	0.320
Central cell, M\$	$2.12 \cdot r_{fw}^c + 3.20$	$2.18 \cdot r_{fw}^c + 3.73$

^aFrom TMR^bBOP - Bechtel^cFirst wall radius, m

Plant capacity factor downtime is assumed to be 20% for maintenance plus time for blanket replacement. Blanket replacement time (t) was taken to be 20 hr per module plus 172 hr per refueling period:

$$t = \frac{\Gamma}{\Phi} \left[\frac{Lc}{\ell m} \times 20 + 172/F_r \right] \text{ hr} ,$$

where:

 Γ wall loading (MW/m²) $Lc/\ell m$ numbers of modules F_r fraction of blanket replaced per refueling period Φ wall exposure at replacement (MWy/m²)

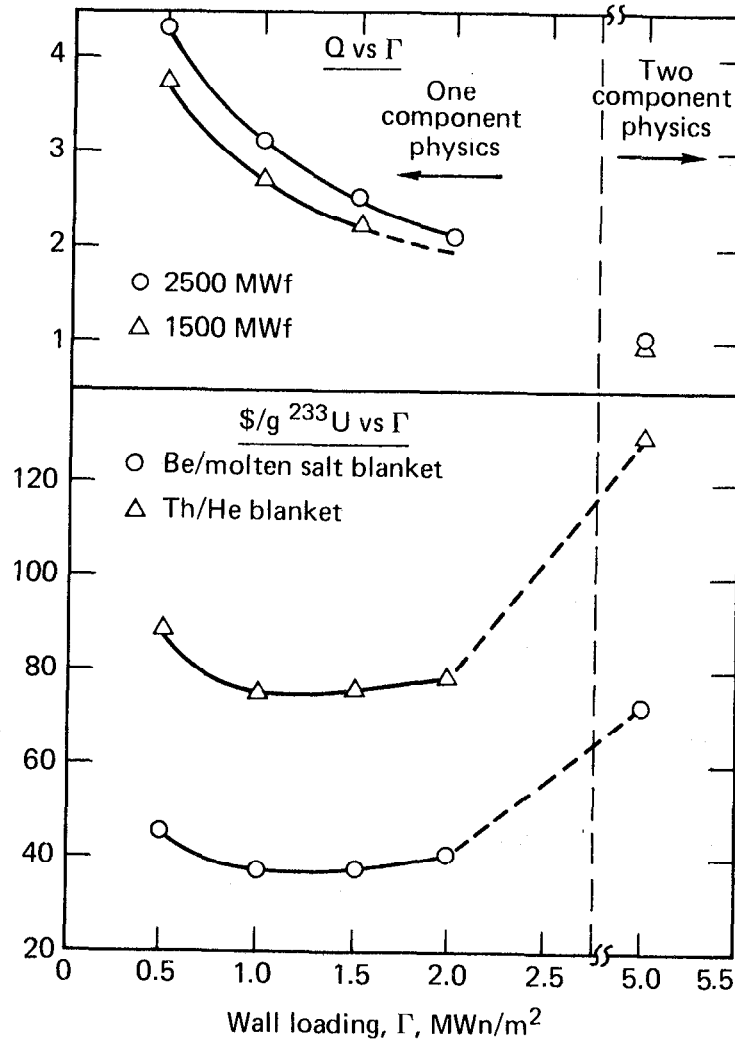


Fig. 8-9. Optimization of performance in Q, Γ space.

Table 8-12. Summary of results.

Case: Burner Physics Blanket	LWR				HTGR			
	One component		Two component		One component		Two component	
	Th/He	Be/MS	Th/He	Be/MS	Th/He	Be/MS	Th/He	Be/MS
Results:								
P-fusion, MW	1333	2857	1333	2857	1333	2857	1333	2857
Q	2.71	3.15	1.0	1.1	2.23	2.54	1.0	1.1
P-net, MWe	999	811	164	- 840	894	599	164	- 840
Γ , MWn/m ²	1.01	1.0	5	5	1.5	1.5	5	5
²³³ U production rate, kg/yr	3456	9874	3456	9874	3456	9874	3456	9874
Direct cost, M\$	2416	3364	2479	3691	2263	3111	2479	3691
Fissile cost, \$/g								
Capital	95.0	45.8	106	52.3	89.9	42.6	106	52.3
Fuel cycle + O&M	34.1	4.82	34.1	4.82	34.1	4.82	34.1	4.82
Power	-52.9	13.4	9.96	15.4	36.4	7.52	7.4	11.4
TOTAL	<u>76.2</u>	<u>37.2</u>	<u>130</u>	<u>72.5</u>	<u>87.6</u>	<u>39.9</u>	<u>132</u>	<u>68.5</u>
Support ratio								
Nuclear	8.91	25.5	8.91	25.5	13.6	38.9	13.6	38.9
Electric, net	11.4	40.2	69.4	-38.8	25.6	98.9	126	-70.4
Direct cost ratio	1.24	1.14	1.34	1.22	1.13	1.08	1.19	1.12
Fission burner, Mills/kWhe								
Capital	9.91	9.91	9.91	9.91	9.91	9.91	9.91	9.91
Fuel cycle (w/o fiss.) plus O&M	6.61	6.61	6.61	6.61	2.59	2.59	2.59	2.59
Fissile	4.27	2.08	7.27	4.06	3.50	1.60	5.29	2.74
TOTAL	<u>20.79</u>	<u>18.60</u>	<u>23.79</u>	<u>20.58</u>	<u>16.00</u>	<u>14.09</u>	<u>17.79</u>	<u>15.24</u>

Fissile Cost (\$/g)

Fuel cycle + O&M (input). At present O&M includes only blanket replacement costs.

Power. Cost of hybrid selling (-) or buying (+) electric power at the same price the fission burners, fueled by the hybrid, are producing electric power.

Support Ratio. The power levels of the supported burners divided by the hybrid power level.

Direct Cost Ratio. Direct capital cost (\$/W) of the system (hybrid + supported burners) divided by the direct capital cost (\$/W) of the burners.

Examination of results (Table 8-12) shows that based on operating economics, the Be/molten salt blanket is best, and that even if fuel cycle and blanket replacement costs are increased to the level estimated for the Th/He blanket, the Be/molten salt blanket would still be the economic winner. The Be/molten salt blanket also gives the highest support ratios. On the other hand, the Th/He blanket results in a positive power balance for both physics cases; the Be/molten salt blanket results in a positive power balance with only the one component physics cases. To break even with the Be/molten salt blanket requires plasma Q's above 1.8. Additionally, the Be/molten salt blanket design requires a fusion driver that is two times larger than the Th blanket design. Comparing burner types shows that the HTGR example of an ACR results in cheaper power and much higher support ratios.

Looking at all the combinations considered here shows that ^{233}U cost varies over a factor of 3, between 37 to 132 \$/g; and power cost varies almost 10 mills/kWhe, between 14.1 and 23.8 mills/kWhe. The nuclear support ratio varies a factor of 4, between 9 and 39.

A major factor in economic superiority of the Be/molten salt blanket is its low fuel cycle costs. But even if these costs are increased to the level used for the Th/He blanket, the Be/molten salt blanket still results in better economics. Also, the capacity factor and noncash flow economics methods penalize the Be/molten salt case relative to the Th/He case.

The Be/molten salt case is the best choice based on this comparison.

Phase III Results

The third series of system calculations was performed to determine the performance potential of the water-cooled blankets being investigated by GE and to compare their performance with the Th/He and Be/molten salt blankets studied during Phase II. To do this we calculated TMH performance with three representative water- (single- and two-phase) cooled blankets. The three are the water-cooled Th pool design and two boiling water linked assembly designs; one fueled with Th and the other with uranium silicide (U_3Si). Performance and economic parameters for these water blankets provided by GE are listed in Table 8-13. Balance-of-plant parameters for the water blanket cases provided by GE are listed in Table 8-14. Parameters for the He and molten salt cases provided by Bechtel are included for comparison.

Results of the three water blanket cases are summarized in Table 8-15. Results for the He and molten salt cases are included for comparison. Base-case thermal plasma (one-component) physics and a nuclear power level (hybrid) of 4000 MW are used for each case. Note that we increased M for the Th/BW and Th/W blankets to 2.0 and 3.0 from 1.01 and 2.1 (GE's beginning of life values), respectively to reflect exposure averaged values. Fissile breeding ratios were not changed from the GE values. Examination of these results show the water-cooled Th blankets to be inferior to the He-cooled Th blanket. The linked assembly Th/BW blanket has too low a fissile breeding ratio, and the pool Th/W blanket heat is at too low a temperature for either to be competitive. The U/BW case competes economically with the Th/He case but has a lower support ratio.

As with previous comparisons, the Be/molten salt blanket results in the best performance from the standpoint of economics and support ratio.

Phase IV Results

For this final phase of the FY79 system study effort, a head-to-head comparison of the two blanket finalists (Th/He and Be/molten salt) was done using the latest performance and cost information available. The thermal plasma mode of tandem mirror physics is used for the driver. Fusion power levels are set to result in 4000-MW peak nuclear power. Plasma Q's are scaled from the Q vs Γ vs power curves, as shown in Fig. 8-9.

Table 8-13. Summary of blanket information.^a

Concept	Blanket	Coolant	Average energy multiplication, M	Average net breeding ratio, f/n	Blanket structure C' (\$/m) direct cost, r _{fw} = 1.5 m	Fuel cycle cost, \$/gm fissile sold	Structural - O&M cost, \$/gm fissile sold	Annual refueling time, ^b days
Pool	Th	Water	2.1	0.84	3,100,000	27.2	3.8	15
Linked assy.	Th	Boiling water	1.01	0.36	690,000	29.7	5.0	30
Linked assy.	U ₃ Si	Boiling water	8.48	1.2	690,000	28.0	8.3	12
Cartridge	Th	Boiling water	1.09	0.36	1,170,000	27.8	4.9	75
Cartridge	U ₃ Si	Boiling water	9.07	1.2	1,170,000	24.1	8.3	21

^aMajor assumptions:

- 2% fissile enrichments.
- 4-yr fuel lifetime (25% of fuel removed annually).
- 4% discount rate; 6.48% effective interest rate; constant 1979 dollars.
- First-wall loading: 1 MW/m²

^bRoutine annual maintenance (6 to 8 weeks) may dominate.

- T/n = 1.0

Table 8-14. Economic variables for the various blanket cases.

Blanket type	Linked assembly		Pool	Axial modules	
	Th/BW	U/BW	Th/W	Th/He	Be/MS
BOP, M\$					
Fixed		10.4	10.4	387	425
Per meter		0.69	0.69	1.09	0.91
Per MW thermal		0.01	0.24	0.11	0.11
Per MW _e -gross		0.74	0.05	0.05	0.05
Thermal conv. eff.		0.32	0	0.35	0.38
Blanket, M\$/m (included					
25% spares)	1.08	0.86	4.84	4.21	4.15

Table 8-15. Performance comparison of boiling water, water, helium, and molten salt blankets.^a

Blanket type	Linked assembly		Pool Th/W	Axial modules	
	Th/BW	U/BW		Th/He	Be/MS
Fiss. atoms/n	0.36	1.2	0.84	0.60	0.80
M	2.0	8.48	3.0	3.5	1.5
Q	2.23	2.23	2.23	2.23	2.12
n, MW/m ²	1.5	1.0	1.5	1.5	2.0
P _f , MW	2222	573	1538	1333	2857
L _{cc} , m	95	51	66	57	86
R _{fw} , m	2.0	1.5	2.0	2.0	2.1
Fissile production					
- Rate, kg/hr	3456	2969	5583	3456	9874
Pe-net, MW	428	1060	- 647	893	381
Direct cost, M\$	3105	1885	2441	2242	3070
Fissile cost, \$/g					
- Capital	133	88	61	89	42
- Fuel cycle + O&M	35	36	31	34	5
- Power	- 27	- 65	23	- 47	- 6
TOTAL	141	59	115	76	41
Support ratio					
- Electric	27	6.3	- 28	13	86
- Nuclear	8.9	5.2	14	8.9	25
Direct cost ratio	1.40	1.27	1.27	1.23	1.14
LWR burner electricity					
cost, mills/kWhe					
- Capital	9.9	9.9	9.9	9.9	9.9
- Fuel cycle (w/o fissile + O&M)	6.6	5.8	6.6	6.6	6.6
- Fissile (from hybrid)	7.9	4.9	6.5	4.2	2.3
Total	24.4	20.7	23.0	20.8	18.8

^aHybrid nuclear power level of 4000 MW and base-case thermal plasma (one-component) physics are used for each case.

Blanket performance and cost parameters used for the comparison are listed in Table 8-16. The high cost of the Be/molten salt blanket is dominated by 5.6 M\$/m for Be at 330 \$/kg. Fuel cycle cost for the Be/molten salt case is not listed because the online reprocessing system cost is included in the direct BOP cost at 200 M\$. Bechtel has since suggested that 40 M\$ is a more likely cost so the 200 M\$ should be a very conservatively high cost.

Fusion driver component costs are listed in Table 8-17. Costs of magnets are from preliminary scaling of the MFTF magnet costs.* Injection and direct converter systems costs includes power supplies and cryopanels.¹

System power flow diagrams for these Th/He and Be/molten salt cases are shown in Figs. 8-10 and 8-11. The double-valued powers listed in the Th/He case are peak/average values for equilibrium cycles where 1/4 of the blanket is removed after each cycle.

Balance-of-plant costs for the Th/He and Be/molten salt case are calculated with the algorithm developed by Bechtel.

Capital costs for the two cases are listed in Table 8-18.

To uniquely determine hybrid fissile and electricity costs the hybrids are assumed to be providing makeup fissile material to LWR's operating on the denatured ²³³U-Th fuel cycle with Pu recycle. Parameters used to represent this burner are listed in Table 8-19.

System performance for the base Th/He and Be/molten salt cases as well as an improved Be/molten salt case are compared in Table 8-20. The design point chosen for the driver (Q vs Γ vs R_{fw}) is not optimized but should not be far off based on the tradeoff shown in Fig. 8-9. The high cost Be/molten salt blanket would most likely optimize at a higher wall loading lower Q point but the power self sufficiency requirement will keep us from dropping Q much lower. The cost of hybrid-produced fissile material and LWR burner electricity cost are coupled by requiring the prices of buying and selling fissile material and power to be the same for both hybrid and burner. For example, in the Th/He case the 70.6 \$/g cost of fissile material produced by the hybrid is based on a power cost of 20.5 mills/kWhe produced by the LWR burners, which is based on a fissile material cost of 70.6 \$/g.

* Personal communication from W. Neef, 9/17/79.

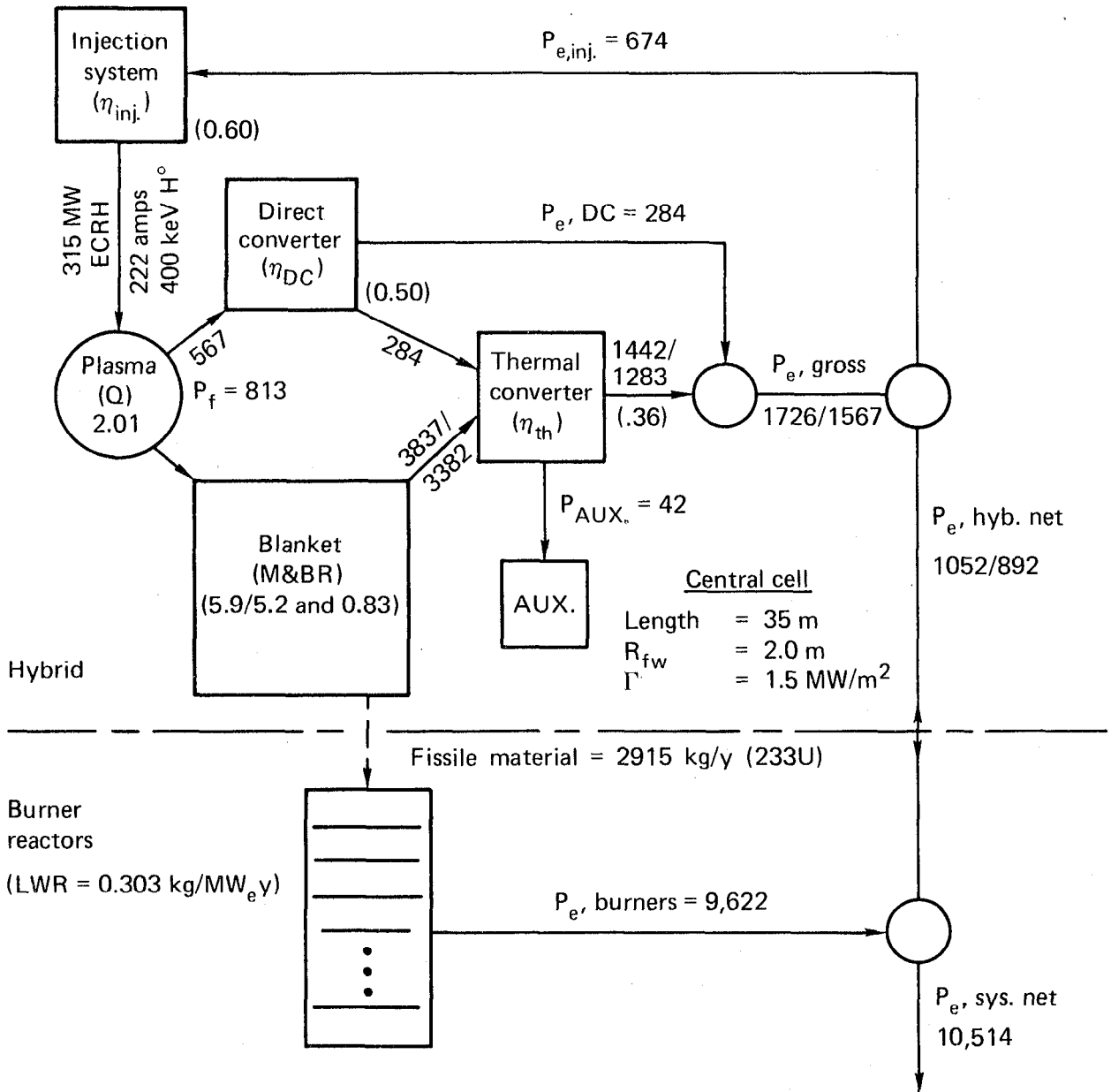
Table 8-16. Blanket performance and cost parameters.

Blanket type	Th/He	Be/MS
Tritium breeding ratio, T	1.06	1.05
Fissile breeding ratio, f/n (av)	0.83	0.62
Energy multiplication, M		
Cycle peak	5.9	1.43
Cycle av	5.2	1.43
Blanket coverage, % (used to determine f/n and M)	94	97.5
First-wall radius, m	2.0	2.1
Blanket and shield cost, M\$/m	4.05	8.72
First-wall loading, MW/m ²	1.5	2.0
Blanket life, MW-yr/m ²	9.6	8.0
Fuel cycle cost, \$/kg-HM or \$/g-fiss	495 14.6	(Inc. in cap. cost)
Blanket replacement cost, M\$/m	3.57	1.29
Fuel cycle and/or blanket replacement, \$/g	20.6	3.5
O&M cost, \$/kWth-yr	6.6	6.6
²³³ U to Th ratio, max	3.4%	0.1%

Table 8-17. Fusion driver component costs and performances.

Magnets (coils plus structure)	
End plugs	282 M\$
Central cell	1.58 M\$/m (@r _i = 3.9 m)
Injection system	
Cost	320 \$/kW _e input
Efficiency	60%
Direct conversion system	
Cost	130 \$/kW input
Efficiency	50%
Other	140 M\$

Hybrid
$$P_f = \frac{P_{nuc. \text{ MAX.}}}{(0.2 + 0.8 \cdot M_{\text{MAX}})} = \frac{4000}{(0.2 + 0.8 \cdot 5.9)} = 813$$



#/# ≡ peak/average

Fig. 8-10. System power flows (Th/He case).

$$P_f = \frac{P_{nuc. \text{ MAX.}}}{(0.2 + 0.8 \cdot M_{\text{MAX}})} = \frac{4000}{(0.2 + 0.8 \cdot 1.43)} = 2976$$

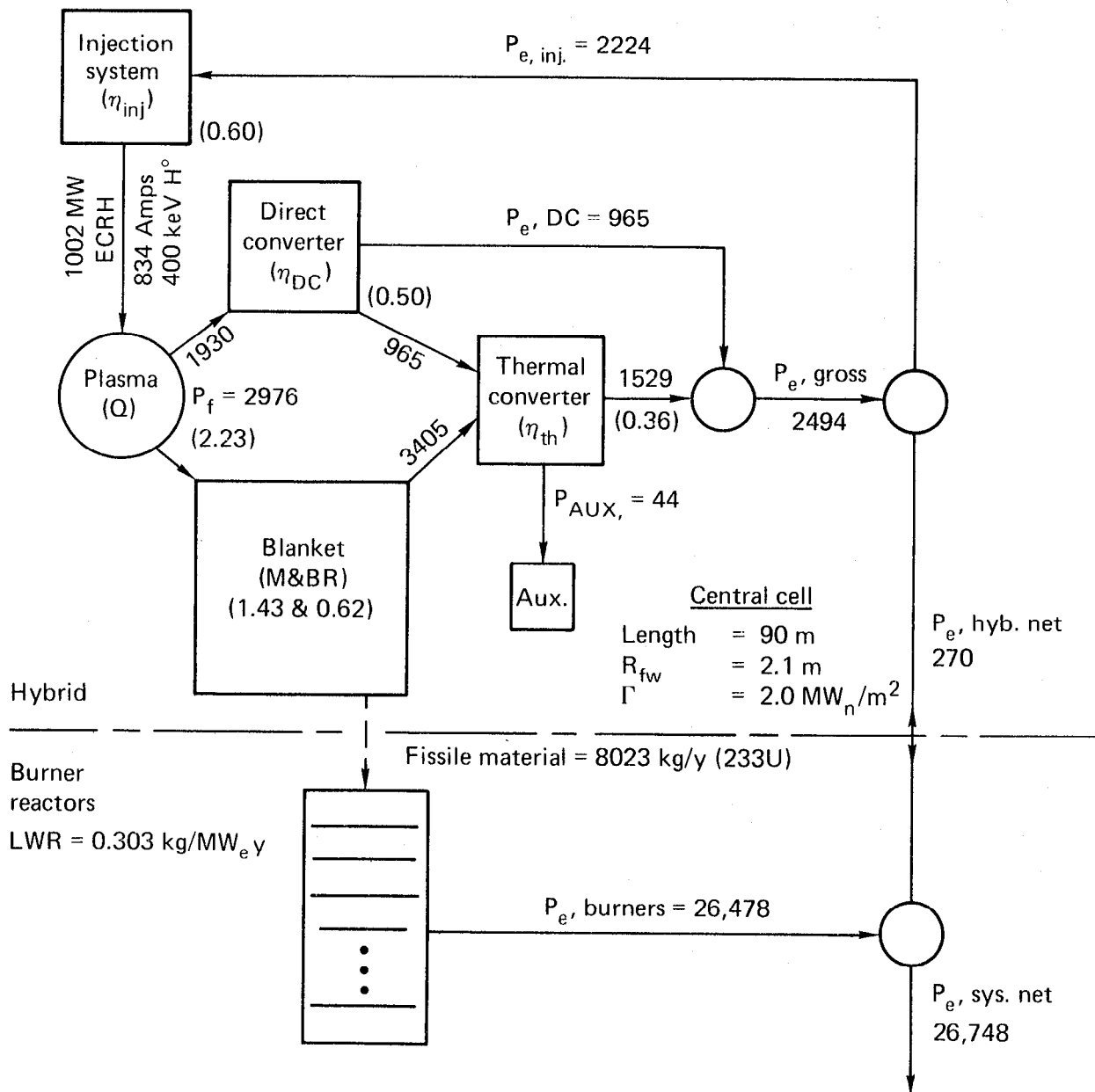


Fig. 8-11. System power flows (Be/molten salt case).

Table 8-18. Hybrid capital costs (in millions of dollars).

Blanket type	Th/He	Be/MS
Driver components	767	1538
End cell magnets	282	282
Central-cell magnets	55	153
Injection system	216	712
Direct converter	74	251
Other	140	140
Blanket and shield (including 25% spares)	177	977
BOP	1050	2071
Civil and structure	182	366
Mechanical	435	672
Instrumentation	40	40
Piping	264	520
Electrical	129	273
Reprocessing plant	-	200
Total direct cost	1994	4585
Indirect costs (58% of direct costs)	1156	2660
Total capital cost	3080	7245

Table 8-19. LWR parameters.

Capital cost, $\$/kW_e$	
Direct	600
Total	900
Fissile inventory and depletion costs, mills/ kWh_e / $\$/g$ -Fiss.	0.056
Fuel fabrication and reprocessing cost, mills/ kWh_e	4.11
O&M cost, mills/ kWh_e	2.5
Fissile (^{233}U) makeup, kg/yr for 1 GW_e at 75% capacity factor	227
Net efficiency	0.32
Capacity factor	0.70

Table 8-20. System performance comparison vs blanket type.^a

Blanket type	Th/He	Be/MS (base)	Be/MS (improved)
Fissile breeding ratio	0.83	0.62	0.81
M, av	5.2	1.43	1.58
Driver parameters			
Fusion power, MW	813	2976	2733
Wall loading, MW _n /m ²	1.5	2.0	2.0
Wall radius, m	2.0	2.1	2.1
Solenoid length, m	35	90	82
Plasma Q	2.0	2.2	2.2
Fissile production, hybrid, kg/yr	2915	8023	9554
Electric power, hybrid net, MW	892	270	362
Hybrid direct cost, M\$	1993	4585	4126
Hybrid fissile cost, \$/g			
Capital	97.1	81.1	61.3
Fuel cycle	14.6	(Inc. in cap. cost)	
Blanket replacement	6.0	3.5	1.4
O&M	8.0	3.3	2.8
Power	-55.1	- 6.2	- 6.6
TOTAL	<u>70.6</u>	<u>81.7</u>	<u>58.9</u>
LWR electricity cost, mills/kWh			
Capital	9.9	9.9	9.9
O&M	2.5	2.5	2.5
Fuel cycle (less fissile makeup)	4.1	4.1	4.1
Fissile makeup (from hybrid)	4.0	4.6	3.3
TOTAL	<u>20.5</u>	<u>21.1</u>	<u>19.8</u>
Power support ratio, P _{LWR} /P _{HYB}			
Nuclear	8.5	20.7	24.6
Electric	10.8	98.1	87.0
System cost ratio, \$/kW _e system/ \$/hW _e -burner			
	1.23	1.28	1.20

^aAll hybrids are 4000-MW peak nuclear power and have a 75% capacity factor. Capital charge rate is 6.74% based on noninflating constant dollars.

Comparing the performance shows that the economics of the Th/He case is somewhat better than the base Be/molten salt case (20.5 vs 21.1 mills/kWh_e and 70.6 vs 81.7 \$/g-fissile), while an improved Be/molten salt case is somewhat better than the Th/He case (19.8 vs 20.5 mills/kWh_e and 58.9 vs 70.6 \$/g-fissile). The support ratios of the Be/molten salt cases are much higher than for the Th/He case.

The improved Be/molten salt blanket case differs from the base case in three ways:

- Better breeding achieved by increasing the mole fraction of ThF₄ in the salt from 12 to 27% and increasing solid Be volume fraction from 65 to 75% while decreasing molten salt volume fraction from 25 to 15%.
- Lower blanket cost by reducing the product of Be mass and cost by a factor of 2.
- By doubling the blanket life from 8 to 16 MW/m².

The approximate percentage decrease in fissile cost resulting from these three changes are 16, 10, and 2%, respectively.

Based on the comparison between the Th/He and the Be/molten salt cases shown in Table 8-20, economics (\$/g-fissile or mills/kWh_e) is not a major factor; thus, the criteria for choosing between a Th/He and Be/molten salt blanket must be based on other factors.

It is important to emphasize that the system modeling effort described herein is an interim effort intended to aid in the selection of blanket type, plasma physics mode (or modes), and fusion technology range to concentrate on during the second year of our 2-year tandem hybrid study. The intent is to expand and improve the model during the second year so more accurate economic estimates of the tandem hybrid design(s) can be made. Parameter and sensitivity studies are also planned.

FISSION BURNER REACTOR ASSUMPTIONS

Two different fissile fuels, ²³⁹Pu and ²³³U, along with varying amounts of electricity, can be produced in the hybrid reactor by changing the blanket design. To evaluate the performance of the different blanket designs and fertile fuels, the LLL evaluation model compares the cost of generating electricity from a system of fission burner reactors and supporting hybrid reactors. In this evaluation the cost and performance of the fission burner

reactor significantly affect the performance and cost effectiveness of the TMHR blanket design.

This subsection provides cost and performance characteristics for two fission reactor systems, the LWR and the HTGR, for use in evaluating TMHR blanket designs. The LWR is representative of the dominant fission reactor technology currently in use throughout the world; and the HGTR is representative of many advanced converter reactor technologies yet to be extensively deployed. It is important to recognize that both reactor systems will require additional fuel R&D, reactor R&D, and the development of supporting fuel cycle facilities before either technology may fully utilize TMHR-bred ^{239}Pu or ^{233}U fuels.

Light Water Reactors

The development of the LWR has proceeded to the stage of commercial use on a worldwide scale. In many nations as in the U.S., the LWR has also dominated reactor sales and R&D. There is considerable evidence to suggest that the LWR may continue to lead reactor sales while other reactor options are evaluated. For the U.S. the following issues reinforce this belief:

- Implementation of new reactors and fuel cycles takes time and money that government and industry are reticent to invest.
- There are four reactor manufacturers selling LWR's, each with in-place manufacturing capabilities.
- There will remain a buyer's (reactor) market to minimize LWR prices. (Any two manufacturers have capacity to meet near-term market demands.)
- The problems of the LWR are known by experience.
- There is a long standing government R&D commitment to the LWR.
- Incremental fuel savings by early advanced converter reactors may be matched by improving LWR fuel designs.

LWR Fuel Characteristics and Fissile Fuel Requirements. The fuels in use today in the LWR utilize low enriched ^{235}U as the fissile fuel. To utilize the ^{239}Pu and ^{233}U fuel generated by hybrid reactors, new fuel designs are necessary. Tables 8-21 and 8-22 provide fuel characteristics for boiling water reactors (BWR's) and pressurized water reactors (PWR's) operating on ^{239}Pu and ^{233}U fuel cycles with Table 8-23 as a summary.

Table 8-21. Plutonium-fueled LWR cycles with Pu-recycle (1000 MWe).

Fuel utilization characteristics
(kg/GWe-yr at a 75% capacity factor)

	Load	Discharge	Net consumption.
PWR			
^{239}Pu plus ^{241}Pu	1153	858	295
^{235}U	<u>173</u> (natural U)	<u>108</u>	<u>38</u>
Pu inventory ^a	1225 ^b	N/A	333
BWR			
^{239}Pu plus ^{241}Pu	N/A	808	370
^{235}U	<u>71</u> tails	<u>38</u>	<u>0</u>
Pu inventory ^a	1178	N/A	378

^aAll isotopes equally weighted.

^bAdjusted to a depleted 0.3% (tails) U base.

Table 8-22. Denatured ^{233}U -fueled LWR cycle with Pu credit (1000 MWe).

Fuel utilization characteristics
(kg/GWe-yr at a 75% capacity factor)

	Load	Discharge	Net consumption
PWR			
^{233}U	750	446	304
^{235}U	29 tails	43	- 14
^{239}Pu plus ^{241}Pu	<u>0</u>	<u>63</u>	<u>- 63</u>
^{233}U inventory ^a	750	N/A	227
BWR			
^{233}U	770	452	318
^{235}U	15 tails	17	- 2
^{239}Pu plus ^{241}Pu	<u>0</u>	<u>55</u>	<u>- 55</u>
^{233}U inventory ^a	770	N/A	261

^aAll isotopes equally weighted.

Table 8-23. Recommended LWR fuel characteristics (1000 MWe - 100% PWR).

Fuel cycle	Fuel life, ^a yr	Burnup, MWD/kg HM	Initial bundle inventory, ^b kg fissile	Net consumption, ^a kg/yr
Pu/U (non-denatured)	2.9	30.4	3430 kg	(^{239}Pu plus ^{241}Pu) 333 kg ^{233}U
$^{233}\text{U}/\text{Th}$ (non-denatured)	3.2	33.4	2400 kg ^{233}U	227 kg ^{233}U
Denatured $^{233}\text{U}/\text{Th}$ (no Pu recycle)	3.2	33.4	2400 kg ^{233}U	290 kg ^{233}U

^aAt a 75% capacity factor.

^bFuel life times load inventory. Out-of-core requirements not shown.

Table 8-21 also includes a reduction in Pu use due to the burnup of ^{235}U in the diluent, U tails. This reduction results from the assumption that ^{235}U consumption in the Pu cycle is not chargeable to the Pu cycle. The ^{235}U enters the Pu/U cycle with the tails as a diluent. In the denatured ^{233}U cycles no net consumption of ^{235}U takes place; thus this benefit only occurs to the Pu/U cycle. When the tails have been depleted (late in the 21st century), this bonus will disappear.

LWR Capital Costs. Capital costs for nuclear power plants have traditionally been difficult to reconcile because of scope, accounting, and labor-rate differences throughout U.S. utilities. Unanticipated changes in plant costs have occurred due to the ratcheting of environmental standards and due to increased rates of inflation. This tendency to slip schedules and increase the work scope and inflationary costs in nuclear projects has probably not yet come to an end.

The capital costs for LWR's for this analysis have been derived⁶ by the addition of one additional year of escalation at 12.5% (Table 8-24).

Table 8-24. Capital investment costs (1979 \$/kWe, including interest during construction).

Power plant type	Capital cost, \$/kWe ^a		
	600 MWe	1000 MWe	1300 MWe
LWR	1190	900	780

^aIncludes 7% owner's cost during construction.

LWR Fuel Service Costs. The annual operating costs of an LWR are made up of six components that occur during the fuel cycle at different times:

- Conversion
- Enrichment
- Fabrication
- Reprocessing
- Shipping and waste disposal
- Operation and maintenance

Conversion. Conversion costs are a small fraction of the annual fuel cost of a converter reactor, and the material (F) requirements are not expected to rise significantly in price due to depletion of the resource. The conversion of U_3O_8 to UF_6 occurs for two important reasons: (a) to further purify the U product from the mill; and (2) principally to convert U into a form suitable for enrichment in diffusion or centrifuge plants. This step has not been necessary for the natural enriched fuels of the CANDU.

The reference cost of conversion for this analysis is \$4.4/kg U (1979 \$)⁶ by the inclusion of one year of escalation at 10% per year.

Enrichment. The future of U.S. enrichment has become more clear with time. The relative economics of the diffusion process and the centrifuge process are now well publicized, and the next unit of enrichment capacity will be based on the centrifuge. Additionally, the cancellation of a joint government industry project has shown the desire of Congress to keep U.S. enrichment totally under government ownership and control.

The U.S. long-term strategy for pricing the enrichment service, however, still remains undefined. Today, prices are \$85/SWU in the U.S. based on recovery of government costs. (Overseas prices are currently higher, in the range of \$115 to \$130/SWU.) The question on pricing strategy has been whether the U.S. will switch to commercial pricing (with profit) or maintain the current cost recovery strategy.

This report assumes that the U.S. converts to a commercial pricing strategy by the year 2010. The reference enrichment cost for this analysis is \$110/SWU (1979 \$), slightly less than current non-U.S. commercial rates because of superior U.S. technology.⁶ Additionally the reference operating tails assay is 0.2%, ^{235}U .

Fabrication. The fabrication costs for LWR fuels for this analysis are shown in Table 8-25. These costs are as recommended for a high capacity industry.

Reprocessing. The reprocessing costs for LWR fuels for this analysis are shown in Table 8-26. The costs are recommended for a high capacity industry.

The two sets of reprocessing costs given in Table 8-26 are representative of two alternate philosophies on spent fuel reprocessing, the so-called AGNS-type and Canyon-type facility costs.

Table 8-25. LWR fabrication costs (1979 \$/kg HM).

Fuel type	LWR
LEU5 - Standard	121
- High burnup	132
Natural UO ₂	-
DU5/Th	132
DU3/U	594
DU3/Th	627
Pu/U	407
Pu/Th	418
Pu/U - Spiked	638
Pu/Th - Spiked	638

Table 8-26. Reprocessing cost for LWR fuels (1979 \$ kg HM).

Fuel type (oxide)	Semiremote, AGNS-type facility	Fully-remote, Canyon-type facility
Pu/U	275	407
Pu/U - Spiked	297	451
DU/Th	297	451

The AGNS-type facility costs are for plants similar to the AGNS plant at Barnwell, S.C. These estimates assume current perceived regulations with semi-remote maintenance. The investment cost estimate for the 1500-MTHM/yr, LWR-Purex AGNS reprocessing plant is based on recommendations made by the U.S. INFCE Technical and Economic Assessment Crosscut Group.^{7,8} The direct investment cost of such a facility was estimated at \$1 billion and an annual operating cost of \$50 million.

The Canyon-type facility costs are based on work by the Savannah River Laboratory (SRL). This facility, as well as having fully remote maintenance, is designed in anticipation of much more stringent safeguards and operating criteria than required by current regulations. SRL personnel estimate that the capital investment required for a 1500-MTHM/yr plant is \$1.6 billion with annual operating costs of \$50 million.

Shipping and Waste Disposal. The spent-fuel shipping and waste disposal costs used in this report are those recommended,⁶ but with one additional year of escalation added at 10% per year. These costs are shown in Table 8-27.

Table 8-27. Converter-spend fuel shipping and disposal costs (1979 \$/kg HM discharged from reactor).

Service	After reprocessing option	No reprocessing option
	LWR	LWR
Spent fuel shipping	16.5	16.5
Waste shipping	11.0	-
Waste storage	<u>55.0</u>	<u>132.0</u>
	82.5	148.5

Operation and Maintenance. The operation and maintenance costs used in this report are recommended,⁶ but with one additional year of escalation added at 10% per year. These costs are shown in Table 8-28.

Table 8-28. Converter operation and maintenance costs (1979 \$).

Reactor	Fixed, \$/kWe-yr	Variable, \$/kWe-yr	Total, mills/kWh
LWR	14.3	1.1	2.3 ^a

^a75% capacity factor for LWR.

LWR Fuel Cycle Costs. The cost of fuel for the conventional low-enriched, U-fueled LWR is expected to change with time, principally due to real changes in the cost of U. Table 8-29 lists LWR fuel cycle costs for various fuel cycle alternatives based on the cost and performance characteristics of Tables 8-21 through 8-28 and \$220 per kg/U (U_3O_8) determining the values of ^{233}U and ^{239}Pu . These values might be expected while U (U_3O_8) is the principle nuclear fuel source.

Once the hybrid reactor industry has developed, the price of bred ^{239}Pu and ^{233}U should drop to the hybrid's production cost. The cost of LWR fuel then would depend on this production cost. Table 8-30 provides LWR fuel cycle costs on a per unit fissile fuel cost basis.

High-Temperature, Gas-Cooled Reactor

A fusion-fission hybrid reactor has the potential to produce bred fissile fuel, electricity, or both. To determine the bred fuel requirements, the characteristics of the burner reactors must be considered. A potential market for bred fuel produced by the hybrid reactor is the High-Temperature, Gas-Cooled Reactor (HTGR). Development of the HTGR has been pursued in the U.S. and in Europe to the point where the technology can be considered a developed technology,⁹ although it has not yet been commercially deployed. Small prototype HTGRs have been successfully operated in Europe (the 15-MW_e AVR German pebble bed HTGR) and the U.S. (the 40-MW_e Peach Bottom HTGR). The 330-MW_e Fort St. Vrain demonstration HTGR is now in operation at 220 MW_e on the Public Service of Colorado grid, and the 300-MW_e THTR pebble bed HTGR is under construction in West Germany.

HTGR Characteristics. The HTGR is characterized by its He gas coolant and graphite neutron moderator. The HTGR neutronically is not efficient using the enriched Th/U fuel cycle, but its fuel-cycle characteristics are quite flexible. The German HTGRs to date have used the low-enriched U/Pu fuel cycle and because of nuclear proliferation concerns, use of medium-enriched U with the Th/U fuel cycle using denatured ^{233}U recycle is being considered in the U.S. In addition, use of the Th/U fuel cycle with ^{233}U feed¹⁰ and the U/Pu fuel cycle with plutonium feed¹¹ have been investigated and appear quite feasible.

Table 8-29. One-cycle LWR fuel cycle costs--mills/kWh
(\$220/kg U₃O₈ basis, 1979 \$).

Fuel cycle ^a	Fabrication	Reprocessing and waste disposal	U ₃ O ₈ and Th	Enrichment	Pu and ²³³ U	Fuel total	O&M
LEU ²³⁵ U/ ²³⁸ U	0.60	0.54	7.49	1.76	-	10.4	2.3
LEU ²³⁵ U/ ²³⁸ U (with _____ credits no Pu recycle)	0.60	1.31	6.39	1.73	-	10.0	-
LEU ²³⁵ U/ ²³⁸ U (with Pu and ²³⁵ U credits)	0.60	1.31	6.39	1.73	(1.53) ^b	8.5	2.3
Pu/U (with Pu credits)	2.02	1.31	-	-	5.17 ^b	8.5	2.3
97-8 Pu/U-spiked (with Pu credits)	3.15	1.31	-	-	4.29 ^c	8.5	2.3
HEU ²³³ U/Th (with ²³³ U credits)	2.86	1.25	0.16	-	4.23 ^b	8.5	2.3
DEN ²³³ U/Th (with uranium credits no Pu credit)	2.86	1.25	0.14	-	5.78 ^d	10.0	2.3

^aDesign as described in Tables 8-21 through 8-23.

^bBased on indifference values of Pu (\$62/gm Pu) and ²³³U (\$14/gm ²³³U).

^c\$52/gm Pu.

^dBased on indifference value of ²³³U (\$89/gm) between no Pu recycle cases using ²³³U and Pu.

Table 8-30. One-cycle LWR costs (1979 \$).

LWR cycles	Fab.	Rep.	Th	O&M	Total, m/kWh	Fuel cost, m/kWh/\$/unit fissile
$^{235}\text{U}/^{238}\text{U}$ (no recycle)	0.60	0.54	0	2.3	3.44	0.0925 ^a lb U_3O_8
$^{235}\text{U}/^{238}\text{U}$ (U-recycle)	0.60	1.31	0	2.3	4.21	0.0812 ^a lb U_3O_8
$^{235}\text{U}/^{238}\text{U}$ (full recycle)	0.60	1.31	0	2.3	4.21	(0.2469) g Pu 0.0812 lb U_3O_8
Pu/U	2.02	1.31	0	2.3	5.63	0.0833 g Pu
Pu/U-spiked	3.15	1.31	0	2.3	6.76	0.08333 g Pu
$^{233}\text{U}/\text{Th}$	2.86	1.25	0.16	2.3	6.57	0.05624 g ^{233}U
Den. $^{233}\text{U}/\text{Th}$	2.86	1.25	0.14	2.3	6.55	0.06518 g ^{233}U

^aCalculated at 220 \$/kg U_3O_8 and \$110/SWU (1979 \$).

The HTGR has a number of desirable characteristics that make this concept particularly attractive. The high-temperature helium coolant allows use of modern steam conditions with approximately 40% efficiency with a steam cycle power conversion system. The same reactor core and fuel design could be used with a direct cycle gas turbine power conversion system that would allow use of dry cooling with the same high efficiency or use of a bottoming cycle for a net plant efficiency of more than 50%. The high temperature capability of the graphite-base fuel makes the HTGR the prime candidate for high temperature process heat applications.¹² The low power density and high heat capacity of the HTGR core and the use of a single phase chemically inert coolant offer significant safety advantages to the HTGR compared to alternate nuclear power systems.¹³

The capital cost of the HTGR appears to be comparable with that of LWRS.¹⁴ HTGR capital cost estimates for a 900 MW_e plant from a recent DOE-sponsored evaluation of the steam cycle HTGR are shown in Table 8-31.

HTGR Fuel Market Scenario. To assess the market for bred fissile fuel from the TMHR in the time frame of the early 21st century, an estimate must be made as to what the fission reactor economy will be at that time. Given the present uncertain state of the fission reactor business in the U.S., such a prediction is difficult. Hybrid application of fusion power, and perhaps even pure fusion, is highly unlikely unless a reasonably healthy nuclear power economy exists. It has been assumed, therefore, that by the early 21st century the fission reactor economy has returned to state of normality and acceptance. It is expected that the HTGR will have been successfully commercialized using the thorium/uranium fuel cycle with high- or medium-enriched fuel.¹⁵ Recycle facilities will be in operation for HTGR fuel, including reprocessing and re-fabrication, that could utilize ²³³U bred by hybrid reactors. Use of Pu in the HTGR, although technically possible, is not expected to be available. The HTGR deployed in the U.S. will use prismatic block fuel. The pebble bed HTGR is not expected to be commercialized in the U.S. As a result, direct enrichment of pebble bed balls in the hybrid for subsequent use without reprocessing in the HTGR¹⁶ is not expected to be possible. The HTGR recycle facilities would be able to handle hybrid-bred ²³³U with minimal modification. The re-fabrication processes are all totally remote and could use hybrid-bred ²³³U without modification despite the higher level of radiation expected due to a higher ²³²U content than HTGR-bred ²³³U. The aqueous solution THOREX process reprocessing operation could be used directly for all Th fuel forms proposed for a Th-based hybrid blanket. The HTGR reprocessing head-end, crush-burn-leach processes are suited only for graphite-base, HTGR-type fuel, and a new head-end would be required for metal-clad hybrid blankets. This could be added to the HTGR reprocessing lines expected to be in operation.

The impact of using ²³³U feed in the HTGR has been investigated extensively. The reference ²³⁵U feed HTGR with ²³³U recycle has roughly equal quantities of ²³⁵U and ²³³U loaded at each reload, and the nuclear characteristics of the two fuels are similar. The change to all - ²³³U is thus not a large perturbation. The fuel loadings are lightened somewhat due to the superior nuclear properties of ²³³U compared to ²³⁵U. The moderator temperature coefficient of a ²³³U system is somewhat less negative than for ²³⁵U,

Table 8-31. HTGR-SC total plant cost summary. First plant and follow-on unit 1 of a twin (January 1978, dollars in millions).^{a,b}

Item	First plant	Follow-on plant-unit 1
Net electrical output, MW _e		898
<u>NSS</u>		
Direct cost	164.7	145.7
Indirect cost	<u>75.0</u>	<u>16.8</u>
Subtotal NSS	239.7	162.5
<u>BOP</u>		
NSS-related items	24.6	35.7
Direct cost	315.9	300.6
Indirect cost	<u>149.0</u>	<u>137.7</u>
Subtotal BOP	<u>489.5</u>	<u>474.0</u>
Direct plant cost	505.2	482.0
Total plant cost (w/o contingency)	<u>729.2</u>	<u>636.5</u>
Budgetary contingency	39.5	36.2
Total plant cost (w/contingency)	<u>768.7</u>	<u>672.7</u>
\$kW _e - direct	562.6	536.7
\$kW _e - total	856.0	749.1

^aExcludes owner's costs and other contractor costs.

^bRef. 6.

but the prompt Th doppler effect ensures a strong total negative temperature coefficient. The delayed neutron fraction, β , is less for ^{233}U than for ^{235}U but is quite adequate for normal operation and control procedures.

HTGR Fuel Consumption. The HTGR has a very flexible fuel cycle. Because the fuel rods are composed of ThO_2 , UC_2 and carbon-shim particles, the fissile-to-fertile ratio and the fertile-to-moderator ratio may be easily changed without affecting the mechanical design or thermal/hydraulic characteristics of the fuel. The power density, moderator-to-fertile ratio (carbon/thorium or C/Th ratio), fuel-residence time and fuel reload interval may all be adjusted to optimize the fuel cycle characteristics. The power density is the only characteristic that would affect the rest of the reactor design, so the other fuel cycle characteristics could be altered on existing reactors to adapt their fuel cycles to changing economic conditions.

The fuel consumption requirements for several ^{233}U -fed HTGR fuel cycle options are shown in Table 8-32. With ^{233}U feed and low power density and low C/Th ratio, the HTGR conversion ratio can actually exceed unity. Except for reprocessing losses, it would be a breeder reactor. The choice of fuel cycle characteristics must be optimized to best match the economic conditions that will be present in the 21st century. This has not been done. To represent the HTGR in TMHR calculations, the characteristics of the lead plant HTGR have been assumed. This has an average power density of 7 W/cc and a C/Th ratio of 180. As shown in Table 8-32, with self-generated ^{233}U recycle, it requires a ^{233}U makeup of 134 kg/GW_e · yr at 80% capacity factor.

Conclusions. The role of the HTGR in providing a potential market for fuel bred by the TMHR has been assessed. Interest in the HTGR could be sustained because of its inherent safety characteristics and its capability for high temperature operation for gas turbine and process heat applications. During the time frame of interest, which is the early 21st century, the HTGR could be commercially established at capital costs comparable with those of LWRs with recycle facilities in operation for the reprocessing and refabrication of ^{233}U . The HTGR could therefore provide a market for TMHR-bred ^{233}U . The fuel consumption for the HTGR is 134 kg/GW_e · yr, which is 40% smaller than that of the LWR. This will allow one TMHR to support a large number of burner reactors, thus making the total system electricity cost fairly insensitive to the cost of the hybrid reactor.

TABLE 8-32. HTGR fuel consumption characteristics.

(Annual ^{233}U feed requirements with self-generated ^{233}U recycle for a 1-GW_e reactor with 80% capacity factor using annual refueling and a 4-yr fuel cycle.)

C/Th	Power density, W/cc	Conversion ratio	Initial core, kg	Makeup, kg/yr
60	5	1.00	8550	66
90	5	0.97	1350	67
120	5	0.95	2850	75
150	5	0.92	2150	88
180	7	0.85	1545	134
180*	7	0.76	2040	242

^aLead-plant HTGR with high-enriched ^{235}U feed and self-generated ^{233}U recycle.

RESOURCE AND MARKET ECONOMIC ASSESSMENT

Introduction

The Resource and Market Economic Assessment (RMEA) for the TMHR is an on-going effort to evaluate the competitive strengths and weaknesses for the hybrid. From research on the fusion process, we recognize that the most easily achieved fusion reaction is the deuterium-tritium reaction. With an energy release, a neutron and a He atom are formed. The neutron is subsequently used to produce replacement tritium fuel or to produce nuclear fuel for fission reactors. In the hybrid concept, the fusion reactor produces both its tritium fuel plus saleable fission reactor fuels such as ^{239}Pu and ^{233}U .

The hybrid reactor's ability to make a variety of different products, such as electricity, electricity plus Pu, etc., at different rates and to compete in a number of market places has introduced some confusion into the design of the hybrid. No inclusive market-oriented study has been produced to determine the reactor characteristics that would best meet market needs and provide a clear objective for the hybrid designers.

This hybrid marketing study has the goal of addressing a number of key economic and logistic issues that affect the design of the hybrid reactor from the point-of-view of the marketplace. This study includes a partial cost/benefit study to estimate the national benefit of some of the design options

and of the program itself. Issues such as determining the optimum hybrid plant size and economics of the various fuel production modes are analyzed separately.

Market Place in Year 2010

The market in the year 2010 for synthetic nuclear fuels and by-product electricity from fusion hybrid reactors will depend to a large degree on five key factors that influence the use of fission energy. These factors are:

- Electrical load growth.
- Rate of addition of nuclear capacity.
- Extent of high grade U_3O_8 resources.
- Alternate nuclear fuel and reactor options.
- Public acceptance of nuclear energy.

How these factors will combine by the year 2010 is difficult to foretell. What is hoped is that with a description of each of these issues a clearer understanding of the potential role of the hybrid might be provided, and that a range of market conditions might be found for use in optimizing plant characteristics. In general, this analysis bounds the role of many advanced technologies that do not use conventional resources such as uranium, coal, and oil.

Electrical Load Growth. Electrical energy use in the U.S. has over the last four to five decades increased at an average rate of about 7% per year. The actual year-to-year increases (Fig. 8-12) have, however, been erratic, with electrical growth varying from as high as a 17% growth to a low of a 9% drop. In the U.S. and internationally, the economic disruptions following the 1973 Arab oil embargo caused another perturbation in the pattern of energy and electrical load growth. There was no growth in 1974 over the prior year 1973. Since then load growth returned to near historic levels in 1976 and 1977.

	<u>U.S. electrical load growth</u>	<u>Overall U.S. energy growth</u>
1974	-0.1%	-2.6%
1975	+1.9%	-2.8%
1976	+6.7%	+5.3%
1977	+5.1%	+2.0%
1978	+3.7%	-

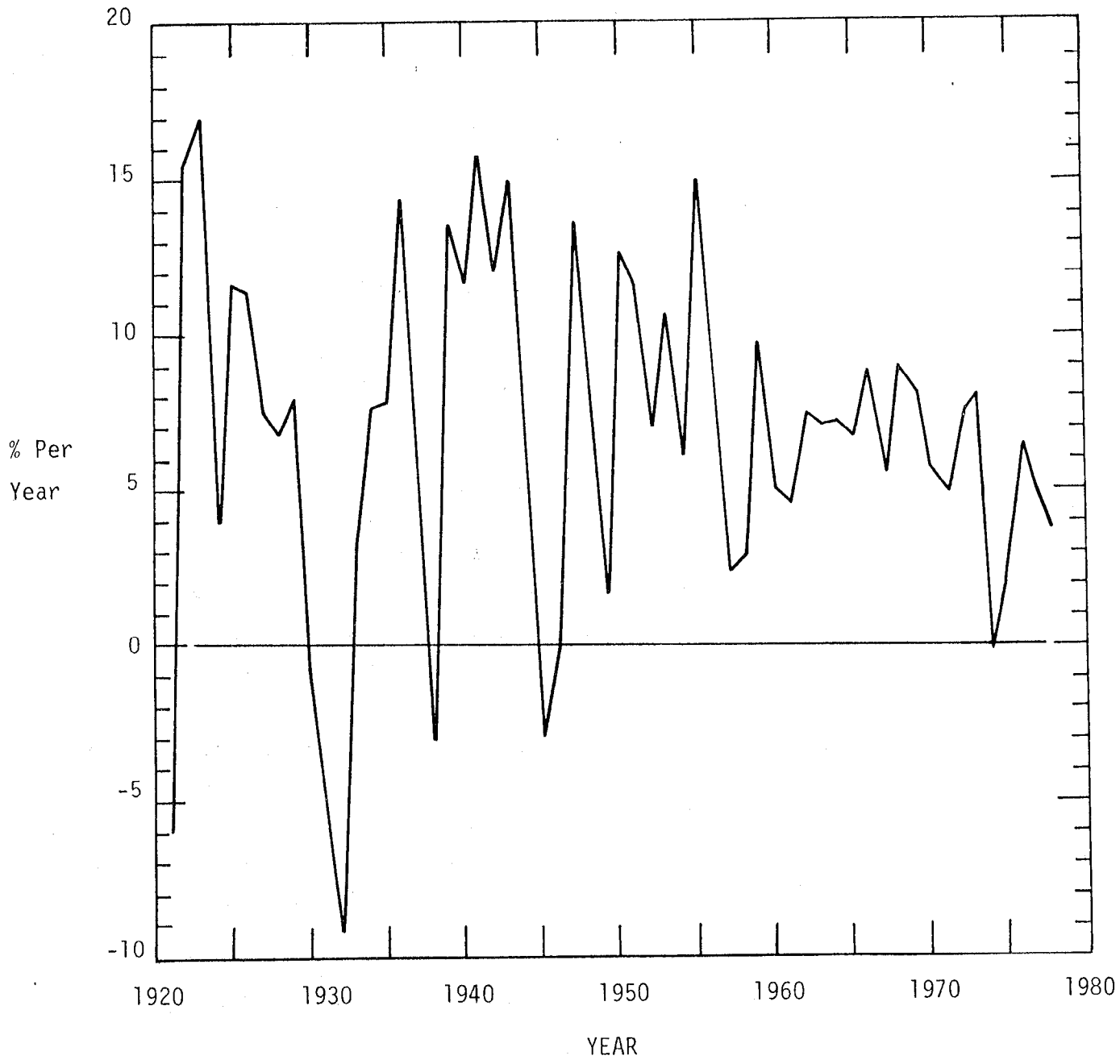


Fig. 8-12. U.S. electrical demand growth.

Many have argued that the relatively low electrical growth from 1973 until the present (3.4% average per year) reflects voluntary conservation along with the impact of higher prices. They furthermore believe that load growth in the next 20 years could be as low as 2 to 3%, citing higher prices, a declining energy/GNP ratio, and conservation.

A growth rate of 5% is in the range of what many studies are now predicting for the next 10 to 15 years. For example, the Edison Electric Institute, a professional association of the electric utility industry, now projects future electrical growth will decrease to 5.3% to 5.8% per year based on the effects of conservation, improved end use efficiency, and price elasticity. This will require either significant conservation or major institutional changes relative to the use of electricity.

A high growth rate, such as 7%, is in the range of what might occur should it become necessary sometime prior to the turn of the century to convert the nation's homes from gas and oil heating to electricity. Providing new homes with electric heating and converting older homes to electricity would by itself add about 3-1/2% to the annual electrical growth rate from now to the turn of the century for the residential sector. In this event, a total electrical growth rate in the range of 7% might result. Should it be necessary to also phase out the use of gas and oil for commercial and industrial use, the growth rate in electrical usage could be higher yet.

For this study, three electrical growth rates will be considered as part of the driving force for the use of nuclear energy. These rates will be 3%, 5%, and 7%. The rate of growth after the year 2000 is assumed to be reduced by one-third from these values. Table 8-33 shows that even modest rates of electrical load growth will lead to sizeable increases in electrical use. Load growth is shown in percent per year.

Table 8-33. Future electrical use (as a multiple of 1978 electrical use).

Load growth, %/yr		2000	2010
1979-2000	2001-2010		
3	2	1.9	2.3
5	3.3	2.8	3.9
7	4.7	4.1	6.6

Domestic Nuclear Energy Usage. Given the uncertainty in forecasting electrical load growth, forecasting nuclear capacity constructions and their fissionable fuel needs is equally or more difficult. Fortunately, nuclear fission appears to be constrained today by institutional and social forces rather than energy demand. If this trend continues through the 1990 planning year, then nuclear constructions would be similar for a variety of electrical energy growth rates through the year 2000. After year 2000, the role of nuclear fission energy should be more defined, possibly maintaining its year 2000 market share. For this analysis, it will be assumed that nuclear fission energy will grow identical to electrical growth after 2000.

We suggest, also, that three different nuclear capacities be considered in the year 2000--a year for which many have forecasted. A low case with 200 GWe in year 2000; a medium case with 400 GWe in year 2000; and a high case with 600 GWe in year 2000. The 200-GWe scenario essentially represents a nuclear moratorium with few plants being committed in addition to those presently planned. The 600-GWe projection represents what could be achieved if the nation were to ease institutional constraints on nuclear plant installations. The 400-GWe projection provides an in-between point of comparison roughly equivalent to many of DOE's current projections.

Using the above guidelines to project to the year 2010 (Table 8-34), the low nuclear scenario shows 240 to 320 GWe; the medium scenario, 490 to 630 GWe; and the high nuclear scenario, 730 to 950 GWe.

Table 8-34. Nuclear capacity projection.

Load growth, %/yr		Projection, GWe		
1979-2000	2001-2010	Low	Medium	High
3	2	240	490	730
5	3.3	280	550	830
7	4.7	320	630	950

Table 8-35 shows the electrical energy contributions implied by the above nuclear scenarios and the relative importance of the fuel supply for fission reactors.

Table 8-35. Nuclear contribution (as a multiple of year 2010 total electrical usage).

Load growth, %/yr		Nuclear capacity projection, GWe		
1979-2000	2001-2010	Low	Medium	High
3	2	0.3	0.6	0.9
5	3.3	0.2	0.4	0.6
7	4.7	0.1	0.2	0.3

World Nuclear Energy Usage. Like domestic forecasts of nuclear capacities, world forecasts are produced by both combining economic forecasting techniques and political realism. The forecasts thus reflect the forecasters own perception of the political constraints that will hinder or expand nuclear constructions. Table 8-36 lists six such forecasts.

In recent years differing views on the magnitude of the role for nuclear fission have developed. The U.S. has swung to the perception that nuclear fission's role has been over estimated and has lowered its forecast. The Europeans, however, have also reduced their forecasts from past years but have consistently produced forecasts with larger nuclear contributions than does the U. S. The uncertainty in world forecasts is thus almost 50% of the forecasts themselves.

For this analysis the reference world capacity forecast (U.S. inclusive) will be one found by averaging the U.S. EIA forecast and the European OECD/IAEA forecasts. It will also be assumed that world nuclear capacity will grow at an average annual rate of 3.3% from years 2000 to 2010. With this basis, the low nuclear forecast is 850 GWe in 2000 and 1180 GWe in 2010. The medium forecast is 925 GWe in 2000 and 1280 GWe in 2010. The high forecast is 1000 GWe in 2000 and 1380 GWe in 2010.

Table 8-36. Comparison of world nuclear forecasts.

Source	Date	Capacity at year's end, GWe	
		Year 2000	Year 2010 ^a
EIA	Oct. 1978	700-850-1050	970-1180-1450
INFCE ^b	Oct. 1978	832-1207	1150-1670
AECL/WEC	July 1978	1142	1580
ERG/WEC	July 1978	967-1284	1340-1780
OECD/IAEA	Dec. 1977	1000 ^c -1890	1380-2620
WAES	May 1977	913-1772	1260-2450

^aAssumes 3.3% per year growth rate from years 2000 to 2010.

^bU.S. contribution to INFCE.

^cPresent trend. No low forecast was supplied.

Internationally, the split of reactor sales may be determined by the vested manufacturing interests of individual nations. It is assumed for determining fuel needs that 15% of these plants will be of the CANDU type (50% of non-European capacity) and 85% of the LWR, Table 8-37.

Nuclear Fuel Resources/Demand. As a fuel producer, the fusion hybrid reactor will compete with mined uranium in a number of ways, such as: to reduce a uranium shortfall; to supply a redundant, alternate fuel source; to develop an unavailable fuel (^{233}U or ^{239}Pu); or as a more economical or ecological option to mining additional uranium.

The following articles describe the availability of uranium domestically and internationally and the demands for fuel supplied by mining uranium or by breeding in the hybrid. Also described are the availability, cost, and demand for thorium.

The economic argument for developing a hybrid reactor capability hinges upon our ability to forecast the extent of future supply and price. Abundant, cheap uranium reduces or postpones the need for the hybrid reactor, while scarce or high-cost uranium implies a compelling advantage and need for hybrids. The evaluation of U.S. and foreign resources thus involves three questions:

Table 8-37. Reference nuclear forecast.

		Capacity at year's end, GWe	
		2000	2010
U.S.			
LWR		200-400-600	280-550-830
	Total	200-400-600	280-550-830
International			
LWR (85% of total)		382-446-510	535-620-705
CANDU (15% of total)		68- 29- 90	95-110-125
	Total	450-525-600	630-730-830
World			
LWR		737-794- 850	1022-1098-1172
CANDU		113-131- 150	158- 182- 208
	Total	850-925-1000	1180-1280-1380

- How much uranium might be discovered?
- What is the expected economic cost of discovering and developing that ore?
- How much of the higher cost (lower grade) ores will be acceptable to mine?

Domestic Uranium Resources. The DOE and mining industry estimates of domestic uranium resources are based on both known reserves and expected but undiscovered resources in and around existing mining districts. Exploration activities throughout the geologically attractive areas since 1960 have not located any new districts in spite of the fact that exploration effort since 1960 is four times greater than all cumulative exploration through 1960.

The 1978 DOE U.S. uranium resource estimate is divided into four informational categories: Reserves, Probable, Possible, and Speculative resources, as shown in Table 8-38. The four informational categories represent ores in differing states of discovery. The Reserves and Probable categories are defined by the largest information base, and the Possible and Speculative categories by progressively less physical evidence.

The known Reserves category represents ore resources for which definitive drilling and mineralogical statistics have been determined and are now being

Table 8-38. 1978 DOE U.S. uranium resource estimate (tons U₃O₈).

Forward cost, \$/lb U ₃ O ₈	Reserves	Estimated resources			Total
		Probable	Possible	Speculative	
Less than 15	360,000	560,000	485,000	165,000	1,570,000
15 to 30	<u>330,000</u>	<u>505,000</u>	<u>635,000</u>	<u>250,000</u>	<u>1,720,000</u>
Up to 30	690,000	1,065,000	1,120,000	415,000	3,290,000
30 to 50	<u>185,000</u>	<u>385,000</u>	<u>350,000</u>	<u>155,000</u>	<u>1,075,000</u>
Up to 50	875,000	1,450,000	1,470,000	570,000	4,365,000
By-product	<u>140,000</u>	<u>---</u>	<u>---</u>	<u>---</u>	<u>140,000</u>
Total	1,015,000	1,450,000	1,470,000	570,000	4,505,000

developed. To many, the Reserves are comparable to those ores that a mining company would be willing to sell today for future delivery.

The Probable resource category is defined as ores surrounding existing mines that have not been as extensively drilled as the Reserves category ores. The Probable resource estimates are found by mapping local ore trends and interpolating data where necessary.

The Possible resource category represents ores that may be found when a mining district is fully explored and those ores in mining districts not currently producing uranium. This estimate is found by multiplying the Reserves and Probable categories by the ratio of the total surface area of known mining districts to the surface area currently well explored in these mining districts.

The Speculative resource category is defined as ores which might be discovered if additional mining districts are located. These additional districts are expected by statistical techniques, but have yet to be found.

DOE believes there is a reasonable prospect that something in the range of 4.5 million tons of U₃O₈ will ultimately be recovered. In contrast, many in industry believe the significance of the DOE estimate lies in the supporting geological information that has been accumulated. They believe that because of the importance of being conservative in projecting national energy

supplies, probabilities should be placed on actually finding and developing the ores. When such a procedure is used, U.S. resources have been estimated to be less than half of an estimate using the above DOE technique. DOE has also recognized the uncertainty of any geological estimating procedure and the importance of conservatism. For planning purposes, DOE considers 2.5 million tons consisting of ore Reserves plus Probable resources, plus by-product sources, as a prudent planning basis.

For this assessment two U.S. uranium resource bases will be used. The first is a prudent planning base of 2.5 million tons. The second is the full DOE uranium estimate of 4.5 million tons (Table 8-39).

Table 8-39. U.S. uranium resource estimate.

	Basis	Estimate
Prudent planning base	Reserves plus probable	2.5 million tons U ₃ O ₈
Full DOE estimate	Reserves, Probable, Possible, and Speculative ores	4.5 million tons U ₃ O ₈

How uranium prices will rise as U.S. and worldwide resources are depleted is difficult to predict, as is the extent of the resources themselves. Today, spot market prices are between \$40 and \$50/lb U₃O₈. For the future, the success of explorations, the cost of developing and operating new mines and mills, and other factors such as environmental protection will all affect the price of uranium.

For this assessment uranium prices will rise as higher grade resources are depleted and lower grade resources are developed. Prices are assumed to rise linearly from \$40/lb U₃O₈ (1979 \$) today to \$110/lb U₃O₈ (1979 \$) when the resource base is completely depleted, as shown in Table 8-40. This rationale implicitly assumes that uranium prices will be independent of the price of other fuel resources and the prevention of domestic cartel pricing schemes.

The preceding resource estimates implicitly assume that there is a fixed uranium resource base; and once it has been mined, that lower and lower grade and higher cost resources will not become productive. For uranium this appears

to be the case. In the West, high grade uranium deposits were formed by river water precipitating through carbonaceous fields leaving behind previously dissolved uranium. This process does not appear to produce large, low or medium grade deposits that are necessary for uranium price to continue to be a function solely of ore grade. And Eastern ores, such as the Tennessee shales* and the Conway Granites, appear to have too low an ore grade to be environmentally mined.

World Uranium Resources. The OECD Nuclear Energy Agency, the International Atomic Energy Agency (IAEA), the U.S. DOE, and individual supplier nations have published uranium resource estimates. Of these organizations, the joint reports of the OECD and IAEA are considered the most authoritative. A current OECD-IAEA world uranium estimate is shown in Table 8-41 as revised by DOE. (The Reasonably Assured and Estimated Additional categories correspond roughly to DOE's Reserves and Probable categories.)

There are two important points to add to the OECD-IAEA estimates to directly compare them to DOE U.S. uranium estimates. First, OECD-IAEA estimates do not include ores with incremental forward costs in the \$30 to \$50 per pound categories; second, these estimates also do not include the more speculative ores such as were included in DOE's domestic forecast. When these factors are included, world uranium resources appear to be between 5.8 and 10.6 million tons (Table 8-42).

*The Tennessee--or Chattanooga--shales occupy a large part of eastern Tennessee, bedded in three layers beneath 150 feet of limestone overburden. Only the upper two layers are normally considered recoverable. The top layer is about 7 feet thick and contains about 70 ppm U₃O₈, while the next layer is approximately 8 feet thick and contains uranium in concentrations 25 to 60 ppm. The top layer is estimated to contain nearly 5 million tons of U₃O₈, while the bottom may contain up to 8 million tons.

The Conway Granites contain 20 to 40 ppm of uranium and are thought to aggregate 25 million tons of U₃O₈; plus byproduct thorium, at costs greater than \$220 per pound or more; plus environmental effects comparable to or worse than that involved in mining the Chattanooga shales.

Table 8-40. U.S. uranium price estimates (\$/lb U₃O₈ - 1979 \$).

Cumulative use (millions of tons)	Price (\$/lb)		Cumulative demand (millions of tons)		
	Prudent planning base	Full DOE estimate	Price (\$/lb)	Prudent planning base	Full DOE estimate
0	40	40	40	0	0
0.5	54	48	50	0.36	0.64
1.0	68	56	60	0.71	1.29
1.5	82	63	70	1.07	1.93
2.0	96	71	80	1.43	2.57
2.5	110	79	90	1.79	3.21
3.0	-	87	100	2.14	3.86
3.5	-	94	110	2.50	4.50
4.0	-	102			
4.5	-	110			
5.0	-	-			

Table 8-41. World uranium resources by continent.

(Excludes Peoples Republic of China, USSR, and associated countries)
 Thousand tons U₃O₈
 \$30/lb

	Reasonably assured	Estimated additional
<u>North America</u>	920	1540
U.S.*	690	1015
Canada*	220	525
Mexico	6	3
<u>Africa</u>	680	200
South Africa and Namibia	400	44
Niger	210	69
Algeria	36	65
Gabon	26	7
C.A.R.	10	10
Zaire	2	2
<u>Australia</u>	380	60
<u>Europe</u>	80	60
France	48	31
Spain	9	11
Portugal	9	1
Yugoslavia	6	7
Germany	2	4
Italy	2	1
Austria	2	0
Sweden	1	4
Finland	2	0
<u>Asia</u>	20	0
India*	5	1
Japan	10	0
Turkey	5	0
<u>South America</u>	50	20
Brazil	24	11
Argentina*	25	4
Chile	0	7
Total (rounded)	2100	1900

*Revised since OECD report.

SOURCE: "Uranium Resources, Production and Demand,"
 OECD Nuclear Energy Agency and the International Atomic
 Energy Agency, December 1977.

Table 8-42. Expanded world uranium resource estimate (millions of tons U₃O₈).

Cost category, \$/lb U ₃ O ₈	Reserves	Resources			Total
		Probable	Possible	Speculative	
0-30	2.1	1.9	-	-	7.3
30-50	<u>1.0</u>	<u>0.8</u>	-	-	<u>3.3</u>
Total	3.1	2.7			10.6

For this assessment a Planning Base and a Full Uranium Base ground rule will be used for estimating world uranium resources, as was done for U.S. resources (Table 8-43). On this basis, there are 5.8 million tons on a prudent planning basis and 10.6 million tons on a full uranium basis. No world uranium price estimate will be made because of the possibility of cartel pricing.

Table 8-43. World uranium resource basis.

	Basis	Estimate
Prudent planning base	Reserves plus Probable	5.8 million tons U ₃ O ₈
Full world estimate	Reserves, Probable, Possible, Speculative	10.6 million tons U ₃ O ₈

Domestic Uranium Demand. Table 8-44 shows the annual and cumulative uranium use in the U.S. for the referenced three nuclear growth projections previously characterized, along with their implied 30-yr uranium needs, called commitments. (Again, the low nuclear forecast assumes 280 GWe in year 2010; the medium nuclear forecast is 550 GWe; and the high nuclear forecast is 830 GWe.)

In summary, Table 8-44 assumes that the uranium enrichment plants operate at a tails assay of 0.2% ²³⁵U, that the reprocessing/fuel recycle industry will be slow in developing, and that the existing reactor fuel use characteristics will exist at the turn of the century. The next subsection, Alternate

Table 8-44. U.S. uranium demand^a--thousands of short tons
 U_3O_8 (75% capacity factor, 0.20% tails).

Year	Low nuclear			Medium nuclear			High nuclear		
	Annual	Cumulative	Committed ^b	Annual	Cumulative	Committed ^b	Annual	Cumulative	Committed ^b
1990	26	350	984	43	437	1983	53	476	2967
2000	38	665	1721	74	1051	3100	110	1386	4455
2010	53	1117	2606	103	1941	4821	152	2689	6799
2020	71	1737	3630	144	3187	7274	213	4532	10830

^aNo recycle.

^bA 30-yr supply is committed at time of plant sale, 10 years before plant startup.

Nuclear Fuel Supply Options, describes what the nation might do to reduce its uranium use below the levels of Table 8-44.

Three conclusions are evident from a survey of Table 8-44. First, the relative importance of fuel from a single hybrid fuel factory varies considerably from the low nuclear to the high nuclear forecast. Second, uranium resources (if mined as demanded) are sufficient to fuel all the nuclear forecasts through year 2010, even if the low uranium availability forecast (prudent planning base) is assumed. Third, uranium prices may only be modestly higher in year 2010 than they are today because cumulative use of uranium lags behind the commitment of the resource base.

The number of hybrid fuel factories necessary to supply fuel to a converter reactor economy depends on such factors as the availability of uranium (^{235}U), the number of converter reactors, the size of the hybrid fuel factory, and the type of fuel produced by the hybrid reactor. One large hybrid reactor of 4000 MW_{th} output with a thorium blanket will produce about 2300 kg of ^{233}U and support about 10 GWe of LWR capacity. With 28 such hybrid plants, no ^{235}U need be mined for the U.S. to support its LWR in year 2010 for the low nuclear forecast; for the medium nuclear forecast, 55 hybrids; for the high nuclear forecast, 85 hybrids. With fewer hybrid fuel factories, different degrees of independence from a mined-fuel fuel cycle result. The hybrid clearly can act as a fuel supply technology should annual ^{235}U production limits exist. (Note that breeders and advanced converters cannot affect near-term uranium supply problems as can a hybrid reactor.)

The hybrid reactor is one of many insurance policies the nation can develop to assure an adequate nuclear energy contribution. The fission technologies, the fission breeder, and the ACR require the development of their industries and their introduction before domestic uranium resources are committed, while the hybrid reactor's potential as a fuel supplier makes it conceptually difficult to introduce prior to the actual depletion of domestic resources. If the nation chooses a multi-program with ACR's or breeders, in addition to hybrid reactors, the ACR's or breeders must be introduced earlier than the hybrid. Thus a successful ACR or breeder program could reduce the demand for hybrids even though its development program was successful.

How well hybrid bred fuels will compete with mined uranium will also depend on the selling price for ^{235}U . The cumulative uranium usage of Table 8-44, in conjunction with the price assumptions of Table 8-45, shows modest

Table 8-45. Domestic uranium prices - \$/lb U₃O₈ (1979\$).

Year	Prudent planning basis assumption			Full DOE estimate assumption		
	Low nuclear	Medium nuclear	High nuclear	Low nuclear	Medium nuclear	High nuclear
2000	59	69	79	50	56	62
2010	71	94	115	57	70	82
2020	89	129	167	67	90	110

uranium prices in 2010 even though all domestic uranium might be committed. The ability of the hybrid to meet mined-fuel short falls may delay introduction of hybrid reactors until instantaneous uranium prices are large (in comparison to projected hybrid bred fuel prices). Yet, they may be introduced earlier based on long-term economics (as might be the first fission breeders or ACR's). The probability of such a case occurring will depend on the number of years of fuel sale losses before hybrid fuels are competitive with lower grade (high cost) uranium ores and how and who is absorbing these losses and risks.

World uranium needs are shown in Table 8-46.

Thorium Availability Demand. Thorium fuel cycles are often mentioned as alternates to the uranium-plutonium cycle because the bred ²³³U can be mixed with ²³⁸U for recycling as fuel. This denaturing precludes the chemical separation of the ²³³U. Separation would require the more difficult enrichment process as does ²³⁵U in natural uranium. For the conventional uranium-plutonium fuel cycle, thorium is not used.

It is important to recognize that the nation and the world have abundant resources of both fertile thorium and ²³⁸U. It is the fissile fuels that are scarce. The availability of thorium is thus generally not seen to be a limiter of thorium-based fuel cycles. This will be the assumption for this report. The price of thorium will be based on the "Draft NASAP Provisional Data Base," with one year of inflation at 10% per year, and thus prices will remain constant at \$41.8/kg HM (1979 \$).

Table 8-46. U.S. uranium demand^a—thousands of short tons
 U_3O_8 (75% capacity factor, 0.20% tails).

Year	Low nuclear			Medium nuclear			High	
	Annual	Cumulative	Committed ^b	Annual	Cumulative	Committed ^b	Annual	Cumulative
1990	111	1495	4203	115	1505	4579	121	15
2000	162	2839	7358	174	2958	7818	188	30
2010	224	4777	11166	241	5041	11799	259	53
2020	303	7436	15502	326	7894	16704	353	84

^aNo recycle.

^bA 30-yr supply is committed at time of plant sale, 10 years before plant startup.

Tables 8-47 and 8-48 provide another reference, based on dollar per gram fissile ^{235}U , that hybrid fuels must meet to be competitive. However, other issues, such as high fabrication costs for fabricating ^{233}U and ^{239}Pu fuels and differing fissile worths, will be important.

Table 8-47. Enriched uranium price for 93% ^{235}U --\$/gm ^{235}U .

Year	Prudent planning basis assumption			Full DOE estimate assumption		
	Low nuclear	Medium nuclear	High nuclear	Low nuclear	Medium nuclear	High nuclear
2000	59	64	69	54	57	60
2010	65	76	87	58	64	70
2020	74	94	113	63	74	84

Table 8-48. Enriched uranium price for 3% ^{235}U --\$/gm ^{235}U .

Year	Prudent planning basis assumption			Full DOE estimate assumption		
	Low nuclear	Medium nuclear	High nuclear	Low nuclear	Medium nuclear	High nuclear
2000	45	49	54	40	43	46
2010	50	61	71	44	50	55
2020	59	78	96	48	59	69

Alternate Nuclear Fuel Supply Options

There are several options that the nation and the world might employ in addition to the hybrid, that will reduce nuclear fuel supply problems. Each may be a competitor to the hybrid. Some, like the hybrid, are long-term solutions while others are only short-term solutions. It is important however to recognize that even short-term options will be potential competitors to a beginning hybrid fuel industry.

Advanced LWR Fuels. Advanced fuels for LWR's may make possible an improvement of from 20 to 50% in uranium use. This improvement will reduce the demand for bred nuclear fuels. The improvements are made possible by the following design changes:

	<u>Uranium savings</u>
Increased discharge burnup	10 to 20%
Discharged fuel rod reinsert	5 to 12%
Coolant density and spectral shift control	6 to 10%
End-of-cycle extension	5 to 10%
Once-through thorium cycle	4 to 10%
Blankets and improved refueling	7%
Reduced fuel density	<u>5%</u>
Total	35 to 55%

The largest uranium savings is made possible by increased discharge burnup. This improvement requires extending the burnup by as much as 50%, while holding the refueling interval at one year. If the refueling interval is also extended, as utilities would probably prefer with longer life fuel, there is almost no uranium saving to be gained from extending the burnup. On a conservative basis, a gradual 25% improvement in LWR uranium utilization and a corresponding reduction in uranium use may occur.

Advanced Enrichment Processes. DOE is sponsoring advanced enrichment processes aimed at developing low cost enrichment so that tails can economically be stripped down to 0.1% ²³⁵U. The uranium savings made possible as a function of tails assay is shown in Table 8-49.

Table 8-49. Uranium savings-function of tails assay.

Tails, %	Natural uranium per pound new fuel, lb	Uranium saved by changing tails assay, %	Required additional enrichment plants, %
0.10	5.1	21	57
0.15	5.4	15	31
0.20	5.9	9	13
0.25	6.4	0	0

The uranium and enrichment requirements for the LWR as a function of tails assay are shown in Table 8-50

Table 8-50. LWR uranium and enrichment requirements as a function tails assay.

Tails, %	U_3O_8 , short tons/GWe-yr _c	Enrichment metric tons/GWe-yr _c
0.10	136	155
0.15	145	129
0.20	157	112
0.25	171	99

The cost of the uranium recovered by reducing the tails assay is thus a function of the quantity of uranium saved and the price of the advanced enrichment process, as shown in Tables 8-51 and 8-52.

How any new enrichment process will be deployed is difficult to foretell. The first facilities might be used initially to strip further the assay of existing tails with later facilities being used to reduce the operating tails assay of the existing enrichment facilities.

Table 8-51. Cost of uranium from advanced enrichment processes -
\$/lb U_3O_8 (feed at 0.3% ^{235}U).

Assay of stripped tails, %	Enrichment price, \$/SWU		
	50	70	90
0.10	27	38	49
0.15	20	28	36
0.20	16	22	28
0.25	12	17	22
0.30	0	0	0

Table 8-52. Cost of uranium from advanced enrichment processes -
\$/lb U_3O_8 (feed at 0.2% ^{235}U).

Assay of stripped tails, %	Enrichment price, \$/SWU		
	50	70	90
0.10	44	62	79
0.15	32	45	58
0.20	0	0	0

Such a process might have a timetable with the introduction of tail stripping plants in 1995 and the change of operating tails assay by 2005. The tail stripping might continue for 20 years before the existing 250,000 MT of tails (at 0.3% enrichment) and the 1,000,000 MT of tails produced between 1979 and 2005 are finally used. With such a program, mined uranium requirements in 2010 could be 15% less than without advanced enrichment, with 0.2% tails (Table 8-53). This one-time uranium savings (from 1995 to 2015) could adversely affect the initial marketability of hybrid bred fuels.

Table 8-53. Year 2010 domestic uranium requirements with advanced enrichment (thousands of short tons).

Tails, %	Without advanced enrichment	With advanced enrichment	% difference for 0.2% tails
0.10	103	89	16
0.15	103	95	8
0.20	103	103	0

Reprocessing of Spent Nuclear Fuel. The problems and issues of developing a reprocessing industry to separate the bred fuels of the hybrid reactor's blankets are identical to developing a reprocessing industry for reprocessing LWR-spent fuels. If hybrid blanket discharges with their bred fuels are to be useful, then a significant reprocessing industry must be in place and have depleted LWR-spent fuel supplies prior to the growth of the hybrid industry. For this study, a significant LWR-spent fuel reprocessing industry will be assumed in the time frame of the hybrid reactor introduction.

National Plan. The recycling of nuclear fuels has long been viewed as an effective means of conserving uranium, and the development of reprocessing plants to recover these fuels has been a common point for many nuclear technologies. Yet the development and use of reprocessing technology may lead to the separation of high grade fissile fuels in many nations.

In April 1977, President Carter stated his intention to postpone the reprocessing of spent nuclear fuel (and the breeder reactor) in the U.S. and

expressed his desire that all nations also postpone reprocessing. He cited his concern for international nuclear weapons proliferation and the possibility of a 75-year supply of uranium for LWR's then operating or on order.

Since 1977, many groups have worked on changing past reprocessing plant designs to a form more proliferation-resistant than the original high decontamination PUREX process. This work has led to designs such as the CIVEX process, whereby some fission products always remain with high fissile content fuels, such as plutonium. Other groups have investigated new fuel cycles using thorium, whereby plutonium production is reduced and ^{233}U production increased. In these fuel cycles, the reprocessing plant again separates the valuable fissile materials, but in addition, all ^{233}U is diluted with ^{238}U to acceptably low fissile enrichments. Such "technical fixes" along with international inspections may represent the reprocessing designs available when the industry begins to develop.

How and when the reprocessing industry will develop is difficult to predict. The current operating mode of the U.S. is to delay reprocessing until necessary, thus creating a spent fuel stockpile or permanent disposal of spent fuel. (The later approach may be impractical without some separation process.) How long this stockpile will compete with hybrid blankets for a source of bred fuels will depend on how fast and when this industry develops.

A Growth Scenario. Table 8-54 shows an LWR-spent fuel reprocessing scenario with three companies developing the industry, each committing to their first large facilities 4 to 5 years after committing to their first medium-sized facility. Such an aggressive schedule may be likely in a favorable government environment with a large stockpile of aged, spent nuclear fuel. The schedule shown in Table 8-54 will be assumed for this study.

Two points from Table 8-54 are of importance. The first is that it will take 18 years to develop the reprocessing industry to the point at which it can reprocess the annual discharges of LWR-spent fuel. Thus, if the first hybrid reactor were to produce fuel before this time, the nation would not gain any usable fissile until the reprocessing industry was larger. Second, to guarantee a lifetime supply of spent fuel for the industry, the industry may decide not to overbuild more than 10 to 20% above the equilibrium level. Under these conditions, it would take 5 to 10 years after equilibrium has been reached (28

Table 8-54. Reference LWR reprocessing industry growth scenario.

Year	New commitments		Capacity at year's beginning thousands of MT/yr		Fuel ^c reprocessed (thousands MT)
	1500 MT/r plants	3000 MT/yr plants	New ^b	Operating	
0	1 ^a	-	-	-	-
0	1 ^a	-	-	-	-
1	1	-	-	-	-
2	1	-	1.5 ^a	1.5	0.5
3		-	-	1.5	1.5
4		1	-	1.5	3.0
5		0	-	1.5	4.5
6		1	-	1.5	6.0
7		1	-	1.5	7.5
8		2	-	1.5	9.0
9	Limited by longterm spent fuel supply only		-	1.5	10.5
10			-	1.5	12.0
11			1.5	3.0	14.0
12			1.5	4.5	17.0
13			1.5	4.5	21.5
14			3.0	7.5	27.9
15			-	7.5	36.0
16			3.0	10.5	45.9
17			3.0	13.5	57.9
18			6.0	19.5	73.8

^aThe existing AGNS plant will require some modifications before startup to meet future licensing requirements.

^bBased on 10-year design/construction/licensing period.

^c30% operation first year, 70% operation second year, 100% thereafter.

to 38 years after a national commitment to reprocessing) to deplete the national stockpile of spent fuel. During this period, the spent nuclear fuel stockpile would further reduce LWR fuel needs.

Table 8-55 shows the quantity of bred fuels available from the reprocessing industry of Table 8-54 , along with the number of LWR's that can be supported.

Reactor Options. Another solution to a uranium supply problem that will compete with the hybrid concept (especially for R&D funds) will be the development of new reactors that use less uranium or no uranium at all. The deployment of a more uranium-conserving reactor would reduce future uranium needs below what might otherwise have occurred. However, because new advanced reactors cannot reduce the uranium need of existing reactors, long-term planning must occur to match life cycle uranium needs with expected uranium production. Such advanced uranium-conserving reactors currently being developed are: the advanced CANDU, the HTGR, the Pebble Bed Reactor, and the LMFBR.

Hybrid's Impact on Fuel Resources

The timing and the need for the hybrid reactor may be viewed in terms of its impact on the nation's fuel resource bases and on the security of the nation's electrical supply. In essence, one of the merits of the hybrid is that it can be developed and produce fissionable fuel unrestrained by material resource availabilities. This fissionable fuel thus may reduce mined uranium supply shortfalls or increase the number of nuclear power plants otherwise available to the nation.

A variety of actual patterns of hybrid reactor additions can be envisioned. Many will depend on the relative success of the hybrid program in developing a technical base, in creating a viable vendor industry, in reducing the financial risks of early hybrids to the owner/operator, and in the willingness of the vendors and potential owner/operators as well as the government to accept the financial costs and financial risks necessary to bring the hybrid into commercial existence. However, all will depend on the development of supporting fuel services.

Table 8-55. Fuels available from reprocessing industry.

Year	Natural uranium equivalent, ^a thousands of ST U ₃ O ₈		Fissile plutonium, thousands of kg		Number of LWR's supportable by recycle GWe
	Annual	Cumulative	Annual	Cumulative	
0	-	-	-	-	-
1	-	-	-	-	-
2	0.5	0.5	3.2	3.2	-
3	1.1	1.6	6.4	9.6	6
4	1.6	3.2	9.6	19.1	12
5	1.6	4.7	9.6	28.7	18
6	1.6	6.3	9.6	38.3	18
7	1.6	7.9	9.6	47.8	18
8	1.6	9.5	9.6	57.4	18
9	1.6	11.0	9.6	67.0	18
10	1.6	12.6	9.6	76.5	18
11	2.1	14.7	12.8	89.3	18
12	3.2	17.9	19.1	108.4	24
13	4.7	22.6	28.7	137.1	36
14	6.7	29.3	40.8	177.9	53
15	8.5	37.8	51.7	229.6	76
16	10.4	48.2	63.1	292.7	96
17	12.6	60.8	76.5	369.2	118
18	16.7	77.5	101.4	470.6	143

^aDischarged uranium is 0.79% ²³⁵U. With a 0.20% tails assay and a 30% penalty for ²³⁶U buildup, 1 kg of discharged uranium = 0.8 kg of natural uranium.

^b1,226 kg of Pu fissile used per GWe-yr_c; 157 ST U₃O₈ used per GWe-yr_c (recycle credits not included).

This subsection considers three possible cases for deploying the hybrid reactor as a means of sampling the impact of the hybrid on the fission reactor and fuel service industries. These hybrid deployment cases point out the interrelationships between the hybrid, fission reactors, and fuel services. No attempt was made at this time to further list those requirements and milestones necessary to actualize the assumed hybrid deployment and fuel service scenarios.

Hybrid Deployment Scenarios. The three hybrid deployment scenarios suggested have been developed to particularly address the program risks involved in committing new hybrids based on the operating experience accumulated at the time commitment decisions must be made. These risks are typical to the introduction of many new power generation technologies. To further reduce the complexity of these introduction scenarios, it has been assumed that the plant size would not change with time. For this study, the study guide-line plant size of 4000 MW_{th} has been used. The three cases are summarized in Table 8-56 and described herein.

Business as Usual Scenario. This case is characterized by a moderate willingness of industry and government to commit hybrid plants before extensive experience with preceding units has been acquired. A small demonstration plant is assumed to have operated successfully prior to year 0. The first large (but prototypical) hybrid TMHR-1 would be committed in year 0 for startup in year 10. The construction permits for this first plant would be awarded in year 3, and it is assumed that a second hybrid, TMHR-2, would be committed at this point. The further buildup of orders is assumed to await initial operation of TMHR-1. Commercial orders begin in year 10 with the first commercial plants assumed to startup 10 years later. This scenario is, therefore, basically a base technology program with a conservative deployment strategy.

Accelerated Deployment Scenario. The second case reflects a more urgent need for hybrids and is characterized by a buildup of commitments beginning during the construction of TMHR-1. This necessary confidence might be fostered by a limited uranium supply picture, a particularly successful hybrid demonstration plant, or appropriate government support. TMHR-1 and TMHR-2 are again committed in years 0 and 3, respectively, with further commitments beginning in year 6.

Table 8-56. Sample hybrid deployment scenarios (4000 MW_{th} plants).

Year	Business as usual			Accelerated deployment			Nati
	New commitments	New additions	Cumulative capacity	New commitments	New additions	Cumulative capacity	New commitments
0	1	-	-	1	-	-	1
1	-	-	-	-	-	-	1
2	-	-	-	-	-	-	2
3	1	-	-	1	-	-	2
4	-	-	-	-	-	-	4
5	-	-	-	-	-	-	4
6	-	-	-	1	-	-	6
7	-	-	-	2	-	-	8
8	-	-	-	3	-	-	10
9	-	-	-	4	-	-	15
10	1	1	1	5	1	1	20
11	1	-	1	6.5	1	2	25
12	2	-	1	8	-	2	30
13	2	1	2	9.5	-	2	35
14	3	-	2	11	1	3	40
15	3	-	2	13	2	5	45
16	4	-	2	15	3	8	50
17	5	-	2	17	4	12	55
18	5	-	2	19	5	17	.
19	6	-	2	23	6.5	23.5	.
20	7	1	3	27	8	41.5	.
21	7	1	4	31	9.5	52	.
22	8	2	6	35	11	63	.
23	9	2	8	40	13	76	.
24	10	3	11	45	15	91	.
25	11	3	14	50	17	108	.

8-78

National Commitment Scenario

This case may illustrate what the hybrid could do for the nation if uranium were limited and a major national commitment were made to a hybrid introduction program. The aggressive introduction of new TMHR's was assumed to be limited by the demand for the TMHR fuel product (not shown).

Fuel Production. The rate at which hybrid fuels will be available is both a function of the number of hybrid reactors operating and, to a lesser extent, of the type of fertile material used in the blanket. Tables 8-57 through 8-60 illustrate the range of fuel production available from the four reference blanket options and the three sample hybrid deployment scenarios previously described. Also shown are the equivalent amounts of natural uranium and uranium enrichment that would be displaced if these hybrid fuels were used in LWR's. (See Table 8-44 for a comparison of U.S. uranium demand.)

As shown in these tables, each of the four reference blanket concepts have fuel production schedules that are 1 or 2 years displaced in time from any of the others. This occurs because in the early years of commercializing and deploying the hybrid, the rate of change in the number of hybrids will be much larger than the differences in fissile production rates between blanket concepts. Thus it appears that the choice between blanket options should not be made on production rates per reactor but on other considerations that will influence the rate of deployment of hybrids, such as public acceptance, economics, and availability of supporting fuel cycle services.

Supporting Fuel Cycle Services. As much a part of the deployment of the hybrid reactor is the deployment of its supporting fuel cycle services, reprocessing, and bred fuel fabrication. Without both fuel services being available, the hybrid concept cannot function. Tables 8-61 through 8-64 show the quantities of reprocessing and fabrication that will be needed with each of the four reference blanket concepts for the three sample hybrid deployment schedules.

As shown in these tables, the choice of blanket concept does not significantly influence the size of the reprocessing or fabrication industries. Rather, the blanket choice will influence whether the proposed LWR or HTGR fabrication or reprocessing industries must be expanded or new ones developed.

Table 8-57. Fuel production schedule - with ²³⁹U blanket.

Year	Business as usual			Accelerated deployment			National	
	Fissile	U ₃ O ₈	Enrichment	Fissile	U ₃ O ₈	Enrichment	Fissile	U ₃ O ₈
	available, ^a MT	equivalent, ^b 10 ³ x ST	equivalent, ^b MT	available, ^a MT	equivalent, ^b 10 ³ x ST	equivalent, ^b MT	available, ^a MT	equivalent, ^b 10 ³ x ST
0	-	-	-	-	-	-	-	-
1	-	-	-	-	-	-	-	-
2	-	-	-	-	-	-	-	-
3	-	-	-	-	-	-	-	-
4	-	-	-	-	-	-	-	-
5	-	-	-	-	-	-	-	-
6	-	-	-	-	-	-	-	-
7	-	-	-	-	-	-	-	-
8	-	-	-	-	-	-	-	-
9	-	-	-	-	-	-	2.0	0.7
10	-	-	-	-	-	-	4.0	1.4
11	2.0	0.9	0.7	2.0	0.9	0.7	8.1	2.8
12	2.0	0.9	0.7	4.0	1.9	1.4	12.1	4.1
13	2.0	0.9	0.7	4.0	1.9	1.4	20	7.0
14	4.0	1.9	1.4	4.0	1.9	1.4	28	10.0
15	4.0	1.9	1.4	6.0	2.8	2.0	40	14.0
16	4.0	1.9	1.4	10.1	4.7	3.4	56	19.0
17	4.0	1.9	1.4	16.1	7.6	5.5	77	26.0
18	4.0	1.9	1.4	24	11.4	8.2	107	36.0
19	4.0	1.9	1.4	34	16.1	11.7	147	49.0
20	4.0	1.9	1.4	47	22	16.1	198	66.0
21	6.0	2.8	2.0	84	39	29	258	120.0
22	8.1	3.8	2.8	105	49	36	329	150.0
23	12.1	5.7	4.1	127	60	43	409	190.0
24	16.1	7.6	5.5	153	72	52	500	230.0
25	22	10.4	7.5	184	86	63	601	280.0

^aPer deployment scenario of Table 8-56 with the hybrid operating at a 70% capacity factor.

^b1 kg Pu = 0.47 ST U₃O₈ and 0.34 MT SWU.

Table 8-58. Fuel production schedule - with Th blanket.

Year	Business as usual			Accelerated deployment			National c	
	Fissile	U ₃ O ₈	Enrichment	Fissile	U ₃ O ₈	Enrichment	Fissile	U ₃ O
	available, ^a	equivalent, ^b	equivalent, ^b	available, ^a	equivalent, ^b	equivalent, ^b	available, ^a	equiva
	MT	10 ³ x ST	MT	MT	10 ³ x ST	MT	MT	10 ³ x
0	-	-	-	-	-	-	-	-
.								
8	-	-	-	-	-	-	-	-
9	-	-	-	-	-	-	2.3	1
10	-	-	-	-	-	-	4.6	3
11	2.3	1.6	1.1	2.3	1.6	1.1	9.1	6
12	2.3	1.6	1.1	4.6	3.2	2.3	13.7	9
13	2.3	1.6	1.1	4.6	3.2	2.3	23	15
14	4.6	3.2	2.3	4.6	3.2	2.3	32	22
15	4.6	3.2	2.3	6.8	4.7	3.3	46	31
16	4.6	3.2	2.3	11.4	7.9	5.6	64	44
17	4.6	3.2	2.3	18.2	12.6	8.9	87	60
18	4.6	3.2	2.3	27	18.8	13.4	121	83
19	4.6	3.2	2.3	39	27	19.0	166	115
20	4.6	3.2	2.3	54	37	26	223	154
21	6.8	4.7	3.3	94	65	46	291	201
22	9.1	6.3	4.5	118	81	58	371	256
23	13.7	9.5	6.7	143	99	70	462	319
24	18.2	12.6	8.9	173	119	85	564	389
25	25	17.3	12.3	207	143	101	678	468

^aPer deployment scenario of Table 8-56 with the hybrid operating at a 70% capacity factor
^b1 kg ²³³U = 0.69 ST U₃O₈ and 0.49 MT SWU.

Table 8-59. Fuel production schedule - with ²³⁸U blanket.

Year	Business as usual			Accelerated deployment			National (
	Fissile	U ₃ O ₈	Enrichment	Fissile	U ₃ O ₈	Enrichment	Fissile	U ₃ O ₈
	available, ^a MT	equivalent, ^b 10 ³ x ST	equivalent, ^b MT	available, ^a MT	equivalent, ^b 10 ³ x ST	equivalent, ^b MT	available, ^a MT	equivalent, ^b 10 ³ x ST
0	-	-	-	-	-	-	-	-
1	-	-	-	-	-	-	-	-
2	-	-	-	-	-	-	-	-
3	-	-	-	-	-	-	-	-
4	-	-	-	-	-	-	-	-
5	-	-	-	-	-	-	-	-
6	-	-	-	-	-	-	-	-
7	-	-	-	-	-	-	-	-
8	-	-	-	-	-	-	-	-
9	-	-	-	-	-	-	2.5	1
10	-	-	-	-	-	-	5.0	2
11	2.5	1.5	1.1	2.5	1.5	1.1	10.0	5
12	2.5	1.5	1.1	5.0	3.0	2.1	15.0	8
13	2.5	1.5	1.1	5.0	3.0	2.1	25	14
14	5.0	3.0	2.1	5.0	3.0	2.1	35	21
15	5.0	3.0	2.1	7.5	4.4	3.2	50	30
16	5.0	3.0	2.1	12.5	7.4	5.3	70	43
17	5.0	3.0	2.1	20	11.8	8.4	95	56
18	5.0	3.0	2.1	30	17.8	12.6	133	78
19	5.0	3.0	2.1	43	25	17.9	183	108
20	5.0	3.0	2.1	59	35	25	246	148
21	7.5	4.4	3.2	104	61	44	321	189
22	10.0	5.9	4.2	130	77	55	408	246
23	15.0	8.9	6.3	158	93	66	509	306
24	20	11.8	8.4	191	112	80	621	366
25	27	16.3	11.6	228	135	96	747	441

^aPer deployment scenario of Table 8-56 with the hybrid operating at a 7-% capacity fa

^b1 kg fissile = 0.59 ST U₃O₈ and 0.42 MT SWU.

Table 8-60. Fuel production schedule - with Be + Th blanket.

Year	Business as usual			Accelerated deployment			Nation	
	Fissile	U ₃ O ₈	Enrichment	Fissile	U ₃ O ₈	Enrichment	Fissile	eq
	available, ^a	equivalent, ^b	equivalent, ^b	available, ^a	equivalent, ^b	equivalent, ^b	available, ^a	l
MT	10 ³ x ST	MT	MT	10 ³ x ST	MT	MT		
0	-	-	-	-	-	-	-	
.								
8	-	-	-	-	-	-	6.5	
9	-	-	-	-	-	-	13.1	
10	6.5	4.5	3.2	6.5	4.5	3.2	26	
11	6.5	4.5	3.2	13.1	9.0	6.4	39	
12	6.5	4.5	3.2	13.1	9.0	6.4	65	
13	13.1	9.0	6.4	13.1	9.0	6.4	92	
14	13.1	9.0	6.4	19.6	13.5	9.6	131	
15	13.1	9.0	6.4	33	23	16.0	183	
16	13.1	9.0	6.4	52	36	26	248	
17	13.1	9.0	6.4	79	54	39	347	
18	13.1	9.0	6.4	111	77	54	477	
19	13.1	9.0	6.4	154	106	75	641	
20	19.6	13.5	9.6	271	187	133	837	
21	26	18.1	12.8	340	235	167	1066	
22	39	27	19.2	412	284	202	1327	
23	52	36	26	497	343	244	1621	
24	72	50	35	595	411	292	1948	
25	92	63	45	706	487	346	2308	

^aPer deployment scenario of Table 8-56 with the hybrid operating at a 70% capacity

^b1 kg ²³³U = 0.69 ST U₃O₈ and 0.49 MT SWU.

Table 8-61. Required fuel cycle services with ^{238}U blanket - thousands of MT
(blanket enriched to 2%; new fuel fabricated at 3% enrichment).

Year	Business as usual ^a		Accelerated deployment		National
	Reprocessing	Refabrication	Reprocessing	Refabrication	Reprocessing
0	-	-	-	-	-
.					
.					
.					
8	-	-	-	-	-
9	-	-	-	-	0.10
10	-	-	-	-	0.20
11	0.10	0.07	0.10	0.07	0.40
12	0.10	0.07	0.20	0.13	0.60
13	0.10	0.07	0.20	0.13	1.0
14	0.20	0.13	0.20	0.13	1.4
15	0.20	0.13	0.30	0.20	2.0
16	0.20	0.13	0.50	0.34	2.8
17	0.20	0.13	0.80	0.54	3.9
18	0.20	0.13	1.2	0.80	5.4
19	0.20	0.13	1.7	1.1	7.4
20	0.20	0.13	2.4	1.6	9.9
21	0.30	0.20	4.2	2.8	13.0
22	0.40	0.27	5.3	3.5	17.0
23	0.60	0.40	6.4	4.2	21.0
24	0.80	0.54	7.7	5.1	25.0
25	1.1	0.74	9.2	6.1	30.0

^aTypical reprocessing plant sizes are 1500 to 3000 MT/yr and typical refabrication plant sizes are 600 to 1200 MT/yr.

Table 8-62. Required fuel cycle services with Th blanket - thousands of MT/yr
(blanket enriched to 2%; new fuel fabricated at 3% enrichment).

Year	Business as usual ^a		Accelerated deployment		National con
	Reprocessing	Refabrication	Reprocessing	Refabrication	Reprocessing F
0	-	-	-	-	-
.					
.					
.					
8	-	-	-	-	-
9	-	-	-	-	0.08
10	-	-	-	-	0.23
11	0.12	0.08	0.12	0.08	0.30
12	0.12	0.08	0.23	0.15	0.69
13	0.12	0.08	0.23	0.15	1.2
14	0.23	0.15	0.23	0.15	1.6
15	0.23	0.15	0.34	0.23	2.3
16	0.23	0.15	0.57	0.38	3.2
17	0.23	0.15	0.91	0.61	4.4
18	0.23	0.15	1.4	0.91	6.1
19	0.23	0.15	2.0	1.3	8.3
20	0.23	0.15	2.7	1.8	11.0
21	0.34	0.23	4.7	3.1	15.0
22	0.46	0.30	5.9	3.9	19.0
23	0.69	0.46	7.2	4.8	23.0
24	0.91	0.61	8.7	5.8	28.0
25	1.3	0.83	10.0	6.9	34.0

^aTypical reprocessing plant sizes are 1500 to 3000 MT/yr and typical refabrication plant sizes are 600 to 1200 MT/yr.

Table 8-63. Required fuel cycle services with ^{238}U blanket - thousands of MT/y
(blanket enriched to 2%; new fuel fabricated at 3% enrichment).

Year	Business as usual ^a		Accelerated deployment		National co
	Reprocessing	Refabrication	Reprocessing	Refabrication	Reprocessing
0	-	-	-	-	-
.					
.					
.					
8	-	-	-	-	-
9	-	-	-	-	0.13
10	-	-	-	-	0.25
11	0.13	0.08	0.13	0.08	0.50
12	0.13	0.08	0.25	0.17	0.75
13	0.25	0.08	0.25	0.17	1.3
14	0.25	0.17	0.25	0.17	1.8
15	0.25	0.17	0.38	0.25	2.5
16	0.25	0.17	0.63	0.42	3.5
17	0.25	0.17	1.0	0.67	4.8
18	0.25	0.17	1.5	1.0	6.7
19	0.25	0.17	2.2	1.4	9.2
20	0.25	0.17	3.0	2.0	12.0
21	0.38	0.25	5.2	3.5	16.0
22	0.50	0.33	6.5	4.3	20.0
23	0.75	0.50	7.9	5.3	25.0
24	1.0	0.67	9.6	6.4	31.0
25	1.4	0.90	11.0	7.6	37.0

^aTypical reprocessing plant sizes are 1500 to 3000 MT/yr and typical refabrication plant 600 to 1200 MT/yr.

Table 8-64. Required fuel cycle services with Be + Th blanket - thousands of (blanket enriched to 2%; new fuel fabricated at 3% enrichment).

Year	Business as usual ^a		Accelerated deployment		National
	Reprocessing	Refabrication	Reprocessing	Refabrication	Reprocessing
0	NA	-	NA	-	NA-
8	NA	-	NA	-	NA
9	NA	-	NA	-	NA
10	NA	0.22	NA	0.22	NA
11	NA	0.22	NA	0.44	NA
12	NA	0.22	NA	0.44	NA
13	NA	0.44	NA	0.44	NA
14	NA	0.44	NA	0.65	NA
15	NA	0.44	NA	1.1	NA
16	NA	0.44	NA	1.7	NA
17	NA	0.44	NA	2.6	NA
18	NA	0.44	NA	3.7	NA
19	NA	0.44	NA	5.1	NA
20	NA	0.65	NA	9.0	NA
21	NA	0.87	NA	11.0	NA
22	NA	1.3	NA	14.0	NA
23	NA	1.7	NA	17.0	NA
24	NA	2.4	NA	20.0	NA
25	NA	3.1	NA	24.0	NA

^aTypical reprocessing plant sizes are 1500 to 3000 MT/yr and typical refabrication plant sizes are 600 to 1200 MT/yr.

With the ^{238}U blanket concept the reprocessing and refabrication industries would be similar to those used for LWR fuels with recycle. These services may be in place at the time hybrids are deployed. Thus, when hybrid fuels are first processed, the processing may be performed in existing LWR facilities. However, some process changes will be necessary in reprocessing because LWR spent fuels have a fuel composition which is 99.3% U (0.9% fissile) and 0.7% Pu, while this blanket concept would have a fuel composition of 98% U (0.3% fissile) and almost three times the Pu volume (2%). Dilution of hybrid fuels may be necessary to use LWR facilities.

With the Th and the Th + Be blanket concepts the reprocessing and refabrication industries may need to be developed, if not already developed for the HTGR. Again, some process changes may be required.

The $^{238}\text{U}/\text{Th}$ blanket concept produces both Pu and ^{233}U . This concept will require the fuel services of both the Pu/U fuel cycle and the U/Th fuel cycle. Again, the development of these fuel services will partially be determined by the availability of LWR and HTGR fuel services.

ECONOMICS

The hybrid reactor's intrinsic worth to the nation is derived from both its value as a reliable domestic fuel source and its value in reducing and stabilizing nuclear fuel and electrical power costs. These values contain elements that are both tangible and subjective; yet comparisons must be made of alternatives. This subsection focuses on the economic features that will be used in the marketplace in evaluating the hybrid. Other benefits due the hybrid that may not transfer to a market analysis are evaluated in the subsection on Incentives.

The comparisons are based on traditional utility accounting practices with a symbiotic relationship between the hybrid reactor and converter reactors assumed. This type of interrelationship between fuel supplies and power producers is also common to the uranium mining industry, the reprocessing industry, the enrichment industry, and the breeder reactor industry and is conceptually well understood.

Economic Ground Rules

In comparing the cost of power from alternate generating sources, a utility will look at the time discounted charges for capital and fuel over some operating period. These charges are to the customer and not to the utility. The utility approach is to minimize revenue requirements from the customer rather than costs to the utility. This approach is fundamentally different than for other industries, which may change their rate of return with time and from product-to-product.

This use of utility financing and accounting practices to cost the fuel and power production (or consumption) will have three major effects on the competitiveness of a hybrid plant. First, the utility's revenue minimization (RM) ground rule, in which the utility makes a constant return on its investment, increases the penalty for long fuel cycle options (due to federal tax) over that seen using a cost minimization (CM) ground rule. Second, the weighted average cost of money and the financing cost of a hybrid will be lower for a regulated utility than for other industries (due to its higher acceptable debt to equity ratio). Third, the number of plant operating years that a utility will use in its decisions will be longer than will be used in other industries and may approach that of a life-cycle analysis.

In determining the annual capital charge, a utility will use a capital charge rate which reflects the rate of inflation. This annual capital charge will be fixed over the life of the plant. The annual fuel charges are determined using the expected rate of inflation over the operating period. The combined charges for capital recovery and fuel purchases are then discounted and cost comparisons are made.

Perhaps the most serious error in estimating and comparing nuclear fuel cycle costs in the past has stemmed from a failure to handle inflation in a financially consistent manner. It is necessary that all carrying charge costs and discount rates be consistent with the assumed rate of inflation and that all costs be escalated at that same rate of inflation. One reason for this error is the desire to avoid the extensive arithmetic that is needed to handle year-by-year escalation. This shortcut fails to escalate fuel cycle costs in accord with the assumed rate of inflation and thus introduces a bias against plants with low fuel-cycle costs and higher capital costs.

Apart from inflation, there is evidence that the real (constant dollar) cost of certain components of nuclear fuel cycles will rise because of

increasing labor and environmental costs. Examples of components that might be affected are fabrication and reprocessing. In order to accommodate these items, it is first necessary to convert the stream of rising real costs (where costs for each year are in unescalated dollars) into a lifetime levelized real cost for the plant. This levelization must be carried out using the inflation-corrected (zero inflation) discount rate. The levelized real cost becomes the point of reference, and the effects of any assumed rate of inflation are superimposed on this.

Determination of the carrying charges, which enter into the cost calculation for each component of the fuel cycle, becomes complicated because each element of the fuel cycle is characterized by a unique time pattern of expenditures and credits. For example, the hybrid fuel blankets may reside in the reactor for 5 to 10 years before sufficient fissile fuel has been bred to warrant reprocessing. During this period, costs are incurred and financed until future fuel sales are realized. This one-cycle pattern would then repeat from three to six times over the life of the reactor.

The engineering-economics approach used in this report is to predict levelized operating costs rather than performing an actual cash flow analysis on revenue receipts. This technique simplifies calculational comparisons to cost multipliers and the levelization of charges to the utility. The cost multipliers reflect both the cost of financing and the length of time between receipt of sales and purchases (or incurred operating expenses) for fuel and capital expenses over one operating cycle. This approach is described in the succeeding paragraphs and in Tables 8-65 and 8-66.

$$\text{Cost} = (\text{levelized cost of services to utility}) \times \frac{\text{Unit cost if financed}}{\text{Unit cost if expensed}}$$

First, the plant's pattern of irregular expenditures and sales are converted into a uniform series in time. The expenditures are then converted into operating costs using a three-step process:

- Reduce each changing cost of the fuel cycle (including inflation) to a levelized cost whose present worth is the same as the present worth of the actual expenditures.

- Determine the use and interest costs of the fuel cycle using the levelized expenditure as a basis. The fuel-cycle costs are made up of two components: a use cost and a carrying cost. The use cost is the cost of the

Table 8-65. Example of a hybrid reactor fabrication cost calculation.

Assumptions

- Payment for blanket fabrication is 6 months before use.
- Four-year, in-core blanket residence.
- Six-month cooling/reprocessing period.
- No money collected from customer until fuel is available.
- \$50/kg HM hybrid blanket fabrication (1979 \$).
- 2% final fuel enrichment.
- 4% discount rate (constant dollar).
- 6.48% effective interest rate (constant dollar).

Fabrication cost calculation

- Purchase cost:
50\$/kg HM
 - Unrecovered cost at time of fuel sale:
 $50\$/\text{kg HM} \times (1.0648)^{(0.5 + 4 + 0.5)} = \$68.44 \text{ \$/kg HM}$
 - One-cycle fabrication cost per kg HM loaded:
 $68.44 / (1.04)^{(4 + 0.5)} = 57.37 \text{ \$/kg HM (1979 \$)}$
 - One-cycle fabrication cost per gram fissile sold:
 $57.37 / (1000 \times 2\%) = 2.9 \text{ \$/gm fissile}$
-

Table 8-66. Example of an LWR fuel cost calculations for uranium.

Assumptions

- Typical LWR schedule.
- \$40 per lb U₃O₈.
- 40 lb of U₃O₈ purchased per million kWe.
- Uranium purchased 2 yr before loading in reactor.
- 4% discount rate.
- 6.48% effective interest rate.

Fuel cycle cost calculations

- Purchase cost:

$$40 \frac{\text{lb U}_3\text{O}_8}{10^6 \text{ kWh}} \times 40 \frac{\$}{\text{lb U}_3\text{O}_8} \times 1,000 \frac{\text{mills}}{\$} = 1.6 \text{ mills/kWh}$$

- Value at time of fuel loading:

$$1.6 \text{ mills/kWh} \times (1.0648)^2 = 1.8 \text{ mills/kWh}$$

- Depreciation and inventory costs (mills/kWh):

<u>Yr</u>	<u>Book value at beginning of yr</u>	<u>Depreciation at end of yr</u>	<u>Interest at end of yr</u>	<u>Total annual cost</u>
0	1.80	0.45	0.117	0.567
1	1.35	0.45	0.087	0.537
2	0.90	0.45	0.058	0.508
3	0.45	0.45	0.029	0.479

- Fuel-cycle cost (levelized by the amount of electricity produced):

$$\left[\frac{0.567}{1.04} \times \frac{0.537}{(1.04)^2} + \frac{0.508}{(1.04)^3} + \frac{0.479}{(1.04)^4} \right] \Bigg/ \left[\frac{0.25}{1.04} + \frac{0.25}{(1.04)^2} + \frac{0.25}{(1.04)^3} + \frac{0.25}{(1.04)^4} \right] = 2.1 \text{ mills/kWh}$$

fuel actually consumed in producing the electricity. The carrying cost is the interest cost on the monies invested in the fuel from time of purchase to time of receipt of payment for the electricity.

- Add the levelized fuel-cycle charges and the levelized capital cost recovery charges to yield the total forecast power cost. (The levelized capital recovery charge is found as the original cost of the power plant multiplied by the capital charge rate.) This procedure determines the levelized cost of operating any plant over the levelization period.

The three charge rates of primary importance in the preceding were: the discount rate for the utility decision making process; the level annual revenue requirement, excluding depreciation for costs; and the level annual revenue requirement with depreciation, property tax, and insurance for levelizing fixed capital charges.

The discount rate is the weighted average cost of debt and equity monies. The level annual revenue requirement, excluding depreciation, is the effective interest rate on non-depreciable assets that the utility must assume so that funds will be available to repay the debt holder's investments and provide the prescribed rate of return, after taxes, to the equity holders. This rate is used in determining the interest charges on nuclear fuels. The third charge rate includes tax and depreciation effects and is used in determining the annual charges for capital recovery over the levelization period. The development of these charge rates is shown in Table 8-67. The rates are shown for both zero and 6% inflation, and the costs of money for these rates are consistent with historical U.S. utility experience.

Converter Reactor

There is considerable evidence to suggest that the domestic converter reactor of the year 2010 will resemble that of today's LWR rather than a newly developed system such as the CANDU, HTGR, or LWBR. Such a reactor may have improved fuels and improved coolant/moderators, but the general design will be that of an LWR. The following issues reinforce this belief:

- There are four reactor manufacturers selling LWR's; each with in-place manufacturing capabilities.
- There will remain a buyer's (reactor) market to minimize LWR prices. (Any two manufacturers have capacity to meet market demands.)

Table 8-67. Coordinated financial assumptions for investor-owned utilities.

Particle	cost	A, %	B, %
1.	Rate of inflation.	0	6
2.	Cost of debt money for zero inflation.	2.75	2.75
3.	Cost of debt money with inflation (1 x 2); e.g., $(1.06 \times 1.0275) - 1 \times (100) = 8.92\%$.	2.75	8.92
4.	Cost of equity money for zero inflation	5.5	5.5
5.	Cost of equity money with inflation (1 x 4); e.g., (1.06 x 1.055) - 1 x (100) = 11.83%.	5.50	11.83
6.	Assumed debt/equity ratio for utility industry capitalization.	55/45	55/45
7.	Assumed federal plus state tax as percent of earnings. ¹	50	50
8.	Return on debt (cost for use of debt portion of money). (3 x 6); e.g., $(0.55 \times 8.92) = 4.91\%$.	1.52	4.91
9.	(a) Return on equity (cost for use of equity portion of money). (5 x 6); e.g., $(10.45 \times 11.83\%) = 5.32\%$, and (b) Federal tax plus state tax (for 50% local tax on earnings). ^a	2.48	5.32
10.	(a) Weighted average interest rate (net-of-taxes) (8 + 9).	4.00	10.24
	(b) Discount rate for utility decision making process (net-of-taxes) (8 + 9).	4.00	10.24
11.	Level annual revenue requirement excluding depreciation (effective interest rate plus taxes) (10a + 9b).	6.48	15.56
12.	Level annual revenue requirement with depreciation. 32-year book-life and 16-year tax life (determined by calculations using the above assumptions - not shown). ²	5.89	11.83
13.	Charge for property tax plus plant insurance.	0.95	1.70
14.	Level annual revenue requirements with depreciation, property tax, and insurance (12 + 13).	6.74	13.53

^a At 50% assumed federal plus state income tax is equal to return on equity.

^b This annual charge is derived from the preceding financial assumptions and duly incorporates the effects of the normalization of accelerated tax depreciation. 16-year asset depreciation range (ADR) taxable, and a capital recovery period of 32 years. This represents the capital charge that a tax-regulated electrical utility might apply.

- The problems of the LWR are known by experience.
- There is a long standing government R&D commitment to LWR.
- Implementation of advanced reactors/fuel cycles takes time and money that government and industry are reticent to invest. (See Appendix C.)
- Incremental early-year savings of ACR's may be matched by LWR improvements.

- Short term uranium problems may eventually be amenable by technical means (lower tails, reprocessing, LWR fuel improvements).

- The nation will most likely be shortsighted on committed uranium problems and prices that might suggest the construction of ACR's.

For this study, the domestic converter reactor will be an LWR with burnup and fuel characteristics similar to today's LWR fuels. The plant will be capable of utilizing either ^{239}Pu , ^{233}U , or ^{235}U fuels. For the national analysis, the converter reactor will be a mixed industry of 75% LWR's and 25% CANDU's. Again, all reactors will be capable of operating using ^{239}Pu , ^{233}U , or ^{235}U fuels.

It is important to realize the importance of the preceding ground rules. Each converter reactor technology uses the three different fissile fuels more or less efficiently than the others. Thus, if the ground rules include a larger fraction of ACR's, the high ^{233}U use efficiencies of epithermal reactors would result in a preference for ^{233}U production by hybrids. The above ground rule also implicitly assumes that the hybrid research and development budget will not be large enough to develop a converter reactor fuel cycle other than in the LWR.

Converter Fuel Characteristics

The information base for ^{239}Pu , ^{233}U , and ^{235}U fuels has developed over the past three decades at rates commensurate with past needs. Thus, ^{235}U fuels are well studied in LWR's, while the ^{239}Pu and ^{233}U fuels have received less attention. Of the two bred fuels (^{239}Pu and ^{233}U), ^{239}Pu has received more attention for use in LWR's than ^{233}U . The immature nature of designs for ^{239}Pu and ^{233}U fuels has lead to some confusion as to the relative worth of these fuels.

The fuel requirements used in this report are averages of the characteristics of the many authors who presented both ^{235}U , ^{233}U , and ^{239}Pu use

information with a consistent set of ground rules. The chosen set of fuel requirements for LWR are shown in Table 8-68 and those of the CANDU in Table 8-69. Additional fuel characteristics are shown in Table 8-70 and 8-71.

Converter Capital Costs

Capital costs for nuclear power plants have traditionally been difficult to reconcile because of scope, accounting, and labor rate differences throughout U.S. utilities. Unanticipated changes in plant costs have occurred due to the ratcheting of environmental standards and due to increased rates of inflation. This tendency to slip schedules and increase the work scope and inflationary costs in nuclear projects has probably not yet ended.

Capital costs for converter reactors (LWR and CANDU) for this analysis have been derived from a "Draft NASAP Provisional Data Base" by the addition of one year of escalation at 12.5%. The reference cost for an LWR and a CANDU are shown in Table 8-72.

The capital investment costs in Table 8-72 include an owner's cost of approximately 75% of direct and indirect costs for nuclear plants. The interest during construction included is based on the deflated average cost of money of 4.5% and a cash flow of 10-yr design, licensing, and construction lead time. Plant costs were scaled by size using a scaling factor of -0.55, based on the DOE "Draft NASAP Provisional Data Base", ORNL, February 6, 1979.

Converter Fuel Service Costs

The annual operating cost of a converter reactor is made up of six components, which occur during the fuel cycle at different times:

- Conversion
- Enrichment
- Fabrication
- Reprocessing
- Shipping and waste disposal
- Operation and maintenance

For this analysis, these costs will be based on the revised (February 12, 1979) "Draft NASAP Provision Data Base".

Table 8-68. LWR fuel requirements (1000 MWe reactor @ 75% capacity factor).

	Fuel cycles with reprocessing			
	$^{235}\text{U}/^{238}\text{U}$	$\text{Pu}/^{238}\text{U}$	$^{233}\text{U}/\text{Th}$	Den $^{233}\text{U}^c$
<u>First core</u>				
U_3O_8 , short tons	392	-	-	-
^{233}U , kg ^{233}U	-	-	2400 ^b	2400 ^b
Pu, kg Pu_f	-	3430	-	-
Separative work ^a , MT SWU	203	-	-	-
<u>Net annual reload</u>				
U_3O_8 ^a , short tons	157	-	-	-
^{233}U , kg ^{233}U	-	-	227	290
Pu, kg Pu_f	(174)	333	-	-
Separative work ^a , MT SWU	112	-	-	-
<u>Lifetime requirements (first core plus 29 reloads)</u>				
U_3O_8 , short tons	4945	-	-	-
^{233}U , kg ^{233}U	-	-	8980	10,800
Pu, kg Pu_f	(5220)	13,100	-	-
Separative work ^a , MT SWU	3451	-	-	-

^aBased on an enrichment plant operating tails assay of 0.20% ^{235}U .

^bFuel life times reload fuel inventory.

^cNo Pu recycle.

Table 8-69. CANDU fuel requirements (1000 MWe reactor @ 75% capacity factor).

	Fuel cycles with reprocessing			
	$^{235}\text{U}/^{238}\text{U}$	$\text{Pu}/^{238}\text{U}$	^{233}U	Den $^{233}\text{U}^c$
<u>First core</u>				
U_3O_8 , ^a short tons	538	-	-	-
^{233}U , kg ^{233}U	-	-	1648	1648
Pu, kg Pu-fissile	-	1020	-	-
Separative work ^a , MT SWU	-	-	-	-
<u>Net annual reload</u>				
U_3O_8 , ^a short tons	30	-	-	-
^{233}U , kg ^{233}U	-	-	70	102
Pu, kg Pu_f	-	214	-	-
Separative work ^a , MT SWU	-	-	-	-
<u>Lifetime requirements (first core plus 29 reloads)</u>				
U_3O_8 , short tons	-	-	-	-
^{233}U , kg ^{233}U	-	-	3680	4610
Pu, kg Pu_f	-	7230	-	-
Separative work ^a , MT SWU	-	-	-	-

^aBased on an enrichment plant operating tails assay of 0.20 ^{235}U .

^bWith Pu credit.

^cNo Pu recycle.

Table 8-70. LWR fuel characteristics (with fuel recycle).^a

	Fuel cycles with reprocessing			
	$^{235}\text{U}/^{238}\text{U}$	$\text{Pu}/^{238}\text{U}$	$^{233}\text{U}/\text{Th}$	Den $^{233}\text{U}^c$
Burnup, MWD/kg HM,	30.4	30.4	33.4	33.4
Fissile charge, kg/GWe-yr				
^{235}U	794	73 ^c		29 ^c
^{233}U	-	-	779	750
Pu_f	-	1226	-	-
Fissile discharge, kg/GWe-yr				
^{235}U	215	38	14	43
^{233}U	-	-	538	446
Pu_f	174	893	-	(63)
Net annual requirements, kg/GWe-yr				
Purchased fissile fuel	405	333	227	290

^a75% capacity factor

^bNo Pu recycle.

^cTails.

Table 8-71. CANDU fuel characteristics.^a

	Fuel cycles with reprocessing			
	²³⁵ U/ ²³⁸ U	Pu/ ²³⁸ U	²³³ U/Th	Den ²³³ U/Th ^b
Burnup, MWD/kg HM	7.5	16	16	16
Equilibrium fissile enrichment, % HM	0.711	1.11	1.46 (93% in U)	1.46 (12% in U)
Fissile charge, kg/GWe-yr				
²³⁵ U	852	112 ^c	-	-
²³³ U	-	-	831	831
Pu _f	-	455	-	-
Fissile discharge, kg/GWe-yr				
²³⁵ U	249	17(N.C.)	-	-
²³³ U	-	-	761	729
Pu _f	340	241	-	(32)
Net fissile requirements				
Purchased fissile fuels	263	214	70	102

^a75% capacity factor.^bNo Pu recycle.^cTails.

Table 8-72. Capital investment costs (1979 \$/kWe, including interest during construction).

Power plant type	Capital cost, \$/kWe ^a		
	600 MWe	1000 MWe	1300 MWe
LWR	1190	900	780
CANDU ^b without heavy water	1280	970	830
CANDU ^b with heavy water	1455	1145	1005

^aIncludes 7% owner's cost during construction.

^bThe CANDU plant has been assumed to cost about the same as a HWR, which uses slightly enriched fuels.

^cHeavy water cost is 175 \$/kWe (0.75 MT/MWe at 107 \$/lb D₂O).

Conversion

Conversion costs are a small fraction of the annual fuel cost of a converter reactor, and the material (F1) requirements are not expected to rise significantly in price due to depleting of resources. The conversion of U₃O₈ to UF₆ occurs for two important reasons: (1) to further purify the uranium product from the mill; and (2) principally to convert uranium into a form suitable for enrichment in diffusion or centrifuge plants. For the natural enriched fuels of the CANDU, this step has been unnecessary.

The reference cost of conversion for this analysis is \$4.4/kg U (1979 \$) based on the "Draft NASAP Provision Data Base" and one year of escalation at 10% per year.

Enrichment

The future of U.S. enrichment has become more clear with the passing of time. The relative economics of the diffusion process and the centrifuge process are now well publicized and the next unit of enrichment capacity will be based on the centrifuge. Additionally, the cancellation of a joint government industry project has shown the desire of Congress to keep U.S. enrichment totally under government ownership and control.

The U.S. long-term strategy for pricing the enrichment service, however, still remains undefined. Today, prices are \$85/SWU in the U.S. based on recovery of government costs. (Overseas prices are currently higher, in the range of \$115 to \$130/SWU.) The question on pricing strategy has been whether the U.S. will switch to commercial pricing (with profit) or maintain the current cost recovery strategy.

This report will assume (as in the "Draft NASAP Provisional Data Base") that the U.S. converts to a commercial pricing strategy by year 2010. The reference enrichment cost for this analysis is \$110/SWU (1979 \$) (based on the Draft and one year of escalation at 10% per year), slightly less than current non-U.S. commercial rates because of superior U.S. technology. Additionally, the reference operating tails assay is 0.2% ²³⁵U.

Fabrication

The fabrication costs for LWR and CANDU fuels for this analysis are shown in Table 8-73. These costs are as recommended in the "Draft NASAP Provisional Data Base" for a high capacity industry but increased by one year of escalation at 10% per year.

Reprocessing

The reprocessing costs for LWR and CANDU fuels for this analysis are shown in Table 7-74. These costs are as recommended in the "Draft NASAP Provisional Data Base" for a high capacity industry but increased by one year of escalation at 10% per year.

The two sets of reprocessing costs given in Table 8-74 are representative of two alternate philosophies on spent fuel reprocessing, the so-called AGNS- and Canyon-type facility costs.

The AGNS-type facility costs are for plants similar to the AGNS plant at Barnwell, South Carolina. These estimates assume current, perceived regulations with semi-remote maintenance. The investment cost estimates for the 1500-MTHM/yr, LWR-Purex, AGNS reprocessing plant are based on recommendations made by the U.S. INFCE Technical and Economic Assessment Crosscut Group. The direct investment cost of such a facility was estimated at \$1.0 billion with an annual operating cost of \$50 million.

Table 8-73. Converter fabrication costs (1979 \$/kg HM).

Fuel type	LWR	CANDU ^a
LEU5 - Standard	121	-
- High burnup	132	-
Natural UO ₂	-	72
DU5/Th	132	88
DU3/U	594	495
DU3/Th	627	539
Pu/U	407	341
Pu/Th	418	352
Pu/U - spiked	638	539
Pu/Th - spiked	638	550

^aThe HWR costs of NASAP Data Base have been used for the CANDU reactor.

Table 8-74. Converter reprocessing costs (1979 \$/kg HM).

LWR and CANDU fuel type (oxide)	Reprocessing cost	
	Semi-remote, AGNS-facility	Fully-remote, Canyon-type facility
Pu/U	275	407
Pu/U - spiked	297	451
DU/Th	297	451

The Canyon-type facility costs are based on work by the Savannah River Laboratory (SRL). This facility, as well as having fully remote maintenance, is designed in anticipation of much more stringent safeguards and operating criteria than required by current regulations. SRL personnel estimate that the capital investment required for a 1500-MTHM/yr plant is \$1.6 billion with annual operating costs of \$50 million.

Shipping and Waste Disposal

The spent fuel shipping and waste disposal costs used in this report are as recommended in the "Draft NASAP Provisional Data Base", but with one additional year of escalation added at 10% per year. These costs are shown in Table 8-75.

Table 8-75. Converter spent fuel shipping and disposal costs (1979 \$/kg HM discharged from reactor).

Service	After reprocessing option		No reprocessing option	
	LWR	CANDU	LWR	CANDU
Spent fuel shipping	16.5	11.0	16.5	11.0
Waste shipping	11.0	5.5	-	-
Waste storage	<u>55.0</u>	<u>27.5</u>	<u>132.0</u>	<u>66.0</u>
Total	82.5	44.0	148.5	77.0

Operation and Maintenance

The operation and maintenance costs used in this report are as recommended in the "Draft NASAP Provision Data Base", but with one additional year of escalation added at 10% per year. These costs are shown in Table 8-76.

Table 8-76. Converter operation and maintenance costs (1979 \$).

Reactor	Fixed, \$/kWe-yr _c	Variable, \$/kWe-yr _o	Total, mills/kWh
LWR	14.3	1.1	2.3 ^a
CANDU	17.6	1.1	2.6 ^b

^a75% capacity factor for LWR.

^b80% capacity factor for CANDU.

HYBRID REACTOR

The Resource and Market Economic Assessment (RMEA) for the TMHR is a parallel effort to the conceptual design of the plant. The intent of this assessment is to provide insights into the hybrid concept to guide future design efforts while not delaying current design efforts. To meet this goal the design parameters for the hybrid RMEA were selected from the first phase of the project, while design efforts continued. The following parameters are different from those more current elsewhere in this report.

The TMHR is best described as a three-component machine where one-component is the fusion driver, the second is the fission blanket, and the third is the balance-of-plant heat transport systems and electrical generation equipment. For the RMEA the fusion driver and blankets were simplified from design specific concepts to a more general concept and the balance of plant reduced to cost and schedule considerations. The five key hybrid design factors used in the RMEA are:

- Fusion driver characteristics.
- Blanket characteristics.
- Hybrid capital cost estimates.
- Fuel service cost estimates.
- Power and fuel sales estimates.

Fusion Driver Performance

The fusion driver element is both the source of high energy neutrons to drive the fission blanket and a source of energy to operate the plant. To operate the fusion driver the device must be supplied with energy in the form of high energy tritium and deuterium ions. These ions fuse, releasing high energy neutrons and helium ions. The neutrons escape and are captured in the blanket, while the helium ions are removed through the TMHR end plugs to generate electricity. The efficiency at which this process can be made to operate is one of the design challenges for the TMHR project.

For the RMEA, two energy yield levels were selected to bound the probable range of operating conditions. The high energy yield design had an energy multiplication (Q) of 4.8 with a wall loading ($\Gamma\eta$) of 2.1. The low energy yield design had a Q value of 1.0 with a wall loading $\Gamma\eta$ value of 1. Thus, the

high energy yield design produced roughly five times the supplied input energy, while the low energy yield design reached the breakeven point. These design levels are summarized in Table 8-77.

Blanket Performance Characteristics

The objective of any hybrid blanket design is to multiply the number of fusion neutrons and to use these neutrons to generate replacement tritium and bred fissile material. The objective can be accomplished in many ways, but the choice of fertile material is the major determinant of the results. Table 8-78 shows performance characteristics of four promising candidate fertile fuel blanket designs.

The ^{238}U blanket design is characterized by the highest fissile breeding ratio and energy multiplication of all the hybrid blanket designs and by the production of Pu. This large energy multiplication in the blanket allows the fusion driver to be of a small size relative to the amount of energy and fissile fuel produced. However, the amount of fuel produced per plant (when the thermal size of the plant is the design constraint) is smaller than that of the other designs.

The Th blanket design is characterized by the production of ^{233}U and the lowest fissile breeding ratio. Because Th has a low fast fission cross section, the Th blanket has a low energy multiplication and a larger fusion driver than the ^{233}U blanket. However, the amount of fuel produced per plant (when the thermal size of the plant is the design constraint) is large and this fissile material (^{233}U) is a particularly good thermal reactor fuel.

The $^{238}\text{U}/\text{Th}$ blanket is characterized by the production of both ^{239}Pu and ^{233}U and by a large breeding ratio. With the addition of the uranium blanket zone this blanket produces more energy than the preceding all Th blanket and more fissile fuel per plant.

The Be/Th blanket is characterized by the largest fissile material production rate but also the largest fusion driver requirements. The blanket produces ^{233}U with the least amount of energy multiplication, allowing the concept to produce the least amount of heat per unit of fissile production. When the comparisons are made based on a specific thermal plant rating, this concept produces the most fissile material.

Table 8-77. Fusion driver performance parameters.

Parameter	High (TMR)	Low
Q	4.8	1.0
First-wall radius	1.6	1.6
Wall loading,	2.1	1.0
P_f' , MW/m	25	12
Injection efficiency	0.72	0.60
Direct conversion efficiency	0.60	0.50
Thermal conversion efficiency	0.35	0.35
Central cell cost, M\$/m	4.73	4.73

Table 8-78. TMHR blanket performance parameters.

Parameter	Blanket Type			
	U^{238}	Th	$^{238}U/Th$	Be + Th
Breeding ratios:				
^{239}Pu	1.5	-	0.6	-
^{233}U	-	<u>0.6</u>	<u>0.7</u>	<u>0.8</u>
Total	1.5	0.6	1.3	0.8
Tritium	1.0	1.0	1.0	1.0
Energy multiplication	11	3.4	7.6	1.6
Fissile production (kg/yr _o)				
^{239}Pu	2880	-	1650	-
^{233}U	-	<u>3250</u>	<u>1930</u>	<u>9340</u>
Total	2880	3250	3580	9340
Power distribution, MW _{th}				
Fusion energy	444	1370	637	2703
Fission energy	<u>3556</u>	<u>2630</u>	<u>3363</u>	<u>1297</u>
Total	4000	4000	4000	4000

Capital Cost Estimates

The TMHR capital cost estimates for the REMA were developed during the first phase of the TMHR project by adopting pure fusion cost estimates to the TMHR. The methodology and equipment costs are shown and summarized by blanket design in Table 8-79.

Table 8-79. Preliminary TMHR capital costs - millions of dollars (4000 MW_{th} plant).

Fusion Driver Performance	Blanket Type			
	²³⁸ U	Th	²³⁸ U/Th	Be + Th
High	1250	2330	1480	3870
Low	890	1210	960	1680

Fuel Service Cost Estimates

The anticipated fuel services for the TMHR are similar in scope to those needed by the converter reactor industry to operate on a closed fuel cycle. The TMHR requires a fertile fuel, Li, fuel fabrication, reprocessing, waste disposal, and fuel transportation. Each of these steps, though similar to those converter reactor fuel service operations, will require some additional research and development.

The fertile fuel for first core and reload blanket will be either U or Th. For those blanket concepts that use U, it will be depleted U available from the enrichment process; and for those blanket concepts that use Th, it will need to be mined. In each case, it is anticipated that no U or Th recycle will occur.

Lithium requirements for the TMHR result from the need for tritium to fuel the fusion driver. The Li blanket absorbs neutrons to provide this make-up tritium. This Li will need to be mined for all TMHR blanket concepts.

The fabrication of the fertile fuel and Li into blanket elements requires steps that might be similar to those processes currently used by converter reactors, depending on the selection of blanket design. These processes may be

simplier and less costly for the TMHR, because of reduced criticality and security concerns when handling depleted U and natural Th.

The reprocessing of TMHR blankets will require either the PUREX process, the THOREX process, or the molten salt process, depending on the selection of blanket type. Of these processes the PUREX process has received the greatest technical development, particularly for the reprocessing of LWR fuels. For each of the processes, however, additional R&D will be necessary to reoptimize reprocessing plant design concepts to the enrichments, flow rate distributions, and material differences of hybrid elements.

The disposal and transportation of waste and the transportation of TMHR blanket elements are expected to be similar to processes currently in use today or proposed for LWR fuels.

The cost of the fuel services varies with the design of the blanket and the selection of fertile material. For the analysis of the REMA the cost of TMHR fuel cycle services has been patterned after those of the converter reactor (LWR and HTGR) industry, as reported in the "Draft NASAP Provisional Data Base."⁶ (These costs are shown in Table 8-80.) When converted to a dollar per gram fissile product, the total of fuel services is generally in the range of \$30 per gram fissile (assuming a 2% enrichment in the TMHR).

Table 8-80. Typical TMHR fuel service costs.

Service	Cost
Uranium (tails)	No charge
Thorium	\$42/kg HM
Lithium	\$73/lb Li ₂ O
Fabrication of blanket elements	\$50-140/kg HM
Reprocessing package	\$490-530/kg HM
O&M	\$6.6/kW _{th} -yr

Power Costs and Fuel Sales

The economic standing of the TMHR will depend on the cost of producing its fissile fuel and electricity and the price at which they may be sold. For the RMEA a systems approach was developed to determine fissile fuel costs and electricity costs by equating the cost of operating the TMHR with the cost of operating the converter reactors it supports.

Table 8-81 summarizes the cost of fuel and power from the TMHR available from the first phase of the TMHR study. These costs have been used in the REMA.

Bred Fuel Prices

Bred fuels, such as Pu and ^{233}U , can be priced in many different ways. The classical indifference value approach assigns prices to Pu and ^{233}U based on equalizing the costs of fuel obtained by mining U with the cost of fuel obtained by buying bred fuel. Such a method has been criticized because it is fuel design specific, it is complex, and it ignores the politics of owning and financing a fuel with a volatile market price. Yet, it does provide a point of reference back to the price of U--a fuel that will compete with any bred fuel.

For this analysis the indifference value approach will be used to predict market prices for bred fuels that hybrid reactors must beat to be competitive. Table 8-82 lists bred fuel prices as a function of uranium price.

Commercial Plant Rating

The power and fuel rating of the commercial plant is fundamentally one of the more important choices for any power technology. Large plant ratings often have led other technologies to cost reductions and more competitive plants. Small sizes however are beneficial in reducing development costs and easing the design and deployment of new technologies. For the hybrid reactor it appears there are incentives to pick a medium sized plant, because relatively few hybrids may be constructed to supply the nation's fissile fuel needs. Yet, the design of the plant, the cost of developing various size plants, and the market for hybrids is not well enough defined to make a size recommendation.

Table 8-81. Typical bred fuel and system costs.

Fusion driver performance Blanket type	High (Q = 4.8, $\beta = 2$)				Low (Q = 1,		
	U	Th	Be	U/Th	U	Th	Be
Fissile cost (\$/g)							
Capital	<u>71</u>	85	38	61	99	163	8
Fuel cycle + O&M	<u>30</u>	30	30	30	30	30	3
Power cost (at fission)							
Burner total mills/kWh)	<u>-61</u>	-50	-18	-48	-48	-6	-1
Total	<u>40</u>	65	50	43	81	187	13
Support ratio							
Nuclear	<u>5.6</u>	12.7	36.5	9.56	5.6	12.7	36
Electric	<u>5.2</u>	12.3	37.5	8.97	7.3	12.5	-42
System direct cost ratio							
	<u>1.07</u>	1.08	1.05	1.06	1.22	1.31	1
Fission burner (mills/kWhe)							
Capital	<u>9.9</u>	9.9	9.9	9.9	9.9	9.9	9
Fuel cycle (less makeup)							
+ O&M	<u>2.7</u>	<u>2.7</u>	<u>2.7</u>	2.7	2.7	2.7	2
Fissile makeup	<u>1.7</u>	<u>1.4</u>	<u>1.2</u>	1.5	3.5	4.3	3
Total	<u>14.3</u>	14.0	13.8	14.1	16.1	16.9	15

Table 8-82. Fissile Pu and ²³³U price.^a

²³⁸ U ₃ O ₈ price, \$/lb	²³⁹ Pu (+241) price, \$/gr	²³³ U price \$/gr
40	22	23
60	29	35
80	36	47
100	43	59
120	50	71
160	64	95
200	78	119
260	100	155

Note: Intermediate prices can be calculated using linear interpolation.

^aBasis (1979 \$)

Fabrication costs, \$/kg HM	4.4
Enrichment cost, \$/kg SWU	110
Fabrication costs, \$/kg HM	
LEU	120
Pu/U	410
DU/Th	630
Recovery costs, \$/kg HM	
(U,Pu) O ₂	360
(U,Pu,Th) O ₂	385
Thorium cost, \$/kg	42

The importance of the commercial plant size will depend on five key factors. These factors are

- Hybrid deployment rates.
- Reprocessing and fabrication.
- Economies in construction.
- Research and development.
- Marketability of program.

Hybrid Deployment Rates

The timing, the need, and the rate at which hybrids will be constructed is important to any decision on plant size. With large numbers of hybrids being demanded, it would be advantageous to build large plants; conversely, if relatively few hybrids are needed, then smaller plants would allow economies of production to outweigh economics of scale, especially for early plant designs.

Thus, a significant issue in the development of the hybrid must be, will hybrids be required to produce all (100%) of the nation's fissile fuel or 20%, 40%, 60%, etc. of it. If 20% of the nation's year 2020 fissile fuel needs are to be supplied, this translates to about six (4000 MW_{th}) hybrids with Th + Be blankets, 18 (4000 MW_{th}) hybrids with Th blankets, 20 (4000 MW_{th}) hybrids with U/Th blankets, and 30 (4000 MW_{th}) hybrids with ²³⁸U blankets. Such small numbers of hybrids may not justify the development of large components for large plant sizes such as 4000 MW_{th}.

Reprocessing and Fabrication Considerations

As much a part of the deployment of the hybrid reactor is the deployment of its supporting fuel cycle services, reprocessing, and bred fuel fabrication. In particular with a hybrid, without these services being available, the concept would be unworkable. The selection of the plant size for the commercial hybrid will set size and process requirements for the reprocessing and fabrication industries. For example:

Economical reprocessing plant sizes appear to be in the range of 1500 to 3000 MT HM/yr. With a hybrid plant size of 4000 MW_{th}, 12 to 15 hybrid plants would commit the fuel services of one

1500 MT/yr plant.* The misoperation of any one hybrid would thus reduce the fuel supply to its reprocessing plant and the reprocessing plant fabrication facilities by 10%. It is unknown at this time whether such a fluctuation in fuel supply is acceptable to potential reprocessing and fabrication plant operators.

Further investigation appears necessary to determine the interrelationship between the fuel service industries and the selection of the size of the commercial hybrid.

Economies in Construction

The competitive position of the commercial hybrid plant will be determined by both its capital cost and the price of its bred fuel and electricity. If the competitive position is to be assured, all areas of cost reduction should be applied, including economies available to large plant sizes and to replication of plant designs. Yet for the hybrid development program, the pursuit of economics of scale may counter production (or replication) economies that would occur with smaller plant sizes.

It is particularly important to recognize that few (ten to thirty 4000 MW_{th}) hybrids may be needed in the U.S. to augment declining domestic U reserves. With only 10 to 30 plants, potential economies of scale may be lost in practice because of changing plant designs; and if true, the multiple construction of small units might be preferable. Unfortunately, cost vs size vs production information, such as for the LWR, is unreliable to assist in making such a decision.

Marketability of Program

There are two stages in the development of the hybrid that plant rating becomes important: during the funding of the demonstration facilities and at the time potential owner/operators consider the construction of hybrids.

* Not applicable for molten salt concept.

During the research stage of developing the hybrid, Congress might be expected to be the sole funding agent. As long as the hybrid program does not involve large financing, the direct involvement of Congress will be small. However, to bring the hybrid to the point of commercial readiness, demonstration plant(s) must be built and funded. Such funding will be large enough to make the hybrid program visible as an expense that could be dropped to balance the budget. A small commercial plant size would allow small demonstration facilities and lower program costs, possibly increasing the chance of a successful commercialization program.

The size of the commercial hybrid is also important to the prospective owner/operators. These owner/operators might be the U.S. government, energy supply companies, or groups of electric utilities. For all three prospective owner/operators, minimum costs that might occur with large plant sizes are important, but the ability to market the bred fuels becomes a major concern with large plants.

Electric utilities are familiar with the joint ownership of power plants, but the ownership of a large hybrid would require significantly more partners in a joint venture than previously accomplished; particularly, if each of the utilities do not wish to rely on a single source of nuclear fuel.* Thus, a small plant size would be more appealing to the electric utility industry.

Energy supply companies have a similar problem with large plant sizes and the accompanying large rates of fuel production. Energy supply companies typically sell fuels on a contract basis, with production levels specified for many years by contract. These companies would compete with other energy supply companies to divide the nuclear fuel market. To each energy supply company, the operation of a single large hybrid may become a significant portion of their product line. Thus, the misoperation (lack of fuel production) from one large hybrid could severely impact the company's ability to supply fuel previously sold. It is unknown at this time what sizes would be acceptable as an energy supply company.

The U.S. Government may not have the same problems in owning a large size plant. If the U.S. government were to operate hybrid fuel factories, it is

*One 4000 MW_{th} hybrid with a Th + Be blanket can support 25 1000-GWe LWR's.

likely it would also be the sole operator of all hybrid factories. By combining all plants under one ownership, capacity reserves become more manageable, possibly eliminating plant size problems.

Small commercial plant sizes appear to have merit in trying to finance the hybrid development program. In addition, if the electrical utility industry or an energy supply company is the intended owner/operators of the commercial plants, small plants would be advantageous to increase supply reliability and to reduce the number of reactors supported. Large commercial plant sizes appear to be acceptable if a redundancy of hybrid reactors can be accomplished, such as when one owner (possibly the U.S. government) builds reserve capacity.

Research and Development Costs

The development of any new technology requires both the development of knowledge on the basic concept and the development of specific equipment designs. To ease development requirements, small plant sizes and components are usually developed first with larger, more economical plants and plant components evolving from previous designs. The selection of the optimum plant size must take into account the lead time necessary to evolve from the small component sizes used in R&D to those typical of commercial service. Such information, however, is not available today for the hybrid to definitively suggest a commercial plant size.

Incentives for Hybrid

The rationale for developing any new energy source involves the weighing of many tangible and intangible benefits and costs in some consistent manner. For the hybrid, there are intangible benefits that are difficult to measure, such as increased energy availability, reduced mining needs, and improved public welfare that might occur with the deployment of hybrids. There are also tangible benefits, such as the reduction in the cost of electricity with hybrids. Additionally, the incentive involves people issues, such as who receives the benefits, when and how much, as well as who must pay for the R&D and the other costs. Such an encompassing technology assessment, of course, is difficult to accomplish during the early R&D stage technology development when information is least available.

For this study the incentive for the hybrid is measured in terms of the change in costs of the basic national resources--labor and material--to the U.S. electric utility industry when the hybrid competes with mined U and enrichment prices.* These costs represent the real costs to society and exclude transfer payments, such as income taxes and financing charges. With transfer payments excluded investments such as nuclear fuel and services are recorded as they occur. Since hybrid capital and fuel costs are very uncertain at this stage of development, a range of financial benefits is suggested to bound the incentives for the hybrid.

Reference Electrical Utility Forecast

The financial benefit of deploying hybrids depends to a great degree on the amount of nuclear fuel needed by the electrical power industry, and thus, the benefit depends on the number of nuclear power plants constructed and the availability and cost of enriched U. Table 8-83 describes an electrical capacity forecast for the medium nuclear capacity case (400 GWe of nuclear in year 2000). This forecast is predicated on large thermal market forecasts assuming a 5% electrical growth rate through year 2000 (3-1/2% thereafter) and the availability of 2.5 million tons of domestic U. The latter U limit restricts U.S. nuclear capacity to about 440 GWe, assuming no recycle as shown. Additional assumptions are shown in Table 8-84.

With the nuclear construction schedule of Table 8-83, a series of fuel and capital expenditures result to the nation. A breakdown of these costs is shown in Table 8-85. If hybrid fuels were to compete with enriched U, then in this scenario the financial benefit of introducing the hybrid would be the cost difference between mining and enriching U and creating hybrid fuels.

From Table 8-86 the utility would purchase, between year 2010 and year 2055, \$1.3 trillion in U and \$570 billion in enrichment services. Thus, if hybrid fuels were free, the utility would save \$1.9 trillion less the additional costs of the more expensive refabrication services requested with hybrid fuels. In terms of discounted dollars (Table 8-82), the benefit would be reduced to some figure below \$19.5 billion (present values to year 1979).

* R&D costs have not been removed.

Table 8-83. Reference electrical capacity forecast.

	INSTALLED LARGE THERM	NEW FOSSIL	INSTALLED FOSSIL	NEW HTGR	INSTALLED HTGR	NEW LWR	INSTALLED LWR	NEW+RLD RECYCLE	INSTALLED RECYCLE	NEW U-FUELED	INSTALLED U-FUELED	NEW FAST
(T H O U S A N D S O F M W)												
78	377.	24.3	320.	0.	0.	6.0	56.	0.	0.	6.0	56.	0.
79	395.	15.2	331.	0.	0.	7.8	64.	0.	0.	7.8	64.	0.
80	415.	17.6	344.	0.	0.	6.5	70.	0.	0.	6.5	70.	0.
81	436.	17.6	357.	0.	0.	7.7	78.	0.	0.	7.7	78.	0.
82	458.	16.4	369.	0.	0.	10.2	88.	0.	0.	10.2	88.	0.
83	481.	11.4	375.	0.	0.	16.5	105.	0.	0.	16.5	105.	0.
84	505.	8.5	379.	0.	0.	20.7	126.	0.	0.	20.7	126.	0.
85	530.	11.7	385.	0.	0.	19.0	145.	0.	0.	19.0	145.	0.
86	556.	17.2	396.	0.	0.	15.0	160.	0.	0.	15.0	160.	0.
87	584.	18.8	409.	0.	0.	15.0	175.	0.	0.	15.0	175.	0.
88	613.	19.5	422.	0.	0.	16.0	191.	0.	0.	16.0	191.	0.
89	644.	21.3	437.	0.	0.	16.0	207.	0.	0.	16.0	207.	0.
90	676.	23.1	454.	0.	0.	16.0	222.	0.	0.	16.0	222.	0.
91	710.	25.6	471.	0.	0.	17.0	239.	0.	0.	17.0	239.	0.
92	746.	27.9	489.	0.	0.	17.0	256.	0.	0.	17.0	256.	0.
93	783.	30.3	510.	0.	0.	17.0	273.	0.	0.	17.0	273.	0.
94	822.	31.8	531.	0.	0.	18.0	291.	0.	0.	18.0	291.	0.
95	863.	34.5	554.	0.	0.	18.0	309.	0.	0.	18.0	309.	0.
96	906.	37.3	579.	0.	0.	18.0	327.	0.	0.	18.0	327.	0.
97	951.	39.3	606.	0.	0.	19.0	345.	0.	0.	19.0	345.	0.
98	999.	42.4	635.	0.	0.	19.0	364.	0.	0.	19.0	364.	0.
99	1049.	45.8	667.	0.	0.	19.0	382.	0.	0.	19.0	382.	0.
00	1101.	48.3	701.	0.	0.	20.0	400.	0.	0.	20.0	400.	0.
01	1140.	45.5	733.	0.	0.	10.0	406.	0.	0.	10.0	406.	0.
02	1180.	50.1	769.	0.	0.	10.0	411.	0.	0.	10.0	411.	0.
03	1221.	57.9	811.	0.	0.	5.0	409.	0.	0.	5.0	409.	0.
04	1264.	65.8	865.	0.	0.	0.0	399.	0.	0.	0.0	399.	0.
05	1308.	68.9	918.	0.	0.	0.0	390.	0.	0.	0.0	390.	0.
06	1354.	72.2	969.	0.	0.	0.0	385.	0.	0.	0.0	385.	0.
07	1401.	75.7	1022.	0.	0.	0.0	379.	0.	0.	0.0	379.	0.
08	1450.	79.3	1077.	0.	0.	0.0	373.	0.	0.	0.0	373.	0.
09	1501.	73.8	1136.	0.	0.	0.0	366.	0.	0.	0.0	366.	0.
10	1554.	76.7	1195.	0.	0.	0.0	359.	0.	0.	0.0	359.	0.
11	1608.	79.7	1257.	0.	0.	0.0	351.	0.	0.	0.0	351.	0.
12	1664.	82.8	1323.	0.	0.	0.0	341.	0.	0.	0.0	341.	0.
13	1723.	86.1	1398.	0.	0.	0.0	325.	0.	0.	0.0	325.	0.
14	1783.	89.5	1479.	0.	0.	0.0	304.	0.	0.	0.0	304.	0.
15	1845.	93.1	1560.	0.	0.	0.0	285.	0.	0.	0.0	285.	0.
16	1910.	96.8	1640.	0.	0.	0.0	270.	0.	0.	0.0	270.	0.
17	1977.	100.7	1722.	0.	0.	0.0	255.	0.	0.	0.0	255.	0.
18	2046.	104.7	1807.	0.	0.	0.0	239.	0.	0.	0.0	239.	0.
19	2118.	108.9	1895.	0.	0.	0.0	223.	0.	0.	0.0	223.	0.
20	2192.	113.2	1985.	0.	0.	0.0	207.	0.	0.	0.0	207.	0.
21	2268.	119.3	2078.	0.	0.	0.0	190.	0.	0.	0.0	190.	0.
22	2348.	124.3	2175.	0.	0.	0.0	173.	0.	0.	0.0	173.	0.
23	2430.	129.5	2274.	0.	0.	0.0	156.	0.	0.	0.0	156.	0.
24	2515.	134.9	2377.	0.	0.	0.0	138.	0.	0.	0.0	138.	0.
25	2603.	140.5	2483.	0.	0.	0.0	120.	0.	0.	0.0	120.	0.

Table 8-83. (continued).

26	2548.	0.	2446.	0.	0.	0.	102.	0.	0.	0.	102.
27	2489.	0.	2406.	0.	0.	0.	83.	0.	0.	0.	83.
28	2428.	0.	2354.	0.	0.	0.	64.	0.	0.	0.	64.
29	2363.	0.	2318.	0.	0.	0.	45.	0.	0.	0.	45.
30	2295.	0.	2270.	0.	0.	0.	25.	0.	0.	0.	25.
31	2239.	0.	2224.	0.	0.	0.	15.	0.	0.	0.	15.
32	2179.	0.	2174.	0.	0.	0.	5.	0.	0.	0.	5.
33	2116.	0.	2116.	0.	0.	0.	0.	0.	0.	0.	0.
34	2051.	0.	2051.	0.	0.	0.	0.	0.	0.	0.	0.
35	1982.	0.	1982.	0.	0.	0.	0.	0.	0.	0.	0.
36	1909.	0.	1909.	0.	0.	0.	0.	0.	0.	0.	0.
37	1834.	0.	1834.	0.	0.	0.	0.	0.	0.	0.	0.
38	1754.	0.	1754.	0.	0.	0.	0.	0.	0.	0.	0.
39	1681.	0.	1681.	0.	0.	0.	0.	0.	0.	0.	0.
40	1604.	0.	1604.	0.	0.	0.	0.	0.	0.	0.	0.
41	1524.	0.	1524.	0.	0.	0.	0.	0.	0.	0.	0.
42	1441.	0.	1441.	0.	0.	0.	0.	0.	0.	0.	0.
43	1355.	0.	1355.	0.	0.	0.	0.	0.	0.	0.	0.
44	1266.	0.	1266.	0.	0.	0.	0.	0.	0.	0.	0.
45	1173.	0.	1173.	0.	0.	0.	0.	0.	0.	0.	0.
46	1076.	0.	1076.	0.	0.	0.	0.	0.	0.	0.	0.
47	975.	0.	975.	0.	0.	0.	0.	0.	0.	0.	0.
48	871.	0.	871.	0.	0.	0.	0.	0.	0.	0.	0.
49	762.	0.	762.	0.	0.	0.	0.	0.	0.	0.	0.
50	648.	0.	648.	0.	0.	0.	0.	0.	0.	0.	0.
51	529.	0.	529.	0.	0.	0.	0.	0.	0.	0.	0.
52	405.	0.	405.	0.	0.	0.	0.	0.	0.	0.	0.
53	275.	0.	275.	0.	0.	0.	0.	0.	0.	0.	0.
54	141.	0.	141.	0.	0.	0.	0.	0.	0.	0.	0.
55	0.	0.	0.	0.	0.	0.	-0.	0.	-0.	0.	0.

Table 8-84. Typical assumptions for incentives analysis.

- 6% general rate of inflation.
 - Average new steam coal prices - \$1.35/MBtu today.
- \$2.50/MBtu in 2000.
 - Uranium prices as described in Tables 8-37 through 8-47.
 - Enrichment prices of \$110/SWU (1979 \$).
 - Fuel service cost as described in Tables 8-37 through 8-47.
 - Social discount rate, without correction for inflation - 6% per year.
 - Social discount rate, corrected for inflation - 12.36% per year.
-

Table 8-85. Current dollar expenditure summary for utility industry (reference cap.

CURRENT DOLLAR CUMULATIVE EXPENDITURES (BILLIONS OF \$) ECONOMIC COST CASE															
YR	CAPITAL INVESTMENTS				EXPENSES										
	FOSSIL	HTGR LWR	FBR	TOTAL	FOSSIL	LWR				FBR					
						FUEL O&M	FABRICATION RECOVERY		URANIUM FEED	SEP WK	PU SALES	PU PURCHASES	FABRICATION RECOVERY O&M	PU SALES	PU PURCHASES
							O&M	O&M							
78	17.54	5.10	0.	22.64	20.16	0.88	1.40	0.50	0.	0.	0.	0.	0.	0.	
79	29.19	12.13	0.	41.32	42.96	1.94	3.17	1.15	0.	0.	0.	0.	0.	0.	
80	43.51	18.34	0.	61.84	68.96	3.18	5.11	1.92	0.	0.	0.	0.	0.11	0.	
81	58.67	26.13	0.	84.80	98.49	4.62	7.44	2.86	0.	0.	0.	0.	0.	0.	
82	73.59	37.08	0.	110.65	131.78	6.35	10.38	4.06	0.	0.	0.	0.	0.	0.	
83	84.58	55.85	0.	140.43	168.51	8.50	14.50	5.71	0.	0.	0.	0.	0.	0.	
84	93.34	80.80	0.	174.14	208.54	11.21	19.90	7.90	0.	0.	0.	0.	0.	0.	
85	106.04	105.09	0.	211.12	252.63	14.49	26.11	10.57	0.	0.	0.	0.	0.11	0.	
86	125.86	125.41	0.	251.27	302.11	18.31	32.87	13.66	0.	0.	0.	0.	0.	0.	
87	148.82	146.95	0.	295.77	357.84	22.71	40.69	17.31	0.	0.	0.	0.	0.	0.	
88	174.05	171.31	0.	345.35	420.58	27.77	49.86	21.65	0.	0.	0.	0.	0.	0.	
89	203.21	197.12	0.	400.33	491.47	33.54	60.43	26.76	0.	0.	0.	0.	0.76	0.	
90	235.83	224.49	0.	461.32	571.84	40.09	72.58	32.70	0.	0.	0.	0.	0.	1	
91	276.32	255.31	0.	531.62	663.01	47.54	86.70	39.67	0.	0.	0.	0.	0.	1	
92	321.87	287.98	0.	609.85	766.72	55.01	102.90	47.75	0.	0.	0.	0.	0.	1	
93	374.30	322.61	0.	696.91	885.13	65.57	121.43	57.07	0.	0.	0.	0.	0.	1	
94	432.69	361.48	0.	794.17	1020.19	76.36	142.84	67.87	0.	0.	0.	0.	0.	2	
95	499.78	402.68	0.	902.46	1174.66	88.52	167.31	80.28	0.	0.	0.	0.	0.	2	
96	576.72	446.35	0.	1023.07	1351.79	102.15	195.24	94.50	0.	0.	0.	0.	0.	2	
97	662.62	495.21	0.	1157.83	1555.24	117.39	227.40	110.74	0.	0.	0.	0.	0.	3	
98	760.98	547.01	0.	1307.96	1789.01	134.44	263.98	129.31	0.	0.	0.	0.	0.	3	
99	873.43	601.91	0.	1475.34	2058.48	153.43	305.61	150.37	0.	0.	0.	0.	0.	4	
00	999.20	663.17	0.	1662.37	2369.68	174.48	353.74	174.17	0.	0.	0.	0.	0.	4	
01	1124.81	695.64	0.	1820.44	2718.29	197.16	403.79	198.90	0.	0.	0.	0.	0.	5	
02	1271.31	730.05	0.	2001.37	3109.42	221.46	459.53	225.27	0.	0.	0.	0.	0.	6	
03	1450.78	748.29	0.	2199.07	3552.91	247.14	518.30	252.61	0.	0.	0.	0.	0.	6	
04	1667.14	748.30	0.	2415.43	4062.10	273.67	579.15	230.09	0.	0.	0.	0.	0.	7	
05	1907.30	748.30	0.	2655.60	4644.18	301.11	643.74	308.51	0.	0.	0.	0.	0.	8	
06	2173.99	748.31	0.	2922.29	5303.89	329.87	712.57	338.72	0.	0.	0.	0.	0.	9	
07	2470.23	748.31	0.	3218.54	6031.26	359.89	786.62	370.12	0.	0.	0.	0.	0.	10	
08	2799.40	748.32	0.	3547.72	6892.80	391.20	861.16	402.87	0.	0.	0.	0.	0.	12	
09	3123.90	748.32	0.	3872.22	7840.83	423.70	939.09	436.88	0.	0.	0.	0.	0.	13	
10	3481.40	748.33	0.	4229.73	8904.78	457.54	1022.79	472.00	0.	0.	0.	0.	0.	15	
11	3875.28	748.33	0.	4623.61	10099.21	492.64	1110.45	508.50	0.	0.	0.	0.	0.	16	
12	4309.28	748.34	0.	5057.62	11441.13	528.77	1200.30	545.78	0.	0.	0.	0.	0.	18	
13	4787.53	748.34	0.	5535.87	12954.88	565.21	1286.78	582.64	0.	0.	0.	0.	0.	20	
14	5314.56	748.35	0.	6062.91	14664.76	601.38	1369.13	618.60	0.	0.	0.	0.	0.	23	
15	5895.41	748.36	0.	6643.77	16589.25	637.32	1452.53	654.39	0.	0.	0.	0.	0.	25	

Table 8-85. (continued)

16 6535.63	748.37	0.	7283.9918744.66	673.42	1540.59	690.72	0.	0.	0.	0.	288
17 7241.31	748.37	0.	7989.6921155.19	709.55	1628.91	726.98	0.	0.	0.	0.	322
18 8019.24	748.38	0.	8767.6223849.28	745.45	1715.31	762.72	0.	0.	0.	0.	354
19 8876.86	748.39	0.	9625.2526856.40	780.95	1800.25	797.89	0.	0.	0.	0.	398
20 9822.40	748.40	0.	10570.8030208.92	815.89	1883.00	832.31	0.	0.	0.	0.	442
2110878.57	748.41	0.	11626.9833944.72	849.88	1960.73	865.39	0.	0.	0.	0.	492
2212044.56	748.42	0.	12792.9238103.17	882.68	2033.86	897.03	0.	0.	0.	0.	542
2313331.95	748.44	0.	14080.3942727.52	914.04	2101.35	926.95	0.	0.	0.	0.	602
2414759.58	748.45	0.	15502.0347667.86	943.45	2159.56	954.38	0.	0.	0.	0.	672
2516323.63	748.46	0.	17072.0953576.67	970.55	2208.88	979.14	0.	0.	0.	0.	742
2616323.63	748.46	0.	17072.0959549.16	994.98	2247.86	1000.81	0.	0.	0.	0.	802
2716323.63	748.46	0.	17072.0965792.00	1016.04	2271.99	1018.42	0.	0.	0.	0.	872
2816323.63	748.46	0.	17072.0972307.68	1033.26	2281.60	1031.65	0.	0.	0.	0.	932
2916323.63	748.46	0.	17072.0979096.99	1046.10	2281.60	1039.93	0.	0.	0.	0.	1002
3016323.63	748.46	0.	17072.0986162.40	1053.66	2281.60	1042.00	0.	0.	0.	0.	1072
3116323.63	748.46	0.	17072.0993512.64	1058.47	2281.60	1043.94	0.	0.	0.	0.	1142
3216323.63	748.46	0.	17072.0901140.56	1060.18	2281.60	1043.94	0.	0.	0.	0.	1222
3316323.63	748.46	0.	17072.0909018.33	1060.18	2281.60	1043.94	0.	0.	0.	0.	1302
3416323.63	748.46	0.	17072.0917108.96	1060.18	2281.60	1043.94	0.	0.	0.	0.	1382
3516323.63	748.46	0.	17072.0925396.63	1060.18	2281.60	1043.94	0.	0.	0.	0.	1462
3616323.63	748.46	0.	17072.0933861.32	1060.18	2281.60	1043.94	0.	0.	0.	0.	1552
3716323.63	748.46	0.	17072.0942478.18	1060.18	2281.60	1043.94	0.	0.	0.	0.	1632
3816323.63	748.46	0.	17072.0951216.79	1060.18	2281.60	1043.94	0.	0.	0.	0.	1722
3916323.63	748.46	0.	17072.0960090.15	1060.18	2281.60	1043.94	0.	0.	0.	0.	1812
4016323.63	748.46	0.	17072.0969066.73	1060.18	2281.60	1043.94	0.	0.	0.	0.	1902
4116323.63	748.46	0.	17072.0978109.07	1060.18	2281.60	1043.94	0.	0.	0.	0.	1992
4216323.63	748.46	0.	17072.0987172.97	1060.18	2281.60	1043.94	0.	0.	0.	0.	2082
4316323.63	748.46	0.	17072.0996206.61	1060.18	2281.60	1043.94	0.	0.	0.	0.	2172
4416323.63	748.46	0.	17072.0905149.63	1060.18	2281.60	1043.94	0.	0.	0.	0.	2262
4516323.63	748.46	0.	17072.0913932.00	1060.18	2281.60	1043.94	0.	0.	0.	0.	2352
4616323.63	748.46	0.	17072.0922472.84	1060.18	2281.60	1043.94	0.	0.	0.	0.	2432
4716323.63	748.46	0.	17072.0930679.09	1060.18	2281.60	1043.94	0.	0.	0.	0.	2522
4816323.63	748.46	0.	17072.0936443.96	1060.18	2281.60	1043.94	0.	0.	0.	0.	2592
4916323.63	748.46	0.	17072.0945645.35	1060.18	2281.60	1043.94	0.	0.	0.	0.	2672
5016323.63	748.46	0.	17072.0952143.91	1060.18	2281.60	1043.94	0.	0.	0.	0.	2732
5116323.63	748.46	0.	17072.0957764.70	1060.18	2281.60	1043.94	0.	0.	0.	0.	2792
5216323.63	748.46	0.	17072.0962323.25	1060.18	2281.60	1043.94	0.	0.	0.	0.	2832
5316323.63	748.46	0.	17072.0965610.11	1060.18	2281.60	1043.94	0.	0.	0.	0.	2872
5416323.63	748.46	0.	17072.0967387.88	1060.18	2281.60	1043.94	0.	0.	0.	0.	2882
5516323.63	748.46	0.	17072.0967387.88	1060.18	2281.60	1043.94	0.	0.	0.	0.	2882

Current Dollar
 Enriched Uranium
 Purchases Between
 Years 2010 and 2055
 = \$1831 Billion
 [2282+1044-1023-472]

Table 8-86. Discounted dollar expenditure summary for the utility industry (reference

PRESENT WORTHED CUMULATIVE EXPENDITURES (BILLIONS OF \$) ECONOMIC COST CASE														
YR	CAPITAL INVESTMENTS				EXPENSES									
	FOSSIL	HTGR LWR	FBR	TOTAL	FOSSIL	LWR			FBR					
					FUEL O&M	FABRICATION RECOVERY O&M	URANIUM FEED	SEP WK	PU SALES	PU PURCHASES	FABRICATION RECOVERY O&M	PU SALES	PU PURCHASES	
78	17.54	5.10	0.	22.64	17.94	0.78	1.40	0.50	0.	0.	0.	0.	0.	
79	27.91	11.35	0.	39.26	36.01	1.62	2.98	1.08	0.	0.	0.	0.	0.	
80	39.25	16.27	0.	55.52	54.33	2.50	4.51	1.69	0.	0.	0.	0.	0.	
81	49.93	21.77	0.	71.70	72.86	3.40	6.15	2.35	0.	0.	0.	0.	0.	
82	59.30	28.63	0.	87.93	91.45	4.36	8.00	3.10	0.	0.	0.	0.	0.	
83	65.44	39.12	0.	104.55	109.70	5.43	10.30	4.03	0.	0.	0.	0.	0.	
84	69.79	51.52	0.	121.31	127.41	6.63	12.98	5.12	0.	0.	0.	0.	0.	
85	75.40	62.26	0.	137.66	144.76	7.93	15.73	6.30	0.	0.	0.	0.	0.	
86	83.21	70.26	0.	153.47	162.10	9.26	18.39	7.51	0.	0.	0.	0.	0.	
87	91.25	77.81	0.	169.06	179.48	10.64	21.13	8.79	0.	0.	0.	0.	0.	
88	99.12	85.40	0.	184.52	196.89	12.04	23.99	10.14	0.	0.	0.	0.	0.	
89	107.21	92.56	0.	199.77	214.39	13.46	26.92	11.56	0.	0.	0.	0.	0.	
90	115.51	99.32	0.	214.84	232.06	14.90	29.92	13.03	0.	0.	0.	0.	0.	
91	124.19	106.10	0.	230.29	249.90	16.36	33.03	14.56	0.	0.	0.	0.	0.	
92	133.11	112.49	0.	245.59	267.95	17.84	36.20	16.14	0.	0.	0.	0.	0.	
93	142.23	118.52	0.	260.75	286.30	19.32	39.42	17.76	0.	0.	0.	0.	0.	
94	151.28	124.54	0.	275.82	304.93	20.81	42.74	19.44	0.	0.	0.	0.	0.	
95	160.53	130.22	0.	290.76	323.89	22.30	46.12	21.15	0.	0.	0.	0.	0.	
96	169.98	135.58	0.	305.56	343.24	23.79	49.54	22.89	0.	0.	0.	0.	0.	
97	179.36	140.92	0.	320.28	363.02	25.27	53.06	24.67	0.	0.	0.	0.	0.	
98	188.92	145.96	0.	334.88	383.24	26.74	56.61	26.47	0.	0.	0.	0.	0.	
99	198.65	150.71	0.	349.36	404.00	28.21	60.21	28.30	0.	0.	0.	0.	0.	
00	208.34	155.42	0.	363.76	425.34	29.65	63.92	30.13	0.	0.	0.	0.	0.	
01	216.95	157.65	0.	374.60	446.59	31.03	67.35	31.82	0.	0.	0.	0.	0.	
02	225.89	159.75	0.	385.63	467.83	32.35	70.75	33.43	0.	0.	0.	0.	0.	
03	235.63	160.74	0.	396.37	489.25	33.59	73.94	34.92	0.	0.	0.	0.	0.	
04	246.08	160.74	0.	406.82	511.15	34.73	76.88	36.24	0.	0.	0.	0.	0.	
05	256.41	160.74	0.	417.15	533.43	35.78	79.66	37.47	0.	0.	0.	0.	0.	
06	266.62	160.74	0.	427.36	555.90	36.76	82.29	38.62	0.	0.	0.	0.	0.	
07	276.71	160.74	0.	437.45	578.55	37.67	84.82	39.69	0.	0.	0.	0.	0.	
08	286.68	160.74	0.	447.43	601.26	38.52	87.08	40.88	0.	0.	0.	0.	0.	
09	295.44	160.74	0.	456.18	624.02	39.30	89.18	41.60	0.	0.	0.	0.	0.	
10	304.02	160.74	0.	464.76	646.76	40.02	91.19	42.45	0.	0.	0.	0.	0.	
11	312.44	160.74	0.	473.18	669.47	40.69	93.06	43.23	0.	0.	0.	0.	0.	
12	320.70	160.74	0.	481.44	692.19	41.30	94.77	43.93	0.	0.	0.	0.	0.	
13	328.79	160.74	0.	489.53	714.99	41.85	96.23	44.56	0.	0.	0.	0.	0.	
14	336.73	160.74	0.	497.47	737.92	42.33	97.47	45.10	0.	0.	0.	0.	0.	
15	344.52	160.74	0.	505.26	760.89	42.76	98.59	45.58	0.	0.	0.	0.	0.	

Table 8-86. (continued)

16	352.16	160.74	0.	512.90	783.78	43.15	99.64	46.01	0.	0.	0.	0.	0.	1485.4
17	359.65	160.74	0.	520.39	806.56	43.49	100.58	46.40	0.	0.	0.	0.	0.	1517.4
18	367.01	160.74	0.	527.75	829.23	43.79	101.40	46.74	0.	0.	0.	0.	0.	1548.9
19	374.22	160.74	0.	534.96	851.74	44.06	102.11	47.03	0.	0.	0.	0.	0.	1579.9
20	381.30	160.74	0.	542.04	874.08	44.29	102.73	47.29	0.	0.	0.	0.	0.	1610.4
21	388.34	160.74	0.	549.08	896.23	44.49	103.25	47.51	0.	0.	0.	0.	0.	1640.9
22	395.25	160.74	0.	555.99	918.18	44.66	103.68	47.70	0.	0.	0.	0.	0.	1670.2
23	402.05	160.74	0.	562.79	939.91	44.81	104.04	47.86	0.	0.	0.	0.	0.	1699.4
24	408.73	160.74	0.	569.47	961.40	44.93	104.31	47.98	0.	0.	0.	0.	0.	1728.0
25	415.29	160.74	0.	576.03	982.64	45.03	104.52	48.09	0.	0.	0.	0.	0.	1755.2
26	415.29	160.74	0.	576.03	1002.41	45.11	104.66	48.17	0.	0.	0.	0.	0.	1776.2
27	415.29	160.74	0.	576.03	1020.81	45.18	104.74	48.23	0.	0.	0.	0.	0.	1794.9
28	415.29	160.74	0.	576.03	1037.90	45.22	104.77	48.27	0.	0.	0.	0.	0.	1812.2
29	415.29	160.74	0.	576.03	1053.75	45.25	104.77	48.29	0.	0.	0.	0.	0.	1828.1
30	415.29	160.74	0.	576.03	1068.43	45.27	104.77	48.29	0.	0.	0.	0.	0.	1842.8
31	415.29	160.74	0.	576.03	1082.03	45.28	104.77	48.30	0.	0.	0.	0.	0.	1856.4
32	415.29	160.74	0.	576.03	1094.58	45.28	104.77	48.30	0.	0.	0.	0.	0.	1868.9
33	415.29	160.74	0.	576.03	1106.12	45.28	104.77	48.30	0.	0.	0.	0.	0.	1880.2
34	415.29	160.74	0.	576.03	1116.66	45.28	104.77	48.30	0.	0.	0.	0.	0.	1891.0
35	415.29	160.74	0.	576.03	1126.28	45.28	104.77	48.30	0.	0.	0.	0.	0.	1900.8
36	415.29	160.74	0.	576.03	1135.02	45.28	104.77	48.30	0.	0.	0.	0.	0.	1909.4
37	415.29	160.74	0.	576.03	1142.94	45.28	104.77	48.30	0.	0.	0.	0.	0.	1917.2
38	415.29	160.74	0.	576.03	1150.08	45.28	104.77	48.30	0.	0.	0.	0.	0.	1924.4
39	415.29	160.74	0.	576.03	1156.54	45.28	104.77	48.30	0.	0.	0.	0.	0.	1930.9
40	415.29	160.74	0.	576.03	1162.36	45.28	104.77	48.30	0.	0.	0.	0.	0.	1935.7
41	415.29	160.74	0.	576.03	1167.57	45.28	104.77	48.30	0.	0.	0.	0.	0.	1941.9
42	415.29	160.74	0.	576.03	1172.22	45.28	104.77	48.30	0.	0.	0.	0.	0.	1946.8
43	415.29	160.74	0.	576.03	1176.35	45.28	104.77	48.30	0.	0.	0.	0.	0.	1950.7
44	415.29	160.74	0.	576.03	1179.98	45.28	104.77	48.30	0.	0.	0.	0.	0.	1954.2
45	415.29	160.74	0.	576.03	1183.16	45.28	104.77	48.30	0.	0.	0.	0.	0.	1957.8
46	415.29	160.74	0.	576.03	1185.91	45.28	104.77	48.30	0.	0.	0.	0.	0.	1960.2
47	415.29	160.74	0.	576.03	1188.26	45.28	104.77	48.30	0.	0.	0.	0.	0.	1962.6
48	415.29	160.74	0.	576.03	1190.24	45.28	104.77	48.30	0.	0.	0.	0.	0.	1964.6
49	415.29	160.74	0.	576.03	1191.88	45.28	104.77	48.30	0.	0.	0.	0.	0.	1965.2
50	415.29	160.74	0.	576.03	1193.19	45.28	104.77	48.30	0.	0.	0.	0.	0.	1967.2
51	415.29	160.74	0.	576.03	1194.20	45.28	104.77	48.30	0.	0.	0.	0.	0.	1968.5
52	415.29	160.74	0.	576.03	1194.93	45.28	104.77	48.30	0.	0.	0.	0.	0.	1969.2
53	415.29	160.74	0.	576.03	1195.40	45.28	104.77	48.30	0.	0.	0.	0.	0.	1969.7
54	415.29	160.74	0.	576.03	1195.62	45.28	104.77	48.30	0.	0.	0.	0.	0.	1970.0
55	415.29	160.74	0.	576.03	1195.62	45.28	104.77	48.30	0.	0.	0.	0.	0.	1970.0

8-124

net enriched uranium
purchases between
years 2010 and 2055
= \$15.4 billion (present
valued to 1979)
[104.77+44.30-91.19-42.45]

The above zero to \$19.5 billion dollars benefit is a function of the price of U, the cost of hybrid fuels, and the additional cost of fabricating hybrid fuels. For many hybrid marketing cases, hybrid fuels may be only marginally competitive to enriched U; thus, this comparison suggests a hybrid benefit to the nation that approaches zero. However, this competitive example does not include the externals.

Electrical Forecast With a Hybrid

The preceding U.S. electrical forecast was predicated on the assumption that the nation would consume its resources of U and would not build new reactors that use imported or much lower grade U. Thus, no new nuclear additions were assumed built shortly after the turn of the century. At this point all new and replacement electrical additions were assumed to be coal-fueled.

With the hybrid available to supply additional fissile fuel, the nation may continue to commit new nuclear units (Table 8-87). This additional bred fuel both delays the depletion and cost rises in existing domestic U as well as saves the burning of expensive coal. Both effects reduce costs to the electrical utility industry and therefore to the public. For the above cases the discounted benefit of the hybrid would be increased by \$107 billion (Table 8-88), plus the savings between U prices and actual hybrid fuel production costs. This total discounted savings may be in the range of \$107 to \$167 billion (present valued to 1979).

Summary of Conclusions

This market assessment had as a goal the addressing of a number of key hybrid design issues from the point-of-view of the marketplace to guide the hybrid program in meeting the needs of the nation three decades hence. The study included a partial cost benefit study to estimate the size of national benefit of the program, as well as studies on the market impact of key design options.

The cost/benefit assessment showed that the benefit for a hybrid occurs in two parts. The first part is the benefit the nation of lower cost nuclear fuel. This benefit is in the range 0 to \$20 billion (discounted to 1979), depending on the cost advantage of hybrid fuels over mined U. The second

Table 8-87. Electrical forecast with hybrid.

	INSTALLED LARGE THERM	NEW FOSSIL	INSTALLED FOSSIL	NEW HTGR	INSTALLED HTGR	NEW LWR	INSTALLED LWR	NEW+RLD RECYCLE	INSTALLED RECYCLE	NEW U-FUELED	INSTALLED U-FUELED	NE FA
(T H O U S A N D S O F M W)												
78	377.	24.3	320.	0.	0.	6.0	56.	0.	0.	6.0	56.	
79	395.	15.2	331.	0.	0.	7.8	64.	0.	0.	7.8	64.	
80	415.	17.6	344.	0.	0.	6.5	70.	0.	0.	6.5	70.	
81	436.	17.6	357.	0.	0.	7.7	78.	0.	0.	7.7	78.	
82	458.	16.4	369.	0.	0.	10.2	88.	0.	0.	10.2	88.	
83	481.	11.4	375.	0.	0.	16.5	105.	0.	0.	16.5	105.	
84	505.	8.5	379.	0.	0.	20.7	126.	0.	0.	20.7	126.	
85	530.	11.7	385.	0.	0.	19.0	145.	0.	0.	19.0	145.	
86	556.	17.2	396.	0.	0.	15.0	160.	0.	0.	15.0	160.	
87	584.	18.8	409.	0.	0.	15.0	175.	0.	0.	15.0	175.	
88	613.	19.5	422.	0.	0.	16.0	191.	0.	0.	16.0	191.	
89	644.	21.3	437.	0.	0.	16.0	207.	0.	0.	16.0	207.	
90	676.	23.1	454.	0.	0.	16.0	222.	0.	0.	16.0	222.	
91	710.	25.6	471.	0.	0.	17.0	239.	0.	0.	17.0	239.	
92	746.	27.9	489.	0.	0.	17.0	256.	0.	0.	17.0	256.	
93	783.	30.3	510.	0.	0.	17.0	273.	0.	0.	17.0	273.	
94	822.	31.8	531.	0.	0.	18.0	291.	0.	0.	18.0	291.	
95	863.	34.5	554.	0.	0.	18.0	309.	0.	0.	18.0	309.	
96	906.	37.3	579.	0.	0.	18.0	327.	0.	0.	18.0	327.	
97	951.	39.3	606.	0.	0.	19.0	345.	0.	0.	19.0	345.	
98	999.	42.4	635.	0.	0.	19.0	364.	0.	0.	19.0	364.	
99	1049.	45.8	667.	0.	0.	19.0	382.	0.	0.	19.0	382.	
00	1101.	48.3	701.	0.	0.	20.0	400.	0.	0.	20.0	400.	
01	1140.	34.5	722.	0.	0.	21.0	417.	0.	0.	21.0	417.	
02	1180.	39.1	747.	0.	0.	21.0	433.	0.	0.	21.0	433.	
03	1221.	41.9	773.	0.	0.	21.0	447.	0.	0.	21.0	447.	
04	1264.	44.8	806.	0.	0.	21.0	458.	0.	0.	21.0	458.	
05	1308.	47.9	838.	0.	0.	21.0	470.	0.	0.	21.0	470.	
06	1354.	46.2	863.	0.	0.	26.0	491.	0.	0.	26.0	491.	
07	1401.	49.7	890.	0.	0.	26.0	511.	0.	0.	26.0	511.	
08	1450.	53.3	919.	0.	0.	26.0	531.	0.	0.	26.0	531.	
09	1501.	47.8	952.	0.	0.	26.0	550.	0.	0.	26.0	550.	
10	1554.	50.7	985.	0.	0.	26.0	569.	0.	0.	26.0	569.	
11	1608.	49.7	1017.	0.	0.	30.0	591.	0.	0.	30.0	591.	
12	1664.	52.8	1053.	0.	0.	30.0	611.	0.	0.	30.0	611.	
13	1723.	56.1	1093.	0.	0.	30.0	625.	0.	0.	30.0	625.	
14	1783.	59.5	1149.	0.	0.	30.0	634.	0.	0.	30.0	634.	
15	1845.	73.1	1210.	0.	0.	20.0	635.	0.	0.	20.0	635.	
16	1910.	81.8	1275.	0.	0.	15.0	635.	0.	0.	15.0	635.	
17	1977.	85.7	1342.	0.	0.	15.0	635.	0.	0.	15.0	635.	
18	2046.	89.7	1412.	0.	0.	15.0	634.	0.	0.	15.0	634.	
19	2118.	93.9	1485.	0.	0.	15.0	633.	0.	0.	15.0	633.	
20	2192.	96.2	1560.	0.	0.	15.0	632.	0.	0.	15.0	632.	
21	2268.	119.3	1653.	0.	0.	0.0	615.	0.	0.	0.0	615.	
22	2348.	124.3	1750.	0.	0.	0.0	598.	0.	0.	0.0	598.	
23	2430.	129.5	1849.	0.	0.	0.0	581.	0.	0.	0.0	581.	
24	2515.	134.9	1952.	0.	0.	0.0	563.	0.	0.	0.0	563.	
25	2603.	140.5	2058.	0.	0.	0.0	545.	0.	0.	0.0	545.	

Table 8-87. (continued)

26	2548.	0.	2021.	0.	0.	0.	527.	0.	0.	0.	527.	0.
27	2489.	0.	1981.	0.	0.	0.	508.	0.	0.	0.	508.	0.
28	2428.	0.	1939.	0.	0.	0.	489.	0.	0.	0.	489.	0.
29	2363.	0.	1893.	0.	0.	0.	470.	0.	0.	0.	470.	0.
30	2295.	0.	1845.	0.	0.	0.	450.	0.	0.	0.	450.	0.
31	2239.	0.	1810.	0.	0.	0.	429.	0.	0.	0.	429.	0.
32	2179.	0.	1771.	0.	0.	0.	408.	0.	0.	0.	408.	0.
33	2116.	0.	1729.	0.	0.	0.	387.	0.	0.	0.	387.	0.
34	2051.	0.	1685.	0.	0.	0.	366.	0.	0.	0.	366.	0.
35	1982.	0.	1637.	0.	0.	0.	345.	0.	0.	0.	345.	0.
36	1909.	0.	1590.	0.	0.	0.	319.	0.	0.	0.	319.	0.
37	1834.	0.	1541.	0.	0.	0.	293.	0.	0.	0.	293.	0.
38	1754.	0.	1487.	0.	0.	0.	267.	0.	0.	0.	267.	0.
39	1681.	0.	1440.	0.	0.	0.	241.	0.	0.	0.	241.	0.
40	1604.	0.	1389.	0.	0.	0.	215.	0.	0.	0.	215.	0.
41	1524.	0.	1339.	0.	0.	0.	185.	0.	0.	0.	185.	0.
42	1441.	0.	1285.	0.	0.	0.	155.	0.	0.	0.	155.	0.
43	1355.	0.	1230.	0.	0.	0.	125.	0.	0.	0.	125.	0.
44	1266.	0.	1171.	0.	0.	0.	95.	0.	0.	0.	95.	0.
45	1173.	0.	1098.	0.	0.	0.	75.	0.	0.	0.	75.	0.
46	1076.	0.	1016.	0.	0.	0.	60.	0.	0.	0.	60.	0.
47	975.	0.	930.	0.	0.	0.	45.	0.	0.	0.	45.	0.
48	871.	0.	841.	0.	0.	0.	30.	0.	0.	0.	30.	0.
49	762.	0.	747.	0.	0.	0.	15.	0.	0.	0.	15.	0.
50	648.	0.	648.	0.	0.	0.	0.	0.	0.	0.	0.	0.
51	529.	0.	529.	0.	0.	0.	0.	0.	0.	0.	0.	0.
52	405.	0.	405.	0.	0.	0.	0.	0.	0.	0.	0.	0.
53	275.	0.	275.	0.	0.	0.	0.	0.	0.	0.	0.	0.
54	141.	0.	141.	0.	0.	0.	0.	0.	0.	0.	0.	0.
55	0.	0.	-0.	0.	0.	0.	0.	0.	0.	0.	0.	0.

Table 8-88. Discounted dollar expenditure summary for electrical utility industry (with

PRESENT WORTHED CUMULATIVE EXPENDITURES (BILLIONS OF \$) ECONOMIC COST CASE																			
YR	CAPITAL INVESTMENTS				EXPENSES														
	FOSSIL	HTGR LWR	FBR	TOTAL	FOSSIL	LWR					FBR				TOT				
						FUEL O&M	FABRICATION RECOVERY		URANIUM FEED	SEP	WK	PU SALES	PU PURCHASES	FABRICATION RECOVERY		PU SALES	PU PURCHASES	WITH PU	
							O&M	O&M						O&M					O&M
78	17.54	5.10	0.	22.64	17.94	0.78	1.40	0.50	0.	0.	0.	0.	0.	43.27					
79	27.91	11.35	0.	39.26	36.01	1.62	2.97	1.08	0.	0.	0.	0.	0.	80.94					
80	39.25	16.27	0.	55.52	54.33	2.50	4.49	1.69	0.	0.	0.	0.	0.	118.52					
81	49.93	21.77	0.	71.70	72.86	3.40	6.11	2.35	0.	0.	0.	0.	0.	156.43					
82	59.30	28.63	0.	87.93	91.45	4.36	7.93	3.10	0.	0.	0.	0.	0.	194.78					
83	65.44	39.12	0.	104.55	109.70	5.43	10.18	4.03	0.	0.	0.	0.	0.	233.89					
84	69.79	51.52	0.	121.31	127.41	6.63	12.78	5.12	0.	0.	0.	0.	0.	273.24					
85	75.40	62.26	0.	137.66	144.76	7.93	15.43	6.30	0.	0.	0.	0.	0.	312.08					
86	83.21	70.26	0.	153.47	162.10	9.26	17.97	7.51	0.	0.	0.	0.	0.	350.30					
87	91.25	77.81	0.	169.06	179.48	10.64	20.56	8.79	0.	0.	0.	0.	0.	388.51					
88	99.12	85.40	0.	184.52	196.89	12.04	23.24	10.14	0.	0.	0.	0.	0.	425.62					
89	107.21	92.56	0.	199.77	214.39	13.46	25.96	11.56	0.	0.	0.	0.	0.	465.15					
90	115.51	99.32	0.	214.84	232.06	14.90	28.72	13.03	0.	0.	0.	0.	0.	503.55					
91	124.19	106.10	0.	230.29	249.90	16.36	31.55	14.56	0.	0.	0.	0.	0.	542.65					
92	133.11	112.49	0.	245.59	267.95	17.84	34.40	16.14	0.	0.	0.	0.	0.	581.92					
93	142.23	118.52	0.	260.75	286.30	19.32	37.28	17.76	0.	0.	0.	0.	0.	621.41					
94	151.28	124.54	0.	275.82	304.93	20.81	40.20	19.44	0.	0.	0.	0.	0.	661.20					
95	160.53	130.22	0.	290.76	323.89	22.30	43.15	21.15	0.	0.	0.	0.	0.	701.24					
96	169.98	135.58	0.	305.56	343.24	23.79	46.10	22.89	0.	0.	0.	0.	0.	741.58					
97	179.36	140.92	0.	320.28	363.02	25.27	49.10	24.67	0.	0.	0.	0.	0.	782.34					
98	188.92	145.96	0.	334.88	383.24	26.74	52.10	26.47	0.	0.	0.	0.	0.	823.44					
99	198.65	150.71	0.	349.36	404.00	28.21	55.11	28.30	0.	0.	0.	0.	0.	864.96					
00	208.34	155.42	0.	363.76	425.34	29.65	58.14	30.13	0.	0.	0.	0.	0.	907.02					
01	214.87	160.10	0.	374.97	446.13	31.07	61.18	31.93	0.	0.	0.	0.	0.	945.28					
02	221.84	164.51	0.	386.35	466.48	32.46	64.21	33.68	0.	0.	0.	0.	0.	983.19					
03	228.89	168.67	0.	397.56	486.46	33.81	67.21	35.39	0.	0.	0.	0.	0.	1020.43					
04	236.01	172.59	0.	408.60	506.19	35.12	70.18	37.02	0.	0.	0.	0.	0.	1057.11					
05	243.19	176.29	0.	419.48	525.68	36.39	73.08	38.59	0.	0.	0.	0.	0.	1093.22					
06	249.72	180.61	0.	430.34	544.64	37.64	76.04	40.18	0.	0.	0.	0.	0.	1128.84					
07	256.35	184.69	0.	441.04	563.17	38.87	79.00	41.73	0.	0.	0.	0.	0.	1163.80					
08	263.05	188.54	0.	451.60	581.19	40.07	81.83	43.25	0.	0.	0.	0.	0.	1197.94					
09	268.72	192.17	0.	460.89	598.81	41.24	84.62	44.72	0.	0.	0.	0.	0.	1230.29					
10	274.40	195.60	0.	469.99	616.00	42.39	87.42	46.16	0.	0.	0.	0.	0.	1261.97					
11	279.65	199.32	0.	478.97	632.74	43.51	90.27	47.58	0.	0.	0.	0.	0.	1293.08					
12	284.91	202.84	0.	487.75	649.11	44.61	93.08	48.96	0.	0.	0.	0.	0.	1323.51					
13	290.19	206.16	0.	496.34	665.25	45.66	95.79	50.28	0.	0.	0.	0.	0.	1353.33					
14	295.47	209.29	0.	504.75	681.25	46.67	98.41	51.53	0.	0.	0.	0.	0.	1382.61					
15	301.58	211.26	0.	512.84	697.27	47.63	100.83	52.68	0.	0.	0.	0.	0.	1411.25					

Table 8-88. (continued)

16	308.04	212.65	0.	520.69	713.30	48.53	103.16	53.77	0.	0.	0.	0.	0.
17	314.42	213.96	0.	528.38	729.33	49.38	105.40	54.80	0.	0.	0.	0.	0.
18	320.71	215.20	0.	535.92	745.36	50.18	107.54	55.76	0.	0.	0.	0.	0.
19	326.94	216.37	0.	543.31	761.36	50.94	109.61	56.67	0.	0.	0.	0.	0.
20	333.08	217.47	0.	550.55	777.31	51.65	111.60	57.53	0.	0.	0.	0.	0.
21	340.11	217.47	0.	557.59	793.43	52.30	113.30	58.29	0.	0.	0.	0.	0.
22	347.03	217.47	0.	564.50	809.68	52.90	114.89	58.98	0.	0.	0.	0.	0.
23	353.82	217.48	0.	571.30	826.03	53.45	116.37	59.62	0.	0.	0.	0.	0.
24	360.50	217.48	0.	577.98	842.44	53.95	117.73	60.20	0.	0.	0.	0.	0.
25	367.07	217.48	0.	584.54	858.89	54.41	118.99	60.73	0.	0.	0.	0.	0.
26	367.07	217.48	0.	584.54	874.15	54.82	120.15	61.21	0.	0.	0.	0.	0.
27	367.07	217.48	0.	584.54	888.28	55.20	121.21	61.65	0.	0.	0.	0.	0.
28	367.07	217.48	0.	584.54	901.34	55.55	122.18	62.04	0.	0.	0.	0.	0.
29	367.07	217.48	0.	584.54	913.39	55.86	123.07	62.40	0.	0.	0.	0.	0.
30	367.07	217.48	0.	584.54	924.48	56.14	123.87	62.73	0.	0.	0.	0.	0.
31	367.07	217.48	0.	584.54	934.77	56.40	124.59	63.02	0.	0.	0.	0.	0.
32	367.07	217.48	0.	584.54	944.29	56.63	125.23	63.27	0.	0.	0.	0.	0.
33	367.07	217.48	0.	584.54	953.08	56.83	125.81	63.51	0.	0.	0.	0.	0.
34	367.07	217.48	0.	584.54	961.16	57.01	126.32	63.71	0.	0.	0.	0.	0.
35	367.07	217.48	0.	584.54	968.59	57.17	126.78	63.89	0.	0.	0.	0.	0.
36	367.07	217.48	0.	584.54	975.42	57.32	127.15	64.05	0.	0.	0.	0.	0.
37	367.07	217.48	0.	584.54	981.68	57.44	127.47	64.18	0.	0.	0.	0.	0.
38	367.07	217.48	0.	584.54	987.40	57.54	127.73	64.30	0.	0.	0.	0.	0.
39	367.07	217.48	0.	584.54	992.65	57.63	127.95	64.39	0.	0.	0.	0.	0.
40	367.07	217.48	0.	584.54	997.44	57.71	128.13	64.47	0.	0.	0.	0.	0.
41	367.07	217.48	0.	584.54	1001.81	57.77	128.25	64.53	0.	0.	0.	0.	0.
42	367.07	217.48	0.	584.54	1005.80	57.82	128.32	64.58	0.	0.	0.	0.	0.
43	367.07	217.48	0.	584.54	1009.41	57.85	128.37	64.62	0.	0.	0.	0.	0.
44	367.07	217.48	0.	584.54	1012.68	57.88	128.38	64.64	0.	0.	0.	0.	0.
45	367.07	217.48	0.	584.54	1015.58	57.90	128.40	64.66	0.	0.	0.	0.	0.
46	367.07	217.48	0.	584.54	1018.12	57.92	128.41	64.67	0.	0.	0.	0.	0.
47	367.07	217.48	0.	584.54	1020.33	57.93	128.42	64.68	0.	0.	0.	0.	0.
48	367.07	217.48	0.	584.54	1022.21	57.93	128.42	64.68	0.	0.	0.	0.	0.
49	367.07	217.48	0.	584.54	1023.80	57.94	128.42	64.68	0.	0.	0.	0.	0.
50	367.07	217.48	0.	584.54	1025.12	57.94	128.42	64.68	0.	0.	0.	0.	0.
51	367.07	217.48	0.	584.54	1026.13	57.94	128.42	64.68	0.	0.	0.	0.	0.
52	367.07	217.48	0.	584.54	1026.86	57.94	128.42	64.68	0.	0.	0.	0.	0.
53	367.07	217.48	0.	584.54	1027.32	57.94	128.42	64.68	0.	0.	0.	0.	0.
54	367.07	217.48	0.	584.54	1027.55	57.94	128.42	64.68	0.	0.	0.	0.	0.
55	367.07	217.48	0.	584.54	1027.55	57.94	128.42	64.68	0.	0.	0.	0.	0.

net enriched uranium
purchases between
years 2010 and 2055
= \$59.5 billion (present
valued to 1979)
[128.42+64.68-87.42-46.16]

benefit however was found to be much larger. It stemmed from the conservation of the nation's U reserves and the availability of a nuclear alternative to coal as a source of electrical energy. This later benefit appeared to be in range of \$110 to 170 billion (discounted to 1979).

Competitors to the hybrid were also identified, such as the use of advanced LWR fuels, advanced enrichment processes, the reprocessing of existing spent nuclear fuel, and the development of more U-conserving reactors. All appear to be potential early year competitors to hybrid fuels, with only the later option having longer term potential. It is also suggested that a healthy reprocessing industry must be developed prior to the introduction of hybrids. It is believed that a stockpile of free, LWR spent fuel would be detrimental to commercialization of the hybrid.

The commercialization studies showed that when blanket concepts were compared for sets of hybrid deployment scenarios, little difference in fuel production occurred. Each blanket concept, though some produced more fissile fuel than others, had a fuel supply schedule that was only 1 or 2 yr different than any other. This occurred because the rate of addition of new hybrids is larger than the fuel production differences of the blanket concepts. This discovery suggests that the selection of the fertile fuel in the blanket be made not on fuel production rates per reactor, but on factors that will affect the deployment of hybrids, such as the availability of fuel cycle services and the size of the fusion driver.

The commercialization cases also suggested that small commercial plant ratings have merits worthy of further investigation. Small plant sizes could reduce problems in linking the hybrid with the reprocessing and bred fuel fabrication industries. Small sizes were seen also to have merit in reducing R&D costs and in increasing the marketability of the hybrid program.

The resource and market economic assessment found that relatively few hybrids are needed to reduce the need for mined U. This advantage allows the hybrid to become a relatively fast acting solution to U supply problems. Few other technologies could act as quickly to solve U supply problems.

REFERENCES

1. R. W. Moir, et al., Preliminary Design Study of the Tandem Mirror Reactor (TMR), Lawrence Livermore Laboratory, Rept. UCRL-52302, July 25, 1977.
2. J. D. Lee, "Nuclear Design of Fast Hybrid Blankets," Lawrence Livermore Laboratory, Livermore, CA, Rept. UCRL-80651, January 23, 1978. Also, prepared for the Proceedings of the 2nd DMFE Hybrid Reactor Meeting, Washington, D.C., November 2-3, 1977.
3. J. D. Lee, "The Beryllium/Molten Salt Blanket - A New Blanket Concept," Lawrence Livermore Laboratory, Livermore, CA, Rept. UCRL-82663, April 25, 1979. Also, prepared for submission to proceedings of the Third US/USSR Symposium on Fusion-Fission; Princeton, New Jersey; January 22-26, 1979.
4. M. J. Saltmarsh, et al., "An Optimization of the Fission-Fusion Hybrid Concept," ORNL/PPA-79/3, April 1979.
5. L. N. Abott, et al., "Interim Assessment of the Denatured ^{233}U Fuel Cycle: Feasibility and Non-Proliferation Characteristics," Oak Ridge National Laboratory, ORNL-5388, December 1978.
6. "Draft NASAP Provisional Data Base," Department of Energy, Oak Ridge National Laboratory, February 1979.
7. "Interim Recommendations for Fuel Reprocessing and Fabrication Cost Estimation by U.S. INFCE Support Groups," Memo from David E. Mathes, ETN/FCE to Members of the INFCE Technical and Economic Assessment Crosscut Group, August 23, 1978.
8. Memo from Edward J. Hanrahan to Multiple Distribution, "Unit Reprocessing Costs for Use in INFCE Support Group 4 Analysis," September 1, 1978.
9. G. M. d'Hospital and M. Simnad, "Status of Helium-Cooled Nuclear Power Systems," GA-A14067, 1976.
10. R. H. Brogli and G. W. Shirley, "High Temperature Gas-Cooled Reactor Near Breeder Cycles," GA-A15130, 1979.
11. L. Nordheim, R. Brogli, and W. Lefler, "Core Design Studies for Plutonium Utilization in HTGRs," GA-A13831, February 1976.
12. See several papers at the American Nuclear Society National Topical Meeting on Nuclear Process Heat Applications, Oct. 1-3, 1974, Los Alamos, New Mexico.

13. W. J. Houghton and V. Joksimovic, "An Update of HTGR Risk Assessment Study," GA-A14569, 1978.
14. "HTGR Steam Cycle Configuration Evaluation Report," GA-A14900, 1978.
15. H. B. Stewart and R. C. Dahlberg, "HTGR Strategy for Reduced Proliferation Potential," 78-WA/NE-11 ASME Winter Meeting, San Francisco, CA, Dec. 10-15, 1978.
16. K. R. Schultz, et al., "Evaluation of the ²³³U Refresh Cycle Fusion-Fission Power System Concept," GA-A15108, to be published.

SECTION 9
ENVIRONMENTAL AND SAFETY ANALYSIS

INTRODUCTION

Much has been written on the environmental and safety aspects of both fusion and fission reactors. Fusion-fission hybrids must unfortunately address most of the problems of the two combined technologies. Some treatment has been made in the literature of these issues regarding hybrids.¹⁻⁵

This section addresses the environmental and safety aspects of the two TMHR coolant designs most investigated, i.e., helium and molten salt. Very little work has been done on the TMHR in this area. Although environmental and safety concerns were important in the selection of the thorium cycle over the uranium cycle and were a primary driving force for investigation of the fission-suppressed molten salt blanket, analysis and quantification of these aspects are planned for the second year of this study. Some design considerations of the blanket-related safety issues are raised in Section 6, and fusion-unique safety concerns are addressed in Sections 3 and 4. The discussions in this section are intended as a preliminary review of the safety issues to be addressed in the second year of this study. The subsection on the helium-cooled design relies very heavily on previous safety evaluation of gas-cooled mirror hybrid reactors,¹ and the section on the molten salt design is intended primarily to identify the important safety issues associated with the novel and innovative molten salt blanket design.

Environmental and safety issues are prominent in guiding the development of fusion system designs. A DOE Fusion Safety Program has been established at the Idaho National Engineering Laboratory, and the STARFIRE Prototype Commercial Tokamak Design Study led by Argonne National Laboratory is emphasizing optimization of the safety aspects of that design. It is important that the increasing prominence of safety concerns be reflected in continuation of the preliminary TMHR safety evaluations in this section.

HELIUM-COOLED DESIGN SAFETY ASPECTS

Since no significant safety analysis has been done on the helium-cooled TMHR design, this subsection is an introduction to the safety concerns to be

addressed later in this study. Also indicated are design approaches used on gas-cooled fission reactors in the past.

Because of the significant level of fission product activity and after-heat that will be present in the TMHR blanket, it is expected that safety considerations for the TMHR will be very similar to those for fission reactors. The radioactive hazard inventories are expected to be dominated by fission products. The use of a continuously purged Li_2O tritium breeder system allows the blanket tritium inventory to be kept to less than 50 g. Although there will be considerably larger tritium inventories associated with the plasma tritium injection and recovery systems (5 to 10 kg is expected), most of this inventory will be contained in storage or processing system vaults and will thus be considerably less vulnerable than the smaller blanket inventory.

The plasma systems associated with the TMHR offer the potential for additional accident initiating events. The neutral beams, plasma, and magnets have sufficient stored energy to be able to initiate a blanket depressurization accident by burning through the module pressure boundary or by severing a module pipe connection. Since these accidents must specifically be considered, the plasma systems do not appear to significantly impact the blanket safety design requirements. Because of the existence of additional initiating events that have not been previously studied in fission reactor safety programs, it is expected that the plasma systems could affect the accident event probabilities, impacting the reliability requirements imposed on various safety systems. Assessment of this possibility requires probable risk assessment techniques and is clearly beyond the scope of this preliminary conceptual design study.

Conventional deterministic fission-related safety concerns are considered, possible safety related problems are identified, and approaches to handling these problems in future studies are presented in this section.

BLANKET SAFETY

Two aspects of blanket safety during accident conditions should be evaluated: fuel heatup rate in the event of loss of coolant flow; and forces on the fuel generated by rapid depressurization of the blanket.

Fuel Heat-Up Rate

Time required to cause fuel melting with loss of cooling following reactor shutdown is an important parameter for safety analysis. In the TMHR blanket the melting point of the fuel (Th-metal) is 1700°C. Heatup rate of the fuel for complete loss of cooling (adiabatic heatup rate) can be obtained by the following equation:

$$\frac{d\theta}{dt} = \dot{q}'''(t) / \rho C_p, \quad (1)$$

where

θ = temperature of fuel, °C

t = time, s

$\dot{q}'''(t)$ = decay heat, W/cm³

ρC_p = volumetric specific heat of the fuel, W·s/cm³·°C.

For the TMHR blanket analysis we assume that the volumetric nuclear heating after shutdown, \dot{q}''' , can be obtained from the standard fission product decay heat curve shown in Fig. 9.1.

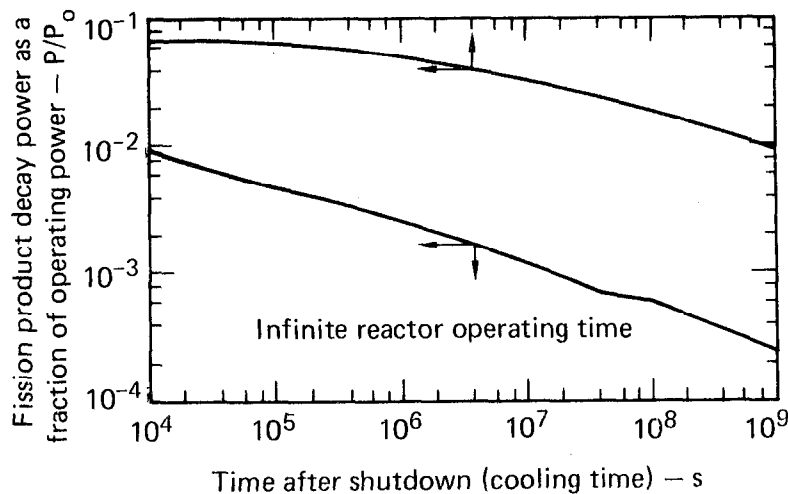


Figure 9-1. Standard fission-product decay-heat curve.

Increase in temperature of the fuel after time t , is given by:

$$\Delta\theta = \int_0^t \frac{d\theta}{d\tau} d\tau. \quad (2)$$

In designing the auxiliary cooling system, the end-of-life maximum decay heat generation, corresponding to 120 W/cm^{-3} peak operating power, should be used. The density of thorium metal is 11.7 g/cm^3 and $C_p = 0.16 \text{ J/g}^\circ\text{C}$.

The nominal peak temperature of the TMHR blanket fuel will be 820°C during normal operation. Hence, the time available before fuel reaches the melting temperature following loss of cooling with reactor shutdown is about 11 min. This heatup time estimate is based on the assumption of totally adiabatic heating and is quite conservative. In fact, coolant flow coast-down, natural convection within the modules, and conduction of heat to the water-cooled module shield are expected to extend the time available before fuel damage occurs even in the event of complete loss-of-coolant flow with depressurization. Further, the auxiliary cooling system should be designed to assure maintenance of adequate cooling even in the event of loss of the main circulators with helium depressurization. Nevertheless, the blanket cooling requirements will impose demands upon the response time characteristics and reliability of the auxiliary cooling system. Further, assurance of adequate cooling during module replacement will be required, which implies the need for reliable and redundant cooling capability to be built into the fuel handling equipment. Although it is expected that these concerns can be adequately addressed, more detailed work in this area is needed.

Forces During Depressurization

A depressurization accident caused by first-wall rupture can result in large pressure differences across the blanket fuel element. To reduce the resulting force, venturis should be provided in the exit manifold of the blanket to limit the flow velocity and the resulting forces on the blanket during depressurization caused by first wall rupture. This action allows a coolable geometry to be maintained.

PLANT SAFETY

In this subsection we analyze the preliminary design of the 4000-MW(t) TMHR so that the adequacy of the proposed design to control expected transients and prevent or mitigate accidents can be evaluated. Safety analyses of those systems that do not directly involve the blanket and power conversion system are not within the scope of this study.

This safety analysis is focused on the more severe expected plant transients and on the design-basis accident. An important objective of the safety analysis is the choice of a postulated accident for use in establishing the design bases for the engineered safety features--emergency cooling and containment atmosphere cleanup--and for the containment system. After examination of potential accidents, the design-basis accident chosen is the postulated gross failure of the helium ducting, which causes rapid depressurization of the blanket coolant into the containment building.

Plant Shutdown Cooling

Assured shutdown cooling, using forced circulation of helium in all normal and emergency situations, is a fundamental safety requirement of the plant. Therefore, much attention is given to provide this function with sufficient redundancy and reliability. The shutdown-cooling capabilities of this design are discussed in this subsection.

Shutdown cooling in the TMHR consists of two phases: an initial period of power reduction, followed by a long-term, decay-heat-removal phase. Reactor trip results in rapid reactor power reduction to the blanket decay-heat level through the trip of the neutral beam injectors together with a trip of the turbine generator. The associated temperature transients are potentially the most severe that a plant would be expected to experience during normal operations.

During the decay-heat-removal phase, the shutdown cooling of the blanket can be accomplished with either the main cooling loops or the auxiliary cooling loops. The parts of both cooling-loop systems necessary to perform emergency cooling in the TMHR plant are designed to provide this function during transients and postulated accidents, including design basis earthquakes, the loss of off-site power, and single equipment failures.

The various signals that initiate reactor trip are generated from the plant protection system. Upon receipt of a trip signal, the plant protection system initiates reactor trip. Power to all the neutral beam injectors is interrupted, causing the plasma to rapidly fall below fusion-producing conditions. Concurrently, a trip signal is sent to the turbine.

Closure of the turbine stop valve causes the control system to change from the normal turbine control mode to the shutdown control mode. Turbine trip causes the opening of the bypass valves around the resuperheaters and the

opening of the loop feedwater discharge lines to the desuperheater. It also causes the programmed closure of the circular turbine throttle valves.

The reactor trip signal also initiates the startup sequence of the auxiliary boilers and associated equipment, the auxiliary circulators and associated equipment, and the emergency diesel generators.

The plant design includes many features that contribute to the reliability of cooling after reactor trip. Each main circulator continues to use steam directly from its associated steam generator. Also, steam from any steam generator can be routed to any circulator to ensure forced convection cooling of the blanket. Separate electrically-driven shutdown boiler feed-pumps are started to supply feedwater to each steam generator. The normal shutdown feedwater supply from the deaerator is backed up by an emergency water supply. However, the water inventory in the steam generators is ample to cover a considerable delay in pump startup or an interruption, such as that required to change from normal to emergency power supply to the pumps.

The system is designed to operate without a significant transient in case of loss of nonseismic equipment, e.g., due to an earthquake. In case of loss of all nonseismic equipment, the steam from the circulator turbine would exhaust to the atmosphere outside the containment building rather than to the condenser, and feedwater would be supplied from the emergency water supply.

During shutdown transients, the feedwater flow to the steam generators and the steam flow through the circulator turbines are controlled. This may be done as follows:

1. The feedwater flow is reduced to zero as the extraction steam supply for the main boiler feedpumps decreases. It remains at zero until 60 s and then is set constant at 2% of full load flow for the remainder of the initial period; i.e., for more than 30 min. The feedwater flow should not be critical because of the large steam generator inventory; the flow could remain at zero for considerably longer than 1 min, and the set value would depart substantially from 2% without important consequences.

2. The circulator-turbine steam flow rate is governed by two valves in parallel located upstream of the turbine. The large control valves are used for plant control during normal operations, whereas the smaller valves, which operate wide open during normal operations, are used to control the steam flow to the circulator turbine after the reactor has been shut down. When the reactor is tripped, the large valves are closed rapidly, and then the shutdown-

control system manipulates the small valves to achieve the desired plant transient behavior.

Initially, after a reactor trip, the helium flow falls rapidly as a consequence of the rapid reduction in power to the circulator turbines with, of course, a rapid drop in circulator speed.

The blanket outlet helium temperature will probably swing down and up during the first 2 min over a small range but should not significantly exceed the initial full load value. The maximum cladding temperature will closely follow the blanket outlet temperature and will also probably remain well within acceptable limits. Gas inlet temperature to the steam generators is expected to vary less than blanket outlet temperature because of the gas volume in the ducting and the heat capacities of walls and other parts.

Thus, these estimates, which are based on the GCFR system design, indicate that this mode of shutdown cooling can maintain metal temperatures and their rates of change within acceptable limits. There is ample margin in steam conditions and supply to provide time for transfer to the decay-heat-removal cooling mode.

Approximately one-half hour after reactor trip, the decay-heat-removal phase will be initiated. If the main cooling loops are used, steam from the auxiliary boilers will be introduced into each main circulator supply line ahead of the circulator turbine throttle. Then the resuperheater outlet isolation valves will be closed, and the steam from the steam generators will be routed through a bypass line to a desuperheater and then to the main condenser.

The auxiliary boilers and associated piping and equipment are independent, so that the loss of a piece of equipment will affect only one auxiliary boiler system. Each auxiliary boiler system is expected to be capable of providing for 100% decay-heat removal.

Decay-heat removal can be provided by the auxiliary loops instead of the main loops. Normally, both loops will be used. However, the operator will not normally initiate the automatic switchover sequence that will make the transfer before 15 min after shutdown, at which time the decay heat being generated in the core can be removed using only one auxiliary loop. After the auxiliary blanket-cooling system equipment startup sequence is completed, cooling is initiated with the auxiliary loops.

Reactivity Insertion Accidents

One of the potential safety advantages of the hybrid reactor concept is the capability to operate in a far-subcritical mode. The TMHR blanket is designed to always be far-subcritical. W. Kastenberg, et al., have studied reactivity insertion accidents for the uranium-fueled Standard Mirror Hybrid Reactor.⁶ They showed that criticality can only be achieved under a series of extremely unlikely events. It is expected that similar analyses for the TMHR would also show that significant reactivity insertion accidents can be considered incredible events.

Local Flow-Blockage Accidents

Local flow-blockage accidents initially involve only a small portion of a blanket. Potential causes for such accidents are localized blockage within a module or flow reduction in an entire module or module assembly. Depending on the failure mode and time sequence and the response of the protection system, serious damage either may or may not be prevented, and the failure may or may not propagate.

Whole-blanket accidents, initiated by overall loop flow reduction or reactivity insertions, are indicated by unambiguous signals that are readily detectable and can be used for initiating protective actions. Local flow-blockage accidents, in which only a restricted area of a module is involved, are more difficult to detect with sufficient assurance to make a decision for reactor shutdown. However, when the signal indicating damage is weak, a fast protective action is presumably not required, whereas a large signal from sizable damage means that fast protective action is desirable.

The objective in detecting a local blockage incident is to limit propagation of the damage. The sensitivity specifications for the protection systems can be defined with regard to an acceptable amount of damage. This maximum tolerable blanket damage may involve more than one fuel element or module, but it must not be so great as to involve extensive loss of blanket-cooling geometry.

The occurrence of major coolant flow blockages caused by foreign matter is highly unlikely. The numerous parallel and rather tortuous coolant flow paths leading into each module would prevent large pieces of foreign matter from completely blocking a whole module. Additionally, it would be essentially

impossible to totally block the flow entry area into each fuel element by any single piece of debris.

Partial Blockage Accidents

Partial fuel element flow blockage could potentially be caused by material being deposited on the fuel-element spacers or support grid, or by fuel-element swelling and thermal distortion. The consequent local under-cooling could result in cladding failure and eventually in fuel-element damage and relocation of fuel and cladding debris.

Because of the complexity of the problem, a simplified model has been used to obtain lower-limit estimates of the periods of time involved for the propagation of failures from element to element. This model is based on the following assumption. After the coolant channels around a particular fuel element have been blocked, the heat transfer between the element and its surroundings is interrupted (no convective or radiation heat transfer). Therefore, the heatup of the rod is adiabatic.

The adiabatic heatup of the fuel rod to the relocation temperature can be represented by

$$\frac{\Delta T}{\Delta t} = \frac{Q}{\rho c_p} \quad , \quad (3)$$

where

ΔT = temperature increase to reach the relocation temperature

Δt = time to reach melting (s)

ρc_p = mean volumetric specific heat of the fuel rod

Q = peak full-power volumetric heat generation in the fuel.

From Eq. (3) the time to reach the melting of the Th-metal at full power amounts to

$$\Delta t = \frac{\Delta T \rho c_p}{Q} = 15 \text{ s}$$

Cladding melting would begin in about 11 s at full power.

Propagation of the failure to other channels is difficult to assess at this time. However, for reference, GCFR propagation (element to element) are on the order of 10-70 s. Propagation times are expected to be larger in the TMHR blanket due to the large amount of structural material between submodules.

Detection of Local Flow-Blockage Accidents

Rapid detection of local failures is desirable in order to initiate protective actions that will limit the damage and reduce the contamination of the primary circuit. According to the present design, the following signals will indicate the occurrence of failures:

- Blanket module coolant outlet temperature.
- Blanket-coolant-activity.

Whereas the coolant outlet temperature is a signal for an alarm, the coolant activity level signal causes a reactor trip after exceeding preset operation limits. In the subsequent paragraphs, the response times of these signals is discussed with respect to the propagation time of local failures. A value of 15 s is used as a representative number for the minimum propagation time of a local failure to an adjacent submodule.

The coolant outlet temperature of each module is monitored. This temperature increases from the beginning of the accident, and, assuming a thermocouple response time of 1 to 2 s, unambiguous signals might be expected after 2 to 3 s in the case of a major flow blockage accident, and thus before propagation of damage to an adjacent submodule. In any circumstance, the thermocouples are intended as operational system devices and are not included as part of the safety related plant protection system.

In cases of cladding failures, the fission gasses would be transmitted by convective flow into the helium coolant. Instrumentation lines monitoring the activity pick up increased activity or delayed neutrons. Estimates indicate that the system response time is less than 5 s for detection of clad melting. This would allow shutdown of the reactor before the damage could propagate to adjacent submodules.

Reactor-Coolant Leakage

The primary hazard associated with reactor-coolant leakage is the radiological exposure from the coolant-borne tritium and fission products that leak out with the coolant.

The TMHR blanket coolant system is different than that of the GCFR in that it uses large-diameter, distributed-metal piping to contain the high-pressure helium rather than a prestressed concrete reactor vessel (PCRVR). Thus, possible pipe-break accidents need to be considered in future studies.

It is expected that most blanket coolant leaks are slow and would arise primarily from failures of small piping. The flow rates can be reduced by orificing at the tap-off points in the main ducts, by going to smaller diameter piping, or by incorporating fast valving in the system to limit the leak after it occurs. Several methods will reduce the potential leak rates at any location to acceptable levels.

The most rapid depressurization accidents would be caused by main helium duct, heat exchanger vessel, or blanket assembly failures. In the light water reactor (LWR) industry, it has been demonstrated that pressure vessels can be designed and built such that the probability of catastrophic failure is so small that a failure does not need to be considered. In both the blanket assemblies and helium ducts, large ruptures must be considered, and efforts must be made to limit the consequences of such ruptures.

A massive failure of a blanket assembly or helium duct is probably unacceptable in the TMHE. Shock waves generated by a massive failure could potentially cause severe structural damage to all cooling systems and possibly put the fuel into a geometry that would prevent cooling. Assessments of these forces and their effects during a depressurization transient are extremely complex. Therefore, it is prudent to ensure that any failure will produce such moderate pressure transients that the shock waves and larger inertial forces will not be limiting. On the other hand it is equally important to choose a large enough limiting rupture size, such that overall design and economics of the plant are not jeopardized.

Methods of limiting the size of a rupture might include the use of rip stops, internal flow restrictions, wire winding, added structural supports, use of prestressed concrete reactor vessel technology, and doubly enclosing all potential failure locations. Since this question has been successfully addressed by existing LWR designs, it is not expected to pose insurmountable problems for the TMHR.

Secondary-Coolant System Leakage

Water or steam leakage from the secondary coolant system can occur within the helium loop, outside the helium loop but inside the containment building, or outside the containment building. Because of the positive pressure differential from steam to helium under all normal and accident conditions (except for the resuperheater), it is impossible for significant amounts of

fission products to leak from the reactor coolant system into the secondary system. Failure of a water or steam line outside the secondary containment is not considered to be a serious safety problem.

Steam in the reactor coolant system of a gas-cooled fast reactor with metal-clad fuel does not result in significant damage to the plant. No exothermic chemical reactions with reactor internals occurs. Any significant metal-water reaction requires temperatures much higher than that of the cladding. The circulators, steam generators, and auxiliary heat exchangers are designed to operate satisfactorily with the higher coolant densities associated with steam-leak accidents. With continuing steam or water addition to the blanket coolant system beyond what the helium purification system can remove, the system pressure increases. The moisture detection system detects the moisture in the leaking loop, and the plant protection system actuates reactor trip, isolates the loop, and dumps the steam-generator inventory into the atmosphere.

If there is no operator or protective action to control the leak, the blanket coolant system pressure continues to increase until the safety valves open and a steam-helium mixture is blown into the containment building. Possible leakage sources of water or steam into the reactor coolant system are the steam generators, the auxiliary heat exchangers and, if water bearings are used, the circulator bearing-water supply.

We estimate that the largest leak of secondary coolant into the blanket coolant system is caused by a rupture of a superheater leadout tube. This is considered to be a credible occurrence and, although a double-ended offset failure is unlikely, it is to be taken into account in the design of the plant. The first protective action is initiated by the plant protection system upon detection of moisture. At a certain moisture level, the plant is tripped, and the loop identified to have the leak shut down. The circulator turbine is tripped, which causes the helium valve to close, the leaking steam generator valves are closed, and the water inventory is released to the atmosphere. This procedure need not be rapid.

Fuel-Handling Accidents

The design of the fuel handling equipment and fuel storage system makes a serious fuel-handling accident an unlikely event.

Continuous and uninterrupted cooling of irradiated blanket modules during fuel-handling operations is essential. Fuel handling machines that handle an irradiated blanket module have two independent cooling systems operating while handling that module. (These systems can be in the form of direct air, helium, or water-cooling.) When the module is transferred from one machine to another, both independent cooling systems of the machine receiving the module will be in operation, providing cooling before the operation of the cooling systems of the machine delivering the module is terminated. At no time during the module handling cycle will cooling be impaired to the point that handling motions could not be terminated and the module remain safety-cooled.

Safety Conclusions and Recommendations

A preliminary assessment of the TMHR blanket and power conversion system indicates that an adequately safe design is technically feasible. However, an analysis must be performed if an optimized and readily licensable design is to be developed.

1. Fusion-related, accident-initiating events should be considered. Failures of fusion-related components that could cause blanket system failures should be investigated, and the impact of the probabilities associated with these events upon safety system reliability requirements should be assessed.

2. Depressurization accident design criteria should be developed, e.g., hole size, flow limiter design/feasibility, and induced forces on critical components.

3. The effects of fission products and plate-out in the helium purification and tritium recovery system due to clad defects should be estimated. Inservice inspection and maintenance could be significantly affected.

4. The potential for and consequences of accidents during fuel handling should be properly assessed so that appropriate design changes can minimize any radiological risks.

5. During any major accident, there is a possibility for the fusion-related equipment to interact with the blanket-related equipment synergistically to produce a more severe accident. This potential problem should be investigated.

6. Possible occurrence of flow maldistribution in the primary circuit following a failure or accident should be investigated. This could prevent adequate blanket cooling even after the plant shuts down. This problem is highly independent on the blanket design and should be evaluated in depth. If found necessary, flow maldistribution could be adequately limited by suitably modifying inlet and outlet ducts to each module or by ensuring that the degree of flow maldistribution generated due to a failure is limited to a small fraction of the blanket cooling flow.

7. The potential for and design requirements of using the vacuum chamber as an extension of the primary coolant boundary in the event of a module first-wall failure should be investigated. It is possible that this may reduce the safety requirements imposed upon the module design. The impact on the direct converter and beam stop must be determined.

8. The interaction of Li_2O with cladding material and with H_2O in the case of steam injection into the blanket module must be considered in more detail.

MOLTEN SALT-COOLED DESIGN

The TMHR molten salt case has three general areas: the fusion driver, the breeding blanket, and the salt processing/balance of plant. We present here the safety and environmental issues for the blanket region and the molten salt processing. The balance of plant issues unique to molten salt will be addressed, but those associated with the fusion system and energy conversion are beyond the scope of this subsection.

This analysis is very preliminary in nature. We intend to look at the safety and environmental issues to identify significant issues requiring further consideration during the detailed design phase should the molten salt system be chosen for further work.

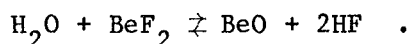
As described in Section 7, the molten salt concept is significantly different than the more conventional clad solid fuel blanket designs. This fundamental difference has both advantages and disadvantages from safety and environmental viewpoints. Fertile material and bred fuel are continuously recirculating through the blanket and then through chemical processing, allowing the system to be continuously cleaned. This cleaning removes the bred uranium-233 and its intermediate protactinium-233, and maintains their concentrations low. Therefore, the fissioning of uranium-233 can be reduced to

the point that it no longer is a significant contribution to the fission product burden, when compared to thorium-232, fast-neutron fissioning.

The disadvantage of this technique is the elimination of the cladding to contain the fuel and fission products. The integrity of the primary piping system must be the "first line of defense" with respect to a leak of significantly radioactive material, as compared to a clad fuel situation where the cladding is usually this "first line of defense."

COMPATIBILITY OF MOLTEN SALT WITH STEAM AND AIR

Molten fluoride-based salts are fairly inert due to their strong chemical bonding. M. W. Rosenthal et al.,⁷ make the following comment concerning safety: "...and the salts do not react rapidly with water or air." W. R. Grimes and S. Canton⁸ discuss the safety issues of using Li_2BeF_4 in controlled fusion reactors and mention a reaction between steam and beryllium fluoride:



They also state that "the reaction of steam with Li_2BeF_4 yields HF and BeO, though the reaction is not particularly exothermic," and conclude that the reactions of molten salt with steam or moist air would cause additional corrosion problems, but that it would not be a significant accident hazard.

TRITIUM HANDLING AND SAFETY ISSUES

To sustain the deuterium-tritium fusion reaction, tritium must be bred in the blanket. In the molten salt blanket case, this means a tritium generation rate of 1.86×10^{-3} g-mole/s or 160 g-mole/d. Not only is this a significant radiation/biological hazard due to tritium's decay to helium, but it is a sizeable chemical explosion source if the tritium is handled as T_2 . The biological hazards of tritium as related to a TMHR have been studied by W. E. Kastenberg et al.⁹

STRUCTURE RADIOACTIVITY DUE TO NEUTRON ACTIVATION

The neutron activation of structural material of the molten salt first-wall and blanket is a significant environmental consideration with respect to

disposal of worn out hardware. This problem was addressed in a DOE Technical Assessment.¹⁰ TZM was indicated as a problem material, having significant activity after 10^6 yr of decay. This long term activation requires appropriate special disposal techniques to ensure that these activated components stay isolated from the environment.

The need for cooling of the blanket after a reactor shutdown and molten salt dump has not been evaluated. In the shutdown and drained mode, the blanket does not contain a significant quantity of fuel or fission products, thus the main afterheat source is the radioactivity of the TZM structure. During the first week after shutdown, TZM has about twice as much as 316 stainless steel. In the molten salt design the helium-cooled first-wall provides a heat sink for the blanket by radiation heat transfer. As follow-on work, an evaluation of the heat removal ability of the first-wall will be needed, and an alternate blanket after-cooling system must be designed if the first-wall proves to be an inadequate heat sink.

ABNORMAL OPERATIONAL SITUATIONS

Reactor and/or turbine trip shutdowns of the molten salt system have not been evaluated. The operating philosophy of draining the molten salt into dump tanks should simplify the handling of problems because the cooling of the molten salt is handled separately from the blanket. This operating philosophy does have the safety/maintenance problem of a salt freeze-up (the freezing temperature is 500°C). If the salt does not drain properly, it forms frozen salt zones in the blanket, which is very difficult to thaw during startup. If startup is attempted with a frozen zone, the nuclear heating may cause local structural overheating due to the poorer cooling capability of frozen molten salt. Further work is needed to evaluate this problem and to design appropriate hardware and instrumentation, as well as develop a reasonable startup technique that guards against frozen salt flow blockages.

Due to the high temperature strength properties of TZM and the high heat capacity of the molten salt, the molten salt system should be capable of withstanding reasonably large fusion driver power fluctuations. However, if these fluctuations cause significant thermal gradients in the blanket, they will probably cause thermal stress cracking because TZM is relatively brittle, especially at welds.

An additional operating problem is associated with a cladding failure of the beryllium pins. If beryllium metal comes in contact with the molten salt, it can cause uranium and thorium metal to plate-out due to the strong reducing nature of beryllium. This situation occurs whenever the oxidation capability of the salt is insufficient to balance the added beryllium. Further evaluation of this beryllium-salt interaction is needed to quantify the problem.

CHEMICAL PROCESSING SAFETY AND ENVIRONMENTAL CONSIDERATIONS

When compared to a conventional clad fuel-type breeding system, the molten salt process generates much less nuclear waste material because the fissioning is greatly suppressed, and there is no activated fuel-cladding material that must be disposed of. The tradeoff is that the chemical processing systems is an integral part of the molten salt system and must be operational, to some minimum degree, for the reactor to operate. Specifically, the molten salt off-gas handling hardware must process the tritium and fission product gases whenever the reactor is operating, although the uranium and non-gaseous fission product removal systems can be offline for short periods. The chemical processing system must also adjust the redox (reduction/oxidation) potential of the salt. An appropriate chemistry balancing technique has not been clearly identified. Failure to keep the salt in chemical redox balance can lead to either excessive corrosion or thorium and/or uranium reduction and plate-out in the system. The excessive corrosion situation can lead to piping failures and subsequent molten salt spillage, while the thorium and/or uranium plate-out can lead to localized high fissioning rates (hot spots) in the blanket. The redox control problem needs further evaluation.

The chemical processing system must handle several toxic and hazardous makeup and reagent chemicals (i.e., beryllium, thorium, and fluorine). The safety and environmental issues may be very significant and should be evaluated as part of any further work, especially for handling beryllium.

DESIGN BASIS ACCIDENT

An analysis of the molten salt case to determine the appropriate design basis accident has not been performed. Based on a superficial evaluation, an accident leading to a major spillage of molten salt into the containment is

suggested. To handle this situation, the balance of plant equipment and containment must be sized and designed to collect the spilled salt in a catch basin and also process the containment atmosphere to remove the airborne contamination.

CONCLUSIONS AND RECOMMENDATIONS

Due to the preliminary nature of the molten salt case study, no hard conclusions can be drawn. Several areas have been identified for further evaluation and study. In general, the design appears to be less demanding from a decay heat removal point of view than a conventional-clad, fuel-type design. The tradeoff is the absence of the fuel cladding as the "first line of defense" for contamination control. Even though the total contamination activity may be much less than a conventional system, the fact that it is in the liquid phase puts a significantly greater burden on the primary piping integrity and contamination control systems.

Based on this preliminary analysis, the following areas as a minimum will require additional study and design:

- Various accident sequences should be considered and one or more selected as a basis for design of the safety hardware systems. Due to the significant stored energy in some of the fusion driver components (i.e., superconducting magnets, fusion plasma, neutral beam injectors, etc.), they should be included as possible accident initiations and/or contributors.

- The tritium handling and environmental concerns are probably significant. Even though this problem is common to all deuterium-tritium fusion machines, the unique design of the molten salt blanket warrants a careful design and evaluation for this approach.

- The control of the molten salt redox potential can have a significant impact on plant safety. Further work is needed to identify an appropriate control technique and then evaluate its capabilities during abnormal and accident situations. Specific consideration should be given to a failed beryllium pin to determine if this situation will propagate to more pin failures, flow blockages, or unacceptable buildup of thorium and uranium metal in the blanket.

- The handling and safety issues of the toxic and hazardous chemicals need further evaluation. The use of large quantities of beryllium pose a significant safety and environmental hazard.

REFERENCES

1. D. J. Bender, Editor, "Reference Design for the Standard Mirror Hybrid Reactor; A Joint Report by Lawrence Livermore Laboratory and General Atomic Company," Lawrence Livermore Laboratory, Rept. UCRL-52478 (1978).
2. W. E. Kastenberg et al., "Some Safety Studies for Conceptual Fusion-Fission Hybrid Reactors," EPRI ER-548 (1978).
3. K. R. Schultz et al., "Conceptual Design of the Blanket and Power Conversion System for a Mirror Hybrid Reactor," General Atomic Company Rept. GA-A-14021 (1976).
4. Proceedings of the US-USSR Symposium on Fusion-Fission Reactors, 13-16 July 1976, CONF-760733.
5. D. Okrent and W. E. Kastenberg, "Fusion Reactor Safety," paper N1.2/5 in the Transactions of the 5th International Conference on Structural Mechanics in Reactor Technology, Berlin, Germany, 13-17 August 1979.
6. W. E. Kastenberg et al., "On the Safety of Conceptual Fusion-Fission Hybrid Reactors," Nuclear Engineering and Design, 51 (1979) 311-359.
7. M. W. Rosenthal et al., "Molten-Salt Reactors--History, Status, and Potential," Nuclear Applications and Technology, 8 2 (1970).
8. D. M. Gruen, Editor, The Chemistry of Fusion Technology, Plenum Press-London, 1972, pp. 161-190, Chapter by W. R. Grimes and S. Cantor, "Molten Salt as Blanket Fluids in Controlled Fusion Reactors."
9. W. E. Kastenberg et al., "On the Safety of Conceptual Fusion-Fission Hybrid Reactors," Nuclear Engineering and Design 51 (1979) 311-359.
10. DOE/ET-0007, "Alloys for the Fusion Reactor Environment--A Technical Assessment," January 1978.

SECTION 10
COMPARATIVE EVALUATION

INTRODUCTION

During the course of this study, four blanket coolant technologies were considered: water, liquid metal, He, and molten salt. For reasons discussed elsewhere the water and liquid metal options were dropped. Considerable further work was then done on He and molten salt. This work is discussed in Sections 6 and 7. The purpose of this section is to compare the two technologies. Conclusions and recommendations are given in Section 11.

Our intentions were to select one of these two technologies as the basis for a reference design that was to be carried out in the second year of the study. Three criteria were to be used as the basis for the decision:

- Performance of the commercial reactor.
 - Minimum \$/g of fissile fuel.
 - Technological risk (unscheduled down time).

- Development program to commercialize the reactor.
 - Time, cost, and risk of developing the requisite technology are to be considered.

- Intangibles.
 - Safety - After heat leading to fuel melt and dispersal of radioisotope.
 - Support ratio - Affects growth rates and has to do with minimizing the number of guarded sites.
 - Proliferation of nuclear weapons technology and materials.
 - Waste generation.

These criteria were elaborated on as follows:

- Performance of commercial reactor.
 - Total system capital cost
(fusion + fission + reprocessing).

- Total system operating cost
- (fusion + fission + reprocessing).
- Total system power produced
(fusion + fission + reprocessing).
- Fissile fuel production rate in fusion reactor
- Minimum \$/gm of fissile fuel.
- Must breed its own tritium.
- Must break even on electricity.

- Technological risks--Evaluated by judgment.

- Uncertainty of designs
 - Mechanical
 - Thermal-hydraulics
 - Neutronics.
- Uncertainty of materials
 - Availability
 - Compatibility.
- Uncertainty of licensing.

- Economic risk--Confidence level in evaluating costs of principle materials (e.g., Be in molten salt) and the market value of the product (e.g., ^{233}U).

- Development program, time, cost, and risk of developing the requisite technology.

- Intangibles--With quantifiable data where possible.

- Safety--Estimation of adiabatic melt time at the end-of-life conditions, activation and fission product inventory (Ci), consideration of mobile fuel safety concerns.
- Support ratio--Can be calculated for LWR, HTGR, and high gain HTGR. Could consider support ratio as function of burner reactor growth rate.
- Proliferation--Can comment on ppm of ^{232}U bred ^{233}U . The ^{232}U would make the fuel naturally spiked but more difficult to handle. The fuel could also be denatured but this reduces performance.

- Waste--Can calculate kg/yr of fission products and reactor structure that are discharged.

HELIUM CASE

Summary of Design Choice

Of the three possible fuel forms (rods with radial or axial flow and plates) shown in Table 10-1, the plate form is recommended because the blanket is thinner and the neutronics performance is better (~7% better than axial rods design and 4% better than radial rods design). The neutronics results are summarized in Tables 10-2 through 10-5.

The case for helium is summarized in Table 10-6. The design approach used by General Atomic in this design was based on a large module (~600 t), where the first-wall is the vacuum boundary and is broken when the module is changed. Some of the features are summarized in Table 10-7. An alternate design approach adopted by General Electric used a separate first wall. The blanket was changed out in much smaller units (<100 t) without breaking the vacuum system, changing the first wall or removing other major structures.

The virtues of these two design philosophies are discussed in Sections 6 and 7 and will not be discussed further here; nor will we make a recommendation on which to adopt for the future.

The He-cooled, Th metal, fast-fission blanket was found to perform well and have modest development requirements and moderately good intangible features, such as risk of release of fission products in loss-of-coolant flow situations.

MOLTEN SALT CASE

The design ended up with somewhat less fissile production than found in the preliminary assessment, principally because of the lower Th metal density of the salt composition based on the MSBR rather than a less well known 50°C higher melting point salt, but which had double the Th density. The other change was the use of somewhat more structural material due partly to the separate first wall. Even so, the fissile production rate is huge--8044 kg/yr

of ^{233}U . Some of the parameters of the molten salt case are shown in Table 10-8. Some advantages and disadvantages of this concept are given in Tables 10-9 through 10-13. Some comparisons between molten salt and He are given in Tables 10-14 and 10-15. Some problems seen for the molten salt are given in Table 10-16.

FISSION-SUPPRESSED BLANKET

In examining the molten salt case we found many problems but were impressed by its outstanding fissile fuel production and safety features, due to suppression of fissioning. There are a number of possibilities for suppressing fissioning, most of which have not been examined to know if they are feasible and perform well. Some of these possibilities are given in Table 10-17, which also shows both a fission-suppressed and a fast-fission configuration. In the fast fission blanket concept the fission rate changes with time due to bred-in fissile material leading to an undesirable power swing in time. Removing the bred-fissile-fuel by on line processing or by suppressing fission reduces this power swing is shown in Fig. 10-1. The fuel produced in the fission suppressed concept has a high purity of ^{233}U compared to the fast-fission case shown in Table 10-18. Table 10-19 gives some advantages and disadvantages for the fission suppressed blanket relative to the fast-fission blanket.

CONCLUSION

The performance of the molten salt concept was somewhat inferior to the He-cooled concept. The molten salt case resulted in 80 \$/g of $^{233}\text{U}^*$ and an add-on capital cost of the supported reactors of 28% to account for the cost of the hybrid, whereas the He-cooled case was 70 \$/g and 23%, respectively.

The development required for the molten salt concept was judged to be considerably more extensive in time and cost than for helium cooling.

*The improved molten salt case resulted in 60 \$/g and 20% capital cost add-on.

The safety advantage resulting from fission suppression was important. The high support ratio was judged important because of the heavy reliance on the known technology of fission reactors and less reliance on a relatively few, highly guarded sites where the hybrid and its support facilities would be located.

The molten salt concept was judged to have higher risk of not performing as well as estimated and of a higher risk of not being able to solve problems, such as fabricating the molten-salt containing wall out of Mo-based alloys.

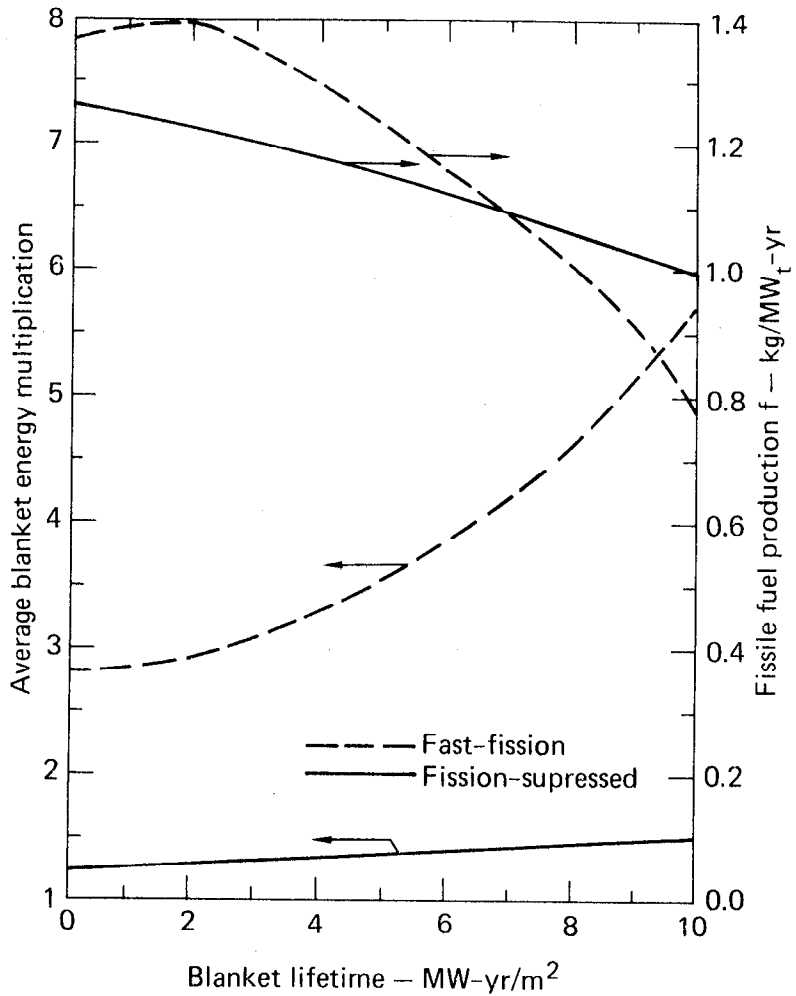


Fig. 10-1. Blanket energy multiplication and fissile-fuel production are plotted vs neutron exposure. The energy multiplication for the fission-suppressed case is much less sensitive to exposure than the fast-fission case.

Table 10-1. Fuel Configuration Thermal-Hydraulic Characteristics for He Case

	Plate	Axial rod, cross-flow	Radial rod, radial flow
Characteristic dimension	Plate thickness: 1.15-1.58 cm	Outer diam: 1.19 cm	1.67 cm
	Coolant channel: 1 mm	Pitch/diam: 1.18	1.05
$\Delta T = T_{out} - T_{in}, \text{ }^\circ\text{O}$	230	230	230
$\Delta P, \text{ kPa}$	20.7	20.7	7.2
$\bar{h}, \text{ W/m}^2 \text{ K}$	2434	2174 (minimum 1087)	1122
$T_{max,CLAD}, \text{ }^\circ\text{O}$	666	663	662
$T_{max,cl}, \text{ }^\circ\text{O}$	939	775	765
Reynolds number	6562	18212	4170
Void fraction, %	7.3	35	17.8
Clad/solid, %	3.6	8.2	5.9

Table 10-2. Helium-cooled blanket neutronics performance at beginning and end of Life (9.6 MW-yr/m² exposure).

	BOL	EOL	Av
⁶ Li (n,α)	0.8925	1.2208	
⁷ Li (n,n'α)	0.0852	0.0872	
Tritium breeding ratio	0.9777	1.3080	1.13
²³³ U production	0.9644	1.2055	
U (n,f)	--	0.3869	
Th (n,f)	0.1184	0.1351	
Net ²³³ U production	0.9644	0.7883	0.88
Blanket energy multiplication	2.8	8.5	5.5
First-wall heating, w/cc	13.4	14.3	
Peak nuclear heating in the thorium zone, w/cc	42	120	
²³³ U enrichment, %	0	3.35	
²³³ U, MT/m	0	5.74 × 10 ⁻¹	

Table 10-3. Shield Parameters.

Shield design:

Thickness	0.7 m
Material	SS-316, B ₄ C
Cost	\$ 10 x 10 ⁶

Possible alternative:

Thickness	~1.4 m
Material	Concrete - Borated Water
Cost	\$ 1.6 x 10 ⁶

Table 10-4. Helium blanket design characteristics.

Parameter	Characteristic
Average power production, MW(th)	~4400
^{233}U production, metric tons/yr	4
Reactor direct capital cost	$\$227 \times 10^6$
Annual fuel replacement and handling cost	$\$81 \times 10^6/\text{yr}$
Materials selected:	
Fertile material	Th-Metal
First-wall	Inconel-718
Fuel cladding and structure	Inconel-718 or HT-9
Tritium breeding (purged flow)	Li_2O
<u>Mechanical design</u>	
Reactor length, m	56
First-wall radius, m	2
Blanket thickness, m	1.72
Number of separable modules	16
Annual changeout time (for two modules), days	24.1
<u>Neutronics design</u>	
Average T/n	1.13
Average M	5.5
Average $^{233}\text{U}/\text{n}$	0.88
^{233}U enrichment at EOL, %	3.4
Wall loading, MW/m^2	1.5
Peak Q, W/cc	120
Blanket lifetime, $\text{MW}\text{-yr}/\text{m}^2$	9.6
<u>Thermal-hydraulics</u>	
Configuraton	Plates
Average plate thickness, cm	1.4
Helium pressure, MPa (atm)	5.6 (55)
Temp. in, $^{\circ}\text{C}$	285
Temp. out, $^{\circ}\text{C}$	515
Thermal cycle efficiency, %	~38
<u>Blanket lifetime, $\text{MW}\text{-yr}/\text{m}^2$</u>	9.6 (8 years, 6.4 operating years)

Table 10-5. Neutronics design, damage level, and material selection.

Neutronics design:

Q_p changes from 1 \rightarrow 2.5; implies flexibility in selection of blanket configuration and materials.

M changes from 2.8 (BOL) to 8.5 (EOL); implies adiabatic afterheat melt-down time \sim 11 min.

Low consequence blanket becomes attractive.

Damage level:

Blanket life: 9.6 MW-yr/m² at \sim 2% burn-up for thorium (swelling).

Optimize lifetime of different radial zones.

Mechanical design improvement.

Material selection:

Fertile material--Th-metal.

First-Wall--Inconel-718.

Fuel cladding and structural material--HT-9 or Inconel-718

Tritium Breeding Material--Li₂O.

Table 10-6. Conclusion and recommendations for a helium-cooled TMHR blanket.

Fertile Material, Th-metal, 4 metric tons yr ^{233}U .

Average thermal power, 4400 MWTh.

A blanket with close coupling between neutronics, thermal-hydraulics, and mechanical designs.

Gas-cooled fission reactor technology.

Thorium fuel cycle.

Takes advantage of TMR cylindrical geometry.

Rapid module changeout.

Technically feasible.

Table 10-7. Mechanical design.

Advantages:

Compact design.

Single module replacement, 18.5 days.

Takes advantage of cylindrical geometry of TMR.

Disadvantages and development program:

High replacement and handling cost, $\$56.4 \times 10^6/\text{yr}$.

Could be improved by selected blanket zone replacement.

Need to develop:

Movement of 600-700 metric tons module.

Fast connect and disconnect devices.

Omega joints.

Table 10-8. TMHR molten salt coolant plant description.

Parameter	Characteristic	
Fusion power, MW_t	2904	} 4000
Induced blanket power, MW_t ^a	1096	
Fission power, MW_t	254	
Blanket length, m	88	
First-wall radius, m	2102	
Blanket power, MW_t		
First-wall	169	
Breeding zone	3247	
Shield	3.5	
Total	3419	
Fuel production	<u>B.R.</u>	<u>Kg/yr</u>
Tritium	1.08	176
^{233}U	0.68	8044

^aBlanket thermal power minus incident fusion neutron power.

Table 10-9. TMHR molten salt design material considerations.

Advantages:

- Nonpyrophoric fuel form.
- No fuel swelling.
- No structural material swelling.

Disadvantages:

- Molten salt very corrosive.
 - TZM difficult to fabricate and weld.
 - TZM a more exotic material than most other considered; more extensive development required.
 - TZM blanket may require annealing prior to any handling operation due to ductile-to-brittle transition during cooldown.
 - Be availability may be limited.
 - Potential corrosion of Be by molten salt.
 - Graphite material uncertainties (swelling properties, cladding integrity).
 - High operating temperatures (to prevent freezing) and limiting temperatures for materials force a narrow operating range.
 - Long half-life of activated TZM.
-

Table 10-10. TMHR molten salt coolant neutronics considerations.

Advantages:

High support and capacity expansion ratios.

Low fission rate:

- Results in He rather than FP.
- Low decay heat.
- Low fission product production.
- Low FP radiation levels.
- Low ^{232}U breeding.

No plutonium production.

Minimum blanket structure volume fraction.

Continuous online removal of some fission products.

Good design potential for minimizing radiation streaming.

Disadvantages:

Fission suppression requires much larger and more efficient fusion driver.

To accomplish neutronic performance objectives, blanket requires large quantities of Be for neutron multiplication.

High activation of structure and molten salt coolant.

Sensitive to mechanical design changes.

Table 10-11. TMHR molten salt coolant mechanical design considerations.

Advantages:

- Low pressure blanket coolant (thinner boundaries, milder leakage blowdown).
- Small coolant conduits (pipes, headers, and manifolds).
- No refueling equipment in reactor compartment.
- No central region penetrations or joints for refueling.
- Blanket maintenance does not require breaking plasma vacuum chamber.
- Design allows possibility of long-lived first-wall (perhaps for the life of the plant).

Disadvantages:

- MHD effects restrict design and configuration options.
 - Environment and molten salt composition restrict material selection.
 - High temperatures and large ΔT s (stress and displacement problems due to high modulus of elasticity of Mo).
 - For performance, first-wall must have separate and different coolant.
 - Additional constraints placed on first-wall design due to need for periodic annealing.
 - Design must accommodate blanket heatup, salt fill, drain refill, and flow with attendant problems (cooldown, preheat, availability, trace heating required).
 - Need for periodic replacement of blanket modules negates some of the anticipated advantageous operational benefits of online refueling (i.e., outages, downtimes, availability, etc.).
 - Design must accommodate incompatible materials.
 - Mechanical joints and valves not developed.
 - Exotic and costly materials.
 - Complex processing if fission products are removed.
-

Table 10-12. TMHR molten salt coolant thermal hydraulic considerations.

Advantages:

- High fuel production per unit power.
- Mild power and flow transient effects due to:
 - Low power density.
 - Coolant high mass density.
- No blanket power swing to impact BOP or fusion driver design.

Disadvantages:

- Increased corrosion due to MHD effects.
 - Difficulties assuring adequate flow mixing to limit structural temperatures.
 - Flow is in laminar/transition regime.
 - Significant differential growth and distortion in structure and bundle due to radial power and flux gradients (TZM very unforgiving).
 - Lack of metal and graphite wetting produces:
 - Difficulties in drainage.
 - Impossibility of utilizing small flow passages.
 - Possible hot spots in reentrant areas.
 - Graphite clad Be exhibits role reversal of cladding in usual load carrying role.
 - Adverse consequences place high reliability requirements on Be cladding:
 - Thermal effects of one large failure.
 - Chemical effects of multiple small failures (exposed Be will locally upset the Redox balance causing Th and U to plate out locally and Be to go into solution).
-

Table 10-13. TMHR molten salt coolant chemical processing and BOP considerations.

Advantages:

- Continuous operation allows ^{233}Pa and ^{233}U removal--suppresses ^{233}U fissioning and ^{232}U formation (high activity) in product.
- Eliminates need for fuel cladding and its disposal as contaminated material.
- Eliminates need to load/unload fuel elements and transport to reprocessing.
- The ^{233}U product form (UF_6) is presently the standard uranium starting material. (Tritium is not trapped in a solid lithium form.)
- After shutdown, cooling system requirements minimized.
- High heat carrying capability reduces equipment sizes (i.e., pumps, pipes, etc.) and pumping power.

Disadvantages:

- Total plant costs high due to high operating temperatures (high equipment costs, exotic materials, high piping costs).
 - Heat transport system for molten salt significantly more expensive than He.
 - High freezing temperature of molten salt and the heatup cycle needed to start up the plant.
 - Must routinely handle large quantities of hazardous materials (Be , F_2).
 - Requires intermediate heat transport loops (IHX).
 - Temperature domain of IHX's greatly exceeds current technology limitations (500°C for LMFBR's).
 - More BOP equipment requires remote operation and maintenance.
 - Requires elaborate contamination control system.
 - Many hardware components not developed; especially valves (that have galling problems).
 - Molten salt requires close Redox control to suppress corrosion and not precipitate uranium and thorium.
-

Table 10-14. Comparisons of helium vs molten salt.

Helium ^a	Molten salt
<u>Materials:</u>	
Good compatibility	Severe concerns: - Corrosion - Radiation damage
<u>Power conversion system:</u>	
Technology developed	Development required: - Steam generator - Pumps - Trace heat system
<u>Fuel cycle:</u>	
Development expected	Development required Separate reprocessing facilities not needed
<u>Tritium control:</u>	
Can be separate from heat transport	In heat transport loop Extraction concerns
<u>Maintenance:</u>	
Transparent gas Nonradioactive	Trace heating needed Opaque, radioactive, drainable
<u>Design:</u>	
High pressure High temperature Heat transfer to helium Large pipe size	Low pressure Higher temperature Heat deposited in salt More compact piping but temperature and materials place severe restrictions
<u>Safety:</u>	
No fuel motion during operation	Radioactive coolant Process loop at high temperature on-site

^aThe helium-cooled blanket concept appears to have strong areas of superiority in lower technical risk and less development.

Table 10-15. Perceived advantages of the Be molten salt blanket.

High support ratio (ratio of supported fission burner power to fusion hybrid power).

Continuous removal and sale of ^{233}U .

Low after heat.

Low fission product burden.

Long life.

Low radioactive waste generation.

High ratio of fissile material energy production.

Table 10-16. Problems with molten salt.

Beryllium availability.

Safety issue of handling such large quantities of Be.

Narrow window of operating temperatures and trace heating requirements.

Development of Be, molten salt, etc., industries.

Lower blanket energy multiplication requires higher Q.

Higher power drivers require larger prototypes.

Extensive materials development programs required (welding of TZM, cladding with graphite, etc.).

Long-lived activation of TZM (^{93}Mo (3000 yr) half life, ^{93}Zr million year halflife).

No other champion for molten salt--hybrid program would have to justify it on its own.

While other development programs are working on Th and He and a hybrid using them would benefit, not only isn't this true for molten salt but it's a dying technology.

With so many problems to be attacked simultaneously, the molten salt design approach appears to be revolutionary, rather than an evolutionary approach normally preferred by prudent planners.

Table 10-17. Other fission-suppressed blanket options.

Li₇Pb₂/Thorium - Helium

LiPb₄ - Thorium eutectic 400°C melt - helium

- water

Li₇Pb₂/Aqueous solution

Li₇Pb₂/Graphite/ThO₂ - helium

Pb/graphite/ThO₂ - helium

Be/graphite/ThO₂/Li₂O - helium

Li (depleted)/Th

.

.

.

etc.

²³³U/n ≈ 0.3 to 0.7

@ T/n = 1.1

M ≈ 1.2

Fission-suppressed blanket:

Plasma | ← Li₇Pb₂ → | ← Th-Metal → | ← Shield → |

Fast-fission blanket:

| ← Th-Metal → | ← Li₂O → | ← Shield → |

Table 10-18. Bred fuel isotopics (ppm).

Isotope	Fast-fission	Fusion-suppressed
^{231}Pa	1770.0	104.0
^{233}Pa	45.7	41.1
^{232}U	41.2	2.7
^{233}U	5560.0	5004.0
^{234}U	50.5	2.9
Total U	5660.0	5010.0
^{230}Th	590.0	35.0

(~400 days irradiation)

Table 10-19. Fission-suppressed blanket (relative to fast-fission blanket).

Advantages:

1. Produces better quality fuel.
2. Lower M (~ 1.2), lower \dot{q}''' .
3. Constant M and \dot{q}''' during blanket life.
4. Higher support ratio.
5. Lower fission and actinide concentration.
6. Ease of T/H design.
7. Longer life fertile zone.
8. Utilize pure fusion technology, implies cleaner, safer system.
9. Lower ^{230}Th content, implies easier handling of fuel during reprocessing.

Disadvantages:

1. Lower M
 - 2.2 Lower U/n (0.4-0.8)
-

SECTION 11
CONCLUSIONS AND RECOMMENDATIONS

This section presents the conclusions resulting from the year-long study and offers recommendations for future work.

SYSTEM PERFORMANCE

The tandem mirror, as expected, makes a good hybrid. The geometry and steady-state operation help simplify the complex engineering of a breeding blanket. The moderately high Q (about 2) results in low cost fissile fuel (40-80 \$/g ²³³U) and allows use of light water reactors with only a 14-24% increase in electricity cost to pay for the hybrid fuel factory. Table 11-1 shows the key parameters for two blanket options. The high support ratio (number of fission reactors of the same nuclear power rating) of 9-25 maximizes the number of dispersed sited conventional nuclear power plants while minimizing the number of fuel production centers. High support ratio and safety are outstanding features of these designs.

BLANKET COOLANT TECHNOLOGY

WATER COOLING

We do not favor water cooling because moderation of the fast neutrons reduces fuel breeding. This reduction is significantly greater for ²³³U production than for Pu production. Another problem with water cooling is the difficulty of tritium decontamination.

LIQUID METAL COOLING

We eliminated liquid metal cooling because of the increased hazard relative to helium and because of MHD-related design problems, such as loss of blanket wall coverage due to inlet and outlet manifolds. If sodium is the primary coolant, a great deal of technology from the liquid-metal, fast-breeder program could be used directly. Feasible design solutions exist for liquid metal cooling, and further work is appropriate if other coolants having greater

Table 11-1. Parameters for the Th/He and Be/molten salt blankets.

Parameter (4000-MW nuclear plant)	LWR burner		
	$\left(\frac{300 \text{ kg rate}}{1000 \text{ MW}_e \text{ yr}} \right)$		
	Th/He	Be/molten salt (base)	Be/molten salt (improved)
U-233			
Production rate, kg/yr	3310	8023	9554
P_{fusion} , MW	915	2976	2733
P_{net} , MW	892	270	362
Q	2.0	2.2	2.2
Γ , MW m ⁻²	1.5	2.0	2.0
Support ratio	8.5	20.7	24.6
System cost ratio	1.23	1.28	1.20
Mills/kWh _e	20.5	21.1	19.8
\$/g	70.6	81.7	58.9

safety prove to have undesirable technical or economic problems. Further, the use of lithium as a coolant allows tritium breeding in the coolant. The technology of tritium extraction from liquid lithium is reasonably well developed, while there may be major technical problems in extraction from other materials.

MOLTEN SALT

Molten salt coolant results inherently in a blanket having the following characteristics:

1. Fission is suppressed by an order of magnitude over fast fission blankets resulting in less hazard from fission products. Consequences of loss-of-coolant accidents should be virtually eliminated, since little afterheat exists.

2. The large number of fission reactors (>20) supported by one fuel producer leads to desirable deployment scenarios and favorable economics compared to fast fission blankets.

3. Online processing allows removal of certain fission products and bred-fissile fuel.

We see great virtue in fission-suppressed blanket concepts; however, the molten salt design has problems in materials, chemistry, and development requirements. We judged that problems posed by molten salt technology applied to the hybrid outweigh the advantages resulting in high support ratios and fission suppression. Because of radiation damage, the Hastelloy alloy developed in the molten salt fission reactor program was unacceptable as a structural material in the reactor high flux region. A potential substitute is molybdenum-based alloys (TZM). We judged the forming, welding, and brazing of molybdenum to be a large development program with high risks of not being successful.

The large amount of beryllium used in the design raised questions of availability, cost, and safety. Since there is no molten salt development program now and not likely to be one in the future, this hybrid application would have to carry the burden of the entire development rather than use technology being developed for fission reactors. If a solution to fabrication of molybdenum for use up to 700°C for the salt-containing structure were found, and ways of reducing the amount of beryllium required by a factor of several, then the molten salt concept would be much more attractive, but would still require an extensive high risk development program.

HELIUM COOLING

We judged the helium-cooled, thorium-metal blanket concept to be better than the molten salt concept. The performance, although good, was under that of molten salt in that fissile fuel cost more. The larger blanket energy multiplication resulted in a lower support ratio (9 vs 25), but this same effect meant the fusion power was down by a factor of 2 for the same hybrid nuclear power rating. The helium-cooled design can take advantage of the rather large world-wide development work in He technology. The fission rate is such that, with no cooling, fuel damage would occur in about 11 min after shutdown, requiring a reliable emergency cooling system. The power density is such, however, than ^{238}U fast-fission blankets would have fuel damage under similar conditions in about 1 min.

FISSION-SUPPRESSED BLANKET CONCEPT

At the beginning of this study, we aimed to select a coolant technology from among several obvious possibilities to base a reference design. We used the case method and have methodically chosen the helium-cooled, fast-fission, thorium-metal blanket. However, the virtue of fission suppression with its passive cooling safety and high support ratio has so impressed us that we strongly recommend further work to find a combination of materials and coolants that will approach the performance of the molten salt concept with less demanding technology.

We recommend a thorough examination of non-fissioning neutron multipliers using combinations of Be, Pb, ^7Li , and mobile fertile (Th) materials such as molten salt, aqueous solutions, slurries, or balls. The emphasis should be acceptable performance, hazard reduction, and minimum extension of technology.

BLANKET DESIGN PHILOSOPHY

Two distinct, mechanical design philosophies appear in this study and are compared in the He-cooled concepts. A selection is scheduled for the second year. One philosophy is called large module and the other small module.

The small module philosophy minimizes the size of the blanket module to be handled, with a target of less than 100 t. The first-wall is separate from

the blanket and operates at an intermediate temperature to achieve lifetimes of 20 years or even perhaps the life of the reactor itself. This first-wall, and therefore the vacuum envelope, is not broken when the blanket modules are replaced. The reactor vault is then not exposed to tritium except from the blanket. This design philosophy results in lower breeding because one extra wall separates the neutron-producing region from the breeding region. However, blanket handling is considered more conventional, is faster, and experience from the fission reactor program is more applicable. Changeout or repair for the first-wall, although done infrequently, is difficult and may take longer than the normal refueling interval. This design philosophy is employed in the water and molten salt blankets and could be extended to the He case as indicated in Section C.

The large module philosophy has one wall separating the plasma vacuum region from the high pressure coolant region. When changing out the module, a large slice (several hundred t) of the cylindrical reactor (including magnet, first-wall, shield and blanket) is removed from the central cell. Special heavy moving equipment with built-in automatic tools is necessary in this concept. The virtue of this approach is minimum structure to degrade breeding and accessible first-wall. The entire unit can be checked out for leaks before installation. The drawbacks are large size, somewhat larger changeout time, and higher risk of problems developing requiring longer shutdown time for changeout machine repair.

A choice between these two philosophies has not been made. More detailed comparisons between the two are needed in the pursuit of the helium-cooled design to facilitate the judgment.

TANDEM MIRROR OPERATING MODES

We considered four physics-operating modes of the tandem for the hybrid. They are:

<u>Q range</u> *	<u>Mode name</u>	<u>Description</u>
Up to 1.1	Two-component	At the end of the solenoid, deuterium atom beams in the 200- to 400-keV range are injected into a relatively cold tritium background plasma.
Up to 1.8	Kelley	Both deuterium and tritium atoms at 200 keV are injected into the solenoid into a hot ($T \approx 100$ keV) deuterium and tritium plasma.
Up to 3	Thermal	The deuterium and tritium plasma in the solenoid are heated by electrons, which are in turn heated by microwave power near the electron cyclotron resonance frequency (ECRF).
Up to about 15	Thermal barrier	This mode is like the thermal mode, except the electrostatic potential is made to drop between the end plug and the solenoid in order to thermally isolate the electrons in the plug ($T_{e\text{ plug}} \sim 200$ keV) from those in the solenoid ($T_{e\text{ solenoid}} \sim 30$ keV).

During this first year's study, we recommended the thermal mode; but during the course of the study, the thermal barrier mode was invented. We now recommend it be selected as the operating mode for the hybrid. The rationale deserves explanation. A simplistic but basically accurate viewpoint is that the higher Q modes employ increasingly uncertain physics. They represent further departures from thermodynamic equilibrium, and therefore are threatened with more plasma instability. They will be proven later in time. Data are now

*The wall loading is 1 MW m^{-2} . For lower wall loading, Q goes up from these values quoted and vice versa, except for the two-component mode, which is independent of wall loading up to 5 MW m^{-2} .

being accumulated in the Tandem Mirror Experiment (TMX) at Lawrence Livermore National Laboratory on the first three modes, but we must wait for construction of the upgraded tandem mirror experiment in 1982 and the tandem version of the Mirror Fusion Test Facility (MFTF-B) in 1984 for testing of the thermal barrier idea. So, generally, the higher Q modes place more demand on the physics.

Conversely, as Q goes up, the injection power goes down. Less reliance is placed on high-power, high-efficiency neutral beams and gyrotron microwave tubes. Even the magnetic field strength comes down for the high Q thermal barrier mode. So, generally, the lower Q modes place more demand on technology.

The risk or demand placed on physics and on technology is non-quantitatively plotted in Fig. 11-1. One would tend to choose some compromise in arriving at an intermediate value of Q, depending on an opinion of success of developments in the future in both physics and technology. If we were to choose an operating mode for a prototype hybrid to be based on likely TMX results, we would choose the two-component mode at $Q = 0.5$. If we were to choose (guess) a mode for a prototype machine whose construction begins after MFTF-B has operated, we would opt for the thermal barrier mode, but probably not the highest Q version, so $Q = 3$ to 5.

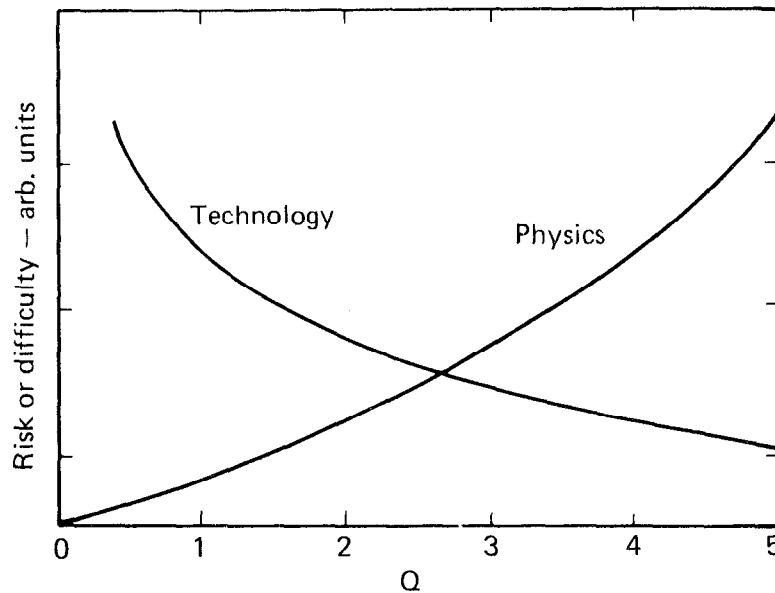


Fig. 11-1. Physics and technology risk tradeoff.

When we look ahead to a commercial fifth-of-a-kind, say, then we can assume even further refinements are made, and can assume even high Q is achieved. We are assuming a primary motivation for developing the tandem mirror will be the pure fusion goal, and therefore there will be motivation to seek Q over 10 operation independently of the hybrid application.

Finally, in choosing operating modes, we are driven by performance to seek out the lowest cost of product fissile fuel. In a study of the standard mirror (Yin-Yang coils, steady neutral beam injection) where Pu production was the goal, the cost of product fissile fuel vs Q was calculated as shown in Fig. 11-2. The Q for this technology-constrained design (8-T magnets and 125-keV beams) was only 0.6. A clear motivation for improving Q to about 1.5 can be seen. We have plotted a similar curve from the present study for ^{233}U production (Fig. 11-2). In this case, Q should be about 2.5. Our design point at $Q = 2.2$ for the thermal mode is somewhat low. A clear motivation for picking a higher Q operation mode is evident.

If greater emphasis is placed on nearer term physics or if problems should develop with the thermal barrier mode, then the two-component mode should be re-examined.

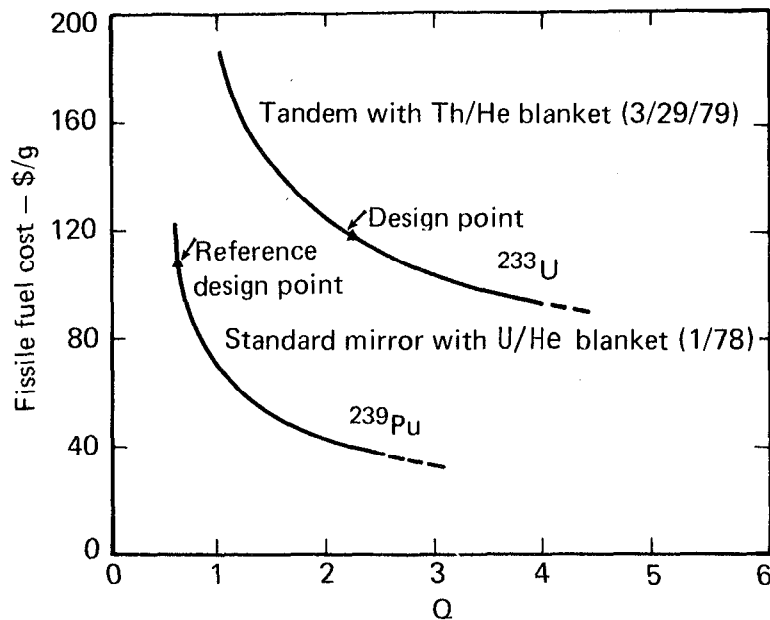
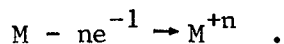


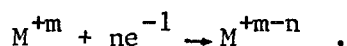
Fig. 11-2. Product fissile-fuel cost vs Q .

APPENDIX A
CORROSION DUE TO MHD EFFECTS

To understand the voltage effects, the corrosion process is considered from an electrochemical point of view (similar to a galvanic cell or battery). (Refer to Fig. A-1.) In any galvanic cell there are two electrodes: an anode and a cathode. The anode and cathode may be on the same metal surface in a corrosion situation. A corrosion process (or galvanic cell) involves two chemical reactions: an oxidation reaction, which occurs at the anode; and a reduction reaction, which occurs at the cathode. The oxidation reaction involves a metal (M) in its ground state valence giving up n electrons and becoming a metal ion with positive charge n:



The reduction reaction involves the opposite effect. Some ionized species M, with a valence of +m in the solution, gains n electrons and reduces its valence:



However, the reducing atom may or may not end up at its ground state valence. Electrical neutrality considerations require that the number of electrons released by the oxidation reaction equal the number of electrons received in the reduction reaction. Therefore, this electron flow can be related to the reaction rate by

$$R = I/nf ,$$

where

R is the reaction rate in g-moles/s.

I is the electric current in A.

n is the number of electrons per reaction.

F is the Faraday constant = 96,493.5 coulombs/equivalent.

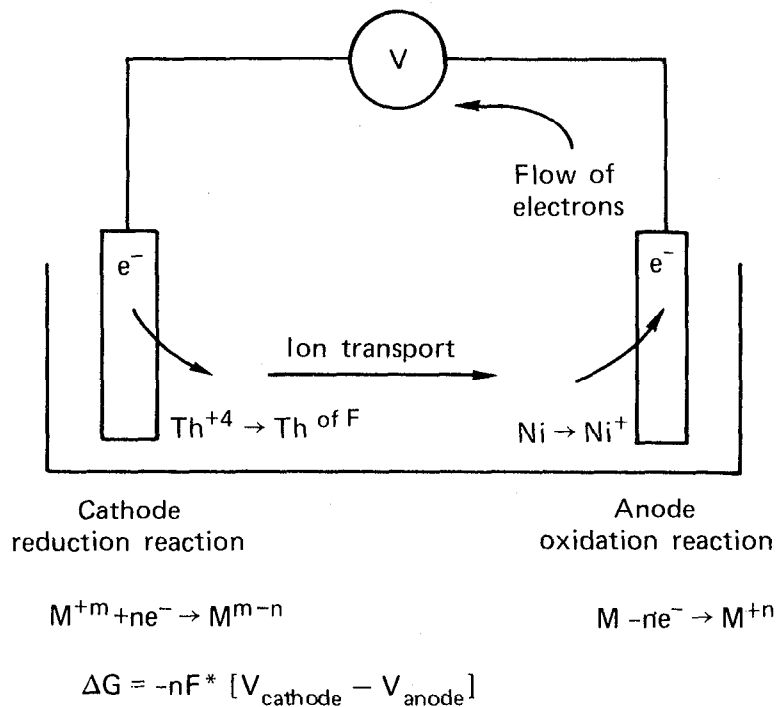


Fig. A-1. Electrical effects on corrosion.

The prediction of the spontaneous corrosion phenomenon involves a chemical thermodynamic evaluation of the oxidation (anode) and reduction (cathode) reactions. Specifically, the gibbs-free energies for these reactions are calculated by*

$$\Delta G_a^0 = + nFV_a^0, \text{ for oxidation at anode, and}$$

$$\Delta G_c^0 = - nFV_c^0, \text{ for reduction at the cathode,}$$

where

ΔG^0 is the standard gibbs-free energy of reaction as measured by a half-cell voltage technique (anode or cathode).

*G. N. Lewis and M. Randal, Thermodynamics, 2nd Edition, McGraw-Hill Book Co., New York, 1961, Chapter 24.

V° is the standard half-cell reaction voltage for the subscript pole (anode or cathode).

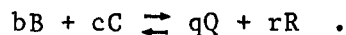
n and F have been previously described.

The net-free energy for the combined process is given by

$$\Delta G^{\circ} \text{ net} = \Delta G_a^{\circ} - \Delta G_c^{\circ} = nFV_a^{\circ} - nFV_c^{\circ} .$$

If this net-free energy is negative, the reactions proceed spontaneously. The above gibbs-free energies are given for the oxidation and reduction reactions when the ions are at their standard states (i.e., the activity of each species is equal to 1). For nonstandard states, the free energy is calculated from:

Consider the arbitrary reaction,



The free energy of this reaction is given by

$$\Delta G = \Delta G^{\circ} + RT \ln \frac{[A_Q]^q * [A_R]^r}{[A_B]^b * [A_C]^c} .$$

This can be converted to a voltage relationship by using the general formula

$$\Delta G = -nFV$$

Thus,

$$V = V^{\circ} - \left[\frac{RT}{nf} * \ln \frac{[A_Q]^q * [A_R]^r}{[A_B]^b * [A_C]^R} \right] ,$$

where

V is the apparent voltage of the cell.

V° is the standard-state voltage based on standard-state, half-reaction voltages.

R is the ideal gas law constant, which in electrochemical units equals 8.31470 J/deg. equivalent.

T is the absolute temperature in $^{\circ}\text{K}$.

n is Faraday's constant 96,493.5 C/equivalent or J/V equivalent.

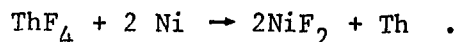
B,C,Q and R are dummy chemical forms.

b,c,q, and r are the stoichiometric coefficients of the B,C,Q, and R chemical forms, respectively.

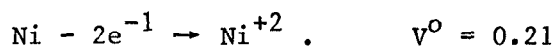
and A_I is the activity of species I.

By analogy to the net-free energy criteria for a spontaneous reaction, if the apparent voltage of the cell is positive, then the reaction proceeds spontaneously.

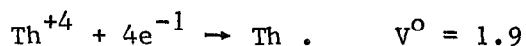
The main point of this thermodynamic evaluation is to determine the corrosion acceleration effects of an MHD-induced voltage. The above voltage equation holds the key to this answer, because the induced voltage drives the above arbitrary reaction. Instead of being zero, the threshold voltage for which the reaction proceeds is lowered by the value of the MHD-induced voltage. As an example, the case of thorium fluoride corrosion of nickel is treated as



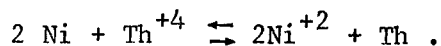
This is made up of two half cell reactions: oxidation and reduction. The oxidation reaction is



The reduction reaction is



To yield the ionic reaction:



$$V^{\circ} \text{ reaction} = V^{\circ} \text{ cathode} - V^{\circ} \text{ anode} .$$

$$V^{\circ} \text{ reaction} = 1.9 - (2 * 0.21) = 1.48 .$$

Putting this standard voltage into the voltage activity relationship gives
 [for 650°C (923°K)]

$$V = 1.48 - \left[\frac{8.3174 \frac{\text{J}}{\text{V equ.}} * 923^{\circ}\text{K}}{4 (\text{elec}) * 9.65 * 10^4 \frac{\text{J}}{\text{V equ.}}} \right] * \ln \frac{[\text{Th}]^{1.0} * [\text{Ni}^{+2}]^2}{[\text{Th}^{+4}] * [\text{Ni}]^{1.0}} .$$

The activities of nickel metal and thorium metal are 1, since they are solids.

Rearranging for the activity of nickel ions gives

$$\frac{[\text{Ni}^{+2}]^2}{[\text{Th}^{+4}]} = \text{EXP} \left[\frac{(1.48 - V)}{1.989 * 10^{-2} *} \right] ,$$

or

$$[\text{Ni}^{+2}] = [\text{Th}^{+4}]^{0.5} * \text{EXP} \left[\frac{(1.48 - V)}{2 * 1.989 * 10^{-2}} \right] ,$$

where

$[\text{Ni}^{+2}]$ is the activity of nickel ions in the molten salt.

$[\text{Th}^{+4}]$ is the activity of thorium ions in the salt.

V is the MHD-induced voltage.

The preceding relationship indicates that the thermodynamic equilibrium concentration of nickel ions in the molten salt is related to the applied MHD voltage by an exponential relationship. One way to consider this exponential effect is to calculate the voltage change that corresponds to a 10-fold increase in nickel concentration. Let V_0 be the reference voltage associated with a reference nickel concentration $[\text{Ni}^{+2}]_0$, and V_n and $[\text{Ni}^{+2}]_n$ represent the new voltage for the new nickel concentration, respectively. For a 10-fold increase in nickel concentration, the voltage difference is given by

$$\frac{[\text{Ni}^{+2}]_n}{[\text{Ni}^{+2}]_o} = 10 = \frac{[\text{Th}^{+4}]^{0.5} * \text{EXP} \left[\frac{(1.48 - V_n)}{2 * 0.01989} \right]}{[\text{Th}^{+4}]^{0.5} * \text{EXP} \left[\frac{(1.48 - V_o)}{2 * 0.01989} \right]},$$

$$10 = \frac{\text{EXP} \frac{1.48}{2 * 0.01989} * \text{EXP} \left(\frac{-V_n}{2 * 0.01989} \right)}{\text{EXP} \left(\frac{1.48}{2 * 0.01989} \right) * \text{EXP} \left(\frac{-V_o}{2 * 0.01989} \right)},$$

$$10 = \text{EXP} \left(\frac{-V_n + V_o}{2 * 0.01989} \right).$$

Thus, a 10-fold increase in the concentration of nickel ions is realized for a voltage of

$$V_o - V_n \ln(10) * 2 * 0.01989 = 0.0916 \text{ V}.$$

The corrosion rate is not necessarily directly related to the thermodynamic equilibrium concentration of the corroded ion. From a thermodynamic point of view, the controlling factor limiting corrosion is the ability of the molten salt to hold that activity of metal ion without having it precipitate. If the voltage potential applied drives the corrosion reaction such that the corrosion product ion concentration exceeds the solubility limit in the salt, then the corrosion reaction is thermodynamically favorable.

Data on the solubility of nickel in the molten salt method have not been found in the literature. Assuming that a nickel concentration of 10^{-3} g moles/l is acceptable and below the solubility limit of nickel in the molten salt, and also assuming that the solution is ideal (the activities of both thorium and nickel are equal to their concentrations), the MHD voltage that can be allowed without producing a spontaneous corrosion reaction is given by

$$V = 1.48 - 0.01989 * \ln \left[\frac{(\text{Ni})^2}{(\text{Th})} \right].$$

The thorium concentration in the molten salt is

$$[\text{Th}] = 0.72 \text{ mole \%} * 3.35 \frac{\text{g}}{\text{cc}} * \frac{1 \text{ mole}}{308 \text{ g}} * \frac{1000 \text{ cc}}{1}$$

$$[\text{Th}] = 10.9 \text{ g moles/l} .$$

For the assumed nickel concentration of 10^{-3} g moles/l:

$$V = 1.48 - 0.01989 * \ln \left[\frac{(10^{-3})^2}{10.9} \right] = -1.16 \text{ V} .$$

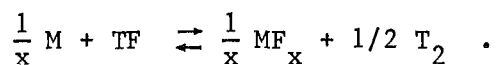
With these assumptions, more than 1 V of MHD-induced voltage is required to cause spontaneous corrosion. This is the basis of the 1-V limit used in the blanket internals design (Section 7).

APPENDIX B
MOLTEN SALT CHEMICAL CONSIDERATIONS

This appendix contains a summary of the review on general molten salt chemistry given by W. R. Grimes during the TMHR molten salt system review at Oak Ridge National Laboratory (ORNL).

In the molten salt blanket neutrons react with molten salt coolant by fissioning of the thorium and uranium and by transmutation of the lithium, beryllium, and fluoride. The fissioning generates three categories of fission products: noble gases, rare earths, and noble metals and metalloids. Each of these classes behaves differently in a molten salt system. The noble gases are slightly soluble in the molten salt and accumulate in any voids. Specifically in the molten salt concept, these noble gases probably accumulate in the void spaces in the beryllium rods. The rare earths and active metals form stable fluorides, which are moderately soluble in the molten salt. The noble metals and metalloids do not form stable fluorides and have a low solubility in the molten salt. Therefore, they tend to precipitate in the low temperature regions of the loop (i.e., the cold leg and the intermediate heat exchanger). In some of the nuclear fissions, the fission product elements do not use up all four of the fluorides from the fissioned atom. In this situation a net increase exists in the oxidative nature (free fluoride ions) of the salt, and it tends to be more corrosive to the structural metals.

Some of the transmutation reactions significantly contribute to the formation of free fluoride, because the cation is transmuted to helium, which does not combine with the fluorine. The tritium breeding reaction produces tritium fluoride that can cause significant corrosion of a metal (M) by



To control this fluoride corrosion, it is necessary to provide a reduction/oxidation (redox) buffer in the molten salt. In the MSRE the uranium (III)/uranium (IV) redox couple was used to maintain the proper redox chemistry. Unfortunately, the uranium concentration proposed for the TMHR

molten salt system is not sufficient to provide adequate protection. A reasonable candidate as a substitute redox buffer is cerium (III)/cerium (IV) fluoride, but there is no experimental molten salt data to verify this fact. "Rough calculations suggest that for a total cerium concentration of 10^{-4} mole fraction in a blanket containing 2×10^6 kg of Li_2BeF_4 , the coolant would have to be processed at a rate of 50 liters/minute to maintain the redox potential of $\text{CeF}_3/\text{CeF}_4$ in a safe range."*

If Hastalloy N is to be used in the system, it will be susceptible to tellurium-induced cracking, similar to the situation observed in the MSRE. This problem has been worked on at ORNL, and small additions of titanium or niobium to the Hastalloy N has been found to reduce this effect. The tellurium corrosiveness is also a strong function of the salt redox chemistry. To reduce the tellurium corrosion, the salt must be kept strongly reductive. In the MSBR, a UF_4 to UF_3 mole ratio of 50 or less was to be used. If a salt maintained this reductive, tritium is predominately in the T_2 form. In this form the tritium easily diffuses through piping system, especially the tubes of the intermediate heat exchanger.

In summary, the TMHR molten salt system requires a molten salt chemistry development program, especially the development of a new redox control system, possibly based on the Ce (III)/Ce (IV) fluoride couple, but there are no obvious unsolvable problems.

*S. Cantor and W. R. Grimes, "Fused-Salt Corrosion and Its Control in Fusion Reactors," Nuclear Technology, Vol. 22, April 1974, pp. 120-126.

APPENDIX C

ARGONNE NATIONAL LABORATORY COMMENTS ON THE MIRROR HYBRID STUDY

During fiscal year 1979, Argonne National Laboratory carried out a hybrid assessment study for DOE. The assessment used the LLL-Mirror Hybrid Study, the Westinghouse-Tokamak Hybrid Study, and other sources. The results will appear in an Argonne report. Some response from the Argonne group to our work is contained in a letter included herein because it offers a more objective perspective than ours.

ARGONNE NATIONAL LABORATORY

9700 SOUTH CASS AVENUE, ARGONNE, ILLINOIS 60439

TELEPHONE 312/972-4836

August 23, 1979

Dr. Ralph W. Moir
Mail Code L-436
Lawrence Livermore Laboratory
P. O. Box 808
Livermore, California 94550

Dear Ralph:

We greatly appreciated the opportunity last week to discuss with you and your team the status of the tandem mirror hybrid reactor study. We believe the staff from LLL, GE, GA and Bechtel have done a good job so far, and we encourage your efforts to communicate the results of your study with us and others in the fusion community. The following are some specific comments that some of our staff made after your presentation. I'm sure that you have already considered most of them; hopefully they will be of some further value to you as you continue the study.

General Comments

- It appears that excellent progress has been achieved in developing a conceptual design.
- Some of the design concepts (molten salts, use of TZM, use of Be, etc.) imply an advanced reactor concept not well suited to "near term" application. Would you adopt the same design features if your objective was to design a hybrid demo plant?
- The dismissal of lithium coolant/breeder seems premature. We do not understand why MHD pumping losses should be such a problem at low fields (~ 2 T).

Molten Salt Design - GE

- The outstanding feature is clearly the on-line reprocessing of fissile fuel and tritium.
- The molten-salt concept shows the best nuclear performance relative to the other blankets under consideration. This performance is due to three assumptions:
 - A tritium breeding ratio of 1.0
 - Minimization of blanket energy multiplication.
 - The use of Be as a neutron multiplier.
- If these three assumptions are changed to reflect a more realistic system, this performance will degrade and perhaps other blanket concepts will look more attractive.

- The utilization of Be-9 as a neutron multiplier involves unresolved problems such as material resources and high helium gas production rates. In addition, the use of Be-9 may pose a problem in regard to a sizeable tritium production in the multiplier region due to the Be(n,t) reaction. According to the UWMAK-II design, a tritium production rate of ~ 6 gr/day is estimated for a 5000 MWth power plant. Is it feasible to replace the Be-9 with a more problem-free material (PbO, for instance) from the material compatibility standpoint? Unless minimizing fissile/fertile burnup is one of the major design criteria, employment of a fast/thermal fission plate (as in the helium-cooled design) might be a desirable option.
- The choice of TZM as a structural material generates some difficult problems which need special attention.
 - Long-term radioactivity
 - Large tritium leakage rate from TZM at high temperature
 - TZM fabrication and joining are difficult, especially in the field
- A permanent first wall/vacuum vessel approach using joined tubes of TZM and He cooling seems very optimistic. There appears to be at least 23000 meters of weld path which must be absolutely leak tight to high pressure helium.
- Clad Be rods will require very special handling. Further work on rod and clad design is required.
- The tritium in this system will be present as TF. This may cause some severe materials problems, especially in the presence of even small amounts of moisture. The shield will be cooled by either helium or water. In the latter case, a severe corrosion problem will result in most metal systems if TF is present.
- Possible decomposition of flibe salt with modest voltages in the blanket should be considered.
- Control of the heat transfer in the breeding blankets is complex, lengthy flow paths appear to be marginal.

He Design - GA

- The large He piping required at high pressure (58 atm), high temperature (430°C) with significant weld lengths, joints, pipe supports, valves, etc., seems to be a real challenge, even in the year 2020.
- Cushion seal (omega) at 6-7 meters will require development and may limit design philosophy.

- Using Li_2O as the breeding material introduces materials problems. With fresh samples, reasonable extraction times for tritium are obtained at 600°C ; however, one would expect that higher temperatures would be required as the system ages, probably in the order of 700°C . The greatest portion of the center line temperature of the Li_2O system is below 600°C at beginning of life and below 700°C at end of life.
- Due to the spectrum softening inherent in the use of Li_2O , the tritium in the Li_2O blanket saturates at its full capability in a relatively shallow blanket region. It is advisable to use a graphite reflector behind a thinner Li_2O blanket.

Maintenance and Balance of Plant

- General concept of modular design is attractive. Movement of magnets appears to be the major concern. Magnets will have to be moved under "cold" conditions, this needs further investigation.
- Overall balance of plant concept has been thought out fairly well for both design concepts.

Sincerely,

Charlie

Charles C. Baker
Director
Fusion Power Program

CCB:cap

OAK RIDGE NATIONAL LABORATORY

OPERATED BY
UNION CARBIDE CORPORATION
NUCLEAR DIVISION



POST OFFICE BOX X
OAK RIDGE, TENNESSEE 37830

September 10, 1979

Dr. Ralph W. Moir
Lawrence Livermore Laboratory
Post Office Box 808
Livermore, California 94550

Dear Ralph:

I think all of our people thoroughly enjoyed the opportunity to go back over some of the technical aspects of the MSR concept with you at our recent meeting.

With respect to your question about the termination of the MSR Program, I think the causes are reasonably well established. Even while the MSR was under full development at ORNL (before about 1970), it was a small program, and it did not generate much outside interest - either from industrial concerns within the US or from foreign organizations. Part of this lack of interest was probably due to the heavy emphasis on the LMFBR by nearly everyone, including the AEC. As a consequence, the MSBR was regarded principally as no more than a backup to the LMFBR.

The program was canceled in 1973, even though there was some evidence of increasing industrial interest. Factors which are presumed to have at least contributed to this action included:

- a. the perennial excess of RD&D funding needs over available funds,
- b. the desire to expedite development of LMFBR technology,
- c. perceived difficulties in "selling" a unique, highly chemistry-oriented reactor technology to the power industry,
- d. the time and cost associated with the demonstration of a new technology, and
- e. perceived problems and potential obstacles to the successful development of MSRs.

APPENDIX D

REASONS FOR TERMINATION OF THE MOLTEN SALT REACTOR PROGRAM

The use of molten salt technology requires further development from the state-of-the-art developed by Oak Ridge National Laboratory over a two-decade period. In assessing the size of the development and the risk involved, we encountered a legacy somewhat like other technologies that are now all but dead, such as steam cars, lighter-than-air ships, and wind-power. We are concerned that the hybrid application would have to carry an extra burden by the lack of interested parties for other uses of molten salt. To assess the reasons for the termination of the molten salt reactor program so we can judge the relevance of these reasons for the hybrid application, we asked J. R. Engel to present his opinion why the program was terminated. His letter is attached.

When the program was reestablished in 1974, it was a technology development activity with reactor conceptual design excluded from the effort. Availability of funds was again a major consideration in the termination of the program in 1976.

Obviously, the above reasons must be regarded as only opinions since the decisions were made within AEC/ERDA/DOE.

Yours truly,



J. Richard Engel
Engineering Technology Division

JRE:jt

cc: L. E. McNeese
M. W. Rosenthal
H. E. Trammell

DISCLAIMER

This document was prepared as an account of work sponsored by an agency of the United States Government. Neither the United States Government nor any agency thereof, nor any of their employees, makes any warranty, expressed or implied, or assumes any legal liability or responsibility for the accuracy, completeness, or usefulness of any information, apparatus, product, or process disclosed, or represents that its use would not infringe privately owned rights. Reference herein to any specific commercial product, process, or service by trade name, trademark, manufacturer, or otherwise, does not necessarily constitute or imply its endorsement, recommendation, or favoring by the United States Government or any agency thereof. The views and opinions of authors expressed herein do not necessarily state or reflect those of the United States Government or any agency thereof.

This work was supported by the United States Nuclear Regulatory Commission under a Memorandum of Understanding with the United States Department of Energy.

Available from
GPO Sales Program
Division of Technical Information and Document Control
U.S. Nuclear Regulatory Commission
Washington, D.C. 20555
and
National Technical Information Service
Springfield, Virginia 22161